FINAL REPORT

NATIONAL SCIENCE FOUNDATION WORKSHOP

POST-LIQUEFACTION SHEAR STRENGTH OF GRANULAR SOILS

Principal Investigators:
Timothy D. Stark – University of Illinois
Steven L. Kramer – University of Washington
T. Leslie Youd – Brigham Young University

NSF Workshop held at University of Illinois - Urbana-Champaign on April 18-19, 1997

NSF Grant CMS-95-31678
Earthquake Hazard Mitigation Program of the National Science Foundation

July, 1998

PREFACE

These Proceedings document the goals, objectives, and results of a two-day Workshop on the Shear Strength of Liquefied Soils that was held at the University of Illinois at Urbana-Champaign on April 18-19, 1997. The original title of the Workshop was the "Post-Liquefaction Shear Strength of Granular Soils", however, discussions during the Workshop suggested that the "Shear Strength of Liquefied Soils" was a more appropriate title for the Proceedings. The Workshop was funded by the National Science Foundation with the primary objective of identifying and prioritizing research needed to improve the state-of-the-art and state-of-the-practice on the behavior and estimation of the shear strength of liquefied soils.

The Principal Investigator would like to thank all of those individuals who contributed to the success of the Workshop through the submission of a written statement and their active participation in the Workshop. Funding for the Workshop was provided by Grant No. CMS-95-31678 from the Earthquake Hazard Mitigation Program of the National Science Foundation (NSF). The National Science Foundation funding and the support of Clifford J. Astill, NSF Program Director, are gratefully acknowledged.

The Proceedings present an executive summary, three keynote lectures, a description of Workshop events and discussions, written summaries submitted by each participant, and the findings, conclusions, and recommendations of the Workshop.

The Proceedings constitute a final report to the National Science Foundation for Grant No. CMS-95-31678. The Proceedings are also available on the World Wide Web. The conclusions and recommendations expressed herein do not necessarily reflect the views of the National Science Foundation.

Timothy D. Stark, Principal Investigator
University of Illinois at Urbana-Champaign
July, 1998

TABLE OF CONTENTS

LIST OF TABLES

LIST OF FIGURES

WORKSHOP ACTIVITIES

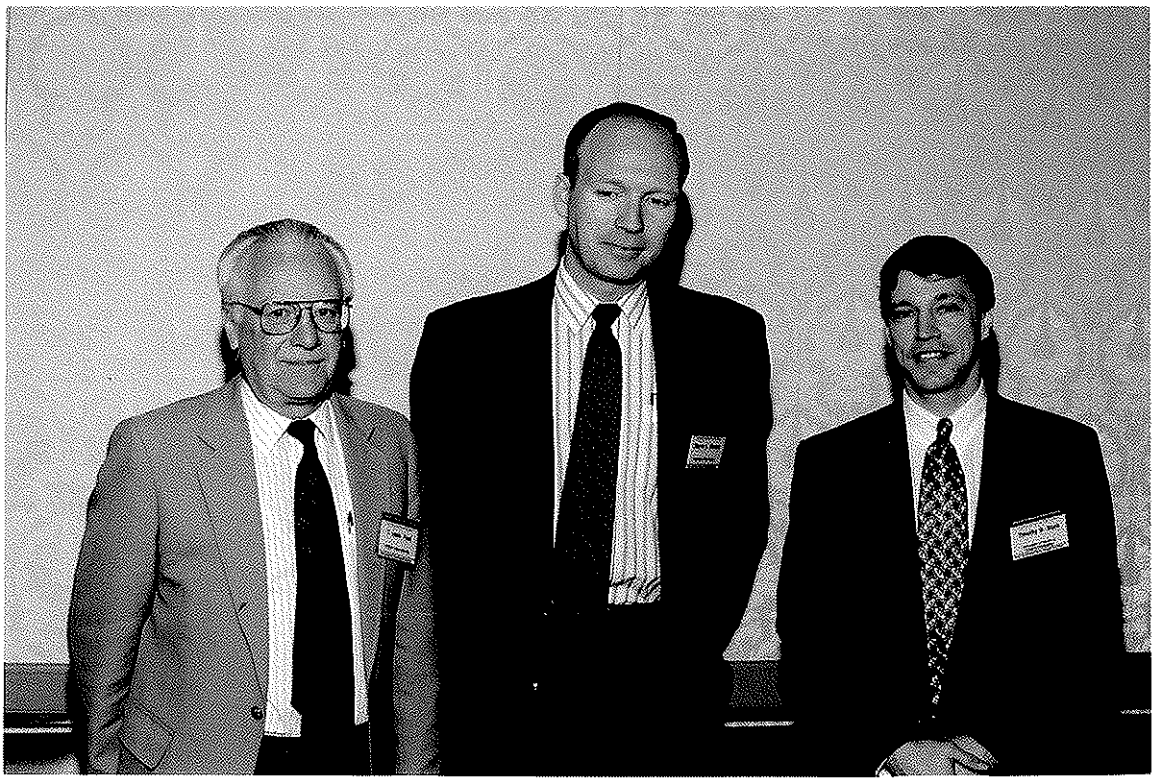

Photo 1

Workshop organizing committee (from left: Professors T.L Youd, S.L. Kramer, and T.D. Stark)

Photo 2

Welcoming remarks by Professor T.D. Stark

Photo 3

National Science Foundation Program Director Dr. C.J. Astill with University of Illinois Civil Engineering Department Head, Professor D.E. Daniel

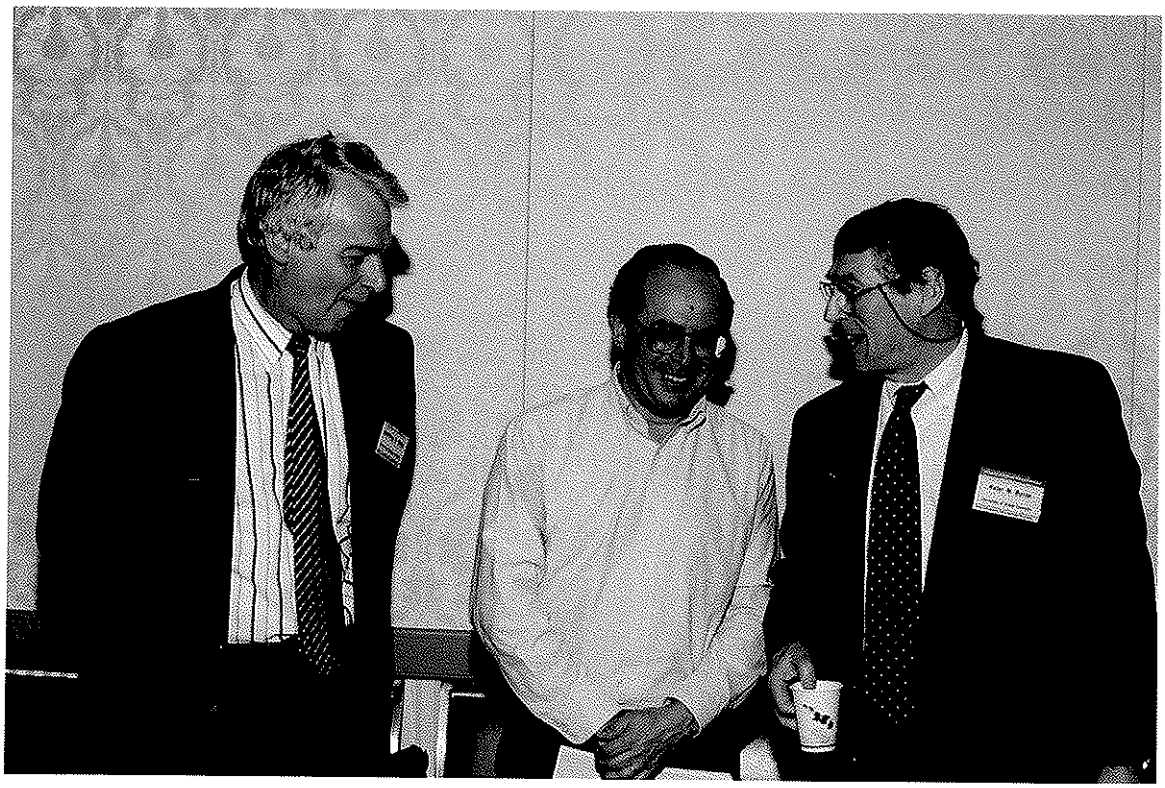

Photo 4

Keynote lecturers (from left to right: Prof. G.R. Martin, Dr. G. Castro, and Prof. P.M. Byrne)

Photo 5

Keynote lecture presentation by Professor P.M. Byrne

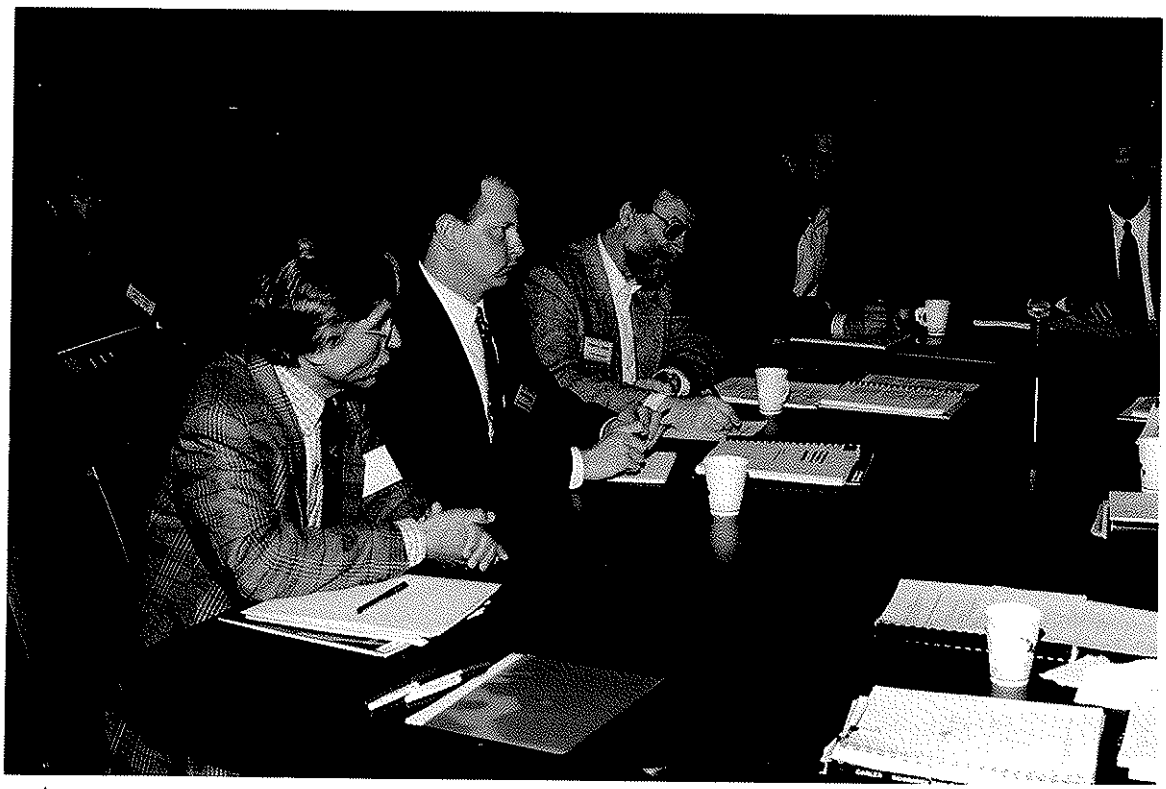

Photo 6

Discussion group meeting (from left to right: Prof. G. Mesri, Mr. J.E. Hedien, Prof. W.A. Charlie, Prof. B.L. Kutter, and Mr. S.M. Olson)

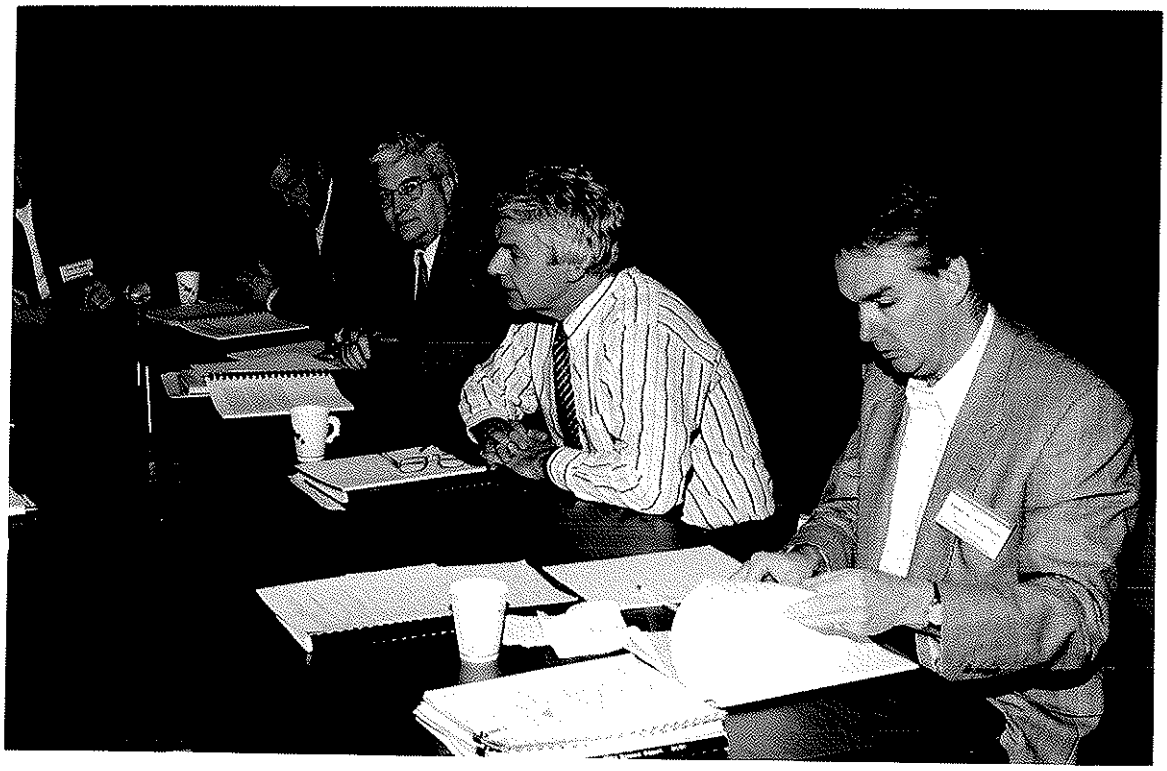

Photo 7

Discussion group meeting (from left to right: Prof. M.F. Riemer, Dr. S.J. Poulos, Keynote Speaker Prof. G.R. Martin, and Prof. P.K. Robertson)

Photo 8

Discussion group meeting (from left to right: Dr. L.F. Harder Jr., Prof. I.M. Idriss, Prof. T.L. Youd, Keynote Speaker Dr. G. Castro, Prof. R. Dobry, Dr. W.-J. Su, Mr. K. Ghiassi, and Dr. A.G. Franklin)

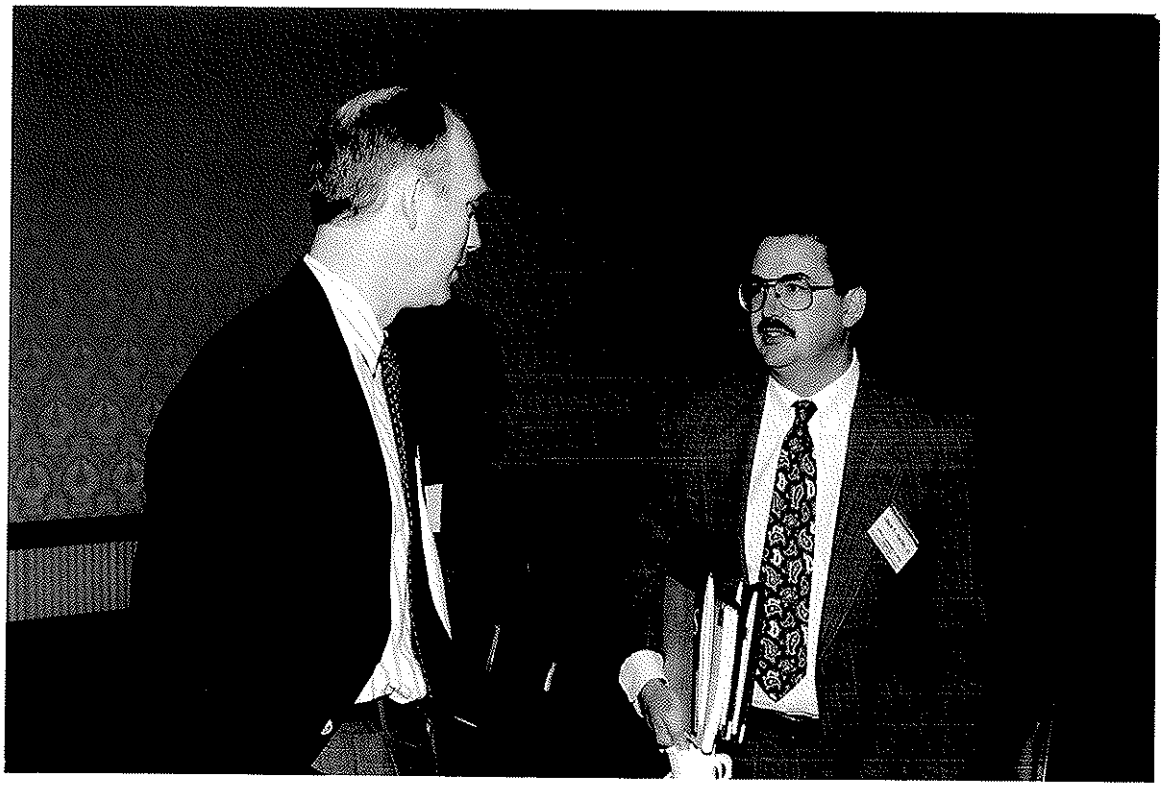

Photo 9

A coffee break shared between Prof. S.L. Kramer and Dr. L.F. Harder Jr.

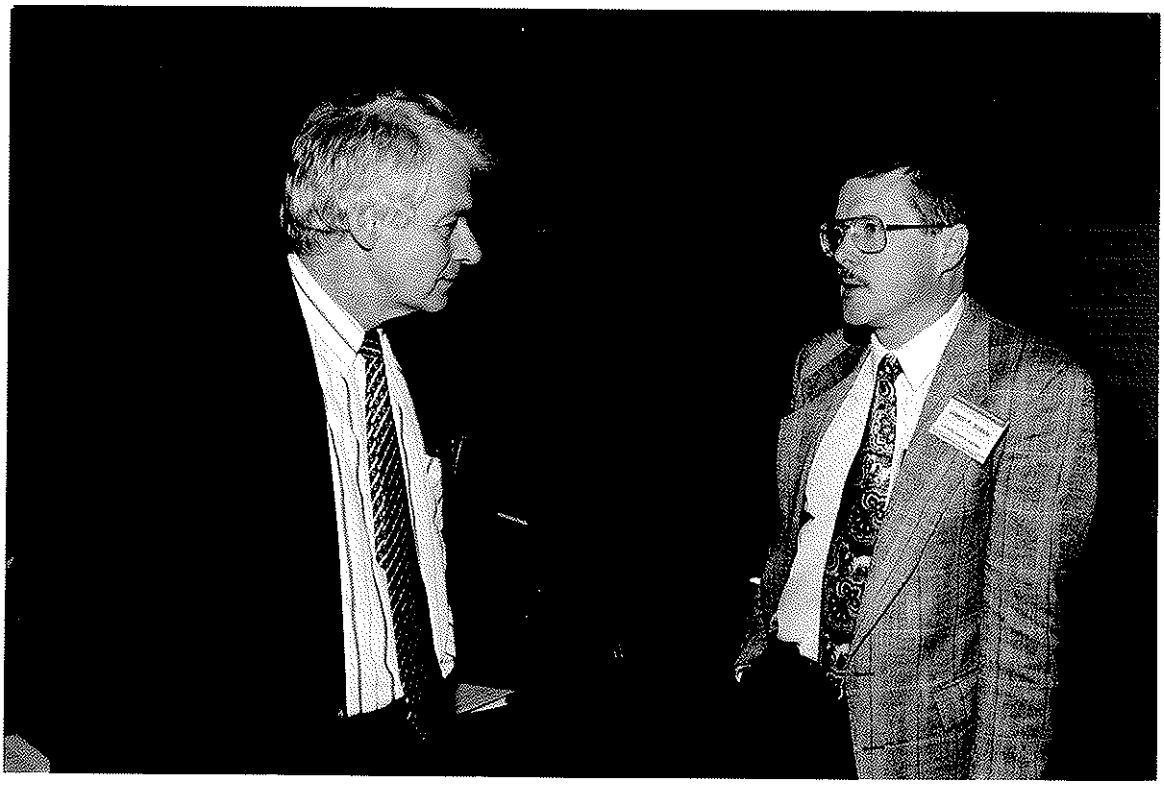

Photo 10

A coffee break shared between Prof. G.R. Martin and Dr. J.P. Koester

The mix had zero strength at the average water content and so flowed through cracks in the rock. The effect of the mixing on the cone trace is shown in Fig. 8. It may be seen that at Site 5, where the flow took place, the trace has been greatly changed and the layering effect on the cone has been lost, as compared to site 2 which is outside the sinkhole zone. Penetration tests on the mixed material show that the average $(N_1)_{60}$ value was reduced to about 5.

Mixing of sand and silt layers under undrained conditions can lead to a very large reduction in residual strength. Such a reduction has occurred at a mine site in African caused by sinkhole formation. Could seismic movements result in mixing, and a similar loss in residual strength?

Was mixing a factor at the Lower San Fernando and Mochikoshi Dams that underwent very large liquefaction-induced strains and displacements?

STRAINS TO MOBILIZE RESIDUAL STRENGTH

The strains required to mobilize the residual strength are important because for many structures the displacements associated with these strains may be too large to tolerate. Provided both the residual strength and the strain required to mobilize it are known, the associated displacements can be estimated for any soil structure system.

Stress-strain response for both monotonic and cyclic loading of loose sand under undrained loading conditions are shown in Fig. 9a. The associated effective stress paths are shown in Fig. 9b. Once the stress path crosses the "collapse" surface into the unstable zone, the resistance of the soil reduces with increasing strain until it drops below the driving stress, τ_{st}, initiating a flow slide. Figure 9 illustrates that the steady state strength depends on the residual effective stress σ'_r and is independent of whether liquefaction is triggered by monotonic or cyclic loading. In this case, the strain to mobilizes the residual strength is independent of the liquefaction trigger mechanism. This occurs because of the high static bias which has prevented the shear stress from changing sign.

For near level ground conditions, the static bias is essentially zero and the stress strain response is depicted in Fig. 10a. The associated effective stress path is shown in Fig. 10b. Under cyclic loading the undrained shear stress-strain response of sand remains stiff for a number of cycles and then abruptly changes to a dramatically softer response. This softer response is caused by a rise in porewater pressure during each cycle of load which drives the stress path towards the ϕ_{cv} line or the collapse line. This represents the pre-triggering response or phase 1 as shown on Fig. 10. Once the ϕ_{cv} line is reached, large deformations may occur and the stress path moves up the ϕ_{cv} line (actually slightly above ϕ_{cv}), depicted as phase 2. Upon unloading, phase 3, high pore pressures occur that lead to a zero effective stress state (point C, Fig. 10). Very large strains may then occur at virtually zero shear stress. This state is true liquefaction as the material deforms as a fluid. With further strain, phase 5, the soil skeleton dilates, the pore pressure drops and the stress point moves up the ϕ_{cv} line again. Upon reversal, the procedure repeats itself with the strain loops getting larger with each cycle.

This behaviour represents level ground conditions where there is no static driving force on the horizontal plane, and is similar to that observed (Fig. 11) at the Wildlife Site in California during a liquefaction event in 1987. This figure was developed from acceleration recordings above and below the liquefied layer, and essentially represents an in-situ shear test. The average strain in the liquefied layer was obtained by double integrating the acceleration records. The corresponding shear stress is directly proportional to the acceleration of the overlying soil. This process, referred to as imaging shows that the field response is similar to that observed in the laboratory. The strains are, perhaps, a bit smaller than expected for a loose soil, and this may be because it was assumed that the entire loose layer had liquefied. Larger strains would be calculated if only a portion of the layer had liquefied.

If the applied loading is not symmetric, then the post-liquefaction response is also unsymmetric with strains accumulating in the direction of the load as shown in Fig. 12. It is this behaviour that is responsible for the large liquefaction-induced displacements that can be so damaging to earth structures and termed lateral spreading.

Figure 12 shows that although the sand tested was loose, it was quite dilative once the phase transformation or ϕ_{cv} state was reached. Upon unloading, the effective stress drops to zero as the porewater pressure rises sending the stress state back to the origin. Upon subsequent loading, the stress path follows up the ϕ_{cv} line (slightly above) with the shear stress increasing and the porewater pressure dropping due to dilation. As the effective stress increases, further dilation is curtailed and the soil reaches its residual strength at a strain of about 30%.

The strains to reach the residual strength may be very different for monotonic and cyclic loading conditions as illustrated in Fig. 13. A soil element starting at stress state "A" and loaded monotonically, will follow the stress path ABC (Fig. 13a) and the stress-strain path ABC (Fig. 13b) to the residual strength, S_r. If the element is liquefied by cyclic loading with stress reversals, its effective stress state will drop to a zero. If loaded monotonically, it will then follow up the ϕ_{cv} line to reach the residual strength S_r at point C. Although the residual strength may be the same, the resistance of the soil and the strains to reach the residual strength are now very different, being small for monotonic liquefaction and perhaps very large after cyclic liquefaction. In fact, there is no single resistance curve or residual strain value associated with cyclic liquefaction. The strain depends on the magnitude of cyclic stress, number of cycles and degree of non-symmetry in loading as depicted in Fig. 14.

STRESS-STRAIN MODELS

There are numerous stress strain models in the literature ranging from simple to complex. Jefferies and Prevost have developed sophisticated models, and we hope to hear more about these at this workshop. To be useful, models must be able to capture both the characteristic drained and undrained response of sand.

Typical shear stress-strain and volumetric response of loose sand under drained conditions is shown in Fig. 15. This represents the skeleton response. The main features can be captured using a simple elastic-plastic model. The elastic response (unloading) is largely isotropic and the main

features can be captured using stress level dependent elastic shear and bulk moduli, G^e and B^e. The loading response is largely plastic and depends on ***stress ratio*** rather than stress. It can be captured by a plastic shear modulus, G^p that reduces with stress level and approaches zero at failure.

The plastic volumetric strain $\Delta\varepsilon^p_v$ can be captured by a dilation angle, ν, such that:

$$\Delta\varepsilon^p_v = \Delta\gamma^p \sin\nu$$

$$\text{and} \qquad \sin\nu = \sin\phi_{cv} - (\tau/\sigma')$$

This relation for sin ν is essentially that proposed by Taylor (1948) and is similar to Rowe's stress dilatancy theory, i.e., the sand contracts for stress ratios below the ϕ_{cv} line and expand above as shown in Fig. 15c and d.

Undrained response merely prescribes a volumetric constraint on the skeleton that causes the porewater pressure to rise, and the effective stress to drop as shown earlier. A model, if properly formulated, should predict the strain softening that occurs in loose sands under constant volume conditions. In addition, the fabric effect can be captured by varying the plastic modulus with the direction of loading.

Note that the strain softening is not an instability or bifurcation problem as the stress ratio continues to rise and the plastic modulus remains positive during softening. However, development of non-uniformities could occur.

The physics of the undrained response is as follows:

Volumetric strains comprises of elastic and plastic components $\Delta\varepsilon^e_v$ and $\Delta\varepsilon^p_v$. For undrained conditions

$$\Delta\varepsilon_v = \Delta\varepsilon^e_v + \Delta\varepsilon^p_v = 0$$

$$\Delta\varepsilon^e_v = (\Delta\sigma'/B^e)$$

$$\text{and} \qquad \Delta\varepsilon_v^p = -\Delta\gamma^p \sin\nu$$

Hence,

$$\boxed{\Delta\sigma' = B^e\,\Delta\gamma^p \sin\nu}$$

This simple expression indicates that the elastic bulk modulus and the dilation angle control the change in effective stress for a prescribed plastic strain increment, $\Delta\gamma^p$. The plastic increment, in turn, depends on the plastic modulus. For stress states below the ϕ_{cv} line, the effective stress will always drop upon shearing as the dilation angle is negative. When the ϕ_{cv} line is reached, dilation drops to zero and if the sample is loose the dilation stays zero and the sample has reached the

critical state. If the sample is denser or the stress state is very low, the sample will dilate and the stress point will move up just outside the ϕ_{cv} line. As it moves up, the stresses increase and dilation is eventually suppressed, and the sample reaches its steady state strength when no further dilation occurs.

The quasi-steady-state occurs in loose samples when the element first reaches the ϕ_{cv} line. At that point the dilation is zero, but with further strain, dilation occurs and the sample moves up the ϕ_{cv} line (just outside).

Elastic-plastic models that capture the element behaviour indicate that the key parameters controlling the undrained or constant volume response are:

1) the elastic bulk modulus of the soil;
2) the plastic shear modulus; and
3) the dilation, if any, after the ϕ_{cv} state is reached.

The characteristic behaviour observed in the testing can be explained in these terms. The strain softening is due to a low plastic modulus. The effective stress at phase transformation, which controls the quasi-steady state strength is also controlled by the plastic modulus. The steady state strength is controlled by the dilation angle, and its gradual suppression as the stress increases, once phase transformation has been reached. As suggested by Jefferies, the steady state is reached when both the dilation and dilation rates are zero.

SUMMARY

- The post-liquefaction shear strength is the strength that can be relied upon for stability and deformation analyses. It is usually assumed to develop under undrained conditions.

- Laboratory testing indicates that the undrained strength of a given soil depends primarily on void ratio, but that fabric and loading path may also have a large influence. It is possible that at large strain, fabric effects might be wiped out and the soil reach a steady state, but the strains required to do so could be very large.

- The strains required to mobilizes the post-liquefaction strength can be very different depending on the pre- and post-liquefaction stress path. It is suggested that the post-liquefaction stress-strain response should be examined rather than the strength alone.

- Models are of two basic types: particulate and continuum. The particulate model has the possibility of predicting response from fundamental particulate mechanics taking into account particle size, shape, grading, fabric, non-uniformities, etc., but it is very complex.

- Continuum models basically capture observed behaviour. We must first agree on the behaviour before we capture it. Critical state represents an agreement about soil behaviour. The general concept as applied to liquefaction problems is that for a given void ratio, there is a

single valued effective stress at failure at which point both the dilation and dilation rate are zero, and hence, the shear strength - the steady state strength is uniquely specified.

A great deal of testing carried out in the past 15 years on sands and silts suggests that the effective stress at failure for a given void ratio is not unique, and that the shear strength of interest can have a wide range of values depending on fabric and loading path. Thus, critical state, while a useful general concept, should not be adhered to too rigorously.

- The concept of a strength related to the initial vertical confining stress S_r/p' is very attractive in practice. For a given method of deposition, loose states, and similar loading paths, test data support the concept. S_r/p' as a function of relative density or penetration resistance is also supported by the data.

- Fines: Defining fines as the % passing the #200 sieve seems reasonable. However, whether the fines are contained in the voids of the coarse material or occupy contact locations is also important, i.e., the fabric. In addition, whether the fines are plastic or non-plastic would seem important. Tests indicate that the presence of fines seems to curtail dilation and so lower the residual strength.

- Stress-Strain Models: Stress-strain models must capture the observed element skeleton behaviour to be of use. Undrained response involves a volumetric constraint applied to the skeleton, and results in a strain softening response for loose sands. A useful model must predict this from the volumetric constraint.

- Simple modelling shows that the change in effective stress due to shearing under constant volume is controlled by the plastic shear modulus, the elastic rebound modulus and the dilation angle. If from drained testing we find that the material at large strain is strongly dilative, we could be assured of a high residual strength. In-situ tools such as the pressuremeter could evaluate dilation at large strains.

- Models can have three functions:

  1. They should provide a mechanic's basis for understanding the behaviour of granular soils.

  2. They should be capable of predicting element stress-strain and strength response over a range of stress paths for a given soil with a given structure.

  3. The incorporation of such an element model in a stress deformation analysis would allow the complete response of the soil structure to be obtained before, during, and after the earthquake, including drainage effects both local and global.

- Final question: How do we determine post-liquefaction shear strength for field conditions? Recover and test undisturbed samples?

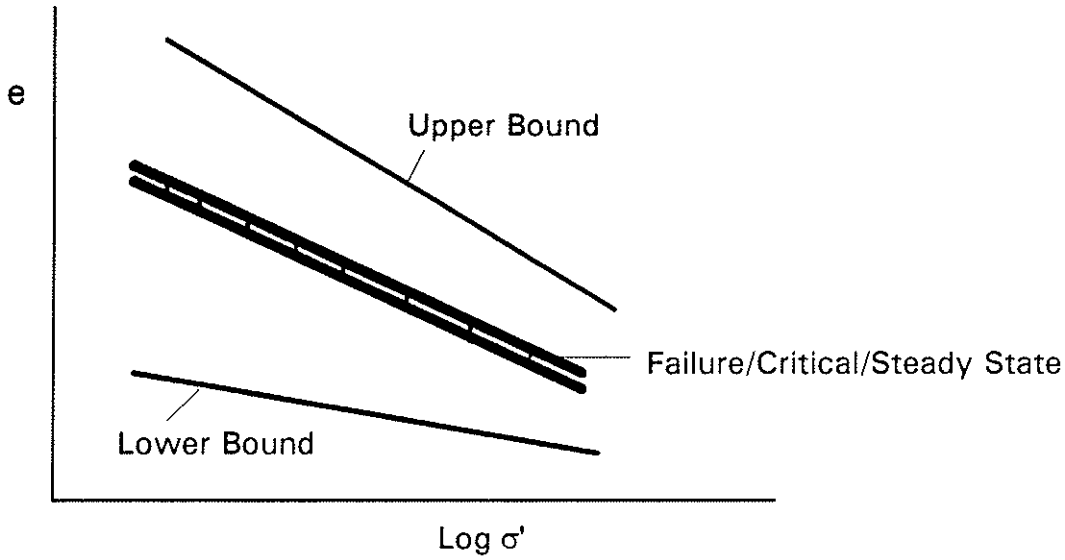

Fig. 1. Void ratio, effective stress states.

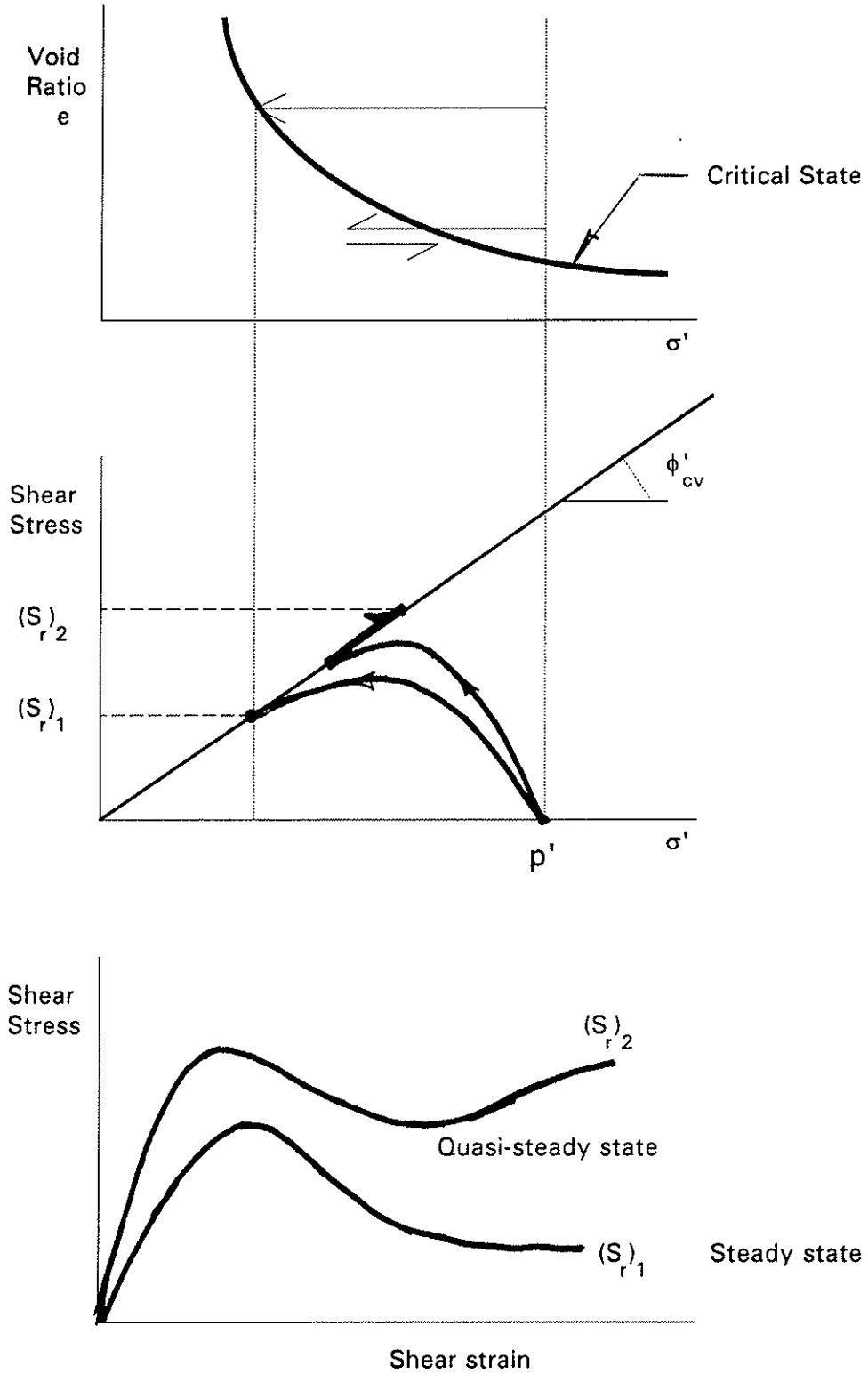

Fig. 2. Characteristic undrained response and critical state concepts.

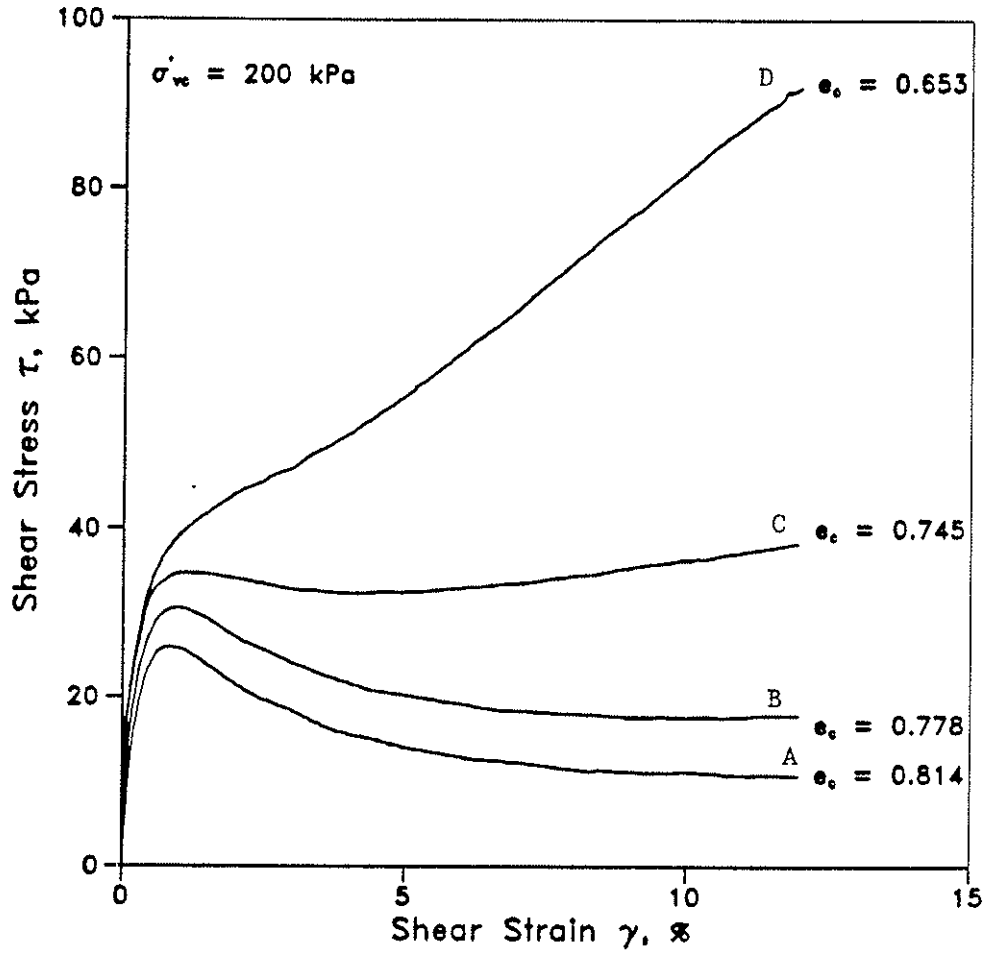

Fig. 3. Undrained response of Syncrude sand at different void ratios for σ'_{vc} = 200 kPa (Sivathayalan, 1994)

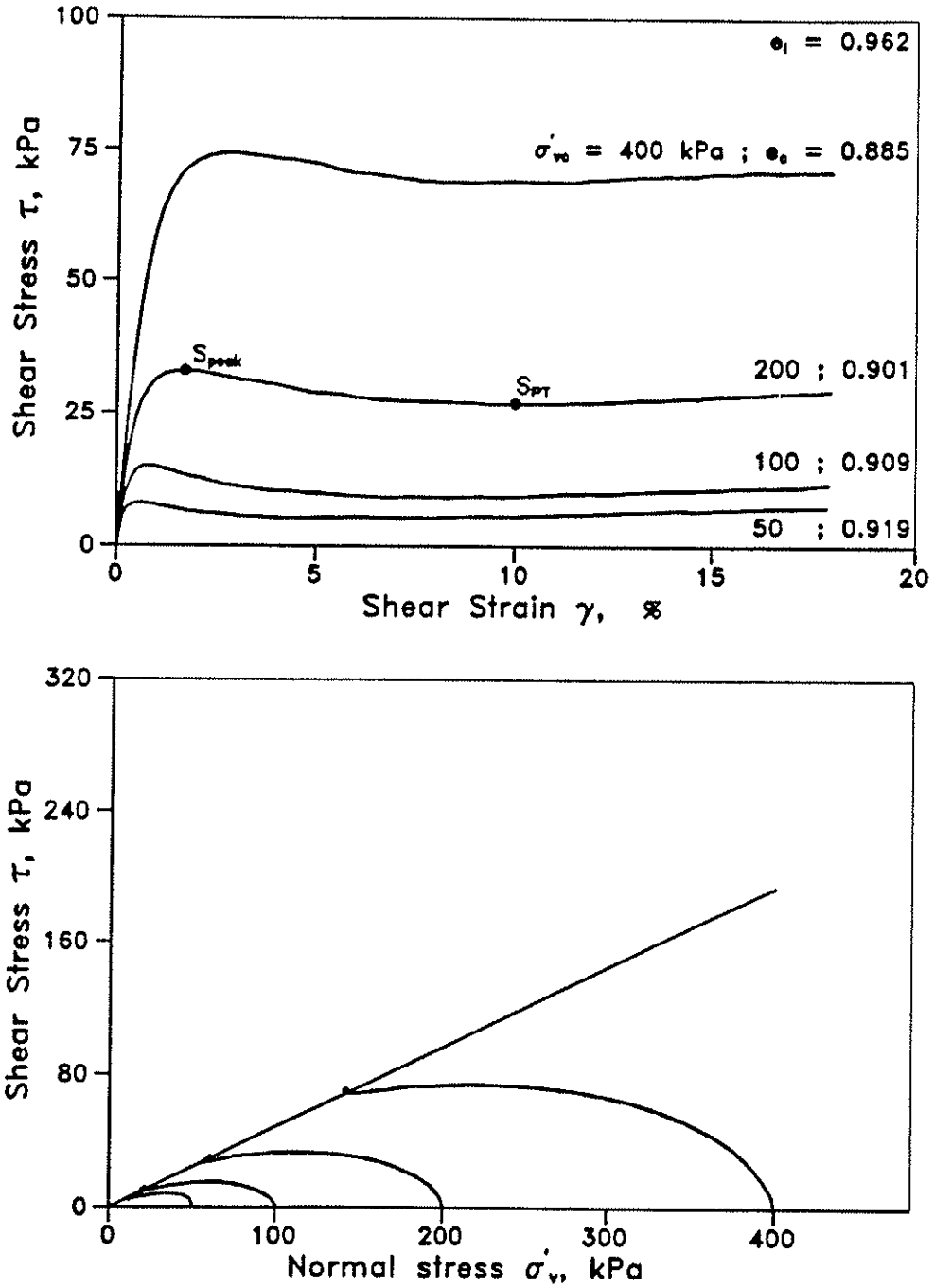

Fig. 4(a). Static undrained simple shear behaviour of loosest deposited Fraser River sand (Sivathayalan, 1994).

(a)

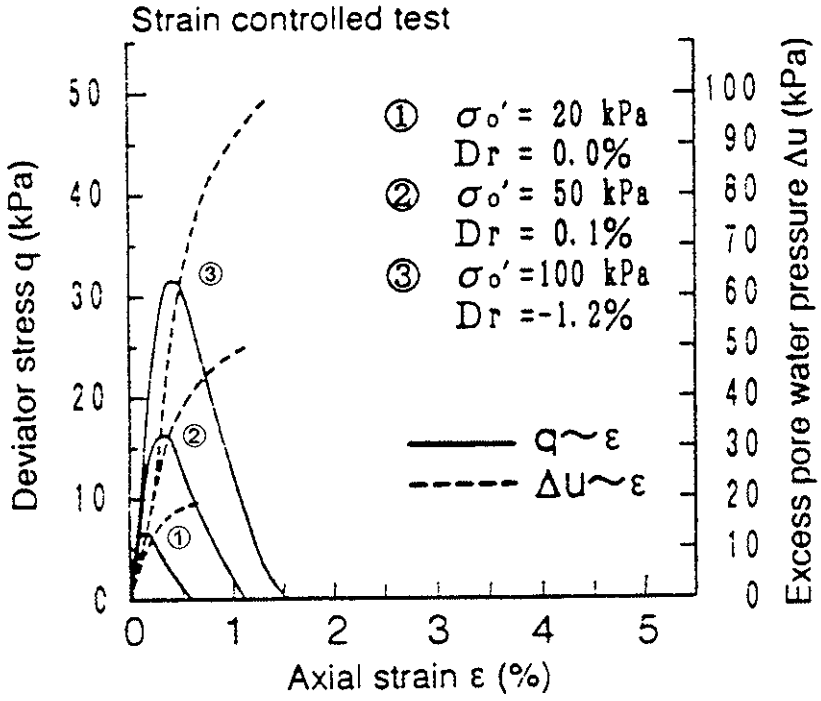

(b)

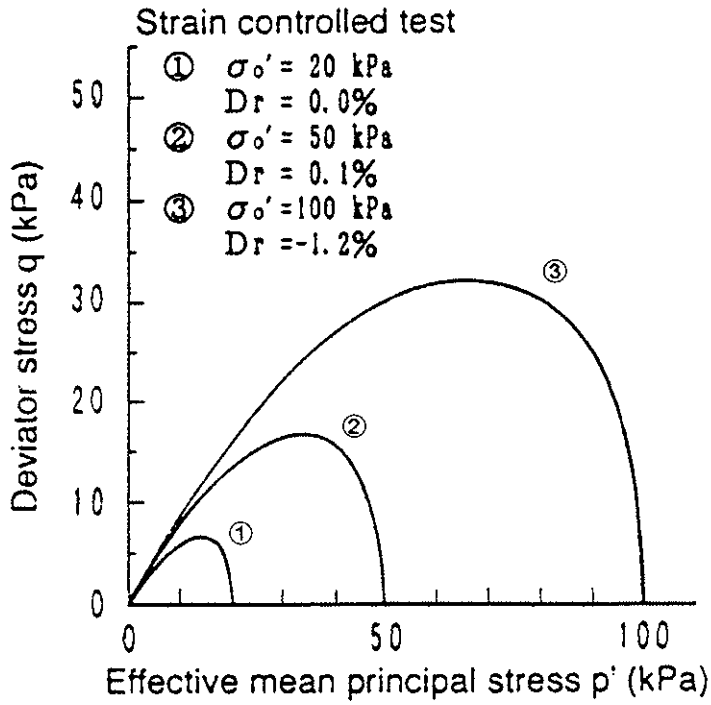

Fig. 4(b). Undrained triaxial compression tests on very loose Toyoura sand (Nagase et al., 1995).

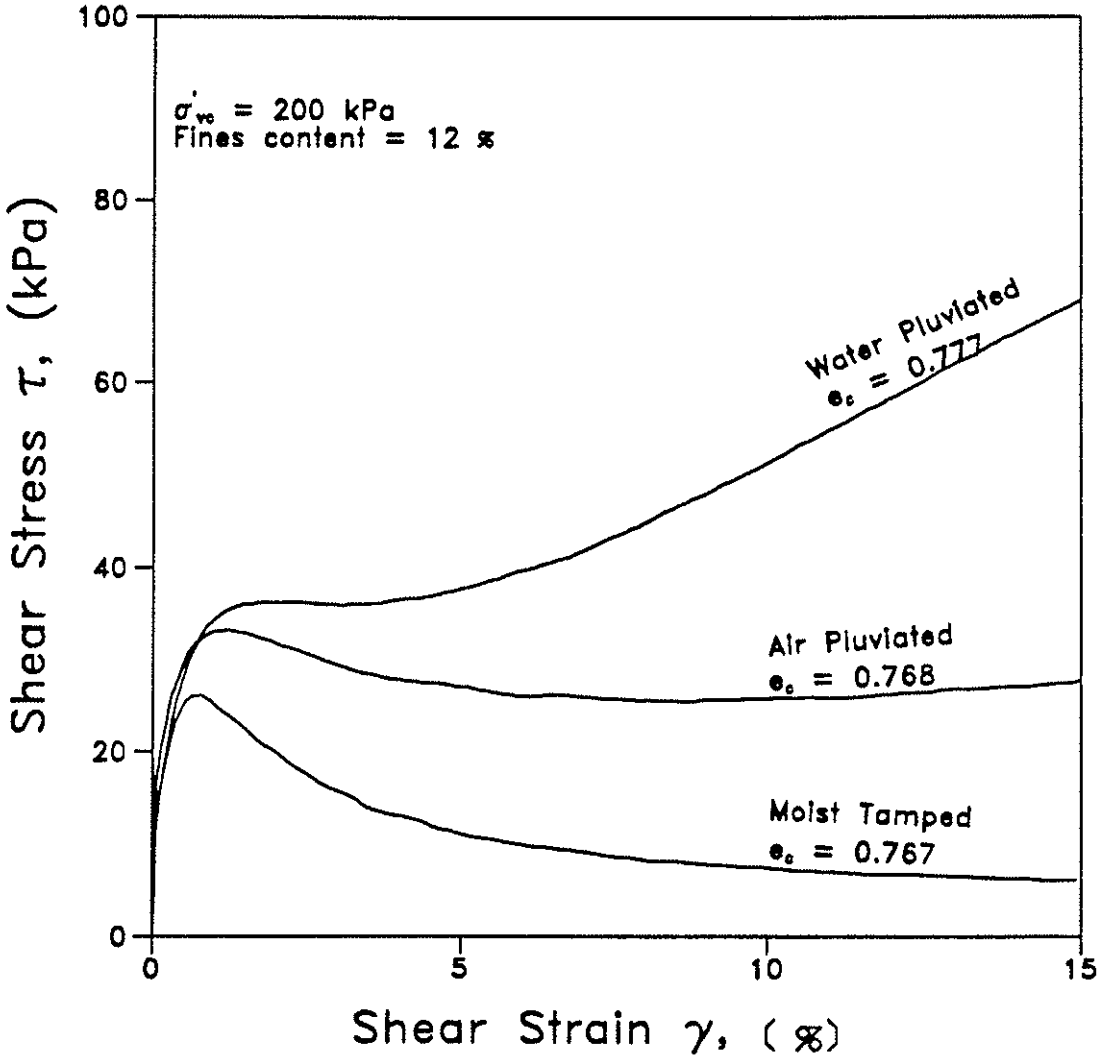

Fig. 5. Effect of specimen reconstituting method on undrained simple shear response of Syncrude sand (Vaid et al., 1995).

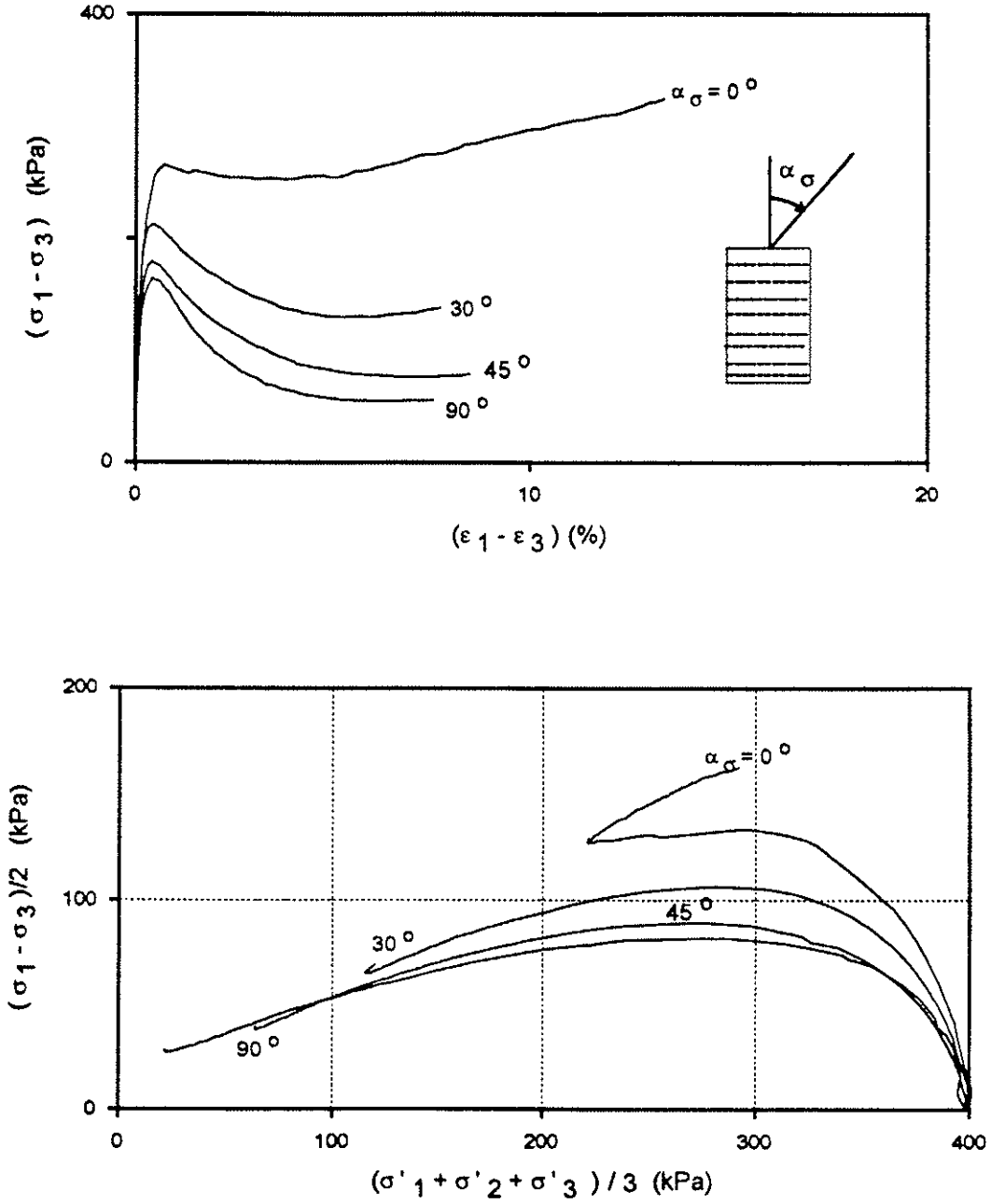

Fig. 6. Undrained anisotropy in water pluviated loose Syncrude sand as measured in the HCT tests (Vaid et al., 1995).

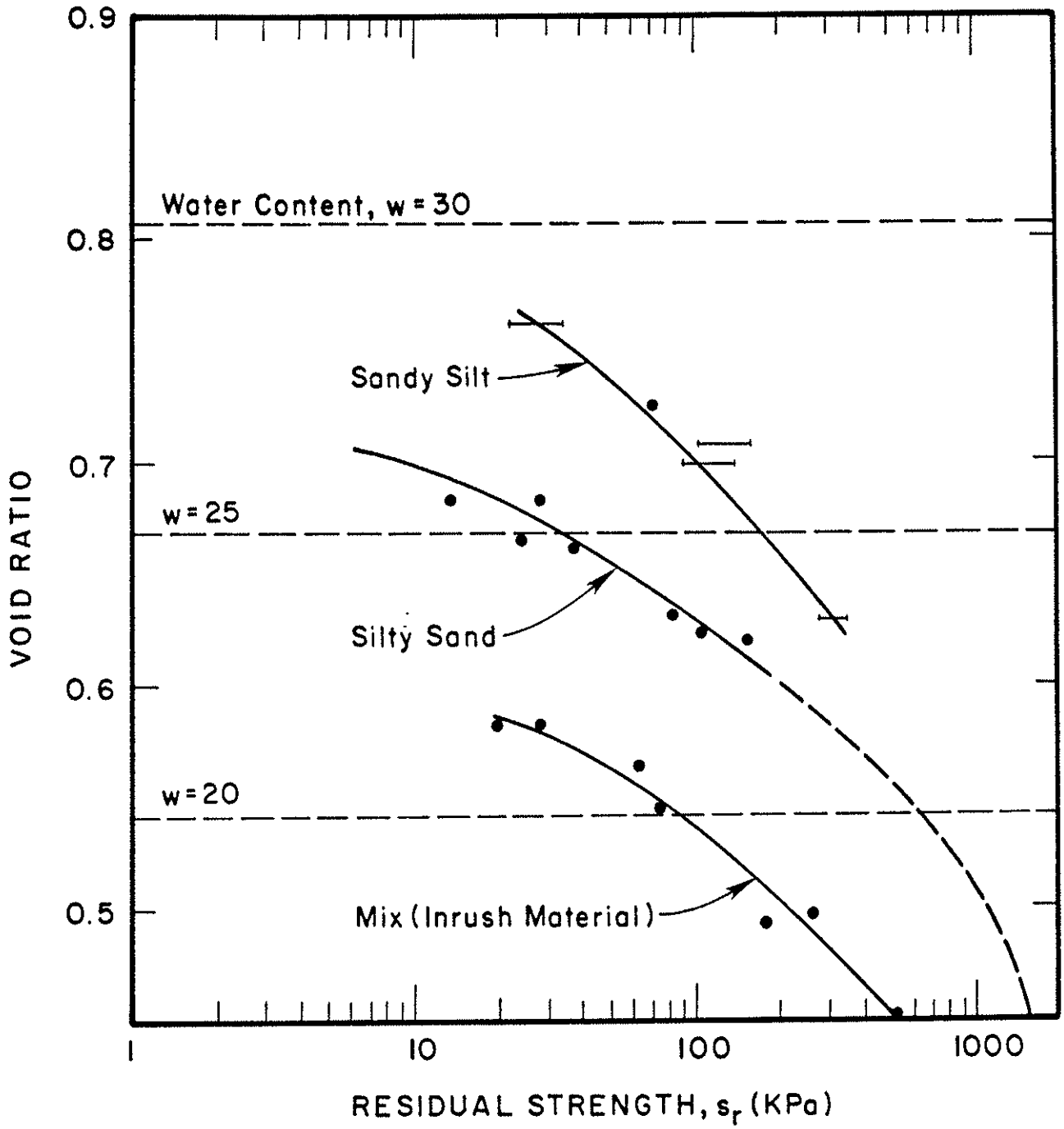

Fig. 7. Residual strength of granular tailings material.

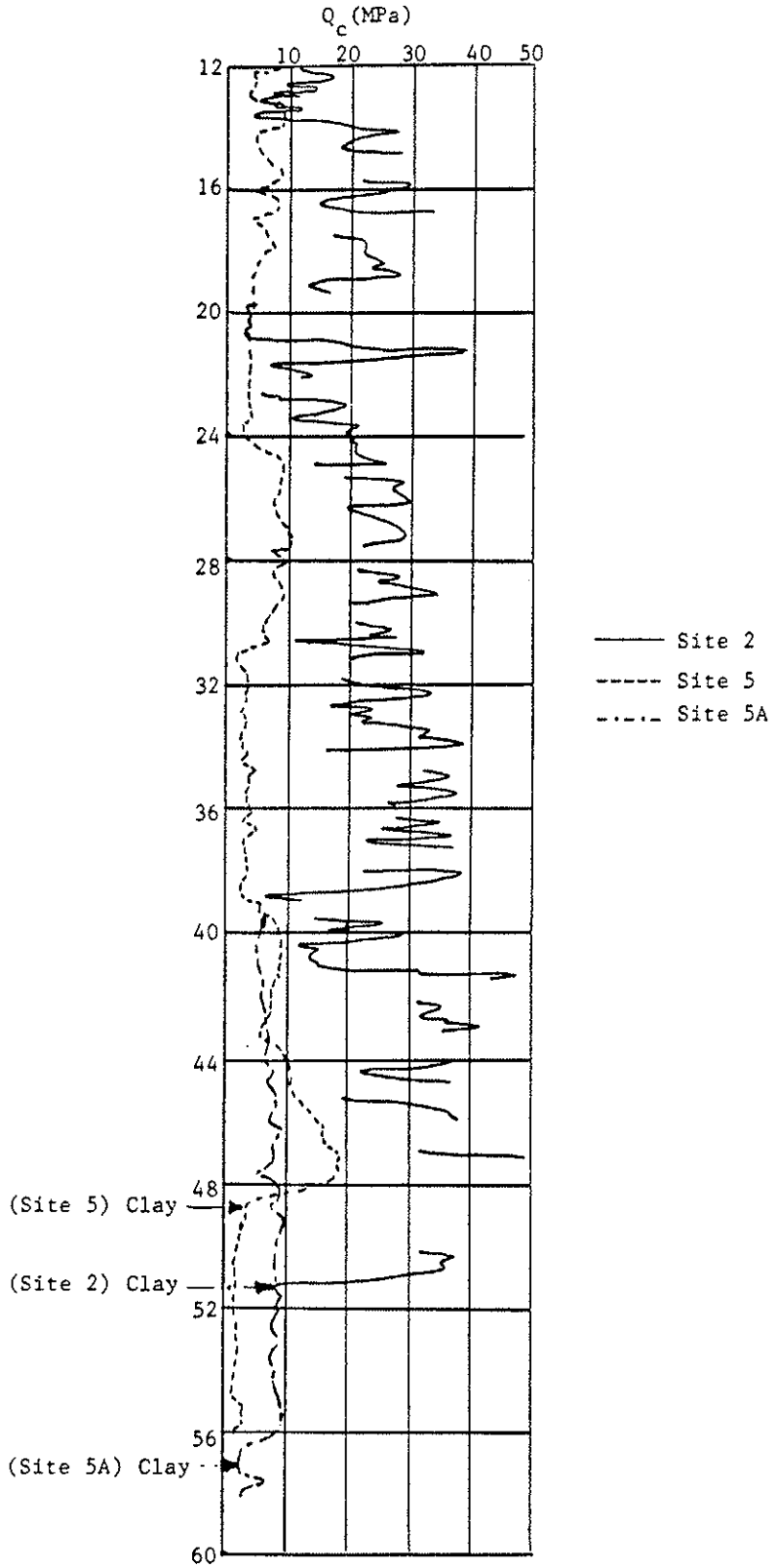

Fig. 8. Comparison of cone penetration resistance at Site 2 and Site 5 (sinkhole site).

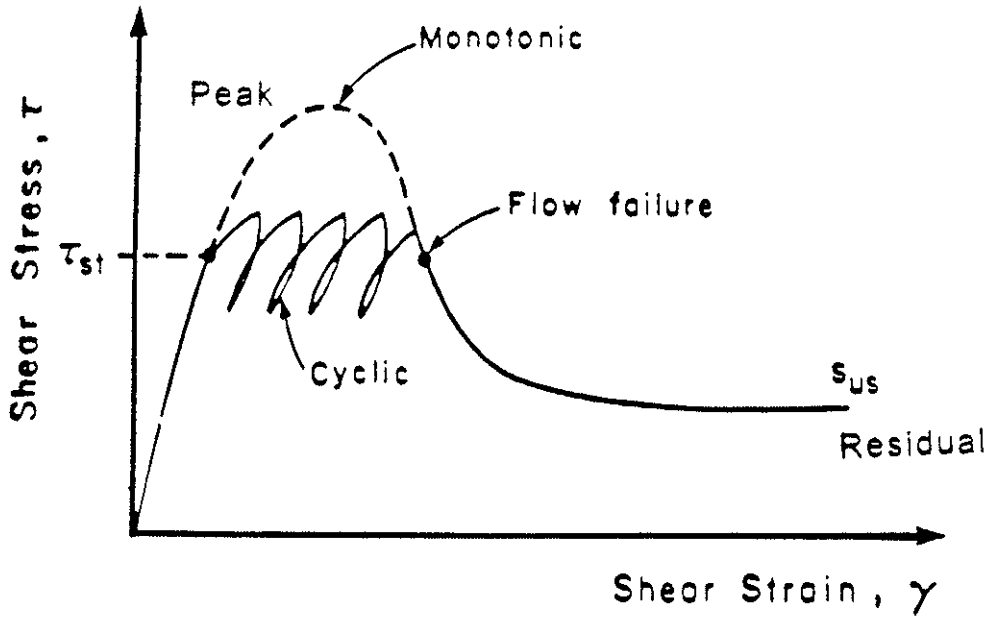

(a)

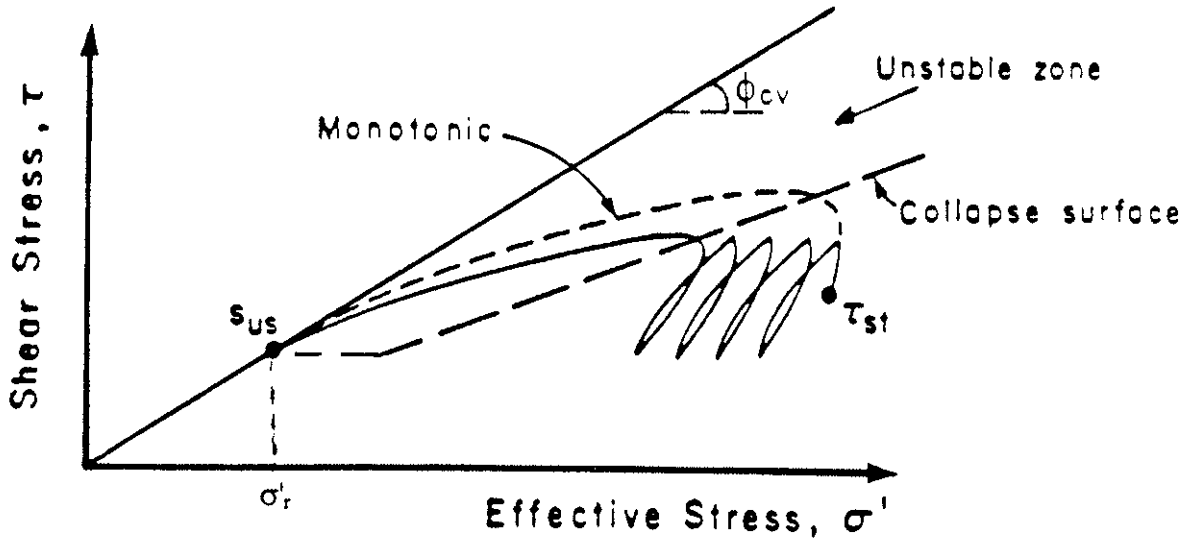

(b)

Fig. 9. Response of loose saturated sand under undrained static and cyclic loading.

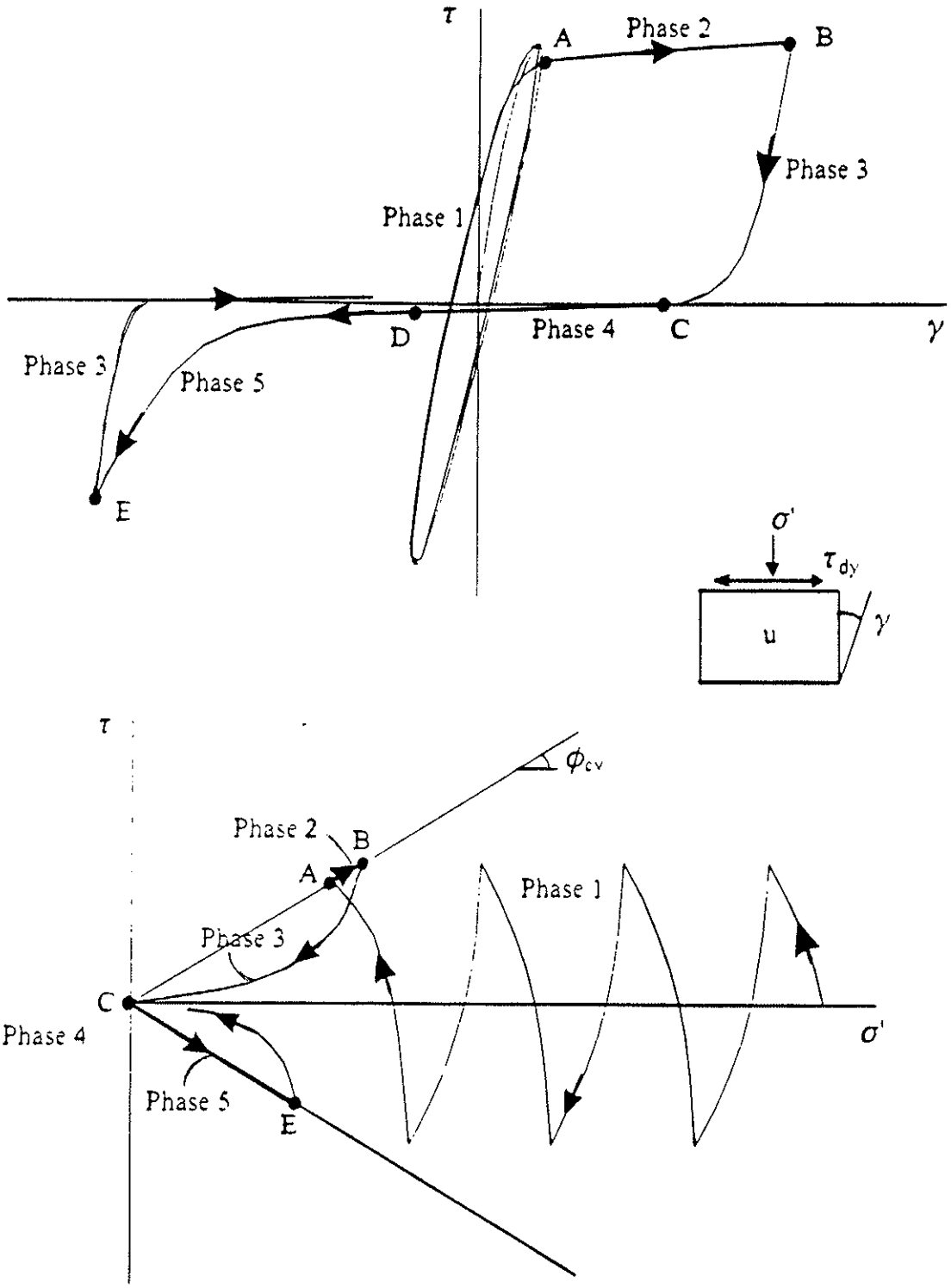

Fig. 10. Characteristic undrained cyclic shear stress-strain and effective path response for sand: (a) shear stress-strain response; (b) effective stress path response.

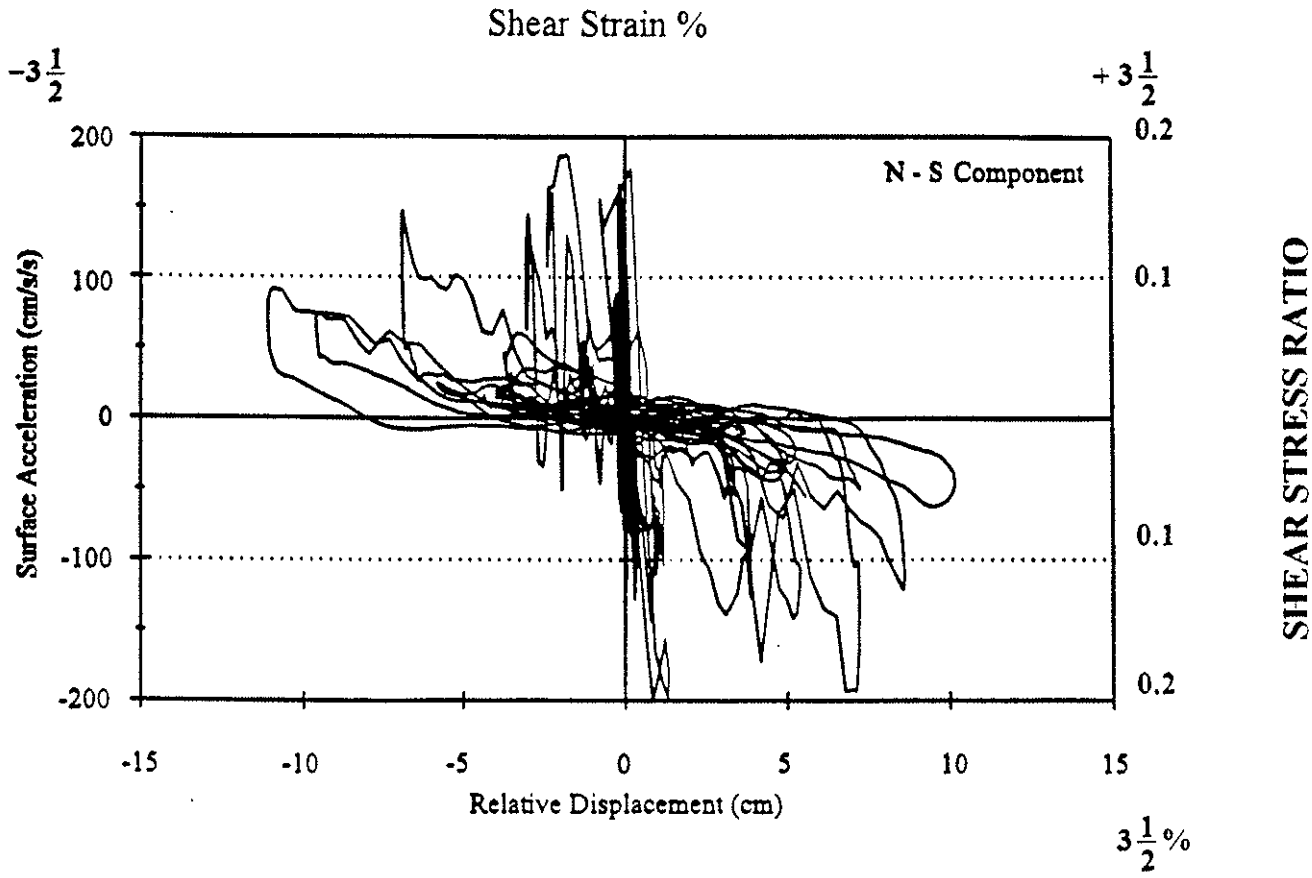

Fig. 11. Surface acceleration vs. relative displacement; N-S component.

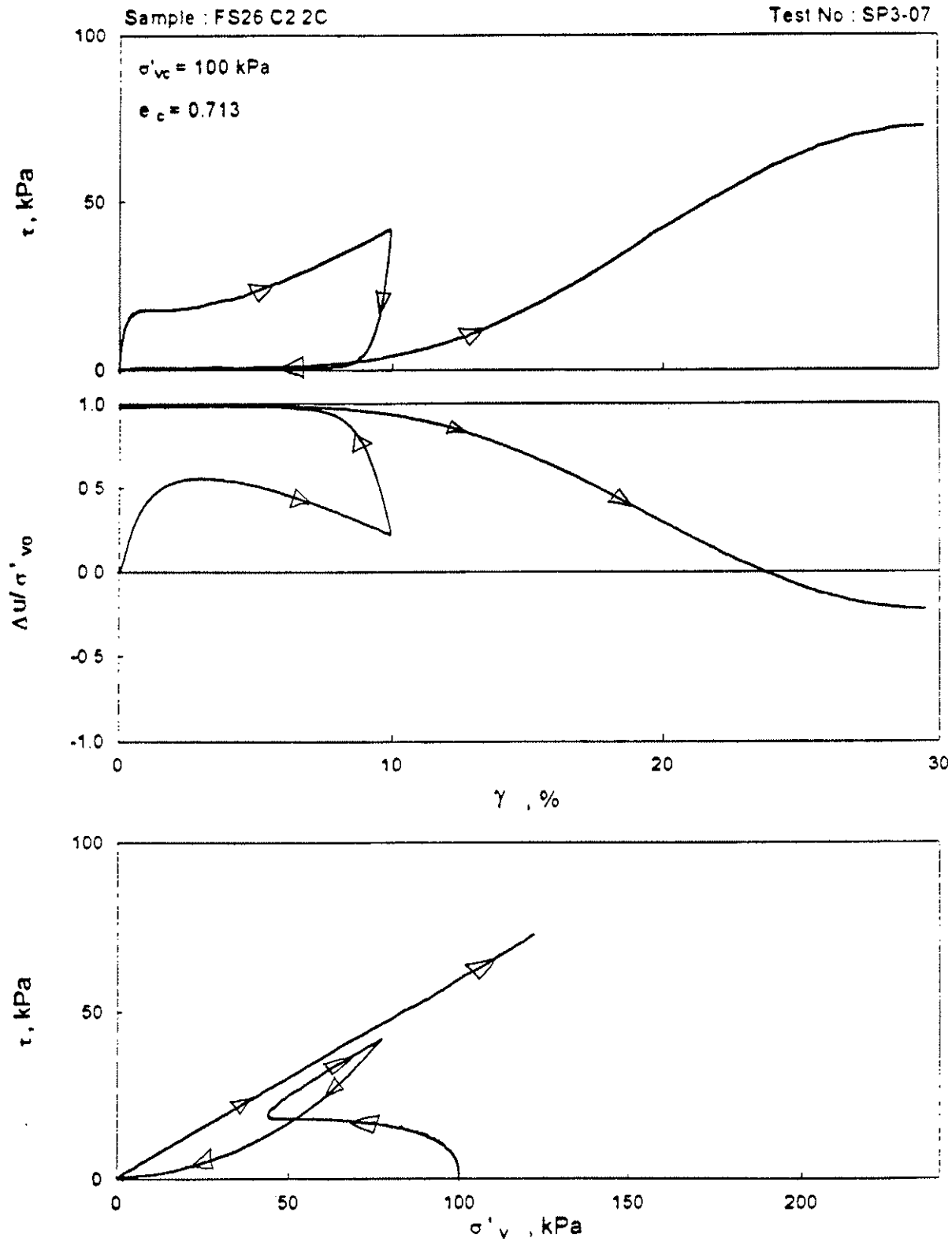

Fig. 12. Undrained response of loose sand to cyclic simple shear loading, Syncrude sand (Vaid, 1996).

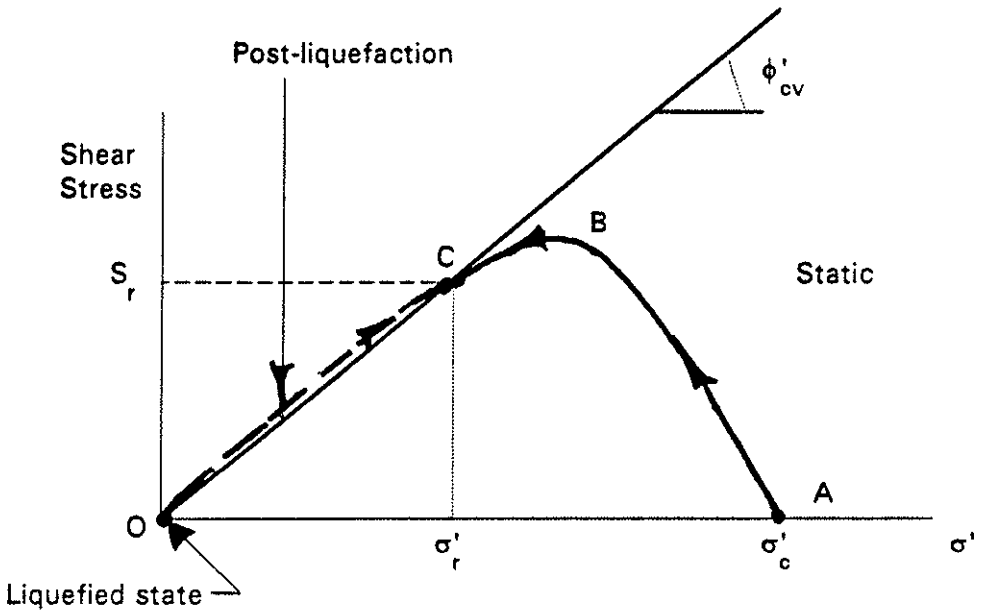

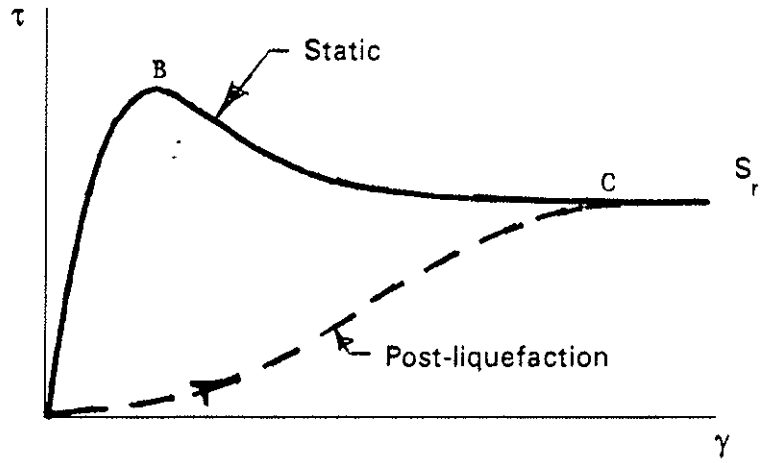

Fig. 13. Static and post-liquefaction stress-strain and strength.

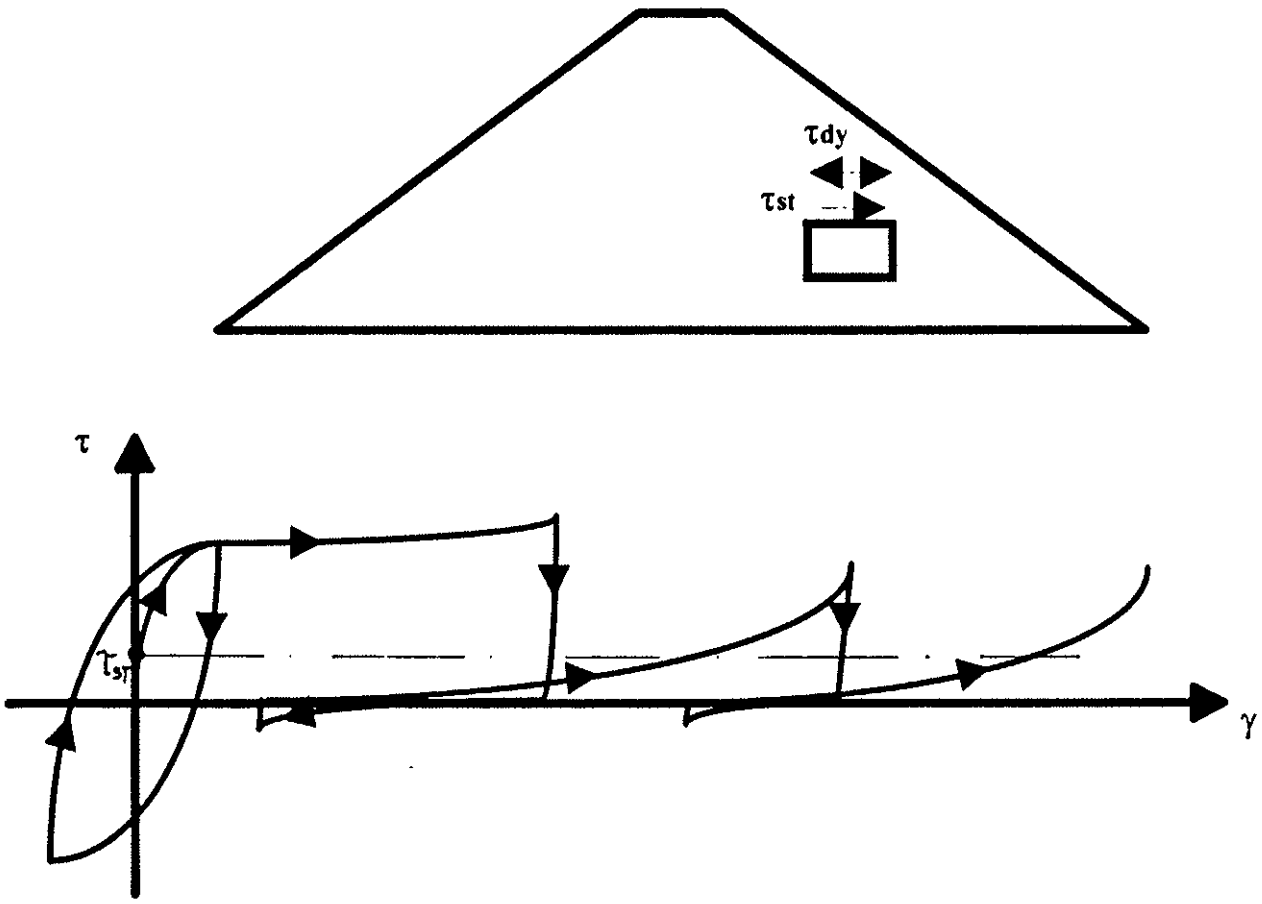

Fig. 14. Undrained cyclic loading with a static bias.

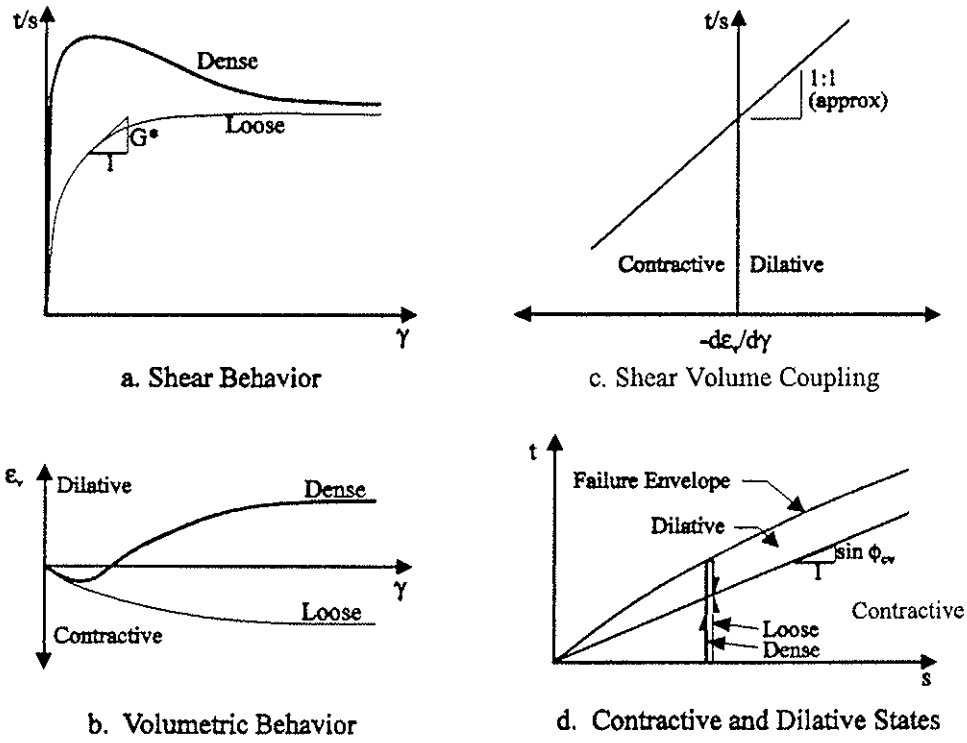

Fig. 15. Response of granular skeleton to monotonic shear loading.

2

"Post-Liquefaction" Shear Strength from Laboratory and Field Tests

Geoffrey R. Martin
University of Southern California

POST LIQUEFACTION SHEAR STRENGTH FROM LABORATORY AND FIELD TESTS

Pre Workshop Summary by Geoffrey R. Martin

1. Introduction:

In the context of laboratory and field tests, the stated main objectives of the workshop are to:

- evaluate the state-of-the-art/practice for determining post liquefaction shear strength for use in stability analyses
- seek consensus re preferred tests and data reduction methods
- seek consensus on fines corrections
- identify and prioritize research needs

Discussion group members were asked to comment on a number of specific topics related the above objectives. Comments received on these topics at the time of writing are summarized below, along with general thoughts and concerns. Research needs identified at a 1989 NSF/EPRI Workshop on the seismic stability of sloping ground are also summarized to provide a measure of progress and a building block for identifying present research needs.

2. Laboratory Tests

Questions posed to group members in relation to post liquefaction shear strength determined from laboratory tests, were generally interpreted by group members within the framework of critical state soil mechanics and the concept of undrained steady state or residual undrained strength. Within this framework the idealized behavior of sands during monotonic undrained loading and undrained cyclic loading is illustrated in Figure 1. In the case of contractant sands where the static stresses are greater than the steady state strength, and where accumulated cyclic strains exceed the strain softening strength, collapse and further strain softening will result with associated high pore pressure increases linked to a liquefaction state. In a slope stability context, this is equated to a liquefaction related flow failure.

Recomendations regarding terminology are proposed by Peter Robertson and Steve Poulos, and definitions or terminology will undoubtedly be discussed at the workshop.

In the context of slope stability, flow related liquefaction is easily identified as a major concern. However, the practising profession is also regularly confronted with ground deformation problems involving essentially level ground and earthquake induced liquefaction (cyclic mobility), particularly in port and bridge river crossing environments. In these cases static driving stresses are usually less then the steady state or residual strength, and the problem becomes one of prediction of the magnitude of lateral spreads (a few or several feet). Analyses (such as Newmark sliding block approaches) require the determination of the "residual shear resistance" prior to

dilation and the magnitude of strain required to mobilize dilatant strength as illustrated by the liquefaction test results shown in Figure 2. In many cases, the latter values are assumed equal to the residual strength from blowcount correlations. These concerns should be addressed during the workshop.

In the context of the residual shear strength for use in stability analyses, I believe it is clear that the steady state strength determined from laboratory tests is not necessarily the strength mobilized under field conditions. Questions related to pore pressure redistribution and associated void ratio changes, and the influence of interface conditions associated with stratified silty and sandy soils, all impact the residual strength mobilized in the field. Bruce Kutter in his written comments makes a strong argument that the strength of liquefied soils is not a material constant, but is dependent on boundary conditions and layer geometry. The results from centrifuge tests to examine these questions should be an important discussion component of the workshop.

The specific questions posed to group members and a brief summary of responses is given below.

2.1 Is the undrained steady state shear strength proportional to the initial effective vertical stress or some other parameter?

Within the critical state concept the steady state undrained shear strength is dependent only on the initial void ratio. Group members clearly felt that void ratio (for given soil composition) is the primary variable governing the residual shear strength. Mike Riemer noted that because granular soils can exhibit a wide range of relative densities at a given stress level (unlike normally consolidated clay) there is little theoretical basis for correlating the residual shear strength to effective vertical stress. However, it was also noted, that for a given depositional environment, relative densitites would decrease due to increasing consolidation vertical stress. This would be particularly the case for more compressible silty sands or sandy silts as opposed to clean sands. Given that the relationship between effective vertical stress and void ratio is is generally parallel to the steady state line, one could expect the ratio of steady state strength to vertical effective stress to be a constant. Experimental data from a number of researchers has indicated such a relationship with values of s_u/p' dependent on soil composition. Peter Robertson also notes the relationship between the undrained shear strength ratio (s_u/p') and the state parameter as proposed by Been and Jeffreies (1985).

2.2 What are the suitable sampling (e.g. freezing), specimen preparation, and laboratory testing procedures for estimating the post liquefaction shear strength?

Group members have no direct experience with use of freezing. However there is extensive experience with this technique, and it would appear that with appropriate care in controlling propagation of the freezing front and careful thawing, freezing could be a very reliable method of

obtaining specimens with a density representative of deposits in the field. From a practical standpoint, freezing is not a viable option for every day use.

The use of piston sampling techniques including careful monitoring of changes in void ratio during sampling to enable to establishment of an in situ undisturbed void ratio are also noted in paragraph 2.8. The determination of a steady state line from reconstituted samples and assuming parallelism with an "undisturbed" sample steady state line was not cited by group members. However, the inherent difficulties with this procedure and the sensitivity of the residual undrained strength to small changes in void ratio is well established in literature. The concept of using laboratory sedimentation of silty sand samples to replicate natural stratified soil deposits as described by Baziar and Dobry (1995) is also worthy of discussion

On the question of laboratory testing procedures, a variety of opinions were expressed by group members. Steve Poulos considers that triaxial compression tests can be successfully used for narrowly graded rounded or subrounded sand grain structures, where samples are prepared in a very loose state under a high consolidation stress to provide a highly contractive state. Steady state can be reached with strains as low a 5%. However difficulties are identified for well graded and angular sands, which require high strains to reach a steady state.

Pedro deAlba suggested that triaxial devices cannot successfully model post liquefaction behavior, because of the high strain levels which can occur in the field. Model and field case histories show flow slides concentrate in relatively narrow shear zones were shear strains could be of the order of several hundred percent. In addition, it was noted that residual strength is extremely sensitive to minor changes in soil gradation and void ratio, hence requiring extensive field sampling to obtain representative soil samples. It was suggested that a new larger scale test configuration for laboratory testing is needed.

Mike Riemer brings up the difficult issue of determining the appropriate testing method, namely triaxial compression, extension, torsional shear, or simple shear, etc. Test data shows differences in steady state strengths for the various methods, with traxial compression yielding the highest values. It is suggested that this is not necessarily a result of the effective stress path, but it could be due to the different mode of deformation in the test.. On the subject of triaxial compression versus triaxial extension tests, Steve Poulos considers that it is impossible to maintain uniform void ratio in specimens subjected to extension, and this contributes to the reason why the steady state line differs between compression and extension tests.

2.3 Effects of consolidation stress and undrained stress path on laboratory measured post liquefaction shear strength.

For a given test type there appears agreement that the stress path has no measurable effect on the undrained steady state shear strength. With respect the effects of consolidation stress, Reimer notes that for samples prepared at a constant void ratio, the level of consolidation stress affects the observed level of quasi steady state strength. The quasi steady state strength is defined the lower bound undrained strength for strain softening contractive behavior prior to limited dilation occuring at very large strains. This raises the question as to whether in some cases steady state residual strength requires very large strains for mobilization, and should one use the quasi steady state strength as recommended by Ishihara (1993).

2.4 Effects of "fines" on laboratory measured post liquefaction shear strength

Clearly this issue is of particular practical significance, as many field soils have high fines or silt content. Group members have a number of comments on the effects of fines. Bruce Kutter notes that the undrained assumption with increased fines is more tenable and a rapid void redistribution becomes of less concern due to the lower permeability. Mike Reimer notes the complexity of the problem. Whereas a small percentage of silt rattling around within the void structure will have little or no effect on the post liquefaction shear strength, it can significantly alter the density of the soil. A high percentage of fines also makes it difficult to accurately replicate the fabric of field conditions through reconstituted laboratory specimens. Steve Poulos considers that the void ratio at the start of shear and the soil composition are the only two parameters that control the undrained steady state strength. Hence, composition (as reflected by fines content) is of primary importance. This is illustrated for two soils with different uniformity coefficients.

Cyclic liquefaction tests in the laboratory have clearly indicated the importance of silt content. In interpreting laboratory test data with varying silt contents, it can be argued that in the case of sands with a low silt content, the sand fabric, that is the skeletal void ratio of the sand, will control behavior, whereas for a very high fines content, the fines void ratio will control the behavior. The relationship between the global void ratio of a soil and the skeletal void ratio of the sand or fines, can be determined from a knowledge of the fines content as shown in Figure 3. The effects of silt content on conventional liquefaction strengths, that is cyclic stress ratios causing 5% double amplitude strain, has been researched by a number of investigators as for example shown in Figure 4. For tests at a constant global void ratio, it can be seen that as the silt content increases, the cyclic stress ratio reduces as the void ratio of the controlling skeletal sand fabric reduces. With a sufficiently high silt content, the cyclic stress ratios are controlled by the silt skeletal void ratios, and at a 100% silt content, effectively the cyclic stress ratio is associated with a pure silt. If one knows the variations in cyclic stress ratio as function of void ratio for both the sand and silt fractions making up a silty sand soil, then one can theoretically compute the effects of fines on

cyclic stress ratios as shown in Figure 4. Consequently in an idealistic sense, one could argue that is not the global void ratio controlling the residual strength of silty soils but rather the skeletal void ratio of the dominant constituent. Noting the sensitivty of the skeletal void ratio of a sand to silt content (Figure 3), is not surprising that variations in silt content (or composition) for a given global void ratio can cause large changes in steady state strength .

2.5 Effects of grain size distribution on laboratory measured post liquefaction shear strength

As grain size distribution can effect effective skeletal void ratios as discussed above, and some soil particles may take an inactive role in influencing strength, grain size distribution can have an influence on post liquefaction shear strength.

2.6 Effects of particle shape on laboratory measured post liquefaction shear strength

At the same void ratio, Steve Poulos makes the argument that sands having angular grains would usually have higher undrained steady state shear strengths than sands having rounded grains.

2.7 Effects of strain rate on laboratory measured post liquefaction shear strength

This seems to be a general consensus that over a reasonable range of strain rates, the effects of strain rate are not significant.

2.8 Suitable techniques for estimating in situ void ratio and state parameter

The use of careful piston sampling using thin-walled-tubes with corrections for void ratio changes on disturbance, are discussed by Steve Poulos. The potential application of electrical methods to measure in situ void ratio are also mentioned, but group members do not have the experience with this technique to comment specifically.

3. Field Tests

It is generally recognized (as noted by Peter Robertson) that the utlization of undisturbed sample tests to estimate post liquefaction undrained shear strength of site soils, is a difficult and expensive approach. The other option is to make use of insitu field tests using empirical correlations. Four techniques have been explored for this purpose, namely the SPT, CPT, shear wave velocity measurements and field vane tests. The use of the field vane test equipped with piezometer to measure pore water pressure is described by Wayne Charlie. The use of self boring pressuremeter is an another approach more amenable to direct consitutive modelling of pressuremeter test data, and is worthy of further discussion but not highlighted in any detail by group members.

The written contribution to the topic of field tests using SPT, CPT or shear wave velocity measurements by Scott Olson is very comprehensive and addresses all requested specific topics on the subject. Rather than attempting to summarize, I will make only supplementary comments on a few aspects of Scott Olsen's response.

3.1 Advantages and limitations of different field tests

With respect to the CPT, I note that CPT equipment can utilize small diameter push samplers which are available commercially, but which are rarely used. In addition, the CPT is routinely adopted to the use of a piezocone and also a seismic cone for downhole shear wave velocity measurements.

3.2 Suitable procedures for estimating the post-liquefaction shear strength.

The SPT based procedure described by Seed and Harder (1990) is clearly the state-of-the-practice in the profession. However, it is recognized that both uncertainties in relation to back analyses of case histories and the "mechanics" of residual strengths mobilized on a case by case basis, lead to a range of residual strengths for a given blowcount. More guideance is needed by the profession to clarify the source of uncertainties and to provide a methodology for determining a "best guess" versus being conservative.

The normalized SPT based procedures described by Stark and Masri (1992) and Ishihara (1993) warrant more detailed discussion at the workshop, particularly the use of laboratory databases which are used to add to back analysis data from case histories. The CPT based procedure described by Olson and Stark has yet to be studied by many, but because of the interent advantages of the CPT as an insitu testing method, needs to be discussed at the workshop.

3.3 Uniqueness of a relationship betwen SPT/CPT and post liquefaction strength

If the conclusion is one where uniqueness does not exist for all sands and conditions, then the parameters most influencing the variability need to be defined.

3.4. Effect of fines

This is clearly a critical issue due to the sensitivity of undrained strength to fines content, and also the depositoinal fabric. In utilizing CPT data to study this problem, more use should be made of side friction measurements in correlation studies as opposed to using the end tip resistance only. The underlying basis for presently published fines content corrections are by no means clear, and a more mechanistic understanding is needed. The use of laboratory based CPT test cells such as the facility at WES, could be of value in resolving the problem.

4. Research Needs

The following extract from the Proceedings of a 1989 NSF/EPRI Workshop on Dynamic Soil Properties and Site Characterization may provide a useful starting point for evaluating both progress and present research needs. The extract relates to the question of stability of sloping ground sites involving liquefiable soils.

Steady State Strength

There is still some uncertainty related to the definition of steady state and how it should be determined. There is a need for continued research to clarify the soil variables and the testing method. At present, S_{us} for a given soil is assumed to be only a function of void ratio. However, questions have been raised as to whether S_{us} is a function of other variables such as stress path, initial soil fabric, rate of strain, and in termediate principal stress. Since the determination of SUs is of primary importance to any evaluation of stability, further research is required to clarify whether these variables affect S_{us}. There is also a clear need to define a standard testing procedure to deter mine S_{us}.

Current practice in laboratory steady-state research and engineering applications is to prepare laboratory samples with a high degree of homogeneity. However, in nature, deposits are often highly nonhomogeneous, and further research is required to study the influence of nonhomogeneous sample site conditions on the determination of S_{us}.

Within the framework of the steady-state concept, the precise and reliable definition of void ratio is a critical issue. Inadequate knowledge of void ratio has negative implications with regard to both interpretation of laboratory experiments and application of the steady-state concept to field problems. This question raises the issue of the physical scale of the determination. At which scale are spatial variations in void ratio and other nonhomogeneities significant? Image analysis studies show large variations of void ratio within laboratory specimens that would be classified as uniform from a macroscopic standpoint. Such variations can also be illustrated from simulation studies. Their physical and statistical significance is not known, and the scale at which they should be determined is also unknown. Obviously, variations in void ratio relate to variations in fabric (e.g., clusters of grains, number of contacts, orientation of contact forces).

The above remarks made for laboratory specimens raise other important interrelated questions for both laboratory and field investigations:

a) Do in situ materials exhibit spatial variations in void ratio and fabric that are similar to or different from laboratory specimens?

b) Are efforts made in specimen preparation techniques to maximize the level of uniformity warranted when compared to *in situ* materials?

c) Are "microscopic" effects more important for cohesionless materials with significant amounts of fines?

d) How much refinement should be given to assessing these variations (both *in situ* and in the laboratory): i.e., at which "microscopic" scale do the variations become insignificant with respect to overall behavior?

e) Is void ratio a sufficient descriptor for defining steady-state conditions, or should some descriptors of fabric possibly on a statistical basis) be considered?

At a more fundamental level, these questions relate to a better understanding of the process of shearing from a micromechanistic standpoint.

In the absence of standardized and economical laboratory testing procedures for deter mining steady-state strength, correlations with field test values have been proposed as an alternative technique for estimating this important parameter. Research by Seed and others has developed preliminary relationships between residual strength or steady state strength and corrected standard penetration resistance $(N_1)_{60}$. Research should continue to develop these correlations further. Such results will augment laboratory research by providing economical methods to define stratigraphy and material proper ties of soil layers and to extrapolate results from tests on a few laboratory specimens to soil layers in the field.

Avenues of research that will address these questions include:

a) Better physical and statistical characterization of void ratio and fabric of laboratory specimens before, during, and after shearing. Image analysis techniques could play a role.

b) Continued development of techniques to evaluate the void ratio, and, in general, the state of a soil *in situ*. Electrical resistivity techniques are one example; however, other approaches could be developed.

c) Evaluation of the fabric and subsequent laboratory testing of undisturbed soil specimens. This raises the need to develop improved procedures to obtain undisturbed samples reliably and efficiently. Freezing is one possibility; however, more cost-efficient and simpler technologies can be considered, such as impregnation with different chemical products.

d) Theoretical and numerical modeling of the micromechanisms of shearing, i.e., providing a better understanding at the particulate level of the processes that lead to phenomena of engineering interest, such as steady-state deformation. This could also support research in the area of progressive failure phenomena.

Current practice to evaluate *in situ* values of S_{us} is either to obtain samples and per form laboratory tests (as described above), which require some correction to the *in situ* void ratio, or to empirically correlate S_{us} with a field measurement such as penetration resistance. Major areas of uncertainty relate to the difficulty in obtaining undisturbed samples and monitoring their changes in void ratio and in the uniqueness of the existing empirical correlations between penetration resistance and Sus for all soil types. Hence, a major priority should be to develop improved methods for the determination of S_{us}. This is closely related to the *in situ* determination of *in situ* state.

Pore Pressure Redistribution/Dissipation. For most practical situations, particularly for those involving fine sands and silts, it is often assumed that there is relatively little pore pressure redistribution or dissipation during earthquake loading and reconsolidation will be a post-earthquake process. However, it has been suggested that, for coarser sands or stratified cohesionless soils, significant redistribution or dissipation may occur both during and following earthquake loading. It has been observed in past earth quakes that, in some instances, large slope displacements have been initiated sometime after the earthquake ground shaking ceased. This suggests that pore pressure redistribution may be affecting the overall shearing resistance of the soil mass.

For the case of a layer of sand located beneath an impervious clay boundary, it has been suggested that pore pressure redistribution effects under conditions of constant volume may tend to increase void ratios in the upper half of the layer and decrease those in the lower half. It has been postulated that, in the extreme, a thin zone of water may accumulate at the upper sand-clay interface. Clearly, the above phenomena could greatly influence the available strengths that can be mobilized.

The key parameter controlling the redistribution of earthquake-induced excess pore pressures, both before and after the earthquake, is the coefficient of consolidation, C_v ($= k/m_v\gamma$, where k = coefficient of permeability and m_v = coefficient of volume decrease). During the initial stages of pore pressure buildup during an earthquake, it is reasonable to assume constant values of k and m_v to evaluate redistribution or dissipation effects. However, when effective stresses become very low, values of m_v will increase significantly and, hence, c_v values will decrease. Large cyclic shear strains, say in excess of 1 percent, which may accompany low effective stresses, may also influence m_v and k as a result of changes in soil structure.

Clearly, the pore pressure redistribution/dissipation process is very complex; nevertheless, it may play an important role in the assessment of the earthquake stability or deformations of saturated cohesionless soil slopes or strata. Research on the changes in mv and k would provide an essential database on values of C_v to use in analytical studies addressing the role of redistribution/dissipation of pore pressures on stability analyses. Laboratory studies should address gravel, sands, and silts to cover the full range of k and m_v values.

Triggering of Stability Failure. If a soil mass is deemed to be potentially unstable, if the strength of the soils were to decrease to S_{us}, one needs to determine whether the expected earthquake shaking will be sufficient to trigger the failure. In sands, very small strains (about 1 percent) are sufficient to overcome the peak and trigger the failure. In clays, the strains required to trigger are typically very large; thus, earth quake shaking will seldom trigger slope failures in clays (except, of course, sensitive clays that have a low strain at peak). Triggering criteria based on

mobilized effective stress ratio have been proposed for sand. The triggering of the failure will be a progressive phenomenon. Initially, a limited zone of the soil mass may research S_{us}, and then the failure will propagate until the soil mass researches overall instability.

Research is required in two main areas: (1) stresses and strains that are required to cause a soil element to decrease in strength towards S_{us} and (2) consideration of the progressive nature of the failure in numerical analyses. In the first area, one needs to consider the potential effects of creep (rate of loading) and whether triggering correlates better with an accumulation of strain, an increase in pore pressure, or the development of particular value of effective stress ratio.

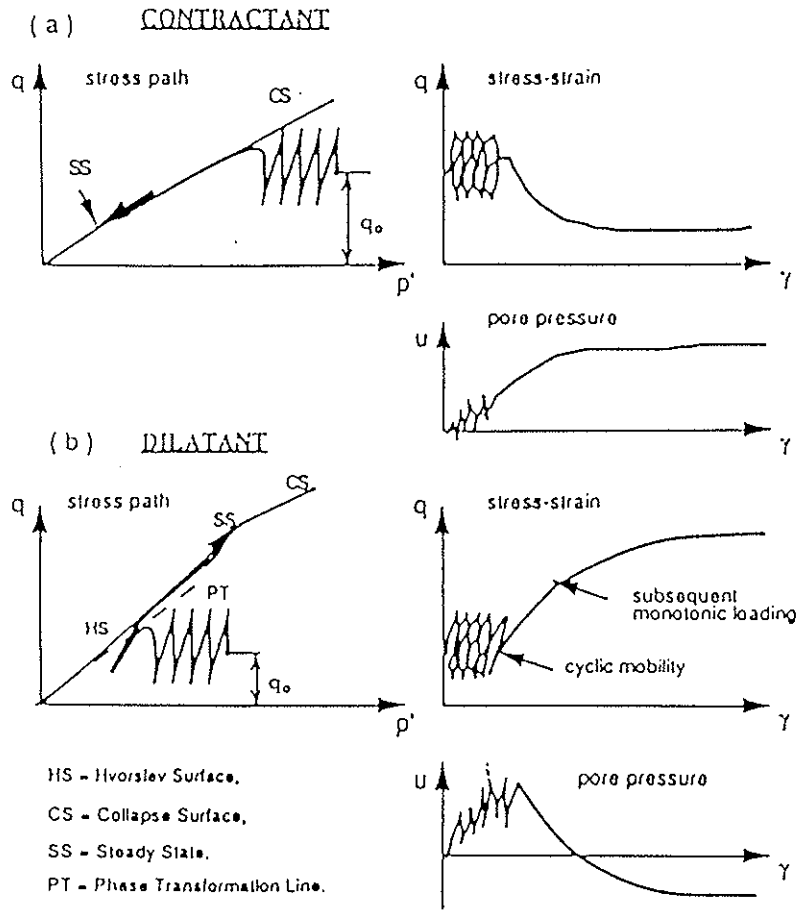

Idealized Soil Behaviour under Undrained Cyclic Loading.

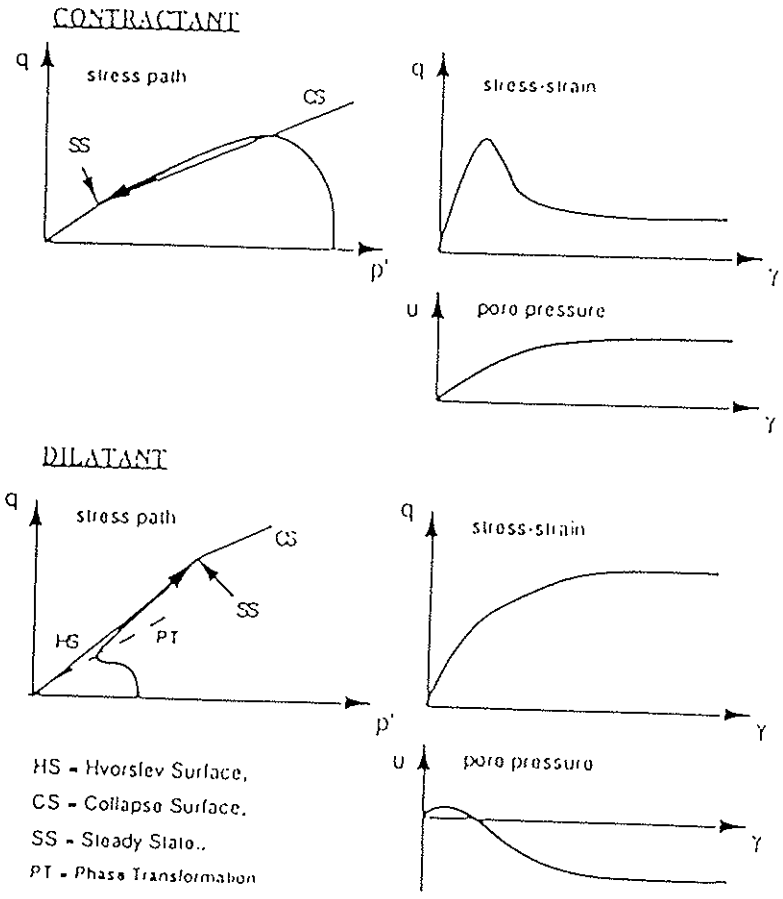

Idealized Soil Behaviour Under Undrained Monotonic Loading.

Figure 1 Idealized Undrained Behavior (after Gu et. al. 1994)

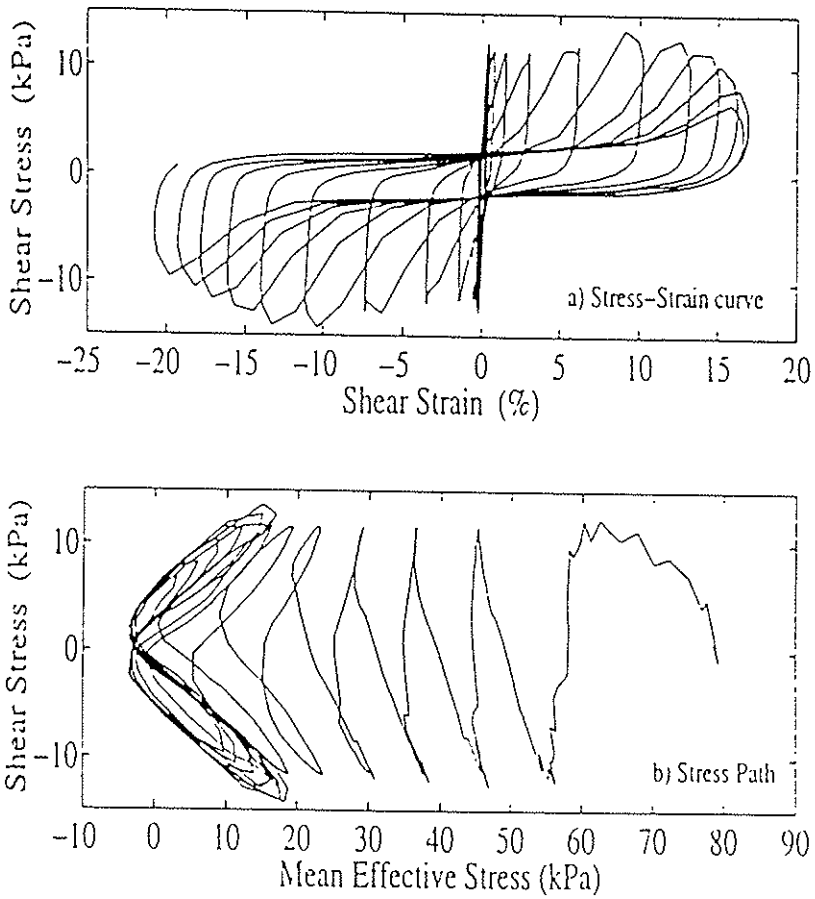

Stress-strain curve and stress path for Nevada Sand with D_r = 60% obtained from undrained cyclic simple shear (CSS) test (Arulmoli *et al.*, 1992).

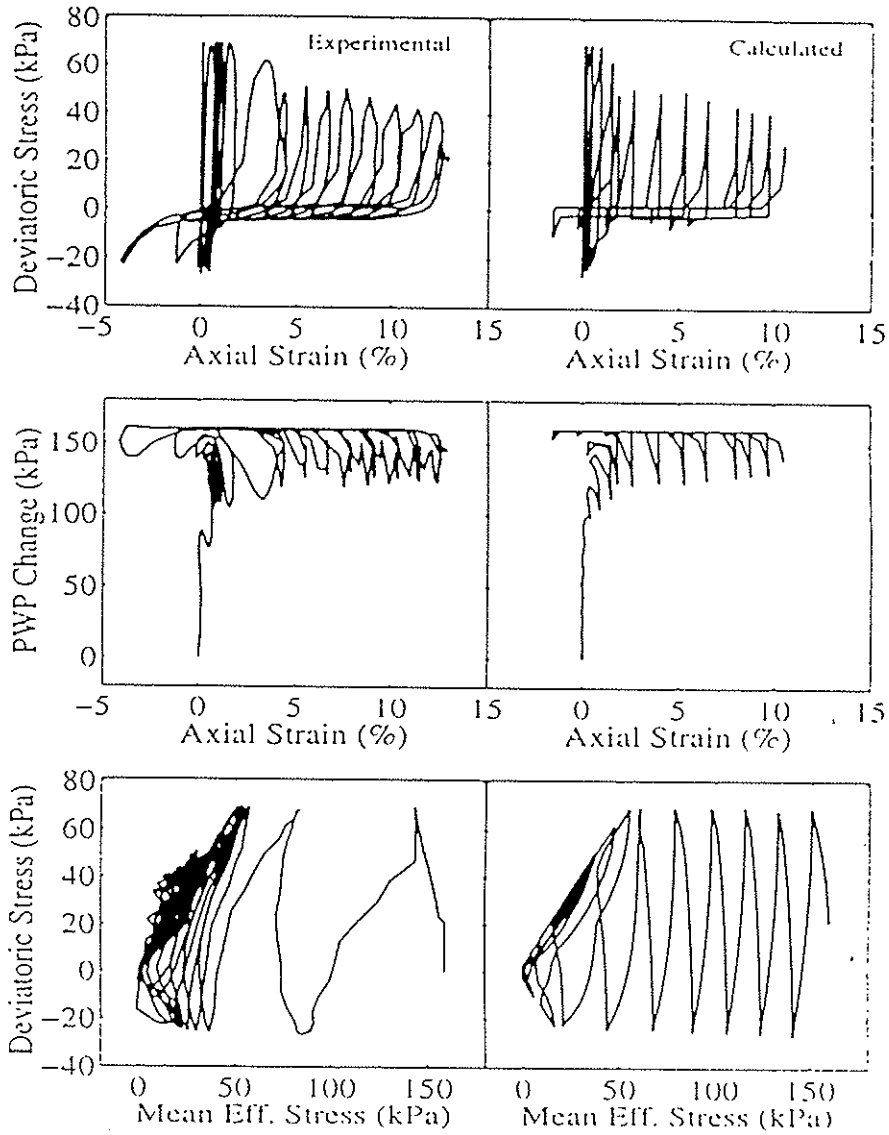

Computed and laboratory results for a cyclic triaxial undrained test with stress bias ($CIUC_{cyclic}$ - VELACS Test No. 40-58 Earth Technology) - Stress-strain, PWP, and stress path behavior.

Figure 2 Cyclic Liquefaction Test Data (after Parra, 1996)

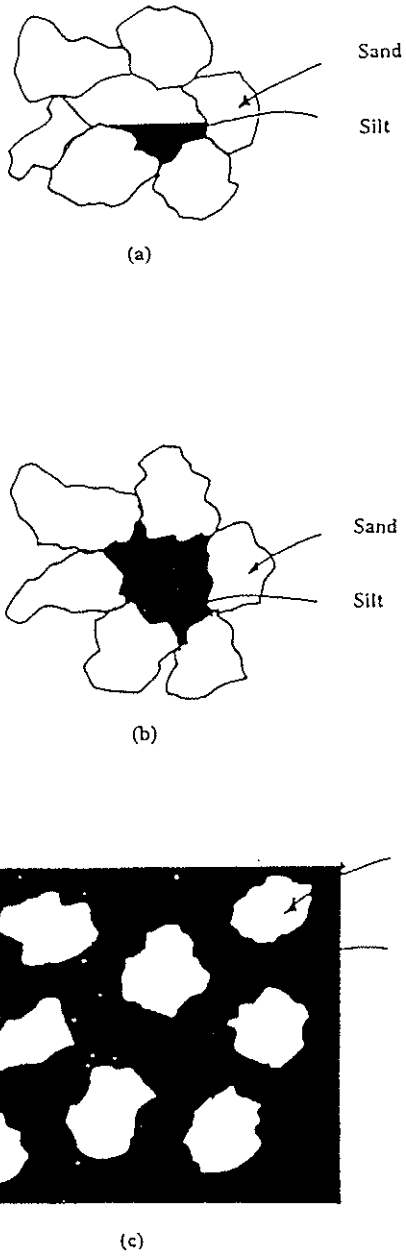

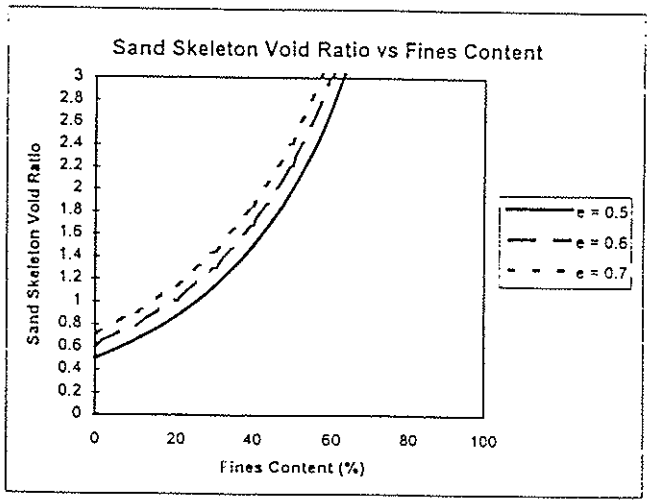

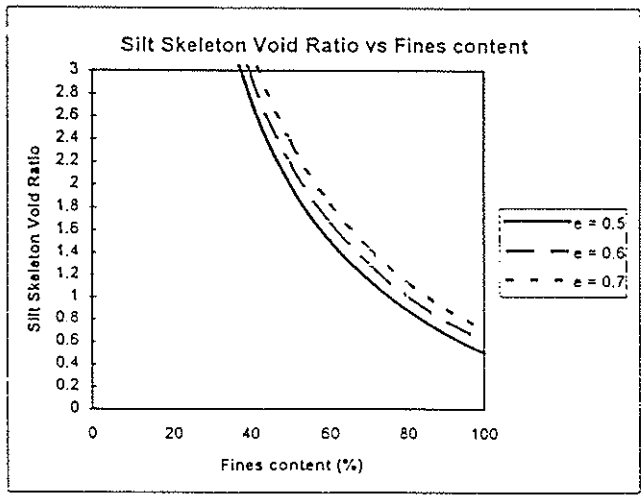

Combinations of Sand and Silt Grain Structure

Skeleton Void Ratios vs. Fines Content (after Andrews, 1997)

Figure 3 Skeleton Void Ratios vs Fines Content (after Andrews, 1997)

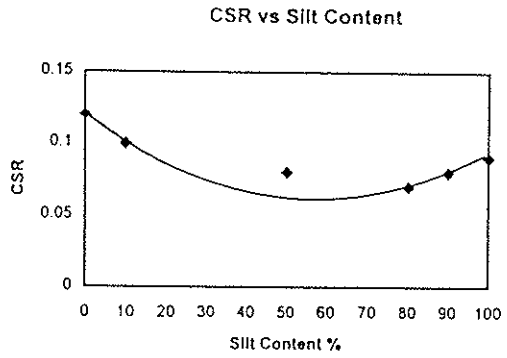

e= 0.92
30-35 cycles

(Replotted from Cao and Law, 1991)

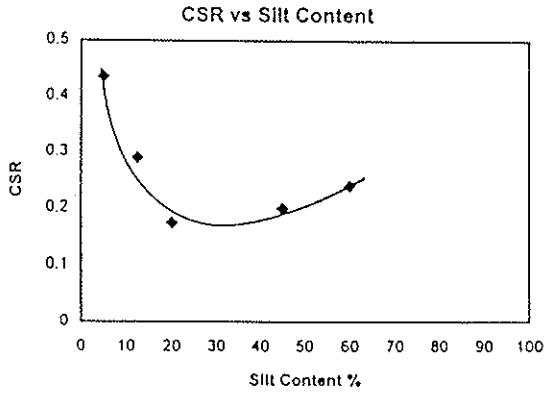

e= 0.56
10 cycles

(Replotted from Koester, 1994)

Effect of Silt Content on Liquefaction Strengths (after Andrews, 1997)

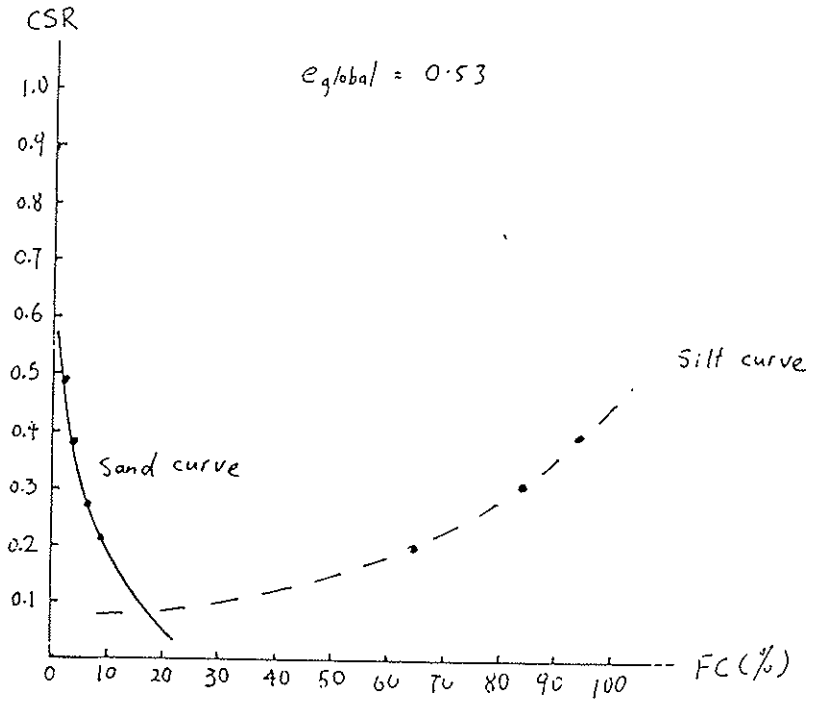

Theoretical Cyclic Stress Ratios to Induce Liquefaction vs. Fines Content (10 Cycles, e_{global}= 0.53) (after Andrews, 1997)

Figure 4 Effect of Silt Content on Liquefaction Strength (after Andrews, 1997)

"Post-Liquefaction" Shear Strength from Case Histories

Gonzalo Castro
GEI Consultants, Incorporated

"Post-Liquefaction" Shear Strength from Case Histories

by Gonzalo Castro, Principal, GEI Consultants, Inc.

These notes are intended to be an outline for our workshop discussions and to form the basis for our post-workshop report. I have included in these notes pre-workshop comments that were sent by discussion group members. Consideration was also given to the list of questions proposed by the organizers. The enclosed paper is referred to in this outline as it contains more detailed explanations of some issues.

The first point that needs to be discussed is how we define the strength that we are trying to back-figure from the case histories. To define the strength, it is helpful to have in mind the type of case history that we will be looking at. The typical case history (e.g., Lower San Fernando) is one in which a stability failure developed in sandy soils involving large, relatively fast deformations . The failure was triggered by sufficiently rapid loading so that the sandy soil behaved undrained. The strength we would backfigure from such a case history would be the undrained strength in the soil in question that is mobilized at large strains after the peak strength, if any, has been overcome. Thus it is the strength that will determine whether instability is possible and, if so, how far will the failure mass move. The term post-liquefaction is, in my opinion, inappropriate to designate such strength because it implies that the large strain strength will be reached only if momentary states of zero effective stress are reached first. This is certainly not the case if the triggering event is an increment of static load (Ft Peck, Calaveras) and does not need to be the case even for seismically induced failures. In any case, the pore pressure history while the stability failure is initiated is not relevant; what is relevant is the strength that is available to resist the driving forces during the large deformations. Of course, the strength at large strains we have been discussing is the undrained steady-state strength referred to by others as the undrained residual strength, hereafter referred to as S_{us}.

A reference was made earlier to "large" strains. How large is large? For sandy soils laboratory test results indicate that the peak strength is overcome at 1% strain or less, and a constant S_{us} is reached at strains typically of about 10%. To put it in perspective in the case of Lower San Fernando, it would mean that the strain at peak in the failure zone was reached with displacements of only about one inch, and the resistance reached S_{us} after about one foot of displacement and then remained constant for the remaining 150 feet or so of displacements. There may be other secondary effects that may affect S_{us} such as possible drainage (probably negligible for Lower San Fernando), or mixing with water as the failure mass entered the reservoir, or mixing of layers at very large deformations, as suggested by Dobry.

Based on the above discussion, the ideal case history is one in which large deformations occurred as a result of instability. Ideally, as in the Lower San Fernando case, the large deformations take place after the earthquake shaking has ended, and thus the forces driving the movements are best defined: they are due to gravity only. A distinguishing feature is that there is a substantial difference

EXECUTIVE SUMMARY

On April 18-19, 1997 an international Workshop titled "Shear Strength of Liquefied Soils" was held at the University of Illinois at Urbana-Champaign. The Earthquake Hazard Mitigation Program of the National Science Foundation, of which Dr. Clifford J. Astill is the Program Director, sponsored the Workshop. The Principal Investigator for the project was Timothy D. Stark of the University of Illinois. The Steering Committee for the Workshop consisted of Timothy D. Stark, Steven L. Kramer, University of Washington, and T. Leslie Youd, Brigham Young University. To the Principal Investigator's knowledge, this was the first multi-disciplinary Workshop pertaining solely to the topic of the behavior and shear strength of liquefied soils.

Approximately twenty-five international experts in the fields of soil liquefaction, granular fluid flow, seismic slope stability, and seismically-induced permanent deformations attended the Workshop. The participants represent industry, government, and academia and provided a broad range of background and perspective on the problems discussed at the Workshop. In addition, other members of the profession and University of Illinois students and faculty attended the Workshop.

One of the major problems facing the earthquake engineering profession is the evaluation of seismic stability of dams, embankments, and slopes. This information is needed to determine how the structure will perform during an earthquake and the magnitude of permanent deformation that the structure will undergo as a result of an earthquake. This is critical for an earth dam to ensure that the reservoir is not released during or after an earthquake because of a potential reduction in the freeboard of the dam.

One important input parameter to this evaluation is the shear strength of soils predicted to liquefy. This strength, initially called the post-liquefaction shear strength, is generically termed the shear strength of liquefied soil or liquefied shear strength throughout these Proceedings. The shear strength of liquefied soil is used because discussions during the Workshop indicated that the term post-liquefaction may be inappropriate. The uncertainties surrounding the behavior and shear strength of liquefied soils are complicating a number of major projects.

The main objectives of the Workshop were to: (1) evaluate the state-of-the-art and state-of-the-practice for determining the shear strength of liquefied soils, (2) provide recommendations for the use of the liquefied shear strength in stability and deformation analyses, (3) seek consensus on a number of practice-related issues concerning the shear strength of liquefied soils, and (4) identify and prioritize research needs on the shear strength of liquefied soils and the subsequent stability analyses.

To facilitate the discussions, the participants were assigned to one of the following three discussion groups: Theoretical/Conceptual Issues, Liquefied Shear Strength from Laboratory and Field Tests, and Liquefied Shear Strength from Case Histories. The three keynote speakers and discussion group leaders were: Professor Peter M. Byrne of the University of British Columbia, Professor Geoffrey R. Martin of the University of Southern California and Dr. Gonzalo Castro of

GEI Consultants, Incorporated, respectively. Each participant was asked to write a 2-3 page (not including figures and tables) statement that addressed several issues/questions assigned to their discussion group and any other ideas or thoughts on the shear strength of liquefied soils that they would like to have discussed.

These Proceedings present an executive summary, an introduction, the keynote lectures, a description of the working group discussions, written statements submitted by the participants, and the findings, recommendations, and conclusions of the Workshop to the National Science Foundation and the practice. The Workshop Proceedings are available for electronic transmission in ASCII file format and posted on the World Wide Web.

INTRODUCTION

Ever since the major earthquakes of 1964 in Prince William Sound, Alaska and Niigata, Japan focused attention on the problem of soil liquefaction during earthquakes, considerable research has been conducted to develop a better understanding of the mechanics of liquefaction in saturated cohesionless soils. Excellent summaries of observed field performance of sands during earthquakes and the state-of-the-art in liquefaction potential evaluation can be found in publications by Seed (1968), Yoshimi et al. (1977), Seed (1979), Finn (1981), Ishihara (1985), National Research Council (1985), Castro (1987), Marcuson et al. (1992), Ishihara (1993), Finn et al. (1994), Dobry (1995), and Youd and Idriss (1998).

As a result of the San Fernando Earthquake near Los Angeles, California, in February 1971, a massive slide occurred in the upstream slope of the Lower San Fernando Dam. An investigation of the slide, including trenches, borings, in situ density tests, and analyses, was performed and reported by Seed et al. (1973), Seed et al. (1975a), Seed et al. (1975b), and Lee et al. (1975). The field investigation showed that the slide occurred because of liquefaction of a zone of hydraulic sand fill near the base of the upstream shell. The analysis of the dynamic response of the dam, performed as part of the investigation in 1973, was made using a method of analysis proposed by Seed, Idriss, and Lee at the University of California at Berkeley (Seed et al., 1975b). Application of the 'Berkeley' method to the Lower San Fernando Dam led to the conclusion that it provided a reasonable basis for evaluating the location and extent of the zone of liquefaction in the upstream shell. When the liquefied soil was considered to have no shear strength the computed factor of safety of the upstream shell was approximately 0.8 and thus it was concluded that the analysis would indicate that failure would have occurred. As a result of its application to field case histories, such as the Lower San Fernando dam and Sheffield Dam (Seed et al., 1969), the Berkeley method has been used for seismic stability evaluations of a number of dams in the past 15 years (Babbitt et al., 1983; Marcuson et al., 1983; Smart and Von Thun, 1983). During that period, however, some limitations of the method have been identified, including:

1. The method does not provide a basis for evaluating the shear strength of liquefied soil in zones that are predicted to liquefy.

2. The method sometimes predicts large potential deformations accompanying soil liquefaction that may not develop in the field. This overestimation is probably caused by the omission of the liquefied shear strength from the analysis.

In addition, the cost and extent of remedial measures required for a liquefiable deposit are greatly influenced by the magnitude of the liquefied shear strength. As a result, considerable interest has developed concerning the shear strength of liquefied soil and post-liquefaction stability and deformation analyses.

TERMINOLOGY

Studies of the shear strength of liquefied soils by Castro (1969) showed that even after liquefaction, many sands do retain a significant resistance to shear deformation. Several procedures have been developed to evaluate this shear resistance, which has been referred to as

the undrained steady-state strength by Poulos et al. (1985), undrained residual strength by Seed (1987), and undrained critical strength by Stark and Mesri (1992).

To clarify the shear strength of liquefied sands, Figure 1 illustrates the undrained behavior of a loose cohesionless soil using the results of an isotropically consolidated-undrained triaxial compression test conducted by Castro (1969). The monotonic loading test was performed on a uniform, clean, fine quartz sand, referred to as a Banding sand. The test specimen was initially consolidated to an equal all around confining pressure, σ'_{3c}, of approximately 400 kPa. The minimum and maximum void ratios of the sand are 0.50 and 0.84, respectively. The void ratio of the specimen after consolidation was 0.71, corresponding to a relative density of 37%. The specimen exhibited an undrained yield strength of approximately 110 kPa at an axial strain of approximately 1%. After the yield strength was mobilized and the specimen liquefied, it deformed from an axial strain of about 1% to 19% in just 0.18 seconds. (σ_d is the deviator stress, σ_1-σ_3, where σ_1 is the major principal stress and σ_3 is the minor principal stress. σ'_{3c} is the effective minor principal stress after consolidation and before undrained shear. u_d is the porewater pressure measured during undrained shear.)

At an axial strain of approximately 10%, the deviator stress and porewater pressure became essentially constant. The liquefied shear strength is approximately 45 kPa. Poulos (1981) termed this strength the undrained steady-state shear strength. The undrained steady-state shear strength is defined as the shear strength available in a steady-state of deformation. The steady-state of deformation is achieved after all particle orientation and breakage has reached a steady-state condition such that the mass continuously deforms at a constant volume, constant effective normal stress, constant shear stress, and constant rate of shear strain. Casagrande (1936) first defined this shear strength while developing the "critical void ratio" concept. As a result, Stark and Mesri (1992) termed this shear strength the undrained critical strength. Stark and Mesri (1992) concluded that the undrained critical strength is the shear strength available after liquefaction has been triggered and is applicable to post-liquefaction stability analyses. Seed (1987) referred to the shear strength of liquefied soil as the undrained residual strength because it represented the minimum shear strength available to a liquefied soil during a flow failure.

LABORATORY APPROACH

Poulos et al. (1985) developed a procedure for estimating the undrained steady-state shear strength of liquefied soils using the results of monotonically loaded, consolidated-undrained triaxial compression tests with porewater pressure measurements on undisturbed and reconstituted soil samples. Figure 2 illustrates this procedure for estimating the steady-state strength from laboratory triaxial compression tests. The test results from reconstituted specimens are used to determine a relationship (the steady-state line) between undrained steady-state shear strength and void ratio. This steady-state line is used to adjust the results of tests on undisturbed test specimens for densification during sampling, handling, transportation, laboratory preparation, and laboratory consolidation. The steady-state strength corresponding to the in situ void ratio is estimated by drawing a line through the laboratory void ratio-steady-state strength data point, parallel to the steady-state line. This technique assumes: (1) that the slope of the steady-state line is the same for reconstituted and undisturbed samples, and (2) that the slope of the steady-state line is independent of the method used to reconstitute the samples in the laboratory.

As pointed out by Poulos et al. (1985) the slope of the steady-state line is mainly affected by the shape of the grains in a given soil, while the vertical position of the steady-state line is affected

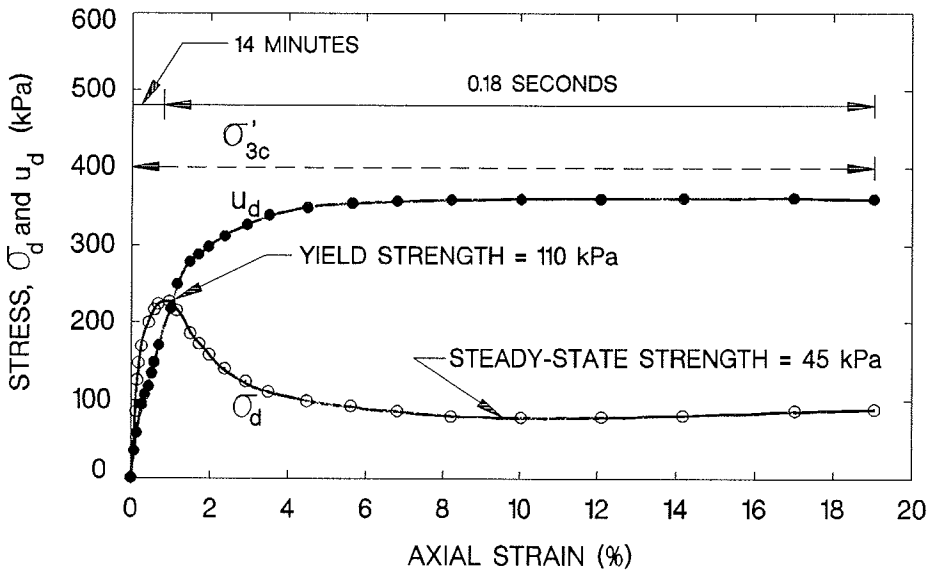

Figure 1. Typical Stress-Strain Curve from Isotropically Consolidated-Undrained Triaxial Compression Test on Loose Banding Sand (after Castro 1969)

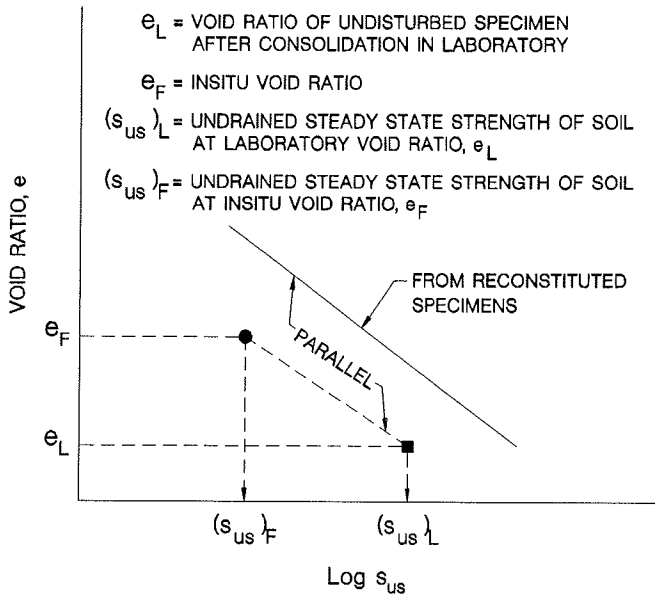

Figure 2. Poulos et al. (1985) Procedure for Determining Undrained Steady State Shear Strength for Soil at In Situ Void Ratio

by small differences in grain-size distribution. However, recent studies by Vaid and Chern (1985), Vaid et al. (1990), Konrad (1990a and 1990b), and Vaid and Thomas (1995) indicate that the steady-state line may be influenced by the mode of shear and the effective confining pressure. Dennis (1988) also states that sample preparation technique and method of loading, i.e. strain-controlled versus stress-controlled, affect the steady-state line. In addition, Kramer (1989) showed that the steady-state procedure is sensitive to parameters of uncertain magnitude and that the steady-state strength must be significantly reduced in order to decrease the probability of overestimating the steady state strength to an acceptably low value.

CASE HISTORIES APPROACH

Seed (1987) presented an alternative approach for estimating the shear strength of liquefied soils based on field case histories. This approach is based on the results of back-analysis of liquefaction case histories where values of the undrained shear strength were calculated for soil zones in which Standard Penetration Test (SPT) results were available. The values of residual shear strength were back-calculated using limit equilibrium analyses, the final geometry of the slide mass, and different failure surfaces to determine a lower-bound residual shear strength. Seed and Harder (1990) re-evaluated these data and a few additional case histories to develop a relationship between the residual shear strength mobilized during liquefaction flow failure and corrected equivalent clean sand blowcount, $(N_1)_{60\text{-}cs}$, shown in Figure 3.

CASE HISTORIES APPROACH USING A STRENGTH RATIO

Stark and Mesri (1992) presented an approach for estimating the undrained shear strength of liquefied soils as a function of the effective vertical stress based on field case histories. This approach is also based on the results of back-analysis of liquefaction case histories where values of the mobilized critical strength ratio were calculated for soil zones in which SPT results were available. The values of mobilized critical strength ratio were back-calculated using limit equilibrium analyses, the final geometry of the slide mass, and different failure surfaces to determine a lower-bound critical strength. Stark and Mesri (1992) used these data to develop a relationship between the undrained critical strength ratio mobilized during a liquefaction flow failure and $(N_1)_{60\text{-}cs}$, shown in Figure 4. This allows both the effects of soil grain characteristics (normalized blowcount) and the stress-dependent nature of the shear strength to be incorporated in stability analyses. This aids stability analyses of upstream and downstream slopes of existing dams because a stress-dependent shear strength is used along the potential failure surface instead of a single value as proposed by Seed (1987). Stark and Mesri (1992) also suggested that many of the liquefaction failures experienced drainage during flow, resulting in a back-calculated shear strength that did not represent an undrained condition.

NEED FOR WORKSHOP

In light of new developments in sampling techniques and procedures for evaluating the shear strength of liquefied sands and silty sands, it was concluded that considerable benefits and clarification of the current state-of-knowledge and state-of-practice might be gained through an international Workshop. One of the major problems facing the earthquake engineering profession is the evaluation of seismic deformations in embankments and slopes. A number of equivalent linear, e.g., Idriss et al. (1973), and nonlinear dynamic effective stress, e.g., Prévost (1981), Roth

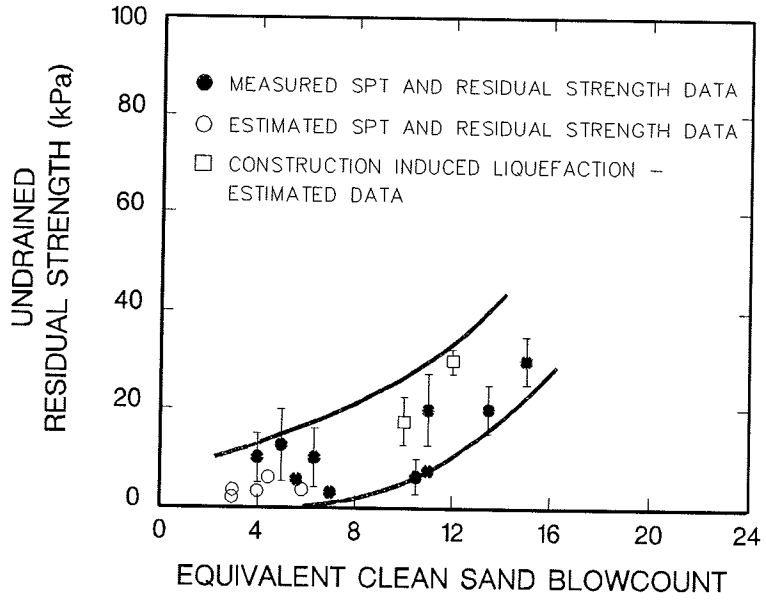

Figure 3. Relationship between Undrained Residual Strength from Liquefaction Case Histories and Equivalent Clean Sand Blowcount (after Seed and Harder 1990)

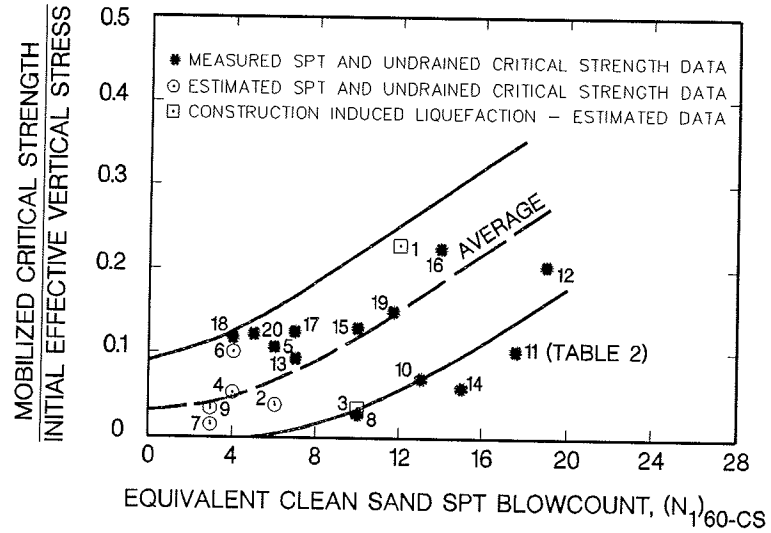

Figure 4. Relationship between Normalized Shear Strength of Liquefied Soil from Liquefaction Case Histories and $(N_1)_{60\text{-}cs}$ based on Yield Strength Fines Content Correction/Adjustment (after Stark and Mesri 1992)

(1985), and Finn et al. (1986), finite element procedures are available to estimate seismic deformations in embankments and slopes. However, a major input to these sophisticated numerical models is the behavior and shear strength of the liquefied soil. In particular, the stress-strain relationship and/or shear strength of the liquefied soil is required to estimate the seismic deformations that may be induced after the triggering of liquefaction.

OBJECTIVES OF WORKSHOP

The main objective of the Workshop was to provide a forum for the exchange of knowledge and experience among experts with a wide variety of viewpoints and perspectives on the behavior of liquefied soils, the shear strength of liquefied soils, and post-liquefaction stability and deformation analyses. The specific goals of the Workshop were to: (1) evaluate the state-of-the-art and state-of-the-practice for determining the shear strength of liquefied soils, (2) provide recommendations for the use of the liquefied shear strength in stability and deformation analyses, (3) seek consensus on a number of practice-related issues concerning the shear strength of liquefied soils, and (4) identify and prioritize research needs on the shear strength of liquefied soils and the subsequent stability analyses.

WORKSHOP ORGANIZATION

The principal investigator, working closely with a steering committee, coordinated the details of planning and organization of the Workshop. The steering committee consisted of the following individuals:

Timothy D. Stark	University of Illinois at Urbana-Champaign
Steven L. Kramer	University of Washington
T. Leslie Youd	Brigham Young University

Because of the breadth of the topics considered in the scope of the Workshop, the participants have a variety of backgrounds and interests, ranging from those who work almost exclusively in the earthquake engineering area to those who work primarily in the area of fluid flow. Working discussion groups were formed for the following three main topic areas pertaining to the behavior of liquefied soils: (1) theoretical/conceptual issues, (2) liquefied shear strength estimation from laboratory and field testing, and (3) liquefied shear strength estimation from case histories. The purpose of the theoretical/conceptual group was to provide some insight into the liquefied/fluid flow behavior of soils and numerical simulation of such behavior to those participants who are not active in that area. The laboratory and field testing group addressed the main issues involving quantification and measurement of the behavior and shear strength of liquefied soils. The case histories group addressed the issues involved in back-calculating the liquefied shear strength from field case histories and the use of the back-calculated shear strengths in design, retrofit, and remediation. After selected invitations and a public e-mail announcement, approximately nine individuals were assigned to each of the three main discussion groups. The following list presents the individuals that agreed to participate in the Workshop and discussion group assignment:

1) Theoretical/Conceptual Issues

*Peter M. Byrne (University of British Columbia)
J. David Frost (Georgia Tech)

Marte Gutierrez (Norwegian Geotechnical Institute)
Richard M. Iverson (U.S. Geological Survey)
Michael G. Jefferies (Golder Associates, Incorporated)
Joseph P. Koester (U.S. Army Corps of Engineers)
**Steven L. Kramer (University of Washington)
Jean H. Prévost (Princeton University)

2) Liquefied Shear Strength from Laboratory and Field Testing Issues

Wayne A. Charlie (Colorado State University)
Pedro A. de Alba (University of New Hampshire)
Jason E. Hedien (Harza Engineering Co.)
Bruce L. Kutter (University of California @ Davis)
*Geoffrey R. Martin (University of Southern California)
Gholamreza Mesri (University of Illinois @ Urbana-Champaign)
Scott M. Olson (University of Illinois, formerly Woodward-Clyde Consultants)
Steve J. Poulos (GEI Consultants, Incorporated)
Michael F. Riemer (University of California @ Berkeley)
**Peter K. Robertson (University of Alberta)

3) Liquefied Shear Strength from Case Histories Issues

*Gonzalo Castro (GEI Consultants, Incorporated)
Ricardo Dobry (Rensselaer Polytechnic Institute)
A. Gus Franklin/Mary Ellen Hynes (U.S. Army Corps of Engineers)
David R. Gillette (U.S. Bureau of Reclamation)
Leslie F. Harder, Jr. (California Department of Water Resources)
John C. Horne (Clemson University)
I.M. Idriss (University of California @ Davis)
William F. Marcuson, III (U.S. Army Corps of Engineers)
Timothy D. Stark (University of Illinois @ Urbana-Champaign)
Wen-June Su (Illinois State Geological Survey)
Robert V. Whitman (Massachusetts Institute of Technology)
**T. Leslie Youd (Brigham Young University)

The individual in each group denoted with one asterisk was the Keynote Speaker and Group Leader. The keynote speaker submitted a paper and presented a lecture describing the state-of-the-art, state-of-the-practice, main uncertainties, and topics that warrant future research in their designated area. The two asterisks denote the individual that assisted the group leader in organizing, conducting, and summarizing the discussion sessions of the group.

The Workshop participants were assigned to one of the three discussion groups in advance and each was asked to prepare and provide in advance a brief (2-3 page) report on their assigned research area. For example, a participant assigned to the laboratory and field measurement group prepared a brief report on the use of laboratory and/or field tests to estimate the behavior and shear strength of liquefied soils, uncertainties associated with the measurements, and current research needs. These reports were collected approximately one month prior to the Workshop and distributed to the appropriate keynote speaker. The keynote speakers reviewed and assimilated the short reports into a keynote paper/report for their discussion group.

KEYNOTE PAPERS

"Post-Liquefaction" Theoretical/Conceptual Issues

Peter M. Byrne and Michael Beaty
University of British Columbia

Granular soils whether deposited by man or nature tend to be layered or laminated. At very large strains, mixing of these layers may occur. This generally has the effect of greatly reducing the residual strength. This is so because a uniform soil generally has a higher void ratio than a graded soil at the same relative density. When the two soils are mixed, without allowing volume change, the mix is now graded and will have a lower residual strength than its individual components.

The residual strength and stiffness arise from the constraint of the water which prevents or curtails volume change during and shortly after the earthquake. This fixes the void ratio at its pre-earthquake value which in turn largely controls the strength. It is usually assumed that the response is undrained. However, this is not necessarily conservative because both dilation and contraction occur in soil, and it is possible that some zones may expand to a looser state and a lower strength.

While the strength after liquefaction may be independent of the trigger mechanism static or dynamic, the associated stress-strain response may be very different. Dynamic or seismic loading has two effects: it applies a significant transient inertia load to the soil structure; and it may trigger soil liquefaction. Provided the strength of the soil after liquefaction is sufficient for static stability, then a flow slide will not occur. However, because the stiffness of the soil may drop by a factor of 100 to 1000 due to liquefaction, very large displacements may still occur. In addition, the transient inertia forces may cause the stresses to temporarily reach the strength of the soil causing yielding and plastic displacement as considered by Newmark. Large displacements may, therefore, occur even if the strength is sufficient for static stability.

The focus here is on conceptual issues and modelling. A framework and model to be useful should capture the observed laboratory element behaviour. Before further consideration of a framework and models, the specific questions posed by the workshop and the contributions of the other panel members will be presented.

SPECIFIC QUESTIONS TO BE ADDRESSED

Continuum Mechanics/Soil Mechanics Approach

- How is the shear strength of liquefied soil influenced by consolidation stress and undrained stress path?
- How do "fines" influence residual strength?
- How should "fines" be defined?
- Is the post-liquefaction shear strength proportional to the initial vertical effective stress? Under what conditions?
- What is the applicability of the quasi-steady state or minimum undrained strength concept?

POST-LIQUEFACTION SHEAR STRENGTH OF GRANULAR SOILS: THEORETICAL/CONCEPTUAL ISSUES

by

Peter M. Byrne[1] and Michael Beaty[2]

INTRODUCTION

This workshop is concerned with the shear strength that can be relied upon for stability after liquefaction has been triggered - the post-liquefaction shear strength. It is a very important item when dealing with the stability of soil structures such as dams, bridge foundations, storage tanks, docks and lifeline facilities when liquefaction prone soils are present. Liquefaction refers to a severe loss in stiffness and/or strength that can be triggered by static or dynamic loading. The purpose of this session is to examine theoretical and conceptual issues related to post-liquefaction strength.

The stress-strain and strength of soil can be modelled in two basic ways: (1) as a particulate medium; and (2) as a continuum. The particulate approach has the possibility of predicting response from first principles. It is, however, very complex and requires a great deal of information about the soil grains and their arrangement. It is likely to be much simpler to directly test the material for its strength than to determine the fundamental parameters required for this model.

In continuum modelling, we basically first agree on how soil behaves and then capture its behaviour. This type of model, therefore, cannot really tell us anything we don't know. However, it can give insights into behaviour, if it is a good model. The list of questions posed (effect of consolidation stress, undrained path, fines, etc.) therefore, cannot be answered from a continuum model. Direct tests must be carried out to observe such effects. Once known, it should be possible to account for them with a good model. Also, such a model or framework should help to explain the observed behaviour.

Direct tests to determine post-liquefaction strength are generally carried out under consolidated undrained conditions. In principle, the samples should be consolidated to the in-situ stress state and then subjected to the expected load path, both prior to and after liquefaction.

A great deal of testing has been carried out in the past 30 years. The results indicate that for a given soil, void ratio is a key factor affecting shear strength. However, strength does not appear to be a unique function of void ratio. Other factors such as the loading path, and the fabric or grain arrangement also influence shear strength. In principle, the effect of fabric should disappear at large strains. However, it is not clear that it does, or the strains required to destroy the initial fabric may be very large.

[1]Professor, and [2]Graduate Student, Department of Civil Engineering, University of British Columbia, 2324 Main Mall, Vancouver, British Columbia V6T 1Z4, Canada

Particulate Mechanics/Granular Flow Approach

- To what extent can information from other technical fields be used to gain insight into the behaviour of liquefied soils?
- How does grain-size distribution influence granular flow?
- How does particle shape influence granular flow?
- How does drainage influence granular flow and post-flow shear strength?
- Does granular flow exhibit a rate-dependent shearing resistance? Under what conditions? What is the nature of the rate dependency?

COMMENTS BY PANEL MEMBERS

Continuum/Soil Mechanics Approach

Definition of Residual Strength/Critical State Line

Frost and Ashmawy suggest that post-liquefaction strength should be determined after the dissipation of excess pore pressure. They question most of the available results on residual strength from laboratory tests and from centrifuge studies.

Jefferies suggests that much of the observed non-uniqueness in the critical state line comes from an incorrect determination of steady state from the laboratory data. He suggests that the steady state condition is when both the volume change, and the rate of volume change, are zero.

Gutierrez states that much of the recent laboratory test results suggest the existence of a unique steady state for clean laboratory sands. However, there are still major disagreements such as whether the steady state is uniquely a function of initial void ratio, whether the steady state line is straight and parallel to the consolidation line, and how laboratory results can be applied to in-situ materials.

Kramer defines residual strength simply as the strength of liquefied soils at large strain. He prefers this definition because it is uncertain if true steady state conditions are reached in either the field or the laboratory.

Kramer notes that the first systematic treatment of the residual strength of liquefied soil came in the form of the steady state approach of Castro and Poulos. This approach assumes the development of an amorphous flow structure at large strains such that the effects of initial conditions are erased. However, the degree to which the requirements for steady state deformation are satisfied, either in the field or in the laboratory, is questionable.

Role of Fines

Frost and Ashmawy propose that a fundamental approach is needed to understand the role of fines in residual strength. They suggest that techniques such as digital image processing can

improve our understanding of fines as an inhibitor or instigator of structural collapse, as an inhibitor of pore pressure dissipation, and as a factor in post-liquefaction strength. The shape of the fines, their relative size, and the initial soil structure are all expected to play a role.

Jefferies defines fines as the fraction passing the #200 sieve. He has performed laboratory testing to investigate the effect of fines, and found that whether the fines improve the residual strength for any density depends on the stress level.

Gutierrez proposes that plasticity be considered as proposed by Ishihara (1993). He also poses the question of whether global void ratio (sand + fines) or clean sand void ratio (skeleton only) be used to characterize sands.

Kramer notes that using the #200 sieve to define fines is arbitrary, but has the important advantages of being straightforward, objective, and easy to determine. He also remarks that fines can affect both the residual strength as well as the in-situ tests often used to estimate the strength. The relative effect of fines on these two aspects is not clear. Also, since fines might affect different in-situ tests in different ways, it may be desirable to have a different definition for fines depending on the test used. Kramer also suggests that plasticity is likely an important component of any definition. He notes that plastic fines might increase the potential for different fabrics.

Koester has found that the residual strengths of sand mixtures containing 25 to 30% fines, regardless of plasticity, were very low and essentially constant to large strain in torsional simple shear. This was true for monotonic or cyclic loading. The clean sands dilated under the same tests. Based on this and data published by others, Koester is convinced that the residual strength of clean sands is higher than for sands with fines (more than 15%?). The presence of the fines appears to prevent dilation, and the beneficial contribution of plasticity is slight. Koester recommends using the #200 sieve to define fines. He also suggests performing consistency testing on just the minus #200 material when evaluating soils for residual strength.

Pseudo- or Quasi-Steady State

Jefferies proposes that the usefulness of the pseudo steady state strength should be interpreted in light of the potential instability and localization which can occur during a strain softening response. He suggests that the pseudo steady state value provides a good lower bound estimate to the instability condition, and is in favour of using the pseudo steady state strength as a reasonable engineering approximation while research into localization continues.

Gutierrez notes that steady state and quasi steady state strengths coincide for very loose materials, but are very different for dense sands. The quasi steady state strength may be difficult to experimentally determine for dense sands due to shear banding. The steady state strength is a function of void ratio only, while the quasi steady state is a function of both void ratio and initial effective stress. Gutierrez also suggests there is a unique relationship between the peak undrained strength and the quasi steady state strength for a given void ratio.

Kramer notes that the quasi steady state occurs at lower strain levels and is therefore influenced by the original fabric. The quasi steady state is not unique, does not control flow failure stability, and is not a fundamental state upon which constitutive models can be based.

Koester expressed some uncertainty on the definition of quasi steady state. He also states that the proportionality of yield cyclic strength to post-liquefaction shear strength observed by Stark and Mesri (1992) does not appear to agree with the results from laboratory tests he performed.

Soil Fabric

Frost and Ashmawy use digital image processing and analysis to provide a quantitative measure of the soil structure. One parameter they discuss is the local void ratio distribution, and note that there are slight but observable differences in the local void ratio distribution between air pluviated samples and samples from moist tamping. They suggest these changes in local void ratio distribution correlate to differences in observed behaviour. They also state that local void ratio distribution changes with strain level in both monotonic and cyclic loading.

Stress Path

Jefferies states that the effect of stress path is large.

Gutierrez states that both the steady state and quasi steady state strengths are affected by stress path. Theoretical ratios relating the steady state or quasi steady state strength for different standard laboratory loading paths have been determined.

Validity of S$_r$/p'

Jefferies generally supports this concept, in a broad sense.

Gutierrez states that since the steady state strength is a function of void ratio alone, it cannot be normalized with respect to initial effective stress. However, the quasi steady state might be normalized under certain conditions.

Kramer remarks that the normalized strength concept is valid when the consolidation curve is parallel to the steady state line. He suggests this is approximately true based on experimental data, though variability of the consolidation curve due to method of deposition and overconsolidation would be expected to influence Sr/p'. Because of these effects, correlation of Sr/p' to $(N_1)_{60}$ or q_c appears logical, so long as factors such as fabric and OCR are consistently reflected in the in-situ test results. The validity of Sr/p' appears to be weakest at low effective stresses.

Koester wonders if remediating soils will affect the Sr/p' ratio by permanently increasing the horizontal stresses.

Consolidation Stress

Jefferies emphasizes that increased consolidation stress decreases the void ratio and, as long as all else is equal, a decreased void ratio increases the post-liquefaction strength. The relative effect may be influenced by gradation, fines content, overconsolidation ratio, etc. Decreasing the consolidation stress leads to a minimal change in strength because of the induced overconsolidation.

Koester is often responsible for post-earthquake stability evaluations of large embankment dams, and therefore fervently hopes there is a strong positive influence of consolidation stress on

residual strength. He notes that residual strength determined from the Seed and Harder (1990) relationship are often too low to resist sliding within these dams.

Constitutive Models

Jefferies emphasizes that stress and strain are related, even for liquefied soils. He then suggests that "a proper understanding of liquefaction will only follow in the context of a theoretical model that sensibly reproduces soil behaviour." Such a model must adequately and consistently account for all significant aspects of liquefied behaviour (such as density, drainage, and stress path) and should not treat each behaviour in a piecemeal fashion. Jefferies briefly presents NorSand, a previously published constitutive model based on two concepts: there is a unique critical state line and the soil state moves to the critical state through shear.

Kramer states that all constitutive models presented at the most recent VELACS workshop were based on critical state concepts. Therefore, knowledge of the residual strength is important even for problems where the residual strength is never fully mobilized.

Particulate Granular Flow

Iverson notes the contribution of Bagnold (1954) to the understanding of granular flow problems, and highlights later refinements by Savage (1984) and Iverson and LaHusen (1993).

Iverson discusses the importance of grain velocity fluctuations. These fluctuations might be likened to the fluctuating motions of molecules in a dense gas, and can be described by a quantity called the granular temperature, T. T can be used as a state variable to determine whether a granular mass exhibits rate-independent Coulomb behaviour (dominated by enduring frictional contacts between the grains), or rate-dependent behaviour (where inelastic grain collisions dominate). The less variability there is between the velocities of individual grains (low values of T), the more rate-independent is the behaviour. Higher values of T imply easier movement of grains past one another, as well as higher rates of energy dissipation. Therefore, it can be inferred that there is no unique rheological model for a shearing granular material in which T is non-zero.

Iverson provides a relation for estimating whether rate effects are significant. He suggests that typical strain rates encountered in many geotechnical problems are not great enough for strong rate dependent behaviour, at least for non-liquefied soils. However, rate effects become more important as the effective stress approaches zero during liquefaction.

FRAMEWORK

Granular soil can be modelled either as a particulate medium or as a continuum.

Particulate Modelling

Soil is a collection of particles, and so we should be able to predict its stress-strain and strength behaviour from the application of particulate mechanics. This has been done to some extent by a number of researchers. We need to know the particle, size, shape, grading, and fabric or arrangement. However, such modelling becomes very complex as it is necessary to keep track of

the particle contacts and the associated forces and directions, and the re-arrangement of particles with the loading. In the short term, it would seem simpler and more reliable to directly test the soil for its response. However, in the long term, the particulate approach might provide useful insights into the soil behaviour in a "flow" state and, perhaps, answers the specific questions posed in the previous section. Iverson suggests that rate effects could become important at low effective stresses during liquefaction. Nemat-Nassar's contribution on this topic should be very helpful.

Continuum Modelling

Here we replace the soil with a continuum. We assign properties to the continuum that best captures what we observe. This approach does not really predict element behaviour, but captures the behaviour that we have observed. However, if we capture the skeleton behaviour in a drained loading test, we should be able to predict its undrained response, since the prevention of drainage merely provides a volumetric constraint on the skeleton. In addition, the response of a soil structure comprising a collection of such elements can be predicted from such a model.

In this approach we must first agree on how the soil skeleton responds. This is essentially the approach taken by Professor Roscoe, and his colleagues and students at Cambridge University, in the late 1950's and early 1960's, in the development of critical state soil mechanics. As pointed out by Kramer, all of the models used in the VELACS predictions were based on critical state.

There are two parts to the process:

1) a general agreement about how soil behaves under controlled conditions - laboratory tests; and

2) a stress-strain model that captures the observed behaviour.

The Cambridge group expended most of its efforts on clay, rather than sand. They collected existing data. In addition, they carried out additional testing of clay.

Early data on sand suggest that the major factor controlling the residual strength, S_r, is the residual effective stress on the failure plane at the time of failure, σ'_r.

$$S_r = \sigma'_r \times \tan \phi'_{cv} \qquad (1)$$

where $\sigma'_r = \sigma_r - u$ and ϕ'_{cv} = the constant volume effective friction angle (generally about 33° for sand, regardless of loading path). While σ_r is generally known at all times, the pore pressure u depends on the drainage state. For the special case of no drainage, σ'_r also depends on void ratio and hence void ratio is a major factor in the residual strength.

The interplay of void ratio and effective stress is a fundamental concept in critical state soil mechanics as depicted in Fig. 1. The soil state exists between the upper and lower bounds shown in Fig. 1. The upper bound represents soil placed and loaded in its loosest possible state, while

the lower bound represents soil placed in its densest possible state. When the soil is sheared it moves towards the failure or critical state. This failure or critical (steady) state may be unique (a line) or there may be a failure band depending on fabric and the path followed to failure.

Assuming for the moment that a failure line rather than a band exists, then for any void ratio there is only a single σ'_r and hence, a single residual strength, $S_r = \sigma'_r \tan \phi_{cv}$. This is depicted in Fig. 2 for both a very loose and a loose sample both of which start from a known effective consolidation pressure p', and have residual strengths $(S_r)_1$ and $(S_r)_2$. Stress-strain relations associated with these stress paths are shown in Fig. 2c. Sample B exhibits a quasi-steady state as well as a steady state.

Critical state concepts have been used in both clays and sands for many years (Taylor, Casagrande, Roscoe and Castro). They represent a framework to evaluate the residual undrained strength. In summary, the concept is that for any void ratio there is a unique residual effective stress, σ'_r at failure. The associated residual strength is $S_r = \sigma'_r \tan \phi'_{cv}$. In practice, there is probably a σ'_r band for each void ratio leading to a range of shear strengths rather than a unique value.

Tests carried out by Y.P. Vaid and his students at the University of British Columbia over the past 15 years, indicate that the important variables for a given sand are: (1) void ratio or relative density; (2) type of compaction (fabric); and (3) direction of loading. These effects are illustrated by considering each separately while keeping other factors the same.

1) Relative Density or Void Ratio

The effect of relative density, while keeping all other factors the same, is shown in Fig. 3 for Syncrude sand. The loose sample, A, strain softening to a residual strength value of about one-half its peak value at a shear strain of about 12%. Sample B strains softens to a quasi-residual strength value of about 2/3 the peak at a shear stress of about 8%. Sample C strain softens marginally to a quasi-steady state at a strain of about 4% before hardening, while the denser sample D strain hardens at all strain levels.

2) Effect of Confining Stress

The effect of confining stress on response is shown in Fig. 4a for a loose sand. The results indicate that the residual strength increases approximately linearly with confining stress and given by $S_r \approx 0.19$ p' for this Fraser River sand. However, very loose samples may have zero residual strength as shown in Fig. 4b for Toyoura sand, i.e., $S_r/p' = 0$. These samples were prepared by freezing.

3) Type of Compaction, or Sample Preparation

The effect of type of compaction or sample preparation is shown in Fig. 5. Samples were prepared at essentially the same void ratio using three different methods of sample preparation: (a) moist tamping; (b) air pluviation; and (c) water pluviation. It may be seen that their residual strengths are different by an order of magnitude, with the moist tamped sample having the lowest

strength and the water pluviated the highest strength. In fact, the water pluviated sample is not even strain softening. The results indicate that shear strains of 15% are not enough to destroy the initial fabric.

4) Stress Path

The effect of stress path on undrained response is shown in Fig. 6. The direction of loading (major principle stress) was varied between α_σ = 0 and 90°, where α_σ = 0 represents vertical loading and α_σ = 90° represents horizontal loading. The results show a factor of five difference in strength between vertical and horizontal loading with vertical loading giving the highest strength, and horizontal loading the lowest strength.

It should be noted that while the α_σ = 0 sample is barely strain softening, it is quite contractive until the stress path reaches the phase transformation or ϕ_{cv} line (σ' drops from 400 to 225 due to shear induced porewater pressure rise). A critical examination of test data shows that all sands, whether loose or dense, contract for stress ratio less than ϕ_{cv}, and denser sands expand for stress ratios greater than ϕ_{cv}. This will be discussed later.

5) Effect of Mixing on Residual Strength

Granular material is generally nonhomogeneous comprising looser and denser zones. In addition, finer and coarser layers often occur. These layers in themselves may have adequate residual strength, but if the strains are large enough, they may mix to form a new more graded material occupying the same volume. This mix material may have a greatly reduced residual strength which could result in a flow failure. Such a situation occurred at the Mufulira Mine in Zambia in 1970 and resulted in the death of 90 miners.

Mine tailings were deposited above the working area of the mine to a depth of 70 m. The tailings were deposited hydraulically and comprised of layers of silty sand and sandy silt. $(N_1)_{60}$ values ranged between 10 and 30 blows with 2/3 of the values greater than 15. The water contents ranged between 20 and 30% with an average value of 24%. Sinkhole formation triggered liquefaction of the tailings causing 1/2 million cubic yards to flow through cracks in the rock and into the working area 500 m below.

The steady state lines for silty sand, the sandy silt and the mix are shown in Fig. 7. For the average water content of 24%, the residual normal stress, σ'_r, and residual strengths are as shown in Table 1.

Table 1

Material	σ'_r (kPa)	S_r (kPa)
Sandy Silt	200	130
Silty Sand	40	26
Mix	≈0	≈0

between the strength required for equilibrium in the pre- and post-failure configurations; in other words, the post-failure configuration is substantially flatter than pre-failure. Whitman suggests that stability (flow) failures will be recognized as those in which the displacements exceed 3 m for small slopes/dams and 10 m for large slopes/dams and movements occurred/continued after ground shaking has essentially ceased. In order to estimate S_{us} from such a failure, one needs both pre- and post-failure configuration; characterization of the soils within the soil mass (e.g., dam and foundation) in terms of soil types, blowcounts, cone, shear wave velocities, laboratory test data; timing and duration of the large movements; observations of the failed mass to ascertain the failure surface or zone and deformation pattern; reservoir level at the time of the failure. Obviously, it reads like a wish list, and it is. (In his note for the workshop, Horne has a good list). Practically, it is highly unlikely that all of the above information will be available. Note that the seismic input is not listed because it does not affect the computation of S_{us} since the extent of the failure is governed by gravity forces and soil strengths. The earthquake of course triggered the failure and affected only the initial movements.

Given the fact that for sandy soils the S_{us} value is reached after relatively small displacements, very soon into the failure there is a condition of instability in which the applied stresses exceed the available resistance and the mass accelerates during roughly the first half of the large movements. The applied stresses drop as the configuration becomes flatter, and the resistance may increase as the length of the failure surface increases, so that at about the midpoint they become equal, the acceleration becomes zero and the velocity reaches a maximum. Thereafter the resistance is larger, and the mass decelerates until the velocity becomes zero and the mass comes to rest. An example of an analysis based on this model was presented in Davis et al, 1988, for the Lower San Fernando Dam, the results of which matched the estimated elapsed time of the failure. Practically, analysis of this type will result in a backfigured S_{us} equal to about the average of the strengths required for a factor of safety of one for the pre- and post-failure configurations. For example, for Lower San Fernando in the pre-failure configuration, the driving shear stress was about 950 psf in the lower part of the hydraulic fill, while in the post-failure configuration the value was about 250 psf. The analysis described above resulted in a value of S_{us} of 520 psf, i.e., close to 600 psf (average of 950 and 250 psf). The use of this average will certainly comply with Dobry's idea of keeping the backcalculations simple!

Unfortunately, there are very few cases of stability failures in sandy soils of the Lower San Fernando type. A much more common occurrence is that of seismically induced limited deformations such as lateral spreads. Unfortunately, the physical mechanism responsible for the movements in such cases is much more uncertain. Any back computation of S_{us} needs to assume a mechanism, as was described for the stability type failure. Inasmuch as the mechanism for limited deformations remains uncertain so will any computation of S_{us} from such case histories.

A postulated mechanism for the limited deformations case was presented in Castro, 1987, and is also described in the enclosed paper. It was assumed that the deformations could be analyzed as a Newmark-type phenomenon in which the yield strength was S_{us} and the movements were caused by the static plus seismic stresses exceeding momentarily S_{us} and thus accumulating movements. In such cases S_{us} exceeds the strength required for equilibrium, which is about the same for both the pre- and

post-seismic configuration. An analysis of this type for Heber Road indicated an S_{us} value of about 100 psf, while the static shear stress was only about 40 psf. The seismic stresses were substantial so the value of 100 psf was exceeded several times during the earthquake, causing accumulation of displacement of up to 7 feet. Note that this analysis requires as an input the seismic shaking the site was subjected to. The note from Mabey and Youd for this workshop appears to have used the same methodology for a large number of lateral spreads, indicating apparent S_{us} values that are rather insensitive to blowcount.

It is questionable whether the Newmark-type analysis is the appropriate mechanism, particularly when the displacements are small (say a couple of feet). Such deformations could well accumulate even in cases in which S_{us} is high, as pointed out by Dobry based on field observations and centrifuge tests. Thus in these cases S_{us} will not control the deformations, and thus it follows that S_{us} cannot be backfigured from such case histories. Whitman indicates that these cases involve repeated contraction-dilation cycles, which this author interprets as the mechanism being other than yielding at S_{us}. The estimation of relatively small but potentially damaging movements is an important matter but may not relate to the value of S_{us}.

Based on the above discussion, cases of limited deformations should not be used for backfiguring S_{us} unless and until a better understanding of the physical mechanism of the deformations were to indicate that they can be related to S_{us}. As noted by Hynes "we need to get the mechanism right."

The question as to whether drainage may have occurred in a specific case history needs to be explicitly addressed in a case-by- case basis. A judgment needs to be made based on the size of the zone of failure, proximity to drainage boundaries, soil permeabilities, and duration of the failure movements. In some cases the answer is clear, e.g., this author believes that drainage in the Lower San Fernando case was negligible. If in a particular case drainage seems probable, one should be aware that the backfigured strength may be higher than S_{us}.

The question as to whether S_{us} is proportional to the initial effective overburden stress (sigma v) cannot be answered at this time from the very few available good case histories. The answer must be obtained from the results of laboratory testing. The results of tests performed in many sands by the author and others have indicated that in a plot of void ratio (arithmetic scale) vs say sigma 3 effective (log scale), the 1D compression curves are flatter than the steady-state line (SSL). A flatter compression curve means that as the sand is consolidated to higher pressures, the soil becomes more contractive (or less dilative), and thus S_{us} does not increase proportional to the consolidation stress. An exception may be angular sands at very high consolidation stress where the two curves become roughly parallel, and thus S_{us} would be proportional to consolidation stress. Of course for clayey soils the compression curve and the SSL are parallel, and thus S_{us} is proportional to consolidation pressure. Where the boundary line is between the two types of behavior is not clear at this time. Relative to this point, Marcuson indicates that if one needs a ratio of S_{us} to consolidation stress of only 0.05, he would feel comfortable that such small strength would be probably available. This author is not sure whether such a conclusion would be correct for a clean sand.

A representative *in-situ* test parameter to catalog the case histories, such as SPT or CPT, is a useful tool. The question was raised as to which value to choose as representative. There is no clear answer to this question. Assuming one has a representative set of values from the failure zone, this author would favor choosing something like the 33 percentile (67% of the values are higher) because the failure would occur preferentially along the weaker soils. Of course, one must be consistent in the parameter selection so as to compare a new site to the case histories on the same basis.

It should not be assumed a priori that a correlation between S_{us} and SPT or CPT applicable to all sandy soils is to be found, as these tests are at least partially drained while S_{us} is an undrained property. Rather the case histories will represent a lower bound.

Published analyses of case histories have led to substantially different interpretations as noted by Gillette, see enclosed paper. There is a need to carefully reevaluate the few available reliable case histories given the strong reliance on these data in practice, which in this author's opinion is unwarranted.

Another limitation of the data, noted by Mabey and Young, is the absence of data at higher blowcounts, say higher than 15, which includes many real structures for which major decisions need to be made on their seismic safety.

Other subjects worth discussing and not listed by the organizers for our discussion group are noted below.

A fines correction to the blowcount was introduced by H. B. Seed and has been used later by Seed and Harder and others. Since most of the available cases are for silty sands, the effect of the correction is to move the data points to the right. The basis for the correction appears to be an extension of the observations from the pore pressure development empirical chart. Since the two phenomena are quite different, the fines correction seems unfounded. Furthermore, even for the pore pressure development chart, the effect of fines can be explained in a way that does not imply a larger resistance to pore pressure development in silty sands, see enclosed paper.

The effect of mode of failure (simple shear, axial compression, and extension undrained shear) in S_{us} has been the subject of several recent papers and discussions. This author has yet to see published undrained tests other than axial compression where S_{us} has been reached within the limitations of the testing apparatus. Unpublished tests by Poulos using drained rotation shear (akin to simple shear) indicates essentially identical steady-state line to that obtained from axial compression tests.

It has been postulated that redistribution of water may cause S_{us} to be lower than the value corresponding to the pre-earthquake void ratio. The issue is far from clear. Some centrifuge tests that were claimed to have demonstrated the occurrence of redistribution in the opinion of the author actually proved the opposite. Certainly it is a crucial issue. Of course, any backfigured S_{us} from a good case history will reflect any redistribution. If this were to be proven an important factor, we have a major challenge: how to predict the amount of such redistribution. The degree of

redistribution, if any, would be a function of the time available during the failure, permeability and size of the failure zone, and other boundary zones. Of course, these site conditions will in no way be reflected in the results of SPT or CPT index tests. Thus there would be another powerful reason why it would be wrong to assume that a specific case will behave similar to a known case history because their soils have the same SPT or CPT.

Whether or not a careful review of case histories leads or not to a "correlation" of S_{us} with an index test such as an SPT or CPT, it is important to continue to investigate case histories. Case histories are ultimately the key element in understanding the physical mechanism of liquefaction failures and of accumulation of limited deformations.

WORKING GROUP DISCUSSIONS

After the three Keynote Lectures, the discussion groups convened to discuss the writing of summary reports and Consensus Topic A. Following the discussion, the subject matter and conclusions of the groups were presented to a Plenary Session comprised of all of the Workshop participants. On the second day, the discussion groups met to discuss Consensus Topic B. Following the group meetings, a Plenary Session was held to discuss Consensus Topic B. Consensus Topic C (Future Research Needs) was discussed only during a Plenary Session, with Steven L. Kramer leading the discussion. A list of research needs was assembled by Steven L. Kramer, Timothy D. Stark, T. Leslie Youd, and the discussion group leaders prior to the Plenary Session. This list served as a starting point for the discussions in the Plenary Session. The Plenary Session resulted in the list of research needs presented under Consensus Topic C in this report.

CONSENSUS TOPICS A

THEORETICAL/CONCEPTUAL DISCUSSION GROUP

Topic 1. Terminology for the Shear Strength of Liquefied Soils

The group discussed the terminology that should be used to describe the shear strength of liquefied soil. In addition, the physical behavior controlling this shear strength and the observed phenomena were discussed. The observed phenomena include flow failure and limited deformation. Limited deformation consists of lateral spreads where the pre-existing shear stresses are relatively low, e.g., Juvenile Hall, and other cases where the pre-existing shear stresses are large, e.g., Upper San Fernando Dam. As illustrated in Figures 1 and 5, the shear strength that controls deformation in flow slides and limited deformation cases, respectively, may not be the same. Figure 1 presents the results of an undrained triaxial compression test on loose Banding sand, conducted by Castro (1969), that exhibits a steady-state shear strength of approximately 45 kPa. Figure 5 presents undrained cyclic simple shear tests results on medium dense to dense Nevada sand, conducted by Arulmoli et al. (1992), that exhibits a cyclic shear strength of approximately 3.3 kPa. The group concluded that at this time, these two shear strengths should be considered and evaluated separately.

With regard to flow failure, the following terminology to describe the shear strength available to a liquefied soil after large strain were reviewed during the Workshop:

- Steady State Strength (Poulos et al. 1985)
- Residual Strength (Seed 1987)
- Critical Strength (Stark and Mesri 1992)

The term 'undrained' was not included with these terms because it is unclear whether or not undrained conditions exist at all times during flow failures. The group commented that the appropriate terminology was complicated because of the lack of understanding of the actual behavior of a soil during a liquefaction flow failure, i.e., whether or not a steady/critical state is reached, the effect of pore-water pressure redistribution, etc. Therefore, the group anticipated that a term that did not reflect any predisposition to laboratory tests would be preferable to describe the behavior of soils during flow failure.

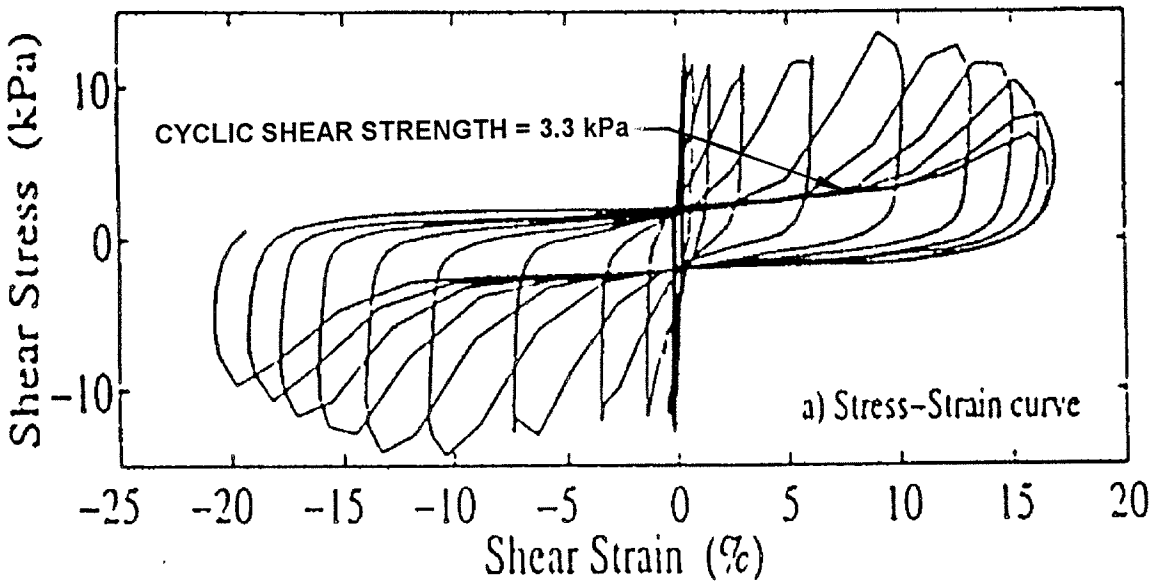

Figure 5. Typical Stress-Strain Curve from Undrained Cyclic Simple Shear Test on Nevada Sand with Relative Density of 60% (after Arulmoli et al. 1992)

The Theoretical/Conceptual Issues group proposed the term 'Apparent Flow Resistance' to the Workshop participants in the following Plenary Session. 'Apparent Flow Resistance' was defined as the available shear resistance during liquefaction flow failure, as influenced by boundary conditions, spatial variability, drainage or void redistribution, time or strain rate, and initial stresses. This term was anticipated to accommodate most, if not all, of the variability that exists in the field during flow failure, and does not restrict the observed shear strength to represent behavior observed in laboratory tests. As understanding of the physical mechanisms during liquefaction flow failure increases, the Theoretical/Conceptual Issues discussion group indicated that it may be appropriate to revise the term used to describe this strength.

The term 'Apparent Flow Resistance' met considerable opposition in the Plenary Session. The main apprehension voiced was that this term introduced a completely new nomenclature for a phenomenon that had been described with other nomenclature for decades. I.M. Idriss expressed reservation about moving away from the term 'Residual Strength' because it has been in use in academia and practice for many years. Ricardo Dobry suggested that 'Residual Strength' has a strong connotation to the large strain strength of overconsolidated clay soils, as first proposed by Skempton (1964). Dobry stated that a different term may be more appropriate to describe the shear strength of liquefied soil at large strain. Scott M. Olson commented that there can be differences between the liquefied shear strength observed in the field and the laboratory. The laboratory strength has long been referred to as 'Steady State Strength,' or more recently as 'Critical Strength,' and these terms are applicable to laboratory boundary conditions and constraints. The strength observed in the field may be better described by 'Mobilized Steady State Strength' or 'Mobilized Critical Strength' because this is the strength that is *mobilized* by the liquefied soil during failure. In addition, these terms are still linked to the phenomenon of

liquefaction and deformation leading to the steady/critical state. This would provide similarity to overconsolidated clayey soils because the residual strength is measured in the laboratory and the shear strength back-calculated from case histories is referred to as the mobilized residual strength.

Steve J. Poulos first disagreed with the terminology 'Post-Liquefaction,' stating that liquefaction is the process of strength loss during loading, therefore the term 'Post-Liquefaction' has no meaning. Poulos continued stating that there are two strengths available to a loose, contractive sand. These are the 'Peak Strength' and the 'Steady State Strength'. The 'Peak Strength' is the shear strength of the soil as the soil structure begins to yield. The 'Steady State Strength' is the shear strength available to the soil after large strain, and can be measured in the triaxial compression test provided the sample is subjected to a confining stress prior to shear that results in a very loose condition with respect to its steady/critical state line (SSL/CSL).

After considerable debate, Geoffry R. Martin proposed the term 'Apparent Residual Strength'. However, many of the participants expressed reservation about this terminology, partly because the term 'Apparent' is nebulous. As a result, it is proposed herein that two different terms be used: one to describe laboratory behavior and one to describe field case histories. The term 'Apparent or Mobilized Residual Strength' appears appropriate to describe the shear strength back-calculated from liquefaction flow failures, e.g., Lower San Fernando Dam. The terms liquefied shear strength, shear strength of liquefied soil, or shear strength at large strain also appear appropriate. The term 'Steady' or 'Critical State Strength' can be used to describe laboratory-measured shear strength at large strains. The relationship or correlation between the laboratory-measured steady/critical state shear strength and the liquefied shear strength back-calculated from flow failures should be investigated and is a topic for future research under Consensus Topic C.

LABORATORY AND FIELD TESTING DISCUSSION GROUP

Topic 2. Laboratory versus Field Determination (Preferred Test and Data Reduction)

Before discussing the consensus topic of laboratory versus field testing, the discussion group reviewed fundamental behavior and terminology in order to reach a common understanding. The discussion centered on the observed soil behavior shown in Figures 1 and 5. All group members agreed that flow liquefaction involves the loss of soil strength with increasing strain, i.e., strain-softening behavior. The following terminology was mentioned as being used by the profession to describe strain-softening behavior with respect to liquefaction: residual strength, steady state strength, critical strength, and ultimate strength. The behavior and strength observed at the 'quasi-' steady state were also mentioned. The behavior of strain-softening soils was differentiated from the behavior of soils that undergo cyclic liquefaction or cyclic deformation, e.g., lateral spreads (see Figure 5). The term 'Mobilized Cyclic Resistance' was suggested by Peter K. Robertson to describe the shear strength applicable to lateral spreads. As this discussion occurred prior to the Plenary Session, the group did not discuss the terminology 'Mobilized Residual Strength'.

Following this brief discussion, the discussion group moved into the consensus topic. All of the group members agreed that field and laboratory testing for liquefaction studies should be complementary, not contentious. Further, the effort and complexity of field and laboratory testing should be dependent upon project risk, i.e., the size and potential hazards of a project. A flow

chart for guiding the methods of estimating the shear strength of liquefied soil is presented in Figure 6.

Low Risk Projects

For low risk or small budget projects, field testing should consist of cone penetration testing (CPT) or piezocone testing (CPTU) in combination with limited standard penetration testing (SPT). The use of the CPT allows for a more comprehensive site investigation for a given budget. Laboratory testing will probably be limited to index testing to determine grain size characteristics (i.e., D_{50}, fines content, and perhaps clay content) and plasticity of the fines. The liquefied shear strength can be estimated using existing correlations for the SPT (Seed and Harder 1990, Stark and Mesri 1992, Ishihara 1993, Baziar and Dobry 1995) or CPT (Jeffries et. al. 1990, Robertson 1990, Olson and Stark 1998) penetration resistance and back-calculated shear strength from liquefaction flow failures. There is some uncertainty in using existing correlations, however, for low risk projects, additional testing and expenditure are typically not warranted. The use of judgment is often the primary alternative for borderline cases.

Moderate Risk Projects

For moderate risk projects, field testing should consist of CPT and SPT coupled with additional tests, such as geophysical testing or field vane shear testing with pore-water pressure measurements (FVTU, Charlie et al. 1995). Laboratory testing should probably include index testing as described above and perhaps laboratory testing of reconstituted samples to investigate soil response and/or estimate the steady/critical state line. If silty soils are involved, undisturbed samples may be obtained with reasonable effort for laboratory shear testing. The liquefied shear strength is typically estimated using existing correlations based on penetration resistance and observations of soil behavior from the laboratory testing program.

High Risk Projects

High risk projects often involve two-phase investigations to allow screening and subsequent 'intelligent' sampling and additional field testing. The preliminary site evaluation will typically involve CPT, SPT, and probably geophysical testing (shear wave velocity, V_s, and geophysical logging of void ratio or density) to identify critical areas. Critical areas would be defined based on predicted behavior estimated from empirical correlations. A detailed site investigation would be tailored to reduce the uncertainty in the preliminary investigation. This would include additional field testing, e.g., CPT, SPT, V_s, FVTU, and self-boring pressuremeter testing (SBPMT), and probably undisturbed sampling, e.g., ground freezing techniques. Preliminary laboratory testing would resemble that for moderate risk projects, and phase two laboratory testing could include triaxial compression/extension, simple shear, and/or torsional ring shear testing on undisturbed soil samples. The testing would be focused on estimating detailed response characteristics.

Field Testing

The discussion of field testing focused on two objectives: (1) estimation of in-situ state leading to an estimate of the potential for flow liquefaction and/or the magnitude of liquefied shear strength, and (2) direct estimation of liquefied shear strength from correlations using field test results.

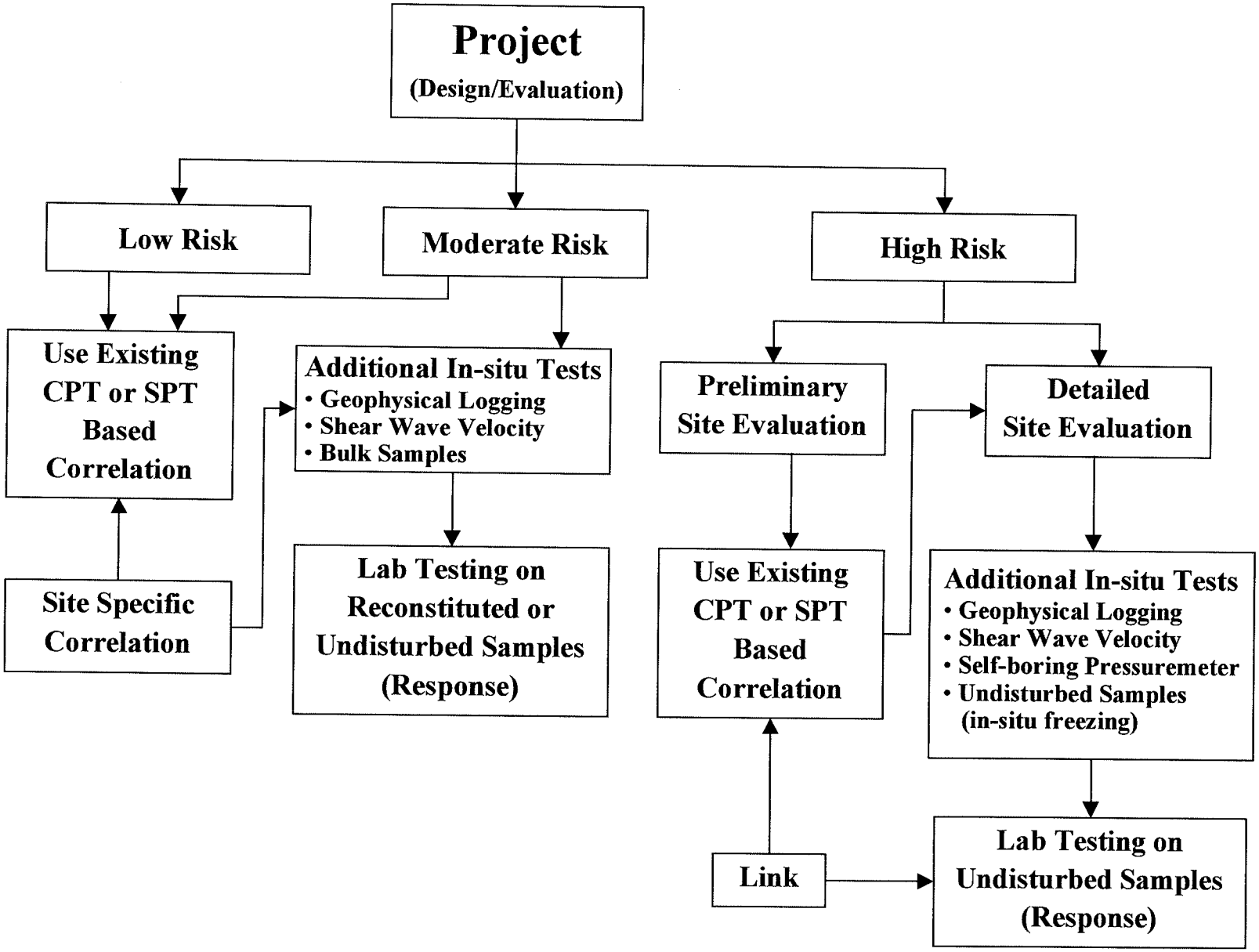

Figure 6. Flow Chart for Assessment of Shear Strength of Liquefied Soil (after Robertson, Workshop Presentation 1997)

In-situ state is described by the effective stress and density of a soil prior to undrained loading. The state parameter is defined as the difference between in-situ void ratio and void ratio corresponding to the steady/critical state line at the in-situ effective stress. In-situ void ratio can be estimated from undisturbed sampling (ground freezing, high-quality piston sampling, or test pit sampling), geophysical logging (gamma-gamma, borehole, or radio-isotope CPT), penetration testing (CPT or SPT), or shear wave velocity testing. All of these techniques are subject to various difficulties and/or uncertainties, require knowledge of the position of the steady/critical state line, and some require values of e_{min} and e_{max}. The state parameter can be estimated directly using the CPT (Been et al. 1986) or SBPMT (Yu 1994) and does not require previous knowledge of e_{min}, e_{max}, and the position of the steady/critical state line.

Estimating liquefied shear strength from field tests utilizes existing correlations where liquefied shear strength or liquefied shear strength normalized to the vertical effective stress back-calculated from liquefaction flow failures is related to a field test parameter, such as penetration resistance. Correlations exist for the SPT (Seed and Harder 1990, Stark and Mesri 1992, Ishihara 1993, Baziar and Dobry 1995), CPT (Jefferies et al. 1990, Robertson 1990, Olson and Stark 1998), V_s (Fear and Robertson 1995), and FVTU (Charlie et al. 1995). Several concerns were mentioned regarding the use of existing correlations, including: (1) the effect (if any) of fines content, plasticity, mineralogy, and grain shape; (2) the appropriate value of test result, e.g., average, median, minimum, or other value; and (3) the reliability of the correlation itself because of the reliability of the case histories and the scatter of the correlation.

The group agreed that despite the uncertainties regarding the influence of fines content and thin layer effects, the CPT/CPTU/seismic CPTU represent an economical and reasonable means for estimating liquefaction resistance and liquefied shear strength of soils. However, the SPT remains useful for verifying CPT results and/or investigating liquefaction resistance because of existing experience and correlations.

Laboratory Testing

The group discussed the relative merits and difficulties associated with 'undisturbed' sampling techniques using ground freezing (Yoshimi et al. 1989), large diameter sampling, and high-quality fixed piston sampling (Poulos et al. 1985). The group agreed that ground freezing is the preferred method to obtain 'undisturbed' samples, assuming the soil conditions are appropriate for the method (i.e., low fines content), successful procedures are strictly followed, and funding is available for appropriate quantity of samples and quality of laboratory testing. Large diameter sampling was considered appropriate only if the utmost care is used to obtain the sample. Fixed piston sampling was least preferred because of the lack of understanding of sampling, handling, and extruding procedures and because corrections are required to estimate the in situ void ratio. However, Steve J. Poulos indicated that fixed piston sampling could provide reasonable quality samples for laboratory testing. The group expressed interest in this technique, provided more documentation of sampling, handling, and extruding procedures is introduced into the literature.

Laboratory tests discussed included triaxial compression and extension, simple shear, and torsional ring shear. No consensus was reached because of the multitude of questions surrounding observed (and sometimes contradictory) behavior in laboratory tests. The uncertainties include stress path effects, mode of shear effects, strains required to reach steady/critical state, whether existing test apparatus could attain these strains, sample preparation, and the significance of quasi-steady state strengths.

Centrifuge testing (Fiegel and Kutter 1994) is model testing, not element testing, and therefore is subject to a different set of difficulties and concerns. In addition, the ability to generate large strains in the centrifuge test was questioned. Test results are limited, but indicate that the liquefied shear strength is not constant due to void ratio and porewater pressure redistribution, and that boundary conditions are critical to the test results. The group concluded that the use of the centrifuge for estimating the liquefied shear strength warranted further research.

CASE HISTORY DISCUSSION GROUP
Topic 3. Classification and Characterization of Liquefaction Field Case Histories

Classification of Liquefaction Field Case Histories

A common feature of liquefaction case histories is that a static driving shear stress, τ_d, was present prior to liquefaction, and that the direction of the permanent deformation is controlled by the direction of τ_d. As a consequence of these permanent deformations, the soil configuration changes and the magnitude of τ_d is reduced. For the purpose of classifying liquefaction field case histories, τ_d is defined as the average undrained shear strength in an undrained strength stability analysis needed to provide a static factor of safety of unity along the most critical failure surface that includes the liquefied zone. This value of τ_d is only for the purpose of classification, and the reduction of τ_d provides a convenient means of classification.

Category 1. Case histories in which the magnitude of τ_d is reduced by more than 10% when comparing the soil configuration before and after the liquefaction incident. This category covers flow slides of earth structures and/or their foundations, as well as the ground movement close to a free face in some lateral spreads. In this category, the permanent ground deformation is primarily driven by the static forces. Case histories applicable to this category include Lower San Fernando Dam, Fort Peck Dam, and Mochikoshi Tailing Dike 1.

Category 2. Case histories in which the magnitude of τ_d is reduced by 10% or less when comparing the soil configuration before and after the liquefaction incident. This category covers most of the ground movements in lateral spreads caused by earthquakes, as well as some case histories of limited deformation of earth structures and/or their foundations. In this category, inertia forces due to earthquake shaking play a major role in the deformations. Case histories applicable to this category include Upper San Fernando Dam, Heber Road, and Juvenile Hall.

The discussion group agreed that only Category 1 case histories will provide information on the 'Apparent' or 'Mobilized Residual Strength'. This strength does not necessarily control the development of limited strains under earthquake shaking (Category 2 case histories).

Characterization of Liquefaction Field Case Histories

A 'good' case history for back-analysis is one in which the liquefied shear strength is the controlling parameter in producing an observed and measurable effect. As a result, the case history can be used to estimate the value of liquefied shear strength, and that strength can be

related to some measurement(s) that can be used to predict the liquefied shear strength in other cases.

Generally, a significant investment of resources is required in an intelligent post-event investigation to permit a comprehensive back-analysis. The investigation must determine: (1) the pre-event conditions, including the site geology, the relevant material properties and conditions, and their distribution; (2) what happened during the event and post-event configuration and conditions; and (3) reliable values of the measurements to correlate with the liquefied shear strength (such as SPT blowcounts, CPT measurements, etc). Table 1 presents a list of the field data that should be obtained in a post-event investigation and the importance of this information for the evaluation of flow slides and lateral spreads.

CONSENSUS TOPICS B

THEORETICAL/CONCEPTUAL DISCUSSION GROUP

Topic 4. Normalization with Initial Vertical Effective Stress

The group began discussions with general acceptance of the concept of normalization of the liquefied shear strength. The stipulations to the normalization are believed to be: (1) the SSL/CSL and the initial consolidation line (ICL) must be parallel; (2) the soil must be loose (i.e., contractive); (3) the soil must be deposited in a consistent manner; and (4) the soil must be subjected to a consistent stress history. It is anticipated that σ'_1 (effective major principle stress) is preferable (although more difficult to determine) to σ'_v (effective vertical stress) for normalization. Some approaches for estimating the normalized liquefied shear strength utilizing the state parameter have been proposed (e.g., Fear and Robertson 1996).

Controversy was expressed regarding the soil types for which normalization is appropriate. In general, the group agreed that normalization is appropriate for compressible soils, such as silty sands and tailings sands. The reason for this is illustrated in Figure 7. For compressible soils, the initial consolidation line (ICL) is often parallel or nearly parallel to the steady/critical state line over a given stress range. Figure 7(a) shows the ICL and the SSL/CSL for remolded layered specimens of silty sand (Batch 7, Lower San Fernando Dam). It can be seen that the ICL and SSL/CSL are approximately parallel over a stress range from 0.3 to 1 tsf. (σ'_{3us} is the effective minor principal stress at the steady/critical state after undrained shear.) Figure 7(b) shows the ICL (for both dry deposition and wet sedimentation) and the SSL/CSL for a sandy silt. (p'_c is the effective mean principal stress after consolidation and p'_s is the effective mean principal stress at the quasi-steady state.) It can be seen that the ICLs and the SSL/CSL are approximately parallel over a larger stress range than those for the silty sand. For these cases, as the effective confining stress increases, the value of state parameter remains nearly constant, and for a given value of state parameter (and steady/critical state parameters), the value of normalized liquefied shear strength is constant. The concept and application become uncertain for clean sands where the ICL may not be parallel to the SSL/CSL. Gonzalo Castro emphasized this point, commenting that the compression and steady/critical state lines are often not parallel for clean, incompressible sands. As a result, the normalized liquefied shear strength may not be constant throughout a thick deposit of clean sand. As indicated here, the compressibility of the sand is critical.

For practical use, it is beneficial to correlate the normalized shear strength at large strain to a normalized penetration resistance. This allows both the effects of soil grain characteristics and the

Table 1. Importance of Field Data Obtained for Liquefaction Field Case Histories

Field Data to be Obtained	Flow Slides	Lateral Spreads
Pre-Failure Geometry	Important/Critical	Critical
Post-Failure Geometry	Critical	Critical
Movements:		
Magnitude, distribution, and areal extent of displacements	Critical	Critical
Sequence/Time Rate	Important	Critical
Type/Mechanism of Movement	Important	Critical
Distress/Cracking/Bulging	Important	Critical
Stratigraphy	Critical	Critical
In-situ Properties:		
Penetration Resistance	Critical	Critical
Unit Weights	Relevant	Relevant
Gradation	Important	Important
Plasticity	Important	Important
Static Shear Strength	Relevant	Relevant
Shear Wave Velocity	Relevant	Relevant
Gradational Changes	Critical	Critical
Stress History	Critical	Critical
Identification and delineation of liquefied soil layer	Critical	Critical
Three-Dimensional Effects	Important	Important
Location of phreatic surface/saturation	Critical	Critical
General Earthquake Characteristics:		
Time Histories	Important	Critical
Magnitude	Important	Critical
Peak Acceleration	Important	Critical
Depositional History	Important	Important
Historic Seismic Performance	Important	Important
Consideration of modified inertial loading through liquefied layer	Relevant	Critical

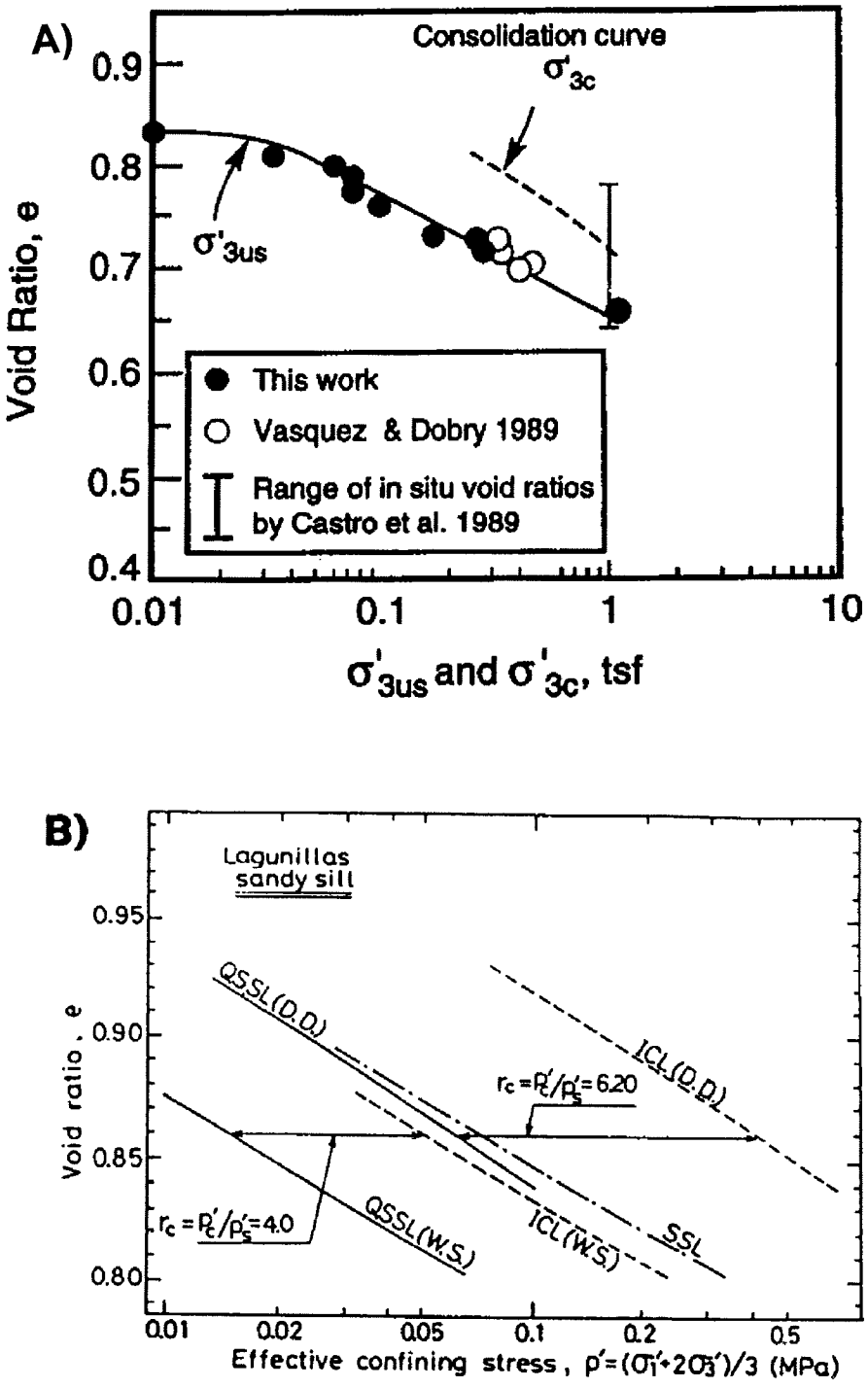

Figure 7. (a) Comparison of Consolidation Curve and Steady/Critical State Line for Remolded Layered Specimens of Silty Sand, Batch 7, Lower San Fernando Dam (after Dobry 1995). (b) Comparison of Consolidation Curve (ICL) and Steady/ Critical State Line (SSL) for Lagunillas Sandy Silt (after Ishihara 1993)

stress-dependent nature of the shear strength to be incorporated in stability analyses. Existing correlations utilize $(N_1)_{60}$ and $(q_c - \sigma_v)/\sigma'_v$, or Q, to estimate normalized liquefied shear strength. The value of $(N_1)_{60}$ is SPT blowcount (N) normalized to 60% hammer energy and corrected to an overburden stress of approximately 1 tsf. The value of q_c is the CPT tip resistance, σ_v is the total vertical stress, and Q is equal to $(q_c - \sigma_v)/\sigma'_v$. However, $(N_1)_{60}$ and Q are not of the same dimension. Blowcount, N_{60}, is a measure of energy, E, imparted to a soil over a given volume, V. This results in N_{60} being proportional to E/V or a unit of stress. It is then normalized by $(1/\sigma'_v)^{0.5}$, the overburden correction (Liao and Whitman 1985). This results in a normalized blowcount, $(N_1)_{60}$, with units of $(\text{stress})^{0.5}$. The parameter Q, on the other hand, is $(q_c - \sigma_v)$, with units of stress, divided by σ'_v, resulting in a dimensionless parameter. Additional research is required to determine which parameter is more appropriate for estimating the liquefied shear strength (or normalized strength), and the Workshop revealed that the subject is controversial. Some of the existing correlations for estimating normalized liquefied shear strength are shown in Figures 4, 8, and 9. (K_o is the ratio between effective horizontal and effective vertical stress at a given point in the soil specimen and V_{s1} is the shear wave velocity normalized to approximately 1 tsf.)

In light of these discussions, it was suggested that future research should investigate the normalization of both clean and silty sands. It is anticipated that normalization is probably appropriate for silty sands, but for clean sands the concept is questionable, and should be applied with caution.

LABORATORY AND FIELD TESTING DISCUSSION GROUP
Topic 5. Fines Content Correction/Adjustment for Field Tests

The group first discussed the development of a fines content correction/adjustment for use in a liquefaction flow analysis based on CPT or SPT results. The fines content correction/adjustment originally stems from the empirical database used to develop cyclic resistance ratio (denoted cyclic or seismic shear stress ratio in Figures 10 and 11) relationships. The correction/adjustment is needed because both penetration resistance and liquefaction resistance are influenced by fines content, soil compressibility, gradation, drainage, permeability, grain characteristics, age, overconsolidation, cementation, etc. Increased fines content is anticipated to lead to a more 'undrained' condition during penetration, resulting in a lower penetration resistance. As noted above, fines content is not the only variable that influences penetration resistance, but is an easily measured and quantifiable parameter to gage the effect of soil grain characteristics on penetration resistance. Therefore, relationships that separate liquefaction from non-liquefaction case histories use fines content (FC) and/or median grain size (D_{50}) to separate soil types (see Figure 10 and 11). (M is the earthquake magnitude and q_{c1} is the CPT tip resistance normalized to an effective vertical stress of approximately 1 tsf.) From these relationships, a general trend of increasing fines content correction/adjustment with increasing fines content can be ascertained.

The main question addressed by the discussion group was: Can the fines content correction/adjustment developed from field case histories of level ground liquefaction and non-liquefaction be used to estimate the shear strength from case histories of liquefaction flow failures or should a separate correction/adjustment be used? The group concluded that a universal correction/adjustment was uncertain, because fines content is not the only parameter that affects penetration resistance and the liquefied shear strength. It was also concluded that available

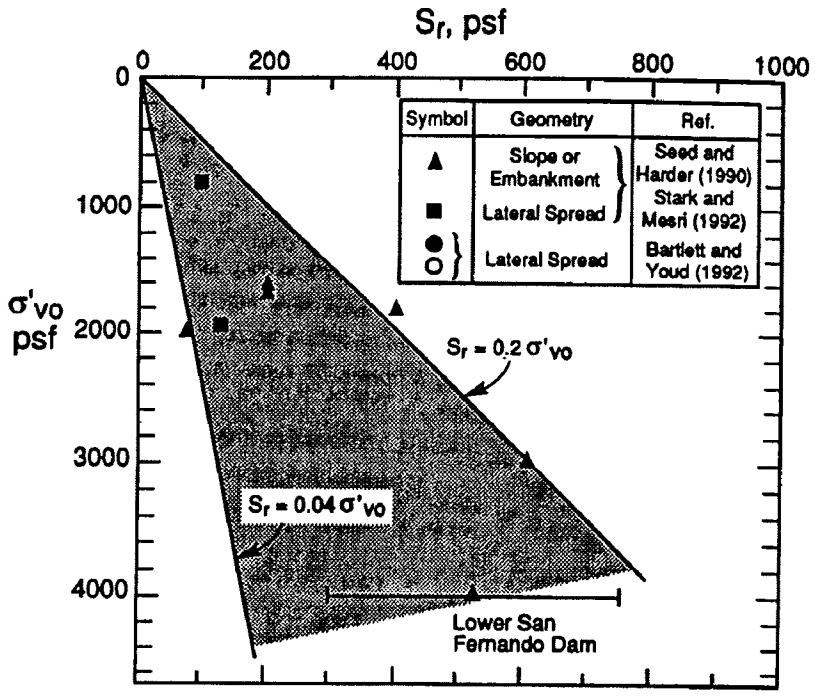

Figure 8. Relationship between Apparent or Mobilized Residual Shear Strength, S_r, and Vertical Effective Stress, σ'_{vo}, for Low Plasticity, Saturated Nongravelly Silt-Sand Deposits with Fines Contents Greater than 10% (after Baziar and Dobry 1995).

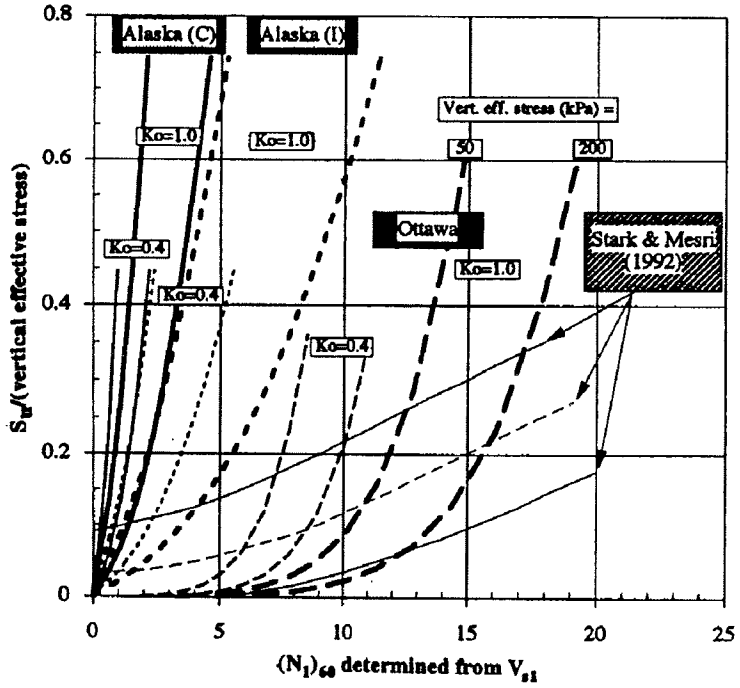

Figure 9. Relationship between Undrained Shear Strength Ratio, s_u/σ'_{vo}, in Triaxial Compression for Ottawa Sand and Alaska Sand Compared with Relationship Developed by Stark and Mesri (1992) (after Fear and Robertson 1995)

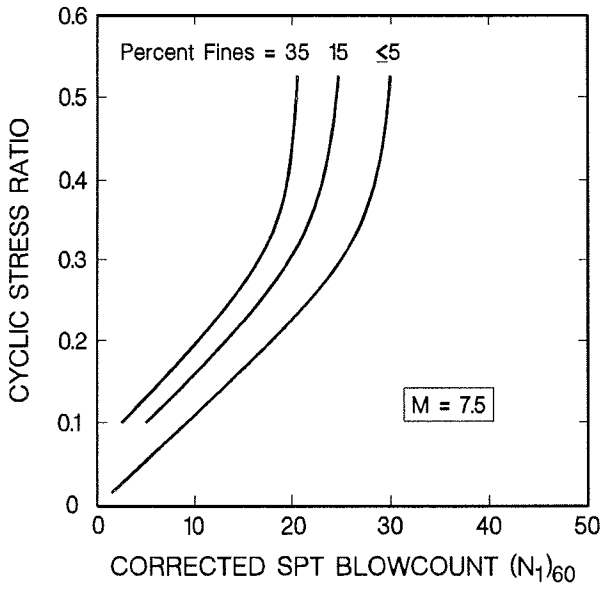

Figure 10. Relationships between Cyclic Stress Ratio Triggering Liquefaction and $(N_1)_{60}$ Values for Sandy Soils and M=7.5 Earthquakes (after Seed et al. 1985)

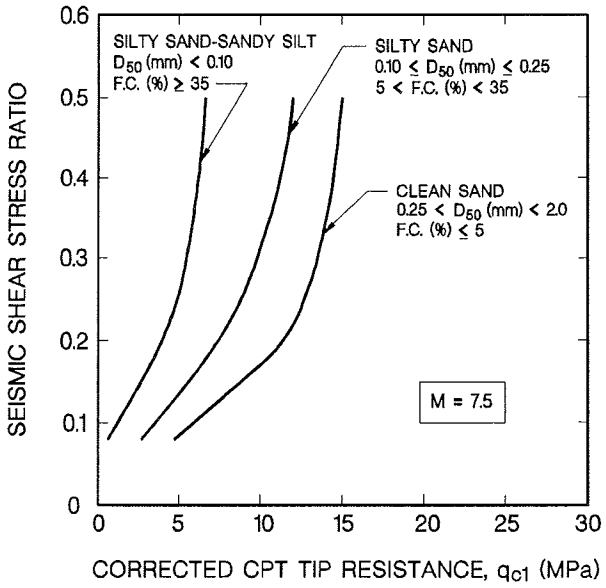

Figure 11. Relationships between Seismic Shear Stress Ratio Triggering Liquefaction and q_{c1} Values for Sandy Soils and M=7.5 Earthquakes (after Stark and Olson 1995)

case histories are inadequate to clarify the issue and additional research should be conducted on this topic.

The CPT shows promise as a means of estimating the normalized liquefied shear strength without relying upon a fines content (or any other) correction/adjustment. Ongoing research is attempting to link normalized liquefied shear strength to a soil behavior index (Robertson, Workshop Presentation 1997). The soil behavior index (Robertson and Fear 1996) is a function of both normalized CPT tip resistance and normalized CPT friction ratio. At this time, it is uncertain as to whether normalized friction ratio or normalized sleeve friction is the more appropriate parameter, but the logic is to remove fines content correction/adjustment from the procedure. In this fashion, the CPT becomes a stand-alone tool, and the SPT can be used as an independent verification of the CPT results.

In summary, the fines content correction/adjustment for the SPT (Seed 1987) should be applied with caution in estimating the liquefied shear strength because parameters other than fines content can affect penetration resistance and/or the liquefied shear strength. Application of a correction/adjustment can lead to invalid and potentially unconservative results. At this time, there are insufficient field or laboratory data to corroborate the correction/adjustment, and additional research is warranted.

CASE HISTORY DISCUSSION GROUP
Topic 6. Re-Evaluation of Liquefaction Field Case Histories

The group agreed that re-evaluation of existing field case histories was appropriate given the current state of knowledge and the availability of new information for some of the cases. However, re-evaluation should consider some or all of the following items.

If pertinent information is available, the re-evaluation should consider momentum effects on the shear strength developed along the failure surface. It is anticipated that using the pre-failure geometry to back-calculate the liquefied shear strength generally results in an unconservative estimate, and using the post-failure geometry generally results in a conservative estimate. During a liquefaction flow failure, the driving stresses initially are larger than the liquefied shear strength, leading to acceleration of the soil mass. The sliding mass therefore continues to move and deform after the geometry is such that the driving stresses are equal to the resisting strengths. Gonzalo Castro suggested that the average geometry (between pre-failure and post-failure) might be appropriate to re-evaluate the liquefied shear strength if information to evaluate momentum effects is not available.

The effect (if any) of fines content (or other parameters) on penetration resistance and drainage is also of importance. It is anticipated that soils with low fines contents could experience drainage and porewater pressure redistribution prior to and/or during flow. The fact that the liquefied shear strength (or normalized liquefied strength) is correlated to penetration resistance requires that investigators consider these effects. If a fines content correction/adjustment is too large, the estimated liquefied shear strength would be unconservative.

The re-evaluation must analyze the proper failure mechanism and soil behavior. For example, flow failures and lateral spreads should not be analyzed using the same technique. These failures result from different mechanisms, and the shear strengths mobilized during each failure may not be the same. As a result, the case histories for re-evaluation should be divided into the following two

categories: flow failures (e.g., Lower San Fernando Dam) and limited deformations. Limited deformations can be further subdivided into lateral spreads (where driving stresses are relatively low, e.g., Juvenile Hall), and other cases (where driving stresses are significant, e.g., Upper San Fernando Dam).

CONSENSUS TOPIC C

ALL PARTICIPANTS
Topic 7. Future Research Needs on the Shear Strength of Liquefied Soils

A Plenary Session was convened near the end of the Workshop to identify research needs on the shear strength of liquefied soils. The research needs are separated into the areas addressed by the three discussion groups. The research needs are not presented in a prioritized manner.

Theoretical/Conceptual Issues

- Appropriateness and/or conditions for normalization of the liquefied shear strength.
- Understanding of the mechanisms and behavior observed during lateral spreads.
- Particle-scale investigations to understand fundamental behavior of particles during shear, from quasi-static to flow-type behavior. This should be accomplished using theoretical, numerical micro-mechanical simulation, and experimental investigation.
- Measurement of shear strength at high shear strain levels. Evaluation of possible effects of fabric, mode of shear, etc., that are seen at low, intermediate, and high strain levels.
- Effect of the state parameter on liquefaction behavior.
- Back-analysis of measurements from SBPMT and CPT.
- Interdisciplinary cooperation with chemists, physicists, etc. to utilize new experimental and imaging techniques to evaluate void ratio and soil fabric.
- Measurement and quantification of soil fabric.
- Improved understanding and quantification of spatial variability and its effects on liquefaction behavior. This research should be conducted at scales ranging from particle scale to prototype scale in the laboratory and field. Investigation of the extent to which spatial variability influences overall response.

Laboratory and Field Testing

Laboratory Testing

- Increased experience with sampling to obtain undisturbed samples of cohesionless soil (type of sampling, transportation/handling/trimming, documentation).
- Use of in-situ freezing versus more conventional sampling techniques.
- Need for standard test procedure to obtain large strains, e.g., modification or development of torsional ring shear test.
- Clarification of stress path effects.
- Modeling of liquefaction phenomena using centrifuge testing.

Field Testing

- Influence of grain characteristics on field test results, and development of correction/ adjustment factors, if appropriate.
- Effects of soil mixing and drainage during post-peak behavior.
- Determination of void ratio/state parameter from field tests.
- Development of new and enhancement of existing field test equipment to characterize potentially liquefiable soil.
- Determination of coefficient of vertical consolidation, c_v, and coefficient of hydraulic conductivity, k, from field testing for use in modeling and post-earthquake considerations.
- Identification, characterization, and potential effects of thin layers.
- Behavior of gravelly soils.

Case Histories

- Re-evaluation of existing liquefaction flow failure case histories, including seeking a consensus on input parameters, observed behavior, momentum effects, and results.
- Understanding the effect of fines content (possibly redefining void ratio to reflect the presence of fines) on liquefied shear strength from laboratory testing and field case histories.
- Re-evaluation of existing lateral spread case histories, with a focus on understanding physical mechanism(s) and the resulting shear strength.
- Augmentation of case histories of flow slides using physical models and full-size field tests.
- Instrumentation of existing sites that are likely to experience some static or seismic liquefaction, e.g., earth dams in seismic zones or coastal facilities.
- Effect of mixing and drainage on liquefied shear strength.
- Organization of investigation teams to quickly examine sites after major occurrences of liquefaction.
- Investigation of sites that did not fail during strong earthquake shaking.
- Understanding of porewater pressure distribution during and after earthquake shaking.

SUMMARY AND RECOMMENDATIONS

A National Science Foundation sponsored Workshop on the shear strength of liquefied soil was held at the University of Illinois at Urbana-Champaign on April 18-19, 1997. The Workshop was organized to foster discussion in three main areas: theoretical and conceptual issues, laboratory and field measurement of the liquefied shear strength, and liquefied shear strength estimation from field case histories. An important function of the Workshop was to identify areas of future research. Some of these areas are presented below, along with some recommendations and conclusions.

Some of the theoretical/conceptual topics for future research are: (1) determining the appropriateness of normalization of the liquefied shear strength with respect to effective stress; (2) understanding the physical mechanisms that control lateral spreading; and (3) investigating the effect of the state parameter on large strain behavior. In regard to field and laboratory testing, some of the future research topics include: (1) improving sampling and laboratory testing techniques to evaluate the shear strength of liquefied soil; (2) investigating the effect of grain characteristics on field test results; and (3) determining the applicability of centrifuge testing to estimate the shear strength of liquefied soil. Some of the topics for future research on field case histories include: (1) re-evaluating existing field case histories, including obtaining consensus on input parameters and back-calculated strengths; (2) evaluating the effect of fines content, drainage, and mixing during flow or lateral spreading; and (3) understanding the mechanism(s) that control lateral spreading. Lastly, augmentation of flow slide case histories using physical models, full-size field tests, and/or instrumentation of existing sites that are likely to experience some static or seismic liquefaction should be undertaken.

The terms 'Apparent' or 'Mobilized Residual Strength' and 'Steady/Critical State Strength' can be used to describe field case histories and laboratory test results, respectively. However, the terms shear strength of liquefied soil, liquefied shear strength, and shear strength at large strain also are appropriate. The CPT represents an economical and reliable means for field testing to estimate the shear strength of liquefied soil. Normalization of the liquefied shear strength appears appropriate for most silty soils, but may not be appropriate for some clean sands. Given the current state of knowledge, it is recommended that existing field case histories of liquefaction flow failures and lateral spreads be re-evaluated. However, the shear strength back-calculated from case histories of these two phenomena should be considered and evaluated separately.

REFERENCES

Arumoli, K., Muraleetharan, K.K., Hossain, M.M., and Fruth, L.S. (1992). "VELACS-laboratory testing program – soil data report." The Earth Technology Corporation, Project No. 90-0562.

Babbitt, D.H., Bennett, W.J., and Hart, R.D. (1983). "California's seismic reevaluation of embankment dams." *Proc., ASCE Symp. on Seismic Design of Embankments and Caverns*, Philadelphia, PA, May 16-20, 96-112.

Bartlett, S.F. and Youd, T.L. (1992). "Empirical analysis of horizontal ground displacement generated by liquefaction induced lateral spreads." *Technical Rpt. NCEER 92-0021*, National Center for Earthquake Engineering Research, SUNY-Buffalo, Buffalo, NY.

Baziar, M.H. and Dobry, R. (1995). "Residual strength and large-deformation potential of loose silty sands." *J. of Geotech. Eng.*, ASCE, 121(12), 896-906.

Been, K., Crooks, J.H., Backer, D.E., and Jeffries, M.G. (1986). "The cone penetration test in sands: part I, state parameter interpretation." *Geotechnique*, 36(2), 239-249.

Casagrande, A. (1936). "The shearing characteristics of soils and its relation to the stability of earth dams." *J. of Boston Soc. of Civil Engineers*, January.

Castro, G. (1969). "Liquefaction of sands." Ph.D. thesis reprinted as Harvard Soil Mechanics Series No. 81, Harvard University, Cambridge MA, 112 pp.

Castro, G. (1987). "On the behavior of soils during earthquakes -- liquefaction." *Proc., Soil Dynamics and Liquefaction*, A.S. Cakmak, Editor, Elsevier, The Netherlands, 169-204.

Castro, G., Keller, T.O., and Boynton, S.S. (1989). "Re-evaluation of the Lower San Fernando Dam: an investigation of the February 9, 1971 slide." *Rept. 1, Contract Rept. D-89-2*, Vols. 1 & 2, U.S. Army Corps of Engineers, Waterways Experiment Station, Vicksburg, Mississippi.

Charlie, W.A., Siller, T.J., Scott, C.E., Butler, W., and Doehring, D.O. (1995). "Estimating liquefaction potential of sands using the CSU piezovane." *Geotechnique*, 45(1), 55-67.

Dennis, N.D. (1988). "Influence of specimen preparation techniques and testing procedure on undrained steady state shear strength." *Proc., Advanced Triaxial Testing of Soils and Rock*, ASTM STP 977, 642-654.

Dobry, R. (1995). "State-of-the-Art Paper: Liquefaction and deformation of soils and foundations under seismic conditions." *Proc., Third International Conference on Recent Advances in Geotechnical Earthquake Engineering and Soil Dynamics*, St. Louis, Missouri, USA, Vol. 3, 1465-1490.

Fear, C.E. and Robertson, P.K. (1995). "Estimating the undrained strength of sand: a theoretical framework." *Canadian Geotechnical Journal*, 32, 859-870.

Fiegel, G.F. and Kutter, B.L. (1994). "Liquefaction induced lateral spreading of mildly sloping ground." *J. of Geotech. Eng.*, ASCE, 120(12), 2236-2243.

Finn, W.D.L. (1981). "State-of-the-Art Paper: Liquefaction potential: developments since 1976." *Proc., First Intl. Conf. on Recent Advances in Geotechnical Earthquake Engineering and Soil Dynamics*, St. Louis, Missouri, USA, Vol. 2, 655-681.

Finn, W.D.L., Yogendrakumar, M., Yoshida, N., and Yoshida, H. (1986). "TARA-3: A computer program to compute the response of 2-D embankments and soil-structure interaction systems to seismic loadings." Department of Civil Engineering, University of British Columbia, Vancouver, Canada.

Finn, W.D. Liam, Ledbetter, R.H., Marcuson, W.F. III. (1994). "Seismic deformations in embankments and slopes." *Proc., Symp. on Developments in Geotechnical Engineering - From Harvard to New Delhi 1936-1994*, Bangkok, Thailand, A.A. Balkema, Rotterdam.

Idriss, I.M., Lysmer, J., Hwang, R., and Seed, H.B. (1973). "QUAD-4: a computer program for evaluating the seismic response of soil structures by variable damping finite element procedures." Report No. EERC-73-16, Earthquake Engineering Research Center, University of California, Berkeley, June, 1973.

Ishihara, K. (1985). "Stability of natural deposits during earthquakes." *Proc., 11th Intl. Conf. on Soil Mechanics and Foundation Engineering*, San Francisco, California, Vol. 1, 321-376.

Ishihara, K. (1993). "Liquefaction and flow failures during earthquakes." *Geotechnique*, 43(3), 351-415.

Jefferies, M.G., Been, K., and Hachey, J.E. (1990). "Influence of scale on the constitutive behavior of sand." *Proc. Canadian Geotechnical Engineering Conference*, Laval University, Quebec, Canada, Vol. 1, 263-273.

Konrad, J.-M. (1990a). "Minimum undrained strength of two sands." *J. of Geot. Eng.*, ASCE, 116(6), 932-947.

Konrad, J.-M. (1990b). "Minimum undrained strength versus steady-state strength of sands." *J. of Geot. Eng.*, ASCE, 116(6), 948-963.

Kramer, S.L. (1989). "Uncertainty in steady-state liquefaction evaluation procedures." *J. of Geot. Eng.*, ASCE, 115(10), 1402-1419.

Lee, K.L., Seed, H.B., Idriss, I.M. and Makdisi, F.I. (1975). "Properties of soil in the San Fernando hydraulic fill dams." *J. of Soil Mechanics and Foundations*, ASCE, 101(8), 801-821.

Liao, S.C. and Whitman, R.V. (1985). "Overburden correction factors for SPT in sand." *J. of Geotech. Eng.*, ASCE, 112(3), 373-377.

Marcuson, W.M.,III, Hynes, M.E., and Franklin, A.G. (1983). "Seismic design, analysis, and remedial measures to improve stability of existing earth dams -- Corps of Engineers approach." *Proc., ASCE Symp. on Seismic Design of Embankments and Caverns*, Philadelphia, PA, May 16-20, 65-78.

Marcuson, W.F. III, Hynes, M.E. and Franklin, A.G. (1992). "Seismic stability and permanent deformation analyses: the last 25 years," *Proc., Stability and Performance of Slopes and Embankments II*, Geotechnical Special Publication No. 31, ASCE, Berkeley, CA, University of California, Vol 1, 552-592.

National Research Council (1985). "Liquefaction of soils during earthquakes." Committee on Earthquake Engineering, Report No. CETS-EE-001.

Olson, S.M. and Stark, T.D. (1998). "Post-liquefaction shear strength of sands from CPT." *Geotechnique*, accepted for publication.

Poulos, S.J. (1981). "The steady-state of deformation." *J. of Geotech. Eng.*, ASCE, 107(5), 513-562.

Poulos, S.J., Castro, G. and France, W. (1985). "Liquefaction evaluation procedure." *J. of Geotech. Eng.*, ASCE, 111(6), 772-792.

Prévost, J.H. (1981). "DYNAFLOW: a nonlinear transient finite element analysis program." Princeton University, Department of Civil Engineering, Princeton, NJ.

Robertson, P.K. (1990). "Evaluation of residual shear strength of sands during liquefaction from penetration tests." *Proc. Canadian Geotechnical Engineering Conference*, Laval University, Quebec, Canada, Vol. 1, 257-262.

Roth, W.H. (1985). "Evaluation of earthquake induced deformations of Pleasant Valley Dam." Report for the City of Los Angeles, Dames & Moore, Los Angeles.

Seed, H. B. (1968). "Landslides during earthquakes due to soil liquefaction." *J. of the Soil Mechanics and Foundation Division*, ASCE, 94(SM 5), 1055-1122.

Seed, H.B. (1979). "19th Rankine Lecture: considerations in the earthquake resistant design of earth and rockfill dams." *Geotechnique*, 29(3), 215-263.

Seed, H.B. (1987). "Design problems in soil liquefaction." *J. of Geotech. Eng.*, ASCE, 113(8), 827-845.

Seed, H.B., Lee, K.L., and Idriss, I.M. (1969). "Analysis of Sheffield Dam failure." *J. of Soil Mechanics and Foundations*, ASCE, 95(6), 1453-1490.

Seed, H.B., Lee, K.L., Idriss, I.M. and Makdisi, F.I. (1973). "Analysis of slides in the San Fernando Dams during the earthquake of February 9, 1971." Report No. EERC-73-2, Earthquake Engineering Research Center, University of California, Berkeley, June, 1973.

Seed, H.B., Lee, K.L., Idriss, I.M. and Makdisi, F.I. (1975a). "The slides in the San Fernando Dams during the earthquake of February 9, 1971." *J. of Soil Mechanics and Foundations*, ASCE, 101(7), 651-688.

Seed, H.B., Lee, K.L., Idriss, I.M. and Makdisi, F.I. (1975b). "Dynamic analyses of the slide in the Lower San Fernando Dam during the earthquake of February 9, 1971." *J. of Soil Mechanics and Foundations*, ASCE, 101(9), 889-912.

Seed, H.B., Tokimatsu, K., Harder, L.F., and Chung, R. (1985). "Influence of SPT procedures in soil liquefaction resistance evaluations." *J. of Geotech. Eng.*, ASCE, 111(12), 861-878.

Seed, R.B. and Harder, L.F. (1990). "SPT-based analysis of cyclic pore pressure generation and undrained residual strength." *Proc., H.B. Seed Memorial Symp.*, Bi-Tech Publishing Ltd., Vol. 2, 351-376.

Skempton, A.W. (1964). "Long-term stability of clay slopes." *Geotechnique*, 14(2), 77-101.

Smart, J.D. and Von Thun, J.L. (1983). "Seismic design and analysis of embankment dams recent Bureau of Reclamation experience." *Proc., ASCE Symp. on Seismic Design of Embankments and Caverns*, Philadelphia, PA, May 16-20, 79-95.

Stark, T.D. and Mesri, G. (1992). "Undrained shear strength of liquefied sands for stability analysis." *J. of Geotech. Eng.*, ASCE, 118(11), 1727-1747.

Stark, T.D. and Olson, S.M. (1995). "Liquefaction resistance using CPT and field case histories." *J. of Geotech. Eng.*, ASCE, 121(12), 856-869.

Vaid, Y.P. and Chern, J.C. (1985). "Cyclic and monotonic undrained response of saturated sands." *Proc., Advances in the Art of Testing Soils under Cyclic Conditions*, ASCE Annual Convention, Detroit, Mich., 120-147.

Vaid, Y.P., Chung, E.K.F. and Kuerbis, R.H. (1990). "Stress path and steady state." *Canadian Geotechnical Journal*, 27(1), 1-7.

Vaid, Y.P. and Thomas, J. (1995). "Liquefaction and postliquefaction behavior of sand." *J. of Geotech. Eng.*, ASCE, 121(2), 163-173.

Vasquez-Herrera, A. and Dobry, R. (1989). "Re-evaluation of the Lower San Fernando Dam." *Rept. 3, Contract Rept. GL-89-2*, U.S. Army Corps of Engineers, Waterways Experiment Station, Vicksburg, Mississippi.

Yoshimi, Y., Richart, F.E., Prakash, S., Balkan, D.D., and Ilyichev, V.A. (1977). "State-of-the-Art Report: soil dynamics and its application to foundation engineering." *Proc., 9th Intl. Conf. on Soil Mechanics and Foundation Engineering*, Tokyo, Vol. 2, 605-650.

Yoshimi, Y., Tokimatsu, K., and Hosaka, Y. (1989). "Evaluation of liquefaction resistance of clean sands based on high-quality undisturbed samples." *Soils and Foundations*, 29(1), 93-104.

Youd, T.L. and Idriss, I.M., eds. (1997). *Proceedings of the NCEER Workshop on Evaluation of Liquefaction Resistance of Soils*, National Center for Earthquake Engineering Research Technical Report NCEER-97-0022, 276 p.

Yu, H.S. (1994). "State parameter from self-boring pressuremeter tests in sand." *J. Geotech. Eng.*, ASCE, 120(12), 2118-2135.

APPENDICES

APPENDIX A.
Written Statements by Theoretical/Conceptual Issues Discussion Group Participants

* =Keynote Speaker
** =Recording Secretary

*Peter M. Byrne (University of British Columbia)
J. David Frost (Georgia Tech)
Marte Gutierrez (Norwegian Geotechnical Institute)
Richard M. Iverson (U.S. Geological Survey)
Michael G. Jefferies (Golder Associates, Incorporated)
Joseph P. Koester (U.S. Army Corps of Engineers)
**Steven L. Kramer (University of Washington)
Jean H. Prévost (Princeton University)

Post-Liquefaction Strength - The Role of Soil Structure

J. David Frost and Alaa K. Ashmawy,
Associate Professor and Post-Doctoral Research Fellow, respectively
School of Civil and Environmental Engineering
The Georgia Institute of Technology
Atlanta, GA 30332, USA

Introduction

Understanding of the behavior of granular soils under earthquake loading has advanced significantly since the mid 1960's as a result of contributions by many researchers around the world. These contributions have involved: (a) the development of practical procedures based on field tests or empirical relationships to permit evaluation of the potential for actual soil deposits to liquefy; (b) extensive studies of the behavior of model soil deposits under simulated conditions such as in centrifuges; (c) the development of a range of innovative laboratory testing systems to apply dynamic loading over a broad range of strains to cylindrical specimens; and (d) sophisticated numerical models to analyze the behavior of virtual soil masses using computer simulations. Obviously, the preceding list is in no way exhaustive but rather of value to illustrate the breadth of approaches which have been used by researchers to gain insight into the behavior of soils under earthquake loading. Despite the accomplishments and contributions of the many researchers that have performed these studies, there still remain some significant "gaps" in our knowledge and hence our framework of understanding. Without doubt, one such "gap" is a clear understanding of the role of soil structure. Equally importantly, not only is it critical in our understanding of the behavior of real undisturbed soil deposits, but it is central to our interpretation of the results of studies using any of the approaches listed above to investigate the behavior of granular soils under earthquake loading. Using results from recent and ongoing digital image analysis based research at Georgia Tech, this paper attempts to provide new insight into the role of soil structure in post-liquefaction strength.

Definition of Post-Liquefaction Strength

Prior to discussing a number of issues related to the role of structure in the strength of granular soils, it is first appropriate to review what is meant by the term post-liquefaction strength in the context of the various investigation approaches listed above .

Investigation Approach	Correct Definition of Post-Liquefaction Strength	Strength Actually Interpreted or Used
Field studies and empirical correlations	Strength after all earthquake induced pore pressure in soil deposit has dissipated	Tests typically performed after earthquake and thus reflect true post-liquefaction strength
Centrifuge model studies	Strength after all simulated earthquake pore pressure in model soil has dissipated	Studies tend to model behavior during event rather than provide post-liquefaction strength values
Laboratory specimen tests	Strength after all laboratory loading induced pore pressure in specimen has dissipated	Steady state or critical state strength values and not post-liquefaction strengths evaluated
Computer models	Strength after all computer simulated loading induced pore pressure in computer model soil has dissipated	Constitutive soil models calibrated with steady state or critical state strength values and not post-liquefaction strengths

Table 1 Definitions of Post-Liquefaction Strength

APPENDICES

APPENDIX A.
WRITTEN STATEMENTS BY THEORETICAL/CONCEPTUAL ISSUES DISCUSSION GROUP PARTICIPANTS

* =Keynote Speaker
** =Recording Secretary

*Peter M. Byrne (University of British Columbia)
J. David Frost (Georgia Tech)
Marte Gutierrez (Norwegian Geotechnical Institute)
Richard M. Iverson (U.S. Geological Survey)
Michael G. Jefferies (Golder Associates, Incorporated)
Joseph P. Koester (U.S. Army Corps of Engineers)
**Steven L. Kramer (University of Washington)
Jean H. Prévost (Princeton University)

POST-LIQUEFACTION STRENGTH - THE ROLE OF SOIL STRUCTURE

J. David Frost and Alaa K. Ashmawy,
Associate Professor and Post-Doctoral Research Fellow, respectively
School of Civil and Environmental Engineering
The Georgia Institute of Technology
Atlanta, GA 30332, USA

Introduction

Understanding of the behavior of granular soils under earthquake loading has advanced significantly since the mid 1960's as a result of contributions by many researchers around the world. These contributions have involved: (a) the development of practical procedures based on field tests or empirical relationships to permit evaluation of the potential for actual soil deposits to liquefy; (b) extensive studies of the behavior of model soil deposits under simulated conditions such as in centrifuges; (c) the development of a range of innovative laboratory testing systems to apply dynamic loading over a broad range of strains to cylindrical specimens; and (d) sophisticated numerical models to analyze the behavior of virtual soil masses using computer simulations. Obviously, the preceding list is in no way exhaustive but rather of value to illustrate the breadth of approaches which have been used by researchers to gain insight into the behavior of soils under earthquake loading. Despite the accomplishments and contributions of the many researchers that have performed these studies, there still remain some significant "gaps" in our knowledge and hence our framework of understanding. Without doubt, one such "gap" is a clear understanding of the role of soil structure. Equally importantly, not only is it critical in our understanding of the behavior of real undisturbed soil deposits, but it is central to our interpretation of the results of studies using any of the approaches listed above to investigate the behavior of granular soils under earthquake loading. Using results from recent and ongoing digital image analysis based research at Georgia Tech, this paper attempts to provide new insight into the role of soil structure in postliquefaction strength.

Investigation Approach	Correct Definition of Post-Liquefaction Strength	Strength Actually Interpreted or Used
Field studies and empirical correlations	Strength after all earthquake induced pore pressure in soil deposit has dissipated	Tests typically performed after earthquake and thus reflect true post-liquefaction strength
Centrifuge model studies	Strength after all simulated earthquake pore pressure in model soil has dissipated	Studies tend to model behavior during event rather than provide post-liquefaction strength values
Laboratory specimen tests	Strength after all laboratory loading induced pore pressure in specimen has dissipated	Steady state or critical state strength values and not post-liquefaction strengths evaluated
Computer models	Strength after all computer simulated loading induced pore pressure in computer model soil has dissipated	Constitutive soil models calibrated with steady state or critical state strength values and not post-liquefaction strengths

Table 1 Definitions of Post-Liquefaction Strength

Definition of Post-Liquefaction Strength

Prior to discussing a number of issues related to the role of structure in the strength of granular soils, it is first appropriate to review what is meant by the term post-liquefaction strength in the context of the various investigation approaches listed above .

Two Load Sequence Laboratory Tests

A review of the strength values interpreted or used in the various investigation approaches summarized in Table 1 shows that there are some significant deficiencies in how we have historically evaluated post-liquefaction soil strength conditions. In the case of investigations which use tests on laboratory specimens, it is not possible to determine post-liquefaction strengths from a test with a single loading sequence only, although this is commonly done. In reality, we should perform a two load sequence test where after the first undrained loading phase in which we liquefy the specimen, we reconsolidate the specimen by allowing drainage to take place, and then reload the specimen under undrained conditions. The strength determined during this second undrained load phase is the post-liquefaction strength. The results of such a two load sequence test are summarized below.

Figure 1 shows the results of a quasi-static undrained torsional shear test performed on a specimen of Ottawa 20-30 sand that was isotropically consolidated to a mean effective confining stress of 100 kPa and a void ratio of 0.682 (Dr = 24%). The maximum shear modulus was determined from a resonant column test to be 82.4 MPa. The specimen was first subjected to a cyclic shear stress of about 14 kPa. Strain softening was initiated at a shear strain of about 0.3% after the application of 9 cycles as shown in the figure at which stage the rate of pore pressure development increased. A steady state condition was reached at a shear strain of about 5% and the test was terminated at a shear strain of 13%. The shear stress was then removed from the specimen and the drainage lines were opened to allow it to reconsolidate isotropically to a mean effective confining stress of about 100 kPa. The void ratio at this stage had decreased to 0.641 (Dr = 41%) and the maximum shear modulus was determined to be 77 MPa. It is noted that for this new combination of confining stress and void ratio, a maximum shear modulus of about 90 MPa would have been expected based on extensive tests on reconstituted specimens prior to the application of large strains. This reduction in maximum shear modulus is attributed to a change in the grain structure during the initial loading and strain softening phase, thus while the specimen is denser following reconsolidation, it has a structure which is less stiff in the direction of the applied torsional vibration loading.

Why the blank space?
We were trying to allow the text to flow to allow "Quantitative Measurements of Structure" (p. 86) to stay where it's at. We can reflow if you'd like.

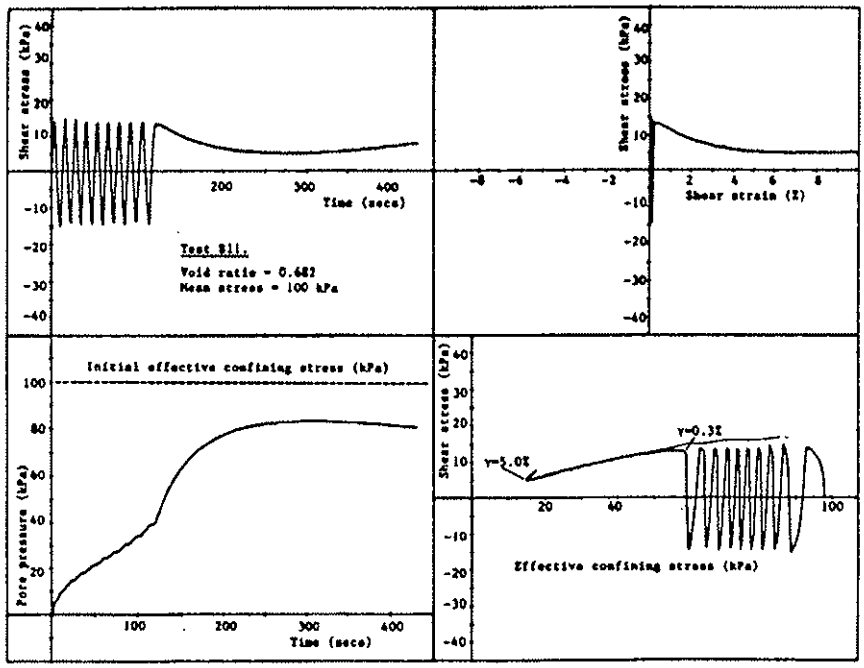

Figure 1 Cyclic Torsional Shear Test Results during Initial Load Sequence

At this stage, it was intended to subject the specimen to a second load sequence of cyclic shear stress of about 14 kPa as in the initial load sequence however, during the first load cycle, strain softening accompanied by the development of large pore pressure was observed (Figure 2) with the specimen reaching steady state at a shear strain of about 3.5%. Several aspects of the results shown in Figures 1 and 2 are of interest. The peak shear strength for the reconsolidated specimen was attained at a shear strain of about 0.7%, compared to 0.3% during initial loading. The application of large shear strains during the initial loading resulted in a particle arrangement which while denser was more conducive to pore pressure build-up during subsequent undrained loading. During the initial loading, the specimen reached a steady state of deformation at a shear strain of 5% at which stage the specimen was able to sustain a shear stress of 5.2 kPa at a mean normal effective stress of 15 kPa. Following reconsolidation, the denser specimen reached steady state at a shear strain of about 3.5% and was able to sustain a shear stress of only 2.6 kPa at a mean normal effective stress of 12 kPa. This difference is clearly of interest in that it has been suggested that the steady state condition is only a function of the initial void ratio for undrained tests. The results of the tests presented above appear to substantiate the argument that the structure may also be reflected in the behavior at steady state. Further they clearly demonstrate the difference between postliquefaction strength and steady state strength and lend credence to the argument that postliquefaction strength determination in the laboratory requires a two load sequence test, one to first liquefy the specimen and the second to determine the post-liquefaction strength.

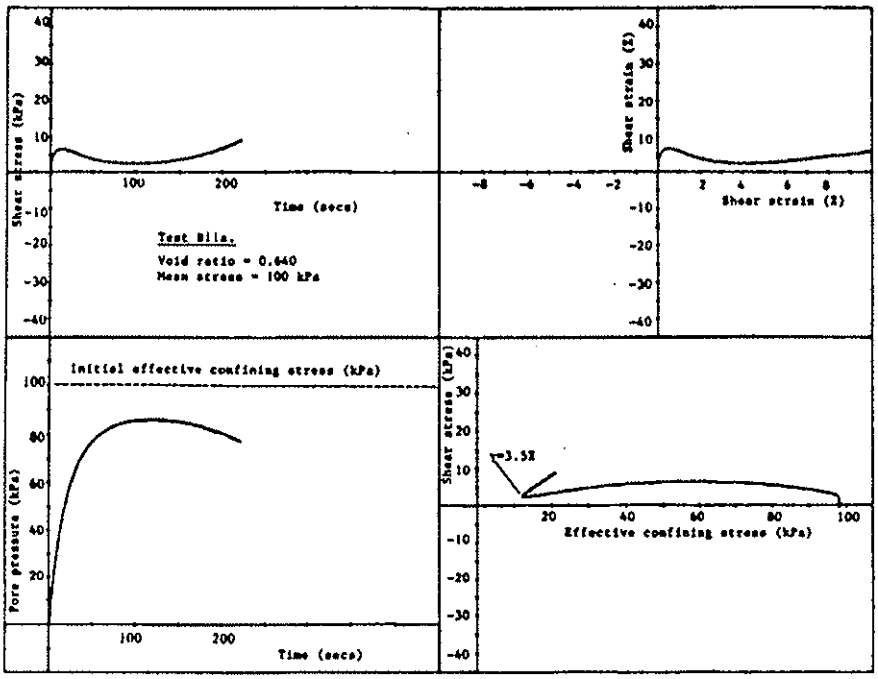

Figure 2 Cyclic Torsional Shear Test Results during Second Load Sequence

Quantitative Measurements of Structure

There is compelling indirect experimental and analytical evidence that soil structure is a critical parameter in the behavior of granular soils under earthquake loading. Ongoing research at Georgia Tech is using digital image processing and analysis to provide quantitative measures of the structure of granular soils. One parameter which is currently being used is Oda's local void ratio distribution. Figure 3 shows the distributions of local void ratio for measurements on two specimens of standard Ottawa sand with the same global void ratios but reconstituted using different methods of preparation (moist tamping and air pluviation). While the distributions appear similar, there are quantifiable and important differences between them as shown in Figure 4. For example, the specimen prepared using air pluviation has a less skewed distribution with more of the voids having values near the mode size. Ongoing measurements are quantifying the evolving local void ratio distribution at different strain levels during monotonic and cyclic loading.

One of the important consequences of data such as shown in Figures 3 and 4 is that the manner in which global void ratio is used may not be sufficiently precise for many future applications, including those to study parameters such as post-liquefaction strength. For example, when referring to tests on saturated specimens, the terms "constant volume," "constant void ratio" and "undrained" are used interchangeably however while this is true in a global sense based on measurements of the mass and volume of the specimen, it may be appropriate to add an additional parameter to our terminology to more correctly describe the soil behavior. One approach to this is illustrated schematically in Figure 5 which shows the undrained behavior of isotropically consolidated specimens at different initial global void ratios. Using q-p'-e space, each test would in fact lie on a single plane parallel to the q-p' axes however, at any stress

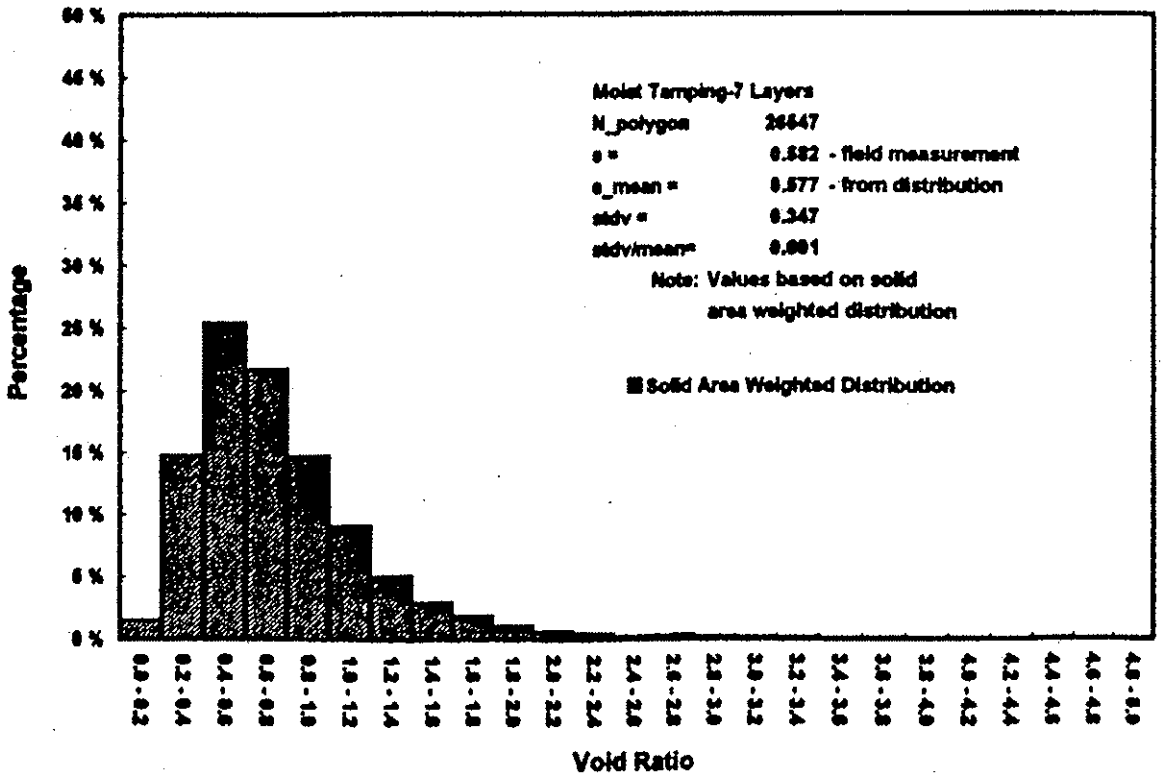

need to be clearer. Anything we can do?

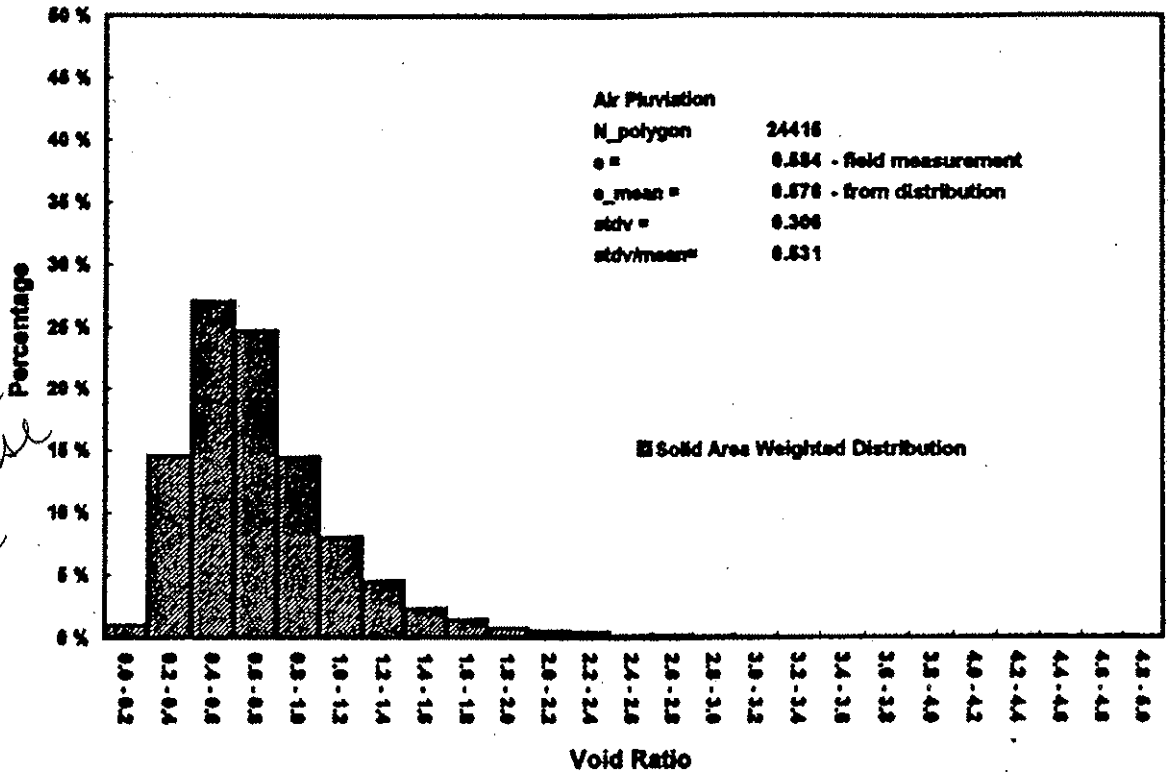

Originals are so small that we'd have to recreate these from scratch to improve them any.

Figure 3 Distributions of Local Void Ratio for Diffenernt Preparation Methods

state within a given constant e plane, the distribution of local void ratio could vary not only as a function of the initial structure but also as a function of the stress path and hence state. This is illustrated in the figure by superimposing the local void ratio distribution plots perpendicular to the lines of constant void ratio to reflect the fact that while the global void ratio and hence the mean of the local void ratio distribution is constant, the distribution of the local void ratio about the mean is changing.

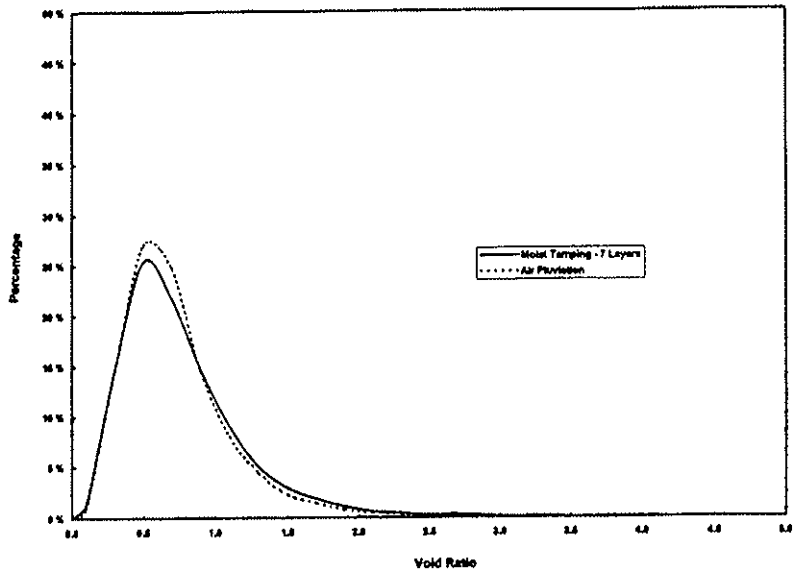

BIGGER

Figure 4 Comparison of Local Void Ratio Distributions

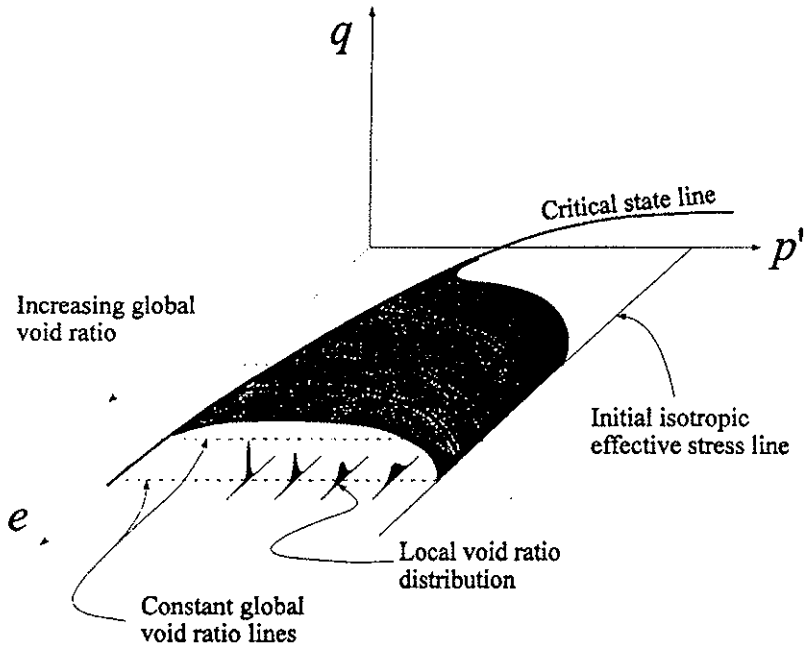

BIGGER

Figure 5 Illustration of the Distinction Between Global and Local Void Ratios

Role of Fines in Post-Liquefaction Strength

A number of researchers have investigated the role of fines in the response of granular materials under earthquake loading. It is suggested that a more fundamental approach is required to gain insight into this topic. In the same manner that quantitative image analysis can provide insight into the role of structure in the behavior of granular soils as has been suggested herein, so too is it considered that similar studies can investigate the role of "fines" as an inhibitor/instigator of structural collapse and hence pore pressure generation, as an inhibitor of pore pressure dissipation and as a factor in post-liquefaction strength. The role that "fines" play in any of these phenomena is expected to be a function of the characteristics of the fines such as their shape and relative size, as well as initial soil structure. Attention is drawn to the importance of relative size as opposed to an arbitrarily selected constant size. In the same manner that it is recognized that characteristic particle sizes such as the D_{10} tend to control the hydraulic conductivity and other characteristics of soil behavior, so too are particles that have some relative relationship to the dominant granular soil size expected to have an impact on the overall soil behavior.

Selected Bibliography

Kuo, C.Y., and Frost, J.D., (1996), "Uniformity Evaluation of Cohesionless Specimens using Digital Image Analysis", ASCE Journal of Geotechnical Engineering, Vol. 122, No. 5, pp. 390-396.

Frost, J.D., and Kuo, C.Y., (1996), "Automated Determination of the Distribution of Local Void Ratio from Digital Images", ASTM Geotechnical Testing Journal, Vol. 19, No. 2, pp. 107-117.

Oda, M., (1972), "Initial Fabrics and their Relations to Mechanical Properties of Granular Materials", Soils and Foundations, Vol. 12, No. 1, pp. 17-36.

Liquefaction and Post-liquefaction Behavior of Granular Soils

Marte Gutierrez
Norwegian Geotechnical Institute
PO Box 3930 Ullevaal Hageby
N-0806 Oslo, Norway

Brief Review of the State-of-the Art

There are currently several procedures for determining the liquefaction potential and the post-liquefaction behaviour of granular soils. The former requires the determination of the yield strength and the latter the residual strength of the liquefiable deposit. The most commonly used procedure for assessing liquefaction potential in the field is the simplified procedure developed by Seed and Idriss (1971, 1982) based on the relation between shaking intensity (represented by the normalized average cyclic shear stress) and the in situ condition (represented by the normalized SPT resistance). Seed's procedure, which was originally intended for level grounds and on a magnitude M=7.5 earthquake, has been extended to account for the effects of earthquake magnitude, pressure effects and static shear by use of correction factors (NRC, 1985). Liquefaction potential have also been estimated based on CPT resistance (e.g., Robertson and Campanella, 1985; Stark and Olson, 1995).

Several other criteria for determining the onset of liquefaction based SPT and CPT resistance and laborartory tests have been proposed as summarized by Ishihara (1993). The different criteria fall within a reasonably narrow band showing not much differences between the procedures. This is especially important as there seems to be good agreement between field-determined liquefaction potential (Seed and co-workers) and liquefaction potential determined from laboratory tests on undisturbed soil samples from deposits of known penetration resistance (e.g., Tatsuoka et al., 1980, Tokimatsu, 1988).

The situation for the determination of post-liquefaction strength is less satisfactory. The main difficulty in the determination of residual strength of liquefied materials is obtaining undisturbed samples for laboratory undrained tests. For disturbed samples, it is not easy determine field conditions and almost impossible to reconstruct samples to field conditions. For clean standard laboratory sands, much of the recent laboratory tests results suggest the existence of a unique steady state (e.g., Verdugo 1992; Ishihara, 1993). However, there are still major disagreements such as whether the steady state is uniquely a function of the initial void ratio, whether is the steady state line is straight and parallel to the consolidation line, and how it can be applied to in situ materials.

In order to account for sampling disturbance and differences in field and laboratory void ratios, Poulos et al. (1985) developed procedures using the field void ratio and the slope of the steady state line from reconstituted samples. The success of this method hinges on the assumption that the steady state lines for the undisturbed and the reconstituted samples are parallel, and on the accurate determination of the in situ void ratio. A more direct correlation of residual strength with in situ condition (as given by the SPT resistance) was made by Seed (1987) and Seed and Harder (1990) again based on case studies. Stark and Mesri (1992) made further studies on the correlation between residual strength and SPT-N taking into consideration the effects of drainage and including results of laboratory tests. Their results show that the residual shear strength is about one-half of that of the yield strength for the onset of liquefaction. Another approach that is becoming more of use in practice is to assume constant ratio of residual shear strength to initial vertical effective stress.

Proposed Workshop Contribution

Several important issues need to be resolved so that current procedures for estimating the liquefaction and post-liquefaction strength of granular soils can be used with confidence. It is proposed that some of these issues be tackled based on theoretical considerations. Based on established postulates in constitutive modelling and well-known correlations developed particularly from drained tests of granular materials, the following will be shown:

1. The steady state (SS) and the quasi-steady state (QSS) coincide for very loose materials. For very dense sand, the SS is very different from the QSS and may be difficult to determine experimentally due to shear banding (Gutierrez, Lacasse and Hoeg, 1992).

2. The SS is a function of the void ratio alone (which can be correlated with relative density Dr and hence with SPT count) and cannot be normalized with respect to the initial effective stress. This is the same assumption as in Critical State Soil mechanics.

3. The QSS is a function of the both void ratio (which again can related to Dr and SPT count) and the initial effective stress. The conditions for normalizing QSS strength with respect to the initial effective stress are discussed.

4. The SS and QSS are both affected by the stress path, i.e., biaxial compression (TC) vs. biaxial extension (TE) conditions. Theoretical ratios of the QSS and SS strengths in TC, TE and PS (plane strain) conditions are given.

5. For a given void ratio there is a unique relationship between QSS strength and the peak undrained shear strength.

Applications of the above results to in situ soils and other practical issues will also be raised during the workshop.

Other issues to be discussed in workshop concerns the effects of fines. For this, it is proposed that the effects of fines plasticity be considered as proposed by Ishihara (1993). Also, the issue of whether the global (sand + fines) void ratio (or relative density), or the clean sand (skeleton) void ratio (or D_1) should be used in characterizing fines containing granular soils.

Also to be presented during the workshop are two recent applications of the steady state theory at NGI:

1. A tailings dam in Poland where undisturbed sampling, DSS testing and cone penetration testing were done.

2. A project on loads on railway ballast in sand where the effects of sample disturbance on the test results are shown.

Proposals for future research will be given.

SHEAR BEHAVIOR OF LIQUEFIED SOILS: INTERDISCIPLINARY PERSPECTIVES

(prepared for NSF workshop on "Post-liquefaction Shear Strength of Granular Soils"
April 17-19, 1997, University of Illinois, Urbana, Illinois)
Richard M. Iverson, U.S. Geological Survey, 5400 MacArthur Blvd., Vancouver, WA 98661

Considerable knowledge gained outside the discipline of geotechnical engineering lends insight to the shear behavior of liquefied granular soils. Below I summarize some areas in which key knowledge is available and identify other areas in which key knowledge is lacking.

Greatly expanded research on post-yield shearing of granular materials commenced about 15 to 20 years ago. Landmark papers such as Savage's (1984) "The mechanics of rapid granular flows" helped propel research expansion. Outside of geotechnical laboratories, most of the research on post-yield shearing has ignored complications of geological materials and has focused instead on simpler granular materials like those used in industrial processes (with grains of uniform size, shape, and composition). Initially most of this work also disregarded the influence of intergranular fluid, but recently increased attention has been focused on mixtures in which grains interact with pore fluid as well as one another. A compendium edited by Roco (1993) provides an excellent summary of state-of-the-art work on solid-fluid mixtures by chemical and mechanical engineers as well as materials scientists. Although some of this work emphasizes mixtures in which the fluid is a compressible gas, other work emphasizes mixtures of grains with nearly incompressible, viscous fluid such as water. Recently physicists have also begun to research the behavior of granular materials (*e.g.*, Jaeger and Nagel, 1992; Jaeger *et al.*, 1996). Although physicists' perspectives are unique and worthwhile, much of their effort thus far has resulted in rediscovery and reinterpretation of phenomena already documented in the engineering literature.

A key concept that has emerged from recent work on shear behavior of dry granular materials involves the role played by grain velocity fluctuations. (The same concept applies to water-saturated granular materials, albeit in a modified manner.) Grain velocities can fluctuate about a mean value due to energy derived from the shearing motion itself or from external energy inputs, such as earthquake shaking. From a mathematical standpoint, the fluctuating motions of grains have been likened to the fluctuating motions of molecules in dense gases, and because of this analogy the mean-squared amplitude of the fluctuations has been expressed by a quantity dubbed the granular temperature, T (*cf.* Campbell, 1990):

$$T = \langle (\vec{v} - \bar{v})^2 \rangle$$

in which $\vec{v}$ is the instantaneous grain velocity, $\bar{v}$ is the time-averaged mean grain velocity, and $\langle\ \rangle$ denotes the ensemble average over all grains. Defined in this manner, T may be interpreted as twice the fluctuation kinetic energy per unit mass of grains. Recognition of the importance of T has several ramifications: (1) T can be viewed as a "state" variable that determines whether a granular mass exhibits quasistatic, rate-independent Coulomb behavior dominated by enduring frictional contacts between grains — or more complicated rate-dependent behavior in which inelastic grain collisions dominate. Behavior becomes fully rate-independent as $T \to 0$. (2) Larger values of T enhance the ability of a granular mass to flow by facilitating ease of movement of grains past one another. However, larger values of T also imply greater rates of energy dissipation, and in this respect granular materials differ

fundamentally from dense gases. Nonzero values of T can be sustained only through continual energy extraction from the mean shearing motion (typically driven by gravity) or from an external (*e.g.*, earthquake) energy source. (3) Owing to the influence of T on flow behavior and energy dissipation, we can infer that there is no "correct" rheological model for a shearing granular material in which T is nonzero. Instead, the apparent rheology depends on T, which in general varies both in space and time. (4) Dependence of apparent rheology on T significantly complicates the simplistic view of grain flows espoused by Bagnold (1954). Although Bagnold's work was extraordinarily insightful, his focus on neutrally buoyant spheres and uniform shear fields renders his equations insufficient for assessing most realistic grain-flow problems (Iverson, 1997).

Despite the complications associated with nonzero T, almost all experiments conclude that the shear-to-normal-stress ratio (τ/σ) in dry granular materials remains remarkably constant over a great range of shear rates, just as Bagnold (1954) suggested, and the ratio differs little from the quasistatic Coulomb value (τ/σ = constant). However, both τ and σ are functions of the local shear rate where T is nonzero. This is an important but subtle point that has lead to considerable confusion. Although the rate-independent Coulomb rule appears to apply to even rapidly shearing granular materials, the stresses τ and σ are themselves rate-dependent if shear is rapid. A dimensionless parameter S identified by Savage (1984) and dubbed the Savage number by Iverson and LaHusen (1993) helps discriminate conditions under which rate-dependent stresses are important:

$$S = (\dot{\gamma}^2 \delta) / g$$

Here $\dot{\gamma}$ is the shear rate, δ is the characteristic grain diameter, and g is the magnitude of gravitational acceleration. Limited data indicate that if $S > 0.1$, rate-dependent stresses dominate. For grains of 1 mm diameter, this criterion implies that shear rates must exceed about 30 s^{-1} for strong rate dependence. Such shear rates probably exceed those encountered in many geotechnical problems.

The presence of pore fluid in general and excess pore-fluid pressure in particular enhances the potential significance of rate-dependent stresses. For cases where pore fluid is present, Iverson (1997) demonstrated that the Savage number should be modified to a form similar to

$$S = \frac{\rho_s}{\rho_s - \rho_f} \frac{(\dot{\gamma}^2 \delta)}{g}$$

in which ρ_s and ρ_f are the mass densities of the solid grains and pore fluid, respectively. Thus buoyancy forces due to static pore fluid increase the value of S. Moreover, if excess pore pressures are present, the pressures can mimic the effects of increased pore-fluid density. In a state of complete liquefaction, pore pressures bear the complete load due to the weight of the solid-fluid mixture, mimicking the condition $\rho_f = \rho_s$. In this case $S \to \infty$, and stresses due to grain interactions become wholly rate-dependent, analogous to the situation investigated by Bagnold (1954). Rate-dependent stresses due to shear of the viscous pore fluid can also be important in such circumstances, depending on the value of the Bagnold number (Iverson, 1997). In summary, depending on the degree of liquefaction, a particular soil-water mixture shearing at a particular rate can exhibit predominately rate-dependent or rate-independent stresses. In this respect the pore pressure P can be regarded as a crucial "state" variable, whose role and importance is equal to that of T. However, a complete theory for the integrated effects of P and T remains lacking.

Because the degree of liquefaction appears so critical to shear behavior of soil-water mixtures, our recent experiments at the USGS debris-flow flume have focused on understanding the degree and causes of liquefaction. We have found that nearly complete liquefaction is commonplace in debris flows except in coarse-grained snouts that form at the heads of surges. Liquefaction initially occurs during shear failure of loosely packed soil mixtures (Iverson *et al.*, 1997). Liquefaction persists owing to the low hydraulic diffusivity (~ consolidation coefficient) of the flowing debris, which results from the low permeability and high compressibility of the poorly sorted, agitated granular matrix and high viscosity of the pore fluid, which contains suspended silt and clay (Major, 1996). Thus the grain-size distribution plays a crucial role in sustaining high pore pressures and the potential for rate-dependent shearing. Granular temperature plays a synergistic role by making the agitated debris orders of magnitude more compressible than most granular soils (Iverson, 1997). Some of the same phenomena might be important in liquefied soils outside the highly energetic environment of debris flows.

REFERENCES CITED

Bagnold, R.A., 1954, Experiments on a gravity-free dispersion of large solid spheres in a Newtonian fluid under shear, *Proceedings of the Royal Society of London, 225A*, 49-63.

Campbell, C.S., 1990, Rapid granular flows, *Annual Review of Fluid Mechanics, 22,* 57-92.

Iverson, R.M., 1997, The physics of debris flows, *Reviews of Geophysics*, 35, in press.

Iverson, R.M., and R.G. LaHusen, 1993, Friction in debris flows: inferences from large-scale flume experiments, *Hydraulic Engineering '93 (Proceedings of the 1993 Conference of the Hydraulics Division of the American Society of Civil Engineers), 2*, 1604-1609.

Iverson, R.M., Reid, M.E., and LaHusen, R.G., 1997, Debris-flow mobilization from landslides, *Annual Review of Earth and Planetary Sciences, 25*, 85-138.

Jaeger, H.M. and Nagel, S.R., 1992, Physics of the granular state, *Science*, 225, 1523-1531.

Jaeger, H.M., Nagel, S.R., and Behringer, R.P., 1996, The physics of granular materials, *Physics Today, 49(4)*, 32-38.

Major, J.J., 1996, Experimental studies of deposition by debris flows: process, characteristics of deposits, and effects of pore-fluid pressures, unpublished Ph.D. thesis, University of Washington, 341 p.

Roco, M.C. (Ed.), 1993, *Particulate Two-Phase Flow*, Butterworth-Heinemann, Boston, 1002 p.

Savage, S.B., 1984, The mechanics of rapid granular flows, *Advances in Applied Mechanics, 24*, 289-366.

NSF Workshop on Post-Liquefaction Strength of Granular Soils

TOPIC: Is the undrained shear strength influenced by consolidation stress and undrained stress path ? What is the effect of fines ? And, how should fines be defined ?

Contribution from Michael Jefferies, Golder Associates

Introduction

I take it as self-evident that liquefaction, in all its forms, is simply another aspect of the constitutive behaviour of soil. Despite depressingly widespread use of emotive phrases like 'collapse surface' the reality is that even during the most extreme liquefaction stress and strains remain related - we are not dealing with tensile failure of a metal. It then follows that a proper understanding of liquefaction will only follow in the context of a theoretical model that sensibly reproduces soil behaviour. Moreover, a proper model must represent the behaviour of dense, drained dilatant sand and yet still capture liquefaction without introduction of new concepts, parameters etc. That is, the model must explain (predict) the response of soil to different density, drainage and stress path; it must not treat each aspect as a separate behaviour.

In this contribution, one such proper model - NorSand - is outlined. Its fit to some test data is illustrated and then the response of the model to the topic questions is presented. NorSand is especially useful for the topic discussion because it includes the concept of a critical state locus and is intrinsically a large strain model so that issues of post liquefaction strength are readily addressed.

Because contributions are limited in length, it is assumed that readers are familiar with the basic concepts of the liquefaction literature and thus the standard terminology used.

NorSand

NorSand (Jefferies, 1993) is an isotropically hardening - isotropically softening, single yield surface plastic model derived from two axioms of critical state theory which are that: a CSL exists (the First Axiom); and, soil state moves to the CSL with shear (the Second Axiom).

The First Axiom has been discussed by many workers and a detailed experimental investigation for sand was presented by Been et al (1991). Importantly, note that a principal source of error in the past over possible non-uniqueness of the CSL in *e-p* space as a function of stress path, and continuing quite widely, arises through the definition that the critical state is the condition in which the soil deforms without volume change, otherwise expressed as zero dilatancy. While this is a necessary condition, it is not sufficient for criticality. At a critical state there must also be the condition that the rate of change of dilatancy is also zero. This error is found, for example, in many of the contributions to the literature on steady state strength by Vaid & co-workers and by Konrad.

Conventionally, the CSL is represented in *e-p* space using the semi-logarithmic form $e_c = \Gamma - \lambda \log(p_c)$ where Γ, λ are material properties. The validity of this idealization at low mean stress has been questioned (e.g. Ishihara, 1993), but objections to it are merely arguments about detail and not central to the validity of critical state models.

Standard critical state models (e.g. CamClay) assume that any yield surface intersects the CSL so directly coupling the yield surface size to void ratio. Real soils, however, display a far richer behaviour and in particular exhibit an infinity of normal consolidation loci (NCL) which are not parallel to the CSL. It is this rich behaviour that is characterised by the state parameter approach, in essence each NCL being related to a value of ψ (where $\psi = e - e_c$). Overconsolidation ratio (OCR) continues to exist in its usual sense of defining the location of a stress state within a yield locus.

NorSand involves just 3 more soil properties than the familiar CamClay model: an elastic shear modulus, G; a volumetric coupling coefficient, N; and a plastic hardening modulus, h. The range of yield surfaces encountered with NorSand are illustrated on Figure 1. The power of NorSand derives from not requiring that the yield surface intersect the CSL in *e-p* space. Instead NorSand uses a hardening law that forces the yield surface to the CSL with shear strain, exactly in conformance with the Second Axiom. The original form of NorSand was derived in the context of monotonic loading; however, the extension to cyclic loading is not difficult as was accomplished by introducing a third axiom that principal stress rotation anneals hardening (Been et al, 1993).

The ability of NorSand, calibrated using dense sand, to represent static liquefaction of a loose sample of the same sand is illustrated on Figure 2 - an excellent fit is observed, including the slight recovery of strength from the post-peak minimum.

With the basic performance of NorSand established, let us turn to the questions posed.

Responses

Q1: What is the effect of consolidation stress?

Increased consolidation stress changes decreases void ratio, with differing amounts depending upon the gradation, fines content etc. Decreased void ratio means post-liquefaction shear strength increases, all else equal. This is the principal argument against normalizing test results to a stress level of 100 kPa - if the test data is normalized in this way then the inferred strength must be de-normalized (which is rarely done), and this overall process leads to errors. However, consolidating natural deposits can reduce any overconsolidation ratio and so partially offset strength gain because of density increase. Decreased consolidation stress, at least for small decreases, leads to minimal change in strength because of the induced overconsolidation.

Q2: What is the effect of stress path?

Large... Specifically, plane strain is very different from the familiar triaxial test and situations in which means stress decreases leads to a markedly lower strength because the critical friction angle is sensibly a constant (and see below for the consequences of localization).

Q3: How do fines influence residual strength?

Variably... We have tested the post liquefaction strength (in triaxial compression) of several sands systematically varying fines contents. Whether fines improves the residual strength for any given

density depends on the stress level. In our work we have defined *fines* simply as the fraction passing the #200 sieve.

Q4: Is the post liquefaction strength proportional to the vertical effective stress?

move subscript up

Broadly, yes. Specifically, under conditions of constant ψ, NorSand predicts that s_u will be linearly proportional to p given the *e-log(p)* idealization of the CSL for any set of material properties.

Q5: What is the relevance of the pseudo steady state or minimum undrained strength?

Figure 3 shows a sample with a clear pseudo steady state. In fact tl
simulation. The interesting aspect is the softening regime post initia
stability postulate (Drucker, 1959), and as such we would expect bi
conditions no longer maintained locally. Hence the computed stren
undrained conditions should not necessarily be expected (it may ha
of the limited sample volume). Further, if we look at the yield surfa
Figure 3 and which we know because this is a NorSand simulation,
about 3.5% shear strain and we might expect instability to be associ

Something wrong with the subscript There. check. Please

The introduction of instability criteria to geomechanical constitutive
subject so definitive conclusions are, as yet, difficult. However, intri
instability limit is plotted against field scale data for post-liquefactio
get what looks like a very promising explanation of what is observed

So, where does the pseudo steady state strength fit in. Well, it is clear ... the pseudo steady state strength is lower bound to the instability condition, and is certainly a far more realistic proposition that the steady state strength. And, if we plot the computed trends for pseudo steady state on Figure 4 we see a rather good explanation of field behaviour. However, if it was universally true that the pseudo steady state strength controlled undrained strength then we would not be able to record the dilatant undrained behaviour that we do in the laboratory.

Clearly some urgent theoretical work is required to distinguish what controls and under what conditions. The point I'd like to emphasize is that sorting out this issue requires applied mechanics and is unlikely resolvable by experiment alone. There are several such models now available and as I noted earlier investigation into localization is an active research topic.

Meanwhile, I'm in favour of using the pseudo steady state as a reasonable engineering approximation while the theoretical work continues. Where I get nervous is when people confuse the pseudo steady state with the CSL, as done by Vaid & co-workers and Konrad (with the ψ_U,ψ_L idea) - that simply leads to misleading concepts, incorrect mechanics, and prevents understanding.

The idea of an instability limit (in the sense of applied mechanics, not the erroneous collapse surface idea) allowing localization and so controlling post liquefaction strength means that stress path and other parameters such as elastic modulus become important. Which nicely explains the fact that despite a lot of work nobody has found a simple correlation of post-liquefaction residual strength in the various failure case histories to penetration resistance - theoretically, there should not be one!

References

Been, Jefferies, & Hachey, 1991: The critical state of sand. Geotechnique

Been, Jefferies, Rothenberg, & Hachey 1993: Numerical Prediction for Model 2. In Proceeding of VELACS Conf, Vol 1. Balkema.

Drucker, 1959: A definition of Stable Inelastic Material. J Appl Mech.

Ishihara, 1993: 33rd Rankine Lecture. Geotechnique

Jefferies, 1993: NorSand - A simple critical state model for sand. Geotechnique.

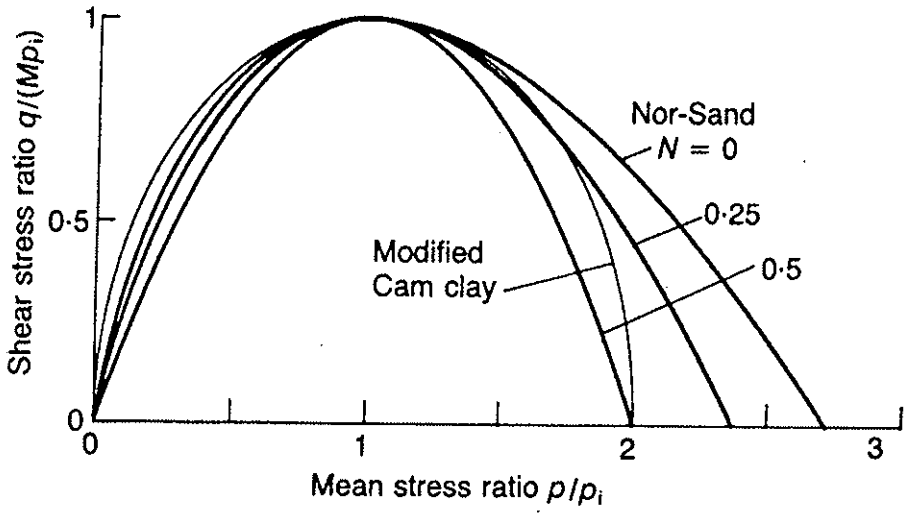

Figure 1: Illustration of NorSand yield surfaces

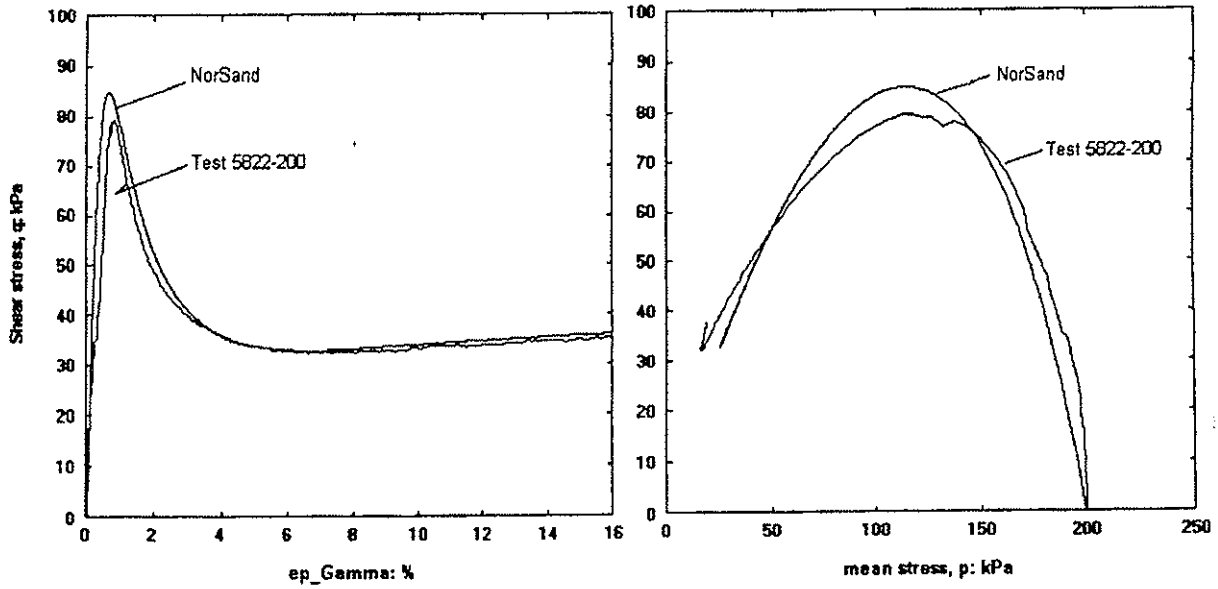

Figure 2 : Illustration of NorSand fit to static liquefaction test

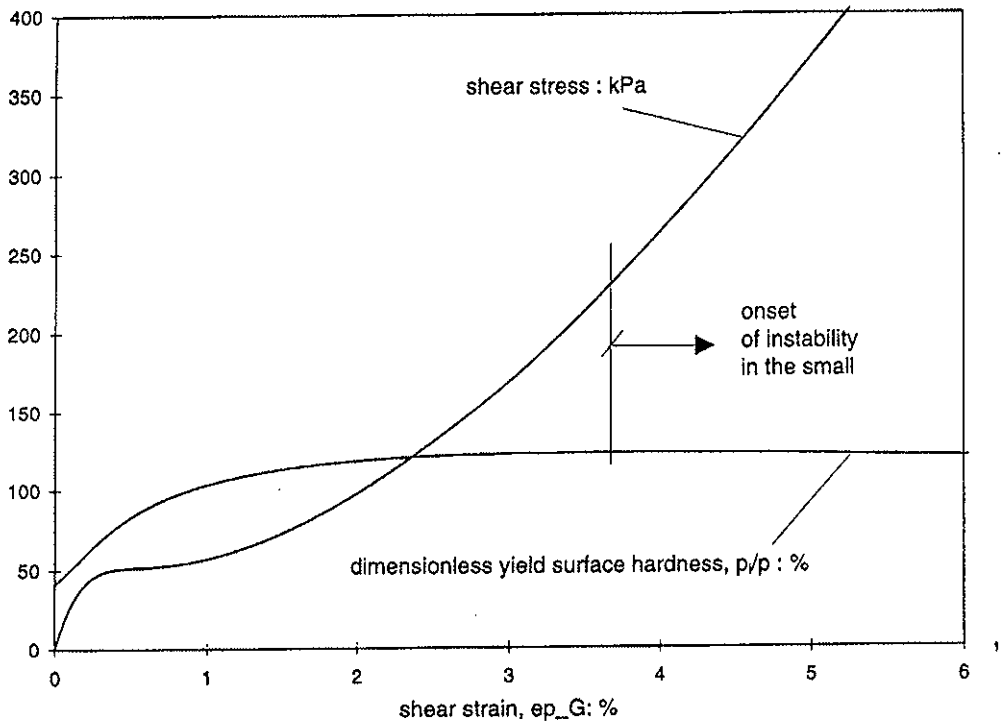

Figure 3: Comparison of NorSand hardening with undrained stress-strain behaviour

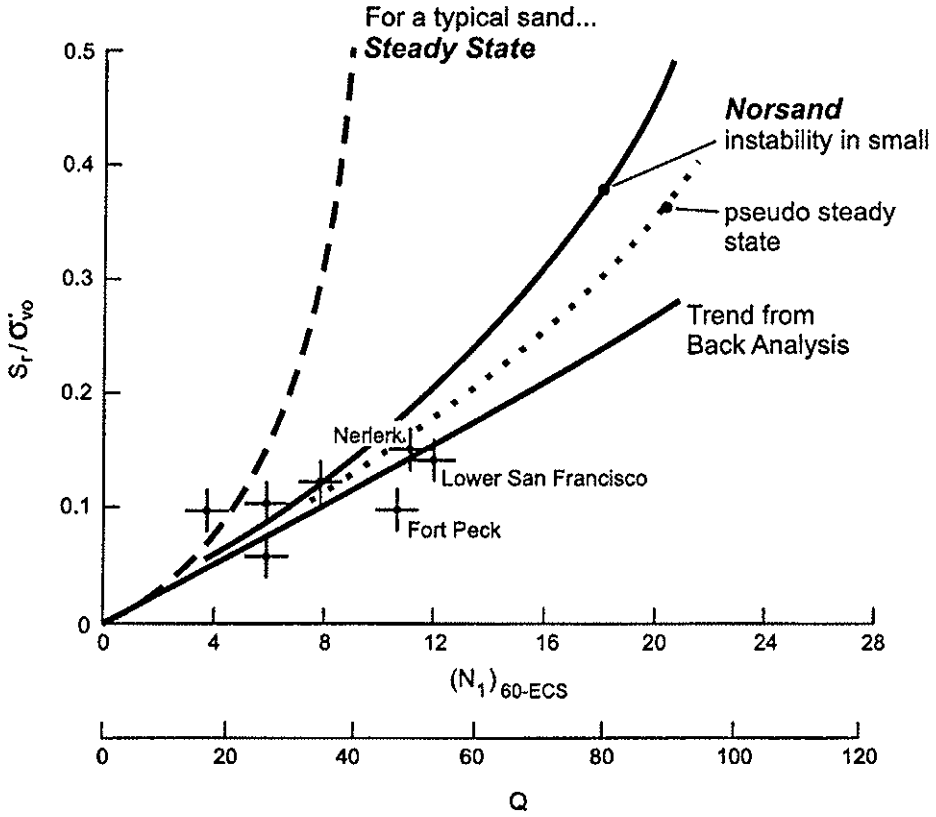

Figure 4: Comparison of field scale residual strengths with theoretical predictions

Submission by Joseph P. Koester, US Army Engineer Waterways Experiment Station, Vicksburg, Mississippi

DISCUSSION GROUP: THEORETICAL/CONCEPTUAL ISSUES

***Soil Mechanics Perspective -**

Question (1): How is the shear strength of liquefied soil influenced by consolidation stress and undrained stress path?

Answer: My office is often charged with post-earthquake stability evaluation of critical facilities, typically large embankment dams, many of which are built from or founded on variously silty or clayey sands and gravels. I therefore fervently hope there *is* a strong positive influence of consolidation stress. If it can be demonstrated that a slope is clearly safe against post-earthquake sliding when shear strength of liquefied soils along the potential failure surface (in a limit equilibrium analysis) is a plausible constant value, there is not likely a worrisome risk. The problem is, however, the term "plausible", in that so-called residual strength values sufficient to resist sliding have generally proven to be larger than determinable from the field performance-based relationship published by Seed and Harder (1990) (i.e., by means of penetration test results) without extrapolation to corrected blowcounts that are so high as to preclude the triggering of liquefaction in the first place. Baziar and Dobry (1995) extended the experience base to include lateral spreads and investigated the influence of confining stress, establishing a range in ratios of (assumedly undrained) residual strength to effective confining stress from 0.04 to 0.2 (see Figure 1). The lower bound ratio is not very helpful, as illustrated by the limit equilibrium analysis result shown in Figure 2, where most of the passive resistance is derived within the residual strength material. Non-circular slip surfaces would exacerbate the problem in that case. When the level of sophistication of analysis rises above limit equilibrium to include soil models and pore pressure generation and dissipation, stress redistribution comes into play and frictional response becomes all the more important.

In a recently completed, but not yet published, study of Sardis Dam, Mississippi, residual strength of liquefied soils (a top stratum clayey silt with characteristics of similar soils that liquefied in major earthquakes in China - I specifically avoid using the term "Chinese clay") were estimated as being 0.075 times the effective overburden stress for use in nonlinear soil model analysis. Peak shear strengths were measured in the field by various means, including vane shear and cone penetration tests, and by best estimates were determined to fall generally into the range of 0.3 times effective consolidation stress. Sensitivity was determined from the vane shear test results to be about 4, thus giving the 0.075 residual strength relation. Additionally, stability analyses were conducted to back-calculate the S_r/p' ratio required to produce a factor of safety against sliding of about 1.5, which was devised from the observation that the dam has been standing for some time, successfully. A ratio of about 0.075 was also found by this means.

With respect to undrained stress path influence, I found in a laboratory experiment series myself that residual strengths of sand mixtures containing 25-30% fines, whatever the plasticity of the fines, were very low and essentially constant to large shear strains in torsional simple shear. This was the case whether virgin specimens were loaded monotonically or specimens that had undergone liquefaction by cyclic loading were loaded, undrained, monotonically to large shear strains. Clean sands, as shown by others, dilated in my experiments (Koester, 1992). I did not vary confining stress enough to judge its effects on residual strength of liquefied mixtures.

Question (2): How do soil "fines" influence residual strength?

Answer: I am convinced, from my own experiments and results published by others, that residual strength of liquefied clean sands is higher than that of liquefied soils containing particles finer than sand. Clean sands tend to dilate when strained in undrained loading, gaining strength quickly. The presence of fines somehow prevents dilation, such that strain potential appears unlimited. I observed this in mixtures containing more than 15 percent fines by weight. I further believe that the beneficial contribution of plasticity of the fines is very slight, once the soil has liquefied. Gradation is the controlling factor, as is the case, I believe, with triggering of liquefaction, as well.

Question (3): How should "fines" be defined, e.g., minus No. 200 sieve?

Answer: I recommend continuing to define fines as minus No. 200 sieve materials. I would like to point out here that I also advocate measurement of consistency using only the fines in assessing potentially liquefiable soils, i.e., not including the material passing the US No. 40 sieve and retained on the No. 200 sieve, as is dictated for Atterberg Limits testing by ASTM. The effect of sand content on consistency measurement is too drastic for the case of low plasticity soils. In some countries, by the way, consistency limits tests are performed on materials passing through a sieve with 0.500 mm openings; the US No. 40 sieve, by the way, passes particles finer than 0.425 mm. The presence of the larger particles would reduce plasticity.

Question (4): Is the post-liquefaction shear strength proportional to the initial vertical effective stress? Under what conditions?

Answer: As I discussed for Question 1, above, I certainly hope so, under most conditions of engineering interest. I suspect, but cannot substantiate, that remediated soils have locked-in horizontal stresses that would affect proportionality with regard to vertical effective stress. Remediated soils would be a very stimulating subject to include in the workshop, if at all possible. They could still liquefy, and it would be interesting to document expert opinions on their residual strength.

Question (5): What is the applicability of the quasi-steady state or minimum undrained strength concepts?

Answer: I do not know what is meant by "quasi-steady state" in the context of post-liquefaction strength. I am reminded of the Stark and Mesri (1992) ASCE Journal of Geotechnical Engineering Division paper on the subject of shear strength of liquefied soils by this question. Stark and Mesri (1992) proposed that post-liquefaction shear strength, or undrained critical strength, s_u(critical), if expressed as a shear stress ratio with effective confining stress, is about half of the yield strength ratio mobilized in the field at liquefaction, s_u(yield, mob)/σ'_{vo}. The latter ratio is defined by the line separating liquefiable and nonliquefiable sands for an earthquake magnitude of 7.5 (15 equivalent uniform loading cycles) as published by Seed et al. (1985) and is approximately equivalent to the equivalent clean sand $(N_1)_{60}$ divided by 90 for $(N_1)_{60}$ up to 20. The authors observed that cyclic triaxial strengths in sands were essentially constant beyond 100 loading cycles, and that the cyclic stress ratio causing liquefaction in 100 cycles was about the same as s_u(critical). Additionally, Stark and Mesri (1992) determined that s_u(critical) was approximately half of the yield strength ratio mobilized in the field at liquefaction in silty sands, as well, when $(N_1)_{60}$ measured in silty sands to estimate yield strength was adjusted according to the procedures suggested by Seed, et al. (1985).

The proportionality of yield cyclic strength to post-liquefaction shear strength observed by Stark and Mesri (1992) from field performance data did not appear to hold in laboratory tests on fine-grained soil mixtures prepared to relatively loose conditions in a cyclic hollow cylinder torsional test program I performed. I offer the two accompanying tables (Table 8.5 and 8.6 from Koester, 1992) from that program for discussion.

REFERENCES CITED:

Baziar, M.H. and Dobry, R. 1995. "Residual strength and large deformation potential of loose silty sands," *Journal of the Geotechnical Engineering Division*, ASCE, 121(12), pp. 896-906.

Koester, J.P. 1992. "Cyclic strength and pore pressure generation characteristics of fine-grained soils," thesis submitted in partial fulfillment of the requirements for Doctor of Philosophy, College of Engineering, University of Colorado, Boulder, CO.

Seed, R. B. and Harder, L. F. Jr., 1990. "SPT-based analysis of cyclic pore pressure generation and undrained residual strength," *Proceedings, H. Bolton Seed Memorial Symposium*, Vol. 2, Ed. J. Michael Duncan, May, pp. 351-316.

Seed, H. B., Tokimatsu, K., Harder, L. F., and Chung R. (1985). "Influence of SPT procedures in soil liquefaction resistance evaluations," *Journal of the Geotechnical Engineering Division*, ASCE, 111(12), 861-878.

Stark, T. D. and Mesri, G. (1992). "Undrained shear strength of liquefied sands for stability analysis," *Journal of the Geotechnical Engineering Division*, ASCE, 118(11) pp. 1727-1747.

Table 8.5 Estimated post-liquefaction shear strengths from undrained hollow cylinder torsional simple shear tests on isotropically consolidated specimens

	Method of Estimation (values in psf, values averaged for multiple tests on replicate specimens)			
Soil Type	$\tau_{cyc}(100)$[1]	$(1/2)\times\tau_{cyc}(15)$[2]	PCM[3]	Monotonic TSS[4]
F11	1080	994	N/A[5]	N/A[5]
F43	346	202	101 (14)[6]	245 (158)[6]
F46	475	346	130 (43)	432 (360)
F64	389	288	634 (547)	648 (562)

[1]Average cyclic shear stress ratio causing liquefaction in 100 cycles x σ'_v
[2]Average cyclic shear stress ratio causing liquefaction in 15 cycles x σ'_v
[3]Post-cyclic monotonic simple shear strength; lower-bound value range at $\gamma = 15\%$
[4]Lower-bound range of shear strength beyond peak shear resistance in virgin monotonic torsional simple shear tests, at $\gamma = 15\%$
[5]Specimen dilative with shear
[6]Values corrected for membrane torque resistance in parentheses

The format for soil type codes is such that each shown is mixed from a fine uniform parent sand; the next two numbers N_1N_2 identify fines content and plasticity index of fines, respectively, in a larger matrix of possible mixtures where: N_1 ranges from 1 through 7, respectively representing fines contents of 0%, 5%, 12.5%, 20%, 30%, 45%, and 60%; and N_2 ranges from 1 through 8, respectively representing plasticity indexes of NP, 4%, 10%, 15%, 20%, 25%, 30%, and 40%.

Table 8.6 Comparison of peak- to residual undrained shear strengths in monotonic torsional shear tests on virgin specimens

Test No. (Type as above)	ϕ'[1]	S_u(peak)[2], psf	S_{ur}[3], psf	reduction[4],
25 (F11)	35°	(dilative)	(N/A)	(N/A)
26 (F43)	33°	2712	158	94%
27 (F46)	28.8°	2296	360	84%
28 (F64)	26.6°	2019	562	72%

[1]Effective angle of internal friction, determined from failure envelope of Figures 8.82-8.85
[2]$\sigma'_m \tan\phi'$, where $\sigma'_m = \sigma'_n$ in these isotropically consolidated tests
[3]membrane-corrected strength at 15% shear strain from Table 8.5
[4]$(S_u(peak)-S_{ur})/S_u(peak)\times 100\%$

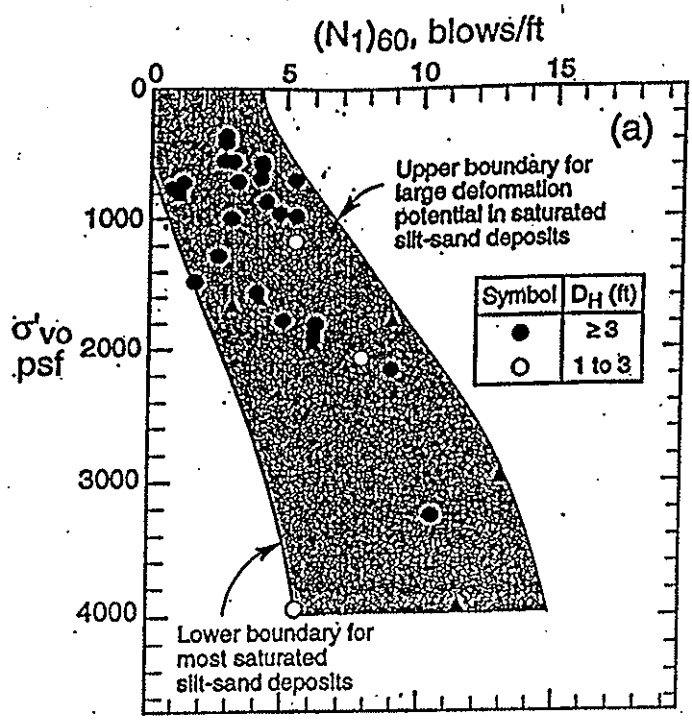

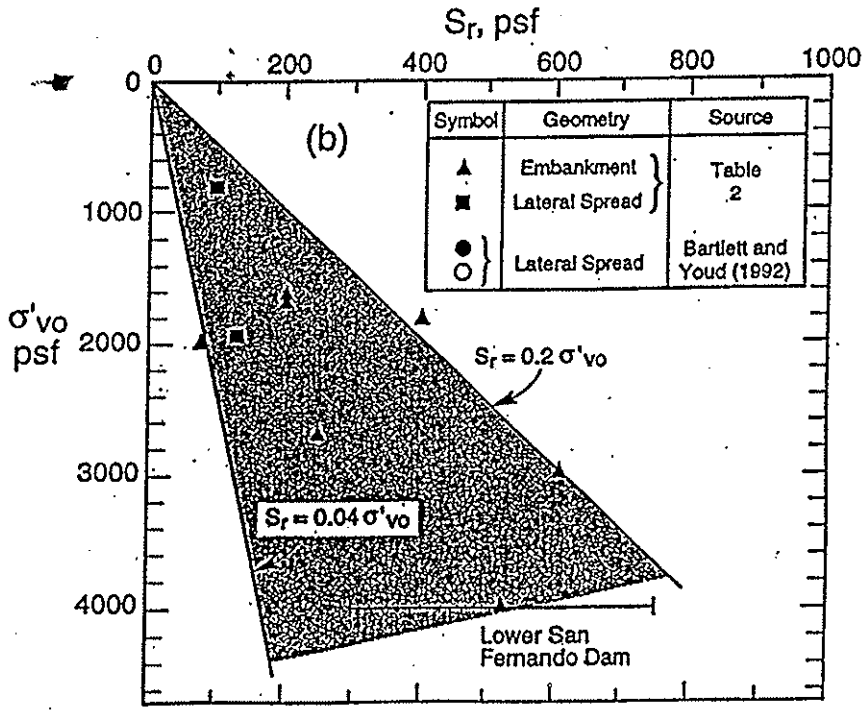

CAN WE CLEAN THIS UP ?

Figure 1 Charts relating normalized SPT resistance ($N_{1,60}$) and residual shear strength (Sr) to vertical overburden pressure (σ'_{vo}) for saturated nongravelly silt-sand deposits that have experienced large deformation (Baziar and Dobry, 1995)

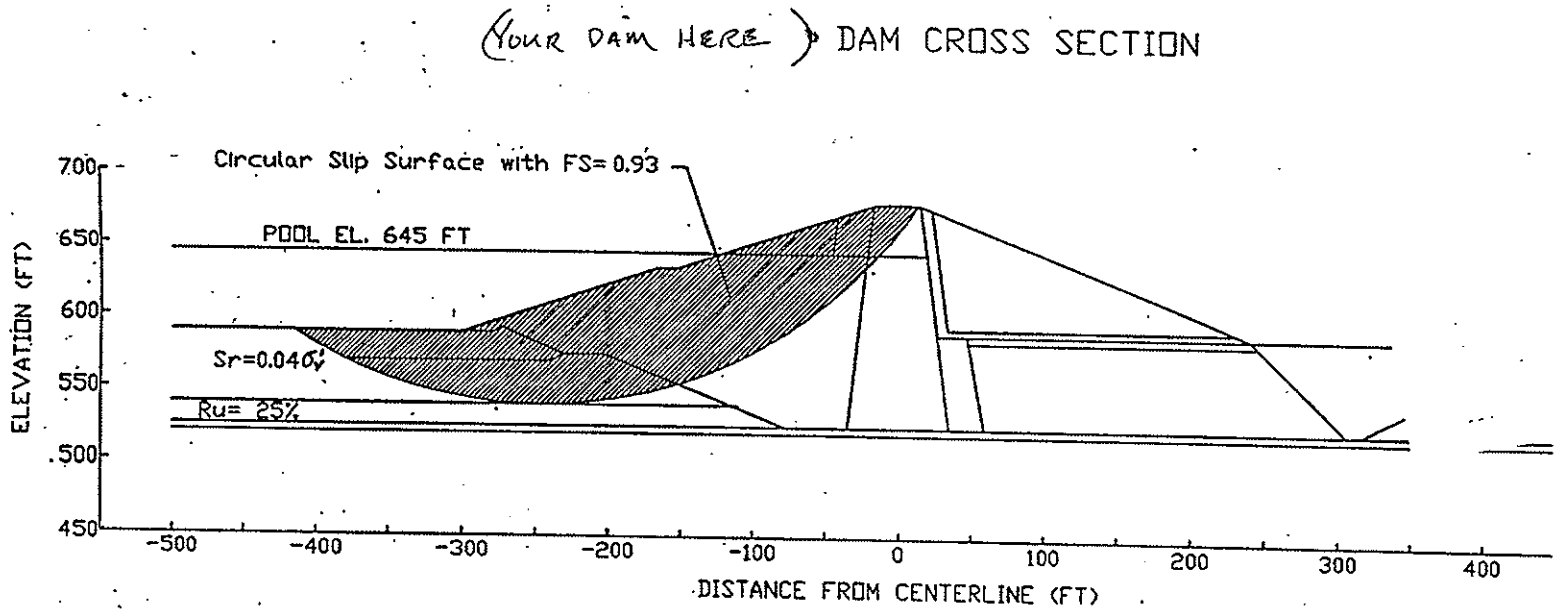

Figure 2 UTEXAS3 results obtained for circular slip surface having the minimum factor of safety under the following conditions: assumed residual strength $S_r = 0.04\ \sigma'_v$ in the silty sands/sandy silts, residual excess pore water pressure of 25% in the foundation sands and pool level of elevation 645 ft

Two Load Sequence Laboratory Tests

A review of the strength values interpreted or used in the various investigation approaches summarized in Table 1 shows that there are some significant deficiencies in how we have historically evaluated post-liquefaction soil strength conditions. In the case of investigations which use tests on laboratory specimens, it is not possible to determine post-liquefaction strengths from a test with a single loading sequence only, although this is commonly done. In reality, we should perform a two load sequence test where after the first undrained loading phase in which we liquefy the specimen, we reconsolidate the specimen by allowing drainage to take place, and then reload the specimen under undrained conditions. The strength determined during this second undrained load phase is the post-liquefaction strength. The results of such a two load sequence test are summarized below.

Figure 1 shows the results of a quasi-static undrained torsional shear test performed on a specimen of Ottawa 20-30 sand that was isotropically consolidated to a mean effective confining stress of 100 kPa and a void ratio of 0.682 (Dr = 24%). The maximum shear modulus was determined from a resonant column test to be 82.4 MPa. The specimen was first subjected to a cyclic shear stress of about 14 kPa. Strain softening was initiated at a shear strain of about 0.3% after the application of 9 cycles as shown in the figure at which stage the rate of pore pressure development increased. A steady state condition was reached at a shear strain of about 5% and the test was terminated at a shear strain of 13%. The shear stress was then removed from the specimen and the drainage lines were opened to allow it to reconsolidate isotropically to a mean effective confining stress of about 100 kPa. The void ratio at this stage had decreased to 0.641 (Dr = 41%) and the maximum shear modulus was determined to be 77.5 MPa. It is noted that for this new combination of confining stress and void ratio, a maximum shear modulus of about 90 MPa would have been expected based on extensive tests on reconstituted specimens prior to the application of large strains. This reduction in maximum shear modulus is attributed to a change in the grain structure during the initial loading and strain softening phase, thus while the specimen is denser following reconsolidation, it has a structure which is less stiff in the direction of the applied torsional vibration loading.

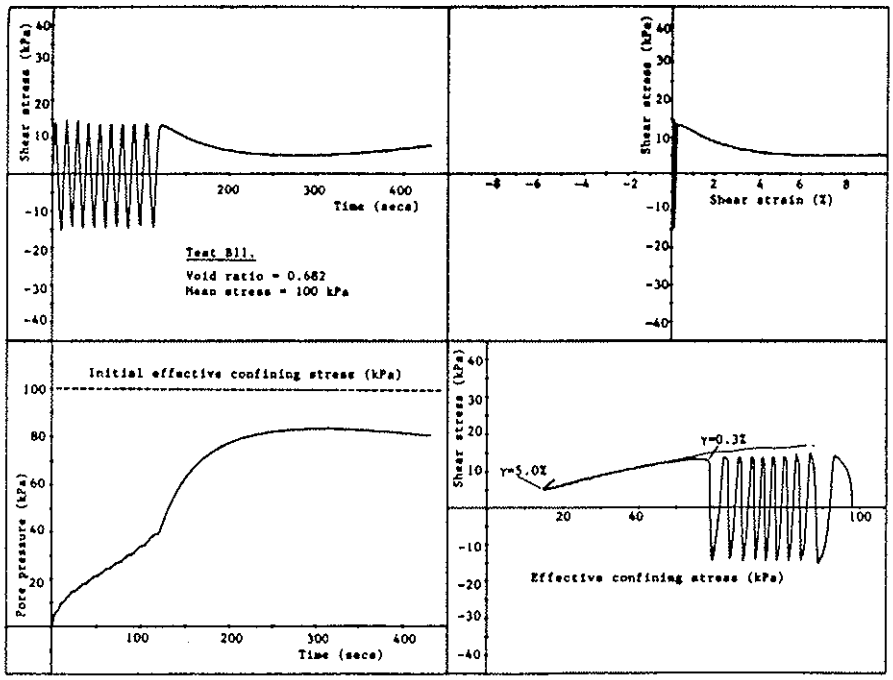

Figure 1 Cyclic Torsional Shear Test Results during Initial Load Sequence

At this stage, it was intended to subject the specimen to a second load sequence of cyclic shear stress of about 14 kPa as in the initial load sequence however, during the first load cycle, strain softening accompanied by the development of large pore pressure was observed (Figure 2) with the specimen reaching steady state at a shear strain of about 3.5%. Several aspects of the results shown in Figures 1 and 2 are of interest. The peak shear strength for the reconsolidated specimen was attained at a shear strain of about 0.7%, compared to 0.3% during initial loading. The application of large shear strains during the initial loading resulted in a particle arrangement which while denser was more conducive to pore pressure build-up during subsequent undrained loading. During the initial loading, the specimen reached a steady state of deformation at a shear strain of 5% at which stage the specimen was able to sustain a shear stress of 5.2 kPa at a mean normal effective stress of 15 kPa. Following reconsolidation, the denser specimen reached steady state at a shear strain of about 3.5% and was able to sustain a shear stress of only 2.6 kPa at a mean normal effective stress of 12 kPa. This difference is clearly of interest in that it has been suggested that the steady state condition is only a function of the initial void ratio for undrained tests. The results of the tests presented above appear to substantiate the argument that the structure may also be reflected in the behavior at steady state. Further they clearly demonstrate the difference between post-liquefaction strength and steady state strength and lend credence to the argument that post-liquefaction strength determination in the laboratory requires a two load sequence test, one to first liquefy the specimen and the second to determine the post-liquefaction strength.

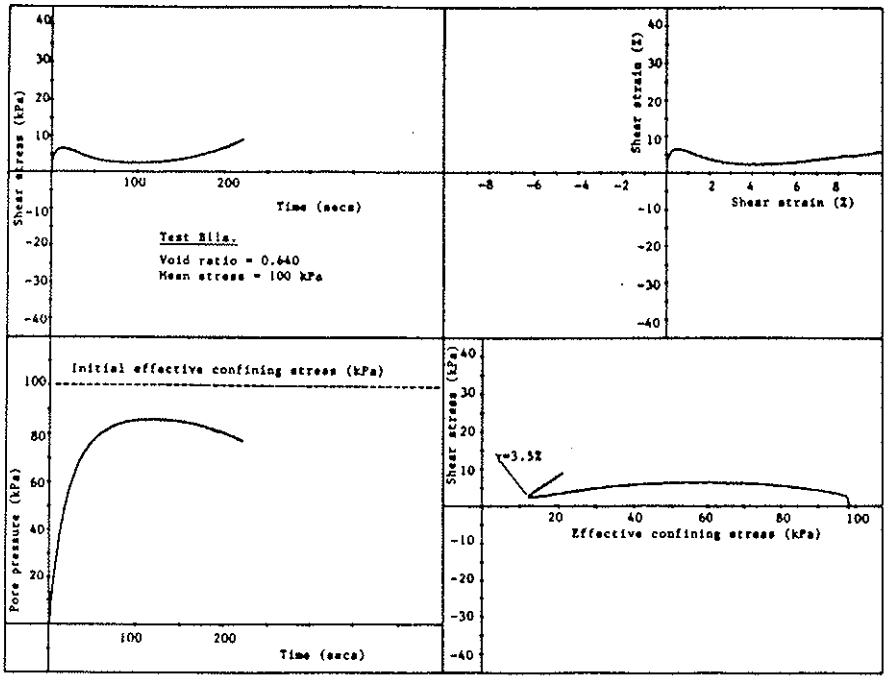

Figure 2 Cyclic Torsional Shear Test Results during Second Load Sequence

Quantitative Measurements of Structure

There is compelling indirect experimental and analytical evidence that soil structure is a critical parameter in the behavior of granular soils under earthquake loading. Ongoing research at Georgia Tech is using digital image processing and analysis to provide quantitative measures of the structure of granular soils. One parameter which is currently being used is Oda's local void ratio distribution. Figure 3 shows the distributions of local void ratio for measurements on two specimens of standard Ottawa sand with the same global void ratios but reconstituted using different methods of preparation (moist tamping and air pluviation). While the distributions appear

similar, there are quantifiable and important differences between them as shown in Figure 4. For example, the specimen prepared using air pluviation has a less skewed distribution with more of the voids having values near the mode size. Ongoing measurements are quantifying the evolving local void ratio distribution at different strain levels during monotonic and cyclic loading.

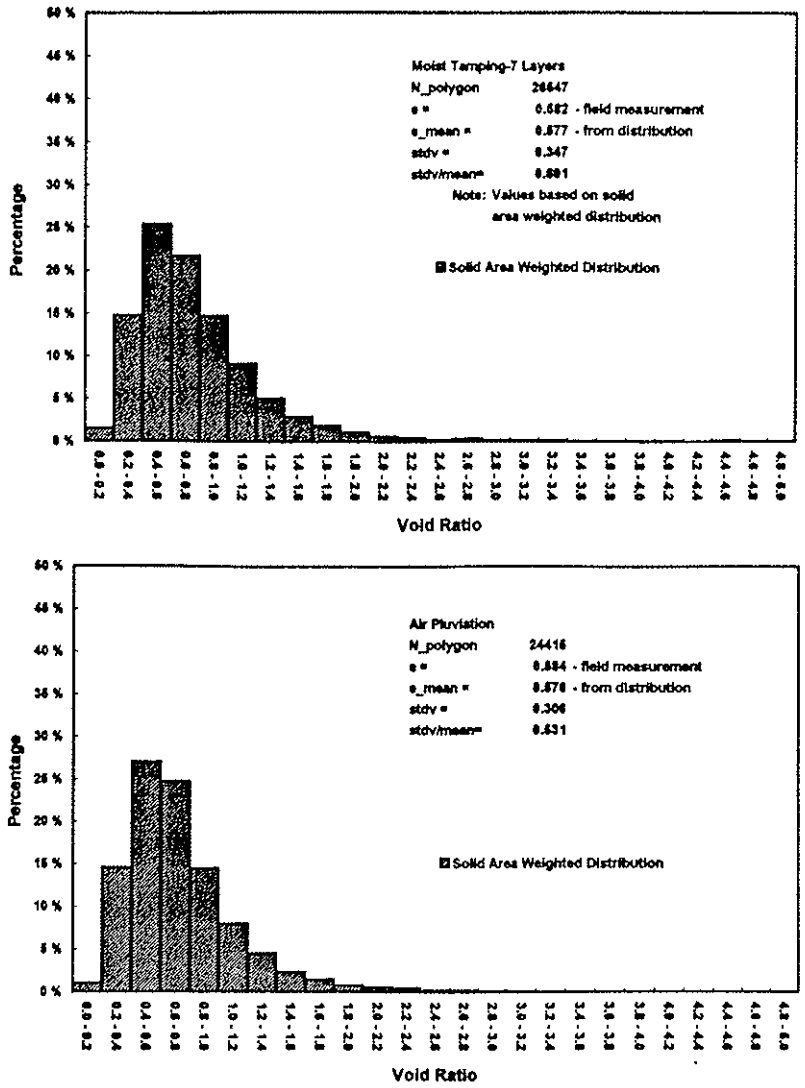

Figure 3 Distributions of Local Void Ratio for Different Preparation Methods

One of the important consequences of data such as shown in Figures 3 and 4 is that the manner in which global void ratio is used may not be sufficiently precise for many future applications, including those to study parameters such as post-liquefaction strength. For example, when referring to tests on saturated specimens, the terms "constant volume", "constant void ratio" and "undrained" are used interchangeably however while this is true in a global sense based on measurements of the mass and volume of the specimen, it may be appropriate to add an additional parameter to our terminology to more correctly describe the soil behavior. One approach to this is illustrated schematically in Figure 5 which shows the undrained behavior of isotropically consolidated specimens at different initial global void ratios. Using q-p'-e space, each test would in fact lie on a single plane parallel to the q-p' axes however, at any stress state within a given constant e plane, the distribution of local void ratio could vary not only as a function of the initial structure but also as a function of the stress path and hence state. This is illustrated in the figure by superimposing the local void ratio distribution plots perpendicular to the lines of constant void ratio to reflect the fact that while the global void ratio and hence the mean of the local void ratio distribution is constant, the distribution of the local void ratio about the mean is changing.

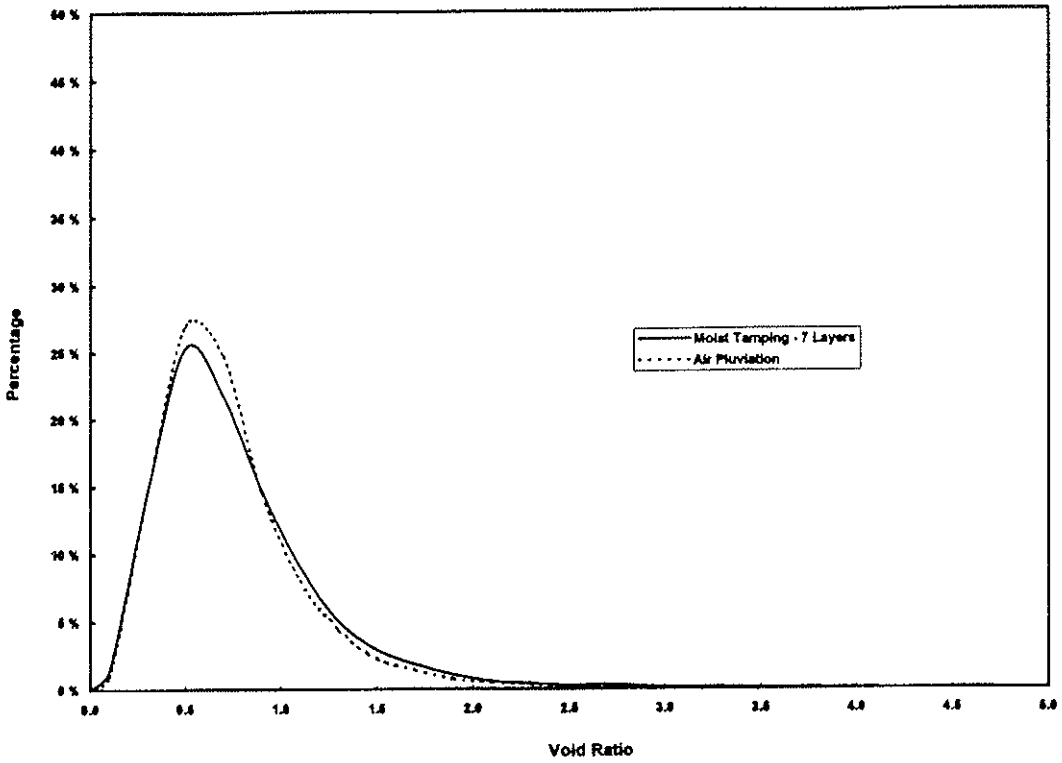

Figure 4 Comparison of Local Void Ratio Distributions

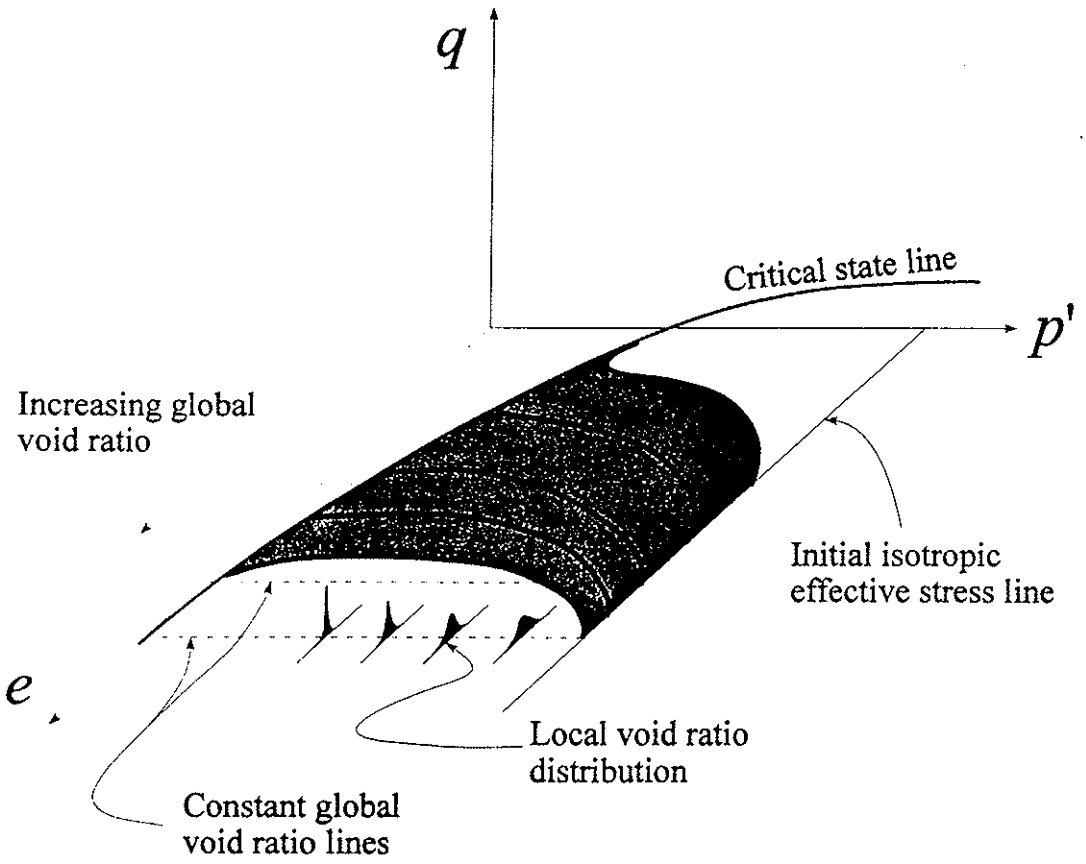

Figure 5 Illustration of the Distinction Between Global and Local Void Ratios

Role of Fines in Post-Liquefaction Strength

A number of researchers have investigated the role of fines in the response of granular materials under earthquake loading. It is suggested that a more fundamental approach is required to gain insight into this topic. In the same manner that quantitative image analysis can provide insight into the role of structure in the behavior of granular soils as has been suggested herein, so too is it considered that similar studies can investigate the role of "fines" as an inhibitor/instigator of structural collapse and hence pore pressure generation, as an inhibitor of pore pressure dissipation and as a factor in post-liquefaction strength. The role that "fines" play in any of these phenomena is expected to be a function of the characteristics of the fines such as their shape and relative size, as well as initial soil structure. Attention is drawn to the importance of relative size as opposed to an arbitrarily selected constant size. In the same manner that it is recognized that characteristic particle sizes such as the D_{10} tend to control the hydraulic conductivity and other characteristics of soil behavior, so too are particles that have some relative relationship to the dominant granular soil size expected to have an impact on the overall soil behavior.

Selected Bibliography

Kuo, C.Y., and Frost, J.D., (1996), "Uniformity Evaluation of Cohesionless Specimens using Digital Image Analysis", ASCE Journal of Geotechnical Engineering, Vol. 122, No. 5, pp. 390-396.

Frost, J.D., and Kuo, C.Y., (1996), "Automated Determination of the Distribution of Local Void Ratio from Digital Images", ASTM Geotechnical Testing Journal, Vol. 19, No. 2, pp. 107-117.

Oda, M., (1972), "Initial Fabrics and their Relations to Mechanical Properties of Granular Materials", Soils and Foundations, Vol. 12, No. 1, pp. 17-36.

Liquefaction and Post-liquefaction Behavior of Granular Soils

Marte Gutierrez
Norwegian Geotechnical Institute
PO Box 3930 Ullevaal Hageby
N-0806 Oslo, Norway

Brief Review of the State-of-the Art

There are currently several procedures for determining the liquefaction potential and the post-liquefaction behaviour of granular soils. The former requires the determination of the yield strength and the latter the residual strength of the liquefiable deposit. The most commonly used procedure for assessing liquefaction potential in the field is the simplified procedure developed by Seed and Idriss (1971, 1982) based on the relation between shaking intensity (represented by the normalized average cyclic shear stress) and the in situ condition (represented by the normalized SPT resistance). Seed's procedure, which was originally intended for level grounds and on a magnitude M=7.5 earthquake, has been extended to account for the effects of earthquake magnitude, pressure effects and static shear by use of correction factors (NRC, 1985). Liquefaction potential have also been estimated based on CPT resistance (e.g., Robertson and Campanella, 1985; Stark and Olson, 1995).

Several other criteria for determining the onset of liquefaction based SPT and CPT resistance and laborartory tests have been proposed as summarized by Ishihara (1993). The different criteria fall within a reasonably narrow band showing not much differences between the procedures. This is specially important as there seems to be good agreement between field-determined liquefaction potential (Seed and co-workers) and liquefaction potential determined from laboratory tests on undisturbed soil samples from deposits of known penetration resistance (e.g., Tatsuoka et al., 1980; Tokimatsu, 1988).

The situation for the determination of post-liquefaction strength is less satisfactory. The main difficulty in the determination of residual strength of liquefied materials is obtaining undisturbed samples for laboratory undrained tests. For disturbed samples, it is not easy determine field conditions and almost impossible to reconstruct samples to field conditions. For clean standard laboratory sands, much of the recent laboratory tests results suggest the existence of a unique steady state (e.g., Verdugo 1992; Ishihara, 1993). However, there are still major disagreements such as whether the steady state is uniquely a function of the initial void ratio, whether is the steady state line is straight and parallel to the consolidation line, and how it can be applied to in situ materials.

In order to account for sampling disturbance and differences in field and laboratory void ratios, Poulos et al. (1985) developed procedures using the field void ratio and the slope of the steady state line from reconstituted samples. The success of this method hinges on the assumption that the steady state lines for the undisturbed and the reconstituted samples are parallel, and on the accurate determination of the in situ void ratio. A more direct correlation of residual strength with in situ condition (as given by the SPT resistance) was made by Seed (1987) and Seed and Harder (1990) again based on case studies. Stark and Mesri (1992) made further studies on the correlation between residual strength and SPT-N taking into consideration the effects of drainage and including results of laboratory tests. Their results show that the residual shear strength is about one-half of that of the yield strength for the onset of liquefaction. Another approach that is becoming more of use in practice is to assume constant ratio of residual shear strength to initial vertical effective stress.

Proposed Workshop Contribution

Several important issues need to be resolved so that current procedures for estimating the liquefaction and post-liquefaction strength of granular soils can be used with confidence. It is proposed that some of these issues be tackled based on theoretical considerations. Based on established postulates in constitutive modelling and well-known correlations developed particularly from drained tests of granular materials, the following will be shown:

1. The steady state (SS) and the quasi-steady state (QSS) coincide for very loose materials. For very dense sand, the SS is very different from the QSS and may be difficult to determine experimentally due to shear banding (Gutierrez, Lacasse and Høeg, 1992).

2. The SS is a function of the void ratio alone (which can be correlated with relative density D_r and hence with SPT count) and cannot be normalized with respect to the initial effective stress. This is the same assumption as in Critical State Soil mechanics.

3. The QSS is a function of the both void ratio (which again can related to D_r and SPT count) and the initial effective stress. The conditions for normalizing QSS strength with respect to the initial effective stress are discussed.

4. The SS and QSS are both affected by the stress path, i.e., triaxial compression (TC) vs. triaxial extension (TE) conditions. Theoretical ratios of the QSS and SS strengths in TC, TE and PS (plane strain) conditions are given.

5. For a given void ratio there is a unique relationship between QSS strength and the peak undrained shear strength.

Applications of the above results to in situ soils and other practical issues will also be raised during the workshop.

Other issues to be discussed in workshop concerns the effects of fines. For this, it is proposed that the effects of fines plasticity be considered as proposed by Ishihara (1993). Also, the issue of whether the global (sand + fines) void ratio (or relative density), or the clean sand (skeleton) void ratio (or D_r) should be used in characterizing fines containing granular soils.

Also to be presented during the workshop are two recent applications of the steady state theory at NGI:

1. A tailings dam in Poland where undisturbed sampling, DSS testing and cone penetration testing were done.

2. A project on loads on railway ballast in sand where the effects of sample disturbance on the test results are shown.

Proposals for future research will be given.

SHEAR BEHAVIOR OF LIQUEFIED SOILS: INTERDISCIPLINARY PERSPECTIVES

(prepared for NSF workshop on "Post-liquefaction Shear Strength of Granular Soils"
April 17-19, 1997, University of Illinois, Urbana, Illinois)

Richard M. Iverson, U.S. Geological Survey, 5400 MacArthur Blvd., Vancouver, WA 98661

Considerable knowledge gained outside the discipline of geotechnical engineering lends insight to the shear behavior of liquefied granular soils. Below I summarize some areas in which key knowledge is available and identify other areas in which key knowledge is lacking.

Greatly expanded research on post-yield shearing of granular materials commenced about 15 to 20 years ago. Landmark papers such as Savage's (1984) "The mechanics of rapid granular flows" helped propel research expansion. Outside of geotechnical laboratories, most of the research on post-yield shearing has ignored complications of geological materials and has focused instead on simpler granular materials like those used in industrial processes (with grains of uniform size, shape, and composition). Initially most of this work also disregarded the influence of intergranular fluid, but recently increased attention has been focused on mixtures in which grains interact with pore fluid as well as one another. A compendium edited by Roco (1993) provides an excellent summary of state-of-the-art work on solid-fluid mixtures by chemical and mechanical engineers as well as materials scientists. Although some of this work emphasizes mixtures in which the fluid is a compressible gas, other work emphasizes mixtures of grains with nearly incompressible, viscous fluid such as water. Recently physicists have also begun to research the behavior of granular materials (*e.g.*, Jaeger and Nagel, 1992; Jaeger *et al.*, 1996). Although physicists' perspectives are unique and worthwhile, much of their effort thus far has resulted in rediscovery and reinterpretation of phenomena already documented in the engineering literature.

A key concept that has emerged from recent work on shear behavior of dry granular materials involves the role played by grain velocity fluctuations. (The same concept applies to water-saturated granular materials, albeit in a modified manner.) Grain velocities can fluctuate about a mean value due to energy derived from the shearing motion itself or from external energy inputs, such as earthquake shaking. From a mathematical standpoint, the fluctuating motions of grains have been likened to the fluctuating motions of molecules in dense gases, and because of this analogy the mean-squared amplitude of the fluctuations has been expressed by a quantity dubbed the granular temperature, T (*cf.* Campbell, 1990):

$$T = \langle (\vec{v} - \bar{v})^2 \rangle$$

in which $\vec{v}$ is the instantaneous grain velocity, $\bar{v}$ is the time-averaged mean grain velocity, and $\langle\ \rangle$ denotes the ensemble average over all grains. Defined in this manner, T may be interpreted as twice the fluctuation kinetic energy per unit mass of grains. Recognition of the importance of T has several ramifications: (1) T can be viewed as a "state" variable that determines whether a granular mass exhibits quasistatic, rate-independent Coulomb behavior dominated by enduring frictional contacts between grains — or more complicated rate-dependent behavior in which

inelastic grain collisions dominate. Behavior becomes fully rate-independent as $T \to 0$. (2) Larger values of T enhance the ability of a granular mass to flow by facilitating ease of movement of grains past one another. However, larger values of T also imply greater rates of energy dissipation, and in this respect granular materials differ fundamentally from dense gases. Nonzero values of T can be sustained only through continual energy extraction from the mean shearing motion (typically driven by gravity) or from an external (*e.g.*, earthquake) energy source. (3) Owing to the influence of T on flow behavior and energy dissipation, we can infer that there is no "correct" rheological model for a shearing granular material in which T is nonzero. Instead, the apparent rheology depends on T, which in general varies both in space and time. (4) Dependence of apparent rheology on T significantly complicates the simplistic view of grain flows espoused by Bagnold (1954). Although Bagnold's work was extraordinarily insightful, his focus on neutrally buoyant spheres and uniform shear fields renders his equations insufficient for assessing most realistic grain-flow problems (Iverson, 1997).

Despite the complications associated with nonzero T, almost all experiments conclude that the shear-to-normal-stress ratio (τ/σ) in dry granular materials remains remarkably constant over a great range of shear rates, just as Bagnold (1954) suggested, and the ratio differs little from the quasistatic Coulomb value ($\tau/\sigma = \text{constant}$). However, both τ and σ are functions of the local shear rate where T is nonzero. This is an important but subtle point that has lead to considerable confusion. Although the rate-independent Coulomb rule appears to apply to even rapidly shearing granular materials, the stresses τ and σ are themselves rate-dependent if shear is rapid. A dimensionless parameter S identified by Savage (1984) and dubbed the Savage number by Iverson and LaHusen (1993) helps discriminate conditions under which rate-dependent stresses are important:

$$S = (\dot{\gamma}^2 \delta)/g$$

Here $\dot{\gamma}$ is the shear rate, δ is the characteristic grain diameter, and g is the magnitude of gravitational acceleration. Limited data indicate that if $S > 0.1$, rate-dependent stresses dominate. For grains of 1 mm diameter, this criterion implies that shear rates must exceed about 30 s^{-1} for strong rate dependence. Such shear rates probably exceed those encountered in many geotechnical problems.

The presence of pore fluid in general and excess pore-fluid pressure in particular enhances the potential significance of rate-dependent stresses. For cases where pore fluid is present, Iverson (1997) demonstrated that the Savage number should be modified to a form similar to

$$S = \frac{\rho_s}{\rho_s - \rho_f} \frac{\dot{\gamma}^2 \delta}{g}$$

in which ρ_s and ρ_f are the mass densities of the solid grains and pore fluid, respectively. Thus buoyancy forces due to static pore fluid increase the value of S. Moreover, if excess pore pressures are present, the pressures can mimic the effects of increased pore-fluid density. In a state of complete liquefaction, pore pressures bear the complete load due to the weight of the solid-fluid mixture, mimicking the condition $\rho_f = \rho_s$. In this case $S \to \infty$, and stresses due to grain interactions become wholly rate-dependent, analogous to the situation investigated by Bagnold

(1954). Rate-dependent stresses due to shear of the viscous pore fluid can also be important in such circumstances, depending on the value of the Bagnold number (Iverson, 1997). In summary, depending on the degree of liquefaction, a particular soil-water mixture shearing at a particular rate can exhibit predominately rate-dependent or rate-independent stresses. In this respect the pore pressure P can be regarded as a crucial "state" variable, whose role and importance is equal to that of T. However, a complete theory for the integrated effects of P and T remains lacking.

Because the degree of liquefaction appears so critical to shear behavior of soil-water mixtures, our recent experiments at the USGS debris-flow flume have focused on understanding the degree and causes of liquefaction. We have found that nearly complete liquefaction is commonplace in debris flows except in coarse-grained snouts that form at the heads of surges. Liquefaction initially occurs during shear failure of loosely packed soil mixtures (Iverson *et al.*, 1997). Liquefaction persists owing to the low hydraulic diffusivity (~ consolidation coefficient) of the flowing debris, which results from the low permeability and high compressibility of the poorly sorted, agitated granular matrix and high viscosity of the pore fluid, which contains suspended silt and clay (Major, 1996). Thus the grain-size distribution plays a crucial role in sustaining high pore pressures and the potential for rate-dependent shearing. Granular temperature plays a synergistic role by making the agitated debris orders of magnitude more compressible than most granular soils (Iverson, 1997). Some of the same phenomena might be important in liquefied soils outside the highly energetic environment of debris flows.

REFERENCES CITED

Bagnold, R.A., 1954, Experiments on a gravity-free dispersion of large solid spheres in a Newtonian fluid under shear, *Proceedings of the Royal Society of London, 225A*, 49-63.

Campbell, C.S., 1990, Rapid granular flows, *Annual Review of Fluid Mechanics, 22,* 57-92.

Iverson, R.M., 1997, The physics of debris flows, *Reviews of Geophysics*, 35, in press.

Iverson, R.M., and R.G. LaHusen, 1993, Friction in debris flows: inferences from large-scale flume experiments, *Hydraulic Engineering '93 (Proceedings of the 1993 Conference of the Hydraulics Division of the American Society of Civil Engineers), 2*, 1604-1609.

Iverson, R.M., Reid, M.E., and LaHusen, R.G., 1997, Debris-flow mobilization from landslides, *Annual Review of Earth and Planetary Sciences, 25*, 85-138.

Jaeger, H.M. and Nagel, S.R., 1992, Physics of the granular state, *Science*, 225, 1523-1531.

Jaeger, H.M., Nagel, S.R., and Behringer, R.P., 1996, The physics of granular materials, *Physics Today, 49(4)*, 32-38.

Major, J.J., 1996, Experimental studies of deposition by debris flows: process, characteristics of deposits, and effects of pore-fluid pressures, unpublished Ph.D. thesis, University of Washington, 341 p.

Roco, M.C. (Ed.), 1993, *Particulate Two-Phase Flow*, Butterworth-Heinemann, Boston, 1002 p.

Savage, S.B., 1984, The mechanics of rapid granular flows, *Advances in Applied Mechanics, 24*, 289-366.

NSF Workshop on Post-Liquefaction Strength of Granular Soils

TOPIC: Is the undrained shear strength influenced by consolidation stress and undrained stress path ? What is the effect of fines ? And, how should fines be defined ?

Contribution from Michael Jefferies, Golder Associates

Introduction

I take it as self-evident that liquefaction, in all its forms, is simply another aspect of the constitutive behaviour of soil. Despite depressingly widespread use of emotive phrases like 'collapse surface' the reality is that even during the most extreme liquefaction stress and strains remain related - we are not dealing with tensile failure of a metal. It then follows that a proper understanding of liquefaction will only follow in the context of a theoretical model that sensibly reproduces soil behaviour. Moreover, a proper model must represent the behaviour of dense, drained dilatant sand and yet still capture liquefaction without introduction of new concepts, parameters etc. That is, the model must explain (predict) the response of soil to different density, drainage and stress path; it must not treat each aspect as a separate behaviour.

In this contribution, one such proper model - NorSand - is outlined. It's fit to some test data is illustrated and then the response of the model to the topic questions is presented. NorSand is especially useful for the topic discussion because it includes the concept of a critical state locus and is intrinsically a large strain model so that issues of post liquefaction strength are readily addressed.

Because contributions are limited in length, it is assumed that readers are familiar with the basic concepts of the liquefaction literature and thus the standard terminology used.

NorSand

NorSand (Jefferies, 1993) is an isotropically hardening - isotropically softening, single yield surface plastic model derived from two axioms of critical state theory which are that: a CSL exists (the First Axiom); and, soil state moves to the CSL with shear (the Second Axiom).

The First Axiom has been discussed by many workers and a detailed experimental investigation for sand was presented by Been et al (1991). Importantly, note that a principal source of error in the past over possible non-uniqueness of the CSL in *e-p* space as a function of stress path , and continuing quite widely, arises through the definition that the critical state is the condition in which the soil deforms without volume change, otherwise expressed as zero dilatancy. While this is a necessary condition, it is not sufficient for criticality. At a critical state there must also be the condition that the rate of change of dilatancy is also zero. This error is found, for example, in many of the contributions to the literature on steady state strength by Vaid & co-workers and by Konrad.

Conventionally, the CSL is represented in *e-p* space using the semi-logarithmic form $e_c = \Gamma - \lambda \log(p_c)$ where Γ, λ are material properties. The validity of this idealization at low mean stress has been questioned (e.g. Ishihara, 1993), but objections to it are merely arguments about detail and not central to the validity of critical state models.

Standard critical state models (e.g. CamClay) assume that any yield surface intersects the CSL so directly coupling the yield surface size to void ratio. Real soils, however, display a far richer behaviour and in particular exhibit an infinity of normal consolidation loci (NCL) which are not parallel to the CSL. It is this rich behaviour that is characterised by the state parameter approach, in essence each NCL being related to a value of ψ (where $\psi = e - e_c$). Overconsolidation ratio (OCR) continues to exist in its usual sense of defining the location of a stress state within a yield locus.

NorSand involves just 3 more soil properties than the familiar CamClay model: an elastic shear modulus, G; a volumetric coupling coefficient, N; and a plastic hardening modulus, h. The range of yield surfaces encountered with NorSand are illustrated on Figure 1. The power of NorSand derives from not requiring that the yield surface intersect the CSL in *e-p* space. Instead NorSand uses a hardening law that forces the yield surface to the CSL with shear strain, exactly in conformance with the Second Axiom. The original form of NorSand was derived in the context of monotonic loading; however, the extension to cyclic loading is not difficult as was accomplished by introducing a third axiom that principal stress rotation anneals hardening (Been et al, 1993).

The ability of NorSand, calibrated using dense sand, to represent static liquefaction of a loose sample of the same sand is illustrated on Figure 2 - an excellent fit is observed, including the slight recovery of strength from the post-peak minimum.

With the basic performance of NorSand established, let us turn to the questions posed.

Responses

Q1: What is the effect of consolidation stress?

Increased consolidation stress changes decreases void ratio, with differing amounts depending upon the gradation, fines content etc. Decreased void ratio means post-liquefaction shear strength increases, all else equal. This is the principal argument against normalizing test results to a stress level of 100 kPa - if the test data is normalized in this way then the inferred strength must be de-normalized (which is rarely done), and this overall process leads to errors. However, consolidating natural deposits can reduce any overconsolidation ratio and so partially offset strength gain because of density increase. Decreased consolidation stress, at least for small decreases, leads to minimal change in strength because of the induced overconsolidation.

Q2: What is the effect of stress path?

Large... Specifically, plane strain is very different from the familiar triaxial test and situations in which means stress decreases leads to a markedly lower strength because the critical friction angle is sensibly a constant (and see below for the consequences of localization).

Q3: How do fines influence residual strength?

Variably... We have tested the post liquefaction strength (in triaxial compression) of several sands systematically varying fines contents. Whether fines improves the residual strength for any given density depends on the stress level. In our work we have defined *fines* simply as the fraction passing the #200 sieve.

Q4: Is the post liquefaction strength proportional to the vertical effective stress?

Broadly, yes. Specifically, under conditions of constant ψ, NorSand predicts that s_r will be linearly proportional to p given the *e-log(p)* idealization of the CSL for any set of material properties.

Q5: What is the relevance of the pseudo steady state or minimum undrained strength?

Figure 3 shows a sample with a clear pseudo steady state. In fact this sample is a NorSand simulation. The interesting aspect is the softening regime post initial peak as this violates Drucker's stability postulate (Drucker, 1959), and as such we would expect bifurcation with undrained conditions no longer maintained locally. Hence the computed strength gain from dilation under undrained conditions should not necessarily be expected (it may happen at laboratory scale because of the limited sample volume). Further, if we look at the yield surface hardening, also plotted on Figure 3 and which we know because this is a NorSand simulation, we see that softening starts at about 3.5% shear strain and we might expect instability to be associated with this.

The introduction of instability criteria to geomechanical constitutive models is a very new and active subject so definitive conclusions are, as yet, difficult. However, intriguingly, if the NorSand instability limit is plotted against field scale data for post-liquefaction strength, Figure 4, then we get what looks like a very promising explanation of what is observed at field scale.

So, where does the pseudo steady state strength fit in. Well, it is clear from NorSand that the pseudo steady state strength is lower bound to the instability condition, and is certainly a far more realistic proposition that the steady state strength. And, if we plot the computed trends for pseudo steady state on Figure 4 we see a rather good explanation of field behaviour. However, if it was universally true that the pseudo steady state strength controlled undrained strength then we would not be able to record the dilatant undrained behaviour that we do in the laboratory.

Clearly some urgent theoretical work is required to distinguish what controls and under what conditions. The point I'd like to emphasize is that sorting out this issue requires applied mechanics and is unlikely resolvable by experiment alone. There are several such models now available and as I noted earlier investigation into localization is an active research topic.

Meanwhile, I'm in favour of using the pseudo steady state as a reasonable engineering approximation while the theoretical work continues. Where I get nervous is when people confuse the pseudo steady state with the CSL, as done by Vaid & co-workers and Konrad (with the ψ_U,ψ_L idea) - that simply leads to misleading concepts, incorrect mechanics, and prevents understanding.

The idea of an instability limit (in the sense of applied mechanics, not the erroneous collapse surface idea) allowing localization and so controlling post liquefaction strength means that stress path and other parameters such as elastic modulus become important. Which nicely explains the fact that despite a lot of work nobody has found a simple correlation of post-liquefaction residual strength in the various failure case histories to penetration resistance - theoretically, there should not be one!

References

Been, Jefferies, & Hachey, 1991: The critical state of sand. Geotechnique
Been, Jefferies, Rothenberg, & Hachey 1993: Numerical Prediction for Model 2. In Proceeding of VELACS Conf, Vol 1. Balkema.
Drucker, 1959: A definition of Stable Inelastic Material. J Appl Mech.
Ishihara, 1993: 33rd Rankine Lecture. Geotechnique
Jefferies, 1993: NorSand - A simple critical state model for sand. Geotechnique.

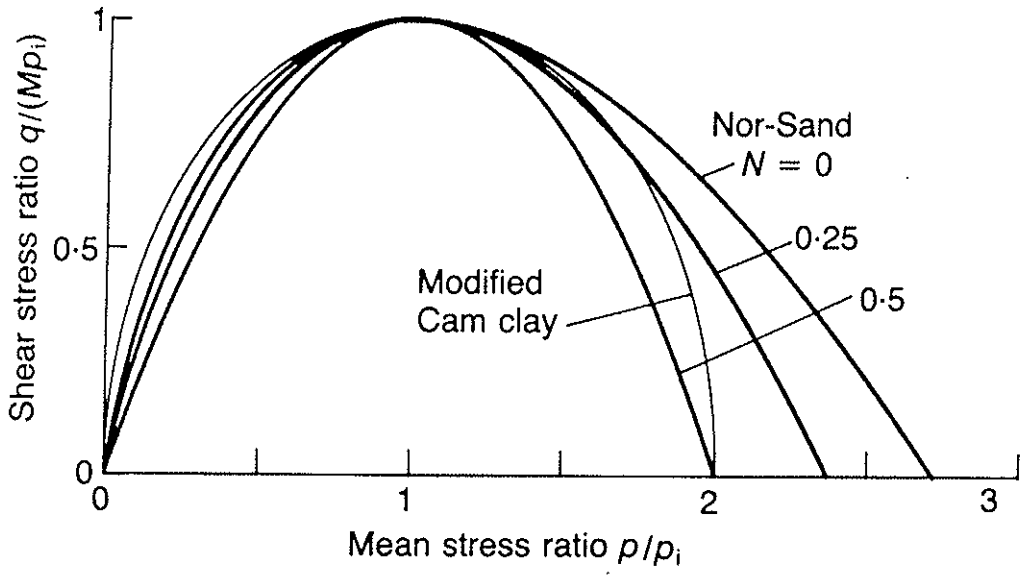

Figure 1: Illustration of NorSand yield surfaces

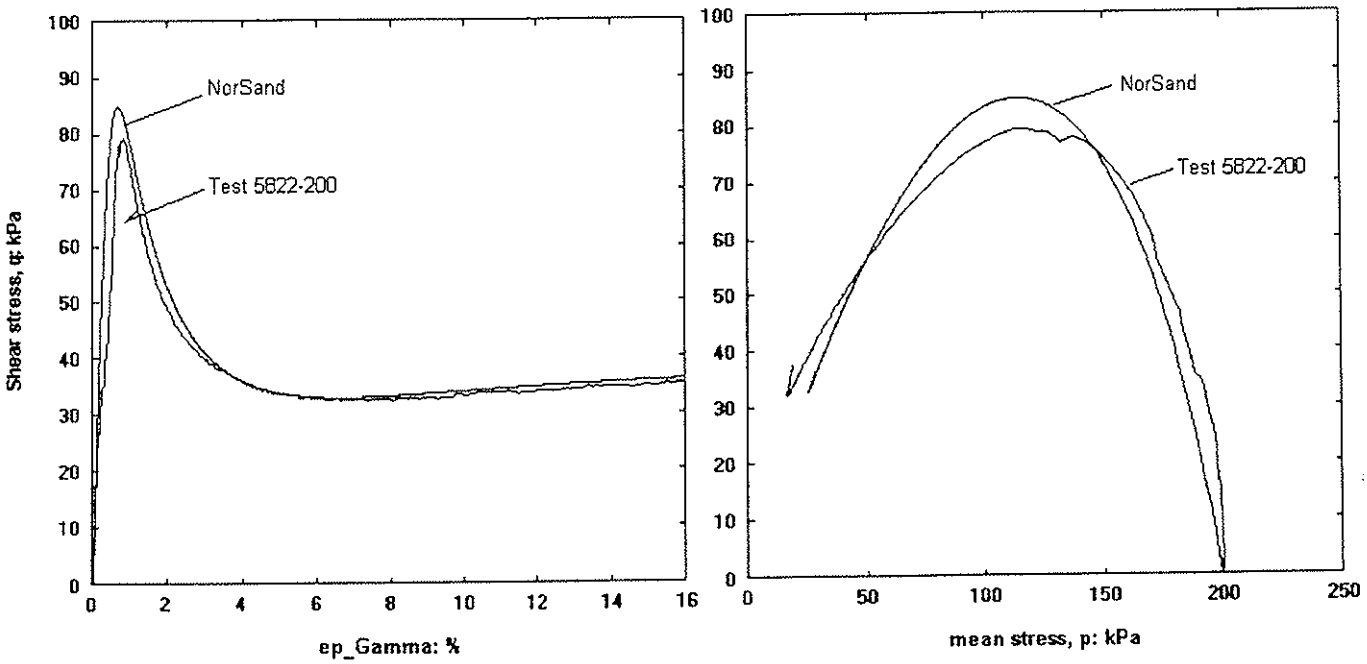

Figure 2 : Illustration of NorSand fit to static liquefaction test

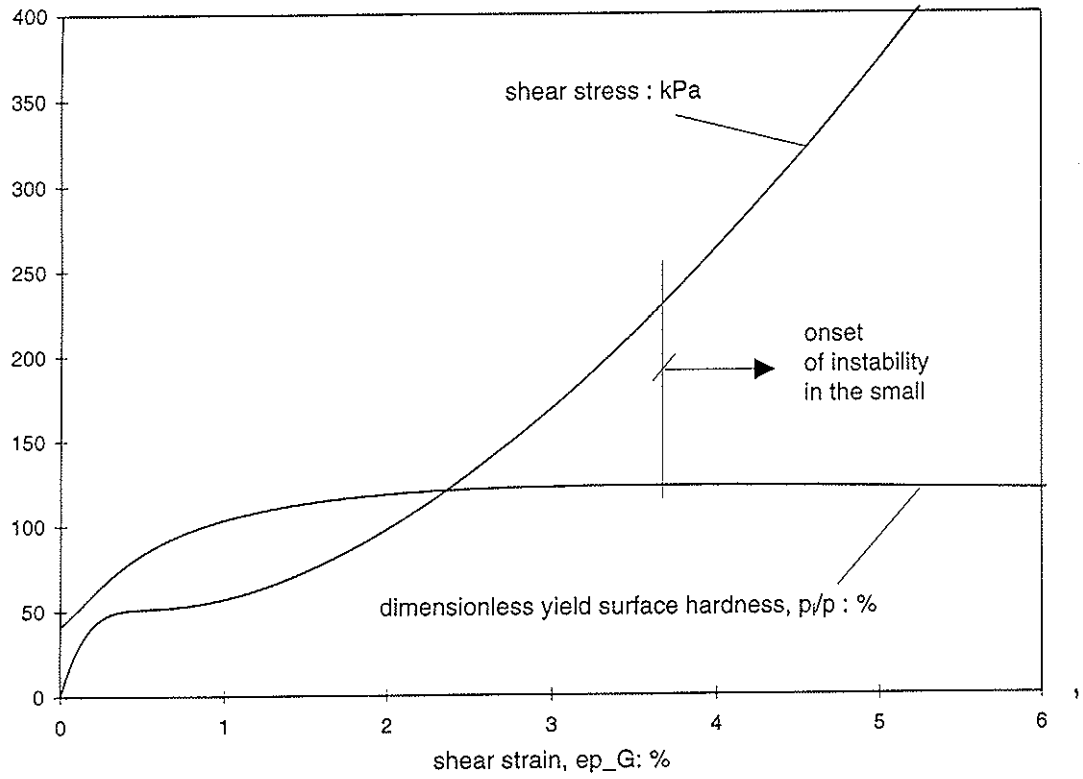

Figure 3: Comparison of NorSand hardening with undrained stress-strain behaviour

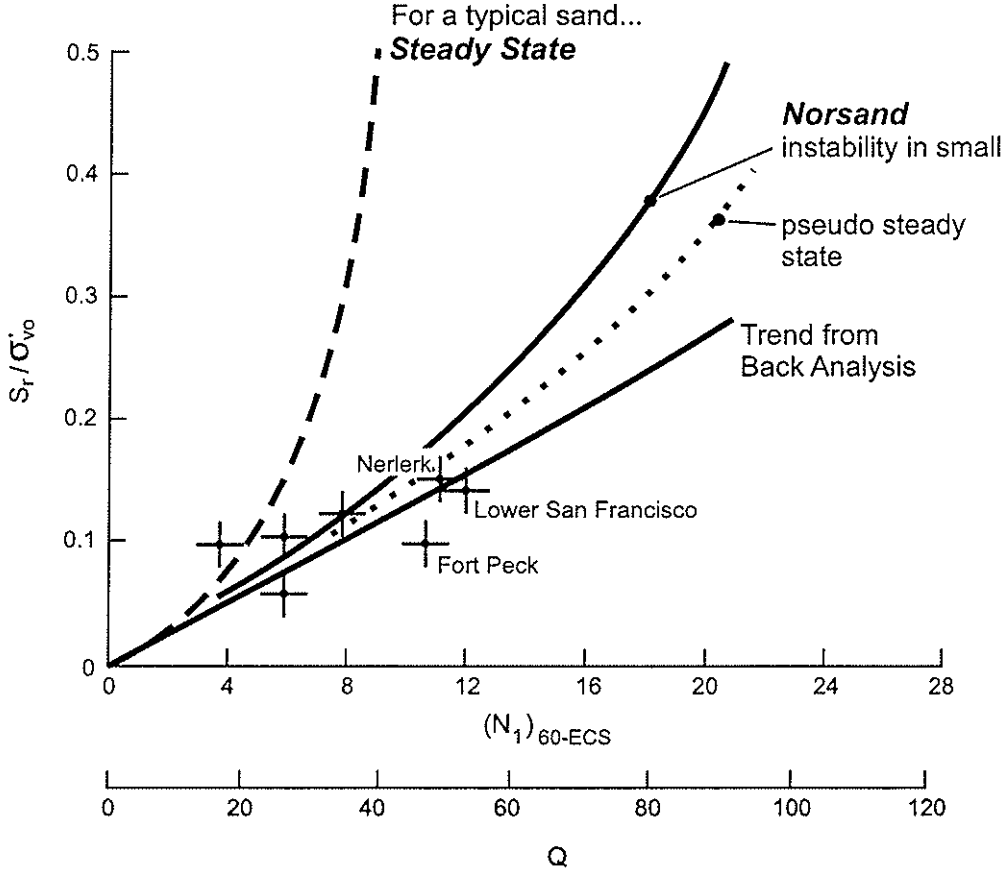

Figure 4: Comparison of field scale residual strengths with theoretical predictions

Submission by Joseph P. Koester, US Army Engineer Waterways Experiment Station, Vicksburg, Mississippi

Discussion Group: Theoretical/Conceptual Issues

***Soil Mechanics Perspective -**

Question (1): How is the shear strength of liquefied soil influenced by consolidation stress and undrained stress path?

Answer: My office is often charged with post-earthquake stability evaluation of critical facilities, typically large embankment dams, many of which are built from or founded on variously silty or clayey sands and gravels. I therefore fervently hope there *is* a strong positive influence of consolidation stress. If it can be demonstrated that a slope is clearly safe against post-earthquake sliding when shear strength of liquefied soils along the potential failure surface (in a limit equilibrium analysis) is a plausible constant value, there is not likely a worrisome risk. The problem is, however, the term "plausible", in that so-called residual strength values sufficient to resist sliding have generally proven to be larger than determinable from the field performance-based relationship published by Seed and Harder (1990) (i.e., by means of penetration test results) without extrapolation to corrected blowcounts that are so high as to preclude the triggering of liquefaction in the first place. Baziar and Dobry (1995) extended the experience base to include lateral spreads and investigated the influence of confining stress, establishing a range in ratios of (assumedly undrained) residual strength to effective confining stress from 0.04 to 0.2 (see Figure 1). The lower bound ratio is not very helpful, as illustrated by the limit equilibrium analysis result shown in Figure 2, where most of the passive resistance is derived within the residual strength material. Non-circular slip surfaces would exacerbate the problem in that case. When the level of sophistication of analysis rises above limit equilibrium to include soil models and pore pressure generation and dissipation, stress redistribution comes into play and frictional response becomes all the more important.

In a recently completed, but not yet published, study of Sardis Dam, Mississippi, residual strength of liquefied soils (a top stratum clayey silt with characteristics of similar soils that liquefied in major earthquakes in China - I specifically avoid using the term "Chinese clay") were estimated as being 0.075 times the effective overburden stress for use in nonlinear soil model analysis. Peak shear strengths were measured in the field by various means, including vane shear and cone penetration tests, and by best estimates were determined to fall generally into the range of 0.3 times effective consolidation stress. Sensitivity was determined from the vane shear test results to be about 4, thus giving the 0.075 residual strength relation. Additionally, stability analyses were conducted to back-calculate the S_r/p' ratio required to produce a factor of safety against sliding of about 1.5, which was devised from the observation that the dam has been standing for some time, successfully. A ratio of about 0.075 was also found by this means.

With respect to undrained stress path influence, I found in a laboratory experiment series myself

that residual strengths of sand mixtures containing 25-30% fines, whatever the plasticity of the fines, were very low and essentially constant to large shear strains in torsional simple shear. This was the case whether virgin specimens were loaded monotonically or specimens that had undergone liquefaction by cyclic loading were loaded, undrained, monotonically to large shear strains. Clean sands, as shown by others, dilated in my experiments (Koester, 1992). I did not vary confining stress enough to judge its effects on residual strength of liquefied mixtures.

Question (2): How do soil "fines" influence residual strength?

Answer: I am convinced, from my own experiments and results published by others, that residual strength of liquefied clean sands is higher than that of liquefied soils containing particles finer than sand. Clean sands tend to dilate when strained in undrained loading, gaining strength quickly. The presence of fines somehow prevents dilation, such that strain potential appears unlimited. I observed this in mixtures containing more than 15 percent fines by weight. I further believe that the beneficial contribution of plasticity of the fines is very slight, once the soil has liquefied. Gradation is the controlling factor, as is the case, I believe, with triggering of liquefaction, as well.

Question (3): How should "fines" be defined, e.g., minus No. 200 sieve?

Answer: I recommend continuing to define fines as minus No. 200 sieve materials. I would like to point out here that I also advocate measurement of consistency using only the fines in assessing potentially liquefiable soils, i.e., not including the material passing the US No. 40 sieve and retained on the No. 200 sieve, as is dictated for Atterberg Limits testing by ASTM. The effect of sand content on consistency measurement is too drastic for the case of low plasticity soils. In some countries, by the way, consistency limits tests are performed on materials passing through a sieve with 0.500 mm openings; the US No. 40 sieve, by the way, passes particles finer than 0.425 mm. The presence of the larger particles would reduce plasticity.

Question (4): Is the post-liquefaction shear strength proportional to the initial vertical effective stress? Under what conditions?

Answer: As I discussed for Question 1, above, I certainly hope so, under most conditions of engineering interest. I suspect, but cannot substantiate, that remediated soils have locked-in horizontal stresses that would affect proportionality with regard to vertical effective stress. Remediated soils would be a very stimulating subject to include in the workshop, if at all possible. They could still liquefy, and it would be interesting to document expert opinions on their residual strength.

Question (5): What is the applicability of the quasi-steady state or minimum undrained strength concepts?

Answer: I do not know what is meant by "quasi-steady state" in the context of post-liquefaction strength. I am reminded of the Stark and Mesri (1992) ASCE Journal of Geotechnical Engineering Division paper on the subject of shear strength of liquefied soils by this question.

Stark and Mesri (1992) proposed that post-liquefaction shear strength, or undrained critical strength, s_u(critical), if expressed as a shear stress ratio with effective confining stress, is about half of the yield strength ratio mobilized in the field at liquefaction, s_u(yield, mob)/σ'_{vo}. The latter ratio is defined by the line separating liquefiable and nonliquefiable sands for an earthquake magnitude of 7.5 (15 equivalent uniform loading cycles) as published by Seed et al. (1985) and is approximately equivalent to the equivalent clean sand $(N_1)_{60}$ divided by 90 for $(N_1)_{60}$ up to 20. The authors observed that cyclic triaxial strengths in sands were essentially constant beyond 100 loading cycles, and that the cyclic stress ratio causing liquefaction in 100 cycles was about the same as s_u(critical). Additionally, Stark and Mesri (1992) determined that s_u(critical) was approximately half of the yield strength ratio mobilized in the field at liquefaction in silty sands, as well, when $(N_1)_{60}$ measured in silty sands to estimate yield strength was adjusted according to the procedures suggested by Seed, et al. (1985).

The proportionality of yield cyclic strength to post-liquefaction shear strength observed by Stark and Mesri (1992) from field performance data did not appear to hold in laboratory tests on fine-grained soil mixtures prepared to relatively loose conditions in a cyclic hollow cylinder torsional test program I performed. I offer the two accompanying tables (Table 8.5 and 8.6 from Koester, 1992) from that program for discussion.

REFERENCES CITED:

Baziar, M.H. and Dobry, R. 1995. "Residual strength and large deformation potential of loose silty sands," *Journal of the Geotechnical Engineering Division*, ASCE, 121(12), pp. 896-906.

Koester, J.P. 1992. "Cyclic strength and pore pressure generation characteristics of fine-grained soils," thesis submitted in partial fulfillment of the requirements for Doctor of Philosophy, College of Engineering, University of Colorado, Boulder, CO.

Seed, R. B. and Harder, L. F. Jr., 1990. "SPT-based analysis of cyclic pore pressure generation and undrained residual strength," *Proceedings, H. Bolton Seed Memorial Symposium*, Vol. 2, Ed. J. Michael Duncan, May, pp. 351-316.

Seed, H. B., Tokimatsu, K., Harder, L. F., and Chung R. (1985). "Influence of SPT procedures in soil liquefaction resistance evaluations," *Journal of the Geotechnical Engineering Division*, ASCE, 111(12), 861-878.

Stark, T. D. and Mesri, G. (1992). "Undrained shear strength of liquefied sands for stability analysis," *Journal of the Geotechnical Engineering Division*, ASCE, 118(11) pp. 1727-1747.

Table 8.5 Estimated post-liquefaction shear strengths
from undrained hollow cylinder torsional simple shear tests
on isotropically consolidated specimens

	Method of Estimation (values in psf, values averaged for multiple tests on replicate specimens)			
Soil Type	$\tau_{cyc}(100)$[1]	$\frac{1}{2}\times\tau_{cyc}(15)$[2]	PCM[3]	Monotonic TSS[4]
F11	1080	994	N/A[5]	N/A[5]
F43	346	202	101 (14)[6]	245 (158)[6]
F46	475	346	130 (43)	432 (360)
F64	389	288	634 (547)	648 (562)

[1]Average cyclic shear stress ratio causing liquefaction in 100 cycles x σ'_v
[2]Average cyclic shear stress ratio causing liquefaction in 15 cycles x σ'_v
[3]Post-cyclic monotonic simple shear strength; lower-bound value range at $\gamma = 15\%$
[4]Lower-bound range of shear strength beyond peak shear resistance in virgin monotonic torsional simple shear tests, at $\gamma = 15\%$
[5]Specimen dilative with shear
[6]Values corrected for membrane torque resistance in parentheses

The format for soil type codes is such that each shown is mixed from a fine uniform parent sand; the next two numbers N_1N_2 identify fines content and plasticity index of fines, respectively, in a larger matrix of possible mixtures where: N_1 ranges from 1 through 7, respectively representing fines contents of 0%, 5%, 12.5%, 20%, 30%, 45%, and 60%; and N_2 ranges from 1 through 8, respectively representing plasticity indexes of NP, 4%, 10%, 15%, 20%, 25%, 30%, and 40%.

Table 8.6 Comparison of peak- to residual undrained shear
strengths in monotonic torsional shear tests on virgin specimens

Test No. (Type as above)	ϕ'[1]	S_u(peak)[2], psf	S_{ur}[3], psf	reduction[4],
25 (F11)	35°	(dilative)	(N/A)	(N/A)
26 (F43)	33°	2712	158	94%
27 (F46)	28.8°	2296	360	84%
28 (F64)	26.6°	2019	562	72%

[1]Effective angle of internal friction, determined from failure envelope of Figures 8.82-8.85
[2]$\sigma'_m\tan\phi'$, where $\sigma'_m=\sigma'_v$ in these isotropically consolidated tests
[3]membrane-corrected strength at 15% shear strain from Table 8.5
[4]$(S_u(peak)-S_{ur})/S_u(peak)\times 100\%$

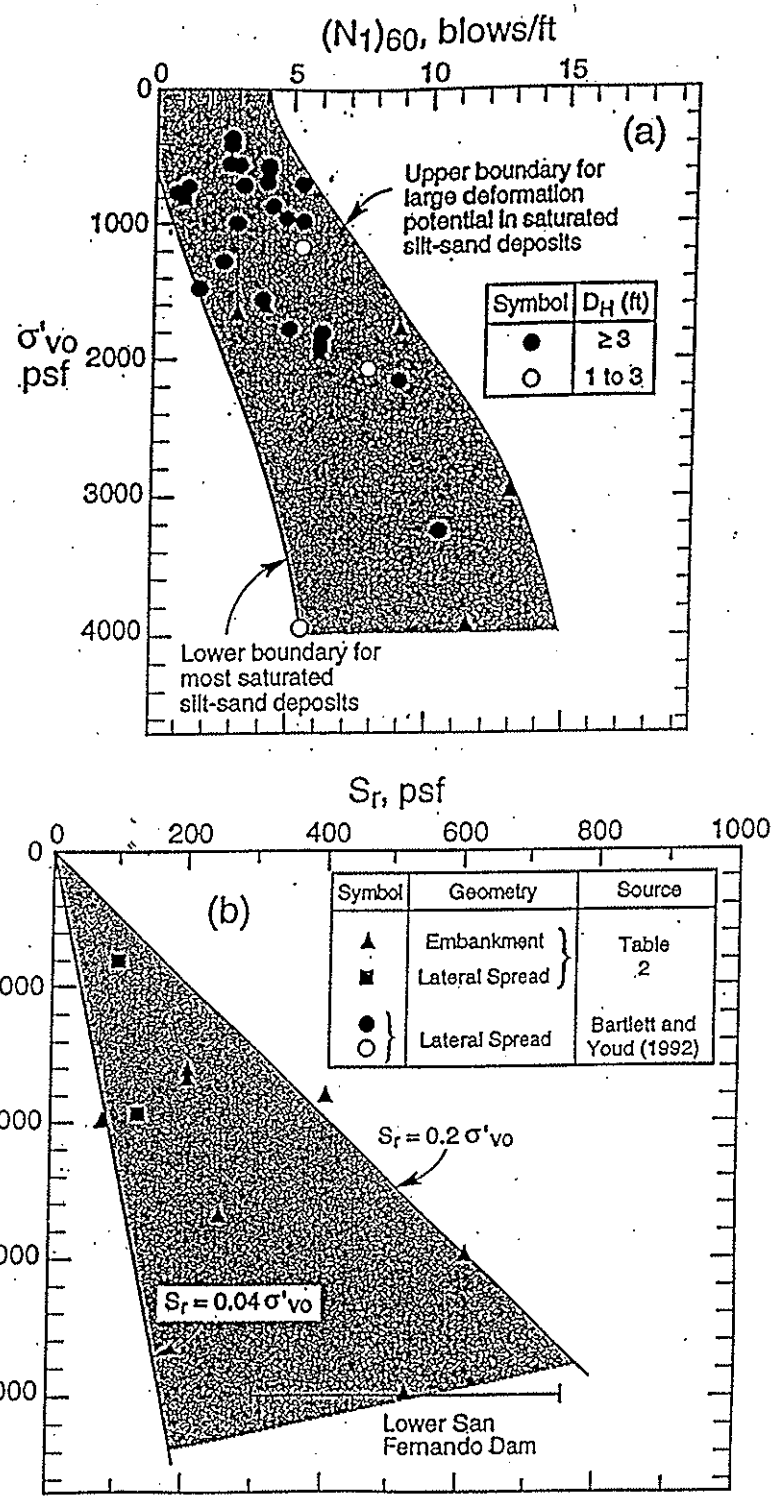

Figure 1 Charts relating normalized SPT resistance ($N_{1,60}$) and residual shear strength (Sr) to vertical overburden pressure (σ'_{vo}) for saturated nongravelly silt-sand deposits that have experienced large deformation (Baziar and Dobry, 1995)

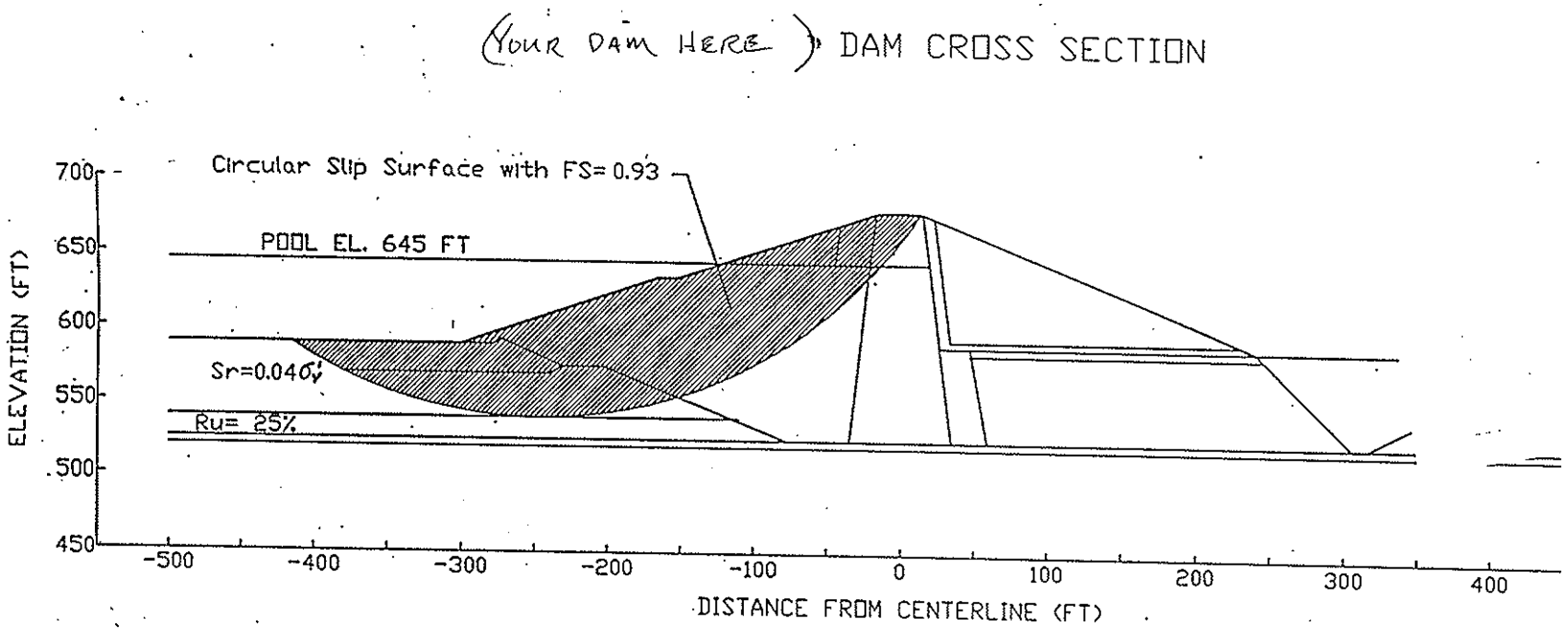

Figure 12 UTEXAS3 results obtained for circular slip surface having the minimum factor of safety under the following conditions: assumed residual strength S_r=0.04 σ'_v in the silty sands/sandy silts, residual excess pore water pressure of 25% in the foundation sands and pool level of elevation 645 ft

Post-Liquefaction Shear Strength of Granular Soils

Pre-Workshop Written Statement

Steven L. Kramer
University of Washington

Measurement and prediction of the residual strength of liquefied soil is a complicated problem; if it wasn't, there would be no need for a workshop of this type. The complexity of the problem results from the complexity of the particle-scale phenomena that contribute to the residual strength, from the spatial variability of the particle-scale parameters that influence the residual strength, from the sensitivity of the residual strength to those parameters, and from the lack of information that typically exists in practical problems. While improvements in the profession's understanding of the fundamental mechanics of liquefied soil behavior can undoubtedly be made, a significant degree of randomness and uncertainty will always exist and preclude precise prediction of residual strength. As we identify and discuss areas in which improvements can be made in residual strength evaluation, we should also discuss areas where improvements cannot be made and how the inevitable remaining uncertainty should be considered in geotechnical engineering analyses.

Knowledge of the residual strength of liquefied soil is important for a variety of reasons, but perhaps two stand out above the others and deserve special attention during the workshop. The first is the classic reason - evaluation of flow slide potential. The second is as a fundamental parameter upon which constitutive models can be based. At the most recent VELACS workshop, a variety of constitutive models were presented; all were based on critical state concepts and hence strongly dependent on the position of the critical state (or steady state) point that describes the residual strength of the soil. Consequently, knowledge of the residual strength is important even for problems in which the residual strength is never fully mobilized.

The first systematic treatment of the residual strength of liquefied soil came in the form of the steady state approach of Castro and Poulos. The basic tenet of that approach is that the steady state requires development of an amorphous flow structure which occurs at such large strains that the effects of any initial conditions are erased. As a result, the steady state strength is influenced only by the void ratio which controls the nature of the interparticle contacts and collisions that occur during flow. It is difficult to argue with the logic of this concept, even though its validity has been questioned. My personal view is that the steady state concept is perfectly valid as long as the requirements of the steady state of deformation are strictly satisfied; the extent to which they are satisfied in the field or in the laboratory, however, is questionable. For that reason, I prefer to use the term residual strength to describe the large-strain strength of liquefied soils.

Regarding the influence of fines on residual strength, it is important to define what is meant by fines. Use of the No. 200 sieve is clearly an arbitrary approach, but the question of

whether or not it is effective is more important. It is straightforward, objective, and easy to measure - all important advantages. We see that fines corrections are required to correlate residual strength to insitu test parameters, but the extent to which the fines affect the actual residual strength (as compared to affecting the insitu test parameter) is not clear. If fines affect different insitu tests differently, then the definition of fines would desirably be test-specific. Because coarse silts (with bulky particle shape and no plasticity) behave similarly to fine sands, however, it would seem desirable to introduce the notion of plasticity into the definition of fines. As plastic fines are introduced, the potential for different fabrics increases; this may have a significant effect on normalized residual strengths which are influenced by initial conditions.

Simple calculations are all that are required to show that the normalized strength concept is valid when the consolidation curve is parallel (on a semi-log plot) to the steady state line. Experimental data seems to suggest that the two curves are at least approximately parallel, though variability of the consolidation curve for clean sands (depending on method of deposition, etc.) and overconsolidation would be expected to influence the residual strength ratio. Because of these effects, correlation of the residual strength ratio to $(N_1)_{60}$ or q_c appears very logical, at least to the extent that factors such as fabric, OCR, etc. are consistently reflected in insitu test results. The validity of the normalized strength concept appears to be weakest at low effective confining pressures where the consolidation curve and steady state line are flat and unlikely to be parallel.

The quasi-steady state can be reached in monotonic loading tests on moderately loose specimens. Because it occurs at lower strain levels than the steady state, the soil retains enough of its original fabric to be influenced by it. Hence, the quasi-steady state is not unique. Data clearly showing development of a quasi-steady state in cyclic simple shear tests on highly contractive, anisotropically consolidated soils would be useful. However, the quasi-steady state does not appear central to the discussions of this workshop because it does not control flow failure stability and it is not a fundamental state upon which constitutive models can be based.

APPENDIX B.
Written Statements by Shear Strength of Liquefied Soils from Laboratory and Field Tests Discussion Group Participants

* =Keynote Speaker
** =Recording Secretary

Wayne A. Charlie (Colorado State University)
Pedro A. de Alba (University of New Hampshire)
Jason E. Hedien (Harza Engineering Co.)
Bruce L. Kutter (University of California @ Davis)
*Geoffrey R. Martin (University of Southern California)
Gholamreza Mesri (University of Illinois @ Urbana-Champaign)
Scott M. Olson (University of Illinois, formerly Woodward-Clyde Consultants)
Steve J. Poulos (GEI Consultants, Incorporated)
Michael F. Riemer (University of California @ Berkeley)
**Peter K. Robertson (University of Alberta)

MEASUREMENT OF POST-LIQUEFACTION SHEAR STRENGTH FROM PIEZOVANE (Tm) FIELD TESTS

W.A. Charlie[1], T.J. Siller[2], and D.O. Doehring[3]
Colorado State University
Fort Collins, CO 80523

DESCRIPTION

This paper presents the result of the first in-situ field test of the Piezovane, a vane shear device equipped with, 1) a transducer to measure changes in pore water pressure to identify contractive and hence, liquefiable solid and 2) a transducer to measure torque to determine shear strength.

APPLICATION

Piezovane tests were conducted adjacent to the Southern Pacific Railroad Bridge south of Watsonville, California. The bridge is supported on piles driven into saturated, sandy, young sediments deposited in meandering stream and estuarine environments. Ground liquefaction induced by both the 1906 San Francisco and 1989 Loma Prieta earthquake resulted in pile settlement and lateral spreading.

RESULTS

This study applied and evaluated the Piezovane, a new field device that identifies soils susceptible to liquefaction-induced lateral spreading and flow failure. Field measurement of shear induced pore pressure changes indicates that the Piezovane identifies contractive and dilative cohesionless soils. Contractive or dilative soil horizons at the SP Bridge site are shown as zones of positive or negative peak induced pore pressure change during Piezovane shearing. Contractive soil horizons have potential for significant lateral spreading. The contractive zones are located at 5.8, 6.7, and 7.5 meters at the SP Bridge site. Comparison of evidence for liquefaction potential indicated by other site tests and geology support the Piezovane test results (Figure 1). The Piezovane recorded positive pore pressures in soil horizons that appear to be the source of sand boils from the 1989 Loma Prieta Earthquake. Contractive sands identified by the Piezovane are consistently within ground that experienced extensive lateral spreading during the same earthquake. The location of the positive pore pressures are in sands that have the highest level ground liquefaction potential as indicated by standard penetration and cone penetrometer tests.

---

[1]Professor of Civil Engineering

[2]Associate Professor of Civil Engineering

[3]Professor of Earth Resources

This study also measured the torque required to rotate the Piezovane. The soil's shear strength was calculated from the torque by an equation given by Brislawn (1992). Figures 2 and 3 give typical torque and pore water pressure response as a function of angle rotated for contractive and dilative sand, respectively. Peak Piezovane shear strength as a function of depth is shown on Figure 1. Figure 4 shows the relationship between the Piezovane's measured residual shear strength and the SPT blow count for several sites that liquefied and had sliding as a result of the Loma Prieta Earthquake. The Southern Pacific Bridge site (SP 48) plots on the high side of the relationship.

SIGNIFICANCE

The advantage of the Piezovane is that it directly measures the soil property (pore pressure during shearing) associated with liquefaction and measures the soils shear strength and a function of rotation.

ACKNOWLEDGMENTS, TRADEMARKS AND PATENT

Funding for this research was provided by the National Science Foundation (Award No. 9011319; Clifford J. Astill, Program Officer) as part of the National Earthquake Hazards Reduction Program. Additional funding was provided by AFOSR. Drs. Tom L. Holzer, John C. Tinsley, and Michael J. Bennett of the U.S. Geological Survey in Menlo Park, California provided invaluable technical information and advice as well as site access, site maps, and geotechnical data. Professor C. Peter Wroth of Oxford University encouraged us to experimentally test our concept. Piezovane and CSU Piezovane are trademarks of Colorado State University. The concept is protected by U.S. Patent Number 5109702.

PUBLICATIONS RELATING TO THE PIEZOVANE

Atkinson, J.H., and Jessett, J.H., 1990, "Measurement of Relative Density of Saturated Sand Using the Piezovane," Field Testing in Engineering Geology, Engineering Geology Special Publication No. 6, Geological Society of London, 229-233.

Brislawn, J., "Direct Measurement of Liquefaction Potential," M.S. Thesis,Colorado State University, Dept. of Earth Resources, Spring 1992, Advisors: W.A. Charlie and D.O. Doehring.

Butler, L.W., "Development of the Piezovane for Estimating Liquefaction Potential of Saturated Sands," M.S. Thesis, Colorado State University, Department of Civil Engineering, Fall 1994, Advisor: W.A. Charlie.

Charlie, W.A. and Butler, W., " A Method for Determining Liquefaction Potential of Cohesionless Soil: Piezovane," U.S. Patent Number 5109702, Air Force Invention No. 18,634, Declaration for Patent Application (1990), Patent Pending, (1991), Patent Accepted (1992), U.S. Patent and Trademark Office, Washington, D.C.

Charlie, W.A., Doehring, D.O., Brislawn, J.P., Hassen, H.A., Siller, T., "Loma Prieta Earthquake: Piezovane, SPT and CPT Evaluations of Liquefaction in Monterey County California,"

Chapter in Performance of Ground and Soil Structures During Earthquakes, K. Ishihara Editor, Special Volume, Int. Society for Soil Mech. and Fdn. Engineering, January 1994.

Charlie, W.A., Doehring, D.O., "Direct Measurement of Liquefaction Potential of Soils Supporting Pile Foundations," 46th Annual Canadien Geotechnical Conference, Saskatoon, Saskatchewan, Canada, September 27-29, 1993.

Charlie, W.A., Siller, T.J., Scott, C.E., Butler, W. and Doehring, D.O., "Estimating Liquefaction Potential of Sands using the CSU Piezovane," Geotechnique, The Institution of Civil Engineers, U.K., Vol. 45, No. 1, January 1995.

Charlie, W.A., Brislawn, J.P., Doehring, D.O. and Hassen, H., "Site Liquefaction Potential using the CSU- Piezovane: Monterey County, California," NEHRP Report to Congress on the 1989 Loma Prieta Earthquake, USGS Professional Paper, No. 1551-B, 1997 (in press).

Charlie, W.A., Doehring, D.O., Brislawn, J.P., Scott, C.E., and Butler, L.W., "Liquefaction Evaluation with the CSU Piezovane," Int. Society for Soil Mech. and Fdn. Engineering, Vol. 2, No. 13, January 1994.

Seed, R.B., and Harder, L.F., "SPT-Based Analysis of Cyclic Pore Pressure Generation and Undrained Residual Strength," Memorial Symposium for H. Bolton Seed, Edited by Duncan, J.M., BiTech Publishers, Vancouver, B.C., Canada, pp 351-376. May 1990.

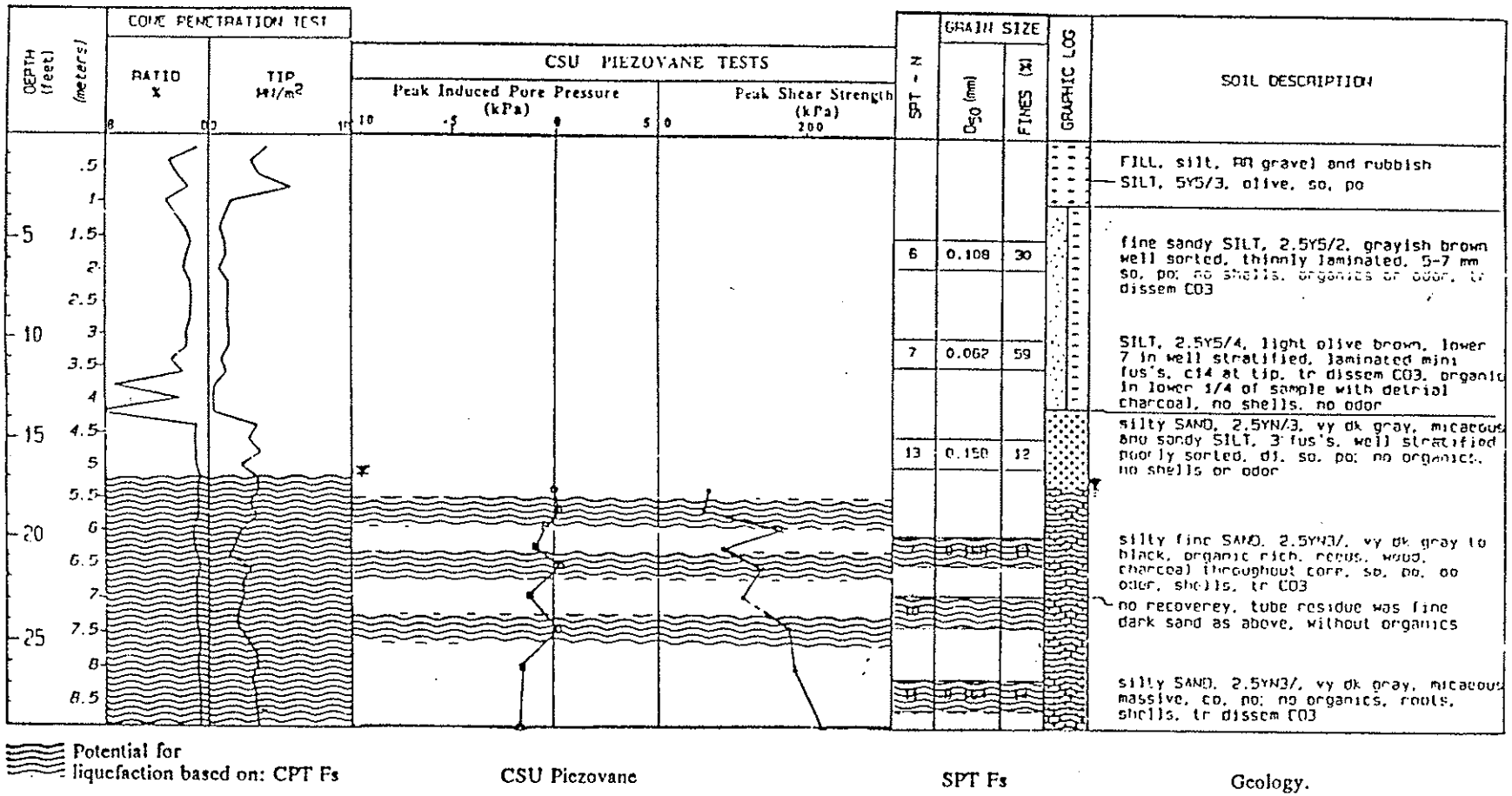

Figure 1. Sediments and testing, SP Bridge BH 48.

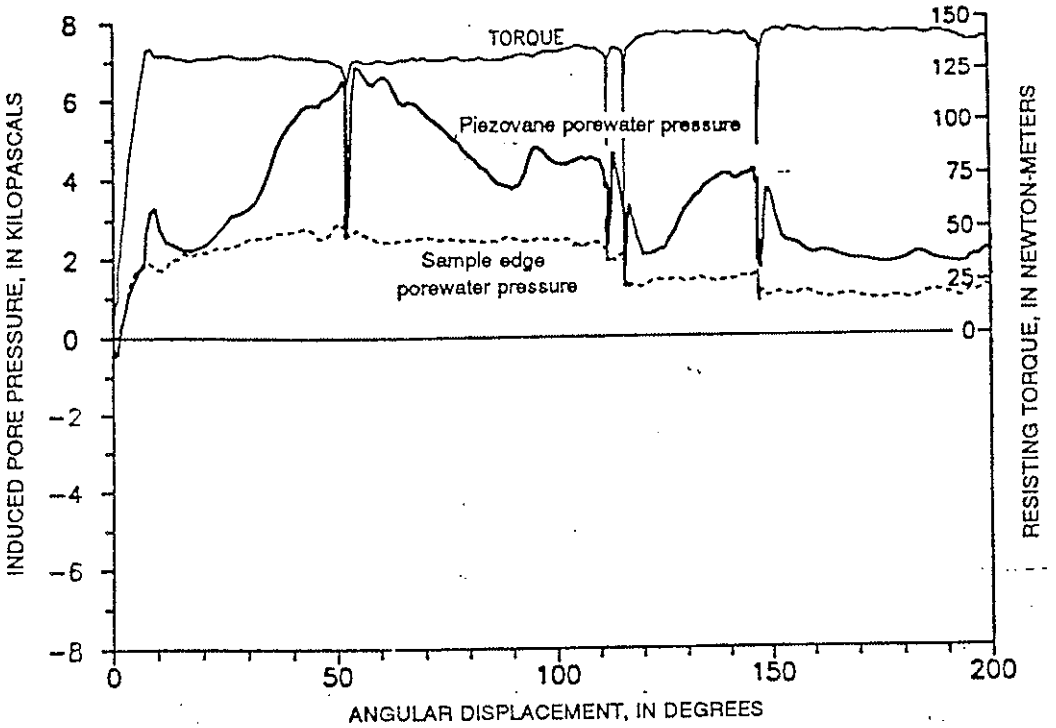

Figure 2. Piezovane induced pore pressure and resisting torque versus angular displacement for contractive sand.

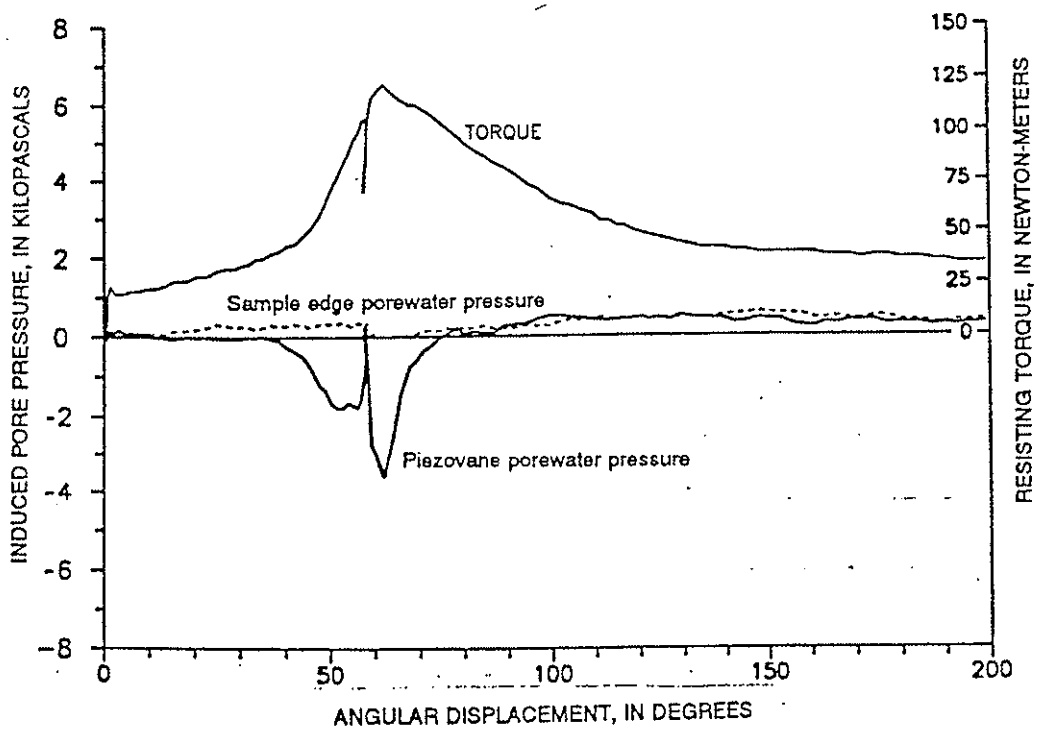

Figure 3. Piezovane induced pore pressure and resisting torque versus angular displacement for dilative sand.

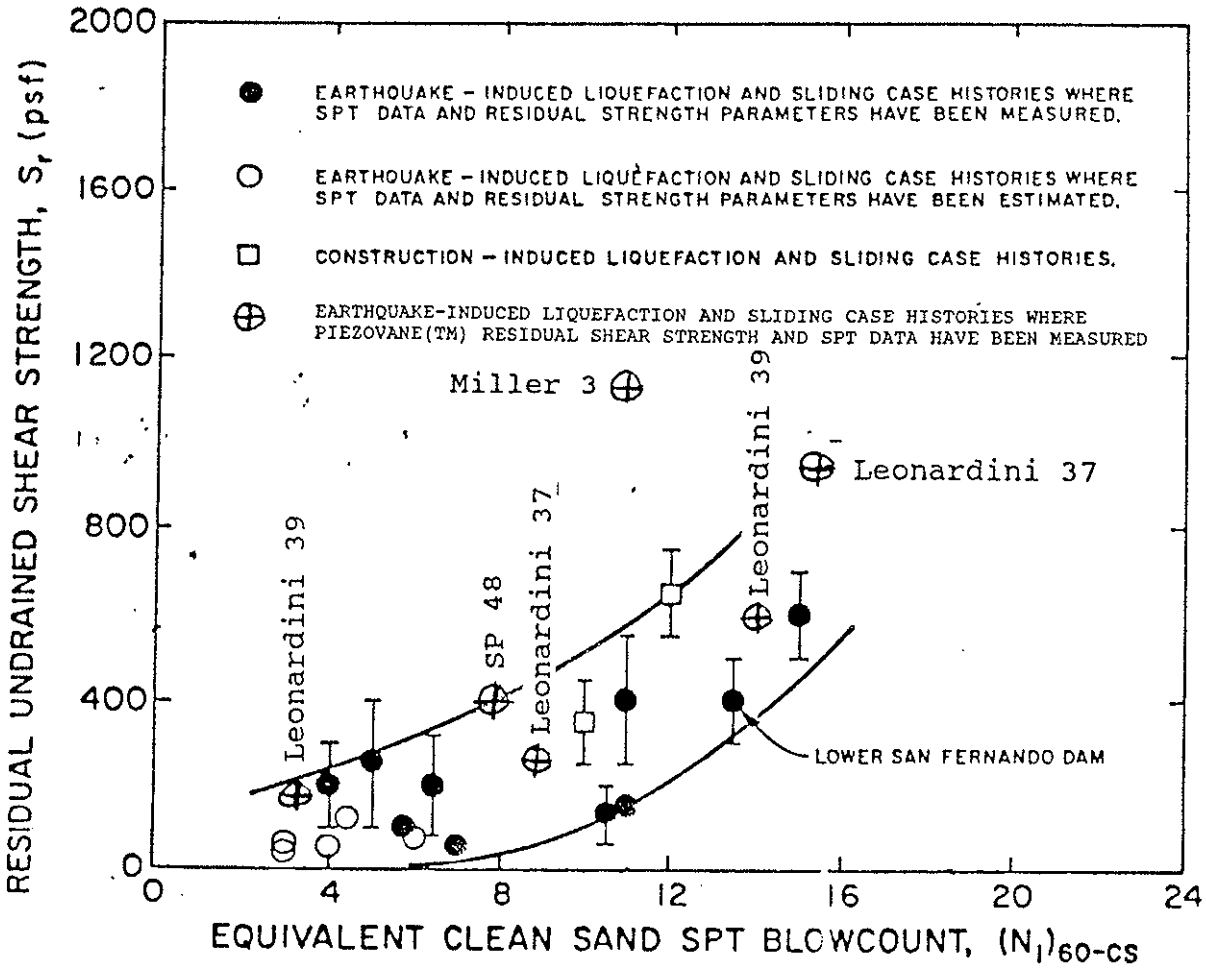

Figure 4. Relationship between Piezovane(TM) measured "undrained" residual strength and SPT blow-count versus undrained residual strength and SPT blow-count reported by Seed and Harder (1990).

Workshop on Post-liquefaction Shear Strength of Granular Soils.

Post Liquefaction Shear Strength from Laboratory and Field Tests.

Issues and Questions

Pedro de Alba, University of New Hampshire

A survey of the substantial literature on post-liquefaction behavior shows basically that, in order to further advance our understanding of this behavior, and in order to transfer laboratory results to the field, we need new types of tests. In 1992, Marcuson et al. stated that "Laboratory testing... is clouded by all the characteristics of an "undisturbed sample" and our inability to properly simulate stress and deformation conditions in the laboratory." This statement certainly remains true as far as current laboratory testing methods are concerned.

It is my contention that we can, with a great deal of trouble and expense, recover undisturbed samples from the field by ground freezing. It is possible that we may soon be able to better characterize the field deposit, and identify critical zones for sampling, by measuring void ratio distribution with the resistivity cone, or other electrical techniques (Bellotti et al, 1994; Morabito, in progress). However, we currently have no way of testing the materials recovered in such a way as to model what actually happens during post-liquefaction failure of contractive soils.

The most logically consistent attempt to relate laboratory test data to field behavior is that of Stark and Mesri (1992). In this approach, cyclic stresses required for triggering of liquefaction of undisturbed samples (presumably obtained by ground freezing) in triaxial compression tests are used to obtain an equivalent SPT blowcount, and this in turn is used to obtain an undrained residual (critical) strength. In this approach, the triaxial yield strength is really used as an index property; this is not an attempt to model actual post-liquefaction field behavior in the lab for a specific case.

As far as actual modeling is concerned, triaxial tests can only be compared to other triaxial tests, and the application of residual strengths measured in triaxial tests to an actual field deposit is a dubious exercise at best. The triaxial device simply cannot model certain critical aspects of post-liquefaction behavior, primarily related to the strain levels which can be produced.

Triaxial samples cannot be deformed beyond 20-25% axial strain without becoming so distorted that stress calculations become meaningless. Verdugo et al. (1995) state that in their triaxial tests, natural non-homogenous structures "... cannot be broken down even at large deformations." To support this conclusion, they point to the fact that the steady-state strengths for "undisturbed" samples of well-graded materials consistently plot above the steady-state line for uniformly reconstituted samples of the same material, even though in theory all initial fabric effects should have been erased. This conclusion is also supported by the tests on remolded discontinuously wet pluviated (RDWP) specimens

of the San Fernando Dam material by Vasquez-Herrera and Dobry (1988), where, again, the steady-state strengths consistently plot above those from uniformly reconstituted samples.

Eckersley's (1990) tests on model embankments of well-graded angular coal clearly show that flow sliding concentrates in relatively narrow shear zones in which the shear strains can be several hundred percent; similar strain levels can be inferred from flow slides in Chilean dams (de Alba et al., 1987). At these very large strain levels, in anything but uniform materials, a flow structure with extensive particle reorientation (and possibly segregation) must develop which cannot be modeled by triaxial, DSS, or torsional shear tests in current use.

There is also the vexing problem of potential water content redistribution, and formation of a layer of very high water content material along an impervious interface after large deformation, first suggested by Seed (1986); this obviously is impossible to model convincingly using current equipment, and until we find ways to observe whether this happens under controlled conditions, may remain a major unknown in interpretation of some field observations. This problem is also related to that of partial drainage; it would be very interesting to see what the effect of allowing some level of dissipation of pore pressures would be, after large deformations. It is interesting to note in this respect that Eckersley (1990) observed that entrapped air in his well-graded coal banks did not seem to inhibit flowsliding.

We have known for a long time that residual strength is extremely sensitive to relatively minor changes in soil gradation and void ratio. Ultimately, characterization of a field deposit will require extensive in-situ testing to identify the most vulnerable zones. Given the difficulties involved in recovering undisturbed samples, and in testing then so as to reproduce field stress and deformation conditions, the only practical way to do this for a specific design problem seems to be by establishing a relationship between a relatively simple and robust in-situ test and the residual strength. Ideally, this test would be capable of much finer discrimination than the SPT.

The major role of laboratory research in establishing such a relationship is in designing a large-scale test or tests which would allow very large strains to develop in undrained conditions. Ideally, these tests would be on a large enough scale that miniature (or full-scale) field tools could be used to make measurements in specimens which would then be liquefied. It is essential in these experiments to test well-graded materials, deposited so as to form the same kinds of complex fabrics which may exist in the field. Parallel triaxial testing would show to what extent triaxial tests are able to model post-liquefaction behavior of soils with complex initial fabric, and to what extent results from these tests can be used as index properties for the study of field deposits.

While discussion to this point has focused on contractive materials subject to flowsliding, there is another important aspect to post- liquefaction behavior, which is the behavior of structures supported on granular soils which are dilative at large strains, but which allow significant deformations to take place during cyclic loading . These soils, with

an $(N_1)_{60}$ of perhaps 15 to 25 bpf, would, in many cases be considered suitable to support structures. Under undrained conditions, model foundations on such materials have been observed to settle significantly as the pore pressure ratio exceeds about 60%-70%, and to continue to settle until shaking stops (de Alba et al., 1976, de Alba, 1983). Further model studies, using shaking tables or the geotechnical centrifuge would be desirable in order to further quantify this behavior, including the effects of partial drainage.

References

Bellotti, R., J. Benoît and P. Morabito (1994), "A Self-Boring Electrical Resistivity Probe for Sands," Proc. XIII ICSMFE, New Dehli

de Alba, P., H. B. Seed and C. K. Chan, (1976), "Sand Liquefaction in Large-Scale Simple Shear Tests," JGED, Vol. 102, No. GT9, September.

de Alba, P. (1983), "Pile Settlement in Liquefying Sand Deposit," JGE, Vol. 109, No. 9, September.

de Alba, P., H. B. Seed, E. Retamal, and R. B. Seed (1988), " Analysis of Dam Failures in 1985 Chilean Earthquake," JGE, vol. 114, No. 12, December.

Eckersley, J. D. (1990), "Instrumented Laboratory Flowslides," Géotechnique, Vol. 40, No. 3, pp. 489-502

Marcuson, W., M. E. Hynes, and A. G. Franklin (1992), " Seismic Stability and Deformation Analyses: the Last 25 years," Proceedings, Stability and Performance of Slopes and Embankments-II, Geotechnical Special Publication 31, Vol. 1, pp. 552-592

Seed, H. B. (1986), "Design Problems in Soil Liquefaction," Earthquake Engineering Research Center Report No. UCB/EERC-86/02, February.

Stark, T, and G. Mesri (1992), " Undrained Shear Strength of Liquefied Sands for Stability Analysis," JGE, Vol. 118, No.11, November, pp. 1727-1747.

Vasquez-Herrera, A. and R. Dobry (1988), "The Behavior of Undrained Contractive Sand and its Effect on Seismic Liquefaction Flow Failures of Earth Structures," Research Report, Dept. of Civil Engineering, Rensselaer Polytechnic Institute.

Verdugo, R., P. Castillo and L. Briceño (1995), "Initial Soil Structure and Steady-State Strength," Proc. Earthquake Geotechnical Engineering, K. Ishihara (ed.), Balkema, pub., pp. 209-214.

STRENGTH OF LIQUEFIED SOIL IS NOT A MATERIAL CONSTANT; LIQUEFACTION IS A BOUNDARY VALUE PROBLEM

Pre-Workshop Written Statement - March 18, 1997

Bruce L. Kutter
University of California @ Davis

INTRODUCTION: CONCEPTUAL ISSUES

From fundamental principles, it is easy to argue that the strength of liquefied soil is not a material constant; it is dependent on boundary conditions and layer geometry. The basic steps in one such argument are:

1. A critical hydraulic gradient exists in a liquefied soil deposit.

2. Upward flow of water occurs due to this hydraulic gradient.

3. Flow of water causes changes in void ratio (void redistribution).

4. Undrained shear strength is highly sensitive to void ratio.

5. Liquefaction causes changes in undrained shear strength.

To evaluate the strength of liquefied soil, we need to answer the following questions:

A) How much void redistribution is likely to occur?

B) Is the void redistribution rapid enough to affect the strength during shaking, and

C) Is it conservative to ignore void redistribution?

The amount of void redistribution is related to the densification of the soil. For example if the average ultimate volumetric strain of a 10 m thick liquefied soil deposit is 1%, then 10 cm of water will be ejected from the densifying soil; this water will be available to be absorbed by a

dilating shear zone. A 10 cm thick layer of water is enough to reduce the dry density of the top 1 m of soil by about 10%; (enough to reduce the relative density by about 50%, say from D_r = 50% to D_r = 0%).

How fast does this water move? By Darcy's law, the flow is v = ki, and i_{crit} is about 1. If the permeability of the liquefied soil is 10^{-2} cm/s (medium sand), then we can estimate that in 10 seconds of shaking, 1 mm of water is produced (enough to fully soften a 1 cm thick sand layer). It might take on the order of 1000 seconds for all 10 cm of water to be ejected (enough to fully soften a 1 m thick sand layer). Observations from centrifuge tests (e.g. Fiegel and Kutter, 1994) indicate that the permeability of liquefied soil can be orders of magnitude larger than that measured in a conventional test. The increase in permeability is consistent with observations of cracks, piping, and boiling that are associated with liquefaction.

Evidence that void redistribution is important comes from the San Fernando case history. The failure did not occur immediately after shaking; it occurred some 90 seconds after the shaking stopped. Pore pressures generated in loose zones could have fed the dilation of a failure zone. When the void ratio increased to the point where the undrained shear strength fell below the driving stresses, a sudden failure developed. The time required for void redistribution in San Fernando Dam might explain the 90 second delay.

Void redistribution can also explain why the back calculated strengths of liquefied soil are less than those determined from undrained compression tests on "uniform" soil elements. The Seed and Harder (1990) relationship between residual strength and blowcount indicates that at a (N1)60 of 10, the residual undrained shear strength can range between 50 and 500. Void redistribution could explain scatter in the back-calculated values. Void redistribution will depend on factors such as the permeability and layer thickness; not accounting for these factors could lead to significant scatter. Recent centrifuge data obtained at UCD and elsewhere point to special cases where the mobilized undrained strength can also fall below the wide range of data given by Seed and Harder (1990).

Research must be focused on attempting to understand and predict the locations, magnitude, and rate of void redistribution. The post-liquefaction shear strength is not a material constant. It will depend on the volumetric strain, thickness, permeability, drainage boundaries, and uniformity of the soil layers.

SPECIFIC ANSWERS TO QUESTIONS POSED BY THE CONFERENCE ORGANIZERS:

Is post-liquefaction shear strength proportional to the initial effective vertical stress or some other parameter?

The critical state concept is applicable, but this states that the shear strength is a function of the void ratio at failure. Because there is some correlation between consolidation pressure and void

ratio (especially for very loose sands), there may be a secondary correlation between consolidation pressure and undrained shear strength. Void ratio will affect the critical state effective stresses, and void ratio will change by void redistribution. Hence there may be a correlation between consolidation stress and post liquefaction undrained strength, but not a unique relationship.

What are the suitable sampling and testing procedures for examining post liquefaction undrained strength?

Because post liquefaction undrained strength is not a unique material property, the answer will depend on sample geometry, permeability, boundary conditions void redistribution and probably other factors. We must admit that post liquefaction undrained strength is not a constant and try instead to determine how to evaluate the many factors that affect the undrained strength. Centrifuge testing is useful for looking at void redistribution. Other laboratory tests may also be used if we analyze them as a boundary value problems, and not as element tests.

Effects of undrained stress path on laboratory measure post liquefaction undrained strength.

There is evidence that sandy soils are much more contractive in triaxial extension than in triaxial compression (e.g., Riemer and Seed 1992). Thus one would expect a smaller strength for extension than compression. Simple shear should be in between.

Effects of fines on laboratory measured post liquefaction undrained strength.

One important effect of fines is the reduction in the permeability. The lower is the permeability, the better is the "undrained" assumption. Permeable soils are subject to rapid void re-distribution. Fine particles are not as sensitive to vibration as coarse grained particles, (their specific surface is greater) hence shaking has a smaller tendency to densify the fines.

Effects of strain rate on laboratory-measured post-liquefaction shear strength.

Strain rate effects are known to be substantial for clayey soils, and less so for granular soils. For a given strain amplitude, the rate of static straining compared to the rate of pore pressure dissipation will affect the amount of drainage that can occur, hence it will affect the mobilized shear strength of permeable soils.

Suitable techniques for estimating in-situ void ratio and state parameter?

There is not too much value in accurately measuring the void ratio if it is likely to change as a result of void redistribution. If one can prove that void re-distribution is not an issue, the procedures outlined by Poulos et al. (1985) is reasonable.

What role should centrifuge tests play in this research. What are the advantages and disadvantages of the centrifuge in estimating the post-liquefaction shear strength? What has been learned about the post-liquefaction shear strength and/or behavior of granular soils from the centrifuge?

By measuring the distributions of pore pressures, accelerations, and by dissecting models to observe deformation mechanisms, centrifuge testing has taught us that liquefaction is a boundary value problem. Cracking, boils, gaps, and interfaces open, slide and close. We have observed large deformations for soils that have huge undrained steady state strengths. Sliding and deformation can occur due to distributed strains with cyclic mobility or localized strains in dilated shear zones as a result of void redistribution. An important research topic that could be addressed on the centrifuge would be to systematically investigate the factors that affect the void redistribution and consequently the factors that affect the steady critical residual "undrained (?)" strength.

REFERENCES

Fiegel, G.F. and Kutter, B.L. (1994) "Liquefaction Induced Lateral Spreading of Mildly Sloping Ground" J. Geotech. Engr., ASCE 120, No. 12, pp. 2236-2243.

National Research Council (1985) Liquefaction of Soils During Earthquakes, National Academy Press, Washington, D.CC., 240 pp.

Poulos, S.J., Castro, G., and France, J.W. (1985) "Liquefaction evaluation procedure," J. Geotech. Engr., ASCE, 111(6), 772-792.

Riemer, M.J., and Seed, R.B. (1992). "Observed effects of testing conditions on the residual strength of loose, saturated sands at large strains," Proc. 4th Japan U.S. Workshop on Earthquake Resistant Design of Lifeline Facilities and Countermeasures for Soil Liquefaction, M. Hamada and T.D. O'Rourke, eds., Tech. Report NCEER-92-0019, National Center for Earthquake Engineering Research, Buffalo, New York, Vol. 1, pp. 223-238.

Seed, R.B. and Harder, L.F. (1990). "SPT-based analysis of cyclic pore pressure generation and undrained residual strength," Proc. H. Bolton Seed Memorial Symposium, University of California, Berkeley, Vol. 2, pp. 351-376.

Undrained Shear Strength of Liquefied Sands

Pre-Workshop Statement by G. Mesri

Liquefaction is here defined as a contractive tendency that when triggered under an undrained condition generates large positive porewater pressures, decreasing shearing resistance to the critical value, s_u (critical), Fig. 1. The shear stresses that trigger the contractive tendency are called yield strength, s_u (yield). Various shearing modes resulting in different shear stress-shear strain paths result in different values of s_u (yield).

Among other topics, the Workshop should consider the following issues:

1. The rationale for normalizing s_u (critical) with respect to vertical consolidation pressure, σ'_{vo}.
2. The best approach for evaluating s_u (critical) for stability analysis of pre-failure geometries.
3. Granular soil deposits and configurations for which partial drainage during liquefaction is possible and should be systematically taken into account in selecting s_u (critical) for stability analysis of pre-failure geometry.

1. The Rationale for Normalizing s_u (critical)

The undrained critical strength of liquefied sands is normalized with respect to vertical consolidation pressure for two separate objectives. The normalizing is done for:

A. Interpreting and explaining the measured or back-calculated magnitudes of s_u (critical).

B. Developing empirical correlations for generalizing and extrapolating an existing database on s_u (critical).

The first objective cannot be criticized even for clean sands because if one has measured s_u (critical, DSS) at consolidation pressure σ'_{vc} or has back-calculated s_u (critical, mob) for a field sublayer with consolidation pressure σ'_{vo}, then filing the data in terms of s_u (critical, DSS)/σ'_{vc} or s_u (critical, mob)/σ'_{vo} is as reasonable as filing them in terms of s_u (critical, DSS) or s_u (critical, mob). The advantage of the former approach, however, is that one can more readily evaluate the magnitude of undrained critical strength and compare it with other normalized strength parameters such as the measured s_u (yield, DSS)/σ'_{vc} or back-calculated s_u (yield, mob)/σ'_{vo}. To illustrate this point consider the s_u (critical, mob) data in Fig. 2, that were back-calculated by Seed and Harder (1990) for liquefied sand zones or layers using post-failure geometries. It is not at once apparent from Fig. 2 whether these back-calculated values are too small, too large or just the right magnitude because a fundamental expression does not exist for s_u (critical) in terms of the angle of internal friction and effective stress condition during liquefaction. The same s_u (critical, mob) data normalized with respect to σ'_{vo} at midddepth of the liquefied zone are shown in Fig. 3 which also includes a relationship between s_u (yield, mob)/σ'_{vo} and equivalent clean sand SPT blowcount from field cases of liquefaction - no liquefaction (Seed et al. 1984). It is at once clear that in a significant number of cases the back-calculated s_u (critical, mob)/σ'_{vo} is greater than s_u (yield, mob)/σ'_{vo}, and therefore s_u (critical, mob) is greater than s_u (yield, mob). This result suggests that undrained shear strength mobilized in the post-failure geometry was increased, most probably, by partial drainage (Stark and Mesri 1992).

A detailed discussion of the second objective, namely normalizing s_u (critical) with respect to the consolidation pressure in order to extrapolate s_u (critical) data on a sand deposit from one depth with consolidation pressure σ'_{vo} to other depths with larger or smaller consolidation pressures, or to use a s_u (critical) database on one sand deposit with a particular value of $(N_1)_{60}$ for other sand deposits with the same penetration resistance, is beyond the scope of this statement. The issue should be considered by the Workshop.

2. An Approach for Evaluating s_u (critical)

Because empirical data such as those by Seed and Harder (1990) may overestimate undrained shear strength of the liquefied sands at the prefailure geometry, and because alternative approaches that require a precise knowledge of in situ void ratio may not be practical, it is necessary to seek another database on s_u (critical, mob) for stability analysis of liquefied sand layers such as the one in Fig. 4. To simplify the present contribution the permanent consolidation shear stresses that may exist in the sand layer are ignored.

A database for s_u (critical) was developed by Stark and Mesri (1992) using the post-yield critical strength from laboratory tests, normalized with respect to the consolidation pressure σ'_{vc}. A limited number of references were located in the literature in which s_u (yield) and s_u (critical) were both measured directly. Therefore, a number of the data points were obtained from laboratory undrained cyclic shear tests using the assumption that is illustrated in Fig. 5. The s_u (critical, DSS)/σ'_{vo} is assumed to be equal to the s_u (yield, DSS)/σ'_{vo} corresponding to a large number of cycles to liquefaction (100 or more cycles) where undrained yield strength versus N_c levels off. The resulting value of s_u (critical, DSS)/σ'_{vo} is correlated to a $(N_1)_{60}$ which is determined from the s_u (yield, DSS)/σ'_{vo} at N_c=15 (for M=7.5), together with the empirical correlation between s_u (yield, mob)/σ'_{vo} and $(N_1)_{60}$ (Seed et al. 1984)

(Fig. 6). The assumption that s_u (yield, DSS)/σ'_{vo} is equal to s_u (yield, mob)/σ'_{vo} was justified by comparing reliable s_u (yield, DSS)/σ'_{vo}, $(N_1)_{60}$ data to the empirical correlation between s_u (yield, mob)/σ'_{vo} and $(N_1)_{60}$ based on field behavior (Seed et al. 1984), (see Fig. 10, Stark and Mesri 1992). Note that all laboratory data on s_u (yield) and s_u (critical), including those from the cyclic triaxial tests reduced by the correction factor C_r, are here denoted by s_u (yield, DSS) and s_u (critical, DSS).

Based on the laboratory data on s_u (critical, DSS)/σ'_{vc}, together with $(N_1)_{60}$ from s_u (yield, DSS)/σ'_{vc}, and assuming s_u (critical, mob)/σ'_{vo}= s_u (critical, DSS)/σ'_{vc}, the following empirical correlation:

$$s_u \text{ (critical, mob)}/\sigma'_{vo} = 0.006\ (N_1)_{60}$$

was recommended for evaluating undrained shear strength of a liquefied sand for stability analysis of a prefailure geometry (Fig. 7). In this approach only σ'_{vo} and $(N_1)_{60}$ are required for evaluating s_u (critical, mob). Note that the proposed correlation between s_u (critical, mob)/σ'_{vo} and $(N_1)_{60}$ is near the lower bound of the back-calculated data by Seed and Harder (1990). This is interpreted to mean that in a number of the field cases analyzed by Seed and Harder (1990) no drainage took place during liquefaction.

3. Potential Drainage During Liquefaction

The workshop should consider the partial drainage issue together with any dilative tendency that may tend to arrest liquefaction.

References

Seed, H.B., Tokimatsu, K., Harder, L.F., and Chung, R.M. (1984). "The influence of SPT procedures in evaluating soil liquefaction resistance," Earthquake Engineering Research Center, Report No. UCB/EERC-84/15, Univ. of California at Berkeley.

Seed, R.B., and Harder, L.F. (1990). "SPT-based analysis of cyclic pore pressure generation and undrained residual strength." Proc. H.B. Seed Memorial Symp., BiTech Publishing, Vancouver, British Columbia, Canada, 2, 351-376.

Stark, T.D. and Mesri, G. (1992). "Undrained shear strength of liquefied sands for stability analysis," J. Geotech. Eng., ASCE, 118, No. 11, pp. 1727-1747.

s_u(yield), Magnitudes of shear stress that trigger liquefaction

s_u(critical), Shearing resistance available after liquefaction

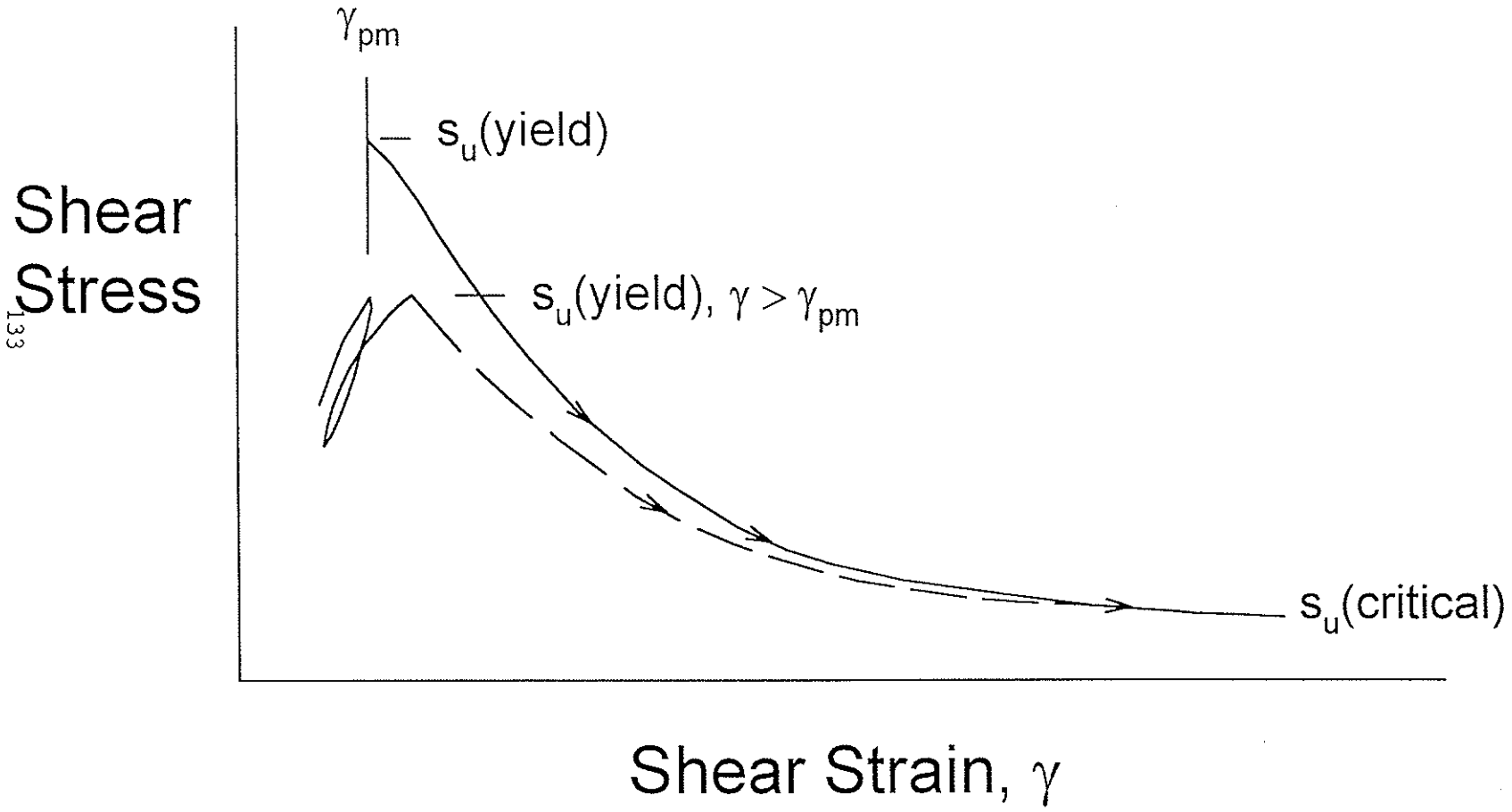

Fig. 1 Definition of s_u (yield) and s_u (critical)

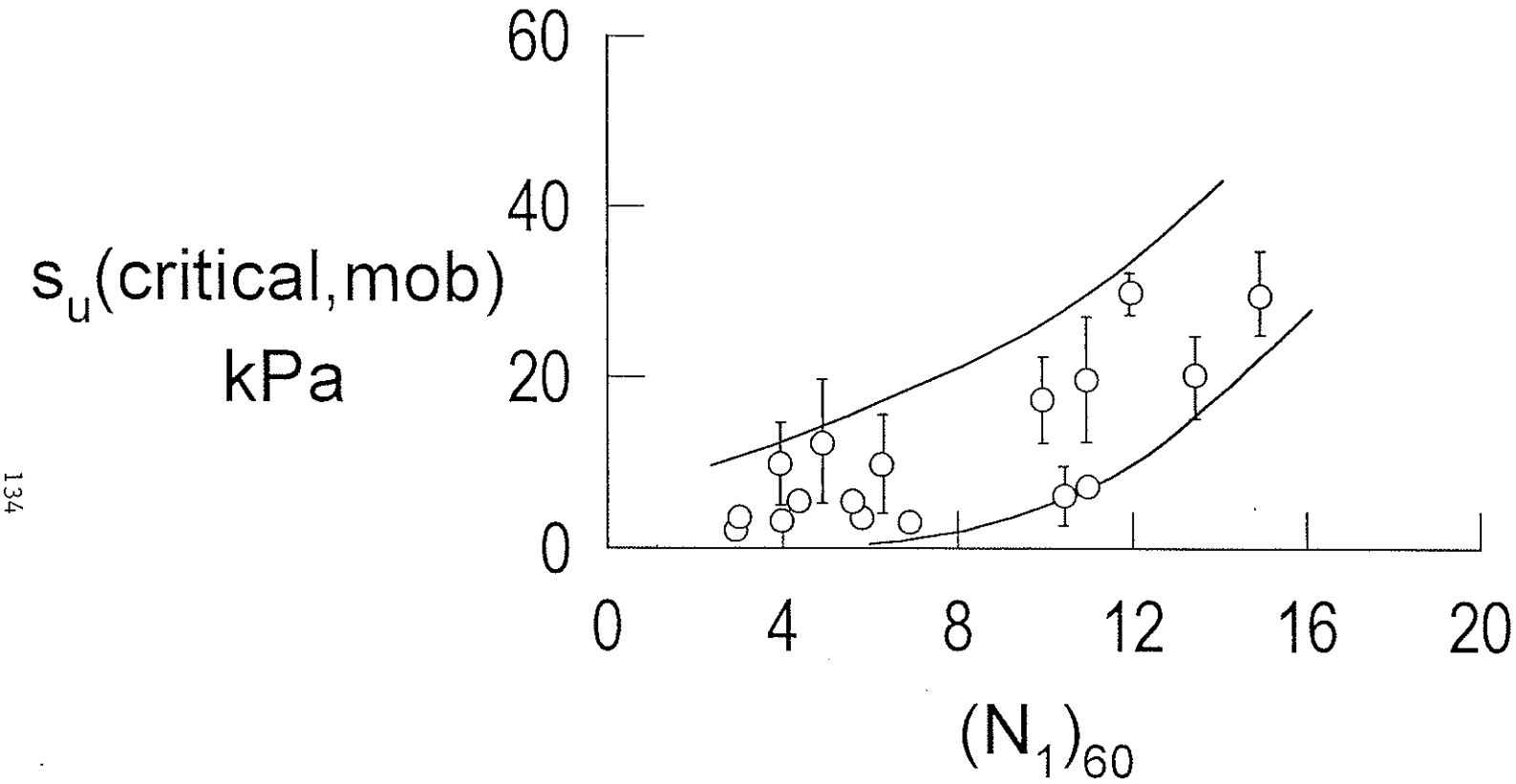

Fig. 2 Undrained critical strength back-calculated from case histories (from Seed and Harder, 1990)

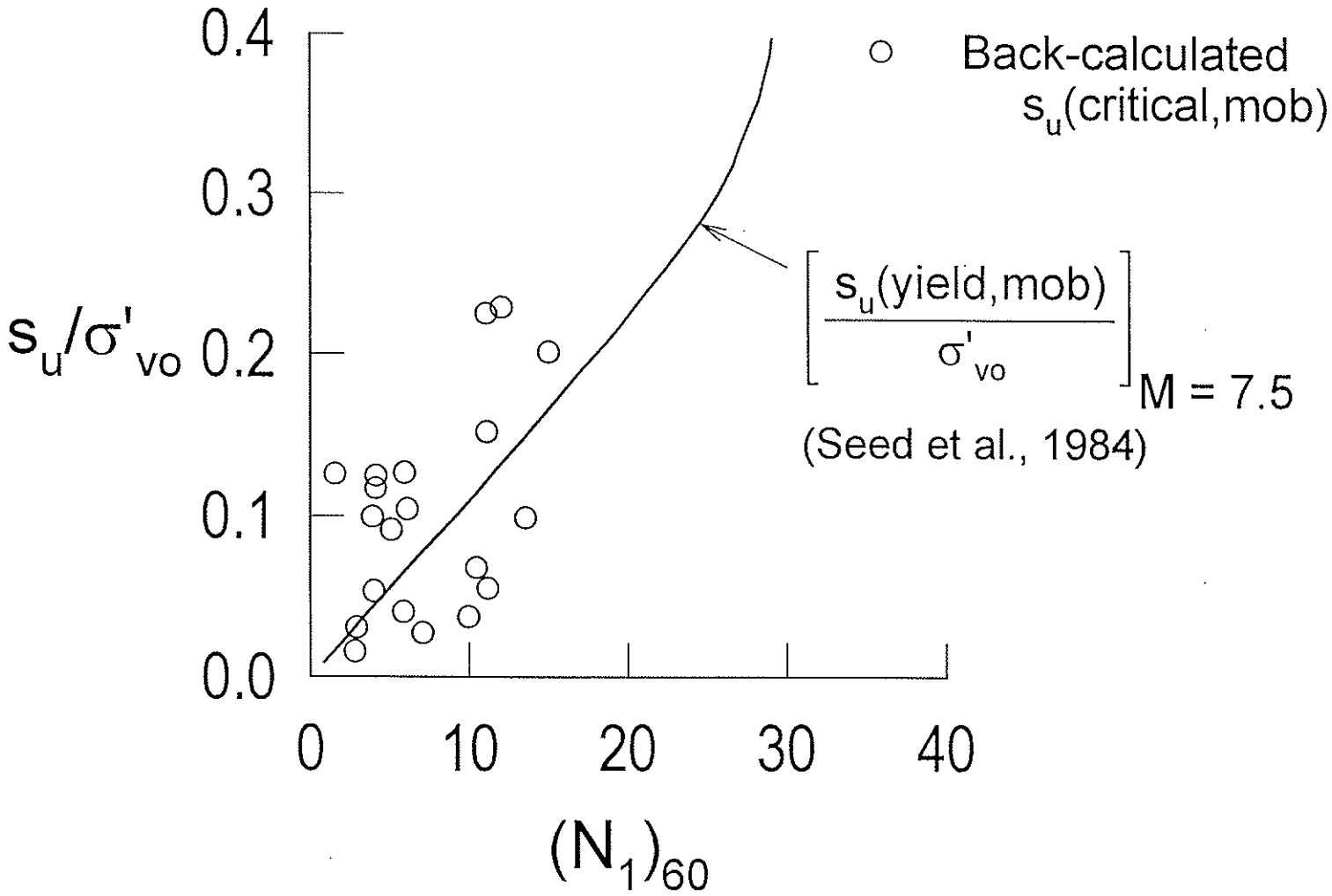

Fig. 3 Back-calculated critical strength normalized with respect to vertical consolidation pressure, σ'_{vo}

Normally Consolidated Young Sand Layer with a Highly Contractive (e_o, σ'_{vo}) Combination

Seismic Response Analysis, M = 7.5, τ(seismic)/σ'_{vo} = 0.15

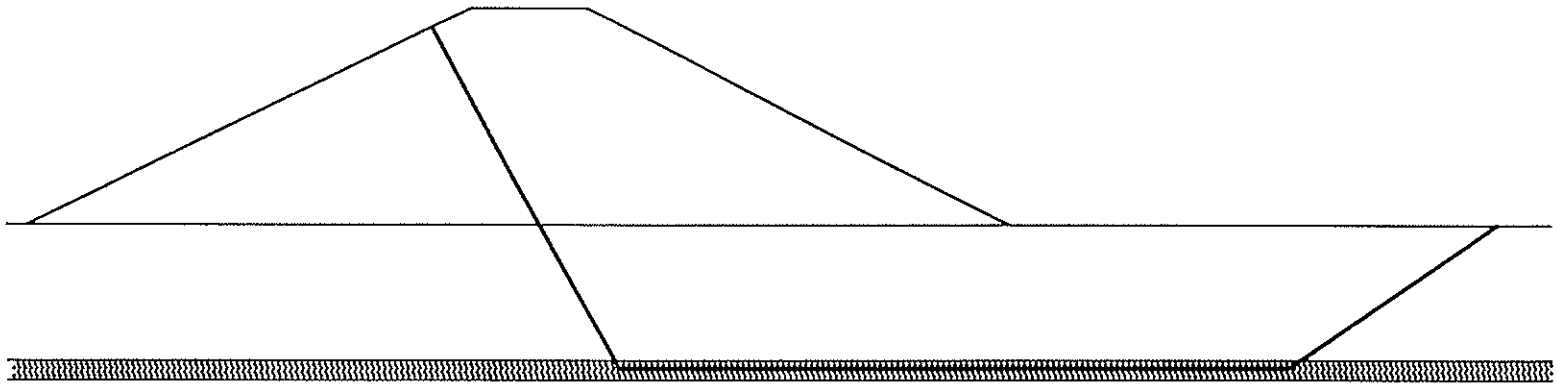

Fig. 4 A liquefied sand layer under an embankment

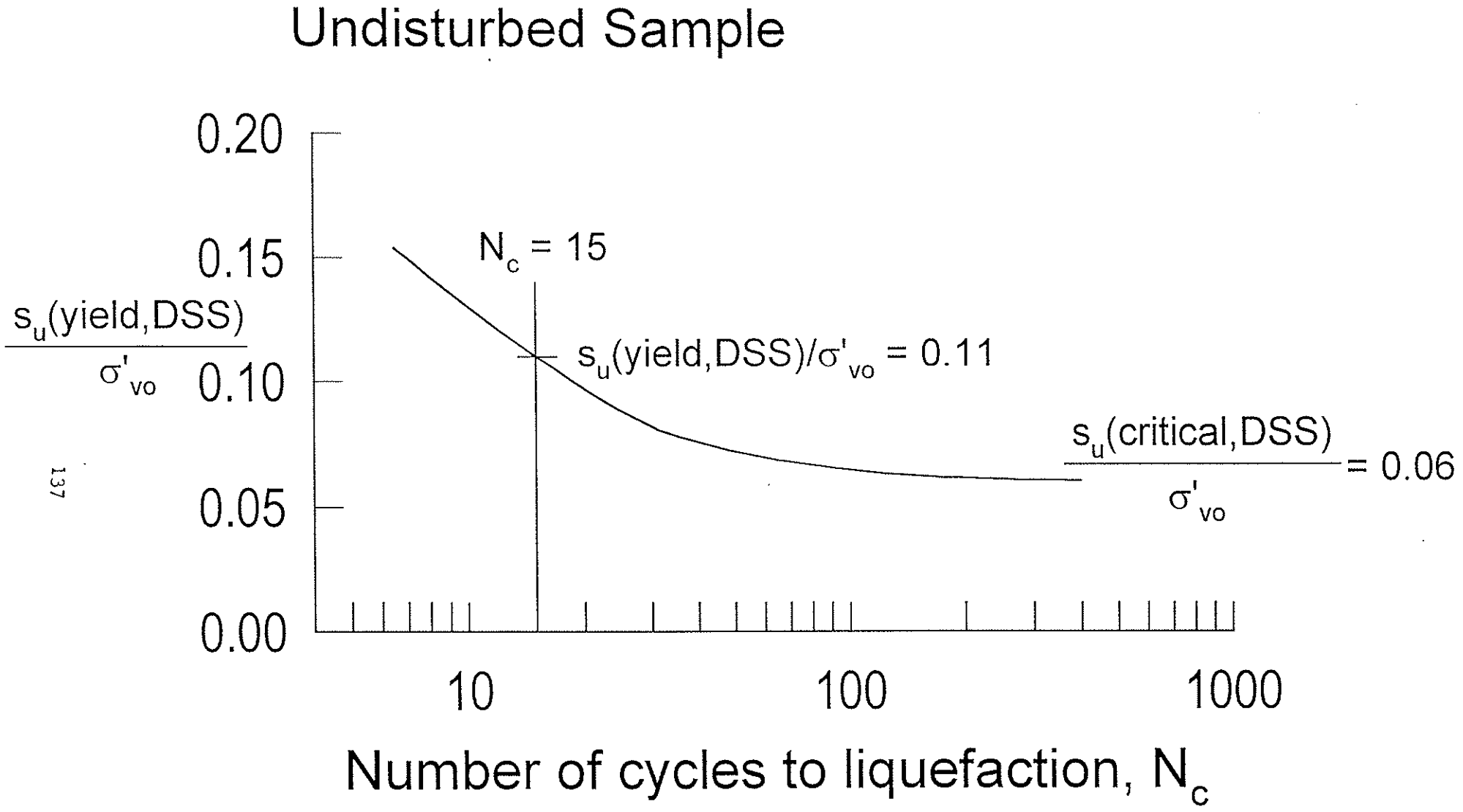

Fig. 5 s_u (critical) estimated from s_u (yield) at a large number of cycles to liquefaction

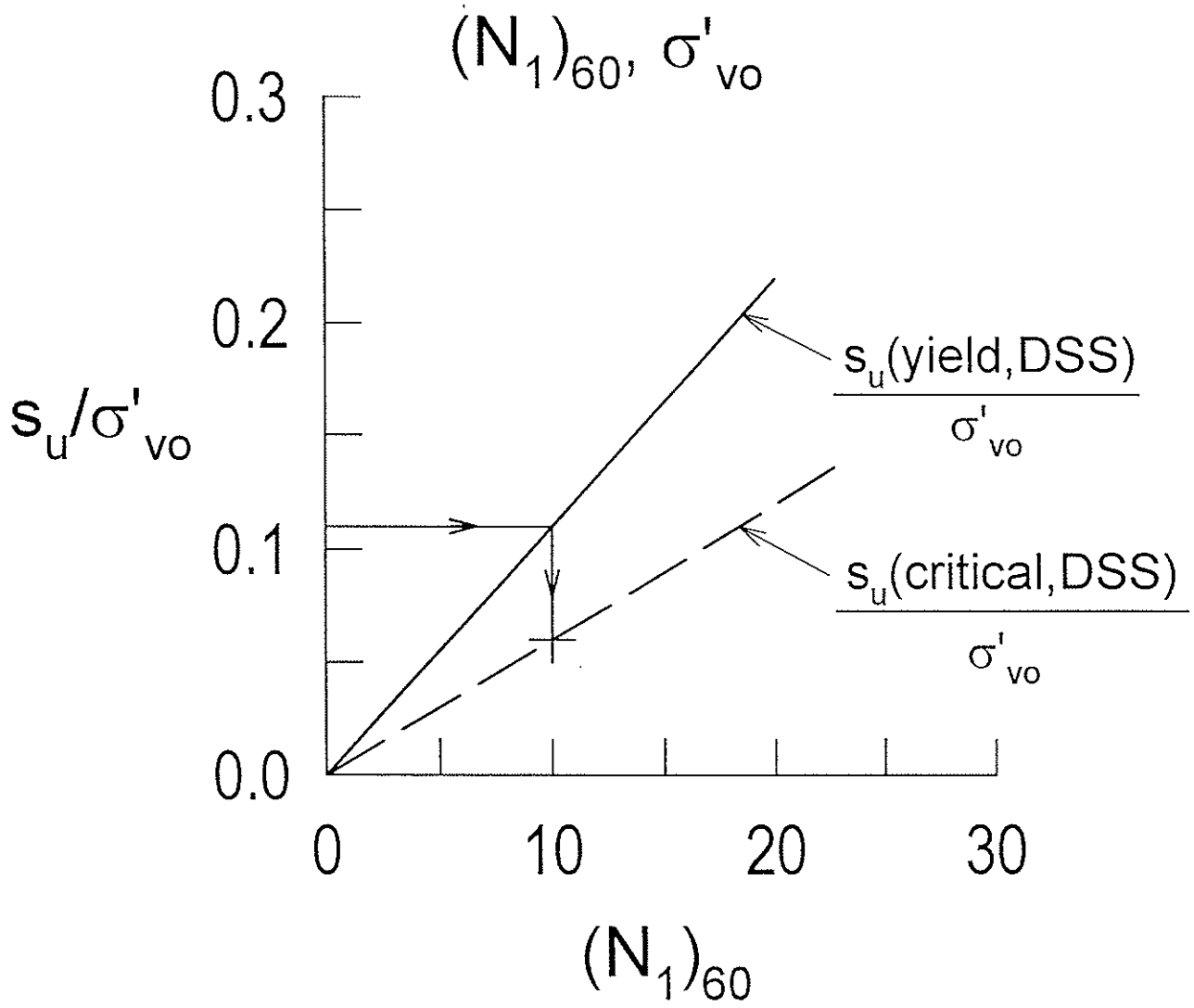

Fig. 6 s_u (critical) correlated to $(N_1)_{60}$ that is estimated using s_u (yield)/σ'_{vo}

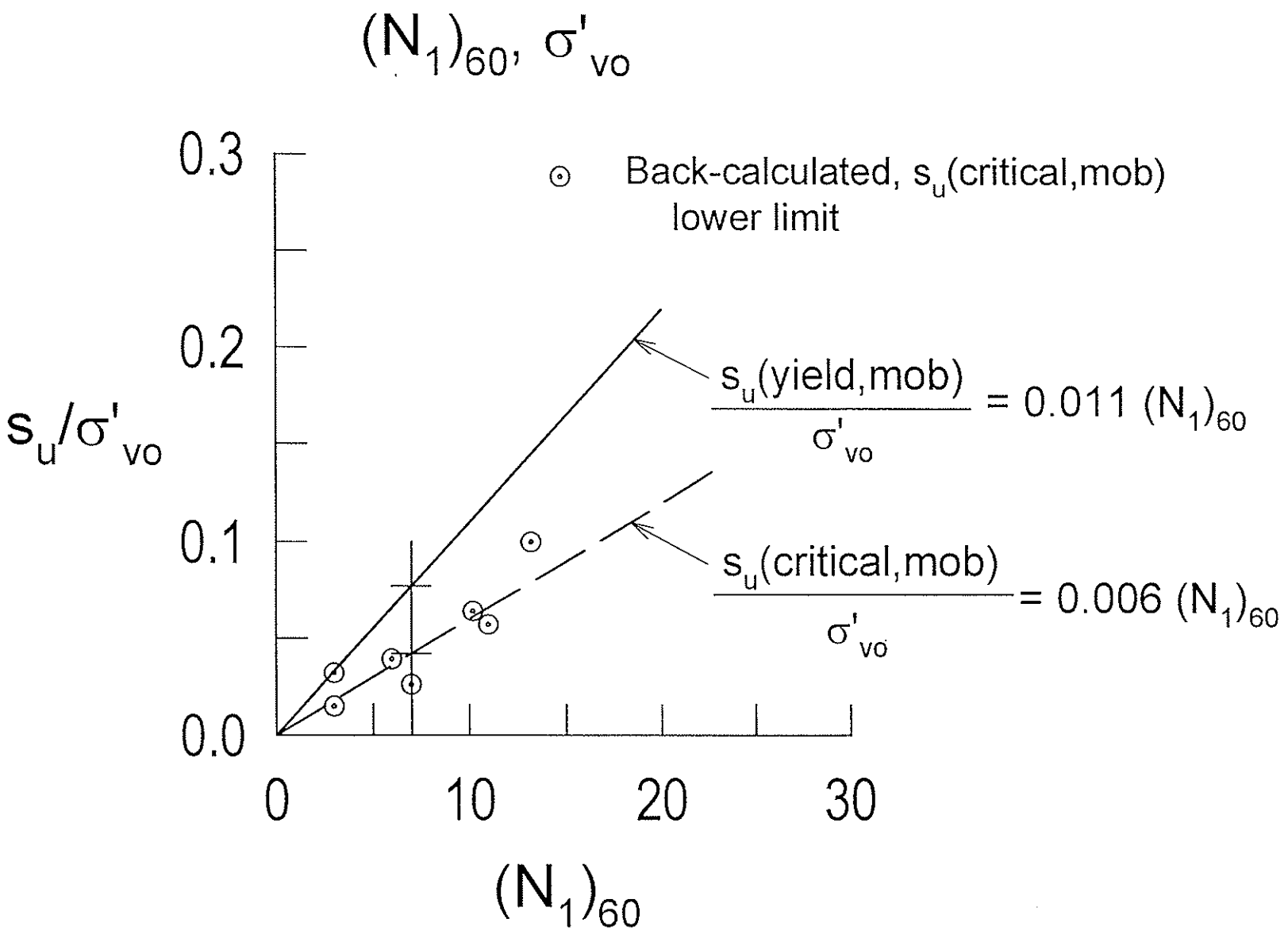

Fig. 7 Empirical correlation between s_u (critical,mob)/σ'_{vo} and $(N_1)_{60}$

DISCUSSION GROUP: POST-LIQUEFACTION SHEAR STRENGTH FROM LABORATORY AND FIELD TESTS:

FIELD TESTS

Scott M. Olson

1.0. FIELD TESTS FOR THE MEASUREMENT OF POST-LIQUEFACTION SHEAR STRENGTH

There are currently (1997), three primary field tests used to estimate the post-liquefaction shear strength of sandy soils. These tests are:

- Standard penetration test (SPT)
- Cone penetration test (CPT)
- Shear wave velocity measurement (V_s)

This section presents the relative merits and limitations of each test method. The estimation of post-liquefaction shear strength from each field test method is discussed in Section 2.0.

1.1. Standard penetration test

The SPT is the most commonly used in situ test for geotechnical exploration. However, the procedures employed for the SPT are different in the U.S. and around the world (Decourt et al. 1988). These differences have resulted in a number of corrections (energy ratio, borehole diameter, rod length, sampling method, etc.) to attempt to "standardize" the SPT. The advantages and disadvantages of the SPT can be summarized as follows.

Advantages	Disadvantages
- Availablity of testing equipment	- Numerous corrections required to "standardize" test
- Extensive experience base and numerous correlations with geotechnical engineering properties	- Lack of reproducibility of test results
- Disturbed sample is recovered for soil classification and laboratory testing	- Inability to delineate thin soil layers sometimes critical for design
- Undrained test used to interpret undrained phenomenon	- Generalizing effect; one value of penetration resistance per 450 mm
- Case histories of liquefaction flow failure and lateral spreading where SPT were conducted are available	- Specific soil properties, i.e., fines content, gravel content, soil compressibility, can significantly affect penetration resistance

1.2. Cone penetration test

The CPT is now considered "the primary field test utilized for evaluation of liquefaction resistance (NCEER 1996)." This statement was based upon the advantages of the CPT over the SPT for estimating the liquefaction resistance of sandy soils. However, at this time (1997), the CPT may also be the most appropriate in situ test for estimating the post-liquefaction shear strength of sandy soils. The advantages and disadvantages of the CPT can be summarized as follows.

Advantages

- Nearly continuous record of penetration resistance with depth (typical measurement interval of 50 mm) allowing delineation of thin soil layers
- Simpler test procedure than SPT or shear wave velocity measurement
- More reproducible test results than SPT
- Lower cost of testing compared to SPT allowing more comprehensive investigation
- Moderate experience base and developing database of correlations with geotechnical engineering properties
- Case histories of liquefaction flow failure and lateral spreading where CPT were conducted are available

Disadvantages

- Lack of sample recovery for soil classification and laboratory testing
- Specific soil properties, i.e., fines content, gravel content, soil compressibility, can significantly affect penetration resistance
- Relatively small area of soil tested
- Drained or partially drained test used to interpret undrained phenomenon

1.3. Shear wave velocity measurement

A growing interest exists in the use of shear wave velocity measurements to estimate liquefaction resistance and post-liquefaction shear strength. Most importantly, available data (Cunning et al. 1995) indicate that a correlation may exist between shear wave velocity and soil state. The advantages and disadvantages of shear wave velocity measurements can be summarized as follows.

Advantages	Disadvantages
- Specific soil properties, i.e., fines content, gravel content, soil compressibility, do not significantly affect test results	- Lack of experience base and database of correlations with geotechnical engineering properties
- Relatively large area of soil tested	- Lack of sample recovery for soil classification and laboratory testing
- Recent research indicates the viability of shear wave velocity measurements to be directly utilized to estimate soil state	- Various methods to estimate shear wave velocity may not provide identical results
	- Case histories of liquefaction flow failure and lateral spreading where shear wave velocity measurements were conducted are not available

2.0. SUITABLE PROCEDURE FOR ESTIMATING THE POST-LIQUEFACTION SHEAR STRENGTH FROM FIELD TESTS

Numerous procedures exist for estimating the post-liquefaction shear strength and normalized post-liquefaction shear strength from in situ test results. Some of the procedures are based upon correlation with field case histories of liquefaction flow failure and lateral spreading, while some are based upon both laboratory test results and some field case histories.

Along with several procedures to estimate post-liquefaction shear strength, several terms have been used in the literature to describe the post-liquefaction shear strength. Many of these terms are mentioned in the following discussion, however, all the terms describe the shear strength available to a soil after liquefaction occurs. These terms are used interchangeably in the following discussion.

The following discussion describes some of the available procedures that utilize field tests, but does not cover methods that are strictly laboratory based, such as Polous et al. (1985). After the existing procedures are reviewed, a preferred method is discussed.

2.1. SPT-based procedures to estimate post-liquefaction shear strength

2.1.1. Seed and Harder (1990)

Updating the work of Seed (1987), Seed and Harder (1990) collected 17 case histories of liquefaction flow failure and lateral spreading to develop an empirical correlation between corrected equivalent clean sand SPT blowcount, $(N_1)_{60\text{-}cs}$, and post-liquefaction shear strength (termed residual strength, s_r, by Seed 1987). The correlation is shown in Figure 1. Seed (1987) developed a correction factor, $\Delta(N_1)_{60}$, (termed N_{corr} in Figure 1) to correct the value of $(N_1)_{60}$ of silty sands and sandy silts to that of clean sands of equal relative density, also shown in Figure 1. This correction factor is based upon the fines content (percent by weight passing the No. 200 standard sieve) of the soil, and is applied as

$$(N_1)_{60} + \Delta(N_1)_{60} = (N_1)_{60\text{-}cs} \quad (1)$$

Increasing fines content of a soil is postulated to decrease penetration resistance because of the increased compressibility of the soil and therefore the increased induced pore pressure during penetration.

Because of its practicality, use of field case histories, and the correlation to a well-known penetration value, $(N_1)_{60}$, this method remains the state-of-practice for estimating post-liquefaction strength of sandy soils.

2.1.2. Konrad and Watts (1995)

Konrad and Watts (1995) proposed a method to estimate post-liquefaction shear strength mobilized in the field from $(N_1)_{60\text{-}cs}$ (referred to as ECS $(N_1)_{60}$) based upon a framework of critical state soil mechanics (CSSM) in conjunction with limited field case histories of liquefaction flow failure. $(N_1)_{60\text{-}cs}$ is estimated using the correction proposed by Seed (1987) (see Figure 1). The idealized approach is shown in Figure 2A. A four step procedure proposed to estimate the post-liquefaction shear strength is as follows.

1. Site characterization - includes SPTs and obtaining representative samples of sand for laboratory testing
2. Laboratory tests - determination of maximum void ratio and critical state line
3. Estimate χ - values of χ estimated from backcalculation of case histories of liquefaction flow failure (see Figure 2B)
4. Estimate mobilized post-liquefaction shear strength using s_{uo} (laboratory-determined post-liquefaction strength corresponding to e_{max}, see Figure 2A), χ, and $(N_1)_{60}$ where

$$\log s_u(\text{field}) = \log s_{uo} + \chi\,(N_1)_{60} \quad (2)$$

This method was used by Konrad and Watts (1995) to correctly predict cases of flow failure and non-flow failure for artificial sand fills constructed in the Beaufort Sea.

2.2. SPT-based procedures to estimate normalized post-liquefaction shear strength

2.2.1. Stark and Mesri (1992)

Expanding on the work of Jefferies et al. (1990), Stark and Mesri (1992) collected 20 field case histories of liquefaction flow failure and lateral spreading to develop a correlation between normalized post-liquefaction strength (referred to as the mobilized critical strength ratio, $s_u(\text{critical, mob})/\sigma'_{vo}$) and $(N_1)_{60\text{-}cs}$. The normalized post-liquefaction strength describes a

relationship between the critical strength *mobilized* during flow failure and the pre-failure effective vertical stress, similar to relationships developed for soft clays. The correlation was defined as a band (to encompass all the case histories) and a lower bound (for use in design), as shown in Figure 3A and 3B, respectively.

Stark and Mesri (1992) suggested that the value of $(N_1)_{60}$ can be corrected by the SPT-based yield strength (or liquefaction resistance strength) fines content correction developed from the liquefaction resistance relationships proposed by Seed et al. (1985), rather than a separate post-liquefaction strength correction, as suggested by Seed (1987). The corrections are shown in Figure 3C. This suggestion is made because the use of the yield strength correction did not affect the position of the band (shown in Figure 3A) that encompasses the case histories.

Stark and Mesri (1992) showed that the lower bound normalized post-liquefaction strength mobilized in the field case histories is approximately one-half of the yield strength ratio mobilized in the field for values of $(N_1)_{60\text{-}cs}$ less than approximately 20 (see Figure 3B). This lower bound relationship is defined as

$$s_u(\text{critical, mob})/\sigma'_{vo} = 0.0055 \times (N_1)_{60\text{-}cs} \quad (3)$$

Despite normalization of the data to the initial effective vertical stress, a wide band of normalized post-liquefaction shear strength is still apparent from the field case histories. Stark and Mesri (1992) attribute this range to the likelihood of drainage occurring during flow failure. If drainage were to occur during flow failure, a constant volume condition would no longer exist, and the mobilized strength would increase. This increase in strength would lead to a higher strength backcalculated from a stability analysis.

2.2.2. Ishihara (1993)

Based on extensive laboratory test data, Ishihara (1993) confirmed the existence of a relationship between post-liquefaction shear strength and initial confining pressure for silty sands and sandy silts. Ishihara (1993) suggested that this relationship is not unique for all sands, but for a given soil (given critical state parameters) and a given K_o, the relationship exists. However, Ishihara (1993) proposed that the quasi-steady state strength, not the critical state strength, should be utilized in post-liquefaction stability analysis, and it is the quasi-steady state strength that Ishihara (1993) related to initial confining pressure. For moderately loose soils, the quasi-steady state is the minimum post-liquefaction shear strength available to a soil, and is often attained at strains of 4 to 10 percent. For these soils, the true steady state occurs after dilation and increase in strength at much larger strains. For very loose soils, the quasi-steady state does not exist.

Ishihara (1993) developed relationships between estimated $(N_1)_{60}$ and laboratory normalized post-liquefaction strength using the logic illustrated in Figure 4A. These correlations are compared with available SPT-based field case histories collected by Stark and Mesri (1992), and the correlations are converted to corrected CPT tip resistance for comparison with available CPT-based field case histories reported by Ishihara et al. (1991). These comparisons are shown in Figures 4B and 4C, respectively.

2.3. CPT-based procedures to estimate normalized post-liquefaction shear strength

2.3.1. Olson and Stark (1997)

Building on the work of Stark and Mesri (1992), Olson and Stark (1997) collected 30 field case histories of liquefaction flow failure and lateral spreading where CPT and/or SPT data were available. The SPT blowcounts were converted to CPT tip resistance using the conversion proposed by Stark and Olson (1995). The relationship developed between equivalent clean sand corrected tip resistance, $(q_{c1})_{cs}$, and normalized post-liquefaction shear strength, $s_u(\text{critical, mob})/\sigma'_{vo}$ is presented in Figure 5A.

Similar to Stark and Mesri (1992), Olson and Stark (1997) concluded that the lower bound mobilized critical strength ratio is approximately one-half of the mobilized yield strength ratio developed from CPT-based case histories for values of $(q_{c1})_{cs}$ less than approximately 10 MPa, and can be expressed as

$$s_u(\text{critical, mob})/\sigma'_{vo} = 0.0085 \times (q_{c1})_{cs} \quad (4)$$

The mobilized critical strength ratio recommended by Olson and Stark (1997) is a lower-bound of the available case histories. As shown in Figure 5A, many of the case histories are near or above the mobilized yield strength ratio. Olson and Stark (1997) attribute this to the possibility of drainage during flow failure and to the various values of state parameter, ψ, possible for the various soils. (State parameter is defined as the difference between in situ void ratio and void ratio at the critical state line at a given effective confining stress.) The effect of initial state on the post-liquefaction strength and normalized post-liquefaction strength is discussed in the Section 3.0.

Olson and Stark (1997) also provide some explanation for the use of the yield strength fines content correction rather than a separate critical strength fines content correction. They note that liquefaction flow failure occurs under conditions of sloping ground, i.e., where the static shear stress is significant. For soils experiencing static shear, the seismic/cyclic stress ratio required to trigger liquefaction is smaller than the stress ratio required to trigger liquefaction in soils with equal penetration resistance (i.e., equal relative density and confining pressure) experiencing no static shear or static shear due to level ground conditions only. Olson and

Stark further suggest that this smaller seismic/cyclic stress ratio to trigger liquefaction in sloping ground may be comparable to the lowest values of seismic/cyclic stress ratio causing field cases of liquefaction in level ground. Based upon this assumption, Olson and Stark (1997) suggest that the minimum yield strength fines content correction (shown in Figure 5B) is applicable to correcting the value of q_{c1} in order to estimate the normalized post-liquefaction strength.

2.4. V_s-based procedures to estimate post-liquefaction shear strength and normalized post-liquefaction shear strength

2.4.1. Fear and Robertson (1995)

In a series of papers (Robertson et al. 1995, Cunning et al. 1995, and Fear and Robertson 1995), Robertson and his co-workers used data from extensive laboratory tests to develop an empirical relationship between soil state and corrected shear wave velocity, V_{s1}. Using the framework of CSSM, the state parameter is related to both post-liquefaction shear strength and normalized post-liquefaction shear strength. Fear and Robertson (1995) then related V_{s1} to both post-liquefaction strength and normalized post-liquefaction shear strength for two sandy soils with different fines contents. These results are presented together with results presented by Sasitharan et al. (1994).

Fear and Robertson (1995) presented the following conclusions:

- Normalized post-liquefaction shear strength is directly related to state parameter for a given sand, however, there is no unique relationship for all sands (see Figure 6A).
- Post-liquefaction shear strength is directly related to V_{s1} for a given sand and a given K_o condition, however, again, there is no unique relationship for all sands (see Figure 6B and Figure 6C where V_{s1} is converted to $(N_1)_{60}$).
- Normalized post-liquefaction shear strength is related to V_{s1} for a given sand and K_o condition, but is stress-level dependent (see Figure 6D where V_{s1} is converted to $(N_1)_{60}$).

2.5. Preferred procedure

Although laboratory based procedures are very promising, not enough field data are available to validate these procedures. Therefore, it is prudent at this time to continue using empirical procedures that analyze field case histories of liquefaction flow failure and lateral spreading to estimate the post-liquefaction shear strength of sandy soils.

NCEER (1996) concluded that the CPT should be the primary tool for evaluating liquefaction resistance. The reasons for this conclusion are summarized above in Section 1.0. It is anticipated that the CPT should also be the primary tool for evaluating the post-liquefaction

shear strength of sandy soils for the same reasons. Olson and Stark (1997) present the most updated compilation of field case histories of liquefaction flow failure and lateral spreading where CPT and/or SPT data are available. They present a lower-bound relationship between corrected CPT tip resistance, $(q_{c1})_{cs}$ and normalized post-liquefaction shear strength backcalculated from the field case histories. It is proposed that this relationship be used as a screening tool, or used solely for less important structures where significant laboratory test results are not available.

3.0. UNIQUENESS OF A RELATIONSHIP BETWEEN PENETRATION RESISTANCE AND POST-LIQUEFACTION SHEAR STRENGTH OR NORMALIZED POST-LIQUEFACTION SHEAR STRENGTH

Available field case histories, as presented by Seed and Harder (1990) (Figure 1), Stark and Mesri (1992) (Figure 3), and Olson and Stark (1997) (Figure 5), appear to indicate a trend of increasing post-liquefaction strength and normalized post-liquefaction strength with increasing penetration resistance. However, on the basis of extensive laboratory test data and a framework of CSSM, it appears that the trend exhibited by the field case histories may not represent a single, unique relationship for all sands.

Available laboratory test data and field data suggest the following:

- Field data suggest that post-liquefaction strength is related to initial effective vertical stress, as shown in Figure 7 (Baziar and Dobry 1995).
- Laboratory data suggest that post-liquefaction strength is directly related to initial confining stress for a given initial state parameter, deposition method, and K_o condition, as shown in Figure 6A (Fear and Robertson 1995) and Figure 8 (Ishihara 1993 and Dobry 1995)
- Laboratory data suggest that for a given method of deposition, the initial consolidation line is approximately parallel to the steady-state line and quasi-steady state line in void ratio-log of confining stress space over a given stress range (see Figure 9). This indicates that for a given sand and a given method of deposition, the state parameter will be approximately equal throughout the sample or deposit.

Existing data indicate that relationships between penetration resistance and post-liquefaction strength or normalized post-liquefaction strength may exist for a given sand. Fear and Robertson (1995) suggested that a relationship between post-liquefaction shear strength and V_{s1} exists for a given sand (see Figure 6B and 6C). However, as noted by various researchers (e.g., Jeffries et al. 1990), this relationship is dimensionally incorrect, and therefore it may not be reasonable to expect a relationship between these parameters. Ishihara (1993) and Robertson (1990) suggested that a relationship between normalized post-liquefaction strength and penetration resistance may exist for a given sand (see Figure 4B and Figure 10).

However, Fear and Robertson (1995) indicated that while a relationship between normalized post-liquefaction strength and penetration resistance may exist for a given sand, the relationship is stress-level dependent (see Figure 6D).

It appears that the disagreement in the literature stems from the method used to estimate penetration resistance. Ishihara (1993) and Robertson (1990) utilized correlations between relative density and penetration resistance that are normalized to a vertical effective stress of approximately 100 kPa. Therefore, they obtained relationships between normalized post-liquefaction strength and penetration resistance that are not stress-level dependent. Fear and Robertson (1995) utilized a correlation between shear wave velocity and initial state (directly related to post-liquefaction strength) that is not stress-level dependent. Therefore, when attempting to relate shear wave velocity (or penetration resistance) to normalized post-liquefaction strength, the relationship becomes stress-level dependent.

Unfortunately, insufficient field data are available to clarify the issue. Therefore, no definitive conclusion can be made on the uniqueness of a relationship between post-liquefaction strength or normalized post-liquefaction strength and penetration resistance for a given sand. However, based on current data, it does not appear that a unique relationship between either post-liquefaction strength or normalized post-liquefaction strength and penetration resistance exists for all sands and conditions.

4.0. SUITABLE TECHNIQUE FOR ESTIMATING IN-SITU VOID RATIO AND STATE PARAMETER

Many of the procedures described above for estimating the post-liquefaction shear strength are based upon a framework of CSSM. Accordingly, a key parameter in describing the stress-strain behavior of soil when subjected to shear is the state parameter, ψ. The state parameter is defined as

$$\psi = e_o - e_{cs} \tag{5}$$

where e_o is the in situ void ratio at a given effective confining stress and e_{cs} is the void ratio at the critical state line for the same effective confining stress (Been and Jefferies 1985).

The state parameter can be used to estimate whether a sandy soil is contractive or dilative, and therefore whether a deposit is susceptible to liquefaction flow failure. Furthermore, based on critical state soil mechanics, the state parameter can be used directly to estimate post-liquefaction strength.

4.1. SPT method

No direct correlation between $(N_1)_{60}$ and the state parameter, ψ, exists. Only a crude estimate of in situ void ratio can be made based upon $(N_1)_{60}$. This crude estimate would require an estimate of relative density from $(N_1)_{60}$, and a knowledge of e_{max} and e_{min}. From this very rough estimate of e_o and a knowledge of the critical state line, ψ could be determined. This technique is not used because of the inaccuracies involved in estimating relative density from $(N_1)_{60}$, which could lead to extremely large errors in estimating ψ.

4.2. CPT method

An estimate of the state parameter, ψ, could be obtained using q_{c1} in a similar fashion as described above. However, this estimate would also be crude.

Been et al. (1986, 1987) developed a method to estimate ψ from normalized CPT tip resistance, $(q_c - \sigma_v)/\sigma'_v$. This method was devised predominantly from large calibration chamber tests, which are subject to boundary size effects, on medium dense to dense sands, and extrapolated to the range of ψ expected for loose sands. Sladen (1989) and Cunning et al. (1995) have pointed out uncertainties involved in the method. Despite these reservations, this method may provide a reasonably accurate means to estimate in situ state from CPT results, and may be more practical than the following method based on shear wave velocity measurements.

4.3. V_s method

Cunning et al. (1995) present a procedure to estimate ψ directly from shear wave velocity results. The results of their study indicate that "provided that the in-situ sand deposit is unaged and uncemented, this approach should provide a reasonable estimation of its in-situ state." The conditions that the sand deposit be unaged and uncemented are appropriate for the purpose of determining susceptibility to liquefaction flow failure. Sands that are aged and/or cemented generally show greater resistance to liquefaction than unaged, uncemented deposits, and for practical purposes, are not susceptible to liquefaction flow failure.

4.4. Preferred method

Based upon the above discussion, the preferred method to determine in situ state of sandy deposits appears to be the use of shear wave velocity measurements. As noted by Cunning et al. (1995), if more accurate estimation of ψ is required, a material-specific relationship among shear wave velocity, void ratio, and effective confining stress should be determined.

The CPT method can provide a reasonable estimate of ψ, however, because of uncertainties in the correlations involved, the estimate determined from CPT results are more useful as a screening tool to determine if a soil is contractive or dilative, rather than to accurately estimate the value of ψ.

5.0. EFFECT OF FINES ON ESTIMATING POST-LIQUEFACTION SHEAR STRENGTH FROM FIELD TESTS

5.1. Definition of fines

Fines content are defined as the percent by weight passing the No. 200 U.S. Standard Sieve. The No. 200 sieve has openings of 0.075 mm. The plasticity index and clay content of the fines may also affect post-liquefaction strength, similar to the effect on liquefaction resistance. However, some clays and silts are susceptible to flow failure, and are often termed quick clays and metastable silts, respectively. In the case of quick clays, undisturbed samples can be obtained with relative ease to estimate soil sensitivity and susceptibility to flow failure.

It is more difficult to obtain undisturbed samples of loose sands and non-plastic silts, therefore, it is these soils that are of importance to this discussion. For these soils, the fines content, plasticity index of the fines, and clay content should be determined.

5.2. Effect of fines on post-liquefaction shear strength

Increasing the fines content of a soil has a dramatic effect on its critical state properties. As shown in Figure 11A (Fear and Robertson 1995), increasing the fines content of Ottawa sand up to 10 percent (kaolinite was added to the Ottawa sand) caused the critical state line to move down in void ratio-log effective confining stress space, and also caused the slope of the critical state line to increase. However, the critical state line of Alaska sand, with a fines content of 30 percent, plots above the critical state line of clean Ottawa sand, and the slope of the critical state line is approximately equal to that of Ottawa sand with 10 percent fines. For comparison, the critical state line of kaolin (fines content of 100 percent) plots above that of Alaska sand, and has a steeper slope than that of Alaska sand.

As shown in Figure 6A, the normalized post-liquefaction strength is greater for Alaska sand (with 30 percent fines content) than for clean Ottawa sand at the same initial state. The fines content of the Alaska sand is composed predominantly of carbonate shell material, suggesting that the fines are non-plastic.

Ishihara (1993) suggested that the effect of fines on post-liquefaction strength is likely best described by the plasticity index of the fines. Ishihara (1993) collected several laboratory and field data where normalized post-liquefaction strengths of silty soils were determined. These

data are plotted against plasticity index in Figure 11B, and indicate that the normalized post-liquefaction strength tends to decrease with increasing plasticity index of the fines.

Results from Baziar and Dobry (1995) indicate that for two specimens of the same silty sand with equal percentage of fines, the post-liquefaction strength is also highly dependent upon method of deposition and resulting soil fabric, as indicated in Figure 11C. However, this may be because quasi-critical state strengths were determined from the laboratory tests, rather than the critical state strengths.

The results described above indicate that increasing the non-plastic fines content of a soil may increase normalized post-liquefaction strength, while increasing the plasticity index of the fines decreases normalized post-liquefaction strength.

5.3. Effect of fines on field test results

In general, increasing fines content tends to decrease penetration resistance. This decrease in penetration resistance is realized because increasing the fines content of a soil increases the compressibility and decreases the permeability of the soil. Both of these factors result in a less drained condition during penetration, leading to an increase in excess pore pressure during penetration and thus a lower penetration resistance in a silty sand than in a clean sand at equal relative density and effective confining stress.

This effect has led to the development of a fines content correction to correct the penetration resistance in silty soils to that of clean sands at equal relative density and effective confining pressure, e.g., Seed et al. (1985), Seed (1987), Stark and Olson (1995). Corrections have been developed for both liquefaction and post-liquefaction analysis. However, when Stark and Mesri (1992) applied the yield strength fines content (rather than the lower critical strength fines content correction) to correct penetration resistance in cases where flow failure occurred, the effect was negligible.

5.4. Effect of fines on estimating post-liquefaction strength from field tests

Fines content can have several effects when estimating the post-liquefaction strength from field tests. Increasing the content of non- to low plasticity fines decreases penetration resistance and it may increase normalized post-liquefaction shear strength. Increasing the plasticity index of fines may also decrease penetration resistance, and it may decrease normalized post-liquefaction strength.

It appears that a fines content correction is necessary if a universal relationship between normalized post-liquefaction strength and penetration resistance is to be developed. The reasoning is that for a given state parameter, a soil with non-plastic fines may exhibit a higher

normalized strength, but will also exhibit a lower penetration resistance than a clean sand with the same value of state parameter. Unfortunately, few case histories of liquefaction flow failure are well-documented enough and well-enough understood to clarify the above issues. Therefore, it seems necessary at this time to simply use the correction employed in individual procedures to estimate post-liquefaction strength, as sufficient data do not exist to define a universal fines content correction.

6.0. REFERENCES

Baziar, M.H. and Dobry, R. (1995). Residual strength and large-deformation potential of loose silty sands. *ASCE Journal of Geotechnical Engineering Division*, Vol. 121, No. 12, p. 896-906.

Been, K. and Jefferies, M.G. (1985). A state parameter for sands. *Geotechnique*, Vol. 35, No. 2, p. 99-112.

Been, K., Crooks, J.H.A., Becker, D.E., and Jefferies, M.G. (1986). The cone penetration test in sands: part I, state parameter interpretation. *Geotechnique*, Vol. 36, No. 2, p. 239-249.

Been, K., Jefferies, M.G., Crooks, J.H.A., and Rothenburg, L. (1987). The cone penetration test in sands: part II, general inference of state. *Geotechnique*, Vol. 37, No. 3, p. 285-299.

Cunning, J.C., Robertson, P.K., and Sego, D.C. (1995). Shear wave velocity to evaluate in situ state of cohesionless soils. *Canadian Geotechnical Journal*, Vol. 32, p. 848-858.

Decourt, L., Muromachi, T., Nixon, I.K., Schmertmann, J.H., Thorburn, S., and Zolkov, E. (1988). Standard penetration test (SPT): international reference test procedure. *Proceedings of the 1st international symposium on penetration testing*. Vol. 1, Orlando, Florida, USA, p. 3-26.

Dobry, R. (1995). Liquefaction and deformation of soils and foundations under seismic conditions. *Proc: Third International Conference on Recent Advances in Geotechnical Earthquake Engineering and Soil Dynamics*. Vol. 3, April, St. Louis, Missouri, USA, p. 1465-1490.

Fear, C.E. and Robertson, P.K. (1995). Estimating the undrained strength of sand: a theoretical framework. *Canadian Geotechnical Journal*, Vol. 32, p. 859-870.

Ishihara, K., Verdugo, R., and Acacio, A.A. (1991). Characterization of cyclic behavior of sand and post-seismic stability analyses. *Proc. 9th Asian Regional Conf. on Soil Mechanics and Foundation Engineering*, Chile, BiTech Publishing, Vol. 2, p. 17-40.

Ishihara, K. (1993). Liquefaction and flow failure during earthquakes. *Geotechnique*, Vol. 43, No. 3, p. 351-415.

Jefferies, M.G., Been, K., and Hachey, J.E. (1990). Influence of scale on the constitutive behavior of sand. *Proc. Canadian Geotechnical Engineering Conference*, Laval University, Quebec, Canada, Vol. 1, p. 263-273.

Konrad, J.-M. and Watts, B.D. (1995). Undrained shear strength for liquefaction flow failure analysis. *Canadian Geotechnical Journal*, Vol. 32, p. 783-794.

NCEER. (1996). Summary report to the profession. *NCEER workshop on liquefaction resistance of soils*, Jan. 1996, 49 p.

Olson, S.M., and Stark, T.D. (1997). Post-liquefaction shear strength of sands from CPT. submitted to *Geotechnique* for review and possible publication.

Poulos, S.J., Castro, G. and France, W. (1985). Liquefaction evaluation procedure. *ASCE Journal of Geotechnical Engineering Division*, Vol. 111, No. 6, pp. 772-792.

Robertson, P.K. (1990). Evaluation of residual shear strength of sands during liquefaction from penetration tests. *Proc. of the 43rd Canadian Geotechnical Conference*, Vol. 1, Laval University, p. 257-262.

Robertson, P.K., Sasitharan, S., Cunning, J.C., and Sego, D.C. (1995). Shear-wave velocity to evaluate in-situ state of Ottawa sand. *ASCE Journal of Geotechnical Engineering Division*, Vol. 121, No. 3, p. 262-273.

Sasitharan, S., Robertson, P.K., Sego, D.C., and Morgenstern, N.R. (1994). State-boundary for very loose sand and its practical implications. *Canadian Geotechnical Journal*, Vol. 31, p. 321-334.

Seed, H.B., Tokimatsu, K., Harder, L.F., and Chung, R. (1985). Influence of SPT procedures in soil liquefaction resistance evaluations. *ASCE Journal of Geotechnical Engineering Division*, Vol. 111, No. 12, pp. 861-878.

Seed, H.B. (1987). Design problems in soil liquefaction. *ASCE Journal of Geotechnical Engineering Division*, Vol. 113, No. 8, p. 827-845.

Seed, R.B. and Harder, L.F., Jr. (1990). SPT-based analysis of cyclic pore pressure generation and undrained residual strength. *Proceedings, H.B. Seed Memorial Symposium*, BiTech Publishing, Vol. 2, p. 351-376.

Sladen, J.A. (1989). Problems with interpretation of sand state from cone penetration test. *Geotechnique*, No. 39, Vol. 2, p. 323-332.

Stark, T.D. and Mesri, G. (1992). Undrained shear strength of liquefied sands for stability analysis. *ASCE Journal of Geotechnical Engineering Division*, Vol. 118, No. 11, p. 1727-1747.

Stark, T.D. and Olson, S.M. (1995). Liquefaction resistance using CPT and field case histories. *ASCE Journal of Geotechnical Engineering Division*, Vol. 121, No. 12, p. 856-869.

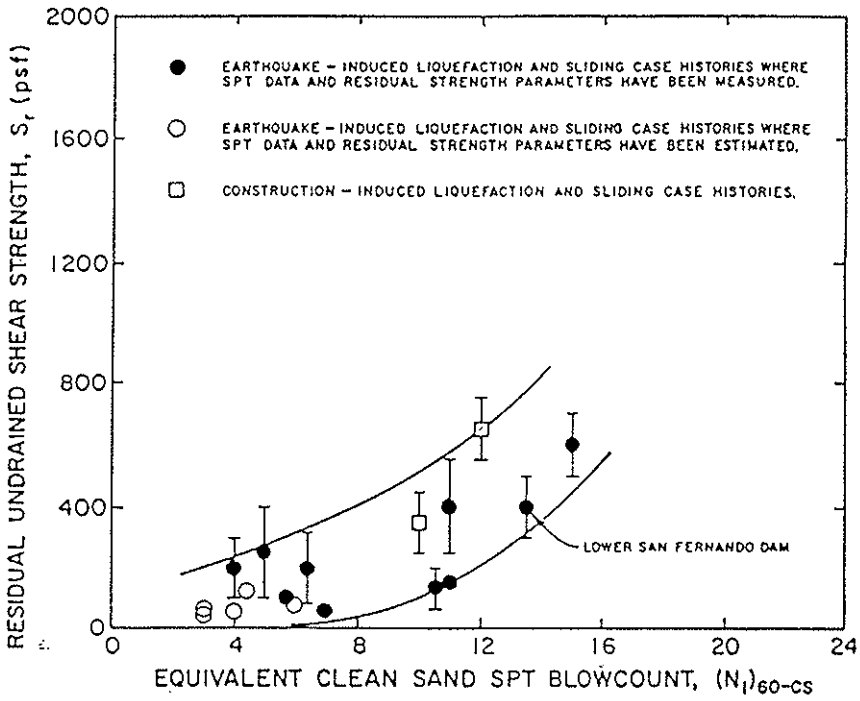

Percent Fines	N_{corr} (blows/ft)
10%	1
25%	2
50%	4
75%	5

Figure 1. Correlation between corrected equivalent clean sand SPT blowcount, $(N_1)_{60\text{-}cs}$, and post-liquefaction shear strength, s_r, and fines content correction for s_r evaluation using SPT data (from Seed and Harder 1990)

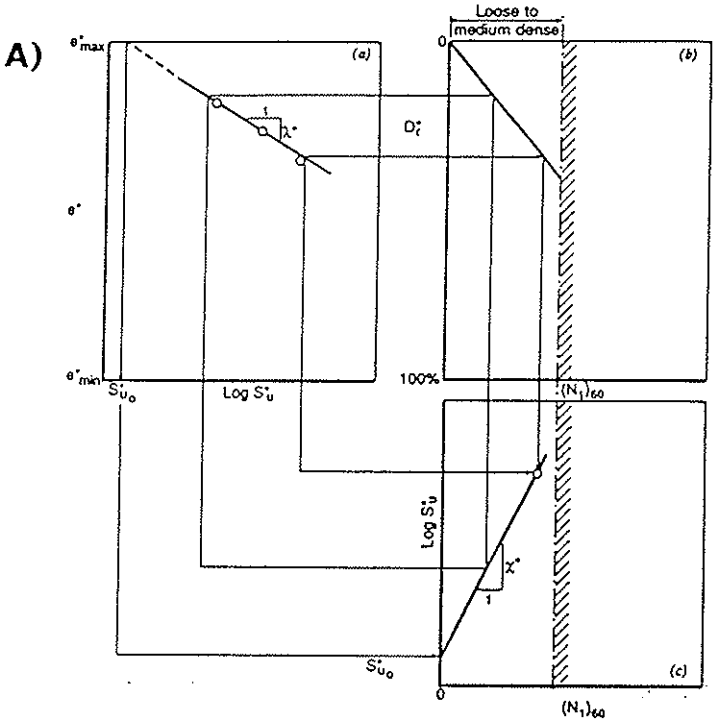

Figure 2. A. Idealized relationship between post-liquefaction shear strength and $(N_1)_{60}$
B. Relationship between χ and λ (slope of critical state line) obtained from field case histories and laboratory tests (from Konrad and Watts 1995)

A)

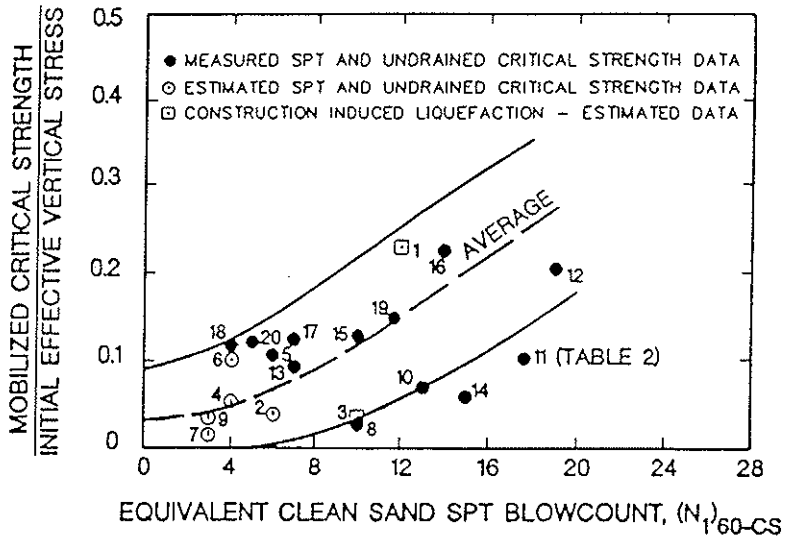

B)

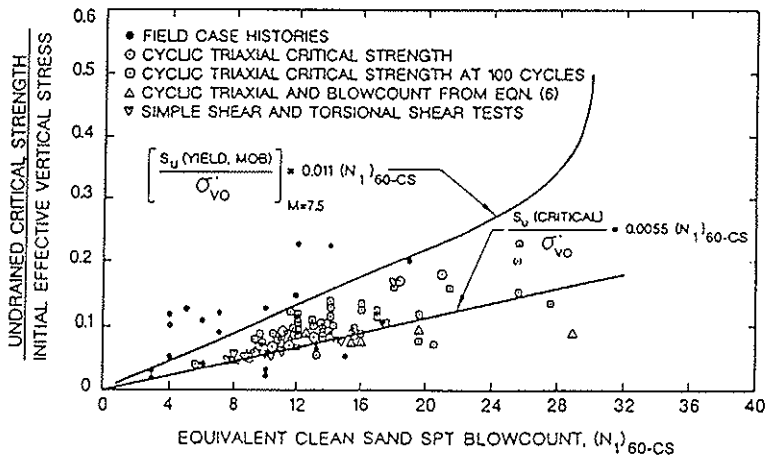

C)

Fines content (%) (1)	Yield strength, $\Delta(N_1)_{60}$ (2)	Critical strength, $\Delta(N_1)_{60}$ (3)
10	2.5	1
15	4	—
20	5	—
25	6	2
30	6.5	—
35	7	—
50	7	4
75	7	5

Figure 3. A. Relationship between normalized post-liquefaction shear strength and $(N_1)_{60-cs}$ based on yield strength fines content correction

B. Relationship between lower-bound normalized post-liquefaction shear strength and $(N_1)_{60-cs}$

C. Liquefaction (yield) strength and post-liquefaction strength fines content corrections (from Stark and Mesri 1992)

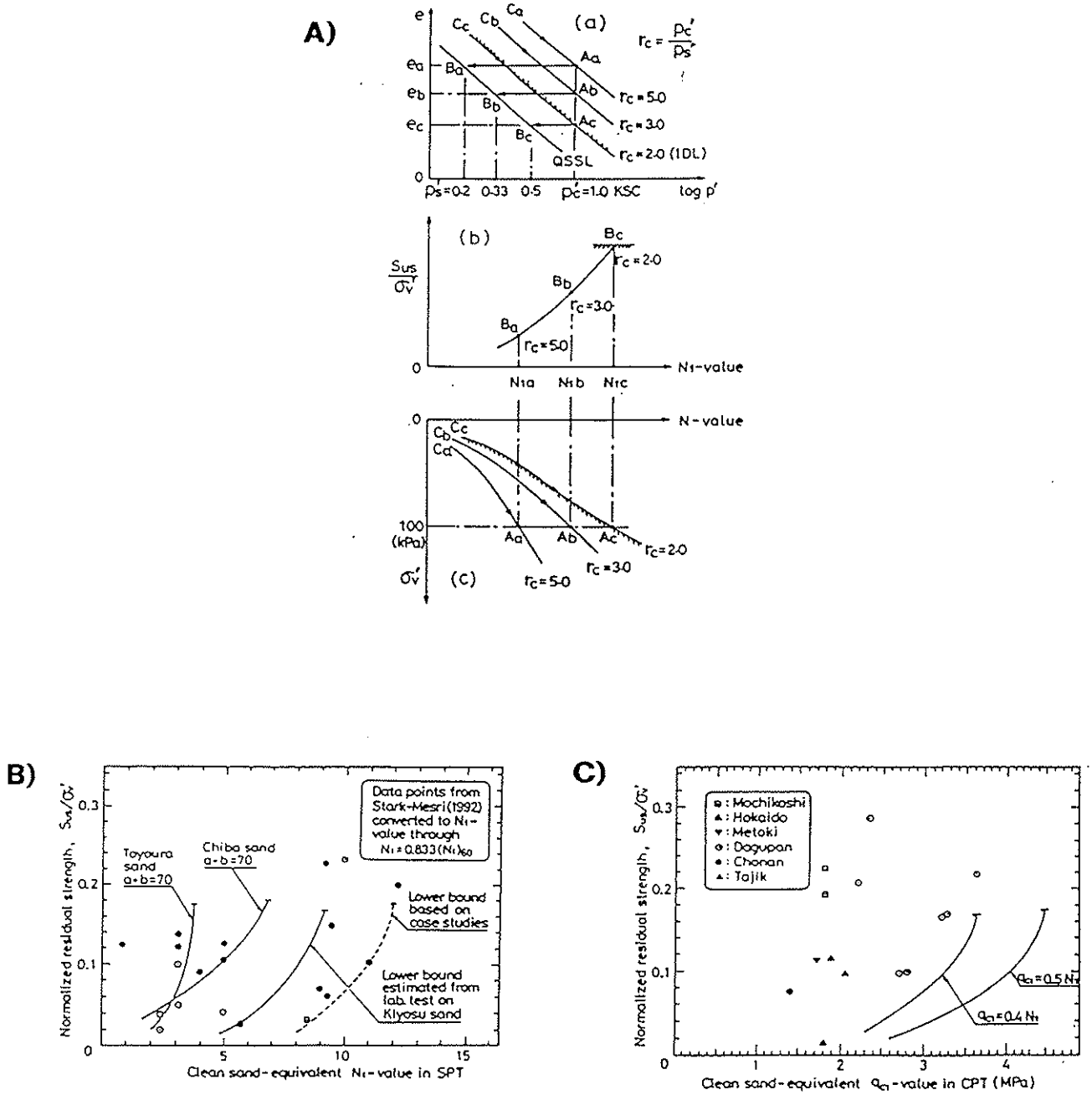

Figure 4. A. Illustration for establishing the relation between the normalized residual strength and $(N_1)_{60}$

B. Relationship between normalized residual strength and $(N_1)_{60}$ based on laboratory-determined quasi-steady state line compared with data from field case histories

C. Relationship between normalized residual strength and q_{c1} based on laboratory-determined quasi-steady state line compared with data from field case histories (from Ishihara 1993)

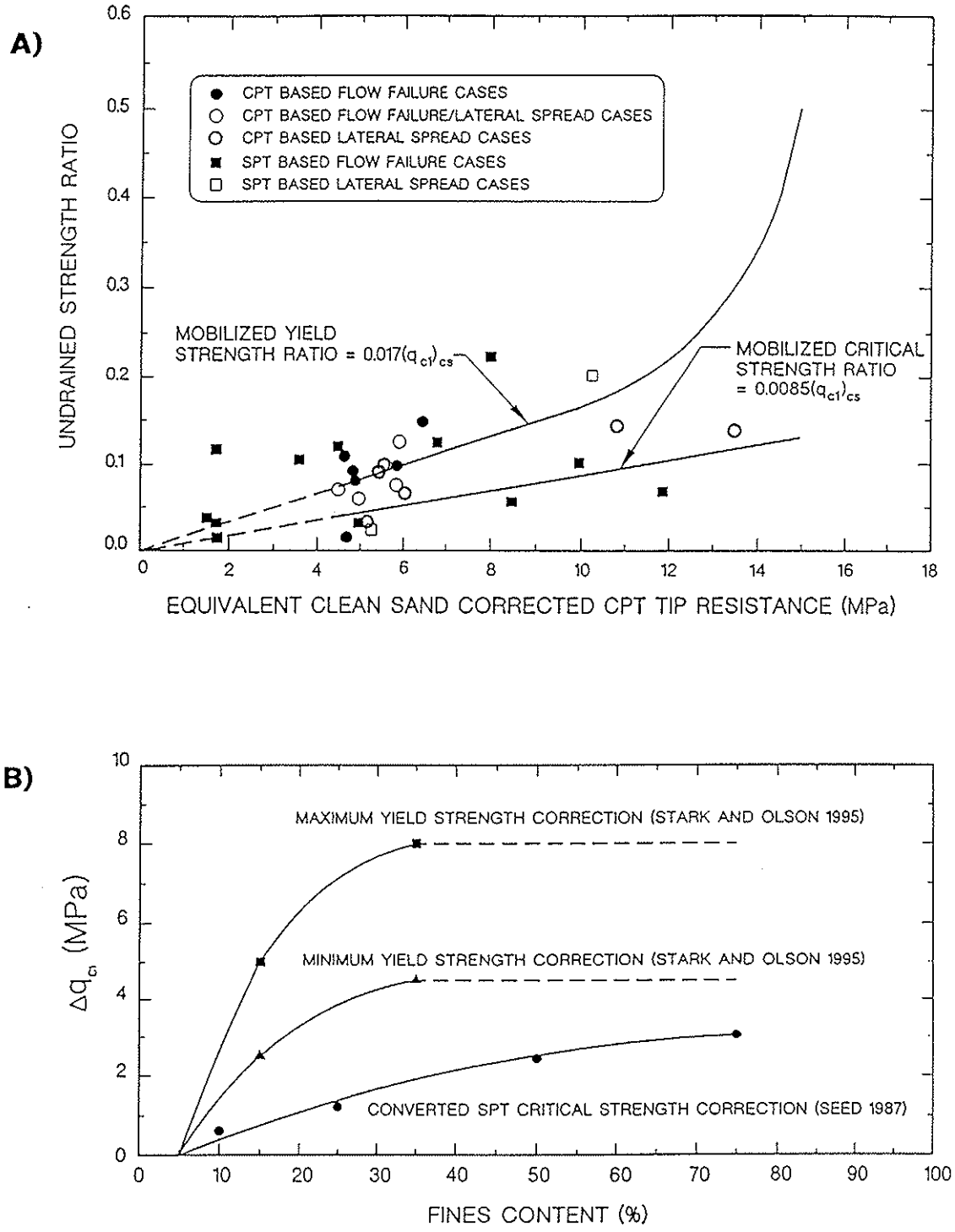

Figure 5. A. Relationship between critical strength ratio estimated from CPT and SPT-based field case histories and $(q_{c1})_{cs}$

B. CPT-based yield strength and critical strength fines content corrections

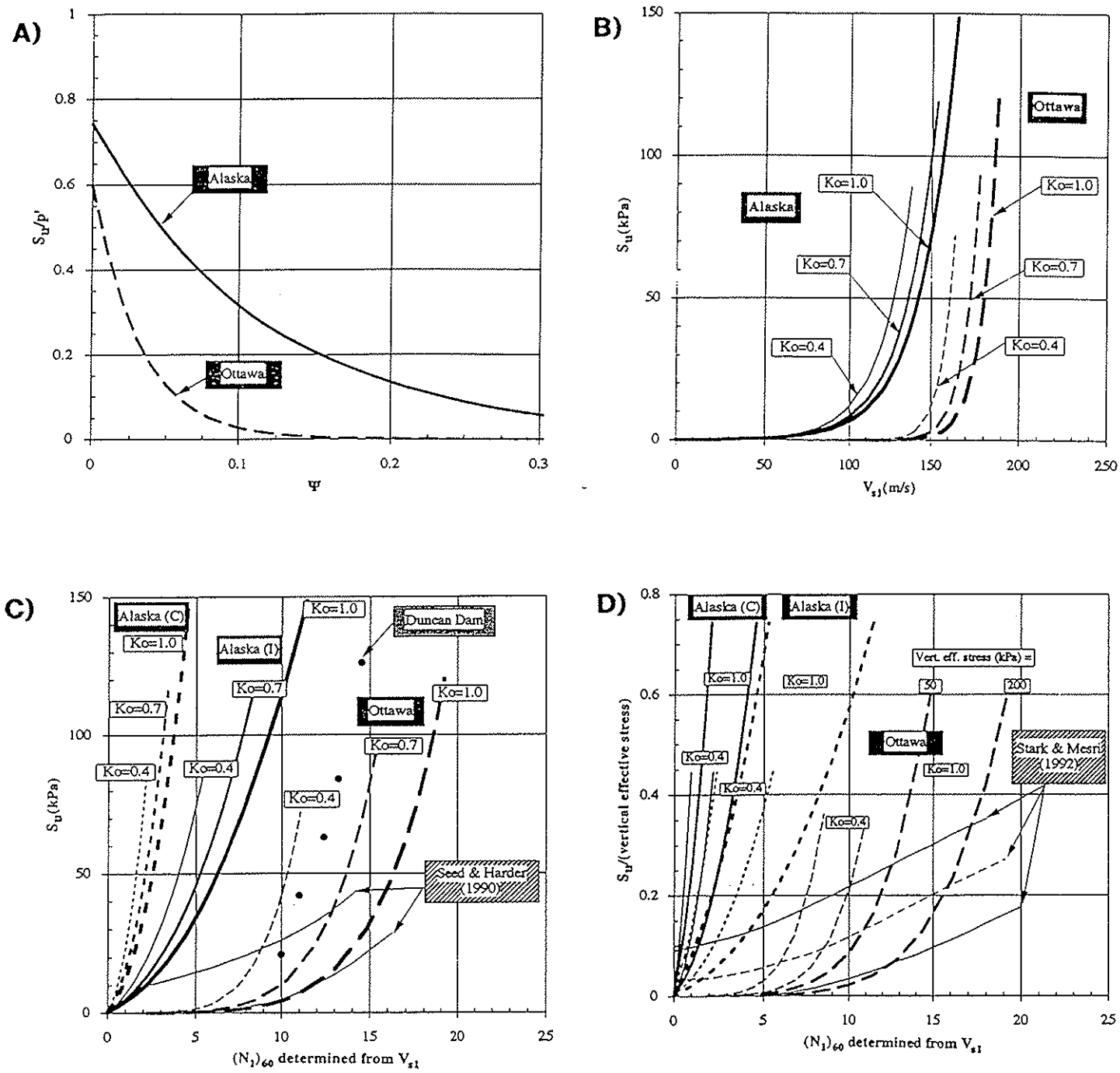

Figure 6. A. Relationship between post-liquefaction strength ratio and ψ in triaxial compression for Ottawa sand and Alaska sand

B. Relationship between s_u in triaxial compression and V_{s1} for Ottawa sand and Alaska sand for a range in K_o

C. Relationship between s_u in triaxial compression and $(N_1)_{60}$ for Ottawa sand and Alaska sand compared with data from Duncan Dam and results from Seed and Harder (1990)

D. Relationship between s_u/σ'_v in triaxial compression and $(N_1)_{60}$ for Ottawa sand and Alaska sand compared with results from Stark and Mesri (1992)

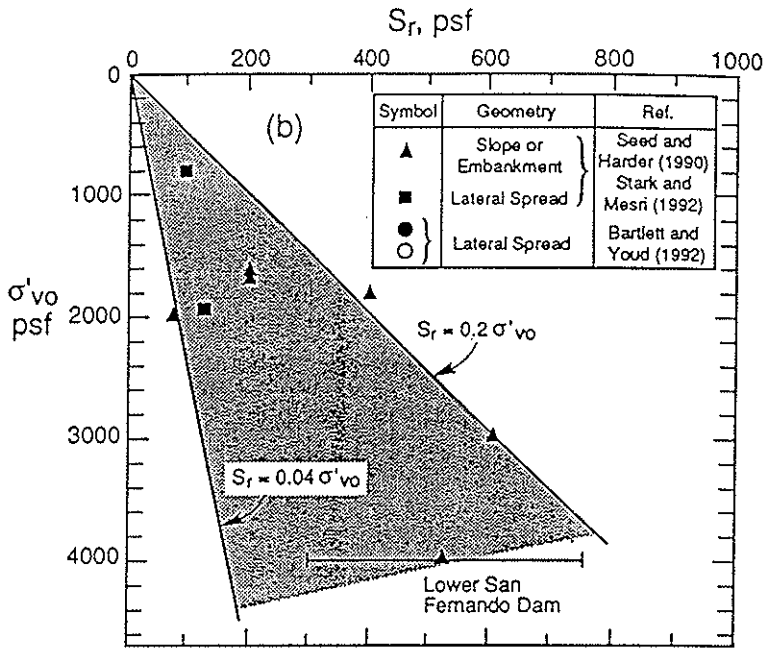

Figure 7. Relationship between post-liquefaction strength, s_r, effective vertical stress for low plasticity, saturated nongravelly silt-sand deposits with fines contents greater that 10% that have experienced large deformations (from Baziar and Dobry 1995)

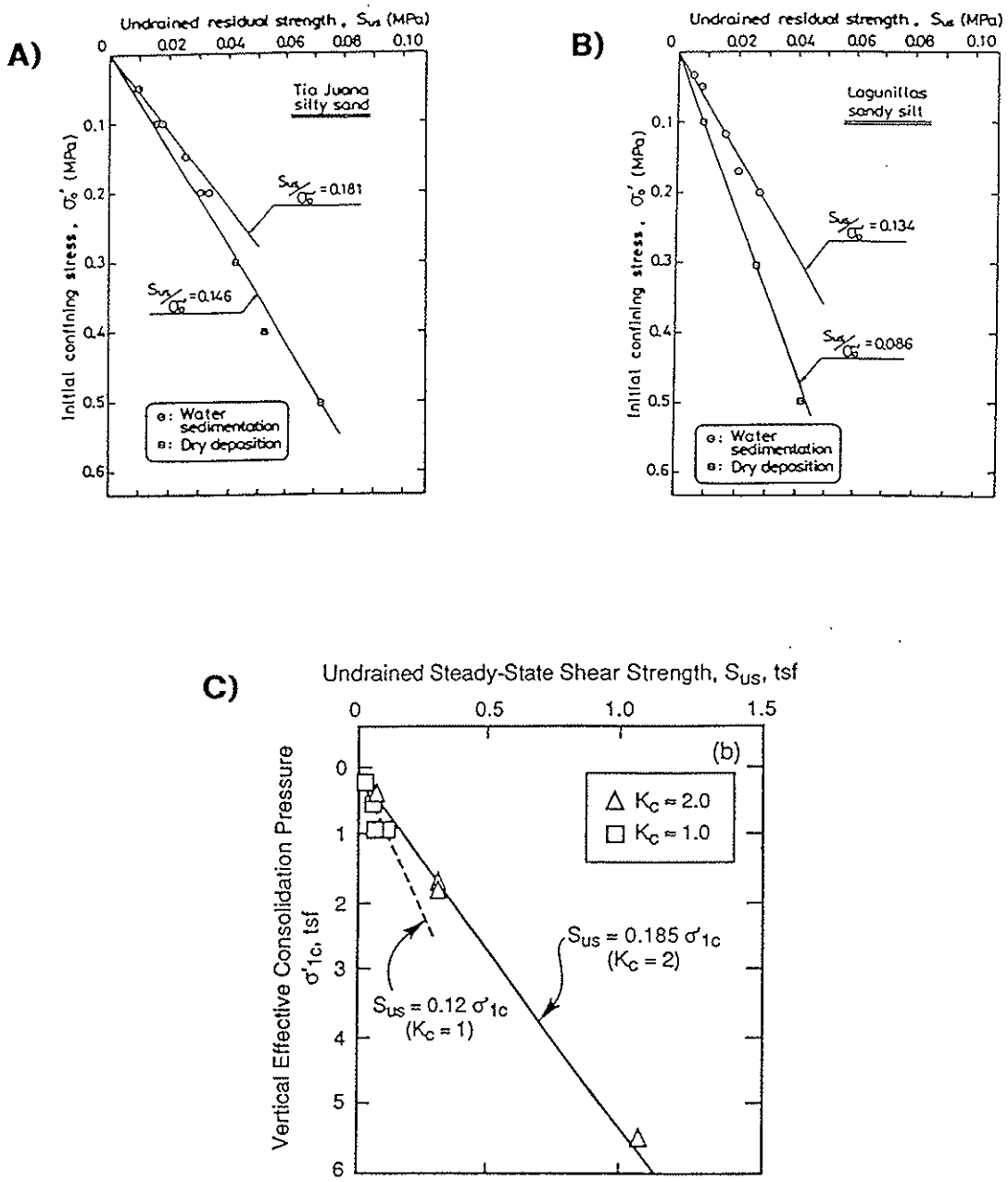

Figure 8. A. Post-liquefaction strength plotted against initial confining stress for Tia Juana silty sand (Ishihara 1993)
B. Post-liquefaction strength plotted against initial confining stress for Lagunillas sandy silt (Ishihara 1993)
C. Post-liquefaction strength plotted against initial confining stress remolded layered specimens of silty sand, Batch 7, Lower San Fernando Dam (Dobry 1995)

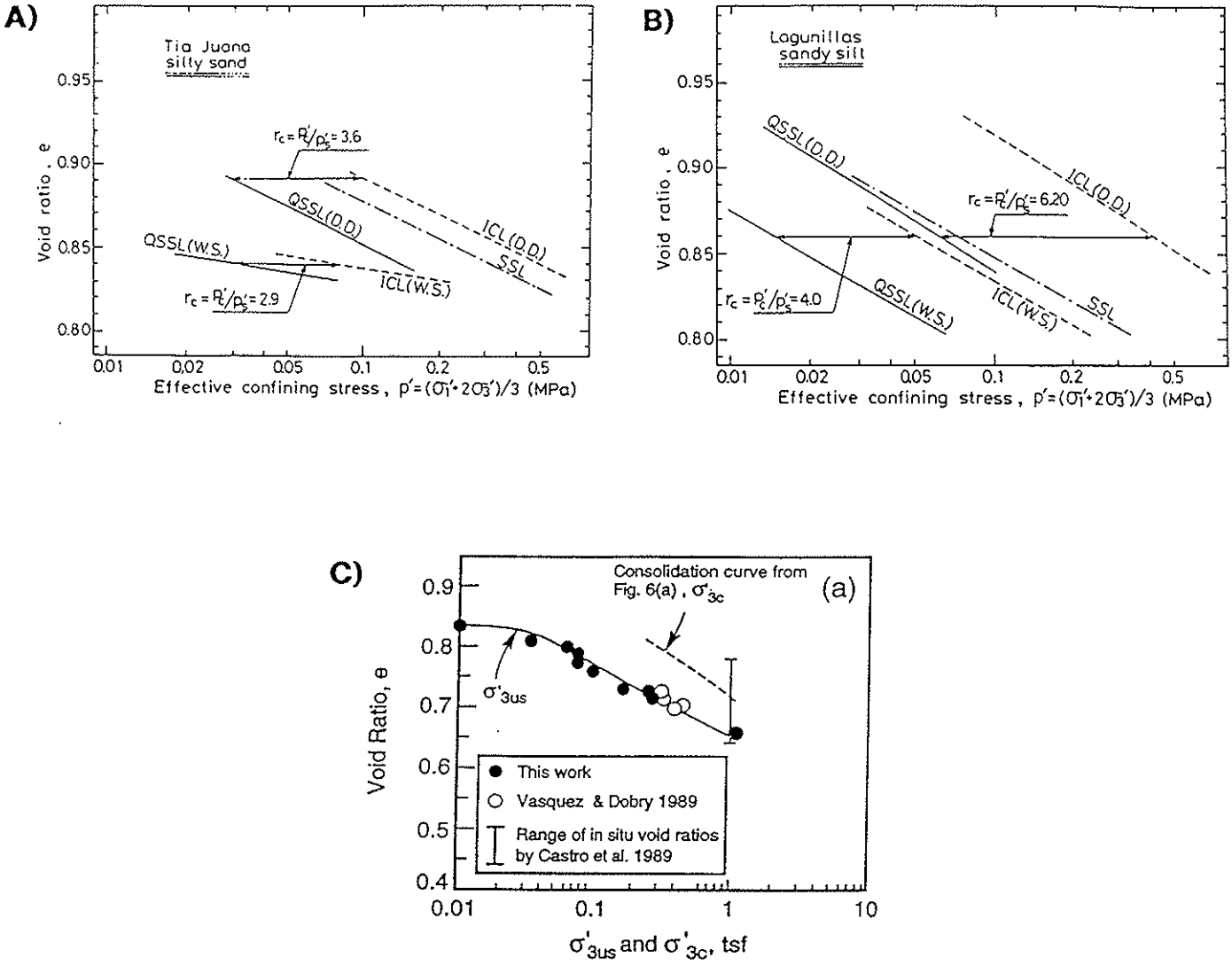

Figure 9. A. Comparison of consolidation curve and steady state lines for Tia Juana silty sand (Ishihara 1993)
B. Comparison of consolidation curve and steady state lines for Lagunillas sandy silt (Ishihara 1993)
C. Comparison of consolidation curve and steady state line for remolded layered specimens of silty sand, Batch 7, Lower San Fernando Dam (Dobry 1995)

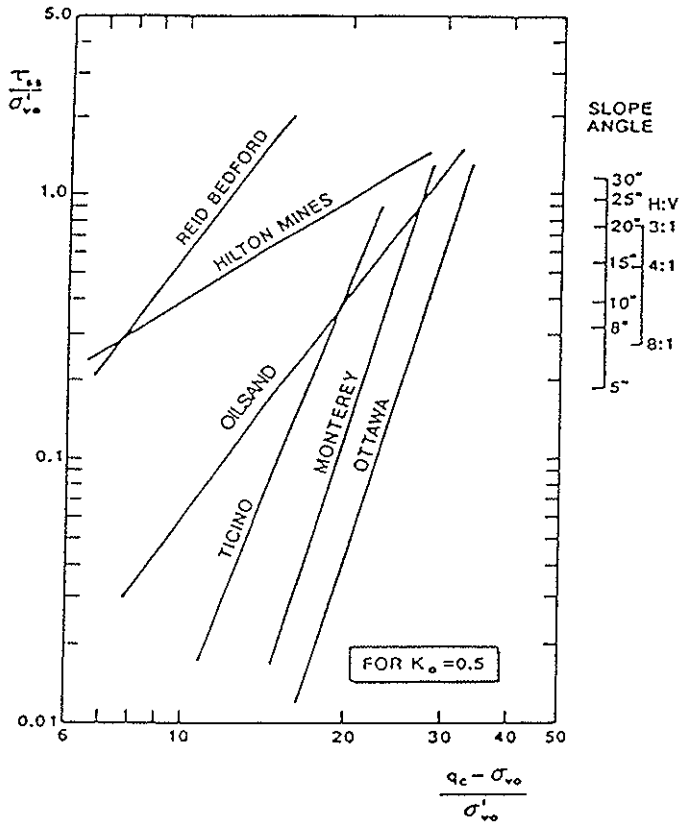

Figure 10. Derived correlations between normalized post-liquefaction strength and normalized CPT tip resistance for normally consolidated sands (K_o = 0.5) (from Robertson 1990)

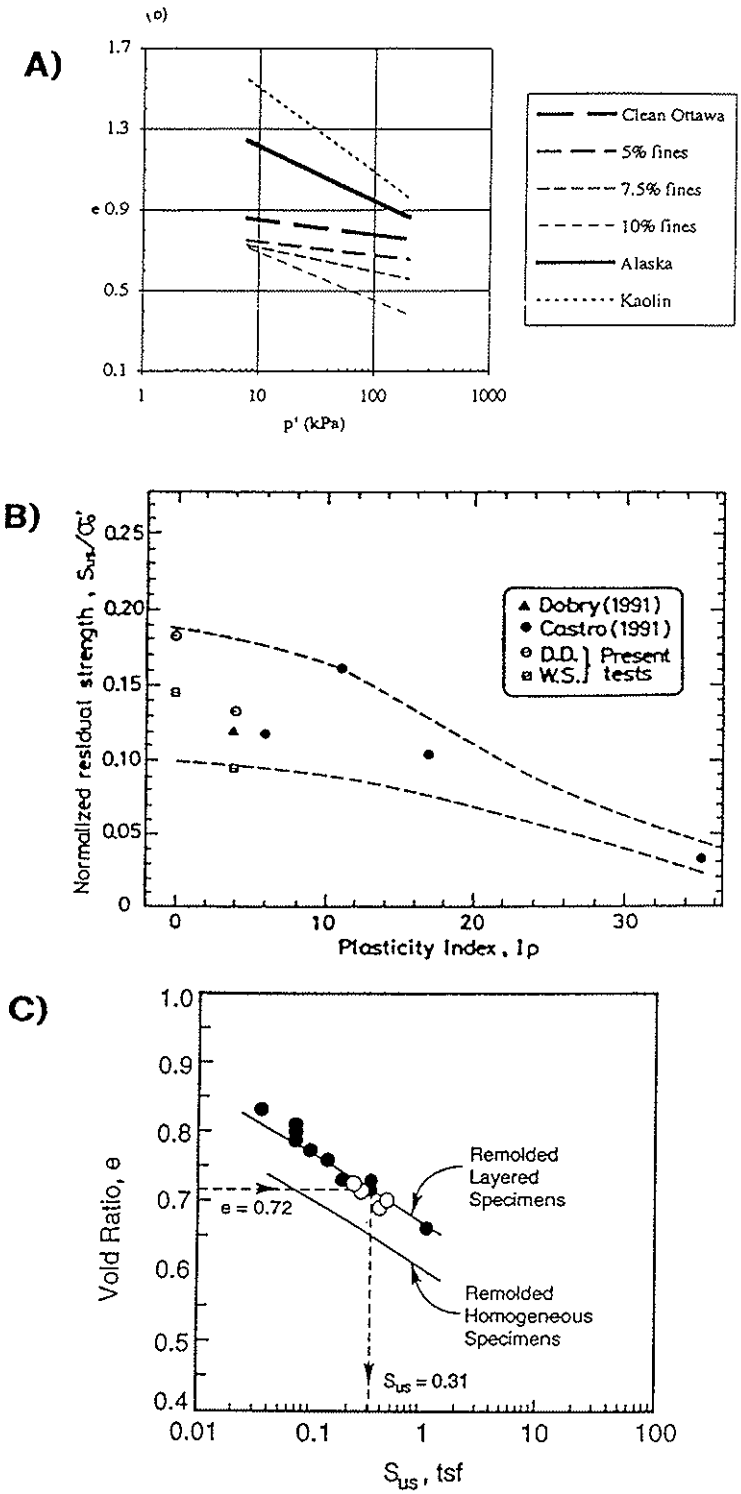

Figure 11. A. Critical state lines for clean Ottawa sand, Ottawa sand with fines and kaolin, and Alaska sand (from Fear and Robertson 1995)
B. Normalized residual strength plotted against plasticity index (from Ishihara 1993)
C. Comparison of critical state lines for remolded layered specimens and remolded homogeneous specimens of silty sand, Batch Mix 7, Lower San Fernando Dam (from Dobry 1995)

COMMENTS ON LABORATORY DETERMINATION OF UNDRAINED STEADY STATE SHEAR STRENGTH

NSF Workshop on Post-Liquefaction Shear Strength
University of Illinois, Urbana-Champaign
April 17-19, 1997

by

Steve J. Poulos
GEI Consultants, Inc.
Winchester, MA 01890

Introduction

The organizers are to be complimented on the format of this conference. It should lead to profitable discussion and useful results both for engineering practice and for teaching.

There are TWO strengths that can be defined from a strength test on any soil specimen. These two strengths are the Steady State Strength and the Peak Strength. They may be measured in drained or undrained shear, or with an intermediate degree of drainage. Not all soil specimens show a peak strength. However, ALL soil specimens show a steady state strength, if the strains are sufficient to reach the steady state.

The term post-liquefaction shear strength should not be used because instead of clarifying the issue about which strength to use for analysis, its use may give the impression that there is a new 'strength' that exists after liquefaction, but which does not exist under any other condition. In addition, most readers associate liquefaction with earthquakes, which indeed do cause liquefaction. However, one of the most notable examples of a liquefaction failure - the partial failure of the Fort Peck Dam in September 1937 - was NOT CAUSED by an earthquake.

In addition, the term liquefaction itself must be defined before the question can be answered, since many in our profession do not distinguish between liquefaction as an

undrained stability failure and "liquefaction" as excessive strain due to repeated loading on dilative (dense) soils.

The definition of liquefaction that I believe should be accepted by all parties before entering the discussions during this Workshop is as follows:

> Liquefaction is the undrained shear failure of a loose sand or a soft clay that results when (1) the in-situ driving shear stresses on the soil mass prior to failure exceed the undrained steady state shear strength of the mass (2) additional shear stresses are applied fast enough to cause undrained shear, and (3) the latter stresses are large enough to cause strains that exceed the strain at peak in the mass such that steady state deformation can be approached.

This use of the term liquefaction will be used in the balance of this discussion.

The term 'liquefaction' also is used for cases in which sufficient repeated loadings are applied to dilative specimens to cause large strains. (Note: Dilative soil specimens or soil masses are not subject to liquefaction, as the term is defined above.) These large strains can be interpreted as "failure" if a structure founded on the affected soil mass cannot tolerate the displacements caused by the strains induced by the repeated loading. The writer would prefer that this phenomenon be referred to as 'cyclic deformation.'

Below are comments on the questions that the organizers of this workshop suggested be considered by the author. In each case the author has taken the liberty of substituting the term 'undrained steady state shear strength - S_{us}' for the term 'post-liquefaction shear strength.'

1. Is the undrained steady state shear strength proportional to the initial effective vertical stress or some other [state] parameter?

The undrained steady state shear strength of a given soil specimen is a function only of its void ratio prior to the start of undrained shear.

If the effective stress at the start of undrained shear increases, but the void ratio is held constant, the undrained steady state shear strength does not change. The peak strength and the strain at peak for the given specimen both increase. But the undrained steady state shear strength remains the same, so long as the soil composition and the void ratio at the start of undrained shear both remain the same.

One might note that with increasing depth, the void ratio of a given deposit might decrease due to consolidation under the increasing vertical stress. Thus one might, in a perfectly homogeneous deposit, correlate void ratio with the vertical effective stress. In that case there also would be a correlation between undrained steady state shear strength and the vertical effective stress, but the ratio of the two would not be constant.

More generally, the undrained steady state shear strength is dependent only on the soil composition and on the void ratio at the start of undrained loading. If a correlation can be found between any parameter, e.g. vertical effective stress prior to shear, and void ratio for a mass of soil with homogeneous composition, then that parameter will be correlated with the undrained steady state shear strength.

2. What are the suitable sampling (e.g. freezing), specimen preparation, and laboratory testing procedures for measuring the undrained steady state shear strength?

a. To measure the undrained steady state shear strength, the sampling must be done in such a manner as to preserve the soil gradation and void ratio of the specimens or, since minor void ratio changes always occur, to preserve the history of changes in void ratio so that the in situ void ratio can be estimated with sufficient accuracy for practical application.

b. Freezing must be done very slowly to help avoid changes in void ratio during freezing. Practically, freezing cannot be sufficiently controlled to avoid volume changes in silty sands.

c. For a soil of given composition, the specimen preparation procedure has no measurable effect on the undrained steady state shear strength. Only the soil composition, including the gradation, must be preserved. However, if the specimens are very non uniform in void ratio, the undrained steady state shear strength may be difficult to measure because one is less likely to be able to strain the specimen enough in the laboratory to cause the steady state to develop. Specimens with a uniform void ratio probably reach steady state at smaller strains than specimens of the same soil with non-uniform void ratio.

d. The laboratory testing procedure to be used depends on the soil composition. The soils that are easiest to test for their undrained steady state shear strength are also the ones that most often exist in deposits that may be subject to liquefaction, namely, narrowly graded sands with bulky (i.e. having small length ratios between the major and the other two axes), rounded or subrounded grains.

For such a sand the undrained steady state shear strength can be measured

consistently in triaxial compression if the specimens are highly contractive at the end of consolidation. To accomplish this state it is necessary to prepare very loose specimens at a very uniform void ratio and then to consolidate them isotropically in small increments until the effective stress is high. The void ratio thereby remains very high under the consolidation stress such that the specimens are in a highly contractive state prior to start of undrained loading. Under this condition the steady state can be reached at axial strains as low as 5%, which is easily attainable in the triaxial compression test.

If the sand is more widely graded, or the grains more elongate or angular, the strain required to reach the steady state increases, and it becomes less likely that a triaxial test can be used to measure the undrained steady state. However, for a variety of cases in which the soils proved to be susceptible to liquefaction, we have found that the triaxial compression test has been the most useful one for measuring the undrained steady state strength.

3. Effects of consolidation stress and undrained stress path on laboratory measured undrained steady state shear strength.

The effect of consolidation stress on the undrained steady state shear strength was discussed under Question 1 above.

The undrained stress path used has no measurable effect on the undrained steady state shear strength.

Tests have been published that show an effect of the undrained stress path, e.g. by comparing axial compression with axial extension tests. However, it is nearly impossible to maintain a uniform void ratio in specimens subjected to extension. If the void ratio were to be measured in the zone of shear (e.g. along the failure plane, if present) when extension tests are performed, which to the author's knowledge has not been done, then the steady state line would be found to be the same in extension and compression.

4. Effects of "fines" on laboratory-measured undrained steady state shear strength?

The void ratio at the start of shear and the soil composition are the only two parameters that control the undrained steady state shear strength.

To ask the effect of fines is equivalent to asking whether soil composition affects the undrained steady state shear strength. Yes, soil composition is the primary factor

that controls the undrained steady state shear strength.

For the purposes of discussion, consider two soils that are composed of sub-rounded quartz grains. Soil A has a coefficient of uniformity of 2, i.e. it is very narrowly graded. Soil B has a coefficient of uniformity of 7, i.e. soil B is more widely graded than soil A. The question is, if a specimen of each of these soils is prepared at the same void ratio after consolidation, which specimen will have the higher undrained steady state shear strength? During steady state deformation, the void ratio is likely to be greater for soil A, at a given principal effective stress, because there are no significant inactive fines present. Inactive fines are those that do not contribute substantially to the process of shear at steady state. Thus, soil A will have the higher steady state line, due to the lack of fines. Note that the steady state line referred to here is the plot of void ratio vs the effective minor principal stress that exists when the steady state of strain is reached.

Therefore, at equal void ratio Soil A, with the narrower gradation, is likely to have a higher undrained steady state shear strength than soil B.

It is probable that the two soils would have similar undrained steady state shear strengths at the same percent compaction. At the same percent compaction soil B would have a higher dry unit weight than soil B, but a similar undrained steady state shear strength.

Tests are needed to demonstrate these effects of gradation.

5. Effects of grain size distribution on the undrained steady state shear strength?

See response to previous issue.

6. Effects of particle shape on laboratory-measured undrained steady state shear strength?

Tests have shown that the steady state friction angle (i.e. the angle of internal friction in terms of effective stress during steady state deformation) is greater for granular soils that have angular grains than those which have rounded grains. Also the steady state line is higher and steeper for angular-grained sands because the angularity of the edges causes more voids to exist during steady state deformation than would be the case for rounded grained sands. Both because of the higher friction angle at steady state and the higher steady state line, the angular-grained sand usually will have a higher undrained steady state shear strength than the rounded-grained sand, so long as both specimens have the same void ratio at the

start of undrained shear.

For the above reason it is more difficult to cause liquefaction in sands with angular grains than in sands with rounded grains.

7. Effects of strain rate on laboratory-measured undrained steady state shear strength?

Tests have shown that for clays and sands, over a wide range of strain rates, the steady state line and the steady state friction angle are not measurably affected. However, it is reasonable to expect that at very high or at extremely slow strain rates, there may be a rate effect.

8. Suitable techniques for estimating in-situ void ratio and state parameter?

The in-situ void ratio is needed to estimate the undrained steady state shear strength in-situ for a soil of given composition. There is no other state parameter needed.
Note: The ***state*** of a soil specimen is defined by the void ratio and the effective principal stresses under which it is consolidated prior to starting undrained shear.

Although the in-situ steady state strength of a granular soil can be measured using published techniques, it is also necessary to be able to estimate the changes in the void ratio, and hence the changes in the undrained steady state shear strength, as a dam or other structure is placed upon the foundation soils, if indeed the foundation soils are loose and are left in place in that state.

One suitable technique for estimating the in-situ void ratio is to measure it directly through careful sampling procedures that have been described in the literature. The procedure involves use of thin-walled-tubes that are properly shaped at the edges and pushed at a rate that will minimize void ratio decrease during sampling but will nevertheless retain the sample during withdrawal of the tube from the ground. It also involves using fixed pistons and measuring the movement of the piston while the sampler is pushed into the ground.

Then the sample length is measured, the tube is properly packed and it is shipped with minimal vibrations. Shipping should be done while capillary stresses are on the sand, so that it will not be much affected by vibrations.

At the laboratory, the in-situ void ratio can be estimated by measuring the volume in the tube, extruding the sample, drying it, weighing it, measuring the specific gravity of the soil solids and then calculating the void ratio as received. That void ratio has

to be increased to account for the effects of shipping and sampling.

Test pits can be used to take specimens directly for measurement of void ratio. Tests have been made to compare void ratios measured in test pits with void ratios measured using thin-walled tube samples as described above. The data show good agreement.

Downhole techniques could be used to measure in situ void ratio, but the author has not investigated their use.

Closing Comments

One question that should be discussed at the Workshop is whether the void ratio of a soil is likely to change during or soon after an earthquake, which would mean that the undrained steady state shear strength also would change. The discussion should include an evaluation of whether any such changes could result in a liquefaction failure that would not be predicted based on the undrained steady state shear strength of the soil at the pre-earthquake void ratio.

Another question that should be discussed is how to measure the undrained steady state strength that applies in-situ for sands that are (1) very gravelly, (2) very widely graded, (3) very non-uniform. It would also be useful to discuss the measurement of the undrained steady state shear strength of clays that are either normally consolidated or heavily overconsolidated, such as clay-shales.

References used for these comments will be provided at the Workshop.

THE STRESS-STRAIN CURVES OF SOILS

Steve J. Poulos

January 1971

GEOTECHNICAL ENGINEERS, INC.
1017 Main Street
Winchester, Massachusetts 01890

THE STRESS-STRAIN CURVES OF SOILS

Steve J. Poulos

January 1971

TABLE OF CONTENTS

THE STRESS-STRAIN CURVES OF SOILS

SYNOPSIS

The steady state of deformation is defined as the state in which a specimen deforms continuously and monotonically without change in shear stress, effective normal stress, volume, or velocity of deformation. Using the steady state as a unifying concept, idealized shapes of stress-strain curves for drained and constant-volume tests are given for bulky-grained and platey-grained soils (Figs. 5,7,15,16). Typical test results are presented in detail.

To illustrate their practical utility, the generalizations made about stress-strain curves are used to evaluate the relative accuracy of typical laboratory tests (Tables 1 and 2), to aid in selecting shear strength for stability analysis (Tables 3 and 4), to understand the relationships between stress-strain curves of sands and clays, and to understand where liquefaction and residual strength fit into the general view of the stress-strain characteristics of soils.

The major factors affecting the shapes of stress-strain curves and the shear strength of soils are: (a) the soil, represented chiefly by its mineralogy and grain shape, (b) the initial structure of the specimen, (c) the initial state (void ratio, effective normal stress, and shear stress), and (d) the method of loading. The effects of each of these major factors on the stress-strain curves are discussed qualitatively.

THE STRESS-STRAIN CURVES OF SOILS

Steve J. Poulos

January 1971

1. INTRODUCTION

The main purpose of this monograph is to provide a systematic qualitative understanding of the shapes of stress-strain curves obtained in triaxial compression, direct shear, direct simple shear and rotation shear tests on fully saturated, uncemented soils. A secondary purpose is to provide insight into the use of this information in geotechnical engineering.

Problems involving the application of stresses to soils may be divided into those in which (a) deformations of the foundation soil (or rock) control design and (b) failure of foundation soil controls design. Those in which failure controls are a special case: i.e., the end point of the class of problems in which deformation controls. Failure problems themselves may be subdivided into shear failures and tension failures, but only shear failures are considered herein. This classification is merely a somewhat more general way of referring to the traditional "settlement" and "bearing capacity" problems of soil mechanics.

The distinction between deformation-controlled and failure-controlled problems may be understood by considering a building on a soil foundation. If the building is rigid or very flexible then the deformations of the foundation soil donot affect the competence of the building and it is only necessary to assure that the foundation soil is safe against failure. Yet, if the building has intermediate flexibility, such that it fails when the deformations of the foundation soil are small (relative to those that are developed when

the foundation soil fails), or if the deformations of the building must be limited for some other reason, then the foundation soil must not deform excessively. In short, if the building fails first, excessive deformations of the foundation soils must be prevented; if the foundation soil fails first, failure of the foundation soil must be prevented.

For problems in which deformations of a mass of soils must be computed, it is well accepted that the computations can be made properly only if the shapes of the stress-strain curves involved are taken into account. But it is less widely appreciated that the shapes of the stress-strain curves must also be known in connection with most failure problems.

For failure problems the precise shape of the stress-strain curve need not be known if the shear stress reaches a maximum and then remains constant even at very large strains. In such a case, the fact that the shear stress varies along a given failure surface in-situ has no practical consequence, because when the strains are sufficient the maximum shear stress will be developed simultaneously along the entire failure surface (assuming that the test used to measure shear strength is a proper model of in-situ conditions). Thus, one would be safe in using the shear strength for computing the factor of safety.

The methods of stability analysis presented in the literature to date include, often only implicitly, the assumption that the stress-strain curve of all soils involved reach a maximum shear stress which then remains constant with further strain. However, the stress-strain curves of soils show a peak under most conditions[5], although conventional tests are usually not carried to sufficient strain to display the drop in shear stress after the maximum is reached. If the stress-strain curve of the soil along a failure surface

does not contain a peak, it is practically never possible to develop the peak shear stress simultaneously along the entire failure surface. The average shear stress mobilized along the failure surface at failure will be smaller than the peak shear stress. The difference between the peak shear stress and the average mobilized shear stress is due to "progressive" failure (Watson, 1940, P.150; Taylor, 1948, P. 348; Casagrande, 1950, P. 237). It is caused by the non-uniform stresses and strains that develop in the failure mass, and it occurs both in the field and in the laboratory.

The occurrence of progressive failure makes it necessary to analyze the distribution of strains within a mass of soil in order to estimate the average shear stress that can be mobilized simultaneously along a failure surface at failure. Alternatively, one can perform model tests to gain insight into the proportion of the maximum shear stress then can be simultaneously mobilized (Rowe, 1969). But the first step that is necessary to estimate the magnitude of the effect of progressive failure in any given case is to determine correctly the shape of the entire stress-strain curve. Only then is it possible to establish whether a given problem is controlled by deformation or by shear failure, and, if it is a failure problem, to make a proper estimate of average shear stress than can be mobilized along a given failure surface.

Progressive failure is but one of many examples that could be used to show why it is important to understand the shape of the entire stress-strain curve of a soil. This monograph is intended as an aid to such understanding.

2. DEFINITIONS

Definitions are given below for the terms: (1) soil, (2) soil structure, (3) steady state of deformation, (4) contractive and dilative behavior, and (5) method of loading. The purpose of these definitions is to facilitate discussion in subsequent chapters of the major variables that affect the shapes of stress-strain curves of soils. The definitions have been prepared with this purpose in mind and, as a result, they differ in some respects from previously published definitions.

2.1 Soil

A soil is a mass of discrete particles that are the products of decomposition and disintegration of rocks and organic matter by natural processes. A soil is assumed to be completely described by: (1) the composition of its solids, (2) the composition of the liquids, gases, and sometimes solids (including dissolved and suspended materials) in its pores, and (3) the distributions of size, shape, and angularity of its grains. Thus the term "soil" refers to the basic soil material and not in any way to the arrangement of the grains relative to each other.

It should not be inferred that it is possible at present to measure quantitatively each of the above-mentioned items, with the exception, in some cases, of the grain size distribution. But it is important to note that if any one of these items is changed, the soil itself and, hence, its properties are also changed.

Although in this paper the principal interest is in soils, the concepts subsequently presented can very likely be applied to any particulate mass, regardless of composition. The numerical values associated with various stress-strain characteristics change with composition, but the basic pattern of stress-strain characteristics of all particulate materials are likely to be the same.

2.2 Soil Structure

The term "soil structure" is used herein to refer to the arrangement of individual grains and groups of grains relative to each other and to the forces that bind these grains and groups of grains into a unit.

To describe the structure of a soil completely, one must observe it at every scale that is pertinent to the engineering application at hand, starting with the scale of individual grains, and moving up to the scale of the entire mass of soil that is involved. On the scale of individual grains one is concerned with the orientation of the grains (Lambe, 1953, P. 38) and with the number of contacts per grain and the magnitudes of forces between grains (Marsal, 1967, P. 40, 46). On a larger scale one might observe layering or stratification, slickensides, joints, and root holes. On a still larger scale one might find old major failure surfaces, holes made by animals, joints and slickensides of very large extent, and hard or soft inclusions of any size and shape. It is not unusual for the large-scale structural patterns to have a far greater influence on the engineering properties of a soil in-situ than does the structure at the scale of individual grains.

The forces between grains or groups can be divided into two types: (1) those that impart strength to the soil only when the effective stress is greater than zero, and (2) those that impart strength to the soil when the effective stress is zero. If the latter forces exist, the soil will exhibit strength when the effective stress is zero. In this monograph the latter forces are referred to as "cementation bonds". Uncemented soils are the main subject of this monograph.

2.3 State of a Soil

The state of a soil is defined by the void ratio and the effective stresses on a specimen at any given moment. For the purposes of this monograph, the state of a specimen will be monitored by the void ratio, e, and the effective minor principal stress*, $\bar{\sigma}_3$, at any stage during a test. A plot of these two variables yields the state diagram, Fig. 1. These coordinates are the same as those used for plotting compression curves from triaxial consolidation tests. They are also used to advantage for following the results of shear tests in which changes in the principal stress ratio, as well as void ratio, occur during shear.**

---

* For tests in which the effective minor principal stress is not known, an appropriate known effective stress will be used. For direct shear tests, the effective stress on the horizontal plane, $\bar{\sigma}_h$, is convenient.

** The changes that occur during shear are better represented in a plot of void ratio versus average principal effective stress, as suggested by Roscoe, Schofield and Wroth (1958 P. 27). However, for many types of tests the three principal stresses are not known. Therefore, it is expedient to compare series of tests of the same type by plotting the void ratio versus one of the known effective normal stresses.

The potential range of changes in void ratio can be visualized with the aid of the sketch at the left in Fig. 1. By viewing void ratio changes with reference to certain void ratio benchmarks, such as $e = o$, $e = e_{max}$, $e = e_{min}$, or the void ratios corresponding to the liquid and plastic limits, one is able to judge whether the results of a given shear test are reasonable or not.

The temperature of the specimen should be included to define its state more completely, but this variable is not considered herein.

2.4 Contractive and Dilative Behavior of Specimens

A specimen is said to be contractive if it tends to decrease in volume when the shear stress is increased during a given test, and dilative if it tends to increase in volume when the shear stress is increased (Casagrande and Poulos, 1964, P. 3).

These terms refer to volume changes that occur due to shear stresses, not to those caused by isotropic changes in effective normal stresses. An isotropic increase in effective normal stress always causes compression and a decrease causes expansion. Such is not the case for shear stresses.

The term "contractive" is applied to a specimen whether or not it actually contracts during a test, and the same applies to the term "dilative." For example, if contraction is prevented, the specimen is nevertheless referred to as contractive. But to prevent contraction, the isotropic effective normal stress must be reduced sufficiently to counterbalance the tendency for volume decrease that is caused by the shear stress. Thus, if the specimen were fully saturated and volume decrease were prevented by maintaining constant water content, the pore pressure would increase sufficiently to cause the required decrease in isotropic effective stress.

The degree to which a specimen is contractive or dilative is dependent on the soil, its structure, its initial state, and the method of loading (Section 2.6).

2.5 The Steady State of Deformation

The "steady state of deformation" is that state in which a particulate material of any composition or particle shape deforms continuously under a constant state of effective stress at constant velocity and at constant void ratio. This constant void ratio is the "steady state" void ratio.*

Therefore, one can measure the steady state void ratio only during deformation, since the soil mass will assume a different void ratio when deformation stops, even in clays. If the velocity of deformation is changed, the steady state void ratio is also changed. If one prepares a specimen of soil at the steady state void ratio, that specimen does not reach the steady state until it has been sheared to very large deformations. The "structure" of the specimen in the steady state is created by the applied shear stresses and is very different from its structure as initially prepared.

---

* The term "steady state void ratio" is synonymous with the term "critical void ratio," which was introduced by Casagrande (1936,P. 18) for the case of sands. The term "steady state" is used for two reasons: (1) It conveys correctly (by analogy to steady state flow of liquids) the concept of flow that the author has in mind. (2) The term "critical state," which, historically, may be applied to the steady state, has been applied by subsequent authors to a completely different condition of soils (Roscoe, Schofield and Wroth, 1958, P. 28; Schofield and Wroth, 1968, P. 19; Schofield, 1970).

Tests on sands (Watson, 1938, Plates BII - 8 and 9) and on steel balls (Roscoe, Schofield, and Wroth, 1958, Fig. 37) have shown that the steady state void ratio decreases with increasing effective stress* as shown schematically in Fig. 1. Although this relationship has not been adequately demonstrated for clays, by analogy the author assumes that a similar relationship will hold.

The principal characteristic that makes the steady state concept so useful is that a soil will tend to the steady state when sheared to sufficiently large strains. Thus, one can expect that specimens prepared at states lying above the steady state line in Fig. 1 will change volume or effective stress during shear such that the state point will move towards the steady state line. These specimens will be contractive. Specimens prepared at states below the steady state line will experience changes that ultimately move the state point towards the same steady state line, i.e., these specimens will be dilative at some stage during a test. The extent to which this behavior applies to real soils is discussed in subsequent chapters. It will be seen that although the steady state line provides an

---

* Watson measured the void ratio at which the specimen would show no net change in volume at peak deviator stress in consolidated-drained triaxial compressions tests. This void ratio was defined by Casagrande (1938, P. BII-8) as the "lower critical void ratio." Casagrande introduced this definition merely for convenience because he recognized the difficulty of measuring the void ratio in the steady state of deformation, which he referred to as the critical void ratio. Watson showed that the lower critical void ratio decreased with increasing confining pressure. From Watson's data Casagrande (1938, P. BII-7, 9) estimated that the critical void ratio varied in the same way but was higher than the lower critical void ratio by about 0.06 for one fine, uniform silty sand (Franklin Falls sand).

important reference in the state diagram, the path by which a soil may move towards the steady state may be rather complicated.

For soils composed primarily of bulky grains, the physical mechanism of steady state deformation is viewed by the author as a continuously changing arrangement of the particles throughout the deforming mass, accompanied by local increases and decreases in void ratio and effective stresses, such that a sufficiently large mass of the material displays no change in the average (or macroscopic) void ratio and effective stresses.

Given a material with bulky grains, there may be little tendency for the development of a preferred orientation of grains in response to the applied shear stresses.* However, materials composed only of platey or elongate grains (e.g., mica, kaolinite, attapulgite and halloysite) ultimately reach a condition in which the grains are orientated parallel with each other in the direction of movement (see Skempton, 1964). In this case, a single or a small number of shiny shear surfaces develop.** At this stage of the shearing process, and at no other stage, such platey-grained soils are able to deform

---

* If the steady state void ratio is a function of particle size, then a material composed of bulky particles with a range of sizes probably would develop a preferred distribution of its grains of various sizes when the steady state is reached. The major movements may then occur between particles in a given size range only, while the balance of the particles move much smaller distances relative to their neighbors. Obviously the steady state void ratio would then be a function of the grain size distribution as well as the size of the particles.

** Whether shiny surfaces would develop in soils with elongate (needle-shaped) grains, such as halloysite and attapulgite, has not yet been established.

continuously at constant velocity, void ratio and effective stress. Therefore, this state is, according to the definition given herein, the steady state of deformation. Clearly the zone in which the steady state develops in platey-grained soils is very thin, and it becomes almost impossible to measure the steady state void ratio. This feature does not diminish the usefulness of the concept, since its use as a working hypothesis for clays as well as sands permits one to view the stress-strain curves of all types of soil in one organized framework.

In real soils the platey particles are never absolutely flat, and the platey or elongate particles are practically always mixed with bulky particles. Therefore, the zone in which a steady state develops in real soils contains a number of particle thicknesses. For example, Fig. 2 contains two scanning electron microphotographs that were taken by viewing normal to the surface of a natural slickenside in Bearpaw Shale which was exposed when a drying crack formed during preparation of the specimen for the microscope (LaGatta, 1971). The photograph at the lower magnification shows that large-scale layering exists. At the higher magnification, layering at the scale of the individual particles in this soil can be seen. Approximately six layers, less than one micron apart vertically, are apparent. If appropriate measurements were made, the void ratio of this zone of the specimen could be determined.

The greater the percentage of bulky particles, the greater will be the volume of soil that reaches the steady state and the less shiny will be the resulting planes of shear. But even small percentages of platey particles may congregate in one zone and cause the steady state strength and void ratio to be controlled by these particles rather than by the entire grain-size distribution of the material.

When a soil is sheared, the contact stresses, if sufficiently great, cause grain breakage. Thus the soil itself changes during deformation. In such cases, the steady state cannot be defined unless the deformations are continued until grain breakage ceases. But in that case, the steady state reached applies to the new soil, not to the original soil.

2.6 Method of Loading

The method of loading is the manner in which a specimen is brought to failure. To define the method of loading, one must know the shear and total normal stresses or the deformations on each boundary of a homogeneously stressed specimen at every stage of a test, and one must describe the degree to which the void ratio is allowed to change. For example, the method of loading is defined for a conventional unconfined compression test by stating that the total minor and intermediate principal stresses are maintained at zero while the total major principal stress is increased from zero, without allowing change in water content of the specimen at any time. As a condition of this test, the top and bottom of the cylindrical specimen, which are major principal planes, are forced to remain plane by the end caps. The friction between the specimen and these end caps causes stress non-uniformities in the specimen. Therefore, the method of loading for this test is not truly known unless these boundary friction forces are known.*

---

* Often the effects of the boundary friction are ignored, for various reasons, but lubrication (Rowe, 1962, P. 507) minimizes the effects.

The changes in effective normal stress and shear stress that are caused by any given method of loading are conveniently followed by plotting them on a Mohr diagram in the form of a stress path, Fig. 3 (Lambe, 1964, P. 45). The stress path shows how the location of the top point of the Mohr circle (in terms of effective stress) changes during the test.*

The state path and the stress path in combination (Figs. 1 and 3) provide a record of the changes in void ratio, effective normal stress and shear stress that result from the method of loading used for any test.

The stress-strain characteristics of soils are strongly dependent upon the method of loading. Therefore, it is essential in laboratory testing that the stress-strain curves be determined for a method of loading that models, as closely as possible, the method of loading that will be applied in-situ.**

---

* The stress path for the plane inclined 45° to the principal planes is used herein because its coordinates are easily computed. The stress paths of the effective principal stresses are superior from the theoretical viewpoint, but all three are not usually known. When some of the stresses are not known, such as in a direct shear test, the stress path is plotted for that plane on which the shear and effective normal stresses are known.

** Alternatively, one must be able to use the results from one method of loading for predicting results for another method of loading. Stress-strain theories are currently being developed with this object in mind (e.g. Schofield and Wroth, 1968). But verification of the utility of such theories remains dependent upon large-scale field tests or on model tests (e.g. Avgherinos and Schofield, 1969).

3. QUALITATIVE DISCUSSION OF FACTORS CONTROLLING SHAPE OF STRESS-STRAIN CURVES

The major factors* that control the shape of stress-strain curves of soils are:

(a) Soil type (particularly mineralogy and grain shape)

(b) Initial structure

(c) Initial state

(d) Method of loading

Each part of a stress-strain curve is affected to a different degree by each of these factors. The author's opinions about these effects are described in Fig. 4, which shows a stress-strain curve with sufficiently general shape for this purpose.

The initial portion (the early part of Zone A, Fig. 4) of the stress-strain curve is affected by all four of the above factors. For example, one can expect that:

(1) As one passes through the range of soils with hard, bulkly grains to soils with soft, platey grains, the stiffness, i.e., the slope $d\tau/d\varepsilon$ should decrease.

---

* Secondary factors, which are important in certain cases, include: (1) rate of loading, (2) temperature of specimen, (3) absolute pressure in pore fluid, and (4) magnitude and frequency of stress cycles, if any. These items are not discussed in this monograph.

(2) As the void ratio increases and the effective stress decreases, i.e., as the initial state moves towards the upper left corner of the state diagram (Fig. 1) the stiffness decreases.

(3) The stiffness changes with structure, be it undisturbed, remolded, compacted wet, compacted dry, etc.

(4) The method of loading affects the measured stiffness substantially. For example, Cornforth (1964, Fig. 17) reported that the strain at maximum shear stress is much lower in plane strain than in triaxial compression.

The shear stress in the steady state (beyond Point s in Fig. 4) is not likely to be influenced by the initial structure, or the initial state, or the stress path followed during loading. Only the soil type and the end point of the stress path are likely to control its value. The specimen loses its memory of how it arrived at the steady state. The strain required to reach the steady state can be expected to be dependent on the initial structure, the initial state, and on the method of loading, as well as the soil type.

The above effects are summarized in the following table:

EFFECTS OF MAJOR FACTORS CONTROLLING SHAPE OF STRESS-STRAIN CURVES

Factor	Qualitative Estimate of Effect of Each Factor on:				
	Initial modulus of deformation	Peak point		Steady State	
		Shear Stress	'Width' of peak and strain at peak	Shear stress	Strain
Soil type	High	High	High	High	High
Initial state	High	High-Med.	High-Med.	None	Low
Initial structure	High	High-Med.	High-Med.	None	Low
Method of loading	High	High	High	Med.-Low	Low

When the grains of a soil are weak, angular, platey, or elongate, and when the soil is tested at sufficiently high effective stresses, significant grain breakage occurs during testing. (In drained tests grain breakage will result in continuous volume decrease with an accompanying change in shear stress. In constant volume tests it will result in a decrease of the effective normal stresses.) Only after grain breakage has ceased (for practical purposes) can the changes in volume and shear stress cease also. The final, steady-state shear stress probably still is dependent chiefly on the soil that was used and on the method of loading, even though the soil has been transformed into a new soil by the shearing process. But the strain required to reach the steady state is likely to be increased by grain breakage.

4. IDEALIZED STRESS-STRAIN CURVES FOR SOILS IN 'DRAINED' SHEAR

4.1 Uncemented Soils with Hard, Bulky Grains

Curve 1 in Fig. 5 (a) shows the stress-strain curve for a triaxial compression test on a very loose (highly contractive) specimen of sand composed chiefly of hard, bulky grains. The shear stress increases gradually with strain until a maximum is reached at Point 's_c'. The shear stress then remains constant with further strain. The volume decreases continuously as the shear stress is applied until a void ratio is reached that remains constant with further strain, Fig. 5 (b). At Point 's_c' the soil has reached the steady state of deformation.

The void ratio change in the state diagram (the state path) is simply a vertical straight line which starts at the initial state and moves continuously down toward the steady state line, Fig. 5 (c), since the effective minor principal stress is not allowed to change during this test. The stress path, Fig. 5 (d), is a straight line inclined at 45°. It ends at Point 's'.

A series of specimens tested in triaxial compression starting from states well above the steady state line and at various effective consolidation pressures would yield stress-strain curves similar in shape to Curve 1 in Fig. 5 (a). The initial tangent modulus would decrease as the void ratio after consolidation, e_c, increased and as the effective consolidation pressure, $\bar{\sigma}_{3c}$ decreased. The strain required to reach the steady state increases with increasing e_c and with increasing $\bar{\sigma}_{3c}$.

In no case would a peak develop. The specimen would be contractive throughout test until the steady state is reached, and the end points of the state paths would define a steady state line as illustrated in Fig. 5 (c). The corresponding steady state strength line, Fig. 5 (d), would be a straight or slightly curved line passing through the origin.

Specimen 2, consolidated isotropically to Point c_d in Fig. 5 (c), which is below the steady state line, first contracts slightly (Watson, 1940, P. 46) and then, as strains become large enough to cause grains to interfere with one another, it dilates until the same steady state void ratio is reached as for Specimen 1, as also shown in Fig. 5 (b). The stress-strain curve for Specimen 2, Fig. 5 (a), displays a peak at Point m when the void ratio is increasing at the maximum rate, due to the energy required to increase the volume against the confining pressure (Taylor, 1948, P. 346; Rowe, 1962, P. 501, 514). At larger strains the same steady state is reached as for Specimen 1.

The ratio of the peak to the steady state strengths from the drained test is defined by the author as the "drained sensitivity." This parameter is analogous to the usual sensitivity that was introduced by Terzaghi (see Skempton and Northey, 1952, P. 30) to describe the sensitivity of saturated soils to remolding at constant water content. To distinguish between the two, the latter will be called "undrained sensitivity" in this monograph. Both are useful indications of the potential magnitude of the effects of progressive failure.*

---

* Bishop (1967, P. 145) has suggested that brittleness be defined by $I_b = (\tau_m - \tau_s)/\tau_m$. This index "has the advantage that it expresses directly the maximum percentage error which can arise due to progressive failure in a brittle soil." The drained sensitivity (τ_m/τ_s) is used here because it is analogous to and has the same utility as the undrained sensitivity which is presently in common use.

The stress path for Specimen 2 is again a straight line inclined at 45°. It crosses the steady state strength line at a strain smaller than peak strain, rises to the peak Point m, and then doubles back on itself to stop on the same steady state strength line as found for Specimen 1. If a series of tests is performed on specimens prepared at the same void ratio as for Specimen 2, but at various values of $\bar{\sigma}_{3c}$, i.e., at states lying on a horizontal line through Point c_d in Fig. 5 (c), the stress paths would pass through a peak and then reverse direction to stop on the steady state strength line. The locus of these peak points would form the curved peak strength envelope shown in Fig. 5(d). This envelope must be curved since: (a) at zero confining pressure an uncemented soil has no strength, so that the peak strength envelope must pass through zero, (b) at sufficiently high confining pressures, the initial state of the specimens would be well above the steady state line, so that no peak would develop and the peak strength envelope would have to merge into the steady state envelope, (c) grain breakage would be more severe at high pressures, which could be expected to cause lower peak strengths than those that would obtain for no grain breakage, and (d) interparticle friction decreases with increasing interparticle force (Rowe, 1962, P. 505). The last two items would also cause a concave downward curvature of the steady state strength line, although it is shown as a straight line in Fig. 5 (d).

Test series on specimens prepared at constant void ratios e_1, e_2, and e_3 in Fig. 6 (a) would yield the series of strength envelopes shown in Fig. 6 (b). The utility of the concept of steady state lies in the hope that regardless of their initial state all specimens of the same soil tested with the same method of loading will show strengths corresponding to a unique steady state strength line (always plotted in terms of effective stress), as shown in Fig. 6 (b), if the tests are carried to sufficient strains.

Specimens prepared at void ratios equal to the steady state void ratio, Points 1, 2, and 3 in Fig. 6 (a), must display a peak in their stress-strain curves in triaxial compression tests. These specimens first contract and then dilate back to their original void ratio, the peak probably occurring at the point of maximum dilation rate. Although such specimens are prepared at the steady state void ratio, they are not in the steady state until they have been sheared to large strains. To form the steady state "structure" the initial structure must be altered appropriately by the shear stresses. This behavior in triaxial compression leads to the conclusion that there exists a line above the steady state line such that specimens prepared at states on or above that line will be contractive throughout a test until the steady state is reached. This boundary, shown dashed in Fig. 6 (a), will be referred to as the DC boundary. It may prove to have significant practical value since specimens prepared at states above this line would show a continuous decrease of the effective minor prinicpal stress during a consolidated, constant-volume test. Thus it may form the boundary between specimens that liquefy and those that do no liquefy under the particular set of test conditions that is used to establish the DC boundary.

The steady state void ratio for bulky-grained soils decreases with increasing effective consolidation stress, yet tests on one sand have shown that the steady state envelope is nevertheless straight for effective normal stresses less than about 4 kg/cm^2 (Castro, 1969, Fig. 19). It appears that in this stress range any decrease in resistance due to the increasing stress level (which would result from decreased interparticle friction and increased grain breakage) is counterbalanced by the lower void ratio of the steady state. Similarly, the void ratios at peak decrease with increasing stress. Thus,

none of the envelopes shown in Fig. 6 (b) are envelopes for constant void ratio at failure. It would be possible to define peak strength envelopes for which the void ratio at peak is a constant. But one cannot do the same for the steady state, if the steady state void ratio and the effective normal stress are uniquely related as postulated.

4.2 Uncemented Soils with Substantial Proportion of Platey Grains

The ideal behavior illustrated in Fig. 5 for hard, bulky-grained soils must be modified for the case of soils that contain large amounts of platey or elongate grains, because as strain occurs the grains become increasingly orientated in the direction of movement (Skempton, 1964, P. 83) and the mobilizable shear stress decreases as a result. At extremely large strains a steady state degree of orientation, and, hence, a steady state strength, is reached.

Specimen 1 in Fig. 7 (c) is prepared at a state well above the steady state line, such that it is contractive throughout shear, as seen in Fig. 7 (b). The stress-strain curve in Fig. 7 (a) has a peak even though the volume is decreasing at a rapid rate at peak (Point m_c). In this case the peak is not the result of dilation, but instead it is due to the loss in strength that follows when the particles in the failure zone become distinctly orientated. The axial strain required to develop the peak is very large because substantial movement between grains is needed to cause the necessary orientation. (Even at 20% axial strain, the relative movement between grains in any soil is still rather small.) Although the void ratio decreases after peak, due to

which a gain in resistance might be expected, the efficiency of the orientated structure is such that a net loss of resistance is observed. If the soil contained a larger percentage of bulky particles, the net effect would be no loss of resistance when the steady state is approached, as in Fig. 5 (a), Specimen 1. The relation between the distribution of particle shapes and the drained sensitivity of such a contractive specimen remains to be investigated.

The maximum shear stress for Specimen 1 occurs at a void ratio that lies above the steady state line (Fig. 7c) by an amount that depends on the initial state, the initial structure, and on the magnitude of the effect of orientation on the grains. The stress path in Fig. 7 (d) also shows the peak at Point m_c. It then reverses on itself to stop at Point s.

Consider a series of specimens prepared at states lying along a virgin compression curve, which will be assumed to pass through Point c_c in Fig. 7 (c). Consolidated-drained tests on these specimens will yield a line of peaks on the state diagram that lies above the steady state line and passes through Point m_c as shown. The location of this line of peaks is dependent on the initial state and structure of the specimen, because at peak the structure of the specimen has not yet been completely altered by the strains. As the effective consolidation pressure is increased, the line of peaks probably merges toward the steady state line, as shown in Fig. 8 (Lines b and c). This change with pressure is anticipated because the difference between the structure of the soil at peak and steady state can be expected to diminish gradually as $\bar{\sigma}_3$ increases. Thus, even for soils with very thin, platey grains one may observe no peak in the stress-strain curve of normally consolidated specimens tested at very high pressures in drained shear.

Corresponding to the line of peaks in Fig. 7 (c) for contractive specimens, the beginning of a peak strength envelope is shown passing through Point m_c in Fig. 7 (d). This peak strength envelope is the one that is usually referred to as the "effective stress envelope" for a given soil. One can see from the discussion in this monograph that this envelope is far from unique. It is a function not only of the soil, but also of the structure, states, and method of loading for the particular test series used to define the envelope. One can obtain very wide ranges in measured "friction angle" for any given soil. But the steady state strength line is likely to be more unique, being dependent only on the soil and the particular set of boundary conditions that exist during steady state deformation.

Specimen 2 in Fig. 7 (c) is prepared at a state below the steady state line and at the same effective stress as Specimen 1. In this case the specimen contracts slightly and then dilates with strain until the steady state is reached. Again, the strain required to reach steady state is very large because of the shape of the grains. The peak point on the stress-strain curve probably corresponds closely to the maximum rate of dilation because the strains required to reach peak in a highly dilative specimen are not sufficient to cause a marked orientation of the grains. (If a specimen were prepared at Point s in Fig. 7 (c), the grain orientation when the shear stress is near its maximum may cause a noticeable difference between the strain at peak and the strain at the point of maximum rate of dilation.)

The peak point for Specimen 2 is shown in Fig. 7 (c) to lie below the steady state line. If a series of specimens were prepared at states lying on a swelling curve, such as that shown dashed, a line of peaks for these dilative specimens could be defined, corresponding to the peak strength envelope passing

through Point m_d in Fig. 7 (d). Again it is seen that this "effective stress envelope" for "overconsolidated" (dilative) clays, is far from unique. Furthermore, the effective stress envelopes for contractive and dilative specimens cannot be expected to be the same (even after the resistance due to dilation rate is taken out), except by rare coincidence. Only when the steady state has been reached can one expect the effect of the initial state and structure of the specimens to be deleted, thus yielding a unique steady state envelope. The postulated relationship between the steady state line, the compression and swelling curves, and the lines of peaks, over the full range up to maximum past pressure, is shown in Fig. 8. The stress level AA' corresponds to the situation shown in Fig. 7 (c).

From Figs. 7 and 8 one can see that normally consolidated specimens have void ratios substantially greater than the steady state void ratio. Their behavior is analogous to that of loose sands. The differences between the shapes of stress-strain curves of normally consolidated clays and loose sands is accounted for chiefly by the distribution of grain shapes, which leads in clays to greater strain at failure and to the possibility of significant grain orientation due to the shear stresses. Quick clays and silts may be compared with extremely loose sands that might be slightly cemented--the cementation bonds being one mechanism through which extremely high void ratios may be maintained in a natural environment.

5. EXAMPLES OF STRESS-STRAIN CURVES FOR SOILS IN 'DRAINED' SHEAR

The stress-strain curves, volume change curves, stress paths and state paths for drained tests are discussed below for the following examples:

(a) Uncemented Soils with Bulky Grains

Highly contractive sand ('very loose') - Fig. 9

Slightly dilative sand ('loose') - Fig. 10

Highly dilative sand ('dense') - Fig. 11

(b) Uncemented Soils with substantial proportion of Platey Grains

Highly contractive clay (normally consolidated) - Fig. 12

Very highly contractive clay (quick) - Fig. 13

Highly dilative clay (heavily overconsolidated) - Fig. 14

5.1 Uncemented Soils with Bulky Grains

(a) Highly Contractive Sand ('Very Loose')

Fig. 9 shows the stress-strain curve, volume change curve, stress path and state path for a consolidated-drained triaxial compression test on a fine quartz sand. The notations at the bottom of the figure have the following meanings:

D_{10} - 10% of grains (by weight) are finer than D_{10}

C_u - Coefficient of uniformity

s_s - Specific gravity of soil solids

e_{max} - Maximum void ratio. Obtained by carefully pouring oven-dried sand into mold.

e_{min} - Minimum void ratio. Obtained by vibrating oven-dry sample.

$\bar{\sigma}_{3c}$ - Effective isotropic consolidation pressure

e_c - Void ratio after consolidation under $\bar{\sigma}_{3c}$

R_{dc} - Relative density after consolidation under $\bar{\sigma}_{3c}$

$$R_{dc} = \frac{e_{max} - e_c}{e_{max} - e_{min}}$$

u_c - Back pressure (applied to saturate specimen)

w - Water content

The stress coordinates in the graphs have been normalized by dividing each by $\bar{\sigma}_{3c}$.

The relative density at start of shear was only 17%, which is below the range of relative density usually encountered in practice. The results of this test are representative of the idealized case shown for Specimen 1 in Fig. 5.

The stress-strain curve shows a gradual rise to the maximum measured resistance at Point m. Even with lubricated ends and the comparatively large axial strain of 24%, the maximum shear stress was not reached. The resistance was still rising and the volume still decreasing when the test was stopped.* At Point m, the shear stress was $1.1\bar{\sigma}_{3c}$ and the volume had decreased 3.0%. If the test had been carried to completion, a steady state would have been reached at a somewhat greater shear stress and slightly lower void ratio. Thus Point m on the state diagram, at a relative density of 32.5%, is probably

---

* Arithmetic plots of stress-strain curves are often misleading because they make it appear that a maximum or a steady state condition has been reached when it has not. A plot of strains on a logarithmic scale quickly demonstrates whether these states truly have been achieved (LaGatta, 1970, P. 2-5).

slightly above the true steady state line, and the friction angle in terms of effective stress, ϕ_m, of 31.6° is somewhat smaller than the steady state friction angle.* The steady state relative density for this effective consolidation pressure (1.0 kg/cm^2) is about 35%, which in practice would be considered a "medium-loose" state (Gibbs and Holtz, 1957, Fig. 5).

The state diagram also contains a plot of the effective normal stress on the 45° plane versus the void ratio. This plot is a 'compression' curve for a test in which the principal stress ratio is continuously increasing, as compared with the more familiar compression curve for one-dimensional consolidation in which the principal stress ratio remains approximately constant (shown dashed in the state diagram). At shear stresses greater than about $0.3\tau_m$, the specimen becomes more compressible in the triaxial test than in one-dimensional compression. This result is reasonable because it is at this point that the shear stresses on the specimen in the two tests begin to deviate from each other. Whether or not the reversal of curvature at the end of the curve is real or an artifact of the test is unknown.

(b) Slightly Dilative Sand ('Medium Dense')

Fig. 10 shows the results of a consolidated-drained triaxial compression test on a slightly coarser (than that used for the test of Fig. 9) but still fine, uniform sand from the Sacramento River. It is composed primarily of

---

* Note that the slope angle, θ_m, of the line from the origin to Point m in the stress path in Fig. 9 is 27.6°. The angle ϕ_m is the slope of a line through the origin tangent to the Mohr circle through Point m. Thus $\sin \phi_m = \tan \theta_m$. In this case, $\sin 31.6^\circ = \tan 27.6^\circ$.

quartz but has some feldspar grains, which are less bulkly and more angular than quartz grains. In this case, the relative density after isotropic consolidation is 39%, which would make the specimen 'medium' dense according to Gibbs and Holtz (1957, Fig. 5). Comparison with Fig. 9 shows that the more contractive specimen was less stiff and required larger strain to reach the maximum shear stress. These differences exemplify the effects of decreasing contractiveness.

The test of Fig. 10 was again not carried to sufficient strain to define the steady state. At point s, the end of test, the shear stress was dropping slowly and the void ratio was increasing slowly. By extrapolating these curves, one can estimate that the steady state void ratio lies between Points c and s on the state path, perhaps at a relative density of 43%. Therefore, this specimen was prepared at a state slightly below the DC boundary (refer to Fig. 6) but probably slightly above the steady state line. The DC boundary would appear to lie about 5% in relative density, or 0.025 in void ratio, above the steady state line. The two lines are rather close together; for practical purposes it seldom would be necessary to distinguish between them for this soil.

Comparison of Figs. 9 and 10 gives:

	e_s	$\bar{\sigma}_{3c}$	C_u	Description of Grains
Fig. 9	0.72	1.0	1.8	Bulky, subrounded to subangular
Fig. 10	0.85	4.5	1.3	Bulky to somewhat elongate, angular to subrounded

The steady state void ratio was considerably higher for the case in Fig. 10 because the soil contained elongate and angular grains and was slightly more

uniform. If the $\bar{\sigma}_{3c}$ values had been equal, the difference would have been even larger. (At $\bar{\sigma}_{3c}$ = 4.5 kg/cm^2 for the soil of Fig. 9, e_s = 0.70.) Differences in grain shape and uniformity of grain size that appear small at first glance have substantial effect on the value of the steady state void ratio.

The peak point friction angle in Fig. 10 is 34.6°. If the test were carried to sufficient strain to define the steady state, a slightly lower friction angle would be obtained at that state.

The upward curl at the end of the state path for $\bar{\sigma}_{45}$ in Fig. 10 reflects the observed dilation at large strains and seems to be a logical change from the corresponding curve in Fig. 9. Therefore, the upward concavity at the end of the curve in Fig. 9 may not be a test error. Of course, a similar error could have occurred in both tests (although the tests were performed in different laboratories) at axial strains greater than about 12%.

(c) Highly Dilative Sand ('Dense')

Fig. 11 contains the results of a consolidated-drained triaxial compression test on the same soil used for the test on the highly contractive specimen in Fig. 9. In the present case, the relative density was 95%, as compared with only 17% before.

A definite peak (drained sensitivity of 1.4) was observed and the specimen dilated substantially. The maximum dilation rate corresponds well with the peak. It is this type of result that permits the idealization shown in Fig. 5.

Comparison of Figs. 9, 10, and 11 shows the transition in shape of stress-strain curves for bulky-grained soils as the density is increased. One

finds increasing stiffness, increasing shear strength, lower strain to reach the maximum shear stress, increasing drained sensitivity, and increasing dilation.

Comparison of Figs. 9 and 11 shows that the steady state void ratio lies for this soil between 0.68 and 0.73 (for $\bar{\sigma}_{3c}$ = 1.0 kg/cm^2), which are values measured at the end of these two tests. In neither case was the strain sufficient to reach the steady state. Because failure planes developed in the highly dilative specimen, the measured volume changes are more suspect. Therefore, it is likely that the steady state void ratio is closer to 0.73, and the previously estimated value of 0.72 (relative density of 35%) may be reasonable.

The shear strength of the dilative specimen is $1.8\bar{\sigma}_{3c}$ as compared with $1.1\bar{\sigma}_{3c}$ for the very loose specimen. These values correspond to ϕ_m = 39.6° and 31.6°, respectively. Increasing the density of this soil is very effective in providing increased shear strength.

The state path for $\bar{\sigma}_{45}$ in Fig. 11 shows in another form that the shear stress caused volume increase, whereas one-dimensional compression from the Point c would yield the dashed curve. The stresses applied during the triaxial test cause compression similar to one-dimensional compression up to the point when the shear stresses reach about one-half of the peak shear stress.

5.2 Uncemented Soils with Substantial Proportion of Platey Grains

(a) Highly Contractive Clay (Normally Consolidated)

Fig. 12 shows the results of a consolidated-drained rotation shear test on a very thin, annular specimen of remolded Pepper shale. This test is representative for the idealized case shown in Fig. 7, Specimen 1. It was consolidated from a water content of 64% (liquidity index = 0.80) to an effective normal stress on the horizontal plane of 4.0 kg/cm^2. The new notations in Fig. 12 are:

$\bar{\sigma}_h$	Effective normal stress on horizontal plane
a	Denotes stage of test after consolidation under the effective normal stress in complete (just before start of loading). The consolidation stresses are anisotropic, hence the use of 'a'.
i	Subscript to denote initial or as-molded state
τ_h	Shear stress on horizontal plane
H	Thickness of specimen
δ	Peripheral displacement
γ	Shear strain (= δ/H_a)
v	Volumetric strain
G_w	Degree of saturation
L_w	Liquid limit
P_w	Plastic limit

The stress-strain curve shows a peak at the extremely large shear strain of 63% and then a very gradual decrease in shear stress, as the grains become better orientated, until a constant shear stress is reached at a "shear strain" of 5260%. Many published stress-strain curves for remolded, normally consolidated specimens in drained shear show a gradual rise to a maximum without subsequent reduction in shear stress. Such results are

obtained if the tests are stopped at conventional low strains. The shear strain at peak of 63% is approximately equivalent to an axial strain of 40% in triaxial compression (assuming the method of loading has no effect on strain at peak). Neither triaxial tests nor direct simple shear tests can be carried to sufficient strain to define the entire stress-strain curve shown in Fig. 12. Two features of this test accentuate formation of a peak: (1) the specimen was anisotropically consolidated at $\sigma_1/\sigma_3 \cong 2$ and (2) it was prepared at w_i = 61% (liquidity index = 80). It is unlikely that their combined effect would reduce the drained sensitivity appreciably below the observed value of S_d = 1.7. If behavior at large strains is to be represented, the assumption that a normally consolidated clay will fail plastically in drained shear must be discarded.

The 'shear strains' that are plotted beyond peak in Fig. 12 are much smaller than the actual strains in the failure zone because a very thin shear zone must begin to form approximately when the peak is reached. (The shear surface observed after test was a very shiny slickenside.) The true shear strains in the failure zone are probably many times greater than those plotted, so it may be more appropriate to speak of the displacements that are required to reach a given point beyond peak. The peripheral displacement at Point m is 0.084 cm, compared with 7.0 cm when the steady state is reached at Point s.

The measured peak shear stress is only 0.22 $\bar{\sigma}_{ha}$ and the steady state shear strength is only 0.13 $\bar{\sigma}_{ha}$, corresponding to a peak friction angle of 12.5° and a steady state friction angle of 7.5°. The very low peak friction angle may be partially the result of grain orientation, which may already have become significant at the large strain at which this peak occurred.

The volume of the specimen decreased throughout the test. In this case, the peak was not formed because of dilation* against $\bar{\sigma}_h$, but instead was the result of grain orientation at large strains. Even at Point s, where it is estimated that the steady state had been reached, the volume was decreasing at a very slow rate. Thus, Point s does not fully satisfy the definition of steady state. When the peripheral displacement was increased from 7 to 23.5 cm the shear stress remained constant and the volume continued to decrease. It seems probable that these volume decreases were due to loss of soil, (although extreme care was taken to contain this fine-grained clay) because one would expect a gain in strength if the void ratio actually decreased from 0.70 at Point s to 0.62 at Point u. Also, a steady state void ratio close to the void ratio at the plastic limit (e = 0.61) seems, intuitively, too low for $\bar{\sigma}_{ha}$ = 4.0 kg/sq cm. Further investigation is needed into the void ratio changes that accompany large deformations in rotation shear. It is likely that none of the void ratios in Fig. 12 represent the void ratio in the very thin failure zone in this specimen, except perhaps at the very early stages of the test.

(b) Very Highly Contractive Clay (Quick)

On the basis of Fig. 7, one would expect that a drained test on a 'quick' clay, which is a very highly contractive soil, would give a stress-strain curve with a substantial peak, since even a remolded, normally consolidated specimen showed a drained sensitivity as high as 1.7 (Fig. 12). Although no drained tests on quick clays have yet been carried to large

---

* In fact, a small amount of energy was being released by this specimen due to volume decrease at peak. This energy causes the magnitude of the peak shear stress to be smaller than it would be if the volume were not changing at peak.

enough strains to prove whether or not a peak does occur, some information on this point may be gained from a study of Fig. 13. It contains the results of a consolidated-drained direct shear test on a Norwegian clay with an undrained sensitivity of 40 to 150. The specimen was consolidated to $\bar{\sigma}_{ha}$ = 0.58 kg/sq cm, which is equal to the in-situ effective overburden pressure. The void ratio after consolidation was about 1.19, as compared with void ratios of 0.70 and 0.56 at the liquid and plastic limits, respectively.

The stress-strain curve showed a break* at $\tau = 0.22\ \bar{\sigma}_{ha}$, rose to $\tau_m = 0.4\ \bar{\sigma}_{ha}$ at a shear strain of 42%, and it displayed no peak. The volume decreased continuously throughout the test. If this test could have been continued to large strains, the shear stress would have increased still further - - to a friction angle greater than 21.9°. It is not clear whether a reduction in shear stress would have occurred at very large strains, but according to Skempton (1964) a soil such as this, with 48% of its grains finer than two microns, would have a steady state friction angle between 10° and 21°. Thus, it is plausible to expect a peak in the stress-strain curve for this quick clay. The drained sensitivity probably would lie between 1.1 and 2.

The state diagram in Fig. 13 shows that the void ratio at Point m was 0.98, which is substantially greater than the void ratio at the liquid limit. One could expect a large volume decrease before reaching steady state in this specimen. The shear stress may therefore increase before decreasing again to the steady state friction angle estimated above.

---

* Bjerrum and Landva (1966, P. 15) explained the presence of the break as due to breakdown of the sensitive, undisturbed structure of the specimen.

(c) Highly Dilative Clay (Heavily Overconsolidated)

Fig. 14 shows the results of a consolidated-drained rotation shear test on a specimen of remolded Pepper shale that was consolidated to 100 kg/cm^2 and swelled back to 1.0 kg/cm^2 before start of rotation. This test is representative for the idealized test shown in Fig. 7, Specimen 2. The stress-strain curve shows the expected sharp peak at a shear stress of 0.5 $\bar{\sigma}_{ha}$ and a shear strain of 20%. This shear strain is equivalent to an axial strain of about 12% in the triaxial cell (assuming no effect of method of loading), which is a reasonable peak strain for a heavily overconsolidated, remolded clay. The peak friction angle is 26.6°. At the steady state the shear stress is 0.14 $\bar{\sigma}_{ha}$, and the friction angle is 8.2°. The drained sensitivity of 3.4 is not unusually high for such a heavily overconsolidated clay.*

The steady state friction angle of 8.2° in Fig. 14 compares well with the value of 7.5° shown in Fig. 12. (Both of these tests were performed on specimens from the same batch of soil.) The small difference between the two results is practically eliminated when the friction against the confining ring is subtracted. The small horizontal tick marks on the stress paths in Figs. 12 and 14 just below Points s show the steady state strength after removal of this friction. This equality of residual (steady state) friction angles for normally and heavily overconsolidated specimens was anticipated by Skempton (1964, Fig. 6).

---

* The degree of progressive failure that takes place in a specimen of these dimensions is probably not sufficient to reduce the measured peak shear stress, and hence the drained sensitivity, by more than 20%.

The volume of the specimen of Fig. 14 increased at the maximum rate near the peak point of the stress-strain curve and continued to increase at larger strains, but the point of maximum dilation rate cannot be determined very precisely from these data. When the steady state was reached at Point s, the volume had increased 8%, and beyond that point there was no change in volume or shear stress. In this case, no effect of squeezing out of soil was apparent. But because a shiny slickenside was formed, the observed volume increase very likely represents changes in only a thin zone of the specimen. It is likely that the actual percent volume increase within the failure zone was substantially greater than the recorded value, and that squeezing out was occurring simultaneously. In any event, the shear stress did reach a constant value.

The best estimates of the steady state void ratios from Fig. 12 and 14, assuming uniform specimens in each case, are:

	$\bar{\sigma}_{ha}$ kg/cm^2	Overconsolidation ratio	e_a	e_s (est.)
Fig. 14	1.0	100	0.68	0.81
Fig. 12	4.0	1	0.84	0.70

Although these values may be grossly in error, they do decrease with increasing effective stress as expected.

6. IDEALIZED STRESS-STRAIN CURVES FOR SOILS SHEARED AT CONSTANT VOLUME

6.1 Uncemented Soils with Hard, Bulky Grains

Fig. 15 shows the idealized relationships among stress-strain curves, changes in effective stress, stress paths, and the state paths followed during constant-volume shear of specimens composed of hard, bulky grains.

For Specimen 1, prepared in a highly contractive state, the stress-strain curve rises to a rather sharp peak and then drops to a steady state shear stress at large strains. The undrained sensitivity shown for this example is about 2. The corresponding stress path shows that the maximum shear stress (Point m) is reached when the effective principal stress ratio is smaller than its value at the steady state (Point s). When Point s is reached, the stress path simply stops--no further change in shear stress or effective normal stress occurs. The state path starts at Point c (Specimen 1) and moves horizontally to the left, since the void ratio is held constant, passing the peak shear stress at Point m and continuing to the left until the steady state line is reached. The line of peaks through Point m lies well above the steady state line. In Fig. 15 (d) the effective minor principal stress is seen to decrease continuously with strain until the steady state is reached. There is no obvious change in curvature as the peak shear stress, Point m, is passed.

Assuming that Specimen 1 was fully saturated and that volume was maintained constant by allowing no change in water content, the stress-strain behavior may be explained qualitatively as the combination of two effects:

(1) the continuous increase in the mobilized effective principal stress ratio with strain, and (2) the simultaneous build-up or pore pressure and consequent reduction of the effective minor principal stress due to the tendency for volume decrease under shear stress.

During the early stages of the test, the shear stress rises because the effect of the increasing principal stress ratio is greater than the effect of the reduction of $\bar{\sigma}_3$. At some point during the test, the effect of the increased principal stress ratio is exactly offset by the effect of the decreasing $\bar{\sigma}_3$. At this point, the peak occurs in the stress-strain curve. At larger strains, the rate of pore pressure build-up is so rapid that, even though the effective principal stress ratio continues to rise slowly, the net effect is a decrease in shear stress, as shown at points beyond Point m in Figs. 15(a) and 15(b). In this case, the drop in shear stress beyond peak is not due to increasing void ratio,as it was in the case of drained tests, nor is it due to orientation of grains. It is merely the effect of a continuous rise in pore pressure as the structure collapses. For this bulky-grained soil, one would expect no decrease of $\bar{\sigma}_1/\bar{\sigma}_3$ even at very large strains, because grain orientation effects should be small.

Specimen 2 is prepared at an initial state that is below the steady state line, Point c, in Fig. 15(c). Again the observed behavior is due to the combined effects of the changes in the effective principal stress ratio and the effective minor principal stress. During the early stages of shear, the pore pressure increases slightly, the effective principal stress ratio rises, and a net increase in shear stress results. The slope of the stress-strain curve decreases up to Point q in Fig. 15(a). But with greater strains,

the soil grains start interfering with each other and the specimen tries to increase in volume. Since the volume increase is prevented by maintaining constant water content, the pore pressure drops so that the effective minor principal stress increases, Fig. 15(d). At this stage, both the changes in $\bar{\sigma}_3$ and in $\bar{\sigma}_1/\bar{\sigma}_3$ tend to increase the shear stress. The combination causes the stress-strain curve to "stiffen," i.e., its slope increases, at Point q in Fig. 15 (a). Subsequently, the pore pressure drops continuously and, therefore, the mobilizable shear stress increases continuously until the steady state is finally reached at very large strains.

The stress path, Fig. 15 (b), shows that the maximum principal stress ratio (Point p) occurs at some stage prior to the stage when the maximum shear stress is reached (Point m). For some time the author felt that such data were the result of test errors. However, Wroth and Bassett (1965, Fig. 7) have shown that the peak principal stress ratio should occur before Point m, at the point when the rate of change of effective minor principal stress is a maximum, i.e., at Point p in Fig. 15 (d). This relationship is analogous to the development of the peak principal stress ratio (or peak shear stress) in drained tests at the point when volume is increasing most rapidly.* Although the principal stress ratio decreases at strains beyond Point p, it does not decrease enough (from this cause) to result in a net decrease in shear stress.

---

* In the present case, an increased principal stress ratio is needed to increase the effective minor principal stress at constant volume rather than to increase volume at constant stress. For contractive specimens in undrained tests, a smaller principal stress ratio is needed because of the continued decrease in effective minor principal stress. Thus the stress path for Specimen 1 should not be expected to cross the steady state envelope in Fig. 15 (b).

By comparing Fig. 15 for constant volume tests with Fig. 5 for drained tests, one can see the value of the concept of steady state as displayed on the state diagram. Given the steady state line, one can predict the end point for a test on a specimen prepared at any initial state, and one can estimate the shape of a stress-strain curve and the changes in volume or effective stress that will occur as the steady state is approached. More information is needed to judge the conditions that develop at peak, but the location of the steady state line relative to the starting point for the test does set certain broad limits on the resistance and effective stresses that develop at peak.

6.2 Uncemented Soils with Substantial Proportion of Platey Grains

Fig. 16 shows the idealized stress-strain curves, stress paths, state paths and effective minor principal stress curves for contractive and dilative specimens of a platey-grained soil in constant-volume shear.

The major difference between Figs. 15 and 16 results from the substantial grain orientation that can occur in a soil containing chiefly platey (or perhaps elongate) grains. The principal stress ratio that can be mobilized first increases and then decreases appreciably at larger strains, as the grains in the failure zone become orientated. Superimposed on these changes are the changes of effective minor principal stress that are caused by the constraint on volume change.

For the contractive case, Specimen 1, the stress-strain curve can be expected to show a substantial post-peak loss of resistance due to the

combined effect of pore pressure build-up and grain orientation at large strains. The effect of grain orientation at very large strains can be expected to be small, if the specimen remains homogeneous, because the void ratio is so high that the particles are not too close together in any case. The undrained sensitivity shown for this example is about 3.7. The stress path shows that in the steady state the principal stress ratio for this type of soil has a value smaller than its maximum at p_c, which is quite different from the result for bulky-grained soils wherein the maximum principal stress ratio occurs at the steady state. The principal stress ratio drops at large strains as a result of grain orientation. Usually, only at very large strains is there sufficient orientation to observe this drop in principal stress ratio in actual tests.

The state path for Specimen 1 shows Point m to the right of the steady state line. The location of the line of peaks through Point m is a function of the initial state and structure of the specimens, as before. The steady state line is reached when the grains have finally reached a steady-state orientation, just as was the case for drained tests.

The shape of the curve of effective minor principal stress vs. axial strain for Specimen 1, Fig. 16 (d), is similar to that for the bulky-grained soil of Fig. 15. In the present case, the effective minor principal stress at peak is 0.4 times its value at the end of consolidation, which corresponds to a value of Skempton's pore pressure coefficient, A_m, of 0.9. When the steady state is reached, the effective minor principal stress is only one-quarter of its original value, and $A_s = 4.2$.

For the dilative case, Specimen 2 in Fig. 15 (a), the stress-strain curve shows the same initial shape as was given for the bulky-grained specimen in Fig. 15. But in this case, a peak does form at Point m because of grain orientation at larger strains. The stress path passes the maximum principal stress ratio and then rises to the peak when the effect of increasing effective minor principal stress is just balanced by the effect of decreasing principal stress ratio, the latter being caused by grain reorientation. The peak point can be expected to lie on an envelope that is steeper than that for the contractive case, because (1) for the dilative specimen $\bar{\sigma}_3$ is increasing and for the contractive specimen $\bar{\sigma}_3$ is decreasing, and (2) the smaller effective minor principal stress for the dilative specimen may mean that a higher principal stress ratio can be mobilized due to higher interparticle friction. At the steady state, the same point is reached as for the contractive specimen, assuming a unique steady state line and ideal tests.

The line of peaks for dilative specimens, Fig. 16 (c), lies to the left of the steady state line and bears no relation to the line of peaks for highly contractive specimens.

Fig. 16 (d) shows for the dilative specimen the usual small decrease of effective minor principal stress, followed by an increase as the grains interfere and try to cause dilation. The effective stress then rises continuously until the steady state is reached. This change increases the shear resistance, but the stress-strain curve nevertheless shows a drop due to the overpowering effect of grain orientation.

Test errors make it practically impossible to observe all of the characteristics illustrated in Fig. 16. The dashed stress paths and state paths show the expected effect of void ratio changes within an individual specimen due to small initial non-uniformities in void ratio and stress distribution. Specimen 1 tries to contract during shear. On one plane in the specimen the shear stress will be more critical than on adjacent parallel planes and that plane will begin to deform more than its neighbors. In the region close to that plane, the grains will become more orientated than in the adjacent zones and the resistance will, therefore, decrease more rapidly with strain than would be expected for a uniform specimen. For a real test, the stress-strain curve beyond the peak strain would lie to the left of the idealized curve shown for Specimen 1, but at very large strains, the measured stress-strain curve would cross the ideal curve because there would be internal drainage away from the failure zone. The stress path would change from that shown as a solid line in Fig. 16 (b) to that shown dashed. A similar argument leads to the stress path shown dashed for the dilative specimen. Therefore, although for ideal constant-volume tests one might expect to reach the same steady state strength for both dilative and contractive specimens, test errors prohibit that oberva-tion. (Specimen non-uniformities also develop in drained tests and they cause errors in measurement of the steady state void ratio. But the steady state strength in drained tests for both contractive and dilative specimens are in closer agreement, as shown in Fig. 6)

In Fig. 16 (d) the Point p (maximum principal stress ratio) is shown at the point where $\bar{\sigma}_3$ is increasing most rapidly, in accordance with the prediction by Wroth and Bassett (1965, Fig. 7). However, observations have not yet confirmed this prediction, as will be seen in Section 7.2.

7. EXAMPLES OF STRESS-STRAIN CURVES FOR SOILS SHEARED AT CONSTANT VOLUME

7.1 Uncemented Soils with Bulky Grains

(a) Highly Contractive Sand ('Very Loose')

Fig. 17 shows the results of a consolidated-constant-volume triaxial compression test on a fine, uniform sand consolidated to an effective stress of 4.0 kg/cm^2 at a relative density of only 27%. This test illustrates the idealized behavior shown for Specimen 1 in Fig. 15.

The stress-strain curve has a sharp peak, at the low axial strain of 1%, followed by a large drop in shear stress and simultaneous decrease of the effective minor principal stress. At peak the A-value was 1.28, which is in the same range as A-values measured in sensitive, normally-consolidated clays. When Point s was reached, the A-value had increased to about 16! These changes correspond to a loss of all but 3% of the effective consolidation pressure, and an undrained sensitivity of about 8, all of which were caused by the collapse of the very loose structure of this specimen. From the stress path, it is seen that the peak point is reached at $\emptyset = 30^\circ$. The maximum principal stress ratio developed only at the larger strains corresponding to Point s. Since grain orientation in this soil probably has small effects, no drop of the principal stress ratio occurred even at 20% strain. The point on the state path corresponding to the peak, Point m, occurred at a substantial distance from Point s.

This test result demonstrates the shape of stress-strain curve that occurs when specimens liquefy in the laboratory under static loading. After

test, such specimens segregate into soil at the bottom with a layer of water at the top. A similar shape of curve may be expected to occur in-situ during liquefaction. But a specimen at the same void ratio in-situ would be more unstable than might be deduced from Fig. 17, because of anisotropic consolidation. For example, assume that in-situ $\bar{\sigma}_1/\bar{\sigma}_3 = 1.5$ and $\bar{\sigma}_3 = 3$ kg/cm^2, corresponding to Point a in Fig. 17. Then the shear stress need be changed by only 0.05 $\bar{\sigma}_{3c}$ to cause liquefaction (Castro, 1969, Fig. 63). Because the strength after liquefaction (.03 $\bar{\sigma}_{3c}$) would be lower than the shear stress at Point a (.19 $\bar{\sigma}_{3c}$), one can expect very large deformations before cessation of movement after liquefaction. Cyclic shear stresses of even smaller magnitude than .05 $\bar{\sigma}_{3c}$ would be sufficient to cause liquefaction in such a specimen.

A. Casagrande has postulated that the liquefied state (Point s in Fig. 17) is a special state in which the particles have adjusted themselves, after collapse of the structure that existed at Point c, so as to offer a minimum resistance to deformation. He referred to this new structure as the "flow structure."* This hypothesis by Casagrande requires investigation, as its implications are important for complete understanding of liquefaction and the interparticle processes that govern the shapes of the stress-strain curves of soils.

---

* Casagrande made this suggestion in his lectures on soil mechanics that the author attended in 1959 and had made it in previous years also, probably for the first time in the early 1950's or perhaps even earlier.

It seems reasonable that such a state might exist over a limited (but very important in practice) range of strain just after the initial structure collapses. At that stage one might visualize that all particles are momentarily practically floating ($\bar{\sigma}_3 \sim 0$) until sufficient strain occurs to cause them to contact each other again and to tend towards the steady state. The movement between particles that is required to achieve an overall axial strain of 20% is very small. Therefore, Point s in Fig. 17 may not be the steady state as defined in this paper, but it may be a temporary neutral state which will be lost at large strains. If so, the stress path would reverse and move up to the right along a strength envelope inclined at about 30°, and the steady state would be reached at some very large strain not achievable in the triaxial cell. In the state diagram, the steady state would then lie to the right of Point s, and could lie even to the right of Point m.

(b) Sand Close to Steady State Void Ratio

Fig. 18 shows the results of a consolidated-constant-volume triaxial compression test on a fine, uniform, river sand. The specimen was consolidated to the high effective minor principal stress of 35.1 kg/cm^2 at a relative density of 48.5%. This curve deserves considerable attention because it represents behavior of soils prepared at a state close to the steady state.

The early portions of the plots in Fig. 18, up to Point q, look much like the early portion of the corresponding plots in Fig. 17. The following points in the two figures are probably analogous:

	Fig. 18	Fig. 17
Maximum shear stress prior to collapse of soil structure	b	m
Maximum pore pressure build-up due to collapse of structure	q	s

It is interesting that at Point b (Fig. 18) $\bar{\sigma}_3 = 0.39\ \bar{\sigma}_{3c}$, which compares well with the value of $0.4\bar{\sigma}_{3c}$ at the analogous point in Fig. 17. But the subsequent pore pressure build-up was much less in Fig. 18, reaching a maximum at Point q, where A = 1.12, as compared with A = 16 at Point s in Fig. 17. Consequently, the drop in shear stress from Point b to Point q in Fig. 18 was slight.

The shape of the curve beyond Point q in Fig. 18 may represent the true behavior of this specimen or it may be due to test error. If it is true behavior, one may explain it with the aid of Casagrande's postulate that just after collapse of the soil structure the particles orientate themselves in such a manner as to offer least resistance to deformation. At this stage, the pore pressure would build up to a maximum value. Subsequent strains would cause the particles to interfere with each other somewhat, resulting in a slight decrease in pore pressure until the steady state is finally reached at large strains. Similar behavior would not be observed in looser specimens (Fig. 17) because extremely large strains would be needed to reach the steady state.

Alternatively, the shape of the stress-strain curve beyond Point q may be due to non-uniform void ratio in the specimen. It may well be that the deformations between Points b and q were concentrated within a small zone that was approaching the steady state of deformation. During this process, the

zone would be contractive and water would flow to adjacent zones. The shear stress would then have to be increased until a fairly large zone of the specimen was in a steady state of deformation. A void ratio variation of only about 0.004 (!) would be sufficient to cause the behavior displayed in Fig. 18. If this interpretation is correct, and if the specimen had a truly uniform void ratio, then the stress-strain curve and the pore pressure curve in Fig. 18 would be as shown dashed. In such a case, one could conclude that this specimen had been prepared at a void ratio almost precisely on the DC-boundary (Fig. 6).

The drop in shear stress at strains beyond Point m is consistent with the probability that grain breakage was occurring during this rather high-pressure test. But if such were the case, the pore pressure probably should have risen simultaneously, which is opposite to what was observed. Therefore, the behavior beyond Point m might be attributed to a test error (due to a slight specimen non-uniformity or slightly incorrect "area correction") or to a combination of grain breakage and test error.

(c) Highly Dilative Sand ('Dense')

Fig. 19 shows results of a consolidated-constant-volume triaxial compression test on a fully saturated specimen of a uniform, medium sand. It was consolidated to $\bar{\sigma}_{3c}$ = 6.6 kg/cm^2 at a relative density of 84%. A very high back pressure of 63.5 kg/cm^2 was used to ensure that full saturation was maintained throughout shear.

The doubly-curved stress-strain curve that results as the specimen passes from the contractive to the dilative state is very well demonstrated.

The explanation for this shape was given qualitatively by Hirschfeld (1958 P. 144). Later this behavior was explained quantitatively by Wroth and Basset (1965, Fig. 7). The maximum principal stress ratio occurs at the second inflection point of the stress-strain curve, which is also close to the point at which the rate of increase of $\bar{\sigma}_3$ is a maximum, as anticipated by Wroth and Bassett. The A-value for this specimen varies from +0.13 at start of loading to -0.42 at peak and, because of the strong negative pore pressures, the peak shear stress is about $9\bar{\sigma}_{3c}$, or 25 times greater than the maximum shear stress measured for the loose specimen of Fig. 18.

The steady state for this specimen is probably near Point m. But grain breakage was occurring at that stage (Wissa, 1970), which means that the steady state could not truly be reached until grain breakage ceased. The reversal of the stress path beyond peak may be due to cavitation of the pore water, grain breakage, and perhaps to small test errors.

7.2 Uncemented Soils with Substantial Proportion of Platey Grains

(a) Very Highly Contractive Clay (Quick)

Fig. 20 shows the results of a consolidated-constant-volume simple shear test on a normally consolidated specimen of a quick silty clay. The undisturbed specimen was consolidated to an effective stress on the horizontal plane, $\bar{\sigma}_{hc}$, of 2.0 kg/cm^2 at a void ratio of 0.76. The void ratio at the liquid limit is 0.67 and at the plastic limit 0.53 for this soil. Therefore, the undisturbed soil must be very sensitive to disturbance of its structure. The measured undrained sensitivity, obtained by vane tests on several specimens ranged from 40 to 150.

The stress-strain curve displays a slight drop after peak. Because of the presence of platey grains, the shear strain at peak is relatively high, 15% (equivalent to $\varepsilon_1 \simeq 10\%$), as compared with only 1% axial strain at peak for the very loose, bulky-grained sand of Fig. 17. At the end of test the shear stress and the effective stress on the horizontal plane are still dropping, and the stress path indicates that the effective principal stress ratio is still increasing. If there is to be any drop in the principal stress ratio due to orientation of grains, as anticipated by the stress path for Specimen 1 in Fig. 16, the strains were not sufficient in this test to display that effect. Judging from the undrained sensitivity of 40-150, one might expect that if strain were continued the stress path would continue its movement downward and to the left. For this soil the strains required to reach the steady state would be very large. The steady state probably has not been even closely approached during this test, although it probably was closely approached when the vane tests were performed to measure undrained sensitivity. The A-value at peak is about 1.2, as for the very loose sand of Fig. 17. The steady state A-value probably would be about 100 for this specimen of quick clay.

(b) Highly Contractive Clay (Normally Consolidated)

Fig. 21 shows the results of a consolidated-constant-volume triaxial compression test for a typical normally consolidated clay. The specimen was fully saturated and consolidated to $\bar{\sigma}_{3c}$ = kg/cm^2 at a void ratio of 1.55.

The void ratio at the liquid limit is about 2.2 and at the plastic limit about 1.1.

The stress-strain curve shows the gradual rise to peak, as usually reported for such soils, and the peak strain of 5% is typical. The effective minor principal stress is still dropping at Point m. Therefore, the steady state has not yet been reached for this specimen. The reported undrained sensitivity of 10 means that the stress-strain curve and stress path would stop approximately on a line where $\tau_{45}/\bar{\sigma}_{3c} = 0.04$, as shown on the stress-strain curve.

The peak point A-value was 0.9 and the A-value at the steady state would probably be about 20. Thus the stress-strain curve shown in Fig. 21 is only part of the entire curve and it does not demonstrate whether the principal stress ratio would drop at large strains due to grain orientation. The balance of the curve cannot be obtained in the triaxial test although its shape can be estimated with the aid of vane tests. The corresponding stress path that might have been followed if the test were carried to large strains is shown dashed.

A slightly more complete stress-strain curve for a normally consolidated clay is shown in Figure 22. A specimen of London clay was consolidated from a slurry at a water content of 163% to an effective consolidation pressure of 60.2 kg/cm^2. It was loaded at constant volume in triaxial compression. In this case the stress-strain curve shows a slight peak--the maximum shear stress occurring at an axial strain of 8.5%, which is not too great when one considers the very high effective consolidation pressure. At peak, $\bar{\sigma}_3$ was still decreasing

and $\bar{\sigma}_1/\bar{\sigma}_3$ was increasing, as for the previous example. But with further strain $\bar{\sigma}_1/\bar{\sigma}_3$ reached a peak and showed a slight drop at the largest strains, as shown by the stress path.

When the test was stopped at 20% strain, ϕ had dropped from a maximum of 16.5° to 15.3°. The latter figure is only 0.3° greater than the steady state (residual) value of 15° reported by Bishop, Webb, and Skinner (1965, Fig. 11) for this soil. This final drop of the principal stress ratio occurred chiefly towards the end of the test where the stress-strain curve turns down slightly. Therefore the change could be due to test error rather than to orientation of grains. Nevertheless, the small difference between the final ϕ-value and the steady state value indicates that the steady state was closely approached in this test. The small difference between ϕ_m and the steady state ϕ is due to the high pressure used. In Fig. 8 it is indicated that the line-of-peaks and the steady state line can be expected to converge at high pressure. It would be expected that the corresponding ϕ-values should converge also.

(c) Highly Dilative Clay (Overconsolidated)

Fig. 23 shows the results of a consolidated-undrained triaxial compression test on a fully saturated, compacted specimen tested at $\bar{\sigma}_{3c} = 2.1$ kg/cm^2 and $e_c = 0.5$. The void ratio at the liquid limit is 0.94 and at the plastic limit it is 0.41. Therefore the specimen could be expected to be dilative at the low consolidation pressure used for this test.

The stress-strain curve shows the expected double curvature and gradual rise to maximum shear stress. At the end of test the shear stress and effective minor principal stress are still rising, indicating that the true maximum, i.e., the steady state, could be developed only after substantial additional strains. The first point of inflection corresponds closely to the minimum value of effective minor principal stress, and the second inflection point approximately to the point at which the maximum principal stress ratio is reached. A small reduction of the principal stress ratio occurs at large strains. This change probably is due to the change in rate of increase of $\bar{\sigma}_3$ rather than to orientation of grains.

The steady state was more closely approached in the example illustrated in Fig. 24. An undisturbed, heavily-overconsolidated specimen of London clay was tested at constant volume in triaxial compression at $\bar{\sigma}_{3c} = 1.05$ kg/cm^2. In this case the reversal of curvature of the early portion of the stress-strain curve was not observed and the effective minor principal stress dropped extraordinarily rapidly - almost to zero - before starting to rise again. The A-value for this portion of the curve was close to one-third, as shown in the stress path, which is the value exhibited by perfectly elastic materials. It may be inferred that this specimen was cemented.* The cementation accounts for the fact that no reversal of curvature is observed in the stress-strain curve for this specimen.

---

* Bishop (1969) has shown that London clay does have tensile strength, i.e., it is cemented.

At the peak Point m, a thin failure zone developed along which subsequent displacements were concentrated. (The horizontal axis was given in percent axial displacement rather than strain, since the strains in the failure zone were unknown beyond peak.) Therefore, the clay grains in the failure zone probably became orientated. Also the failure zone probably increased in water content at the expense of adjacent zones (thus the state path for the failure zone is not truly horizontal for this test). These effects would be expected to cause reduction in shear stress and principal stress ratio from Point m to Point s, as was observed. At 11% axial displacement the strains in the failure zone were already large enough to cause the stress path to approach the steady state strength line very closely. This stress path is related to the dashed stress path for the highly dilative specimen in Fig. 16.

8. APPLICATIONS

Several specific examples of how the information presented in Figs. 5, 7, 15 and 16 can be used to help understand soil behavior are given in the subsequent paragraphs of this chapter.

8.1 Significance of the Terms "Normally Consolidated" and Loose"

The distinguishing quality of normally consolidated specimens of water-deposited clays is that they are contractive if tested at effective stresses equal to or higher than the in-situ stresses. (The degree to which they are contractive, as measured by the height of the virgin compression curve above the steady state line, is dependent upon every detail of their geologic history because their composition and structure are dependent upon this history.) Overconsolidation, on the other hand, causes the state of a clay to move toward or even below the steady state line, and a heavily overconsolidated clay is generally dilative if tested at effective stresses equal to or less than the in-situ stresses.

Residual clays are an exception because they may be normally consolidated, never having been subjected to higher effective normal stress than currently exists, and yet have low enough void ratio to be dilative at low effective stresses.

For sands, the term overconsolidation has little meaning because normal stress alters the state of a sand much less than it does the state of a clay. As one passes from clean sands (or rockfills) to clays, there is an increasing influence of pre-existing effective normal stresses on the void ratio after removal of those stresses.

For sands, the term "loose," as defined by Gibbs and Holtz (1957), refers to specimens that have relative densities in the range 15% to 35%. Such specimens generally lie near the steady state line, or perhaps slightly above, and "very loose" refers to specimens lying well above the steady state line. Therefore, relative to stress-strain behavior, the term "very loose", as applied to sands, and "normally consolidated," as applied to clays, are analogous. Similarly, a "dense" sand specimen, for low effective stresses, lies below the steady state line, as do heavily overconsolidated specimens of clay. But a loose sand or a normally consolidated clay tested at high effective stress will be highly contractive, and a dense sand or a heavily overconsolidated clay tested at high pressure may well be contractive also. Thus, one must not attempt to predict the behavior of a specimen unless the stress level is given together with the terms loose, dense, or normally or overconsolidated.

From the above discussion it becomes clear that,with respect to stress-strain characteristics,the state of any soil specimen may be better measured by its position relative to the steady state line.* For example, one could define a "degree of dilativeness" or a "dilativeness index" as:

$$D_i = \frac{e_s - e}{e_s}$$

If $D_i = 0$, the specimen is at the steady state void ratio. Negative values of D_i would refer to specimens at void ratios above the steady state line, regardless

---

* Wroth (1965) apparently was first to use the distance from his critical state line as a measure of the state of a specimen.

of stress level. It would be of interest to investigate the usefulness of such an index in practice. One problem in use, as with other such indices, is that the location of the reference line, in this case the steady state line, must first be determined.

8.2 Selection of Apparatus for Measurement of Stress-Strain Behavior

The stress-strain curve of a soil depends mainly on (a) the soil, (b) its structure, (c) the initial state of the specimen, and (d) the method of loading. If one assumes that a specimen has been carefully selected to be representative of the soil as it exists in the field, then items (a), (b), and (c) are given. To obtain the desired stress-strain curve, it remains only to select a method of loading for the laboratory test that will model the loading that will be followed at any given point in-situ. None of the available apparatus for laboratory shear testing can model every aspect of the stress and strain that occurs during most field loadings (such as earthquakes, lowering or raising of external water level, cutting of a slope, embanking or other loading at top of slope, erosion at toe of slope, wave forces, lowering of groundwater or seepage within slope from reservoir or rainwater). The only condition that leads to failure and that can be modeled reasonably well in the usual laboratory tests is the loss of strength of the soil with time due to pore pressure increases at practically constant shear stress.

One must then, at this stage of development, consider all laboratory stress-strain curves only as indicators of the stress-strain curves that will develop in-situ.

Given the assumption that the laboratory stress-strain curve is at least a rational indicator of the in-situ stress-strain curve, the specimen non-uniformities that develop in most laboratory tests preclude correct determination of the entire stress-strain curve, even for the boundary conditions that are assumed to exist during the laboratory tests. Any time that a stress-strain curve contains a peak, the zone of the specimen that first reaches peak will account for the majority of post-peak deformations. Thus the strain and the void ratio that correspond to the measured shear stress are those in the failure zone, not the averages for the entire specimen. For cases in which the stress-strain curve contains no peak, a large zone failure will develop because the zone that first fails becomes slightly stronger with strain. The major deformations then are shifted to adjacent zones (Casagrande, 1938, P. 6). But, in the case of tests on dilative specimens, in which the overall volume is held constant, if the specimens are sheared slowly enough to permit internal flow of water, the failure zone may increase in void ratio, get weaker, and account for the remaining deformations. In summary, the effects of non-uniformities depend on the shape of the stress-strain curve, the state of the specimen, the constraint imposed on volume change and, if a constant-volume test, on the rate of strain or loading. In drained tests the measured shear strength is only slightly affected, whereas the corresponding average strains and void ratios are incorrect, and in constant-volume tests the average values of all three parameters - the strength, strain, and void ratio - are affected.

Tables 1 and 2 show the author's estimates of reliability of the measured strengths for several apparatus for the extreme cases of highly contractive and highly dilative specimens of bulky and plate-grained soils.

Several interesting points arise from these tables:

(1) The steady state strength of clays in the constant-volume state probably cannot be measured in currently available apparatus (Table 2). Vane tests may be used to reach the steady state, but the stress conditions at that stage remain unknown.

(2) The simple shear test is rated highly for a wide variety of conditions.

(3) The steady state strength of clays in the drained case (the residual strength) is best measured in rotation shear (Table 1). The rotation shear test may be best for measuring steady state resistance of sands, but this possibility remains to be investigated.

(4) The true triaxial test appears to offer no advantage over the ordinary triaxial test (constant $\bar{\sigma}_3$). However, it provides the opportunity of using a wide variety of stress paths and can therefore be used to model more realistically in-situ stress paths for small strains.

(5) The triaxial or plane strain tests are reasonable tests to use (neglecting the fact that the corresponding stress paths seldom model in-situ stress paths) for determination of peak strength, except that for highly contractive clays it often is not possible to attain the large strains required to reach the peak.

The large variety of test errors not considered when formulating Tables 1 and 2 include: (1) errors in measurements of loads, volumes and deformations, and (2) leakage of soil, water and air from the specimen during tests. It is assumed that the effects of such errors are reduced to tolerable values in each case, although the difficulty of doing so varies considerably from one test to the other.

8.3 Relation Between Failures in Laboratory Specimens and Failures in the Field

The type of failure occurring in a laboratory specimen can be used to infer the type of failure that will occur in the field, so long as the laboratory stress path models the in-situ stress path reasonably well and the specimen is representative.

When the laboratory specimen exhibits a "plastic" failure and no failure plane forms for the range of strain applied in the laboratory, then the stress-strain curve will show no peak for that range of strain. In the field, a very wide failure zone would develop in a mass of such soil. Large deformations would occur in the mass and no distinct failure plane would be observed. Such failures are not catastrophic because the deformations warn

of impending failure. Also, field observations are useful for controlling construction, and one is able to use relatively low factors of safety (high working stress) in design because of the character of the failure. In such cases the deformations usually control the design working stress rather than the strength. Obviously the selection of factor of safety (or working stress) is also a function of the consequences of failure and the reliability of the test data.

When a laboratory specimen fails along a narrow zone, the stress-strain curve usually shows a peak. Prototype failures in soils with this shape of stress-strain curve are usually catastrophic. Examples include: (a) failure of highly dilative clays in the drained condition, (b) failure of highly contractive clays (normally consolidated, sensitive or quick clays) sheared at constant volume and (c) liquefaction of sands.* Such failures are seldom preceded by adequate warning of failure, and even careful observations do not normally provide the necessary warning.

Two approaches are currently being investigated to provide predictions of deformations. One is the use of finite element analysis together with laboratory-measured stress-strain data, and the other is the use of model testing e.g. in large centrifuges. Their simultaneous application should lead in the future to substantially improved predictions of movements in-situ.

8.4 Relation between Pore Pressures before and after Failure In-Situ

For any case of constant-volume shear in which an abrupt failure surface develops it is not correct to use pore pressures measured after failure to

---

* In this last case failure planes are not observed even though the stress-strain curve is sharply peaked. The high pore pressures consequent to liquefaction probably spread rapidly throughout the mass and cause a substantial zone of failure. Perhaps high speed photographs of liquefaction failures in the laboratory would show a failure plane for a brief period.

compute strength parameters in terms of effective stress. After failure the pore pressures in the failure zone are quite different from the pore pressures that existed in the failure zone when the maximum shear stress was acting. Consider the case of Specimen 1 in Fig. 16. At failure (maximum deviator stress) the A-value is 0.9. At the steady state (well beyond failure) the A-value is 4.0 and the shear stress has been reduced to one third of the maximum shear stress. Therefore, the shear stress in unfailed zones adjacent to the failure zone is close to the pre-peak pore pressure, corresponding to A = 0.3 in this example. Piezometers in the failure zone after failure would give higher pore pressures than those that caused failure, and piezometers adjacent to the failure zone would give lower pore pressures than those that caused failure. Only by chance would the correct pore pressures be measured after failure.

To obtain reasonable estimates of the applicable strength parameters in terms of effective stress, pore pressure measurements must be made in the failure zone at, or just before, failure.

8.5 Selection of Shear Strength for Stability Analysis

The conventional method for computing the factor of safety against failure in shear involves two distinct steps: (1) computation of the average shear stress along an assumed failure surface and (2) determination of the average shear strength that can be mobilized simultaneously along the entire failure surface.* The ratio of this average shear strength to average shear stress is the factor of safety.

---

* These two steps are artifically uncoupled, for convenience in analysis of problems in which failure controls, by assuming: (1) a distribution of internal forces in the failure mass and (2) that the stress-strain curve contains no peak.

Stability analysis provides values of shear and normal stress at a number of points along an assumed failure surface. Hence the average shear stress is relatively easily obtained. But to obtain the shear strength that can be mobilized at any point along that surface, one must prepare the soil at the same state (void ratio, effective minor principal stress, and shear stress) and at the same structure as in-situ, and must use the same method of loading (including degree of drainage - which is affected by the degree of saturation, changes in total stresses, strain boundary conditions, and rotation of principal stresses - if any) as will cause failure in-situ.

From the measured stress-strain curves and stress paths one obtains in general, four points that might be chosen to define the shear strength. These are:

- m — Point at which maximum shear stress is reached.
- e — Point at which stress path is tangent to envelope of stress paths.
- p — Point at which maximum principal stress ratio is reached. Points e and p are always identical for straight-line strength envelopes. For curved envelopes they differ slightly. For the purposes of this discussion, this difference -if any - is neglected.
- s — Point at which steady state is reached.

If the test conditions were a true model of those in-situ along the entire failure surface, then Point m would always be used to define strength. But it is not possible to model the degree of progressive failure that occurs along the failure surface in-situ, and it is not even possible to model the

stress path very accurately for a given point on the failure surface.*

Due to these limitations Point m must not be used in all cases to define strength. Recommendations are given below and in Tables 3 and 4 for the point that should be used to define strength and for the factor of safety that should be applied to this strength to account for the effects of progressive failure in-situ. The actual factor of safety to be applied in any given case must be larger than those given in Tables 3 and 4 to account for errors, unknowns, and the seriousness of the failure, if it were to occur. The factors of safety that have been used in the past were developed on the basis of experience with behavior of full-scale embankments and foundations and include, implicitly, the effects of progressive failure. The discussion in this section is aimed at differentiating between the effect of progressive failure and other factors that reduce the working stress.

Hard, bulky-grained soils are considered in Table 3 and platey-grained soils are considered in Table 4. To cover the full range of possibilities, each of these soil types is further divided into the highly contractive and highly dilative cases for both drained and constant-volume shear. To obtain recommendations for intermediate soils, intermediate states, and intermediate constraints on volume change, one may interpolate between the appropriate cases in this table.

---

* Avgherinos and Schofield (1969) advocate the use of models tested in a large centrifuge. In such a device one can model quite closely to the in-situ conditions. Its use will eventually lead to a more rational application of the results of conventional tests.

(a) Soils Containing Chiefly Bulky Grains

For Case A in Table 3 there is no ambiguity since Points m, e, and s coicide. Complete collapse cannot occur until the full shear strength is mobilized at every point along the failure surface. The absence of a peak (drained sensitivity, $S_d = 1$) means that a broad zone of failure will develop in the prototype rather than an abrupt failure plane. Thus large deformations may occur prior to failure, depending on the geometry of the problem and the strain at Point m, and may control the allowable average stress.* These deformations will warn of impending failure.

For Case B in Table 3 the shear stress at Point a, representing the in-situ condition, is greater than the steady state strength. Therefore, the in-situ condition is one of unstable equilibrium. If progressive failure were no worse in-situ than in the laboratory specimen, one could raise the average shear stress to τ_m before causing a sudden collapse (which in this case would be called liquefaction). But the shear stress at some point will reach τ_s. Therefore, the collapse will occur when the average shear stress lies between τ_m and τ_a. Its value will decrease toward τ_a as the undrained sensitivity ($S_u = \tau_m/\tau_s$) increases, as the strain ε_s at Point s decreases relative to ε_m, and as the degree of progressive failure increases (due to stress concentrations caused by hard or soft spots, cracks, holes, sharp corners in the geometry, etc.).

---

* The recommendations in this section apply only if shear failure controls, not is tensile failure or deformations control.

Computations by Bishop (1952) and by Janbu (1971) show that the average shear stress along the most critical surface in a slope composed of an elastic medium is about one-half of the maximum shear stress on that surface. If the stress-strain curve for Case B were linear to Point m and dropped to zero shear strength at all larger strains, and if no progressive failure occurred in the laboratory test, then one would have complete collapse as soon as the average shear stress on the critical failure surface reached about one-half of the peak value measured in the laboratory. At that stage failure would occur locally and the local resistance would drop to zero. Complete failure would ensue shortly. But if the post-peak strength were some positive value, such as τ_s for Case B, then the average stress required to cause failure would be somewhat greater. This reasoning leads the author to suggest that for Case B, the working stress that should be used in stability analysis of a homogeneous slope in such a material is about $1/2\ (\tau_m + \tau_s)$. But if τ_a already has been applied (in the drained condition) and it is higher than τ_s, then the higher working stress given by $1/2\ (\tau_m + \tau_a)$ should be used in the analysis. Thus, to account for progressive failure in Case B, the factor of safety should be at least:

$$F = \frac{\tau_m}{1/2\ (\tau_m + \tau_a)} \qquad \text{for} \qquad \tau_s < \tau_a \tag{1}$$

$$F = \frac{\tau_m}{1/2\ (\tau_m + \tau_s)} = \frac{S_u}{1/2\ (S_u + 1)} \quad \text{for } \tau_s \geq \tau_a \tag{2}$$

This factor of safety must be increased further if the soil is not rather homogeneous but contains discontinuities that accentuate progressive failure. Furthermore, this factor of safety does not account for other uncertainities that may necessitate a still lower working stress.

The failure for Case B will be sudden and only small deformations are likely to precede failure. Therefore one will have little, if any, warning of failure even if field observations are made. To judge when a failure is about to occur in this case it would be necessary to predict the movements that will precede failure and to compare them with measured movements.

For Case C in Table 3 the stress-strain curve has a peak, and the drained sensitivity seldom exceeds 2. Progressive failure would cause the average shear strength along a failure surface to lie between Point m and Point s. The strength may then be defined by Point m, as in the previous case, and modified by the factor of safety given by Eqs. (1) and (2) to account for progressive failure.

Rowe (1969) has made model tests which may be used to check the above recommendation. His soil was a sand with a drained sensitivity, S_d, of about 1.7, as measured in plane strain tests. Using Eq. (2), but substituting S_d for S_u, one obtains a recommended factor of safety of 1.26 to account for progressive failure. Rowe's measurements showed that the peak strength from the plane strain tests was 1.2 to 1.4 t-mes greater than the average shear strength developed in the model tests. Thus Eq. (2) gives a reasonable estimate of the effects of progressive failure in Rowe's tests. But the degree of progressive failure varies somewhat with the geometry of the

problem and the stress level (Rowe, 1969). Additional tests of this type are urgently needed.

For Case D, a highly dilative sand sheared at constant volume, the Points m and s coincide and fall on a line that lies below the strength envelope. To be conservative one would have to choose this lower line to define the strength. But in a dilative specimen one cannot reach Point m without passing Point e. Having reached Point e, large strains will occur unless negative induced pore pressures develop. Casagrande (1959) recommended that one should not rely on development of negative induced pore pressures because gases may exist in the pore water in-situ and because internal migration of pore water toward the most critical zone may occur to greater extent in-situ than in the laboratory. Both of these effects prevent the strength shown at Point m from developing in a test or in-situ. The measured strength is likely to be slightly greater than that given by Point e. Therefore, for practical purposes it is best to use the strength envelope passing though Point e and to assume no net change in pore pressure during the constant volume shear (which is slightly more conservative than using the drained strength) unless evidence is provided to prove that negative induced pore pressures will develop in-situ. (During earthquakes, negative induced pore pressures do develop.)

The stress paths for constant-volume tests on compacted specimens from shallow depths in the upstream slope of earth dams usually have the shape shown for Case D. Therefore, it is this case that is often involved when analyzing stability against sudden drawdown. To obtain strengths for this case one must

perform undrained tests using stress paths that model reasonably well the stress paths that will occur in the dam. If negative induced pore pressures develop, it should be assumed that the pore pressure induced in-situ will be zero.

One of the test errors that occurs when measuring the stress-strain curve for Case D is migration of water toward the failure zone from adjacent zones in the specimen, just as occurs in-situ. This effect may cause development of a peak in the stress-strain curve, or at least a reduction of the shear strength below that for an ideal test. If one chooses to rely on negative induced pore pressures in-situ, then the effect of the difference in the degree of pore water migration between the laboratory and field must be evaluated.

(b) Soils Containing Chiefly Platey Grains

The conclusions listed above for bulky-grained soils apply equally to the case of platey-grained soils. The only significant differences between the stress-strain curves for the two soil types arise from the larger strains usually needed in platey-grained soils to reach a given position on the stress-strain curve, and from the reduction of principal stress ratio that occurs when grains orientate at very large strains. The latter effect causes an increased sensitivity in all cases.

For Case E, Table 4, strains in the range of 10 to 60% are needed to develop the peak. Very large movements will occur in-situ before any localized failure zone develops. The allowable shear stress will be controlled by

the allowable deformation, unless the geometry of the problem is such as to force failure within a narrow zone. Point m should be used to define the strength, but the working stress should be modified somewhat, depending on the geometry, to account for progressive failure. In this case a factor of safety given by Eq. (2) would be quite conservative to account for progressive failure, but should be applied if progressive failure is severe.

For Case F, the constant-volume failure of a contractive, platey-grained soil (e.g., a normally consolidated clay) one must use Point m to define strength, just as for the corresponding case in bulky-grained soils. It makes no sense to use Point e (= s) in this case because collapse occurs before this point is reached. The extreme sensitivity of 100 or more measured in some quick clays (Hoeg, Andersland and Rolfsen, 1969, Table 1) necessitates a substantial factor of safety to account for progressive failure. Under the best of conditions one should use a factor of safety of 2 (as given by Eq. (2)). But because the extreme values of sensitivity are obtained for soils that also have very low strain at peak, the factor of safety must be increased above 2. Tests and field studies are needed to provide information on the appropriate factor of safety for this case.

Case G, a drained test on a dilative specimen containing chiefly platey grains, is the case considered by Skempton (1964). The peak may occur at relatively small strains (15%), but extremely large strains are needed to develop the much lower steady state strength. Here the strength as defined by Point e (=m) must be modified to account for progressive failure. Skempton (1964, P. 81) pointed out that the average shear strength that is mobilized on

the failure plane in highly dilative clay drops continuously with time toward the residual (steady) state strength due to progressive failure, at least in clays or clay-shales that contain slickensides. For short times these soils can sustain shear stresses considerably greater than the steady state strength. The important variables that have to be considered when attempting to account for progressive failure in such soils are: (1) the detailed fabric of the soil. In particular, one must scrutinize the material to determine whether it contains joints, fissures, or other discontinuities. If so, are these surfaces slickensided? What is their inclination relative to the shear stresses in the mass and what is their size and number? (2) The time available for progressive failure. (3) The amount of movement that is needed to reach the steady state.

The nature and extent of discontinuities can be expected to affect severely the rate of drop in strength toward the steady state value. If there are none, then an average shear stress near the peak strength may be mobilized for short times, even when the drained sensitivity is high (S_d = 5 to 10). This suggestion is different from that given for bulky-grained soils (ie., Eq. (2)), because the movements required to reach the steady state are much larger for platey-grained soils than for bulky-grained soils. Although local failure may occur when the average shear stress is as given by Eq. (2), the post-peak rate of drop in shear stress with strain is so small that a substantial proportion of the peak strength can be mobilized. If no macroscopically visible points exist at which shear stresses are highly concentrated, then it seems reasonable to expect that considerable time will be required before creep will lead to substantial orientation of grains at the sites of highest shear stress, and hence to a continuation of

the progressive failure. But the presence of visible discontinuities will speed the process. Even when visible discontinuities do not exist, discontinuities at the scale of the grains do exist and can be expected to lead to progressive failure in time.

The author refrains from making any quantitative recommendations on the effect of these variables. Instead, the reader is referred to Skempton (1964) for information on London clay and for insight into the type of data needed to make a proper judgment. At this time only guesses can be made unless full-scale behavior has been analyzed. In the future, centrifugal model testing may provide a less expensive but satisfactory means for obtaining more data, although the time (creep) effects still will remain unknown.

Case H, constant-volume shear of a highly dilative, platey-grained soil, will be less critical under similar loading conditions than the corresponding drained case, Case G. The discussion given for Case D in Table 3 applies also for Case H. For Case H the stress-strain curve would show a peak and drop-off due to grain orientation at large strains and this peak would be accentuated by the development of a thin failure zone and migration of water toward this zone, both in the laboratory and in-situ. Internal migration of water toward the failure zone in-situ would make this case revert to Case G, and the corresponding discussion would apply. The constant-volume condition cannot be maintained over very long periods of time in-situ, so that the problem of progressive failure with time is unlikely to arise for this case.

(c) Comments on the Use of Tables 3 and 4

To obtain recommended strength to be used in stability analysis, one must first compute the stresses in-situ, then perform a test that models the in-situ stress path on a specimen that is representative (in type of soil, structure, and state). From this stress-strain curve, a strength is selected based on Tables 3 and 4 and plotted as a function of the stresses at Point a. In this manner a "working" strength line is developed. The equation for this line may then be inserted in the stability analysis.

Although the effects of the following factors are not discussed herein, the reader should not neglect to consider their effects on the relation between laboratory and field stress-strain curves:

(1) Disturbance of specimens

(2) Presence of gravel, shells, or other hard inclusions in the specimens

(3) Rate of loading

(4) Effects of repeated loading

(5) Degree of saturation (it should be the same in the laboratory as in-situ, or a conservative value should be used)

(6) Orientation of specimen relative to applied stresses (if the specimen is anisotropic)

(7) Temperature

Finally, it should be remembered that the recommendations given in this section apply only when shear failure controls design, and do not apply when the allowable deformations limit the allowable stress or when tensile failure may occur.

9. CONCLUDING REMARKS

The systematic view presented in this monograph on the stress-strain curves of soils, and the discussion of major factors affecting their shape, permit one to fit any individual stress-strain curve into a pattern that is very useful for: (1) isolating gaps in knowledge about the stress-strain characteristics of a given soil, (2) for minimizing the number of tests required to gain fairly complete insight into its behavior (by performing only those tests needed to define the pattern of change on the state diagram and by separating the important variables in a rational manner), (3) for discovering test errors, and (4) for understanding the application of stress-strain data to practical problems.

A review of stress-strain data that have been reported for drained and constant-volume compression and direct (or simple) shear tests on sands and clays has led the author to idealized relationships among stress-strain curves, stress paths, state paths, and volume change or change in effective minor principal stress. These relationships are illustrated in Fig. 5,7,15, and 16. Typical examples of test data that lend support to the idealizations, and from which the idealizations were extracted, are given in Figs. 9-14 for the drained case and in Figs. 17-24 for the constant-volume case.

The main concepts and test results that led to the generalizations in this monograph are listed below so that areas of departure from previously published work and potential areas of disagreement will be easily isolated.

(1) The steady state of deformation is that state in which a specimen is deforming continuously and monotonically without change in shear

stress, effective normal stress, volume, and velocity of deformation.

(2) The most important factors that control the shape of stress-strain curves of soils are:

(a) The Soil (particularly its mineralogy and grain shape)

(b) Structure (large and small scale, including cementation bonds, if any, and orientation of structure relative to principal stress)

(c) Initial State (void ratio, effective normal stress and shear stress)

(d) Method of Loading (stress path in principal stress space)

Other variables that have important effects in some cases, but are not discussed herein, are: rate of loading, magnitude and frequency of cyclic stressing, temperature, absolute value of pore pressure, and test errors.

(3) It is hypothesized that for any given soil there exists a unique steady state line:

$$e = f(\bar{\sigma})$$

where $f(\bar{\sigma})$ is affected by the velocity of deformation in the steady state but is not affected by the initial structure of the soil, its initial state, and the particular stress path used to reach a given steady state. The steady state cannot be reached unless particle breakage and particle orientation, if any, have been carried to completion. If particle breakage occurs, the steady state line applies only for the resulting soil. This steady state is identical to the critical void ratio introduced by Casagrande (1936), but is quite different, in most cases, from the concept of critical state as used by Schofield and Wroth (1968).

(4) The stress-strain curves of normally consolidated (highly contractive) clays contain a peak in both drained and constant-volume shear tests.

(5) The stress-strain curves of very loose sands in constant-volume shear also contain a peak, which contrasts with the "plastic" stress'strain curve that is often reported. This case is directly analogous to constant-volume shear of a sensitive clay. In sand the failure is called liquefaction, and in clay it is called a flow slide or a shear failure.

(6) The major difference between the shapes of stress-strain curves of clays and sands is the much larger strain required to reach peak stress and the steady state shear stress in clays, due to their content of platey-shaped grains. (Time effects are also greater in clays than in sands, but these are not discussed herein.)

The understanding gained from this empirical study of stress-strain curves leads to many ideas that are useful in practice, some of which are described in Section 8. To help make this information useful to the reader, it is recommended that one perform both drained and constant-volume triaxial tests on specimens of at least one clay and one sand prepared in states on both sides of the steady state line of Fig. 1, and compare the results with the idealizations presented in this monograph.

The important factors that control the shape of the entire stress-strain curve, from small to very large strains, have been clearly stated in qualitative terms. It is hoped that the quantitative effects of each of these factors will be measured in future research programs, so that ultimately one will be able to understand the advantage and limitations of mathematical models of particulate materials.

A warning is given here concerning certain limitations in the contents of this monograph:

(1) The idealized shapes of stress-strain curves apply only for uncemented soils. The effects of cementation are important in practice, but are not covered.

(2) Attention was concentrated on highly dilative and highly contractive specimens and those prepared at states near the steady state line. The shapes of stress-strain curves vary between those shown for these limits. But the case of extremely dilative specimens (e.g., randomly jointed rocks) is not covered.

(3) Practically no mention has been made of degree of saturation. It is assumed to act through its effect on the stress path that develops when the total stress changes, boundary displacements, and permissible volume changes during shear have been sleected. This assumption means that if effective stress is properly defined in a partially saturated soil, the soil's behavior in terms of effective stress will be independent of degree of saturation. The assumption is reasonable for high degrees of saturation (perhaps >80%), but the behavior can be expected to change when one moves to lower degrees of saturation.

(4) No information is given on the detailed effects of the alternative methods of loading that are available, such as axial compression, lateral extension, axial extension, rotation shear, and torsion shear. Rather, it is expected that the type of test will be selected in any given case to model the in-situ stresses and strains reasonably well.

AUTHOR'S NOTE

The information presented in this monograph is the direct outgrowth of the doctoral research carried out at Harvard University by Castro (1969) and by LaGatta (1970) on liquefaction and residual strength, respectively. These topics, both suggested by Professor A. Casagrande, at the time seemed quite unrelated. However, the research showed that both phenomena could be viewed as steady state deformations that are achieved in different ways. The information in this monograph was drafted and presented in essentially its present form during lectures on shear strength at Harvard University in the spring of 1968 and 1969. The paper was finalized while the author was on sabbatical leave at the University of Manchester from January through June, 1970.

The research of Drs. Castro and LaGatta, as well as part of the salary of the author during that time, was funded through grants to Professor Arthur Casagrande from the Waterways Experiment Station of the U. S. Army Corps of Engineers.

LIST OF NOTATIONS

A — Skempton's pore pressure coefficient defined by the equation:

$$\Delta u = B \{\Delta\sigma_3 + A (\Delta\sigma_1 - \Delta\sigma_3)\}$$

a — Subscript to denote stage of a test when a specimen is anisotropically consolidated, just before start of shear at constant water content

c — Subscript to denote stage of a shear test when a specimen is isotropically consolidated

cm — Centimeter

C_u — Coefficient of uniformity

D_{10} — Size for which 10% by weight of grains in a specimen are smaller

e — Void Ratio

e_{min} — Minimum void ratio of a specimen

e_{max} — Maximum void ratio of a specimen

G_w — Degree of saturation

H — Height or thickness of specimen

i — Subscript to denote stage of a test when the specimen is in its initial, as-molded, or as-compacted condition

I.D. — Inside Diameter

in. — Inch

L_w — Liquid limit

m — Subscript to denote stage of a shear test when the shear stress on the specimen is maximum

m — Meter

n — Porosity

o — Subscript used interchangeably with "i"

O.D.	Outside Diameter
p	Subscript to denote stage of a shear test when the effective principal stress ratio is a maximum
P_i	Plasticity Index
P_w	Plastic Limit
R_d	Relative density
s	Subscript used to denote stage of a shear test when the steady state has been reached. Sometimes used for the last point on the stress-strain curve if steady state has not been reached.
S_d	Drained sensitivity ($= \tau_m / \tau_s$ for drained shear)
S_u	Undrained sensitivity ($= \tau_m / \tau_s$ for shear at constant water content)
s_s	Specific gravity of solids
u	Pore pressure
V	Volume
v	Volumetric Strain $(=\frac{\Delta V}{V})$
w	Water Content
w_{nat}	Natural Water Content
w_{opt}	Optimum water content from compaction test
δ	Shear strain $(= \delta/H)$
γ_d	Dry unit weight
ε	Axial strain $(= \Delta H/H = \delta/H)$
Θ	Slope of a line through the origin and any given point on the stress path plotted in terms of τ_{45} vs. $\bar{\sigma}_{45}$.
μ	Micron (10^{-6} meter) ≡ micrometer
σ	Total normal stress
$\bar{\sigma}$	Effective normal stress
$\bar{\sigma}_1$	Effective major principal stress
$\bar{\sigma}_3$	Effective minor principal stress
$\bar{\sigma}_{45}$	$(=(\bar{\sigma}_1 + \bar{\sigma}_3)/2)$ Effective normal stress on plane inclined at 45° to the principal planes.
$\bar{\sigma}_h$	Effective normal stress on horizontal plane
$\bar{\sigma}_1 / \bar{\sigma}_3$	Effective principal stress ratio

τ Shear Stress

τ_{45} $= (\sigma_1 - \sigma_3)/2 = (\bar{\sigma}_1 - \bar{\sigma}_3)/2 = \tau_{max}$ Shear stress on plane inclined at 45° to the principal planes. This plane sustains the maximum shear stress in the specimen.

τ_h Shear stress on horizontal plane

ϕ Slope of line passing through origin and tangent to the Mohr circle (plotted in terms of effective stress) for a selected stage of a shear test. For example, ϕ_m = slope for Mohr circle at stage when the shear stress has reached its maximum value during a particular test.

LIST OF REFERENCES

AVGHERINOS, P. J. and SCHOFIELD, A. N. (1969). "Drawdown Failures of Centrifuged Models," Proceedings Seventh International Conference on Soil Mechanics and Foundation Engineering, Vol.2, PP. 497-505.

BISHOP, A. W. (1952). The Stability of Earth Dams, Ph. D. Thesis, University of London, Imperial College.

BISHOP, A. W. (1967). "Progressive Failure - with Special Reference to the Mechanism Causing It," Proceedings of the Geotechnical Conference, Oslo, Vol. II, PP. 142-150.

BISHOP, A. W. WEBB, D. L., and LEWIN, P. I. (1965). "Undisturbed Samples of London Clay from the Ashford Common Shaft: Strength-Effective Stress Relationships," Geotechnique, Vol. 15, No. 1, PP. 1-31.

BISHOP, A. W., WEBB, D. L., and SKINNER, A. E. (1965). "Triaxial Tests on Soil at Elevated Cell Pressures," Proceedings Sixth International Conf. on Soil Mechanics and Foundation Engineering, Vol. 1, PP. 170-174.

BJERRUM, L. and LANDVA, A. (1966). "Direct Simple-Shear Tests on a Norwegian Quick Clay," Geotechnique, Vol. 16, No. 1, PP. 1-20

CASAGRANDE, A. (1936). "Characteristics of Cohesionless Soils Affecting the Stability of Slopes and Earth Fills," Journal BSCE, January PP. 257-276.

CASAGRANDE, A. (1938). "Investigation of Critical Density of Sand from Franklin Falls, N.H." Pages BII-1 through 16 of Appendix BII from a report by the U. S. Army Engineer Office, Boston, entitled Compaction Tests and Critical Density Investigations of Cohesionless Materials for Franklin Falls Dam and dated June 1938.

CASAGRANDE, A. (1941). Triaxial Compression Tests on Cohesive Soils," Third Progress Report to U. S. Waterways Experiment Station on Cooperative Research on Stress-Deformation and Strength Characteristics of Soils, Harvard University, Cambridge, May.

CASAGRANDE, A. (1950). "Notes on the Design of Earth Dams," Contributions to Soil Mechanics, 1941-1953, Boston Society of Civil Engineers, PP. 231-255. (Reprinted from Journal BSCE, Vol. 37, No. 4)

CASAGRANDE, A. (1959). Lectures at Harvard Univeristy in the courses Soil Mechanics I and II, Engineering 261 (a) and Engineering 261(b).

CASAGRANDE, A. and HIRSCHFELD, R. C. (1962). Second Progress Report on Investigation of Stress-Deformation and Strength Characteristics of Compacted Clays, Harvard Soil Mechanics Series No. 74, Cambridge PP. 1-82

CASAGRANDE, A. and POULOS, S. J. (1964). Fourth Report on Investigation of Stress-Deformation and Strength Characteris of Compacted Clàys, Harvard Soil Mechanics Series No. 74, Cambridge, PP. 1-82.

CASTRO, G. (1969). Liquefaction of Sands, Harvard Soil Mechanics Series No. 81, Harvard University, Cambridge, PP. 1-112. (Ph. D. Thesis)

CORNFORTH, D. H. (1964). "Some Experiments on the Influence of Strain Conditions on the Strength of Sand," Geotechnique, Vol. 14, No. 2, PP. 143-167.

GIBBS, H. J. and HOLTZ, W. G. (1957). "Research on Determining the Density of Sands by Spoon Penetration Testing," Proceedings Fourth International Conference on Soil Mechanics and Foundation Engineering, Vol. I, PP. 35-39. (Also Earth Laboratory Report No. EM-460, Bureau of Reclamation, Denver, 1956).

HIRSCHFELD, R. C. (1958). Factors Influencing the Constant-Volume Strength of Clays, Ph. D. Thesis, Harvard University, Cambridge, PP. 1-390.

HOEG, K., ANDERSLAND, O. B. and ROLFSEN, E. N. (1969). "Undrained Behavior of Quick Clay under Load Tests at Asrum," Geotechnique, Vol. 19, No. 1, PP 101-115.

JANBU, N. (1971). "Slope Stability Computations," Contributions to Embankment-Dam Engineering, Wiley, in preparation Sept. 1971.

LADD, C. C. (1965). "Stress-Strain Behavior of Anisotropically Consolidated Clays During Undrained Shear," Proceedings Sixth International Conf. on Soil Mechanics and Foundation Engineering, Vol. I, PP. 282-286.

LADD, C. C. (1970). Original data for Fig. 21, supplied by letter dated October 15, 1970, to S. J. Poulos.

LAGATTA, D. P. (1970). Residual Strength of Clays and Clay-Shales by Rotation Shear Tests, Ph. D. Thesis, Harvard University, Cambridge.

LAGATTA, D. P. (1971). The Effect of Rate of Displacement on Measuring the Residual Strength of Clays, U. S. Army Corps of Engineers, Waterways Experiment Station, in print Marvh 1971.

LAMBE, T. W. (1953). "The Structure of Inorganic Soil," P roc. ASCE, Vol. 79, Separate No. 315, PP. 1-49

LAMBE, T.W. (1964). "Methods of Estimating Settlement," Journal of Soil Mechanics Division, ASCE, Vol. 90, No. SM5, Part 1, PP. 43-67.

LANDVA, A. (1962). En eksperimentell undersøkelse ay Skaerfastheten i normalkonsoliderte leirer:avhandling. Norwegian Geotechnical Institute Internal Report, F. 175-6.

LEE, K. L. (1970). Letter dated March 11, 1970.

LEE, K. L. and SEED, H. B. (1967). "Drained Strength Characteristics of Sands" Journal Soil Mechanics and Foundations Division, ASCE Vol. 93, SM6, PP. 117-141.

MARSAL, R. J. (1967). Behavior of Granular Soils, Pan-American Soils Course, Universidad Catolica Andres Bello, Caracas, PP. 1-229

ROSCOE, K. H., SCHOFIELD, A. N. and WROTH, C.P. (1958). "On the Yielding of Soils," Geotechnique, Vol. 8, PP. 22-53.

ROWE, P. W. (1962). "The Stress-Dilatancy Relation for Static Equilibrium of an Assembly of Particles in Contact," Proceedings of the Royal Society Series A, Vol. 269, No. 1339, PP. 500-527.

SCHOFIELD, A. N. (1970). Private Communication.

SCHOFIELD, A. N. and WROTH, C. P. (1968). Critical State Soil Mechanics, McGraw-Hill, PP. 1-310.

SKEMPTON, A. W. (1964). "Long-Term Stability of Clay Slopes," Geotechnique, Vol. 14, No. 2, PP. 77-102.

SKEMPTON, A. W. and NORTHEY, R. D. (1952). "The Sensitivity of Clays," Geotechnique, Vol. III, No. 1, PP. 30-53.

SKINNER, A. E. (1970). Letter dated June 9, 1970, containing original data used to prepare Fig. 18.

TAYLOR, D. W. (1948). Fundamentals of Soil Mechanics, Wiley, New York.

WATSON, J. D. (1938). "Investigation of Critical Density of Sand from Franklin Falls, N. H." Pages BII-17 through 38 of Appendix BII from a report by the U. S. Army Engineer Office, Boston, entitled Compaction Tests and Critical Density Investigations of Cohesionless Materials for Franklin Falls Dam and dated June 1938. See also Watson (1940, Chapter V).

WATSON, JOHN D. (1940). Stress-Deformation Characteristics of Cohesionless Soils from Triaxial Compression Tests, Ph. D. Thesis, Harvard University, Cambridge.

WEBB, D. L. (1966). The Mechanical Properties of Undisturbed Samples of London Clay and Pierre Shale, Ph. D. Thesis, University of London. (In two volumes).

WISSA, A. E. Z. (1970). Letter dated March 30, 1970, to S. J. Poulos.

WISSA, A. E. Z. and LADD, C. C. (1965). Shear Strength Generation in Stabilized Soils. MIT Research Report R65-17 (Soils Publication No. 173) to U. S. Waterways Experiment Station, Cambridge, Mass., June, PP 1-290.

WROTH, C. P. and BASSETT, R. H. (1965). "A Stress-Strain Relationship for the Shearing Behavior of a Sand," Geotechnique, Vol. 15, No. 1, PP. 32-56.

TABLE 1 RELATIVE ACCURACY OF PEAK AND STEADY STATE STRENGTHS MEASURED WITH VARIOUS APPARATUS - DRAINED TESTS

Limitations of Table (1) Relative accuracy given for uncemented, highly dilative or highly contractive specimens tested with increasing σ_1. For intermediate states, relative accuracy is intermediate. No attempt made to consider tests with decreasing σ_1. (2) Strengths measured in each apparatus differ due to differences among boundary conditions during loading. Correct apparatus is the one that gives best accuracy and models reasonably the in-situ method of loading. These two needs are often incompatible. (3) Use of lubrication on boundaries or special care to reduce effects of boundary friction has been assumed for triaxial and plane strain tests.

TYPE OF APPARATUS	MAXIMUM ACHIEVABLE STRAIN, %	RELATIVE SPECIMEN UNIFORMITY AT PEAK a)	CHIEFLY BULKY GRAINS				CHIEFLY PLATEY GRAINS			
			HIGHLY CONTRACTIVE (ε = 10-30%)		HIGHLY DILATIVE (ε = 1-15%)		HIGHLY CONTRACTIVE (ε = 5-60%)		HIGHLY DILATIVE (ε = 1-15%)	
			PEAK	STEADY STATE	PEAK	STEADY STATE b)	PEAK	STEADY STATE b)	PEAK	STEADY STATE b)
Triaxial	~30	1	No Peak	2	1	2	4-5	5	1	3 c) -5
Direct Shear	100+	4		2	2	3	4	2-5	2	2 d) -5
Simple Shear	~100	2		1	1	1	1	2-5	1	2 -5
Plane Strain	~20	2		2	1	2	4-5	5	1	3 c) -5
Rotation Shear	8	3		1?	2?	1?	2	1	2	1
True Triaxial e)	~15	2?		2?	2?	2?	4-5	5	1?	3 -5
Hollow Cylinder (Torsion)	?	?		?	?	?	?	5	?	5

Scale of Relative Accuracy

1 Best
2 Good
3 Fair
4 Poor
5 Impractical or Impossible

a) Relative accuracy controlled by achievable strain and uniformity of specimen at each stage, in addition to parameters in table headings. Specimens are less uniform at steady state than at peak, except when both are same.

b) Failure develops in narrow zone, or zones, in which void ratio is quite different from average value. Strains and void ratio in failure zone therefore generally unknown.

c) Shear on pre-formed failure surface will yield a good value.

d) Repeated reversal of shear direction will provide a reasonable value of steady state strength.

e) Independent control of σ_1, σ_2 and σ_3.

TABLE 2 RELATIVE ACCURACY OF PEAK AND STEADY STATE STRENGTHS MEASURED WITH VARIOUS APPARATUS IN CONSTANT-VOLUME TESTS

Limitations: (1) Relative accuracies are given for uncemented, highly dilative or highly contractive specimens tested by increasing σ_1. For intermediate states, relative accuracy is intermediate. No attempt made to consider tests with decreasing σ_1. (2) Strengths measured in each apparatus differ due to differences among boundary conditions during loading. Correct apparatus to use is the one that gives best accuracy and models reasonably the in-situ method of loading. These needs often incompatible. (3) Use of lubrication on boundaries (or special care to reduce effects of boundary friction) assumed for triaxial and for plane strain tests.

TYPE OF APPARATUS	MAXIMUM STRAIN, %	RELATIVE SPECIMEN UNIFORMITH AT PEAK a)	CHIEFLY BULKY GRAINS				CHIEFLY PLATEY GRAINS			
			HIGHLY CONTRACTIVE ε_m = 1-10%		HIGHLY DILATIVE ε_m = 10-20%		HIGHLY CONTRACTIVE ε_m = 5-60%		HIGHLY DILATIVE $\varepsilon_m > 10\%$	
			PEAK	STEADY STATE	PEAK	STEADY STATE	PEAK	STEADY STATE b)	PEAK	STEADY STATE b)
Triaxial	~30	1	1	2?	NO PEAK	2	2-4	5	1	5
Direct Shear	100+	4	3	?		2	4	5	2	5
Simple Shear	~100	2	1	2		1	1	5	1	5
Plane Strain	~20	2	1	3		2	2	5	1	5
Rotation Shear	∞	3	(2)	(1)		(2)	(2)	(5)	(2)	(5)
True Triaxial c)	~15	2?	1?	2?		3	2	5	2	5
Hollow Cylinder (Torsion)	?	?	?	?		?	?	5	?	5

Scale of Relative Accuracy

1 Best
2 Good
3 Fair
4 Poor
5 Impractical or Impossible

( ) Apparatus not available. Estimate included to indicate possible usefulness.

a) Relative accuracy controlled by achievable strain and uniformity of specimen at each stage of test, in addition to parameters in table headings. Specimens are less uniform at steady state than at peak except when both are same.

b) Failure develops along a single plane. Volume of failure zone changes even though overall volume is held constant. Hence measured strength lies between that for drained and constant-volume tests. Peak is slightly affected; steady state strength is strongly affected.

c) Independent control of σ_1, σ_2, σ_3.

TABLE 3 SELECTION OF STRENGTH FOR STABILITY ANALYSIS
HARD, BULKY-GRAINED SOILS

CASE	STATE	TEST TYPE	REPRESENTATIVE STRESS-STRAIN CURVE AND STRESS PATH (Specimens anisotropically consolidated to Point a)	STRENGTH DEFINED @	FACTOR OF SAFETY FOR PROGRESSIVE FAILURE	TYPE OF FAILURE	NOTES
A	CONTRACTIVE	DRAINED	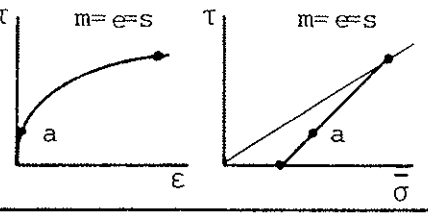	m e s	1	Gradual	Large deformations may precede failure and may control factor of safety. Undrained case is more critical (for same method of loading). If loading is transformed to undrained, liquefaction occurs.
B	CONTRACTIVE	CONS. VOLUME	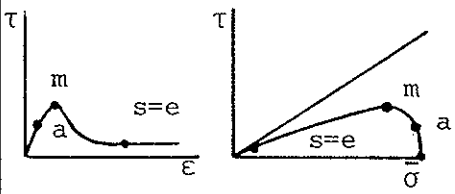	m	$\tau_a > \tau_s$ $\frac{\tau_m}{\frac{1}{2}(\tau_m + \tau_a)}$ $\tau_a \leq \tau_s$ $\frac{\tau_m}{\frac{1}{2}(\tau_m + \tau_s)}$	Abrupt	Small strains precede abrupt failure (liquefaction). Extreme care necessary if in-situ shear stresses exceed steady state strength. For $\tau_a > \tau_s$, the soil is in unstable equilibrium. Larger values of factor of safety needed if conditions in situ are non-homogeneous.
C	DILATIVE	DRAINED	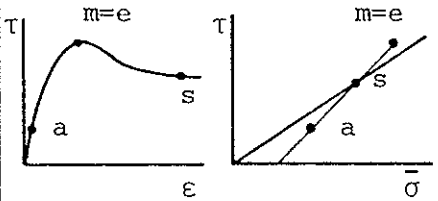	m e	$\frac{\tau_m}{\frac{1}{2}(\tau_m + \tau_s)}$	Abrupt	Failure is abrupt but seldom is a dilative sand loaded sufficiently to cause failure. Rowe (1967) has made model tests that show effects of progressive failure.
D	DILATIVE	CONS. VOLUME	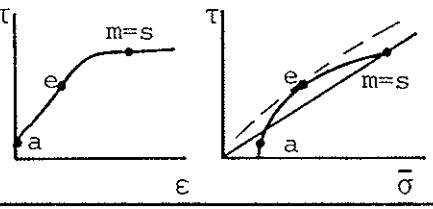	e	1	Gradual	Pore water migration toward zones nearest failure and presence of gas in pore water prevent negative pore pressures from developing in-situ and should not be relied upon. Drained case is lower limit.

MAJOR ASSUMPTIONS

1. Soil tested and its structure are representative of soil at modelled point in-situ.
2. Initial state and method of loading are both satisfactory representations of in-situ conditions.
3. Failure in shear controls, rather than deformations or tensile cracking.
4. Stress-strain curves of all soils along assumed failure surface have similar strains at peak and sensitivity, i.e. similar shape.

TABLE 4 SELECTION OF STRENGTH FOR STABILITY ANALYSIS
PLATEY-GRAINED SOILS

CASE	STATE	TEST TYPE	REPRESENTATIVE STRESS-STRAIN CURVE AND STRESS PATH (Specimens anisotropically consolidated to Point a)	STRENGTH DEFINED @	FACTOR OF SAFETY FOR PROGRESSIVE FAILURE	TYPE OF FAILURE	NOTES
E	CONTRACTIVE	DRAINED	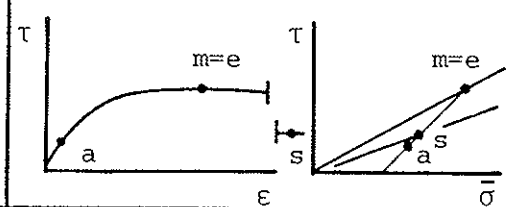	m e	1 (higher if clay lies in a thin seam)	Gradual ↓ Abrupt	Very large deformations precede failure. They are very likely to control factor of safety. The undrained case is more critical (assuming all other aspects of method of loading are identical). Abrupt failure plane forms only after very large strains.
F	CONTRACTIVE	CONS. VOLUME	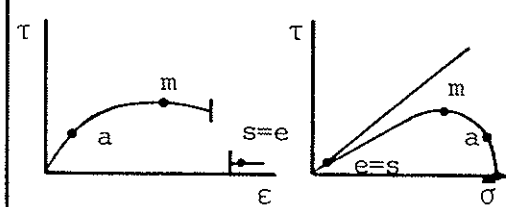	m	1.1 if ε_m is > 20% Same as Case B if ε_m <10%	Abrupt	Large deformations precede failure unless cementation, as exists in some undisturbed clays, results in quite low failure strain. Typical of normally consolidated clays. (Quick clay behavior is more closely related to that of loose sands, so Case B is applicable.) If $\tau_a > \tau_s$, the soil is in unstable equilibrium. The larger that ε_m is, the more likely that deformations control working stress.
G	DILATIVE	DRAINED	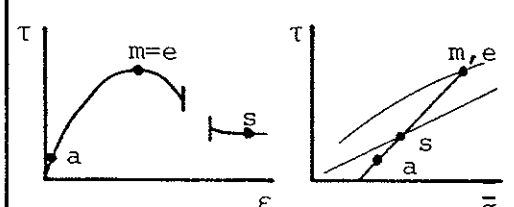	m e	1 to τ_m/τ_s	Abrupt	Usually large strains precede abrupt failure. Factor of safety on peak strength varies with time and with nature of existing discontinuities and with drained sensitivity. See Skempton (1964) and Skempton & Hutchinson (1969). Continuous creep toward failure if $\tau_a > \tau_s$.
H	DILATIVE	CONS. VOLUME	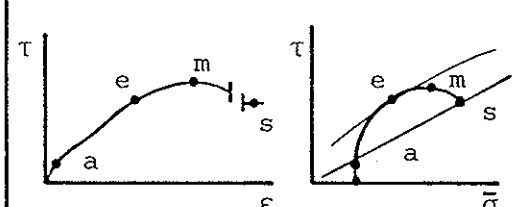	e	For long term, assume drained. For short term, use F=1 with τ_e	Gradual ↓ Abrupt	Pore water migration toward zone of highest shear stress causes strength to be close to drained Case G even though entire mass remainsat constant volume. Large strains needed to define steady state strengths. For very rapid loading, Point m strength could be realizable for short period.

MAJOR ASSUMPTIONS

1. Soil tested and its structure are representative of soil at modelled point in-situ.
2. Initial state and method of loading are both satisfactory representations of in-situ conditions.
3. Failure in shear controls, rather than deformations or tensile cracking.
4. Stress-strain curves of soils along assumed failure surface have similar strains at peak and similar sensitivity, i.e., similar shape.

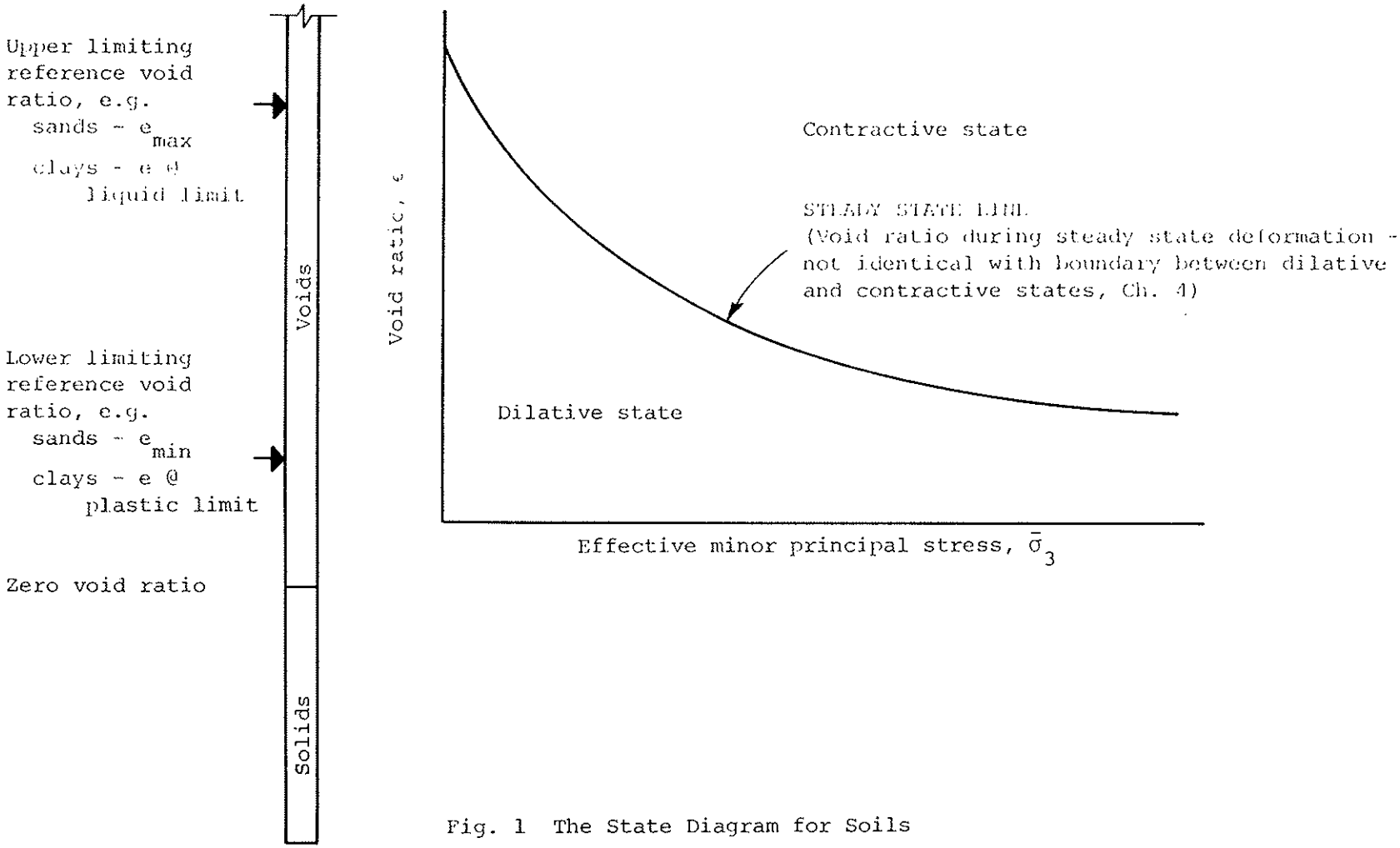

Fig. 1 The State Diagram for Soils

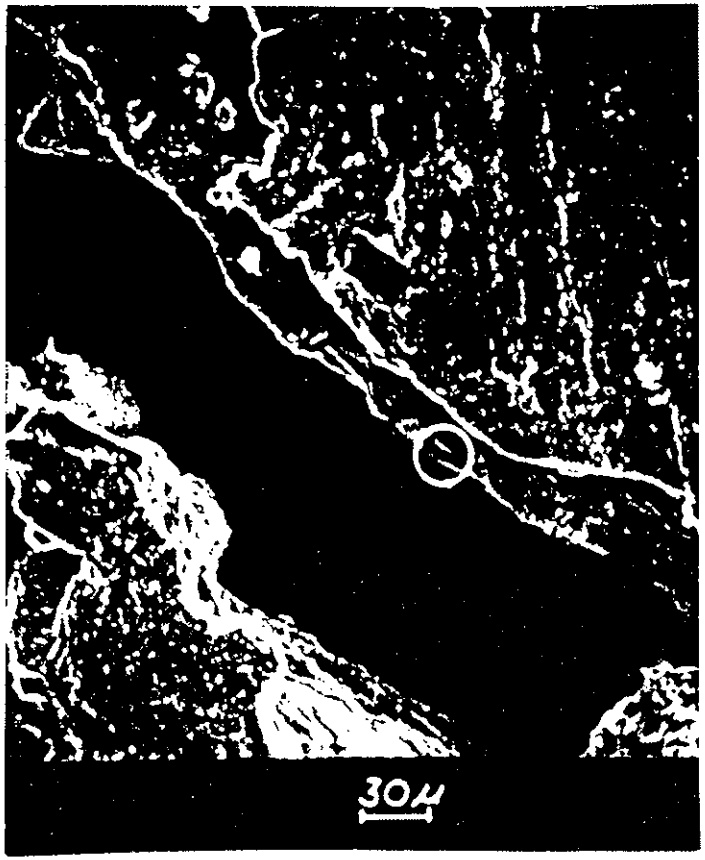

X333

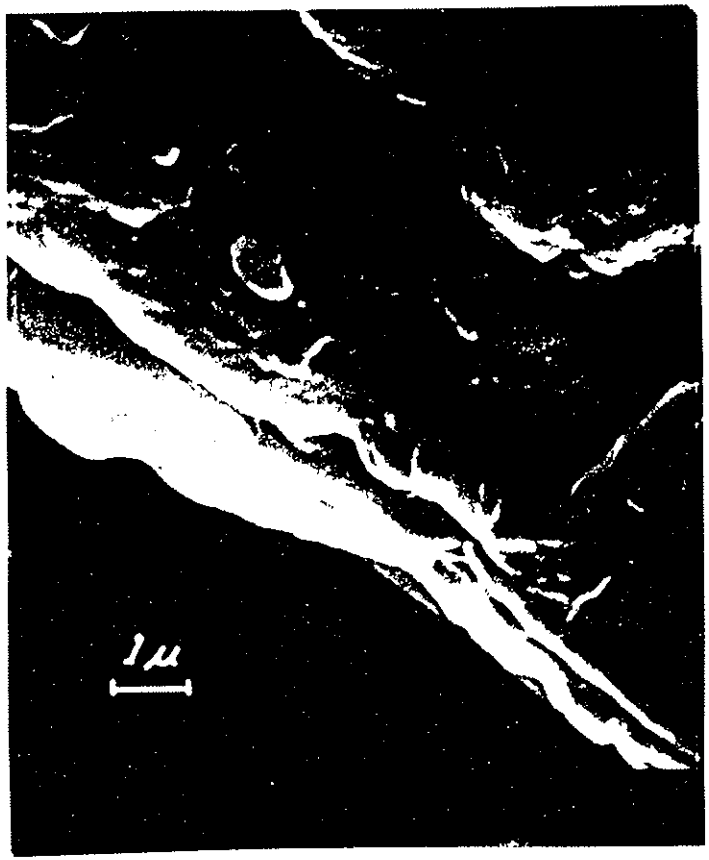

X10000

Fig. 2 Scanning - Electron Microphotographs Viewed Normal to Surface of Natural Slickenside in Bearpaw Clay-Shale

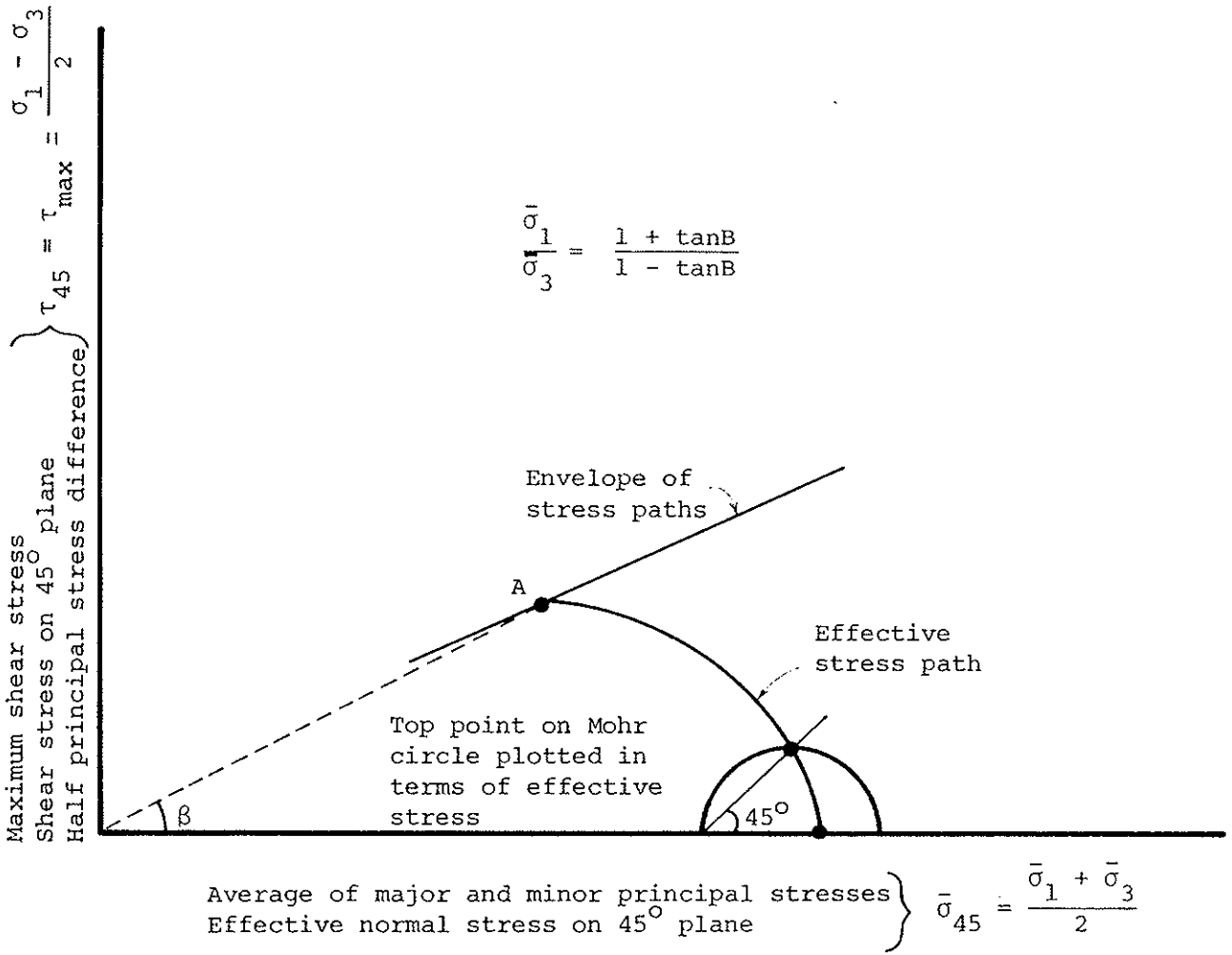

Fig. 3 The Stress Path

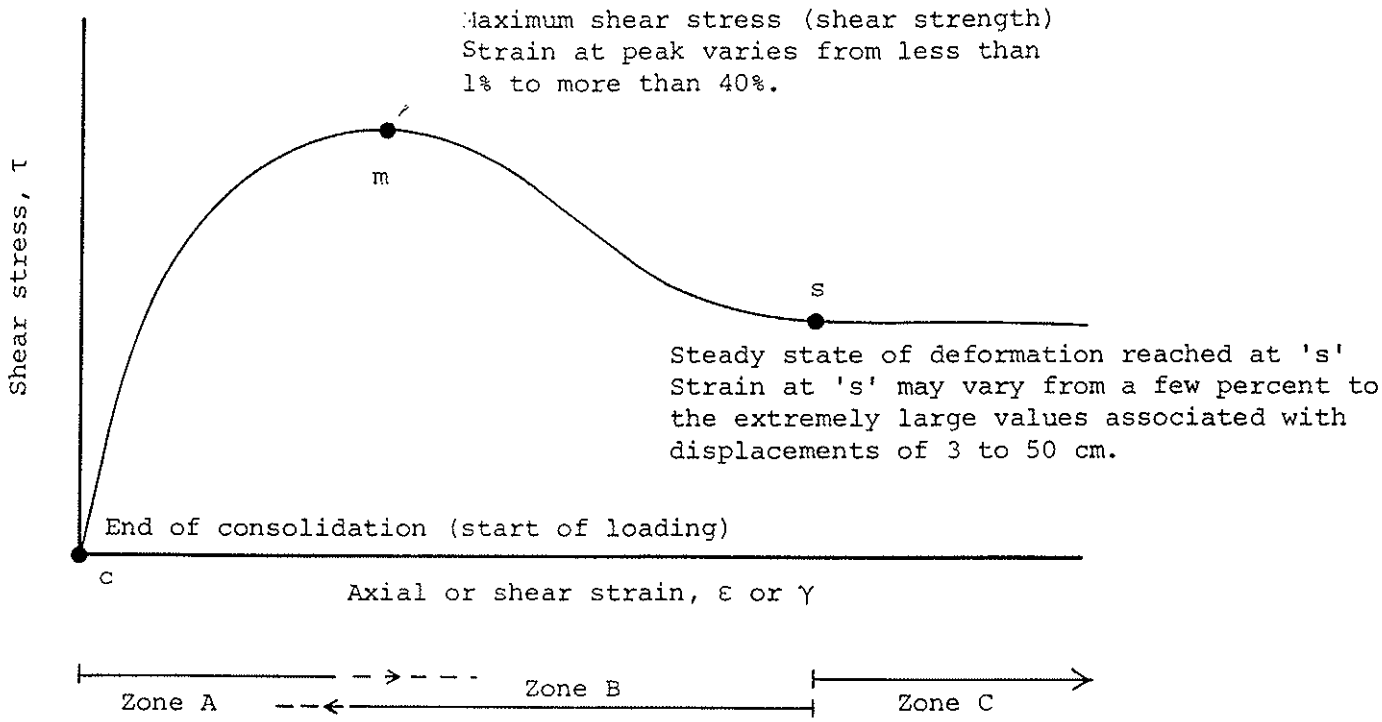

Zone A — Shape strongly affected by soil type, initial structure, initial state, and method of loading. Initial structure (including bonds, if any) and state have more influence here than in any other zone.

Zone B — Initial structure and state increasingly altered by strains until steady state of deformation is reached. Magnitude of drop from τ_m to τ_s is controlled chiefly by initial state, degree of void ratio change that is allowed, and grain shape. Initial structure and method of loading also influence magnitude of τ_m/τ_s.

Zone C — At strains beyond Point 's' crushing has stopped and the grains have reached a steady state "structure." The initial structure and state have been completely altered by the loading process and have no influence on τ_s. Nevertheless the initial conditions do influence ε_s

Fig. 4 Development of a Stress-Strain Curve

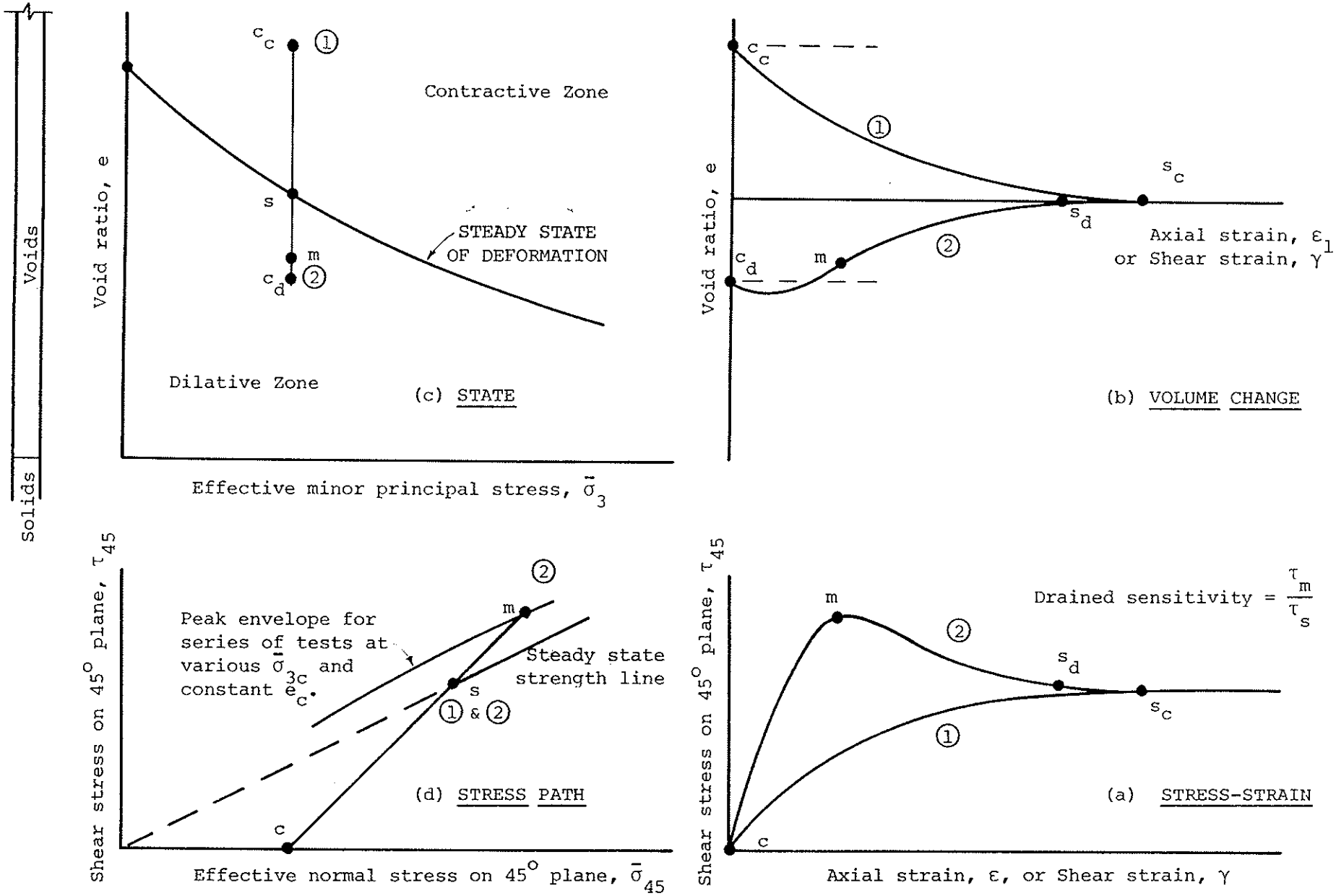

Fig. 5 Consolidated-Drained Triaxial Compression Tests
Idealized For Uncemented Soils With Bulky Grains

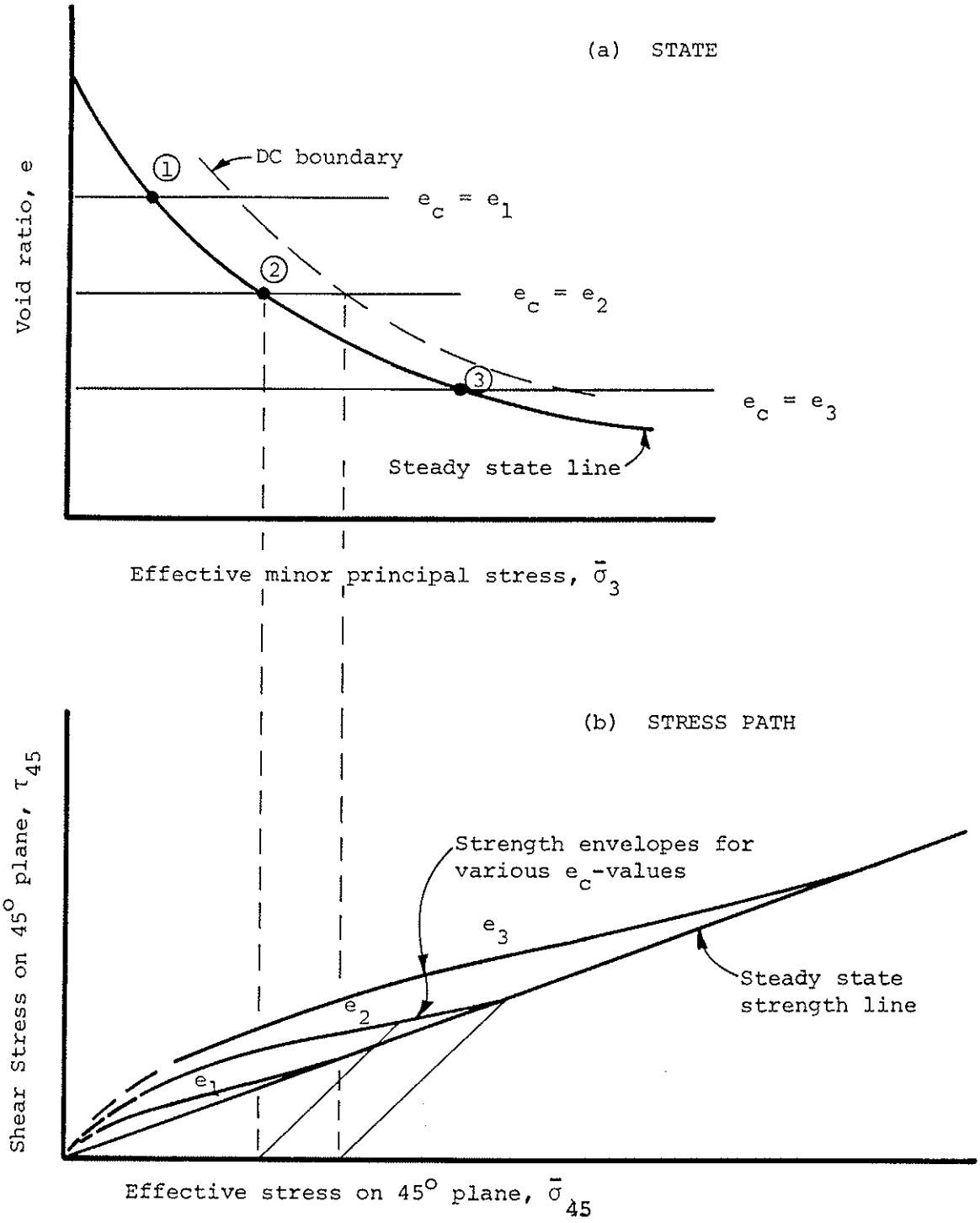

Fig. 6 Strength Envelopes for Specimens Prepared at Constant Void Ratio, e_c. Consolidated-Drained Triaxial Compression Tests.

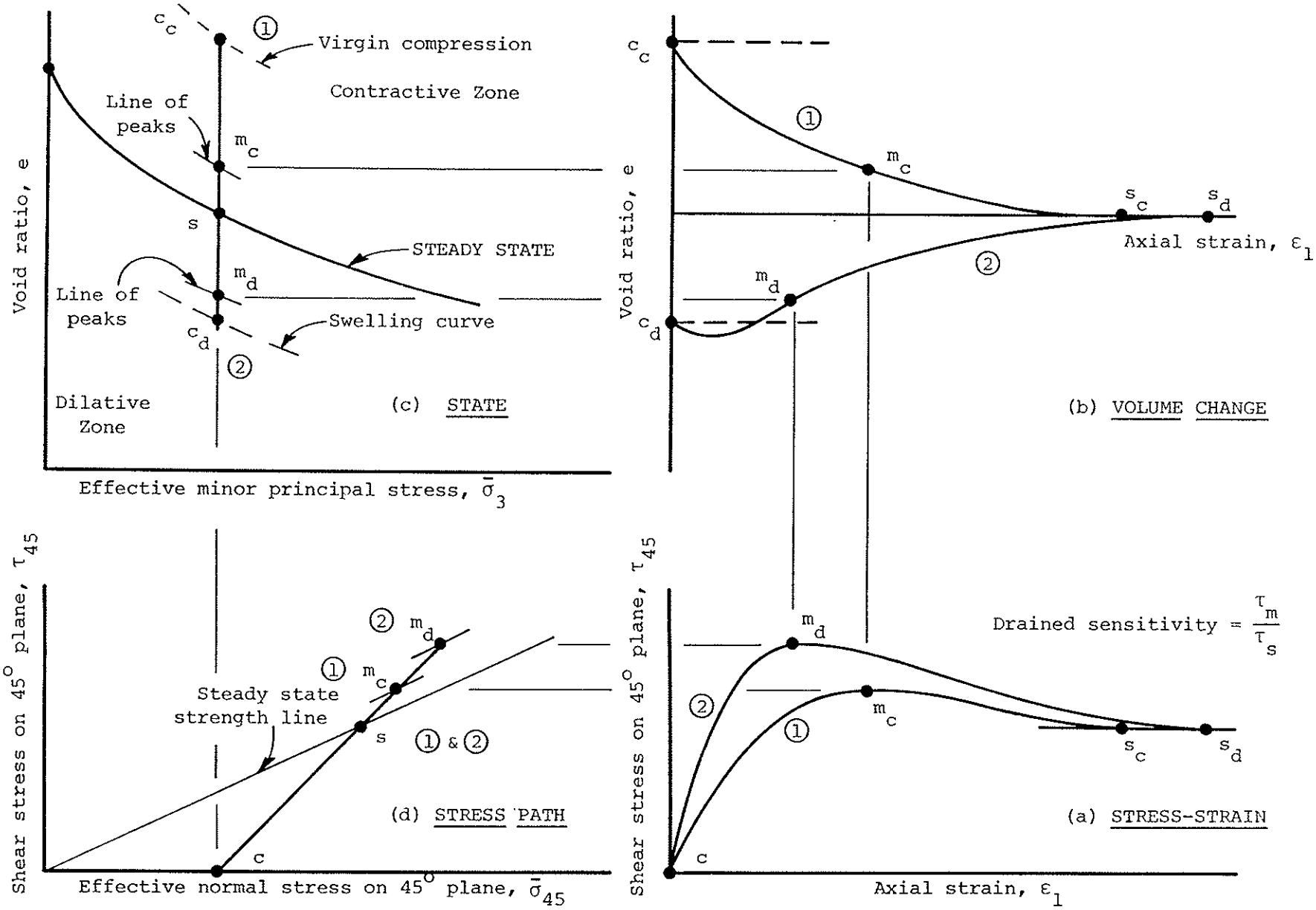

Fig. 7 Consolidated-Drained Triaxial Compression Tests On Soil Containing Substantial Proportion of Flat Grains. Low Stress Levels. Idealized.

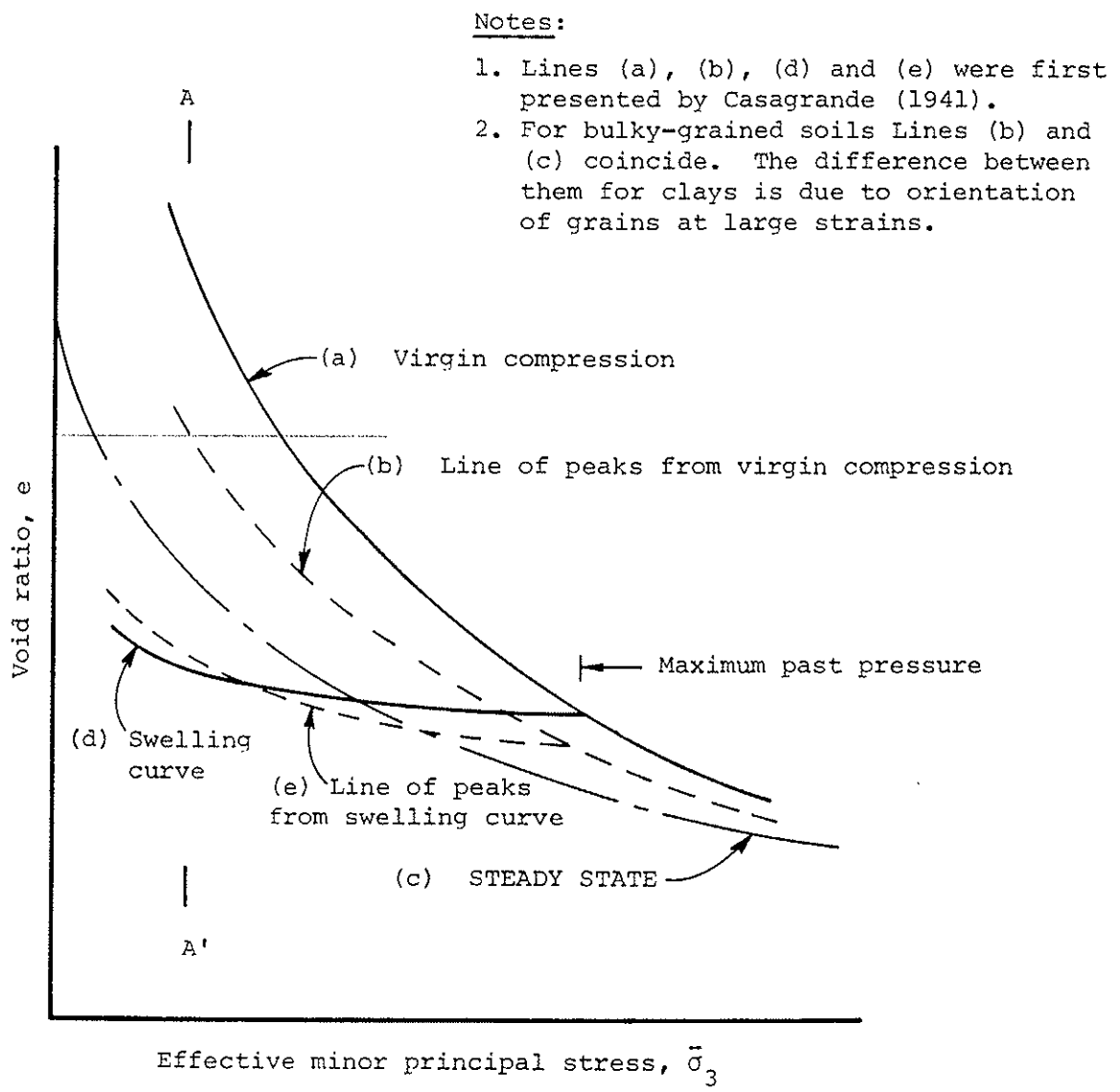

Fig. 8 Postulated Location of Steady State Line Relative to Compression and Swelling Curves for Clays

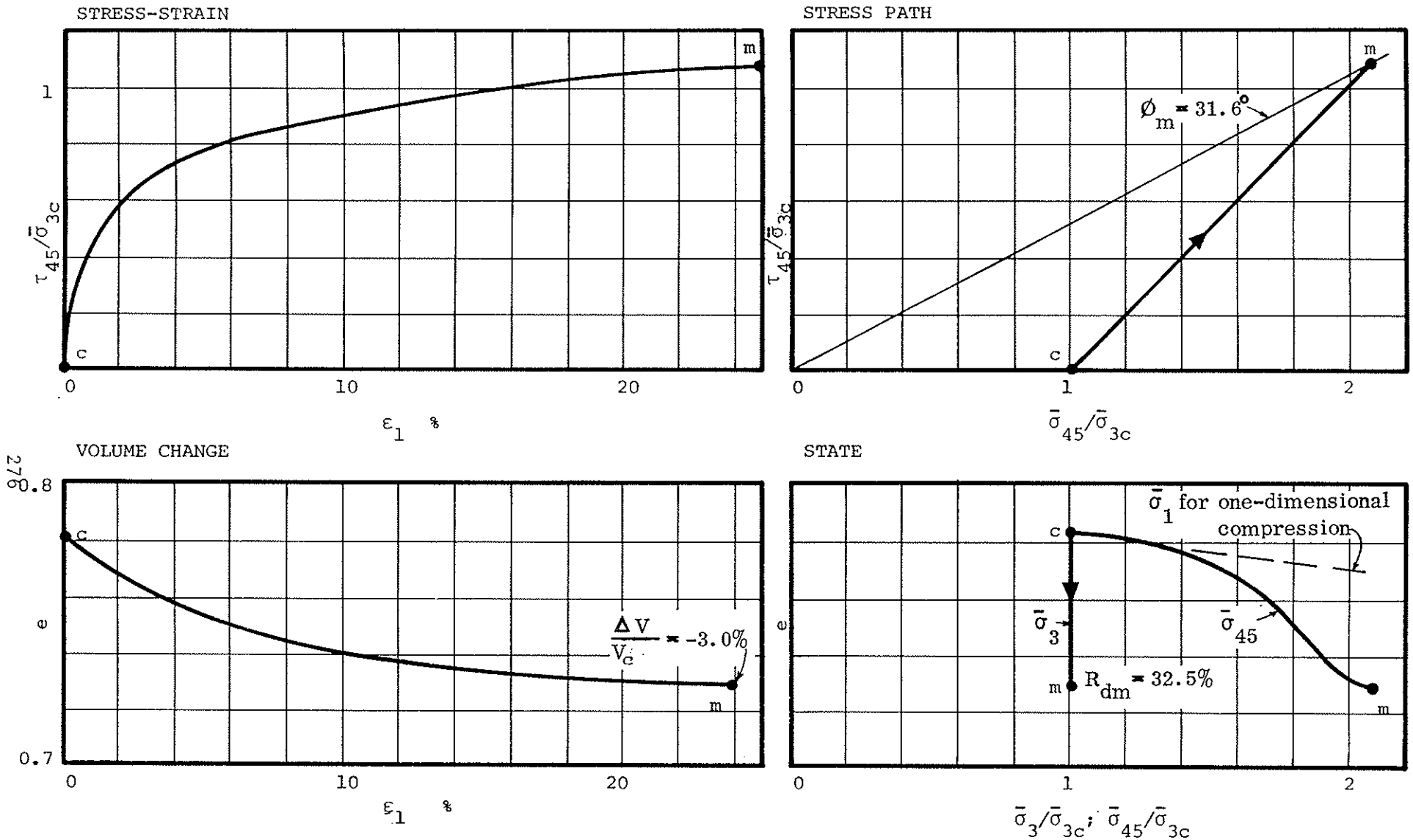

Soil Tested: Fine quartz sand; bulky, subrounded to subangular grains; D_{10} = 0.097 mm; C_u = 1.8; s_s = 2.65; e_{max} = 0.84; e_{min} = 0.50.

Test Conditions: $\bar{\sigma}_{3c}$ = 1.0 kg/cm^2; e_o = 0.783; R_{dc} = 17%; u_c = 4.0 kg/cm^2; strain rate 1%/min; lubricated ends; 1.4 in. dia. by 3.5 in. high; compacted in bulked state (w~5%); fully saturated.

Source: Replotted from Castro (1969), Fig. 66, p. 79.

Fig. 9 Highly Contractive Sand Consolidated-Drained Triaxial Compression

Fig. 9

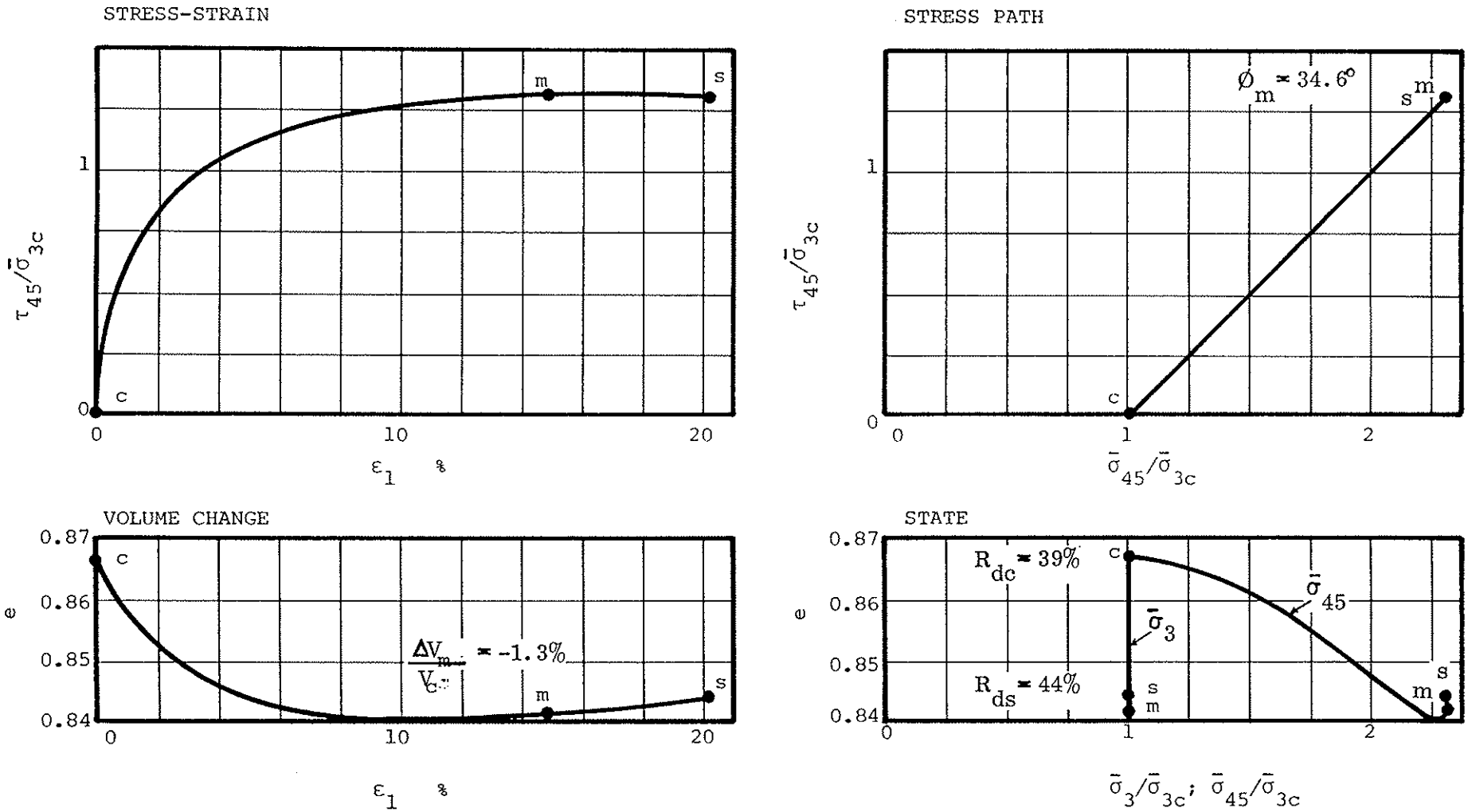

Soil Tested: Fine, uniform Sacramento River sand; bulky, angular to subrounded grains; quartz and feldspar; D_{10} = 0.17 mm; C_u = 1.3; e_{max} = 1.03; e_{min} = 0.61; s_s = 2.68.

Test Conditions: $\bar{\sigma}_{3c}$ = 4.5 kg/sq cm; e_c = 0.867; R_{dc} = 39%; 1.4 in. dia. by 3.4 in. high; strain rate equals 0.18%/min; no back pressure or end lubrication.

Source: Replotted from Lee and Seed (1967), Fig. 4. Original data furnished by Lee (1970).

Fig. 10 Slightly Dilative Sand Consolidated-Drained Triaxial Compression

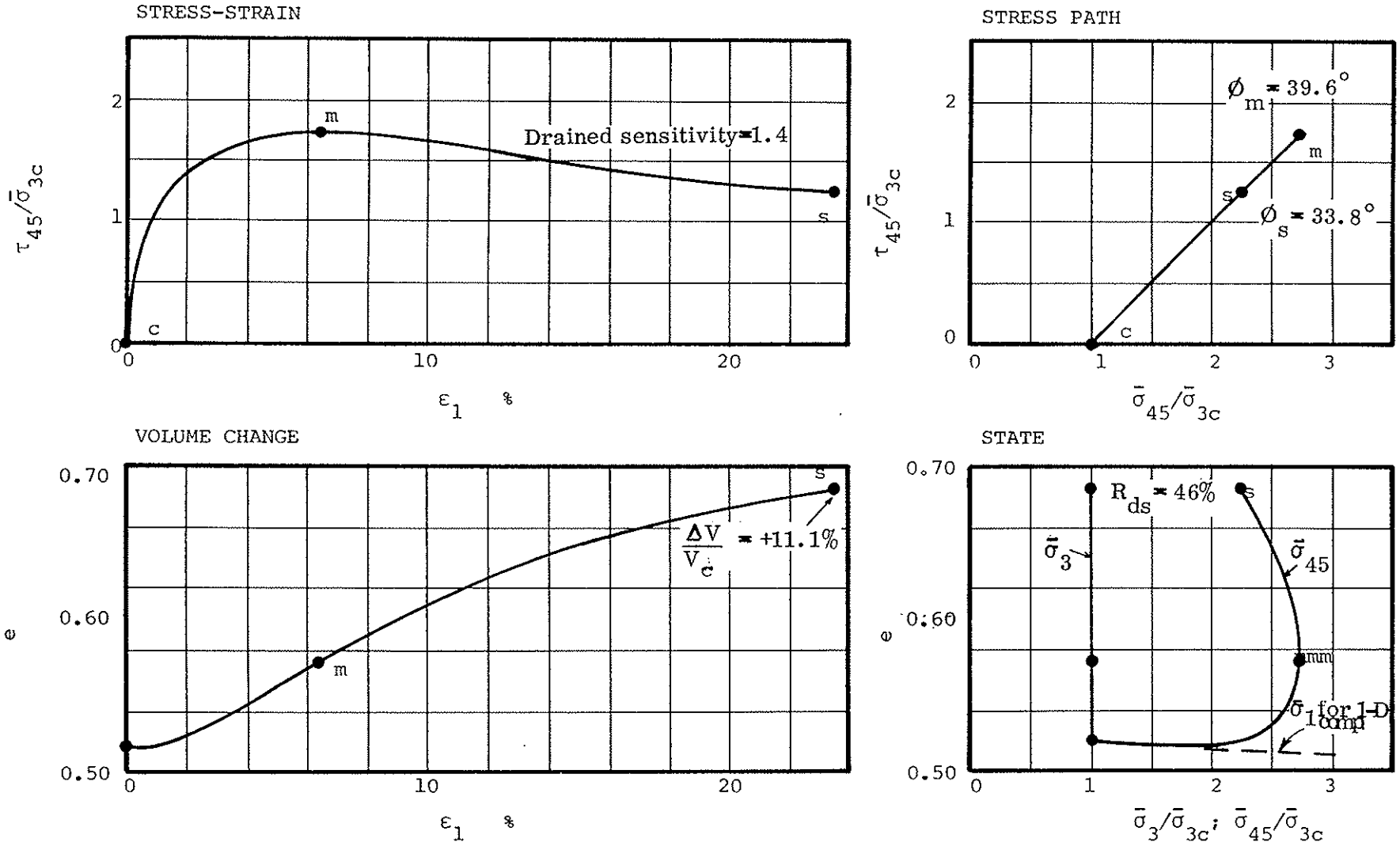

Soil Tested: Fine quartz sand; bulky, subrounded to subangular grains; D_{10} = 0.097 mm; C_u = 1.8; s_s = 2.65; e_{min} = 0.50; e_{max} = 0.84.

Test Conditions: $\bar{\sigma}_{3c}$ = 1.0 kg/sq cm; e_c = 0.518; R_{dc} = 95%; u_c = 4.0 kg/sq cm; strain rate 1%/min; 1.4 in. dia. by 3.5 in. high; lubricated ends; compacted in bulked state (w ~5%).

Source: Replotted from Castro (1969); Fig. 66, p. 79.

Fig. 11 Highly Dilative Sand Consolidated-Drained Triaxial Compression

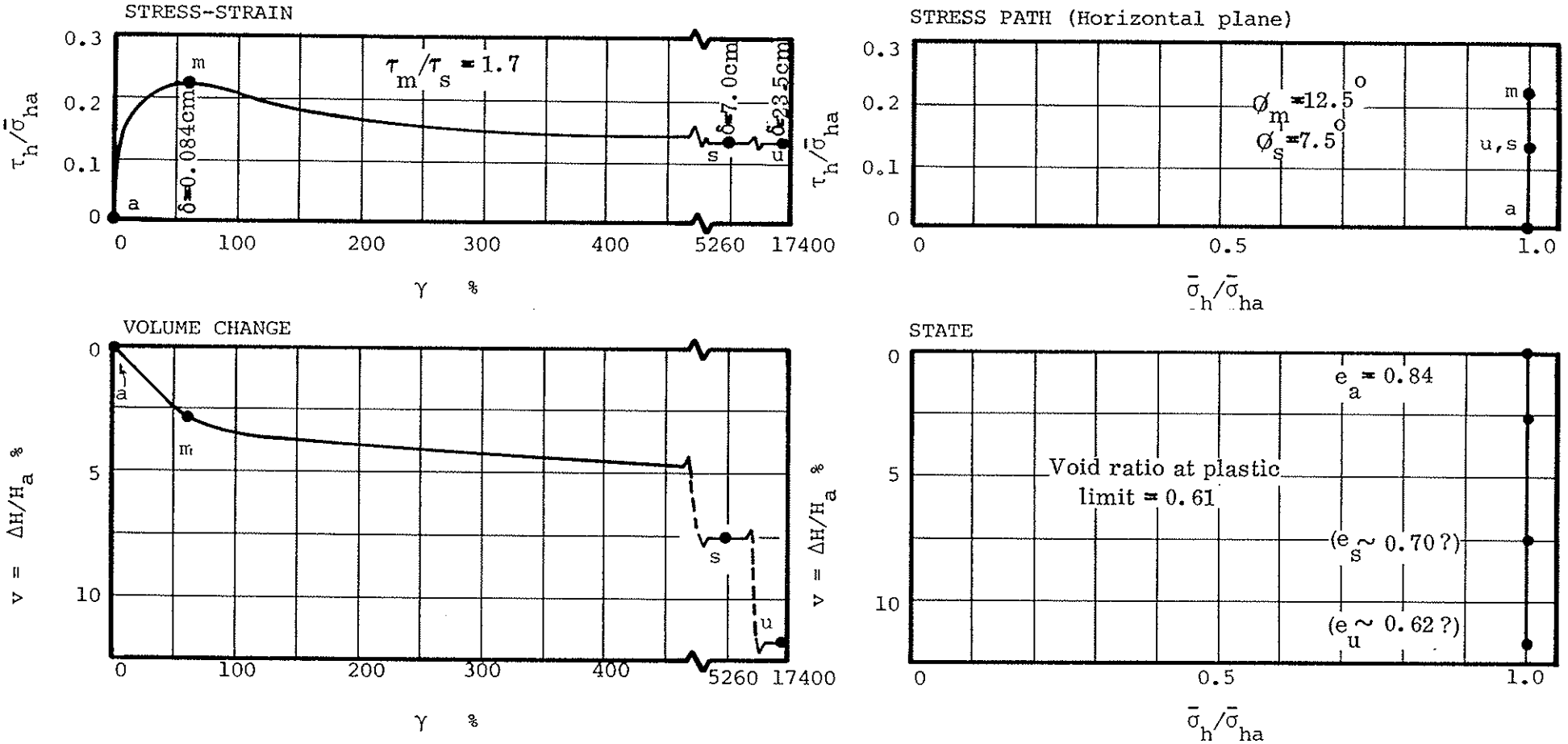

Soil Tested: Pepper Shale; air dried and remolded at w_i = 61%; L_w = 71, P_i = 49; 73% minus 2μ; s_s = 2.76.

Test Conditions: $\bar{\sigma}_{ha}$ = 4.0 kg/cm^2; w_a = 30.5% (e_a = 0.84); displacement rate 0.0056 cm/min on periphery (one rotation in 2.8 days); annular disc, ID = 5.11 cm, OD = 7.11 cm; H_a = 0.135 cm; G_w = 100%; essentially normally consolidated

Source: Replotted from LaGatta (1970), Fig. 7-4.

Fig. 12 Highly Contractive Clay Consolidated-Drained Rotation Shear

Fig. 12

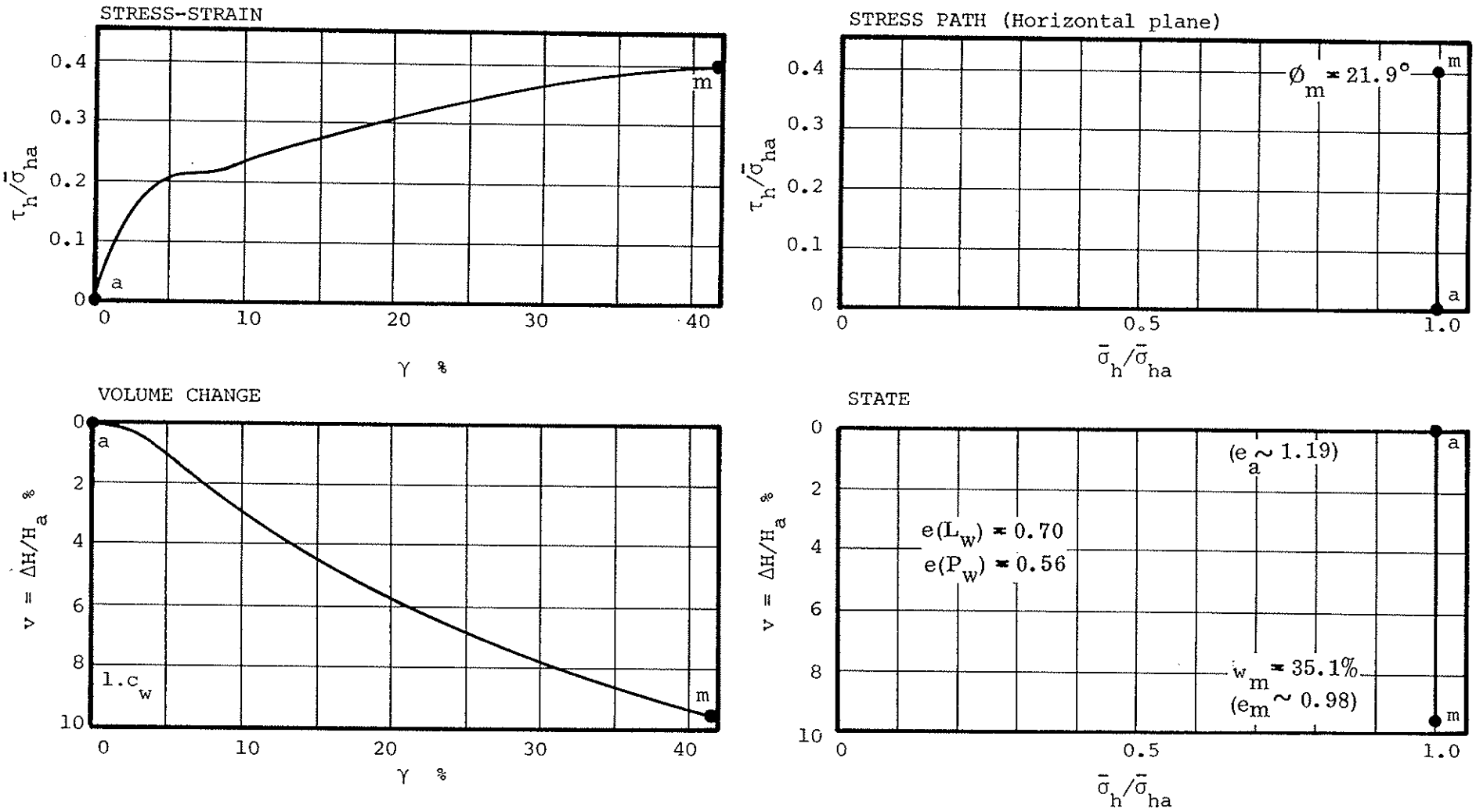

Soil Tested: Manglerud quick silty clay; w_{nat} ~46%, L_w ~25; P_i ~5; undrained sensitivity 40-150; depth 6.30 m (in-situ vertical $\bar{\sigma}$ = 0.60 kg/cm^2); ~48% <2μ; s_s ~2.78.

Test Conditions: $\bar{\sigma}_{ha}$ = 0.58 kg/cm^2; w_a ~43% (e_a ~1.19); H_a = 1.01 cm; 8 cm diameter; average rate of shear strain to 'm' 0.024 %/min; undisturbed.

Source: Replotted from Bjerrum and Landva (1966), Fig. 12, Test 12, p. 15. Additional details from Landva (1962), Table 2, Test K-12.

Fig. 13 Very Highly Contractive Clay Consolidated-Drained Direct Shear

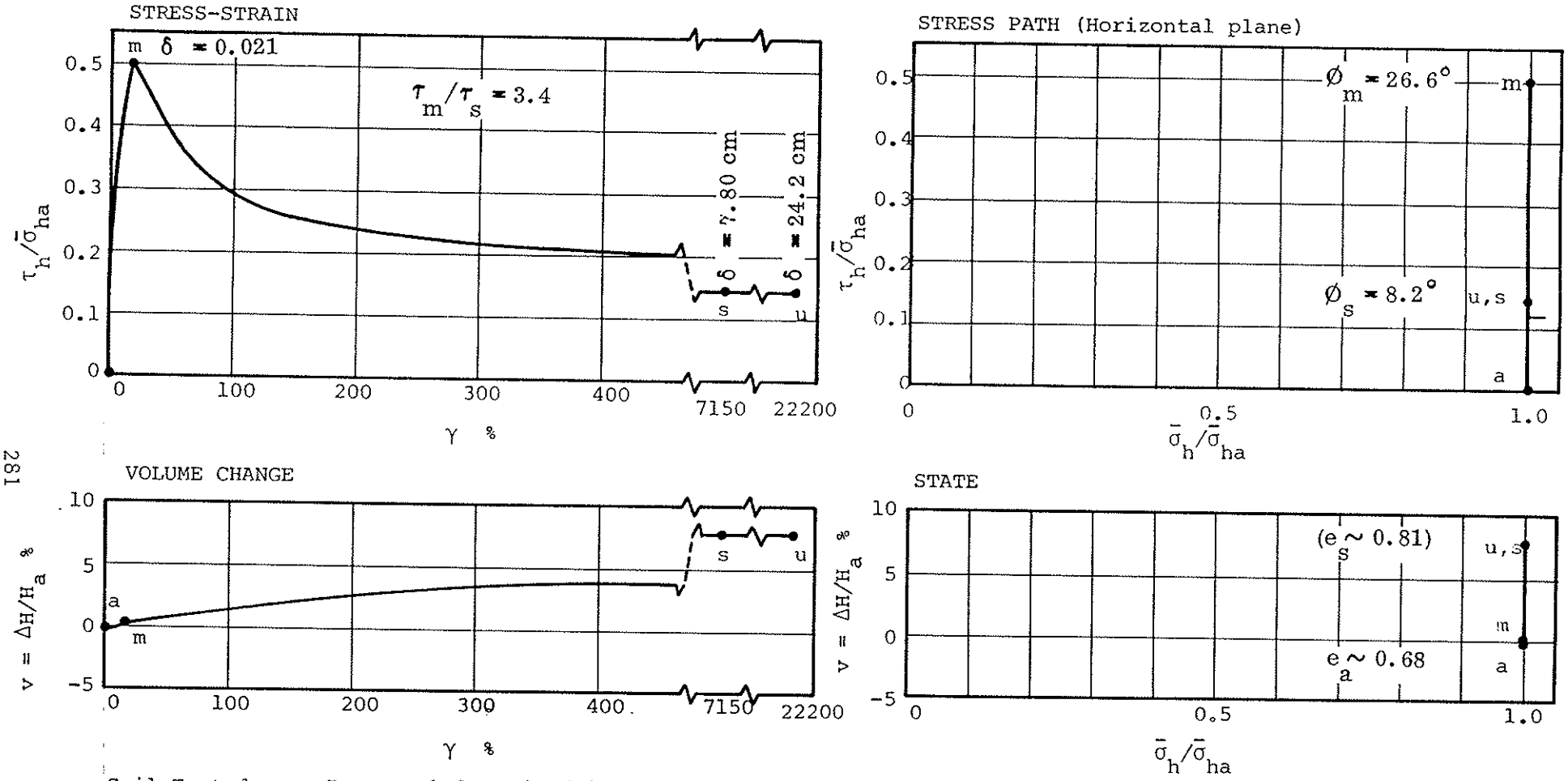

Soil Tested: Pepper shale; air dried and remolded at w_i = 62%; L_w = 71, P_i = 49; 73% minus 2μ; s_s = 2.76.

Test Conditions: $\bar{\sigma}_{ha}$ = 1.0 kg/cm^2; maximum past pressure = 100 kg/cm^2; w_a = 24.7% (e_a~0.68); displacement rate of periphery = 0.0056 cm/min (one rotation in 2.8 days); annular disc, ID = 5.11 cm, OD = 7.11 cm, H_a = 0.109 cm.

Source: Replotted from LaGatta (1970), Fig. 7-16.

Fig. 14 Highly Dilative Clay Consolidated-Drained Rotation Shear

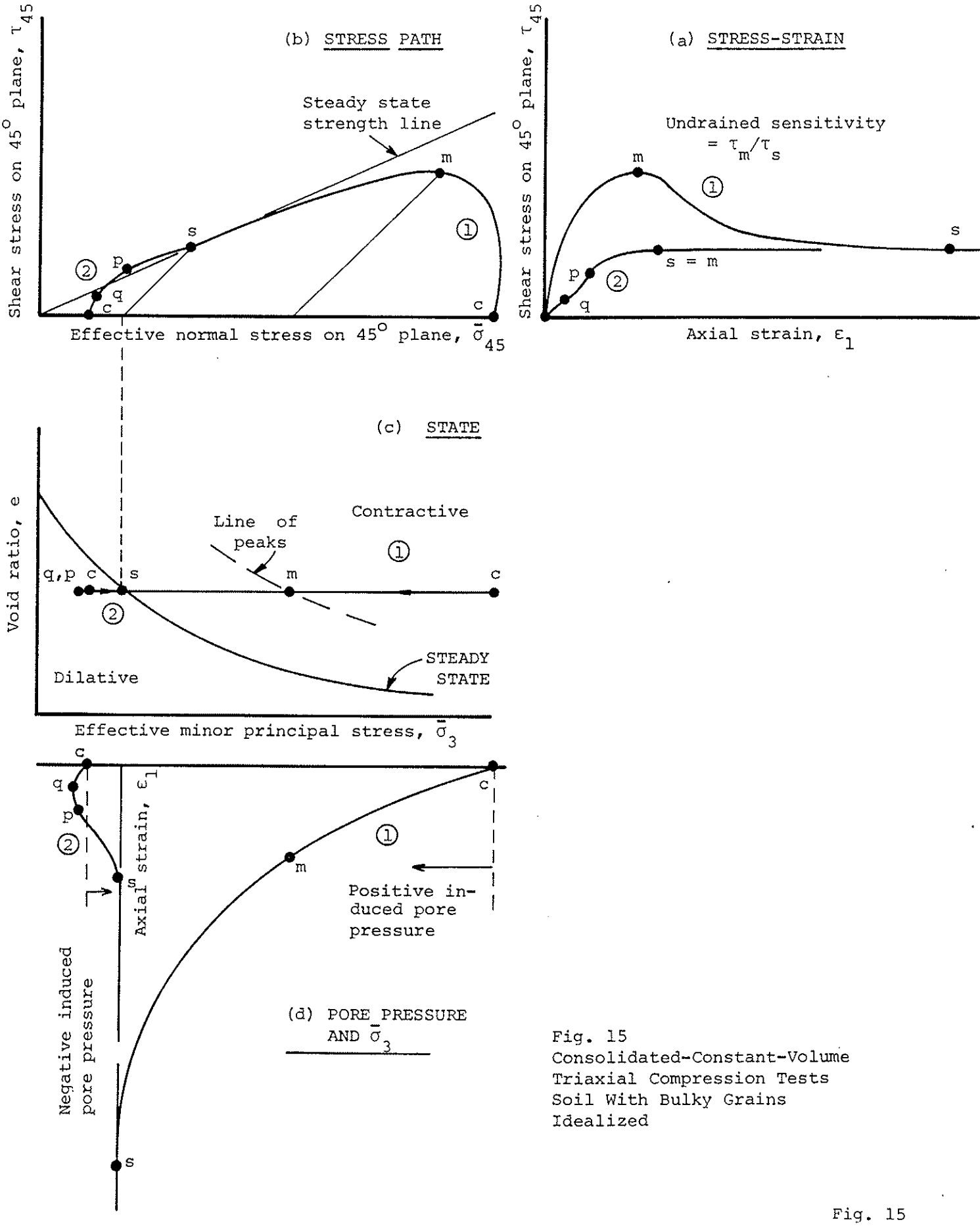

Fig. 15
Consolidated-Constant-Volume Triaxial Compression Tests Soil With Bulky Grains Idealized

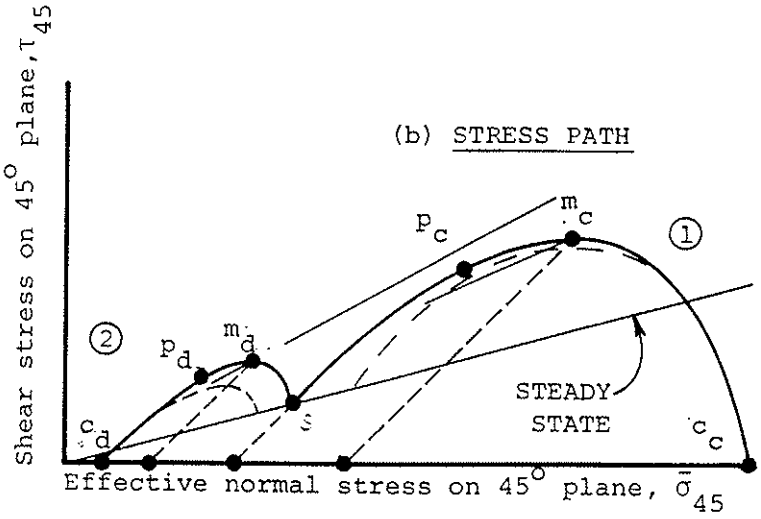

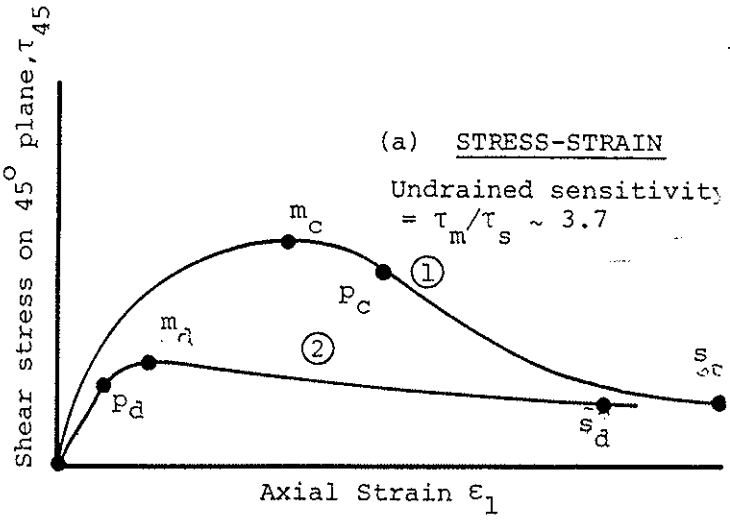

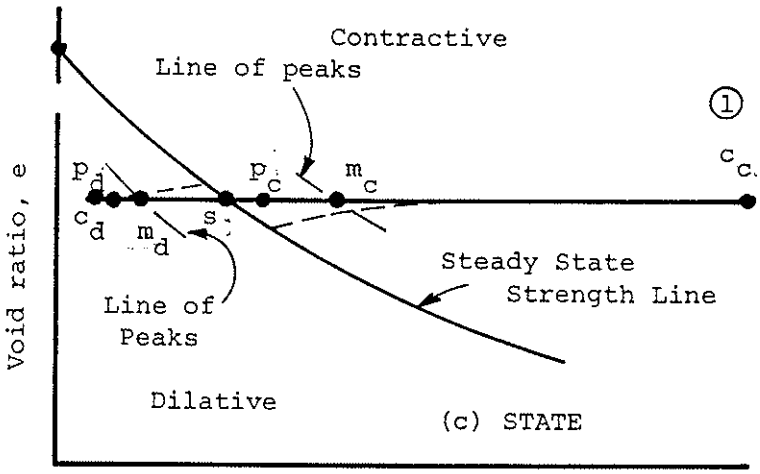

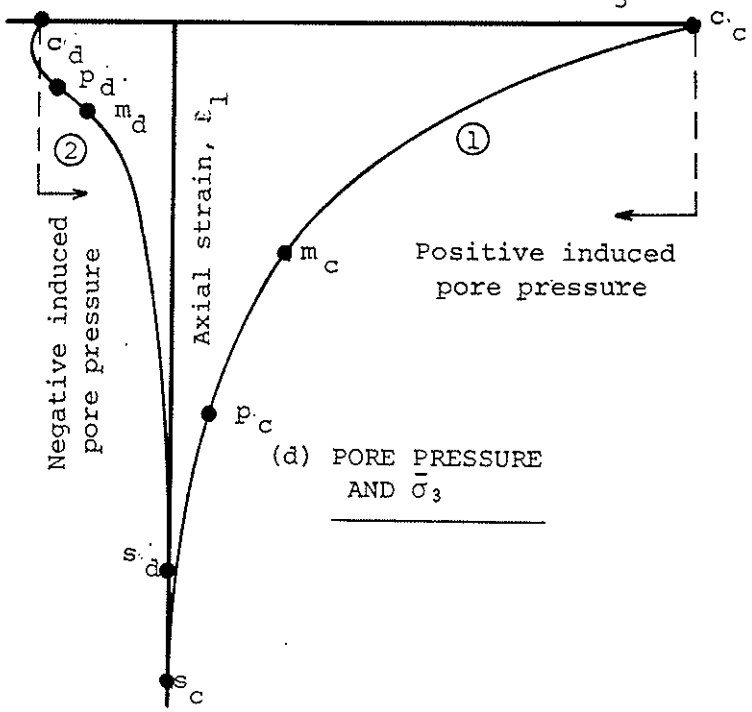

State	A-Values	
	Peak	Steady State
Contractive	0.9	4.2
Dilative	-0·2	-1.1

Dashed stress paths show effect of non-uniformities that develop during actual tests. Corresponding changes on state diagram are also shown dashed.

Fig. 16

Consolidated-constant-volume triaxial compression tests on soil containing substantial proportion of platey-grains idealized

Fig. 16

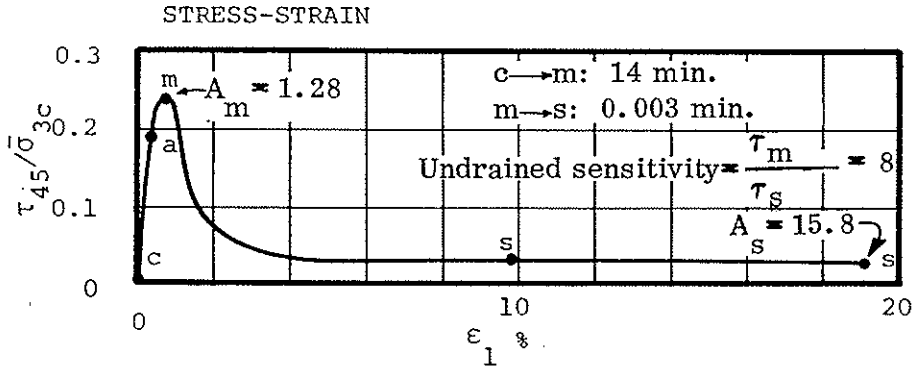

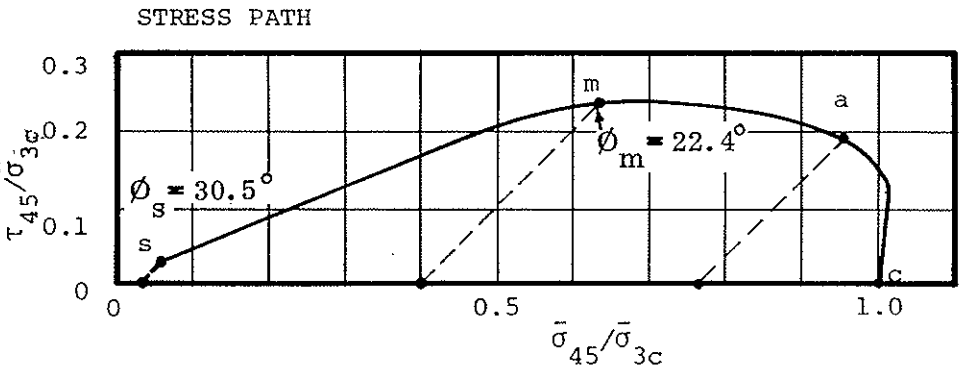

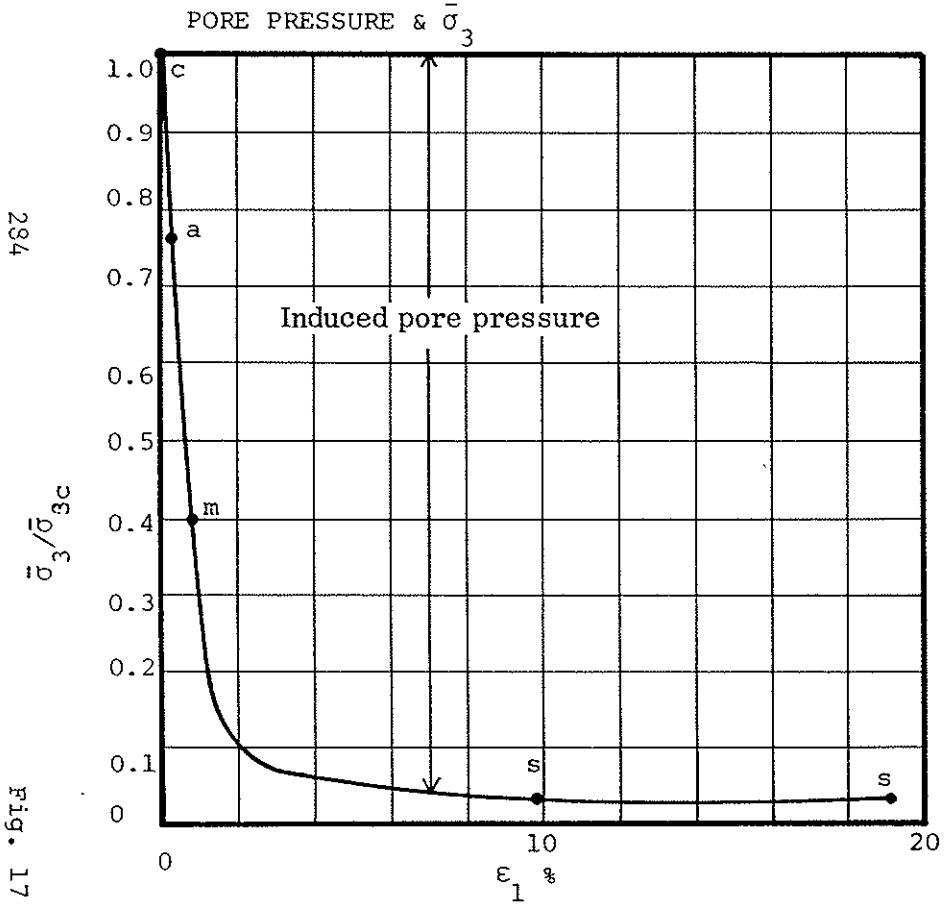

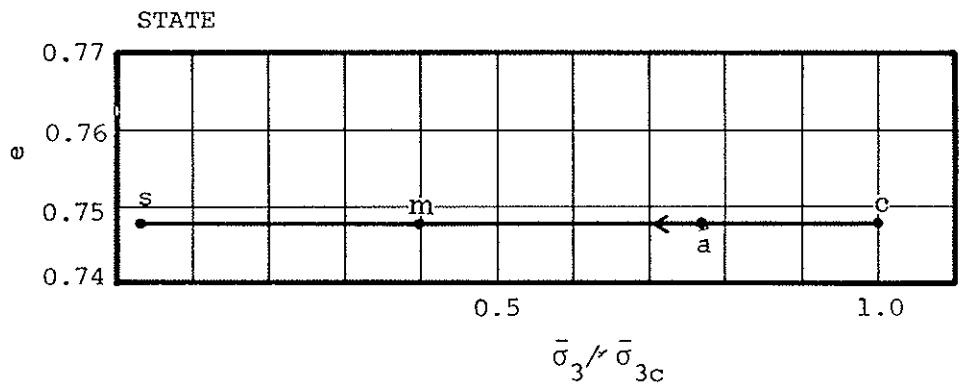

Soil Tested: Fine quartz sand; bulky, subrounded to subangular grains; D_{10} = 0.097 mm; C_u = 1.8; G_s = 2.65; e_{max} = 0.84, e_{min} = 0.50.

Test Conditions: $\bar{\sigma}_{3c}$ = 4.0 kg/cm^2; e_c=0.75; R_{dc}=27%; $\bar{\sigma}_c$=4.0 kg/cm^2; load control (post-peak acceleration); compacted bulked (W ~ 5%); 1.4 in. by 3.5 in. specimen.

Source: Replotted from Castro (1969), Fig. 33, P. 61.

Fig. 17

Highly Contractive Sand
Consolidated-Constant-Volume
Triaxial Compression

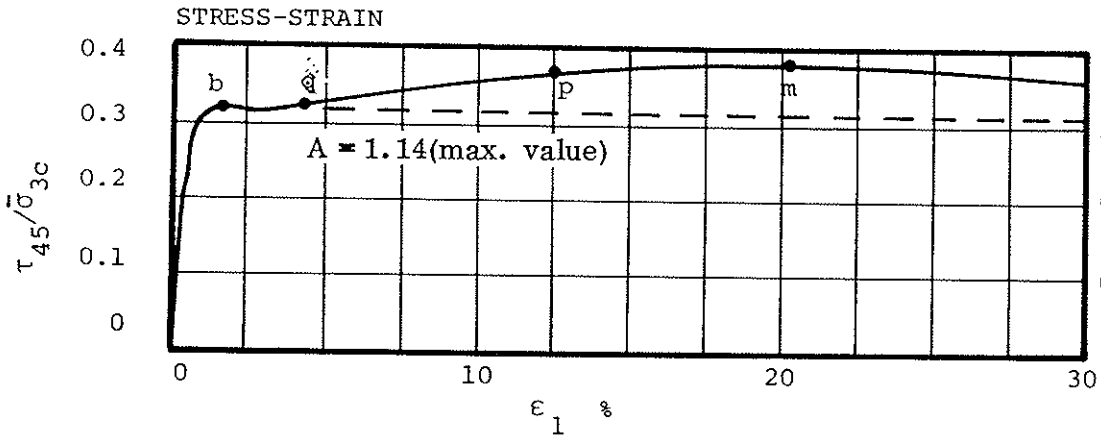

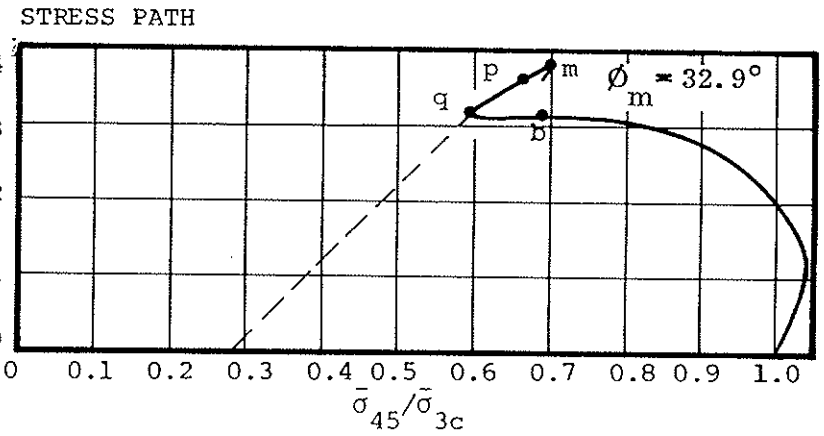

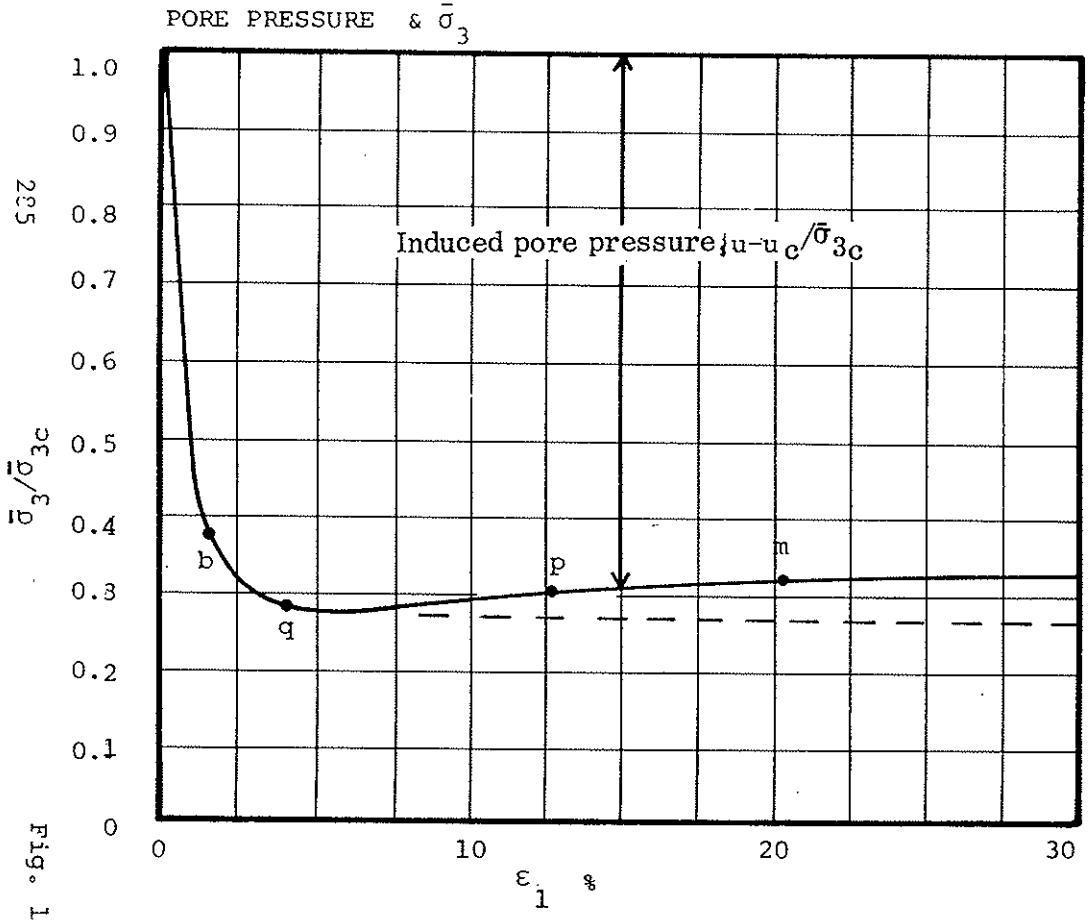

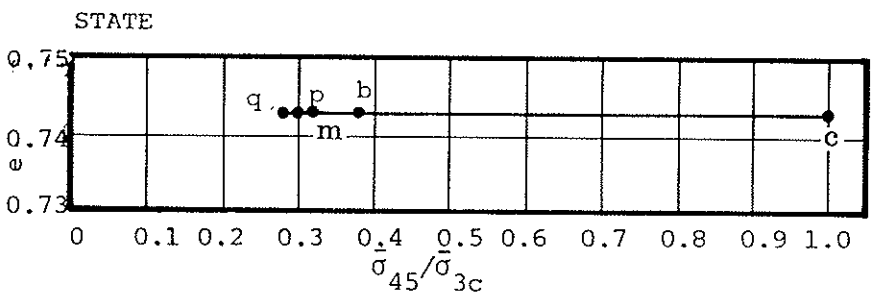

Soil Tested: Ham river-sand, uniform med-fine sand, 96% quartz, Bulky, subrounded to subangular grains D_{10} = 0.15 mm, C_u = 2, s_g = 2.70, e_{max} = 0.877 e_{min} = 0.594.
Test Conditions: $\bar{\sigma}_{3c}$ = 35.1 kg/cm^2; n_c = 42.7%(e_c=0.74); R_{dc} = 48.5%; u_c = 0.70 kg/cm^2; strain rate 0.25%/min; 1.49 in. x 3.04 in. specimen; no lubrication; degree of saturation not given.

Source: Replotted from Bishop, Webb, & Skinner (1965), Figs. 7 & 8, Skinner (1970)

Fig. 18 Sand Near Steady State Void Ratio Consolidated-Constant-Volume Triaxial Compression

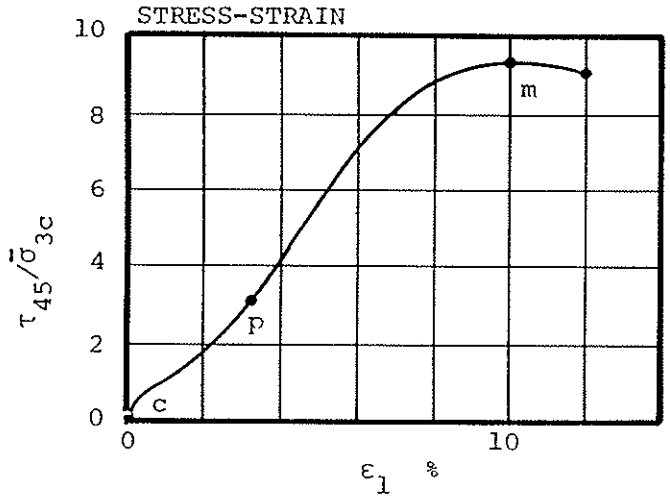

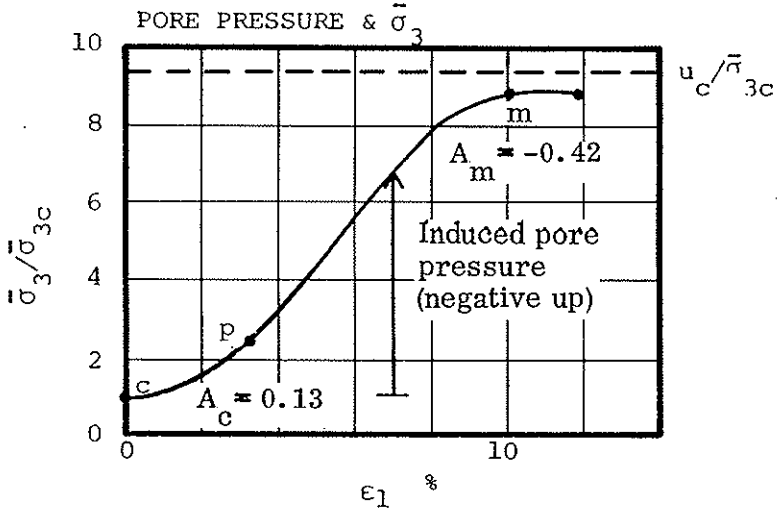

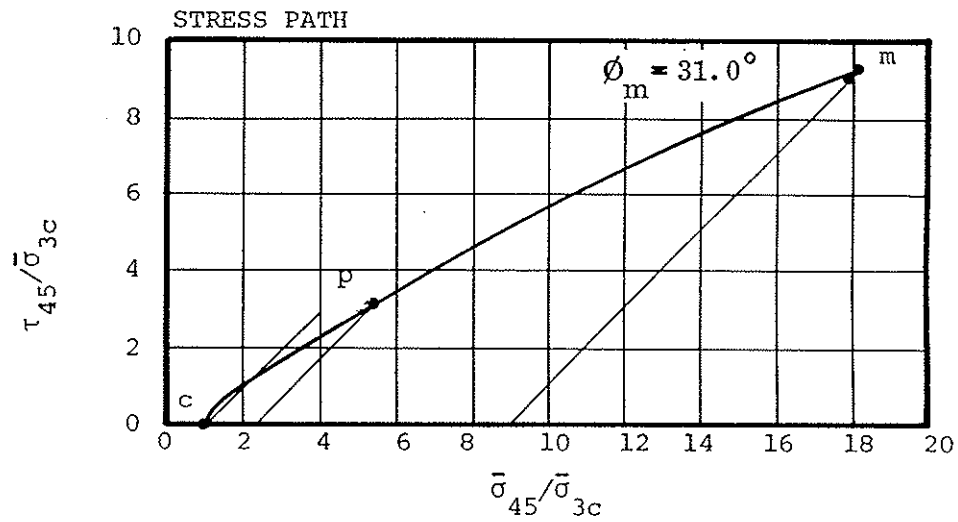

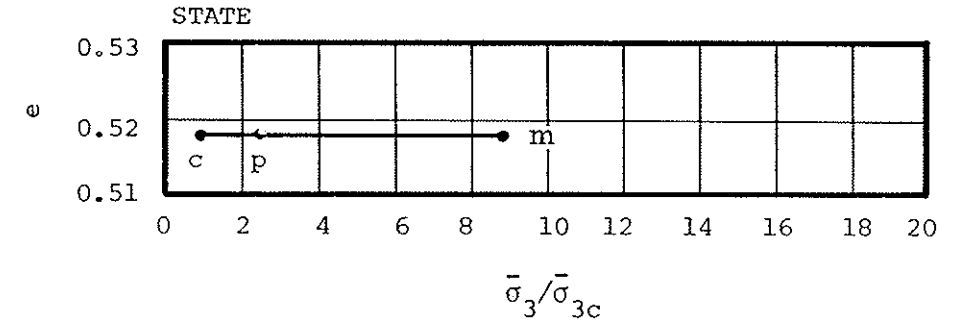

Soil Tested: Coarse Ottawa sand; pure quartz; bulky, rounded grains; D_{10} = 0.65 mm; C_u = 1.2; s_s = 2.67; e_{max} = 0.72; e_{min} = 0.48.

Test Conditions: $\bar{\sigma}_{3c}$ = 6.59 kg/cm^2; e_c = 0.518; R_{dc} = 86%; u_c = 63.5 kg/cm^2; strain rate ~0.033%/min; no lubrication of ends; G_{wc} = 100%.

Source: Replotted from Wissa and Ladd (1965), Fig. 7-7, p. 167.

Fig. 19 Highly Dilative Sand Consolidated Constant-Volume Triaxial Compression

Revised November 25, 1981

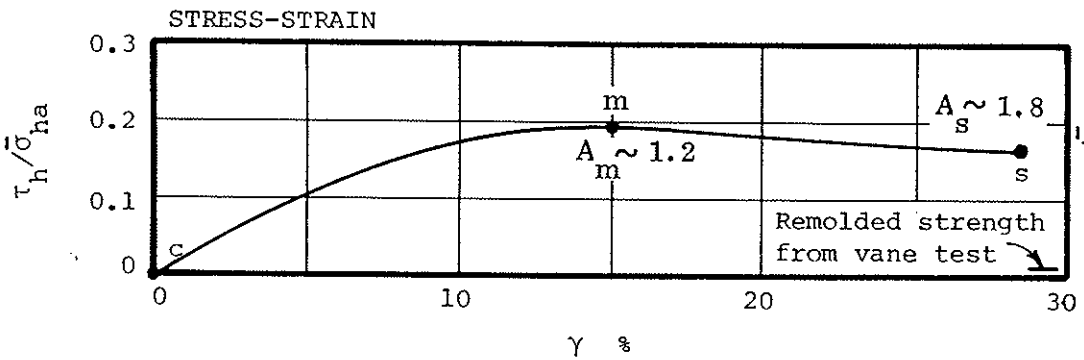

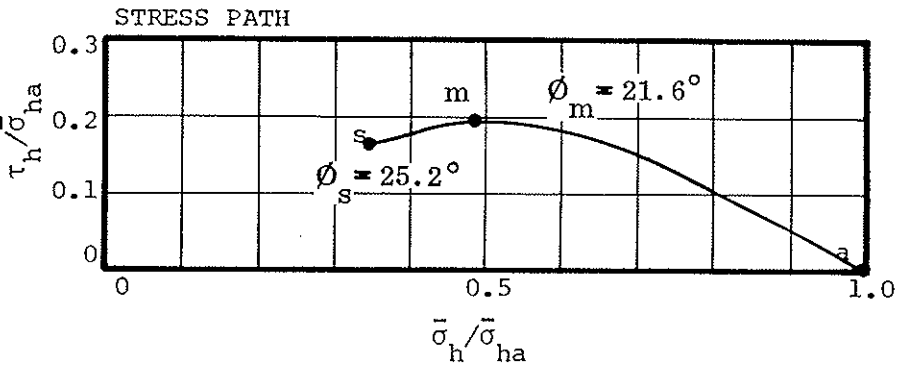

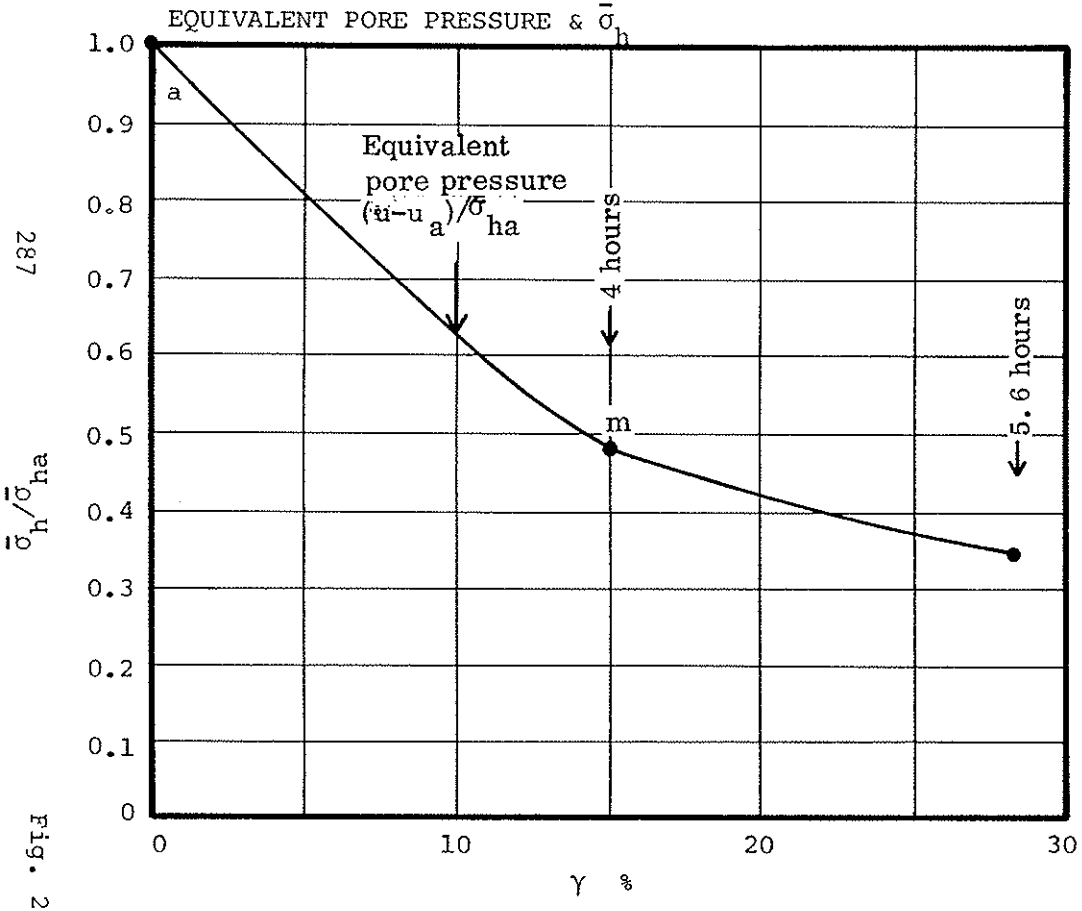

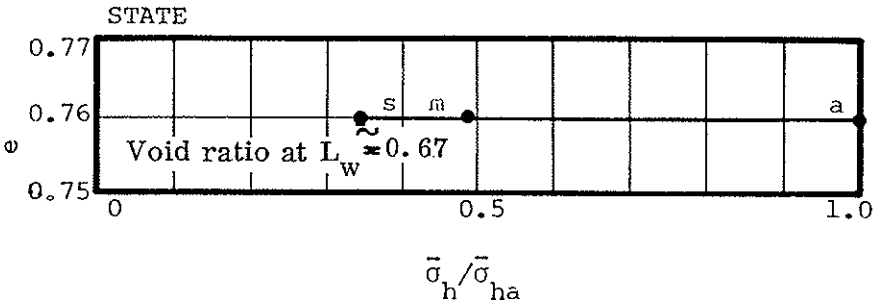

Soil Tested: Manglerud quick silty clay; w_{nat} ~36.4%; L_w ~24; P_i ~5; undrained sensitivity 40-150; depth 8.33 m (overburden = 0.77 kg/cm^2); ~48% < 2μ; s_s ~2.78; undisturbed.

Test Conditions: $\bar{\sigma}_{ha}$ = 2.0 kg/cm^2; w_a = 28.3% (e_a ~0.76); 0.89 cm thick (after consolidation); 8 cm dia.; average rate of shear strain 0.084%/min. to point 's'; thickness maintained constant (u = 0 throughout test).

Source: Replotted from Bjerrum & Landva (1966), Fig. 9, p. 12. Additional details from Landva (1962), Table 1, Test K39.

Fig. 20

Fig. 20 Very Highly Contractive Clay Consolidated Constant Volume Simple Shear

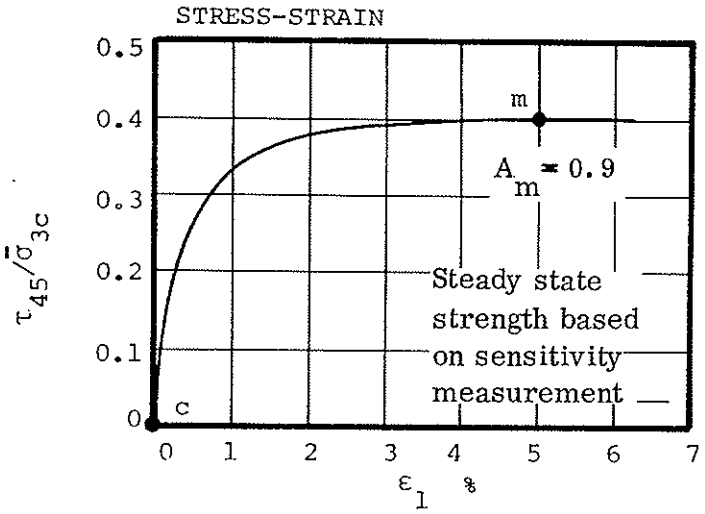

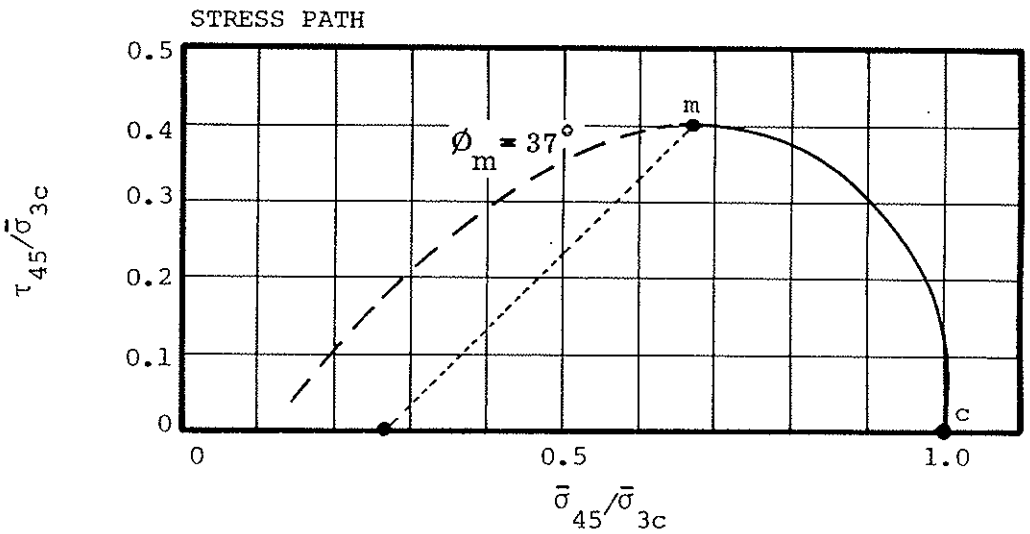

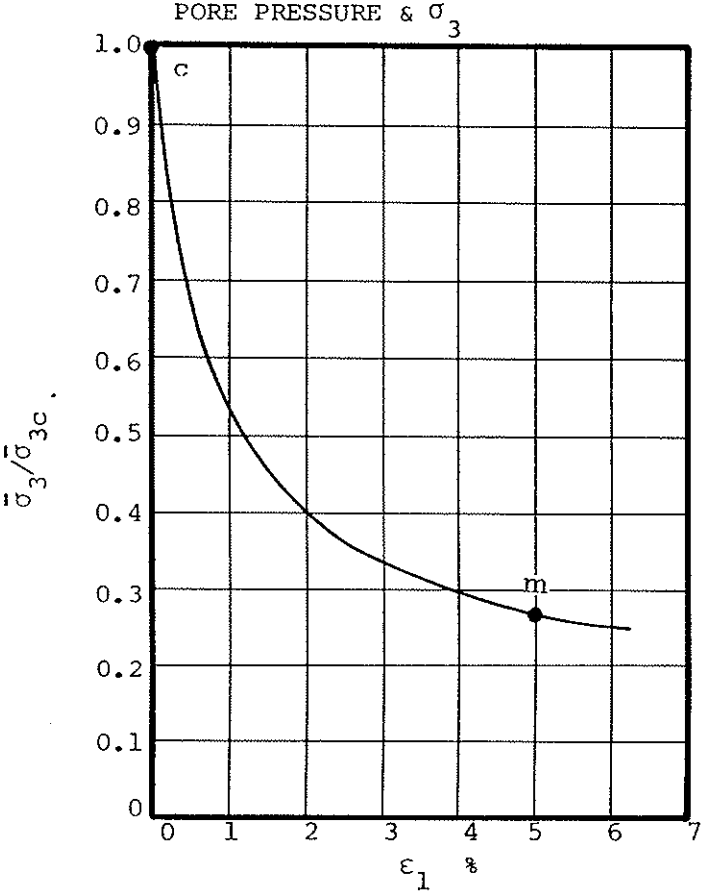

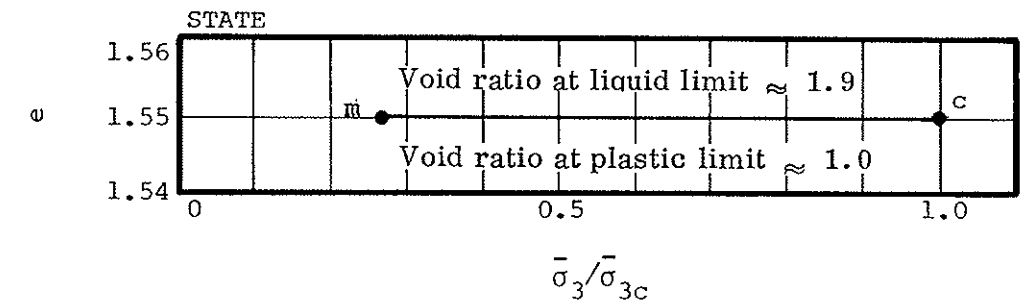

Soil Tested: Kowasaki clay; L_w = 71, P_i ~33, w_{nat} ~72.6%; ~38% <2μ; s_s = 2.68; undrained sensitivity ~10; vertical effective overburden stress = 1.85 kg/cm^2.

Test Conditions: Undisturbed specimen; $\bar{\sigma}_{3c}$ = 3.00 kg/cm^2; pore pressure held constant at 2.00 kg/cm^2; B_c = 1.00; w_{final} = 57.9% (e_c ≃1.55); strain rate 0.016%/min.; 1.4" ϕ x 3.15".

Source: Replotted from Ladd (1965), Figs. 2 & 3, p. 284; additional data from Ladd (1970).

Fig. 21

Highly Contractive Clay
Consolidated-Constant-Volume
Triaxial Compression

Fig. 2

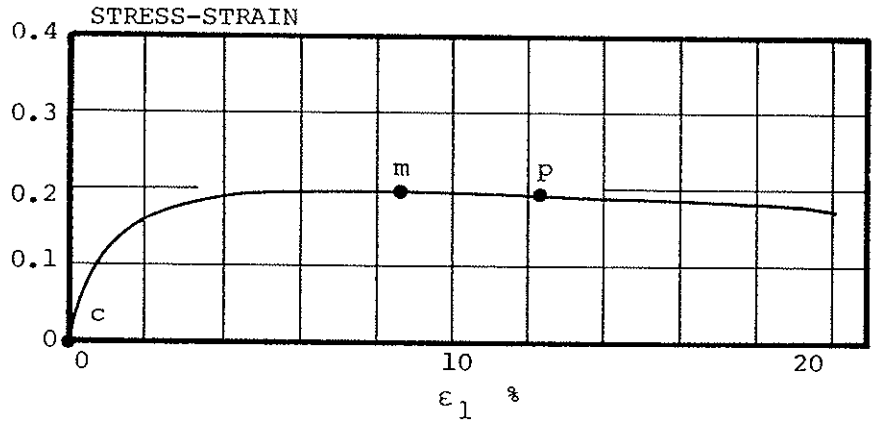

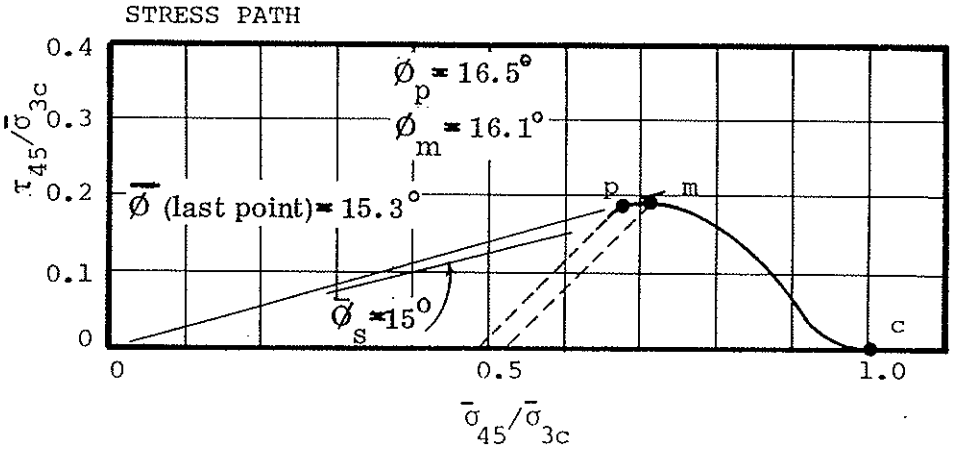

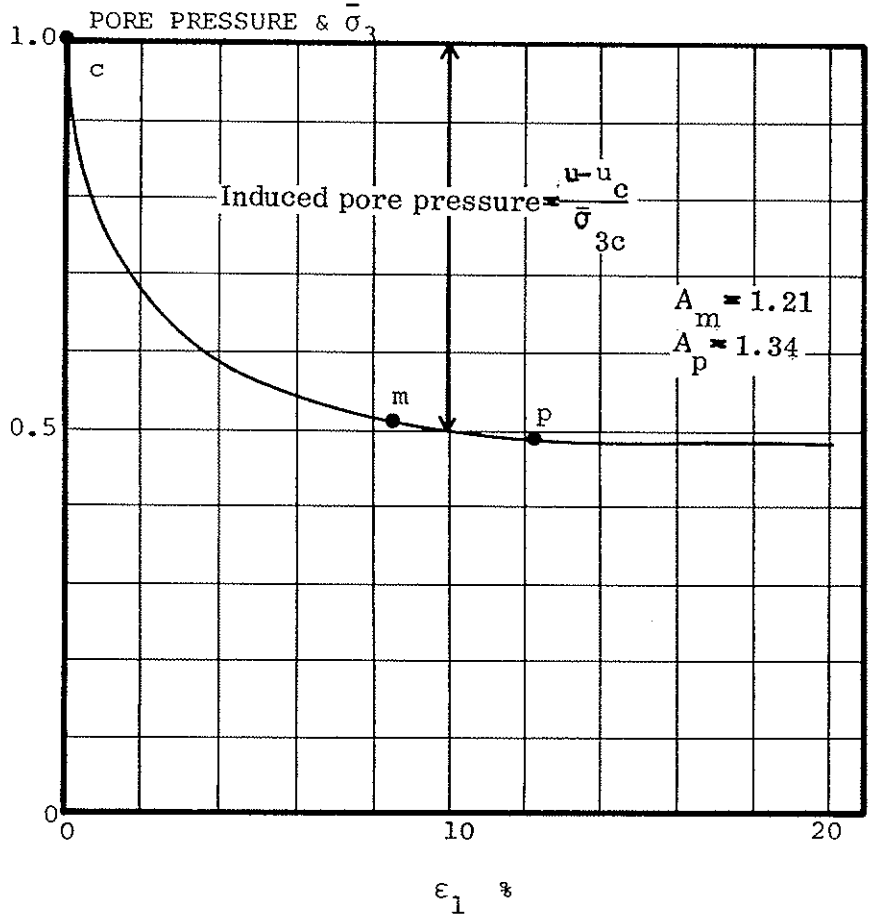

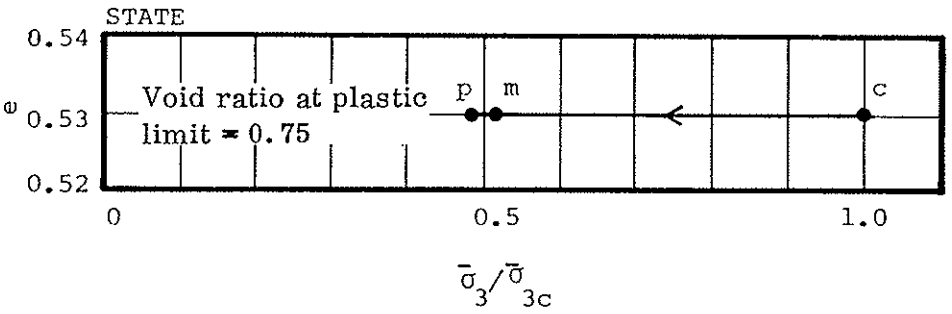

Soil Tested: London clay; w_{nat} = 23.8%; L_w = 68, P_i = 41; depth 114 ft; 59% < 2μ; s_s = 2.77; p_p ~40 kg/cm^2

Test Conditions: Consolidated from slurry at w = 163%; $\bar{\sigma}_{3c}$ = 60.2 kg/cm^2; u_c = 2.81 kg/cm^2; w_c = 19.0%; ($e_c \cong 0.53$); H_o = 7.6 cm, D_o = 3.8 cm; strain rate ≈ 0.0035%/min.; G_{wo} = 99.7%.

Source: Replotted from Webb (1966); Vol. II; Fig. G27. See also Bishop, Webb & Lewin (1965), Test E132.

Fig. 22

Highly Contractive Clay
Consolidated-Constant-Volume
Triaxial Compression

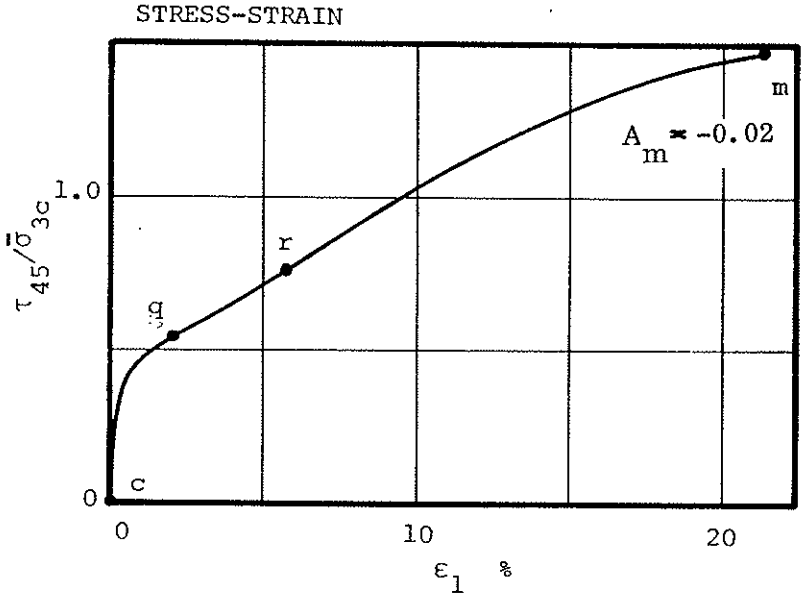

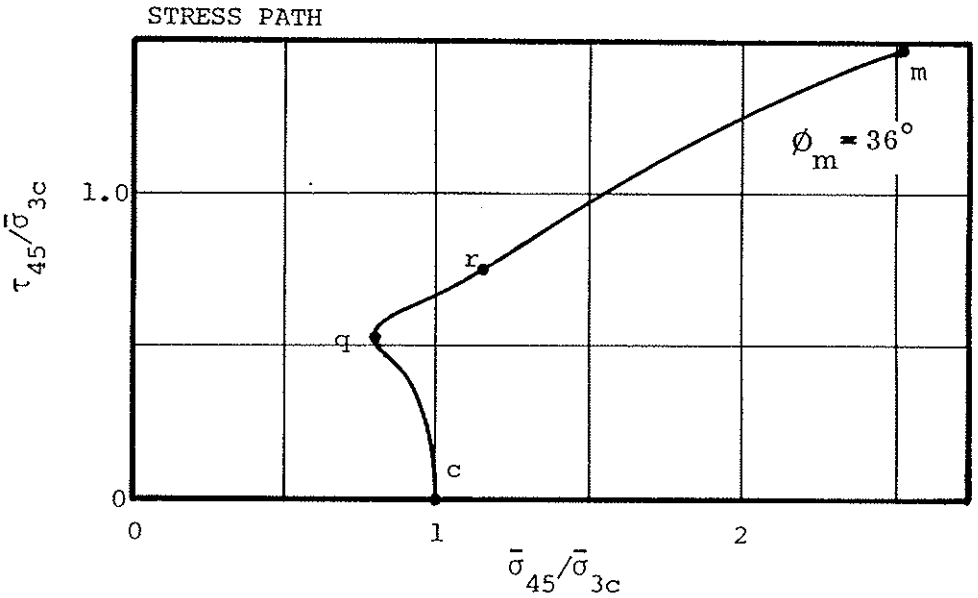

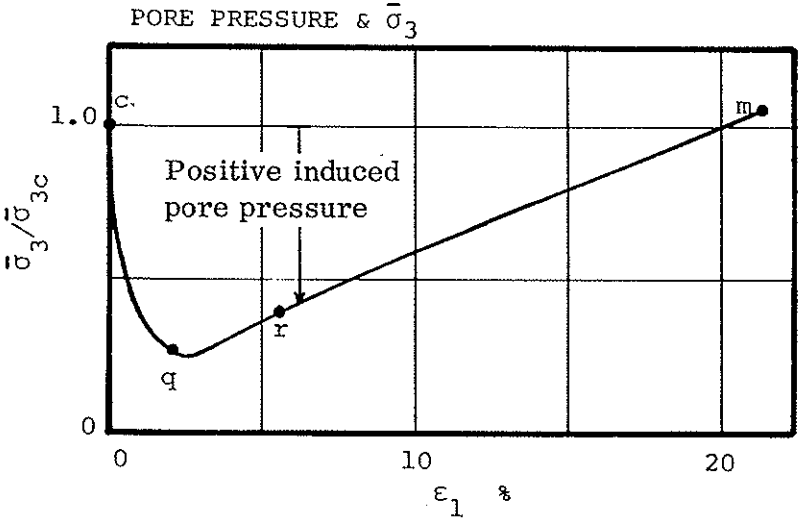

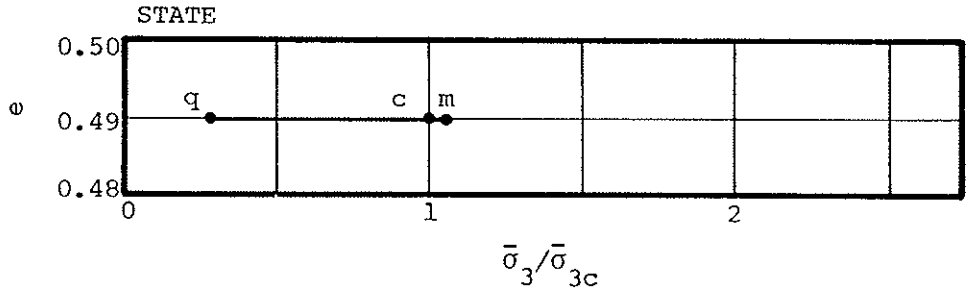

Soil Tested: Canyon Dam silty clay; L_w = 34, P_i = 19; 20% <2μ; s_s = 2.71; air dried, remolded; calcareous, (shells in +40 mesh); ~75% < 0.074 mm; inorganic.

Test Conditions: $\bar{\sigma}_{3c}$ = 2.06 kg/cm^2; e_c = 0.49; Harvard miniature compacted in 10 layers at w_o = 15.8%, $e_o \cong 0.50$; w_{opt} = 16.2%; load control; time to last point = 440 min. (ave. 0.048%/min); H_o=7.14 cm, D_o=3.33 cm; u_c = 5.89 kg/cm^2.

Source: Replotted from Casagrande & Hirschfeld (1962), Fig. 199.

Fig. 23 Dilative Clay Consolidated-Constant-Volume Triaxial Compression

STRESS-STRAIN

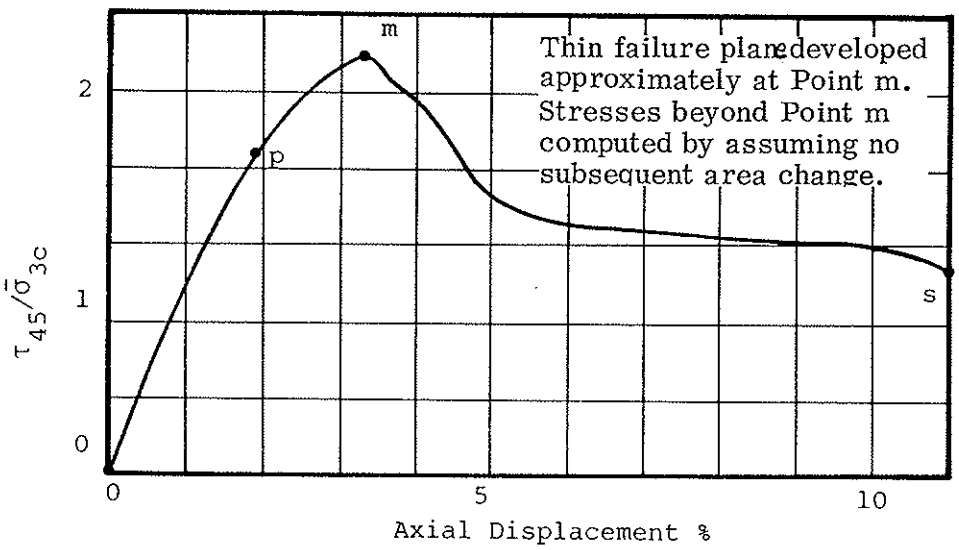

STRESS PATH

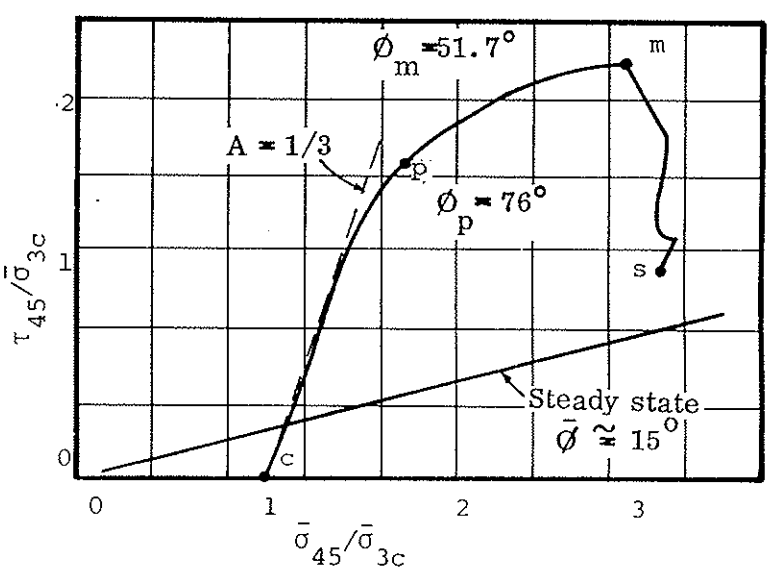

PORE PRESSURE & $\bar{\sigma}_3$

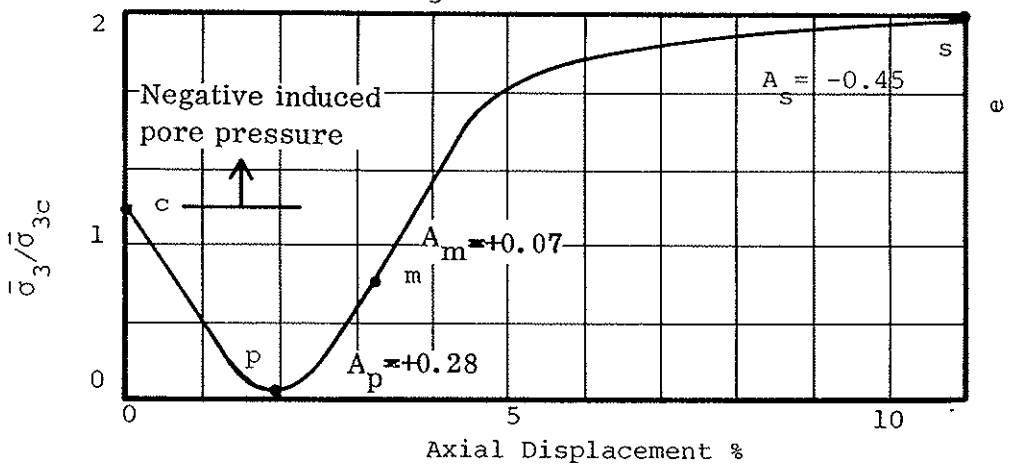

STATE

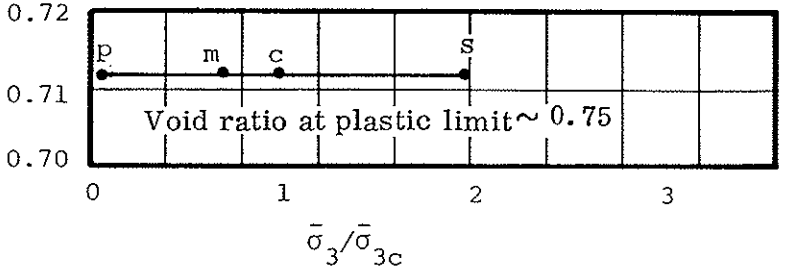

Soil tested: London Clay; depth 114 ft, P_p ~ 40 kg/cm^2; w_{nat} = 23.8%, L_w = 68, P_i = 41, 59% < 2μ; s_s = 2.77.

Test Conditions: Undisturbed, $\bar{\sigma}_{3c}$ = 1.05 kg/cm^2, u_c = 2.11 kg/cm^2, w_c = 25.6% (e_c = 0.712), G_{wo} = 99%, H_o = 7.6 cm, D_o = 3.8 cm.

Source: Replotted from Webb (1966), Vol. 2, Fig. G-14, Test E70. See also Bishop, Webb & Skinner (1965)

Fig. 24

Highly plastic Clay
Consolidated-Constant-Volume
Triaxial Compression

FIGURE CAPTIONS

Fig. 1 The State Diagram for Soils

Fig. 2 Scanning- Electron Microphotographs Viewed Normal to Surface of Natural Slickenside in Bearpaw Clay-Shale

Fig. 3 The Stress Path

Fig. 4 Development of a Stress-Strain Curve

Fig. 5 Consolidated-Drained triaxial Compression Tests: Idealized for Uncemented Soils with Bulky Grains

Fig. 6 Strength Envelopes for Specimens Prepared at Constant Void Ratio, e_c. Consolidated-Drained Triaxial Compression Tests

Fig. 7 Consolidated-Drained Triaxial Compression Tests on Soil Containing Substantial Proportion of Flat Grains. Low Stress Levels. Idealized.

Fig. 8 Postulated Location of Steady State line Relative to Compression and Swelling Curves for Clays.

Fig. 9 Highly Contractive Sand. Consolidated-Drained. Triaxial Compression

Fig. 10 Slightly Dilative Sand. Consolidated-Drained. Triaxial Compression

Fig. 11 Highly DilativeSand. Consolidated-Drained. Rotation Shear.

Fig. 12 Highly Contractive Clay. Consolidated-Drained. Rotation Shear.

Fig. 13 Very Highly Contractive Clay. Consolidated-Drained. Rotation Shear

Fig. 14 Highly Dilative Clay. Consolidated-Drained. Rotation Shear.

Fig. 15 Consolidated-Constant-Volume Triaxial Compression Tests. Soil with Bulky-Grains.

Fig. 16 Consolidated-Constant-Volume Triaxial Compression Tests on Soil Containing Substantial Proportion of Platey Grains. Idealized.

Fig. 17 Highly Contractive Sand. Consolidated-Constant-Volume. Triaxial Compression.

Fig. 18 Sand Near Steady State Void Ratio. Consolidated-Constant-Volume. Triaxial Compression.

FIGURE CAPTIONS (continued)

Fig. 19 Highly Dilative Sand. Consolidated Constant-Volume. Triaxial Compression.

Fig. 20 Very Highly Contractive Clay. Consolidated-Constant-Volume. Simple Shear.

Fig. 21 Highly Contractive Clay. Consolidated-Constant-Volume. Triaxial Compression.

Fig. 22 Highly Contractive Clay. Consolidated-Constant-Volume. Triaxial Compression.

Fig. 23 Dilative Clay. Consolidated-Constant-Volume. Triaxial Compression.

Fig. 24 Highly Dilative Clay. Consolidated-Constant-Volume. Triaxial Compression.

Writing Assignment for NSF Workshop on Post-Liquefaction Strength of Granular Soils

Michael F. Riemer, UC Berkeley
Discussion Group on ***Laboratory and Field Testing***

Is post-liquefaction shear strength proportional to the initial effective vertical stress or some other parameter?

The density (or void ratio) of a given granular material is the most important parameter controlling its undrained post-liquefaction shear strength (PLSS), though other conditions, such as the initial effective stress level and the mode of deformation, can also have very significant effects on the strength. Because granular soils can exhibit a wide range of relative densities at a given stress level (unlike normally consolidated clay), there is little *theoretical* basis for correlating the PLSS to the effective vertical stress for these materials. Empirical observations that show a rough correlation between these conditions owe their usefulness to the fact that for similar materials in similar depositional environments with similar stress histories, the vertical effective stress may also be a good indicator of the relative density of the material. Caution should be exercised, however, in applying such correlations to other deposits with differing conditions

What are the suitable sampling (e.g. freezing), specimen preparation, and laboratory testing procedures for estimating the post-liquefaction shear strength (PLSS) ?

For granular material with little or no cohesive fines, ground freezing may be the only reliable method of obtaining specimens with a density and fabric representative of the deposit in the field. While I have no personal experience with ground freezing to date, I believe there has been sufficient use of these techniques (as for CANLEX) to have confidence in the procedures which have been developed for minimizing disturbance through controlled propagation of the freezing front, appropriate handling, and careful thawing under representative stresses. In contrast, I believe useful and representative specimens of clayey sands can be retrieved through careful application and adaptation of more traditional piston sampling techniques, as even a small fraction of clay fines can successfully bind the sand grains and preserve a largely undisturbed fabric. Careful preparation, including saturation under relatively high effective stress, is required to maintain that fabric up to the time of testing.

The more difficult and contraversial issue is the appropriate testing method for determining the PLSS: triaxial compression, extension, torsional shear, simple shear, others? It is clear from a number of studies (e.g. Miura and Toki, 1982; Vaid et al., 1990; Riemer, 1992; Yoshimine, 1996) that the relationship between the monotonic steady state strength and density can be very different depending on the test type (e.g. Fig. 1). This is not necessarily a result of the effective stress path *per se*, but may be due to the mode of deformation in the different test types. Regardless of whether the variation is due to intrinsic behavior of the soil or inadequacies in some or all of the testing approaches, it raises serious obstacles to selecting a single laboratory method by which a single PLSS is chosen. It should be observed, however, that in all of these studies, undrained triaxial compression tests, which are the most widely performed type of such tests, yield the highest (and therefore least conservative) values of undrained strength.

In addition, there remains the question as to whether static (or monotonic) loading of a specimen will truly reflect the strength available in a post-liquefaction condition. Redistribution of the grains and voids within a globally undrained region of liquefied soil may make the strength of the material at its average density irrelevant. Those familiar with triaxial liquefaction testing know that following liquefaction of clean sands, the region immediately below the top cap is typically looser and weaker than the rest of specimen, but the geometry of triaxial specimens precludes getting realistic strength measurements from such "post-cyclic, static" tests, though a similar approach in torsional and simple shear may be more realistic.

Effects of consolidation stress and undrained stress path on laboratory-measured PLSS?

The level of consolidation stress does effect the observed level of "quasi" steady state strength (Konrad, 1990; Riemer, 1992), with larger consolidation stresses suggesting larger available PLSS over a wide range of strains as shown in Fig. 2. Is this the "truth", or an artifact of testing? If the "true" PLSS is not fully mobilized until very large strains have developed, is that a relevant property to use in design anyway? I feel it is important to investigate this issue of the "quasi" steady state vs. the steady state strength, though it is not obvious how that can best be accomplished.

Although different test types clearly show a major effect on the PLSS, I don't believe that this is a function of the effective stress path itself, since different effective stress paths can be run in the triaxial compression mode, and show the same steady state relationship (see Fig. 3).

Effects of soil characteristics ("fines", gradation, and particle shape) on lab-measured PLSS?

The influence of fines is complex, and depends as much on their nature (clay or silt) and distribution as on the numerical "fines content" as a percentage of the mass. Clearly, a small percentage of silt particles rattling around within the void structure of a medium sand will have little or no effect on the PLSS, though it may significantly alter the density of the soil. The same percentage of clay fines distributed on the sand grain surfaces may have a substantial effect. Great care must be taken in drawing conclusions from comparisons of tests with varying fines contents, since it is difficult to establish what the appropriately comparable densities should be. Because of the much wider variety of possible fabrics, the presence of fines essentially precludes reconstituting specimens from bulk samples of a granular material with any hope of accurately replicating field conditions.

From a practical perspective, the effects of fundamental soil properties such as gradation and particle shape on the PLSS are essentially scientific, rather than engineering questions: the PLSS is sensitive to so many of the soils characteristics and test conditions that it would be difficult to justify the prediciton of one soil's PLSS based on observations of another soil's response in the lab, while "correcting" for differences between the two soils.

Effects of strain rate on laboratory-measured PLSS?

Extremely high rates of strain make accurate measurement of the pore pressure response impossible, and may exaggerate the effects of local density variations if the soil is not able to maintain pore pressure equilibrium. Apart from these testing issues, I do not
believe the strain rate plays a significant role in the PLSS of granular soils.

Suitable techniques for estimating in-situ void ratio and state parameter?

This is crucial to any attempt to link laboratory data to field response, especially for uniformly graded sands, which are extremeley sensitive to small void ratio differences. Careful ground freezing followed by either coring (deep) or block sampling (shallow) would provide an expensive but reliable value of in-situ density. In terms of reasonably rapid and economical methods, I believe that penetration tests (such as SPT and CPT) could be at least roughly correlated to PLSS itself (as for example in Seed and Harder, 1990), rather than working through void ratio as an intermediate step.

References:

Konrad, J.M., (1990). "Minimum undrained strength versus steady-state strength of sands," *J. of Geotech. Eng.*, ASCE, 116(6), pp. 948-963.

Miura, S., and Toki, S. (1982) "A sample preparation method and its effect on static and cyclic deformation-strength properties of sand." *Soils and Foundations,* 22(1), pp. 61-77.

Riemer, M.F., (1992) "The effects of testing conditions on the constitutive behavior of loose, saturated sand under monotonic loading," PhD. Thesis at UC Berkeley.

Riemer, M.F. and Seed, R.B. (1997) "Factors affecting the apparent position of the Steady-State line," *ASCE J. of Geotech. and Geoenv. Eng.*, Vol. 123 No. 3, pp.281-288.

Seed, R.B. and Harder, L., (1990) "SPT-based analysis of cyclic pore pressure generation and undrained residual strengths," Proc. H.B. Seed Memorial Symp., Berkeley, CA, pp. 351-376.

Vaid, Y.P., Chung, E.K.F., and Kuerbis, R.H., (1990) "Stress path and steady state," *Can. Geotech. J,* 27, pp. 1-7.

Yoshimine, M., (1996) "Undrained Flow Deformation of Saturated Sand Under Monotonic loading conditions," Department of Civil Engineering, University of Tokyo.

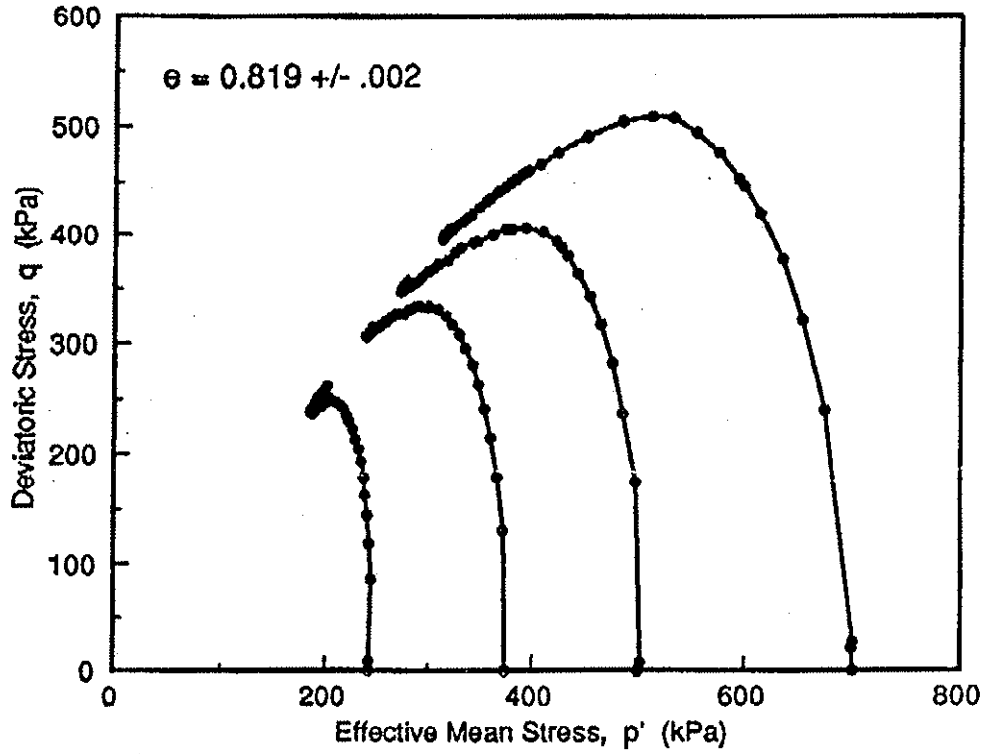

(a)

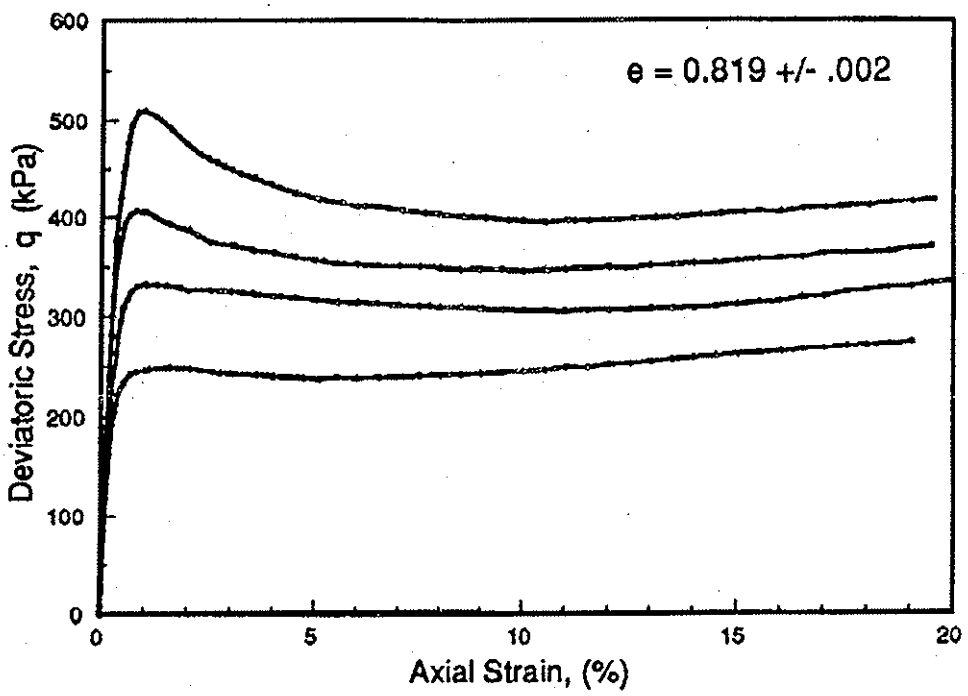

(b)

Fig. 2: (a) Stress path plots and (b) stress-strain plots of tests performed on specimens consolidated to the same void ratio but to different effective stresses (Riemer, 1997).

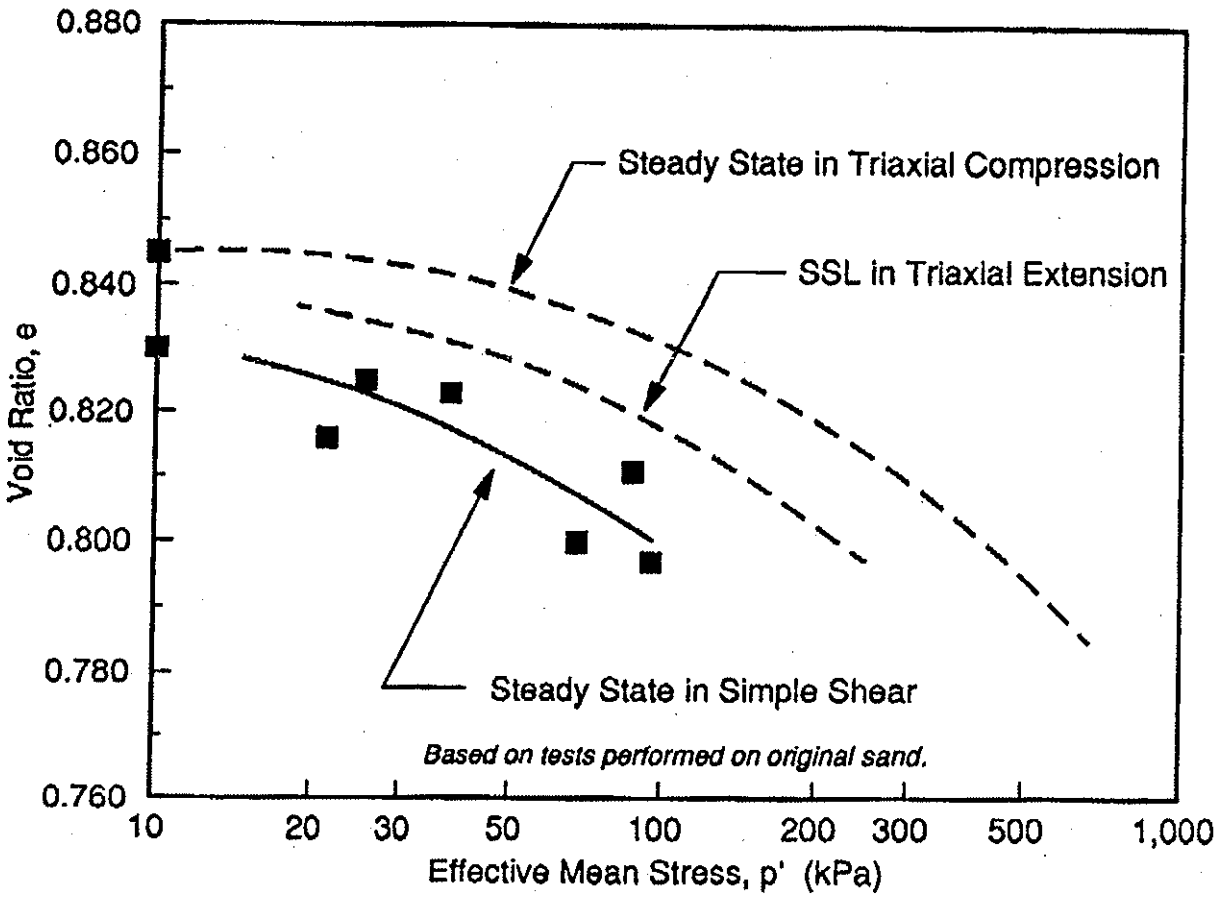

Fig. 1: Comparison of steady state lines from undrained monotonic testing of Monterey #0 sand in simple shear, triaxial compression, and triaxial extension (Riemer, 1992).

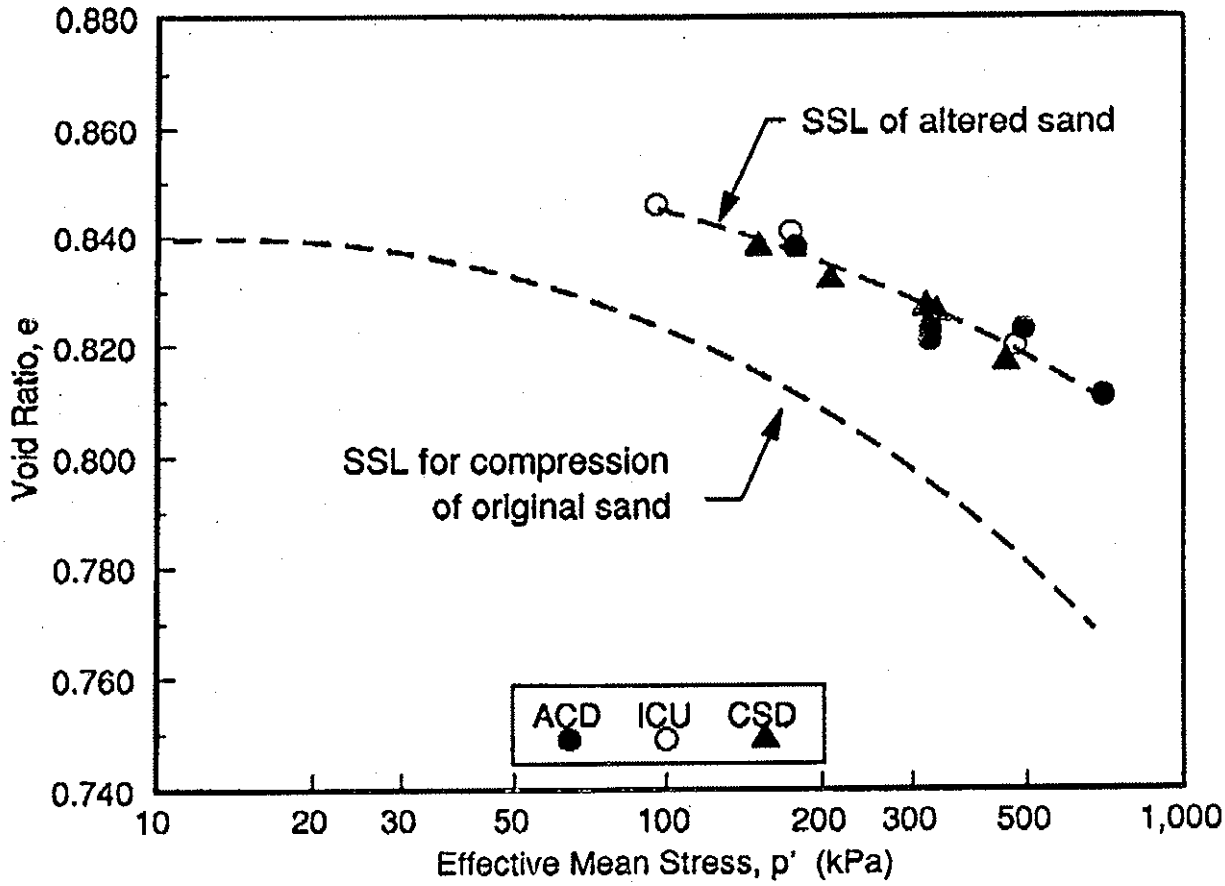

Fig. 3: Comparison of steady state points measured in three different effective stress paths, all of which deform in cylindrical compression (Riemer, 1997).

NSF Workshop
Post-Liquefaction Shear Strength of Granular Soils

Laboratory and Field Tests

Peter K. Robertson
University of Alberta

To aid and guide in the discussion at the Workshop, the following background is provided.

1. Terminology

Based on observed soil behavior in undrained shear the definitions given by Robertson (1994) and Robertson and Fear (1995) can be used to describe either flow liquefaction or cyclic liquefaction.

Post-Liquefaction Undrained Shear Strength, (S_u)

The post-liquefaction undrained shear strength is defined as the ultimate or quasi-steady state undrained shear strength of a soil after either flow or cyclic liquefaction has been triggered. Recent laboratory testing has confirmed that cohesionless soils are similar to cohesive soils in that they have different undrained shear strengths under different directions of loading. The ultimate undrained shear strength in triaxial compression (TC) loading is different than that in triaxial extension (TE) and simple shear (DSS) loading. Typically:

$$(S_u)_{TC} > (S_u)_{DSS} > (S_u)_{TE}$$

Hence, the undrained shear strength required for a design problem will be a function of direction of loading and, hence, ground geometry.

2. Critical State Soil Mechanics

When soils are sheared they tend toward a critical or steady state in which the effective stresses remain constant and no volume changes occur. This behavior was suggested by Castro (1969) and is embodied in critical state soil mechanics (Roscoe et al., 1958). Been et al. (1991) and Ishihara (1993) showed that steady state and critical state are the same condition and in e-p' space are independent of the stress path followed to reach this state. The steady state or critical state represents an ultimate state that can be represented in e-p'-q space, where p' is the mean normal effective stress, q is the deviator stress and e is the void ratio. In this discussion, this ultimate condition will be referred to as 'ultimate state' (US), as recommended by Poorooshasb and Consoli (1991). The critical state or steady state line in e-p'-q space will be referred to as the ultimate state line (USL).

Based on critical state soil mechanics, there is a link between the ultimate undrained shear strength of a soil and the in-situ state of the soil. Based on the state parameter approach by Been and Jefferies (1985), the link between state parameter (ψ) and the undrained shear strength ratio (S_u/p') is shown in Figure 1. Included in Figure 1 are the two extreme relationships for triaxial compression and triaxial extension directions of loading. Note that for a state parameter greater than zero (i.e. loose of the ultimate state line) the undrained strength ratio is very low. In general, post-liquefaction undrained shear strength is important only when the state of a soil is loose of ultimate state and, hence, flow liquefaction is possible.

To estimate the post-liquefaction undrained shear strength there are two approaches:

1 Estimate the in-situ state and then link it to the post-liquefaction undrained shear strength,
2 Estimate the post-liquefaction undrained shear strength directly.

The following sections briefly describe each approach.

3. Estimation of In-situ State

The in-situ state of a sandy soil can be estimated in different ways. The in-situ state can be estimated by first estimating the in-situ void ratio and then linking it with the ultimate state line. This approach requires a knowledge of the appropriate ultimate state line for the soil, which will vary as grain characteristics change. There is also considerable uncertainty on the uniqueness of the ultimate state line. The in-situ state can also be estimated directly using the state parameter approach.

a) Void Ratio

Direct methods to measure in-situ void ratio include: undisturbed samples and geophysical logging. Indirect methods to estimate in-situ void ratio include: penetration testing (SPT, CPT) and shear wave velocity (V_s) measurements. The following is a list of possible techniques:

Undisturbed samples	Yoshimi et al., (1990); Hofmann et al., (1995)
Geophysical logging	Plewes et al., (1988)
SPT	Skempton (1986)
CPT	Baldi et al., (1986)
Shear wave velocity (V_s)	Cunning et al., (1995)

b) State or State Parameter

The in-situ state can be estimated directly in terms of state parameter (ψ) using empirical or semi-empirical correlations based on penetration tests (CPT) and self-boring pressuremeter tests (SBPT). The following is a list of possible techniques:

CPT	Sladen and Hewitt (1989); Been and Jefferies (1992); Plewes et al., (1992).
SBPT	Yu et al., (1996)

4. Estimation of In-situ Response

The response to undrained shear can be estimated in a number of different ways. The direct approach is to obtain undisturbed samples and to test them under the appropriate direction of loading (Yoshimi et al., 1990; Hofmann et al., 1995). This is a difficult and expensive approach and will be limited to only the very largest of projects for which the risk may warrant the expense.

An alternate approach is to estimate the post-liquefaction undrained shear strength from in-situ field tests using empirical correlations. The following is a list of possible techniques:

SPT	Seed et al., (1990); Stark & Mesri (1992); Ishihara, (1993); Baziar & Dobry (1995)
CPT	Ishihara, (1993); Robertson (1990); Jefferies et al. (1990)
Shear wave velocity (V_s)	Fear & Robertson (1995)
Field Vane Test (FVT)	Charlie et al., (1990)

For these approaches to have wide applicability, they must be based on some framework or theory that ensures that the form of the correlation is correct (Fear and Robertson, 1995). Many of these techniques are based on back analyses of case histories. However, there is some uncertainty that the case histories actually involved strain softening soil and hence, there is uncertainty about the back-calculated post-liquefaction undrained shear strength.

An alternate approach is to estimate the soil response using computer aided modeling (CAM) of self-boring pressuremeter tests (SBPT) (Jefferies and Shuttle, 1995; Byrne et al., 1995; Hughes, 1997). CAM requires a constitutive model of soil behavior which can vary from simple elastic, perfectly plastic models (Hughes, 1997) to complex models that require finite element techniques.

a) Influence of Fines

Most of the field methods that attempt to measure soil response are influenced by fines content (e.g. SPT, CPT). Soils with higher fines content tend to produce lower penetration resistances. Hence, techniques have been developed to correct measured penetration resistance to an equivalent clean sand value (Ishihara, 1993). However, these corrections are approximate and different corrections have been suggested for cyclic and flow liquefaction analyses.

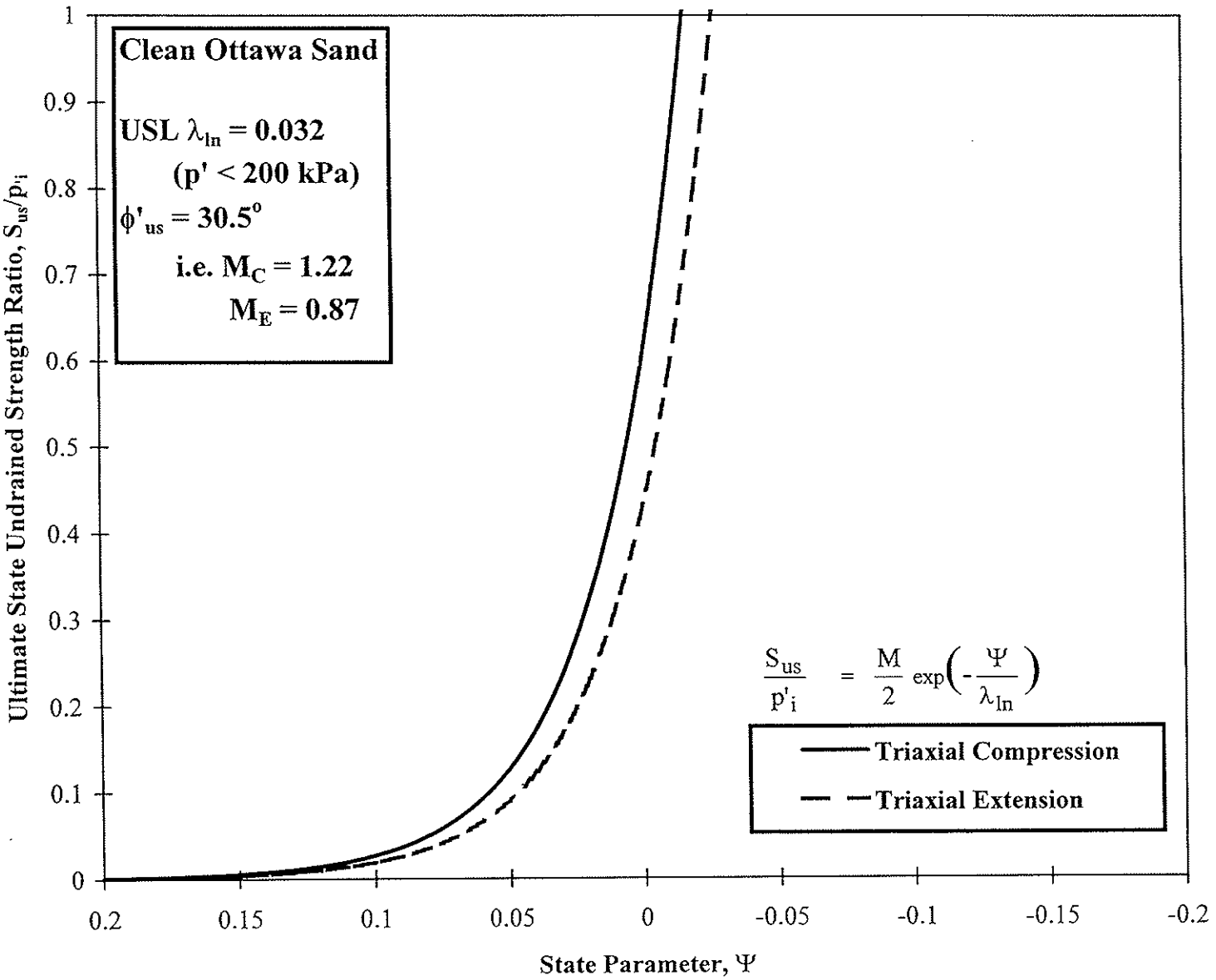
Clean Ottawa Sand
USL $\lambda_{ln} = 0.032$
(p' < 200 kPa)
$\phi'_{us} = 30.5^{o}$
i.e. $M_C = 1.22$
$M_E = 0.87$
$\frac{S_{us}}{p'_i} = \frac{M}{2} \exp\left(-\frac{\Psi}{\lambda_{ln}}\right)$
Triaxial Compression
Triaxial Extension
Ultimate State Undrained Strength Ratio, S_{us}/p'_i
State Parameter, Ψ
1
0.9
0.8
0.7
0.6
0.5
0.4
0.3
0.2
0.1
0
0.2
0.15
0.1
0.05
0
-0.05
-0.1
-0.15
-0.2

APPENDIX C.
Written Statements by Shear Strength of Liquefied Soils from Case Histories Discussion Group Participants

* =Keynote Speaker
** =Recording Secretary

*Gonzalo Castro (GEI Consultants, Incorporated)
Ricardo Dobry (Rensselaer Polytechnic Institute)
A. Gus Franklin/Mary Ellen Hynes (U.S. Army Corps of Engineers)
David R. Gillette (U.S. Bureau of Reclamation)
Leslie F. Harder, Jr. (California Department of Water Resources)
John C. Horne (Clemson University)
I.M. Idriss (University of California @ Davis)
William F. Marcuson, III (U.S. Army Corps of Engineers)
Timothy D. Stark (University of Illinois @ Urbana-Champaign)
Robert V. Whitman (Massachusetts Institute of Technology)
**T. Leslie Youd (Brigham Young University)

Discussion Group on "Post-Liquefaction Strength from Case Histories"

Pre-Workshop Statement by Ricardo Dobry (3/1/97)

It was suggested by the organizers that I write on the following issues related to the topic of backcalculation:

1. Importance of dilative response, especially in lateral spreading case histories
2. Is post-liquefaction shear strength proportional to the initial vertical effective stress or some other parameter?
3. Consideration of consolidation stress and undrained stress path, strain rate, drainage effects, initial effective stress, etc.
4. Suitable analytical method for backcalculation (limit equilibrium vs. stress-deformation analysis)?
5. What is the appropriate geometry for backcalculation (pre-failure vs. post-failure)?
6. Selection of representative in situ test parameter (e.g., minimum, average, maximum cone resistance?)
7. Should existing case histories be re-evaluated based on previous questions?

In the text below I have addressed most of these issues, grouped under two general headings: (A) Lateral Spreads, and (B) Need for Simplicity in Backcalculations.

A. Lateral Spreads

There is significant evidence that dilative response plays a key role in the mechanics of many lateral spreads. The evidence comes from case histories (Figs, 1-2 and 6), centrifuge model tests (Figs. 3-4 and 6-7), and laboratory tests (Fig. 5). Figures 1-2 relate to the pore pressure and acceleration records obtained at the Wildlife site in California in 1987 (Holzer et al. 1989; Zeghal and Elgamal 1994; Youd and Holzer 1994; Elgamal et al. 1995). Figures 3-4 corresponds to a centrifuge test done at 50g centrifugal acceleration at RPI, which simulated a 10-m thick layer of saturated clean sand having a relative density, $D_r \approx 40\%$, inclined a few degrees to the horizontal, and subjected to a base earthquake acceleration of about 0.2g. While this test showed the most extreme dilative response, a number of other centrifuge model experiments of lateral spreading done at RPI and CalTech also exhibit similar acceleration nonsymmetric spikes and simultaneous pore pressure drops such as shown by Figs. 1 and 3 (Taboada and Dobry 1993; Scott et al. 1993; Dobry and Taboada 1994; Dobry et al. 1995). The corresponding shear stress-strain plots interpreted from the acceleration records using Zeghal-Elgamal system identification technique in Figs. 2 and 4 look both very much like the results of the undrained cyclic triaxial test of Fig. 5 (except for the lack of shear strain accumulation in Fig. 2; this

information was not contained in the accelerometer record). Very important in Figs. 2, 4 and 5 are the extremely low values of the residual shear strength in the plateau before the dilative response, with the accumulated shear strain per cycle controlled more by the dilative response than by the height of this residual shear strength plateau.

Additional information on the importance for lateral spreads of the dilative response and of the strain at which dilative behavior starts, and the need to modify the traditional sliding block approach to account for this, is presented in Figs. 6-8 (Taboada et al., 1996). Figure 6 compares the influence of the ground surface slope angle on permanent lateral ground displacement, D_H, measured in the same centrifuge tests at RPI, with that predicted by Bartlett and Youd (1995) empirical correlation obtained from case histories of lateral spreading near a free face. While the comparison in Fig. 6 includes a couple of assumptions that may be arguable, the main point is that both the centrifuge results and Bartlett and Youd's correlation indicate that, as the slope angle increases or as the point on the ground surface moves closer to the free face, D_H increases slowly or stabilizes. On the other hand, the traditional sliding block model with no dilative response predicts a static flow failure, with D_H increasing without bound (Fig. 7a). A modified sliding block model which accounts for the observed dilative response (Fig. 8), predicts much better the observed effects of slope angle (Fig. 7a), frequency of shaking (Fig. 7b) and input acceleration (Fig. 7c).

All centrifuge tests above simulate a homogeneous clean sand deposit. Centrifuge model tests where a more impervious layer lies on top of the liquefiable soil suggest that void ratio redistribution and water accumulation at the boundary between the two layers (Fig. 9), may become a key factor, especially in explaining some lateral spreads in gravels (Fig. 10), with a contractive response developing along this boundary (Andrus et al., 1991; Dobry and Liu 1992; Kutter and Fiegel 1992; Dobry et al., 1995). In this case the sliding block method and the use of a unique post-liquefaction shear strength independent of strain may be the right model, except that this strength is not the same as obtained from undrained laboratory tests unless appropriate correction is made for the void ratio redistribution in the field, which is very difficult.

A third type of soil deposit affected by lateral spreads is silty sands or sandy silts sedimented in water. Due to the high compressibility of these deposits, their density increases rapidly with depth and the residual shear strength, S_r, backfigured from lateral spreads or flow failures, is more or less proportional to the initial effective stress, σ'_{vo} (Fig. 11b). Laboratory tests suggest that at least some of these silty sands are contractive in the field, while others may exhibit dilative response at some strain (Ishihara 1993; Baziar and Dobry 1995). Figure 11b is for soils having at least 10% silts. The S_r/σ'_{vo} concept has been applied by Stark and Mesri (1992) to both silty sands and clean sands (Fig. 12). I am not sure that I agree with this, as clean sands are typically much less compressible and thus their void ratio may be about constant with depth; this could be a subject of discussion at the workshop.

This discussion above suggests two main conclusions. One is the difficulty of defining one type of lateral spread mechanism, method of analysis and way of specifying a post-liquefaction shear strength, valid for all types of soils and soil profiles. Maybe the case histories should be grouped according to their likely lateral spreading mechanism and expected variation of S_r with depth (clean sands, sands/gravels with a silty or clayey layer on top, silty sands/sandy silts, etc.). The second conclusion is that the phenomenon will probably remain complex and difficult to model analytically even after the mechanism is understood, due to things like dilative response, void ratio redistribution, etc. This strongly suggests the need for simplicity in the backcalculations.

B. Need for Simplicity in Backcalculations

A number of charts and correlations have been proposed for the post-liquefaction strength, S_r, calibrated by calculations of S_r from case histories of flow failure or lateral spreading, typically using the SPT, see Figs. 11-13 (Davis et al. 1988; Seed and Harder 1990; Stark and Mesri 1992; Baziar and Dobry 1995). Related SPT and CPT charts and rules have been proposed to separate dilative from contractive, flow failure type behavior (Robertson et al. 1992; Ishihara 1993). These correlations use the same or overlapping case histories. These S_r correlations and the corresponding existing case histories could be re-evaluated using a common set of criteria, in an effort to develop consensual chart(s). This would be similar to the liquefaction triggering chart based on the SPT, originally developed by Seed et al. (1983), and recently updated in the 1996 Utah workshop. The extensive data base of several hundred case histories of lateral spreading compiled by Bartlett and Youd (1992) would enlarge very significantly the list of case histories available for this exercise.

The workshop could perhaps agree on this set of criteria, with the actual calculations done after the workshop. The criteria should be detailed enough so as to be unambiguous; the same criteria used to backcalculate S_r should be applied by users of the backfigured S_r when applying the corresponding charts to predicting factor of safety against flow failure, or the value of D_H in a lateral spread. One initial question is how should the case histories be grouped. The discussion above discloses some of my own opinions on the subject. I would certainly not consider clean sands or gravels when developing S_r/σ'_{vo} correlations. I would eliminate lateral spreading gravel case histories from any correlation using SPT or CPT; the mechanism in these gravel deposits may be controlled by strong void ratio redistribution (Fig. 10), and the SPT or CPT is very difficult or impossible to measure in gravelly soils anyway. While I would like to explore the possibility to separate between clean and silty sands when developing consensual SPT and CPT charts, in an effort to reduce the scatter of the correlations, this may or may not be practical.

Of course, there are several other important issues that would have to be settled before backcalculations of S_r could be implemented on the available case histories. The definition of the input shaking time history, how to model the actual topography/layering, etc., are some of these issues. In deciding all these issues I would stick to three golden rules:

consistency, simplicity and friendliness to future users. Simplicity is absolutely essential, given the uncertainty we have about the actual mechanisms involved, especially of the lateral spreading phenomenon. That is, we should use simple limiting equilibrium and sliding block analysis to backfigure S_r from a measured D_H; this will always give us a clear answer, as in a sense we will have one equation for one unknown (S_r). Even if the actual mechanics assumed for the development of D_H in the field is not correct (e.g., because of dilative response, or because of a lack of a clear failure surface in the field), our chart may still have predictive power to evaluate D_H in future earthquakes. On the other hand, if we use the more complicated stress-deformation analysis, the simplicity is gone as now we have more variables to play with, and thus more than one equation for our one unknown S_r. While we may still be able to fit an S_r to the measured D_H, the resulting chart will have little predictive power and will have to be used with a similar, complicated and ambiguous stress-deformation analysis in practical applications.

Along the same lines of simple rules for backcalculation, I would use always the pre-failure rather than the post-failure configuration, and would eliminate the use of the correction of the SPT for fines contained in Figs. 12 and 13a, which is really not necessary (Fig 13b) and complicates things. In my opinion, a similar simplicity rule should be used to decide any other question arising in connection with the development of the set of criteria for backcalculation and use of S_r charts based on case histories.

References

Andrus, R.D., Stokoe II, K.H., and Roesset, J.M. (1991). "Liquefaction of gravelly soil at Pence Ranch during the 1983 Borah Peak, Idaho earthquake." *Proc. 5th Intl. Conf. Soil Dynamics and Earthquake Engineering.* Karlsruhe, Germany, Sept., 251-262.

Arulmoli, K., Muraleetharan, K.K., Hossain, M.M., and Fruth, L.S. (1992). "VELACS-laboratory testing program—Soil data report." The Earth Technology Corporation, Project No. 90-0562.

Bartlett, S.F., and Youd, T.L. (1992). "Empirical analysis of horizontal ground displacement generated by liquefaction induced lateral spreads." *Tech. Rep. NCEER 92-0021,* Nat. Ctr. for Earthquake Engrg. Res., SUNY-Buffalo, Buffalo, NY.

Bartlett, S.F., and Youd, T.L. (1995). "Empirical prediction of liquefaction-induced lateral spread." *J. Geotech. Engrg.*, ASCE, 121(4), April, 316-329.

Baziar, M.H., and Dobry, R. (1995). "Residual strength and large-deformation potential of loose silty sands." ASCE *Journal of Geotechnical Engineering*, 121(12), December, 896-906.

Davis, A.P., Castro, G., and Poulos, S. (1988). "Strengths backfigured from liquefaction case histories." *Proc., 2nd Int. Conf. on Case Histories in Geotech. Engrg.*, S. Prakash, ed., Univ. of Missouri-Rolla, Rolla, MO.

Dobry, R., and Liu, L. (1992). "Centrifuge modelling of soil liquefaction." *Post Conference Proceedings Volume.* Tenth World Conference on Earthquake Engineering, Madrid, Spain, July 19-24, pp. 6801-6809.

Dobry, R., and Taboada, V. (1994). "Possible lessons from VELACS model No. 2 results." *Proc. of the International Conference on the Verification of Numerical Procedures for the Analysis of Soil Liquefaction Problems.* Arulanandan, K. and Scott, R.F. (eds.), Vol. 2, pp. 1341-1352. Rotterdam: Balkema.

Dobry, R., Taboada, V., and Liu, L. (1995). "Centrifuge modeling of liquefaction effects during earthquakes." Keynote Lecture. *Proc. First International Conference on Earthquake Geotechnical Engineering,* Tokyo, Japan, November 14-16, Preprint Volume, pp. 129-162.

Elgamal, A.-W., Zeghal, M., and Parra, E. (1995). "Identification and modeling of earthquake ground response." *Proc. First International Conference on Earthquake Geotechnical Engineering,* Tokyo, Japan, November 14-16, Preprint Volume, pp. 51-90.

Holzer, T.L., Youd, T.L., and Hanks, T.C. (1989). "Dynamics of liquefaction during the Superstition Hills Earthquake (M = 6.5) of November 24, 1987." *Science*, 244, April 7, 56-59.

Ishihara, K. (1993). "Liquefaction and flow failure during earthquakes." *Géotechnique*, London, England, 43(3), 351-415.

Kutter, B.L., and Fiegel, G.L. (1992). Personal communication to R. Dobry.

Robertson, P.K., Woeller, D.J., and Finn, W.D.L. (1992). "Seismic cone penetration test for evaluating liquefaction potential under cyclic loading." *Canadian Geotechnical J.*, 29(2), 686-695.

Scott, R.F., Hushmand, B., and Rashidi, H. (1993). "Duplicate test of model number 2: Sloping loose sand layer." *Proc. of the International Conference on the Verification of Numerical Procedures for the Analysis of Soil Liquefaction Problems.* Arulanandan, K., and Scott, R.F. (eds.), Vol. 1, pp. 301-314. Rotterdam: Balkema.

Seed R.B., and Harder, L.F. (1990). "SPT-based analysis of cyclic pore pressure generation and undrained residual strength." *Proc., H. B. Seed Memorial Symp.*, BiTech Publishing, Vancouver, B.C., Canada, Vol. 2, 351-376.

Seed, H.B., Idriss, I.M., and Arango, I. (1983). "Evaluation of liquefaction potential using field performance data." *J. Geotech. Engrg.*, ASCE, 109(3), March, 458-482.

Stark, T.D., and Mesri, G. (1992). "Undrained shear strength of liquefied sands for stability analysis." *J. Geotech. Engrg.*, ASCE 118(11), November, 1727-1747.

Taboada, V., and Dobry, R. (1993). "Experimental results of model number 2 and RPI." *Proc. of the International Conference on the Verification of Numerical Procedures for the Analysis of Soil Liquefaction Problems.* Arulanandan, K., and Scott, R.F. (eds.), Vol. 1, pp. 277-294. Rotterdam: Balkema.

Taboada, V.M., Abdoun, T., and Dobry, R. (1996). "Prediction of liquefaction-induced lateral spreading by dilatant sliding block model calibrated by centrifuge tests." *Proc. 11th World Conference on Earthquake Engineering,* Acapulco, Mexico, June 23-28, Paper No. 376.

Youd, T.L., and Holzer, T.L. (1994). "Liquefaction Site, California." *Journal of Geotechnical Engineering,* Vol. 120, No. 6, June, 975-995.

Zeghal, M., and Elgamal, A.-W. (1994). "Analysis of Wildlife site using earthquake records." ASCE *Journal of Geotechnical Engineering,* Vol. 120, No. 6, June, pp. 996-1017.

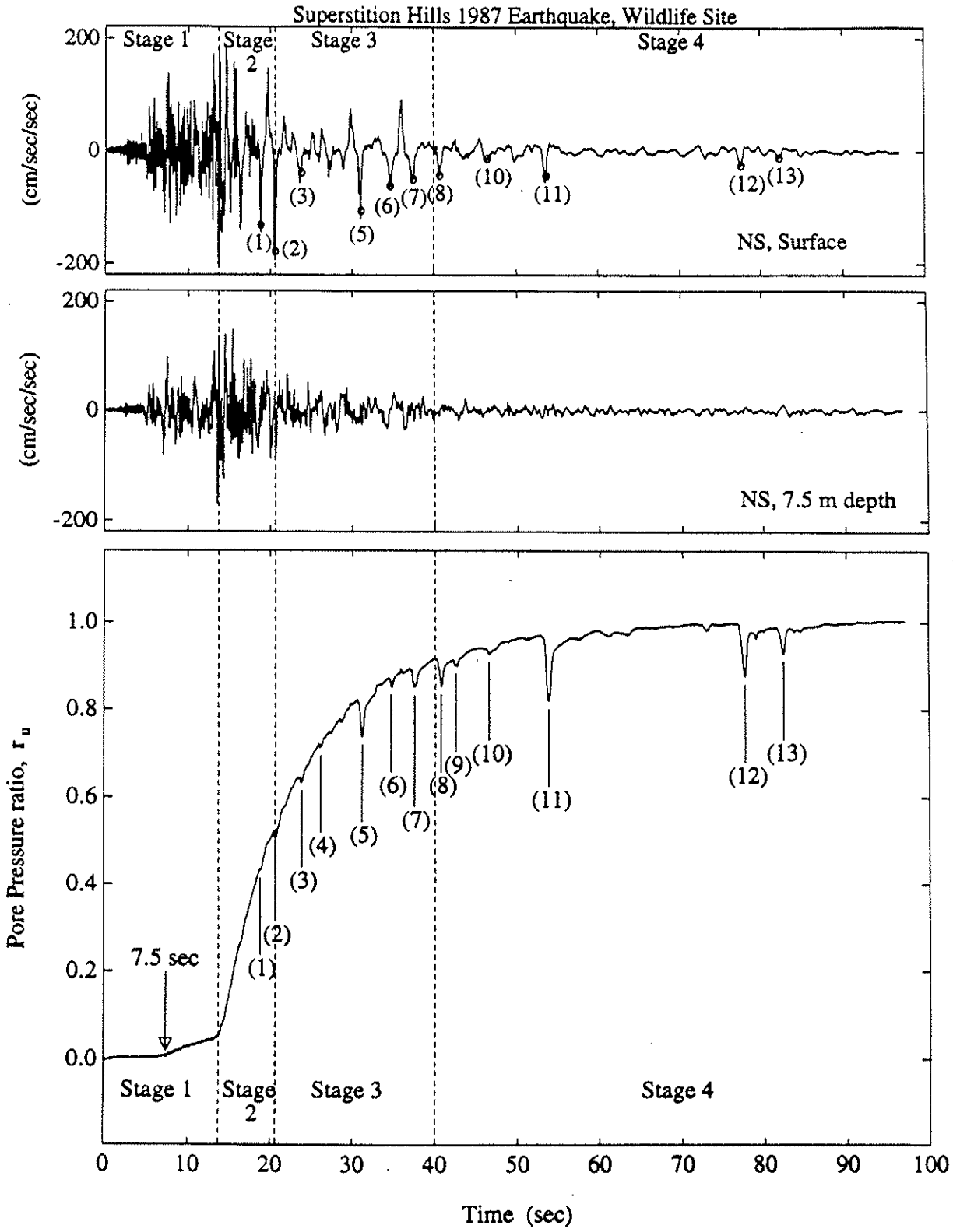

Figure 1 Wildlife Refuge site NS surface and downhole (at 7.5 m depth) accelerations, and associated pore water pressure (at 2.9 m depth) during the Superstition Hills 1987 earthquake.

(Youd and Holzer 1994; Elgamal et al. 1995)

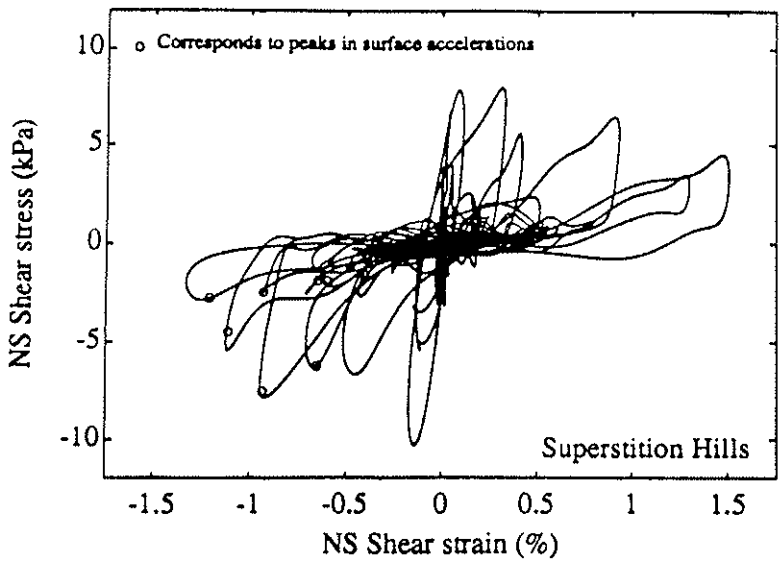

FIG. 2 NS Shear Stress-Strain Histories (at Elevation of P5 or 2.9 m Depth)
(Zeghal and Elgamal 1994)

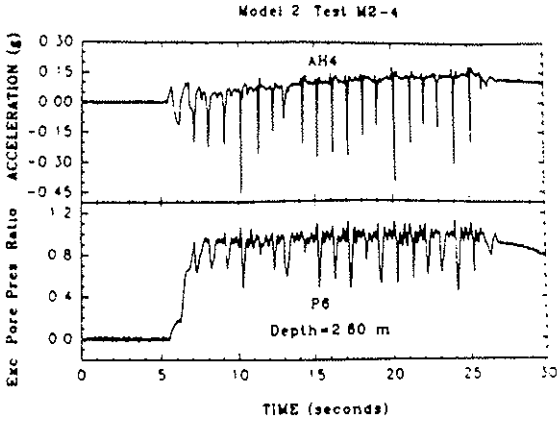

Figure 3 Recorded lateral acceleration and pore pressure in the soil at a depth of 2.6 m, RPI Test M2-4 (Dobry et al. 1995)

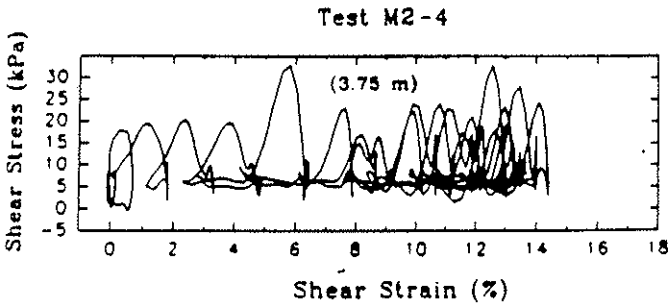

Figure 4 Shear stress-strain history in the soil at a depth of 3.75 m, RPI Test M2-4
(Dobry et al. 1995)

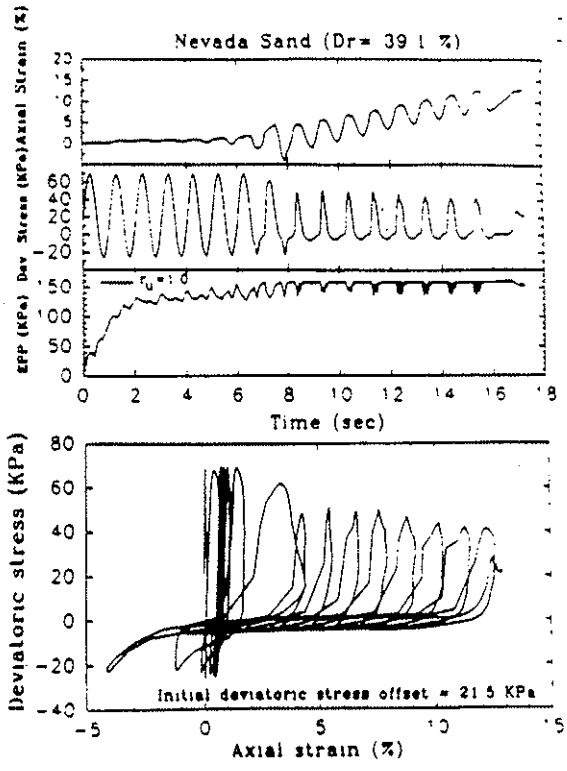

Figure 5 Stress, strain and excess pore pressure histories during an undrained stress-controlled cyclic triaxial test of Nevada sand (Dr = 39.1%)with an imposed static (initial) deviatoric stress (Arulmoli et al., 1992)

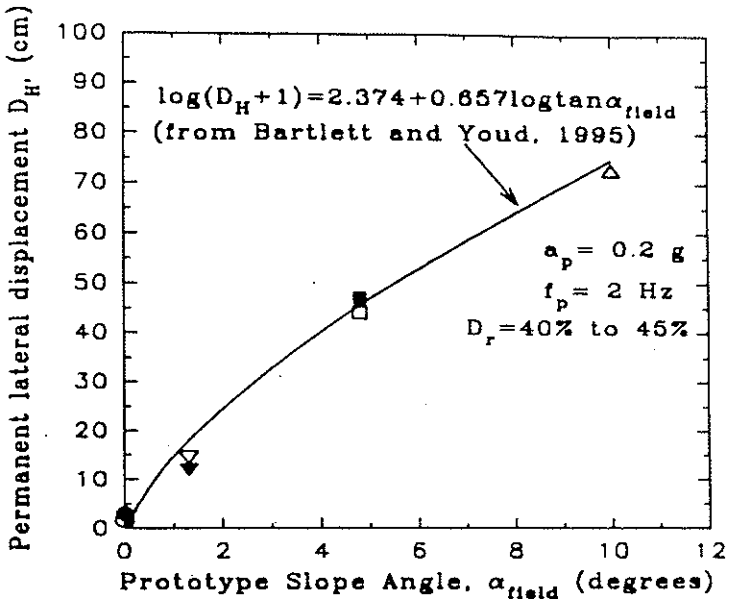

Fig. 6 Variation of D_H with angle of prototype slope measured in centrifuge model tests (data points), and predicted by Bartlett and Youd (1995) empirical correlation (curve). (For Bartlett and Youd's curve, $\tan\alpha_{field}$ = W/H, and D_H = 46 cm for α_{field} = 4.8°, were used) (Taboada et al. 1996)

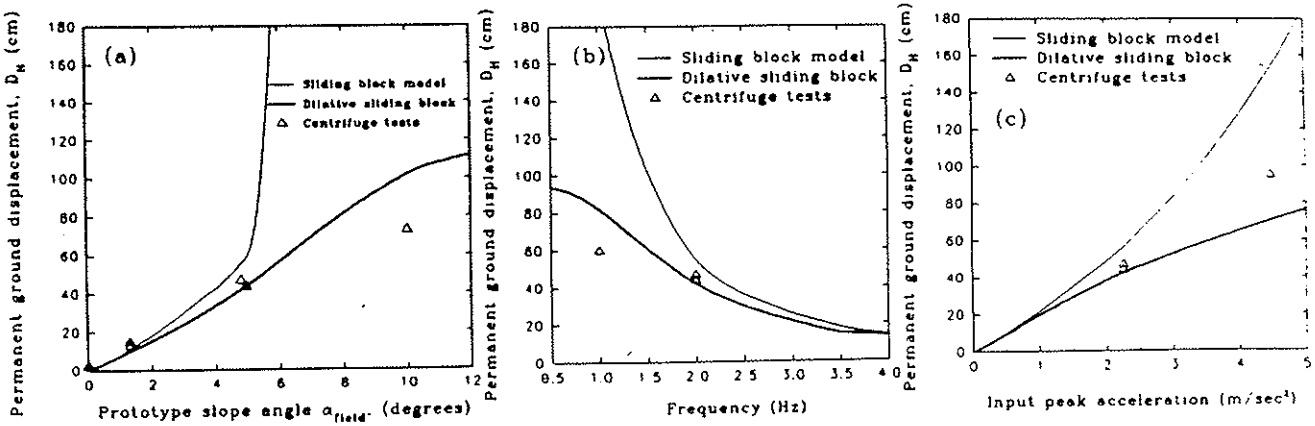

Fig. 7 Comparison of predicted and measured permanent ground displacements D_H versus: (a) slope angle, (b) input frequency, and (c) input peak acceleration. (Taboada et al. 1996)

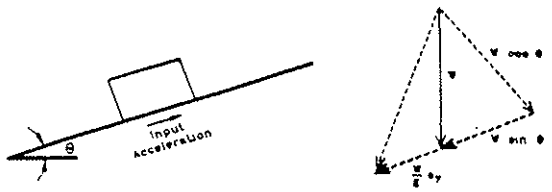

$$W \cos\theta \tan\theta = \frac{W}{g} a_y + W \sin\theta$$

a) Polygon of forces for a block on inclined plane

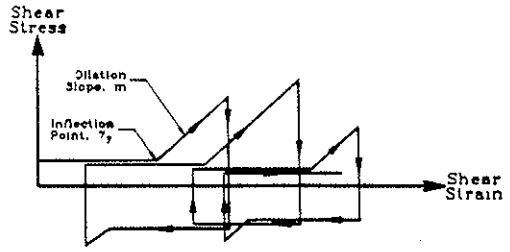

b) Simplified shear stress-strain relation (cycles of arbitrary amplitude with static shear stress offset)

Fig. 8 Sliding block on top of the ramp (slope) and shear stress-strain relation of the dilative sliding block. (Taboada et al. 1996)

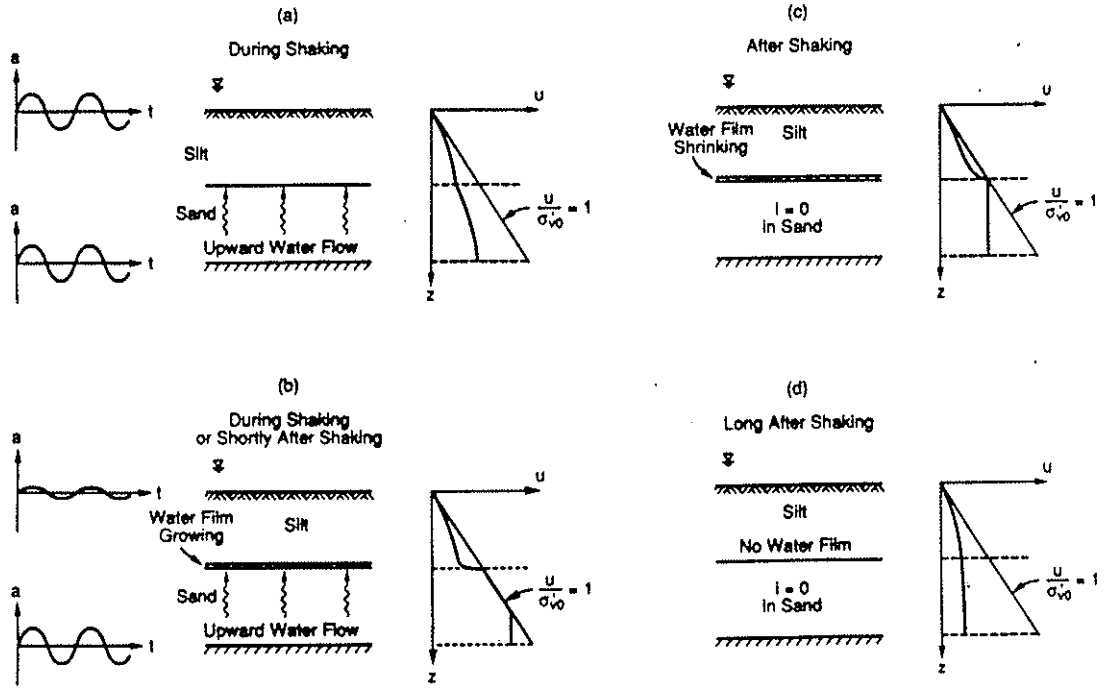

Figure 9 Four stages observed in centifuge test of two-layer deposit. (Dosy and Liu, 1992)

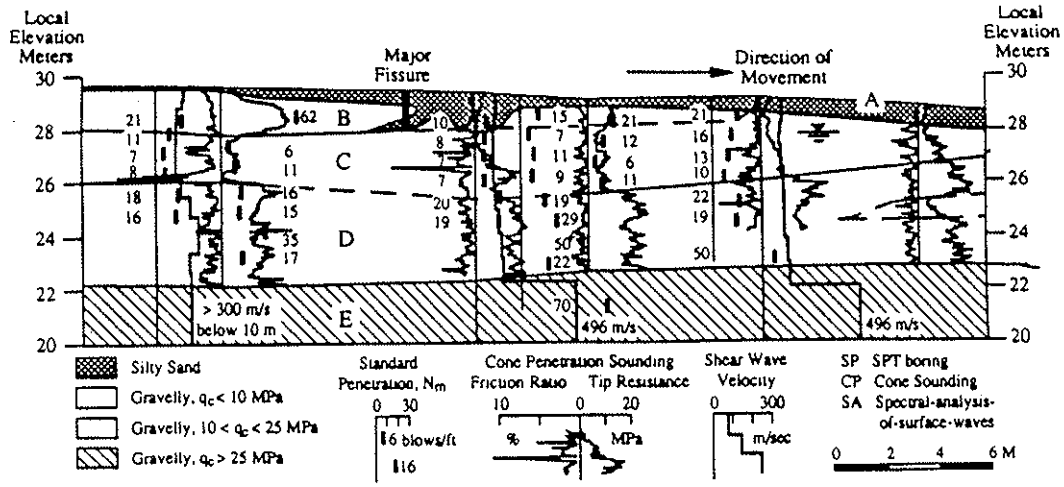

Figure 10 Cross section of liquefaction-induced lateral spread at Pence Ranch site during the 1983 Borah Peak, Idaho earthquake (Andrus, et al., 1991).

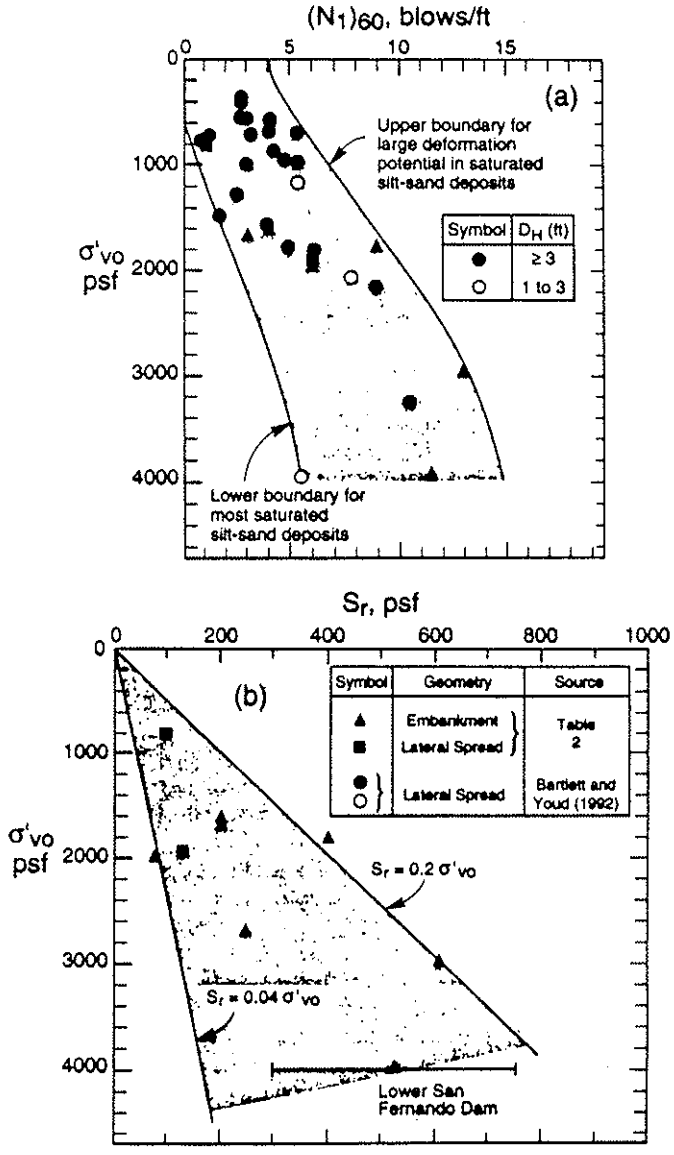

FIG. 11 Charts Relating (a) Normalized Standard Penetration Resistance $(N_1)_{60}$; and (b) Residual Shear Strength S_r, to Vertical Effective Overburden Pressure, σ'_{vo} for Saturated Nongravelly Silt-Sand Deposits that Have Experienced Large Deformations

(Bazier and Dobry 1995)

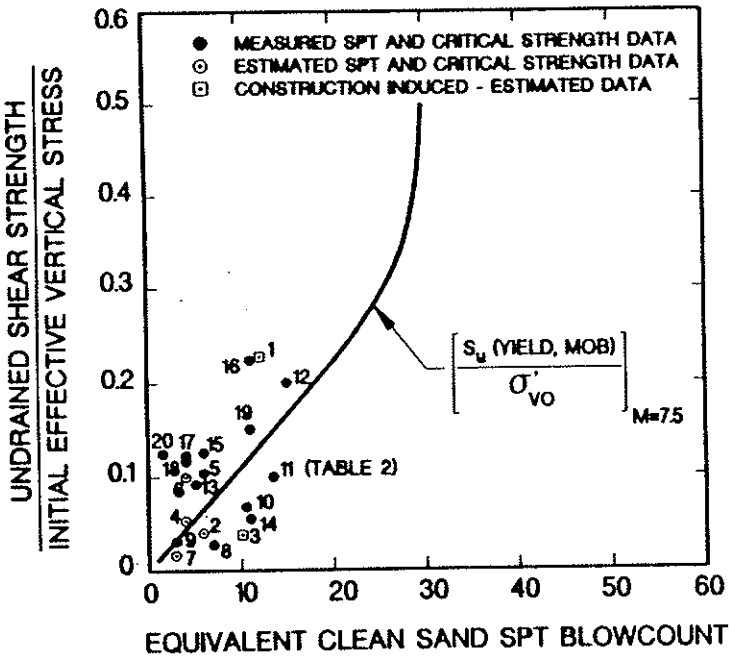

FIG. 12 Comparison of Undrained Critical and Yield Strength Ratios Back-Calculated from Field Case Histories (Stark and Mesri 1992)

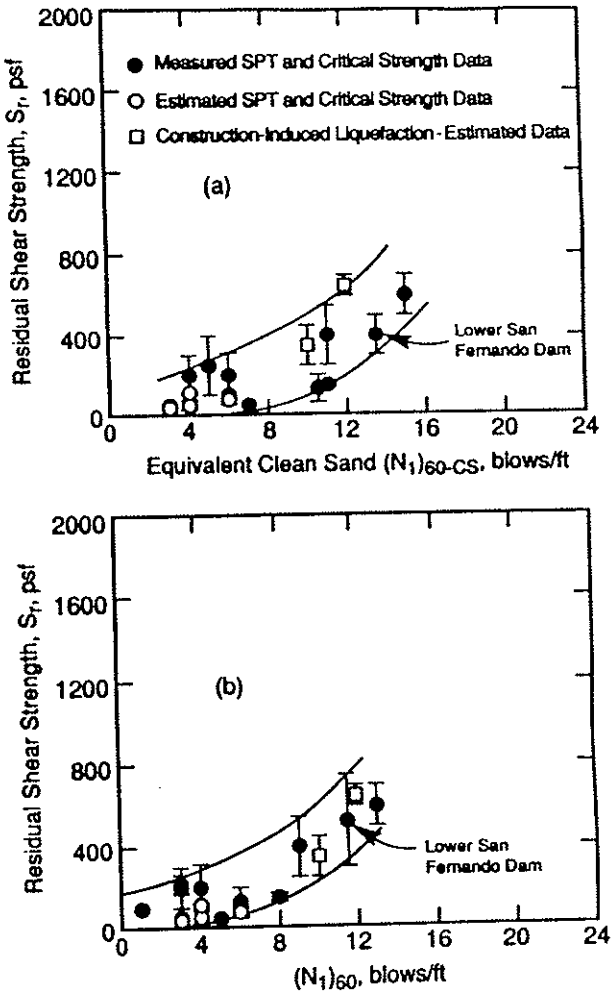

FIG. 13 Proposed Correlations between Residual Shear Strength and Normalized Standard Penetration Resistance for Clean and Silty Sands and Gravels: (a) with Correction for Fines (Seed and Harder 1990); (b) without Correction for Fines, Present Study, Table 2 (Bazier and Dobry 1995)

NSF Workshop on Post-Liquefaction Shear Strength of Granular Soils
University of Illinois, Urbana-Champaign, April 17-19, 1997

By: Mary Ellen Hynes, U.S. Army Engineer Waterways Experiment Station

Discussion Group: Post-Liquefaction Strength from Case Histories
Back-calculation Questions:

1. What is the appropriate geometry for back-calculation (pre-failure vs. post-failure)?

What is failure? In a slope, if sliding movement occurs, it means the available shear strength and stiffness of the sliding mass and materials below it were insufficient to support the sliding mass, at least temporarily. *All you know about the pre-failure geometry is the strength and stiffness required to maintain that geometry.*

The post-failure geometry, alone, also may be insufficient for back-calculation. The simplistic approach to back-calculation in the past has *ignored the effects of aftershocks.* Although limit equilibrium back-calculations have attempted to correct for momentum of the sliding mass, more complicated soil behavior and deformation mechanisms are at work. I believe the residual strength of liquefied materials at Lower San Fernando Dam may indeed be somewhat higher than currently plotted on charts. We have the estimated accelerogram for the sliding mass, thanks to Professor Ron Scott. I suggest this information be utilized in a *reanalysis of Lower San Fernando Dam, to track the effects of the aftershocks, and their impact on the 125-ft trajectory of the toe of the slope.*

2. Selection of representative in-situ test parameter (e.g., minimum, average, maximum cone resistance)?

Use of maximum strength values does not make sense because, whether they are slopes or other soil structures or foundations, *soils failures are not processes that are governed by maximum strength values.* Typically, strength failure will occur over a path of least resistance, thus the minimum. However, *other types of measurements may be governed by maximum values, such as shear wave velocity.* In measuring shear wave velocity, the signal seeks the fastest path, and that is what is measured as the first arrival. The *current practice of using average values seems practical, as long as the average is being limited to the correct zone of interest.* As Dr. Castro has pointed out, different interpretations of limits of the correct zone of interest leads to significant changes in the locations of the few points we have on Professor Seed's correlation between SPT and Sur.

3. Suitable analytical methods for back-calculation (limit equilibrium vs. Stress-deformation analysis)?

Both limit equilibrium and stress-deformation analyses have been used to estimate residual strength in slopes. The limit equilibrium approach has merit because we all have experience and an understanding of the method and its limitations. The stress-deformation approach is much more

complicated and is best done by the few people who wrote the software in the first place. What is lacking is an understanding of the mechanisms at work during the slope failure process.
Model tests performed at WES by Dr. Rick Olsen demonstrated some very interesting mechanisms that are not accounted for in current backcalculations. Dr. Olsen observed that *in a liquefaction failure of a model slope, the sliding mass, sitting atop a liquefied zone, acts as a cantilever. The upper part of the sliding mass (esp. above the phreatic surface) is attached to the original embankment, but is put into tension as bearing capacity support is lost beneath the sliding mass. Eventually, a tension crack forms and then the sliding mass moves--a lot--until it reaches and equilibrium condition.* Dr. Olsen also did some work with aftershocks, and found a similar mechanism at work, even in the deformed slope.

We cannot expect good estimates of residual strength and deformation potential if we are not analyzing the right mechanisms. Although we need information put in terms simple enough to relate to our experience, I feel *a great deal of work is needed, physical model testing in particular, in concert with first-principles based codes, to see that we are modeling numerically what is happening physically.* The centrifuge is the only place where we can perform such physical tests. When we understand the actual soil behavior and deformation processes better, then we can simplify the results and put them in more practical terms. And then we will know how to craft a laboratory or field testing program to obtain the governing engineering parameters.

4. Consideration of consolidation stress and undrained stress path, strain rate, drainage effects, initial effective stress, etc.

This is all part of the answer to no. 3 above. There is no point in investigating this items until we have the mechanisms correct.

5. Is post-liquefaction shear strength proportional to the initial vertical effective stress of some other parameter?

Probably. What do the shear-banding folks have to say?

6. Should existing case histories be re-evaluated based on previous questions?

Yes.

7. Reconsideration of case histories based on previous questions?

Same as no. 6 above.

Consensus Topics A
1) Post-Liquefaction Shear Strength Terminology

If we have a revolution in our understanding of governing mechanisms, there will be significant changes to our terminology. I suspect directional permeabilities, drainage paths and boundary

conditions, deformation potentials (and their gradients) related to stress state and density (and their gradients) will all be important. There is no point in getting locked in to a particular terminology now, as we are seeing being suggested by our Canadian colleagues.

2) Laboratory vs. Field Determination (Preferred Test and Data Reduction)

For and existing structure, there is no doubt that field measurements are preferred. You are measuring the materials at the right stress state and density; you can collect a great deal of information to put the 3-dimensional picture into place; and you can get a lot of high quality information for your money. Going to the laboratory is terribly expensive; the corrections needed for sample disturbance (changes in stress and density state) are not perfected; we cannot subject the sample to the correct stress state and loading conditions as we have in the field; we cannot provide boundary conditions that mimic the field situation; and we do not know how to interpret the test results. It is perfectly clear that the reason there is such a difference between the strengths measured in Castro-type triaxial tests and backcalculations from case histories is that we are not measuring and calculating the right things. We are not performing the back-calculation properly; we are not performing the right laboratory tests; and we do not know how to interpret the laboratory results we get. Let's get the mechanisms right. Then we will better know what we need to measure and how to do it.

3) Identification and Characterization of Field Case Histories

This needs to be revisited, as described above.

Consensus Topics B

4) Normalization with initial vertical effective stress

Let us not be premature. This appears to be the case, but we will know more when we are modeling the right mechanisms.

5) Fines content correction for in-situ tests

Please refer to the work done by Dr. Olsen, for both SPT and CPT corrections, as well as Cn and K-sigma effects.

6) Re-evaluation of field case histories

This needs to be revisited, as described above.

Consensus Topic C

7) Future research needs in post-liquefaction shear strength of granular soils

A) Physical model studies to better understand mechanisms that govern the deformation process and soil behavior.

B) First-principles-based codes to evaluate the results of the physical models and identify the key

engineering parameters.
C) Development of field investigation methods to measure these properties.
D) Re-evaluation of case histories in light of a better understanding of mechanisms as work.

Post-Liquefaction Strength from Case Histories

Dave Gillette, US Bureau of Reclamation
3/4/97

What is the appropriate geometry for back-calculation (pre-failure vs post failure)?

Both, or maybe neither. The pre-failure geometry has a factor of safety less than 1.0 (or it wouldn't fail). We don't know exactly what the factor of safety is, so back-calculation with the pre-failure geometry (assuming FS=1.0) provides an upper bound on the strength. If the velocity of the slide is small, so that inertial effects are of no consequence, the slide would come to rest when FS=1.0. However, if the velocity is significant, the factor of safety for the post-failure geometry would actually be slightly above 1.0. Simple back-calculation (by stability analysis assuming FS=1.0) would yield a lower bound on the shear strength. It may be necessary to explicitly consider the effect of inertia for some slides.

An important design issue (but one which is not addressed by strengths back-figured from failed slopes) is whether large strains are necessary to mobilize the post-liquefaction shear strength. Post-liquefaction stability analyses may show a slope to be stable in its existing form or with proposed modifications. However, if large strains must occur before the shear strength can be fully mobilized, there could deformations so large as to effectively constitute failure, e.g., if a dam crest should fall below the reservoir level. Slopes that did not undergo flowslide movements but did experience high pore pressure and/or movement due to dynamic loading are therefore of at least as much interest as those that slid under gravity loading alone.

Selection of representative in-situ test parameter (e.g. minimum, average, maximum cone resistance)

There is no simple answer to this question. A slide would be expected to occur on the weakest shear surface, but the strength that governs stability is the average over the shear surface. Neither a minimum index property (normalized CPT tip resistance, SPT $(N_1)_{60}$, etc.) nor an average for the deposit would necessarily be appropriate. Our usual practice is to use a "representative" value that is a rough average of the lowest value from each SPT (BPT, CPT...) sounding in the area of the potential slide. Others have sought to accomplish the same thing by using 33rd percentile, mean minus one standard deviation, etc.

Suitable analytical method for back-calculation (limit equilibrium vs stress-deformation analysis)

Ultimately, stress-deformation analyses (FEM or similar method) may prove to be the best tool for evaluating material properties

from failure case histories. However, under the present state of the practice, the greater simplicity and transparency, and wider acceptance of limit-equilibrium analysis make it the preferred method. Given the uncertainties (strengths and piezometric levels in non-liquefied materials, variation of strength within liquefied material, slide geometry, etc.), the more sophisticated and far more labor-intensive stress-deformation analyses may not be able to produce results that are any more useful than the simple limit-equilibrium approach.

Consideration of consolidation stress and undrained stress path, strain rate, drainage effects, initial effective stress, etc.

Ideally, drainage and strain rate should be included in the back-analysis, and may ultimately be necessary to understanding the phenomenon of slope instability during/following an earthquake. However, modelling of drainage is difficult and may involve quite a bit of guesswork to establish material parameters and boundary conditions which are not easily measured. Higher priority should be given to resolving differences in the back-figured strengths and material index properties (SPT $(N_1)_{60}$, fines content, etc.) among various investigators. See Attachment 1 from Fear (1996) for an illustration of the need.

The dominant stress path is commonly considered to be simple shear. Case histories where this is not true should be identified so that the effects (if any) can be studied. This would permit users of a strength correlation to account for the effect of load path as it relates to their site.

Initial effective stress and consolidation stress do not appear to me to be nearly as important as other properties in determining post-liquefaction strength of granular materials. (See response to next question.)

Is post-liquefaction shear strength proportional to the initial vertical effective stress or some other parameter?

Post-liquefaction shear strength may be governed in part by the initial effective stress, but for granular materials, overburden stress is very much secondary to the initial void ratio (density, porosity, relative density, state parameter). In critical-state soil mechanics, or the steady-state concept (Poulos *et al* 1985), the effective stress at large strains (which governs the post-liquefaction strength) is considered a function only of grain shape, grain-size distribution, and void ratio. The initial normal stress does affect the void ratio, but only to a small degree in granular materials, as compared to what occurs in clays, for which the Stress History and Normalized Soil Engineering Properties (SHANSEP) concept has been useful in practice (Ladd 1991). For clays, the void ratio is determined more or less uniquely by the stress history (neglecting desiccation, weathering, etc.). For sands and gravels, the void

ratio at deposition is changed relatively little by overburden stresses except at great depth. (When the overburden stress becomes so high that the material begins to act as a normally consolidated material, stress normalization may work well, but many or most sites where liquefaction is an issue are much too shallow.)

The strongest argument against post-liquefaction shear strength being proportional to effective overburden stress is provided by comparing the Ft. Peck case history with those having similar $(N_1)_{60}$ (actual or fines-adjusted) but much less overburden (Lower San Fernando, Whiskey Springs fan, La Marquesa downstream slope). With an initial effective overburden stress of about 11 ksf (Stark and Mesri 1992), more than double any of the other case histories I am aware of, the strength back-figured for Ft. Peck would be expected to be much higher than most others with similar blowcounts. Instead, it falls in the middle of the band of data from Seed and Harder (1990). (See Attachment 2.) Similarly, Heber Road had the lowest effective overburden, but a number of the other sites had lower strengths, even with higher blowcounts.

Should existing case histories be re-evaluated based on previous questions?

I don't know all the details of the various back-analyses, but strength correlations based on the case histories are heavily used in practice and should be based on the best possible analyses. If they don't meet that criterion, they should be re-evaluated.

References

Fear, Catherine E. (1996), In-Situ Testing for Liquefaction Evaluation of Sandy Soils, PhD dissertation, Department of Civil Engineering, University of Alberta, Edmonton.

Ladd, C.C. (1991), "Stability Evaluation During Staged Construction", ASCE Jnl. Geotech. Engrg., v. 117, no. 4, pp. 540-615.

Poulos, S.J., G. Castro, and J.W. France (1985), "Liquefaction Evaluation Procedure", ASCE Jnl. Geotech. Engrg., v. 111, no. 6, pp. 772-792.

Seed, R.B. and L.F. Harder (1990), "SPT-Based Analysis of Cyclic Pore Pressure Generation and Undrained Residual Strength", Proceedings of the Memorial Symposium for H. Bolton Seed, BiTech Publications, Ltd.

Stark, T.D. and G. Mesri (1992), "Undrained Shear Strength of Liquefied Sands for Stability Analysis", ASCE Jnl. Geotech. Engrg., v. 118, no. 11, pp. 1727-1747.

ATTACHMENT 1

ABSENCE OF CONSENSUS ON WHERE THE DOTS SHOULD BE !

FROM FEAR (1996)

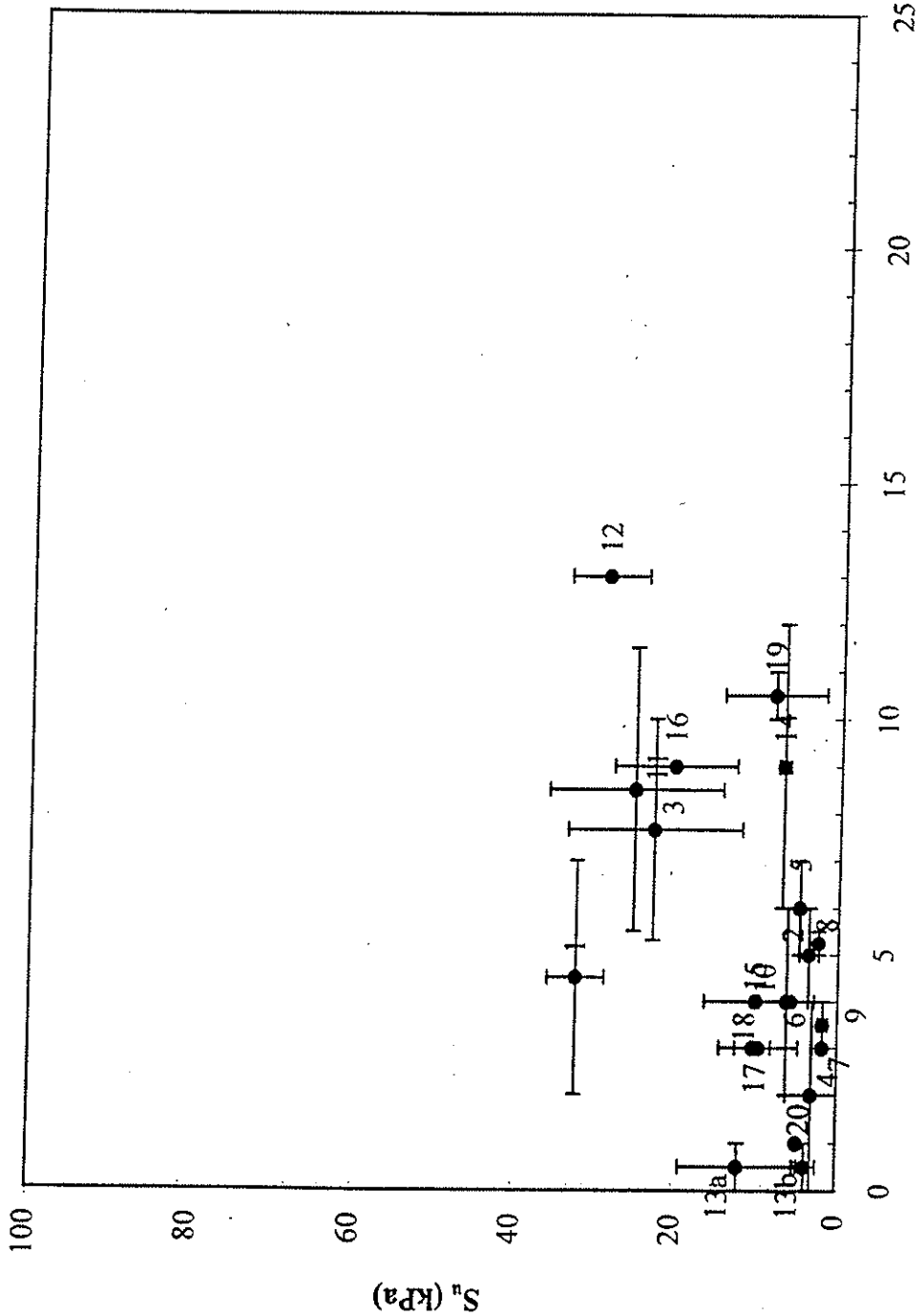

Figure 7-11 Range in S_u and $(N_1)_{60}$ in-situ reported by various authors (see Table 7-4) for the case histories in the Seed and Harder (1990) and Stark and Mesri (1992) database.

INFLUENCE OF INITIAL OVERBURDEN STRESS ATTACHMENT 2.

ADAPTED FROM SEED & HARDER 1990

HEBER RD & σ'_v data from Stark & Mesri 1992

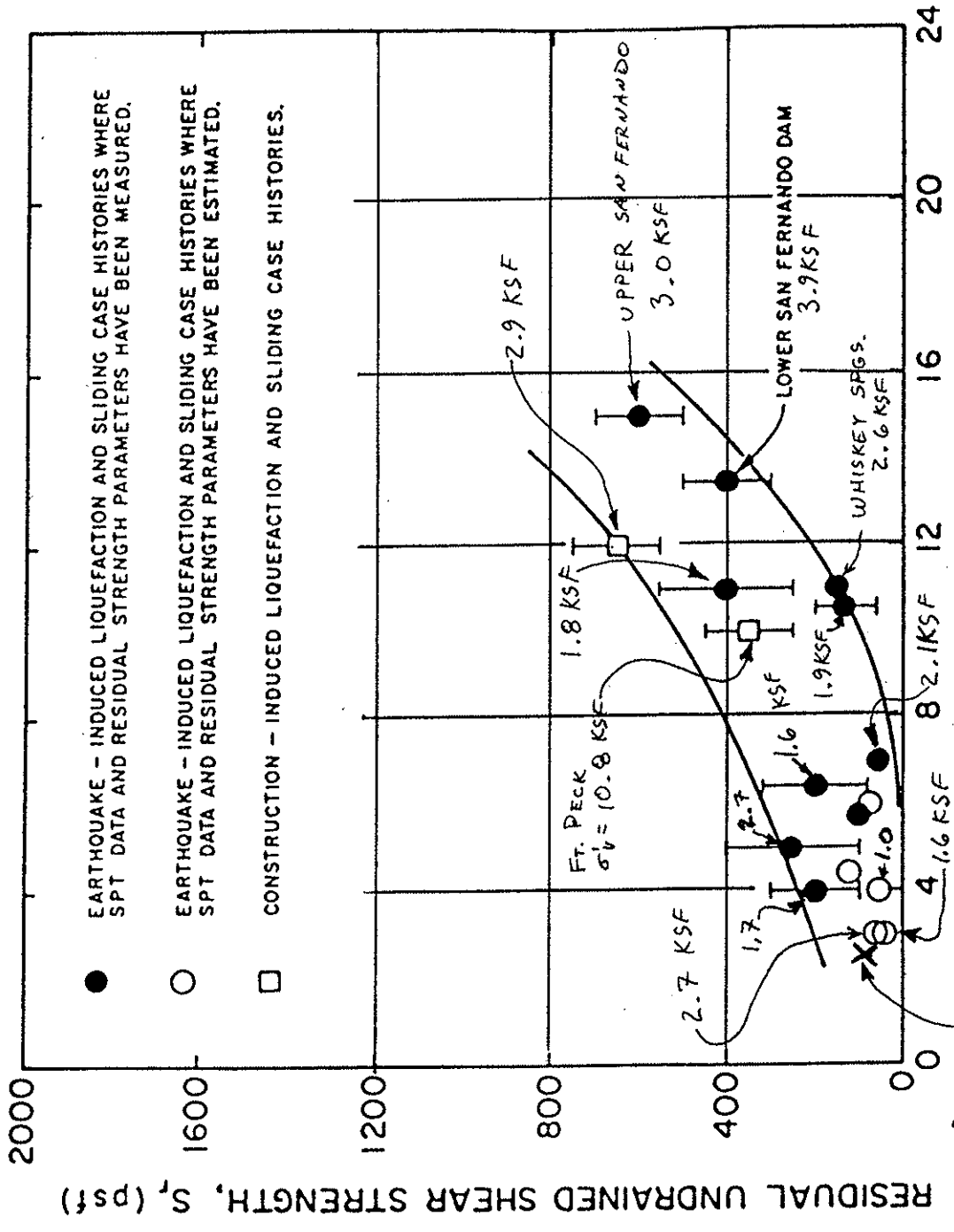

Relationship Between Corrected "Clean Sand" Blowcount $(N_1)_{60-cs}$ and Undrained Residual Strength (S_r) from Case Studies

Workshop on Post-Liquefaction Shear Strength of Granular Soils
University of Illinois
Urbana, Illinois
April 17-19, 1997

Organizers: T.D. Stark, S.L. Kramer, and T.L. Youd

Discussion Group: Post-Liquefaction Strength from Case Histories

Writing Assignment submitted by J.C. Horne

How does one differentiate between flow failure and lateral spreading failure case histories?

Conceptually, flow failure occurs when the static, pre-liquefaction shear stresses exceed the post-liquefaction or "residual" shear strength of the soil. This instability leads to continuous deformation or "flow" until the soil mass reaches equilibrium between the driving shear stress and the resisting shear strength. On the other hand lateral spreading involves static shear stresses that are less than the post-liquefaction strength. During seismic shaking, dynamic shear stresses may momentarily exceed the residual strength, but in general they do not. Permanent strains develop during lateral spreading due to the cyclic nature of earthquake loading coupled with preferential soil yielding during liquefaction.

Without the aid of a detailed post-failure investigation, it is probably impossible to definitively distinguish between the two types. However, flow failures are generally associated with very large surface displacements - on the order of tens or hundreds of meters. Conversely, lateral spreading displacements are typically on the order of centimeters or meters.

What is the minimum data required for valid case histories?

It is problematic to categorize case histories as being either "valid" or "invalid." Rather, case histories run the qualitative gamut from "very useful" to "mediocre" to "meaningless," depending on what information is available. This is why a rating or characterization system should be developed.

Below are listed some of the data that would be useful to assess flow liquefaction and lateral spreading case histories:

- Topographic data obtained both before and after the failure
- Results of a visual field reconnaissance which includes a description of surface features such as ground cracks, sand boils, and structural damage
- Eye witness accounts of the failure

- Measurements of ground surface displacement
- An assessment of the horizontal displacement profile with respect to depth
- Displacements of and damage to in-ground structures such as pipelines and foundations
- The stratigraphy, as obtained from a detailed subsurface investigation
- In-situ strength test data such as from SPT or CPT
- In-situ density data such as from SPT, CPT, or SASW
- In-situ shear modulus data such as from SASW
- Laboratory test data such as grain size distribution
- Acceleration time histories at the top and bottom of the liquefied layer
- Where appropriate, seismological information such as rupture mechanism, earthquake magnitude, epicentral distance, and local intensity

How should the case histories be characterized?

Case histories need to be characterized because they contain varying amounts and quality of the data described above. A simple scheme should be adopted which assigns an index to the case history depending on the quality and type of data available. Such a scheme should be agreed upon by researchers and practitioners active in the geotechnical earthquake engineering arena.

Should quality-based weighting factors be assigned to the case histories?

This really ties in with a rating system. Perhaps numerical factors aren't appropriate, but certainly a "quality index" could be adopted.

Is post-liquefaction shear strength proportional to the initial effective vertical stress or some other parameter?

This is a subject of some debate. The correlation proposed by Seed and Harder (1990) - based on examination of case histories - suggests that post-liquefaction shear strength is dependent solely on SPT blow counts corrected for fines content and overburden stress. Stark and Mesri (1992) reported a correlation - also based on case histories - which indicates residual strength is proportional to both corrected SPT blow count and the initial vertical effective stress. More recently, Baziar and Dobry (1995) reported a residual strength correlation based solely on initial vertical effective stress.

Both the field and laboratory data used to develop residual strength correlations exhibit considerable scatter. As a result, there exists considerable uncertainty in the residual shear strengths that these methods predict.

Does any drainage occur during post-liquefaction flow or lateral spreading?

Yes. Whether or not it is significant is another question. Evidence of sand boils at liquefaction sites suggest that drainage can occur during or shortly after strong ground

shaking of liquefied soils. If significant drainage occurs during flow or lateral spreading failure, effective stresses - and hence shear strength - could conceivably increase with time.

If so, how should this be accounted for in the analysis and use of the back-calculated shear strength?

Without any knowledge of when pore pressure dissipation occurred relative to when displacement occurred (in a given case history), there is no way to account for this in analysis. The alternative to conduct analyses assuming undrained conditions prevail.

Should any case histories be reconsidered based on the previous questions?

It would be appropriate to reclassify all known case histories based on a standardized scheme as suggested above. This would allow future researchers to select those case histories that are most useful for their particular studies.

NSF Workshop on

"Post-Liquefaction Shear Strength of Granular Soils"

University of Illinois, Urbana, Illinois
April 17-19, 1997

Discussion of Requested Topics

by

W. F. Marcuson, III

Identification of flow failure (versus lateral spreading failure)?

I assume the purpose of this question is to try to develop criteria to separate case histories into two categories—flow failure and lateral spreading. From an engineering point of view, sometimes this is important and sometimes it is not, few structures can sustain three or four feet of deformation without catastrophic damage. I guess some earth dams are examples of flexible structures that might sustain several feet of movement without catastrophic damage. I also believe that from a technical point of view, the primary parameters separating flow failures and lateral spreading failures is probably the initial driving shear stress and void ratio. We know that soils depending on the density (void ratio) experience liquefaction, limited liquefaction, and dilation (see Figure 1). Flow failures only occur when the soil behaves as in curve 1 of Figure 1. Geometry is the critical parameter with regard to initial driving shear stress.

Minimum data requirements for valid case histories?

This is an interesting question. It seems to me that all case histories are interesting and provide useful information. However, to try to backcalculate post-liquefaction residual strength from a case history, you need to know the geometry before liquefaction, the geometry after liquefaction, the fact that liquefaction was triggered, and where liquefaction occurred (the layer or depth) and some idea of the density or void ratio of that material. One needs this as a minimum.

How should the case histories be characterized?

Again I assume we are trying to get post-liquefaction shear strength from some sort of correlation similar to the one proposed by Seed and his colleagues relating $N_{1(60)}$ to post-liquefaction residual shear strength. I really see no need to characterize case histories. However, I guess you might code them "1" if no assumptions need to be made, "2" if minor assumptions are made, and "3" if major assumptions are made. Frankly, I believe we should take case histories and use them as best we can. Good, well documented case histories are rare and many times much of the documentation takes place after the earthquake when certain assumptions have to be made to get back to pre-earthquake conditions.

Should a quality-based weighting factor be assigned to case histories?

Off the top of my head, I think this is a bad idea. We need to apply our best engineering judgment and either determine that the case history does in fact provide some useful insights and information or that we do not have enough data to use it.

Is post-liquefaction shear strength proportional to the initial effective vertical stress or some other parameter?

Post-liquefaction shear strength has to be proportional to some parameter. Present information indicates that post-liquefaction shear strength is in fact proportional to initial effective vertical stress and in general, the formula $S_u = c \times \overline{\sigma}_v$ where c is a variable that ranges from something like .04 to .2. As the vertical stress approaches zero, the post-liquefaction strength approaches some lower limit and so this is not a straight line all the way to the origin. While such a correlation may or may not be rigorously correct, it is certainly useful from an engineering point of view. For example, if I assumed that my soil had a post-liquefaction residual strength of $.05 \times \overline{\sigma}_v$ and came up with deformations that were tolerable, I would do no more work.

Does drainage occur during post-liquefaction flow and lateral spreading?

Again, the answer is almost certainly, yes. The question is --- "how much drainage?", "is it negligible?", or "is it important?"

If so, how should this be accounted for in the analysis and use of back-calculated shear strength?

Given the present state of knowledge, I think that we are on the conservative side neglecting drainage. As we all know, drainage is a function of three-dimensional permeability and drainage path length. Since I believe most flow failures and lateral spreads take place in a relatively short period of time, assuming undrained conditions is good engineering.

Reconsideration of case histories based on previous questions?

We can always go back and reconsider and perhaps do a better job, however, given limited resources the question is 'Is this warranted'? My belief is that a great deal could be learned from some centrifuge studies. I hope my colleague Ledbetter covers this.

Shear Stress
Slear Strain
Liquefaction
Limited Liquefaction
No Liquefaction
1
2
3

Figure 1

Workshop on Post-Liquefaction Shear Strength of Granular Soils

Comments re Post-Liquefaction Strength from Case Histories

Robert V. Whitman

Prologue: As most attendees will suspect, I am far from up-to-date re post-liquefaction shear strength, although I have now read or reread more than a dozen of the pertinent papers from the last 10 years. My offerings may best be characterized as "grandfatherly observations and advice." I am now a user of information rather than a researcher generating information - and hence tend to have a relatively short-term viewpoint.

1. Identification of flow failure? I agree that post-liquefaction strength can best be defined and understood if we restrict ourselves to flow failures - since lateral spreading of ground and slumping of dams may well involve contraction-dilation cycles. I suppose that flow failures are characterized by horizontal movements of at least several meters (maybe, say, >3m for small slopes/dams; >10 m for large slopes/dams) and/or by evidence that movements have continued/occurred after ground shaking has essentially ceased.

However, at least in the near future there will in practice be continued interest in using Newmark sliding-block analysis re lateral spreading and crude deformation analyses for dams - and hence a wish for values of shear strength appropriate for such analyses, even if they are only representative or "effective" values rather than some fundamental quantity such as residual or steady-state strength.

2. Minimum data requirements for valid case histories? If you really mean minimum, and if we are concerned only with flow failures, then: Cross-sections (soil profiles) of slope or dam before and after earthquake, including location of water table and with identification for all soils - in particular with location and extent of the soil that liquefied. For lateral spreading or slumping, also need some information concerning ground motions.

3. How should the case histories be characterized? I am not sure what is being asked. A distinction as to whether or not there was flow failure obviously is pertinent. Perhaps the amount of fines in the granular soil is a primary characteristic. Also perhaps by the presence or absence of less pervious caps or strata that might entrap water films.

4. Should quality-based rating factors be assigned to the case studies? Yes, it would be desirable to have such a system, although inevitably the ratings will be subjective and open to controversy.

A first rating factor would concern the confidence in assigning a case to the flow failure category,

A case study of a flow failure should essentially be rated on two matters: How well are pre-earthquake conditions known?, and how much is known concerning the failure? Re the pre-quake conditions: How well is the cross-section known?; and the quality of data (blow counts; laboratory tests) concerning the soils of greatest concern. Re the failure: How well is the zone of flow identified?; has trenching been used, or has the pattern of flow/deformation been inferred from borings?

If the case study involves lateral spreading or slumping, then how well the ground motion is known is another rating consideration.

A careful assessment of the probability distribution (or just plus/minus 1σ) for inferred strengths is itself a form of rating system. Upper and lower bound strengths should be assessed separately in this manner, and should be plotted separately.

5. Is post-liquefaction shear strength proportional to the initial vertical effective stress or some other parameter? I doubt that there is one parameter that is the controlling parameter in all situations. The complexities suggested by questions 6 and 7 almost ensure that matters are not simple. However, I personally find use of the suggested ratio to be very appealing for practical work. Its use provides a simple way of characterizing the range of possible post-liquefaction strengths.

6. Does drainage occur during post-liquefaction flow or lateral spreading? If the question allows for partial drainage, the answer is: Possibly, and probably in some situations. If the question covers the possibility of internal redistribution, including the entrapment of liquid films beneath relatively impervious strata, the answer is: Almost certainly, where such strata exist.

7. If so, how should this be accounted for in the analysis and use of the back-calculated shear strength? As far as evaluation of strength from case studies, I think the question should be ignored. That is, the strength implied by the case history should simply be evaluated directly without correction. As for use of back-figured strengths in practical analysis, Harry Seed's discussion in 1987 still is very pertinent. With time, we possibly will learn to distinguish among cases where drainage or redistribution are factors, and will develop strength estimation procedures applicable to each circumstance.

8. Reconsideration of case studies based upon previous question? As yet, I have not been able to examine many of the case studies in detail. Perhaps I will be able to unearth and study more by the time of the workshop.

Development of a Correlation between Residual Strength and $(N_1)_{60}$ for Lateral Spreads in Natural Materials

by
Matthew A. Mabey and T. Leslie Youd
Brigham Young University

A correlation between $(N_1)_{60}$ and the residual strength was developed by matching calculated sliding-block analysis displacements with actual field measurements of displacements for 66 lateral spreads extracted from case histories compiled by Bartlett (1992). The correlation obtained was subsequently compared with the results of the same procedure using 162 additional field measurements from Niigata. The match was attained by varying the residual strength parameter until agreement was obtained between the displacement calculated for the block and displacements measured in the field. Six different time histories of acceleration were applied to test variation with seismic input. For these analyses, it was assumed that liquefaction occurred instantaneously as strong shaking started and that the strength of the liquefied soil fell quickly to the residual strength. Both a delay in the initiation of liquefaction and a delay in falling to the final residual strength would have the effect of requiring a lower residual strength than calculated. Displacement, thickness and $(N_1)_{60}$ data were extracted from case histories compiled by Bartlett (1992). Most of the measured displacements were from the 1964 Niigata ($M_w = 7.5$) and the 1983 Nihonk1ai-Chubu ($M_w = 7.7$) earthquakes in Japan (originally compiled by Hamada and others, 1986). Nearly all of the sands in these two localities are clean (less than 5 percent fines) and fine to medium grained. Also, these two earthquakes were similar in magnitude and in distance from the lateral spread sites and thus probably generated about the same levels of peak acceleration (about 0.2g) at those sites. Some data were also extracted from lateral spread sites in California and Idaho.

The thickness of the rigid block was defined as the depth to the low $(N_1)_{60}$ in the soil profile. This logical and simple selection facilitated both the compilation of thickness and residual strength information, and was also chosen with an aim of application of the technique to regional mapping. The slope was assumed to be the same as the ground slope.

Residual strength values calculated from these analyses are plotted against $(N_1)_{60}$ in Figure 1. Also shown on Figure 1 are residual strength values calculated by Seed and others (1988) from several case histories, primarily flow slides, plus Seed and others' suggested upper and lower bounds for residual strength.

For $(N_1)_{60}$ greater than 8 and less than 16, many of the residual strength values calculated in this study fall below the lower bound proposed by Seed and others (1988). Several factors likely contribute to the lower estimates of residual strength from lateral spreads.

(1) Most of the strengths calculated by Seed and others are from flow slides, whereas, all the strengths calculated in this study are from lateral spreads. Flow failure generally

continues after earthquake shaking has stopped; thus evaluations of residual strength from flow slides are based on static driving forces generated only by gravitational acceleration. Lateral spreads, on the other hand, generally develop during earthquake shaking with rather complex dynamic interaction between shaking and displacement including oscillatory movements and possible redistribution of pore water within the failure zone (Ishihara, 1991). Thus the strengths that are effective during dynamic lateral spread may be much smaller than those effective during 'static' flow failure for material with equivalent $(N_1)_{60}$s.

(2) Most of the case histories analyzed by Seed and others are from failures in constructed fills, Nearly all of the lateral spreads analyzed in this study were in natural deposits. There may be some fundamental strength differences between these two types of material.

(3) Undoubtedly, there are some incompatibilities between displacements measured in the field and $(N_1)_{60}$ values coupled to those displacements. In many instances, boreholes in which blow counts were measured were some distance away from the locality at which ground displacement was measured. In some instances, the assigned $(N_1)_{60}$ values may not be exactly representative of the liquefiable material in which displacement occurred.

(4) Blow counts are taken at discrete intervals, generally one meter in Japan, and a critical layer may have been missed and thus an incorrect $(N_1)_{60}$ assigned. Also, testing errors and natural scatter of $(N_1)_{60}$ values may have contributed to the scatter in computed residual strengths rather than a systematic bias. In summary, the data plotted on Figures 1, 2, and 3 provide a reasonable estimate of residual strength for evaluating displacement of lateral spreads in natural material.

The paucity of calculated residual strengths in Figure 1 for materials with $(N_1)_{60}$ greater than 16 is specifically noted. That absence is not due to oversight in evaluating strengths for materials with $(N_1)_{60}$ greater than 16. Opportunity for lateral spread of these denser materials has likely occurred during many earthquakes that were subsequently investigated. Based on this observation, it is postulated that there is a major strength increase leading to a discontinuity in the $(N_1)_{60}$-strength relationship for $(N_1)_{60}$ greater than 16. Therefore, residual strength trends and values estimated by the data and curves in Figure 1 and other similar figures in this report should not be extrapolated to $(N_1)_{60}$ values greater than 16. More data and analysis are required to define the relationship between residual strength and $(N_1)_{60}$ greater than 16.

Figure 2 is a plot of the same data as in Figure 1, but with residual strength plotted on a log scale. This figure shows that upper and lower bounds for the calculated residual strengths form straight lines on a semi-logarithmic plot. The data also are rather uniformly distributed between the bounding curves. On a natural scale, as shown in Figure 1, that distribution of data is greatly skewed toward the lower bound.

Recognizing that the data set can be characterized as being distributed between some minimum and maximum bounds, a Beta distribution was selected to describe the distribution of points between the maximum and minimum (Ostle and Malone, 1988, Ross, 1988). Figure 3 shows the match between how the actual data is distributed and the distribution predicated by a Beta distribution for parameters a=1.2 and b=6.2. Figure 4 is a cumulative distribution plot of the chosen Beta distribution and demonstrates the characteristic of a very steep increase in probability. This characteristic is desirable because it means that a very narrow range of strength can be chosen that has a high probability of being correct. The fact that it is skewed towards the minimum bound has the effect that values chosen will under predict displacements less often than over predicting. This insures conservative results.

The relative position of the data points between the bounding curves was analyzed to check for cross correlation with other model parameters. Of particular concern was the possibility of cross correlation between plotted position and $(N_1)_{60}$. While it is highly desirable that residual strength be strongly correlated with blow count, it would be undesirable for residual strength values to be systematically closer to one bound or the other as a function of $(N_1)_{60}$. Most undesirable would be a correlation residual strength and displacement. Such a correlation would require the impossible situation that the displacement be known in order to choose a residual strength for computing the displacement. The correlation factor for position for each of the parameters tested is listed in Table 1.

As mentioned previously the results of the analysis of the original 66 data points was subsequently compared with 162 additional data points. Figure 5 shows this comparison and it can be seen that the additional data points are consistent with the original results with perhaps less scatter of the data into the higher residual strength range.

In conclusion, analysis of these lateral spread case history data seems to imply significant differences in the implied residual strengths as compared to a previous correlation of residual strength to $(N1)_{60}$. These differences are significant in their implications regarding the hazard due to lateral spreading in natural materials.

Table 1.

Tested Parameter	Coefficient of correlation	Degree of dependence
Blow count	-0.089	Insignificant
Thickness	0.576	Possible correlation
Displacement	0.260	Slight
Strength	0.835	Strong (as expected)
Acceleration	0.278	Slight
Duration	-0.205	Slight
Slope	0.450	Possible correlation
Thickness of the liquefiable layer	0.245	Slight

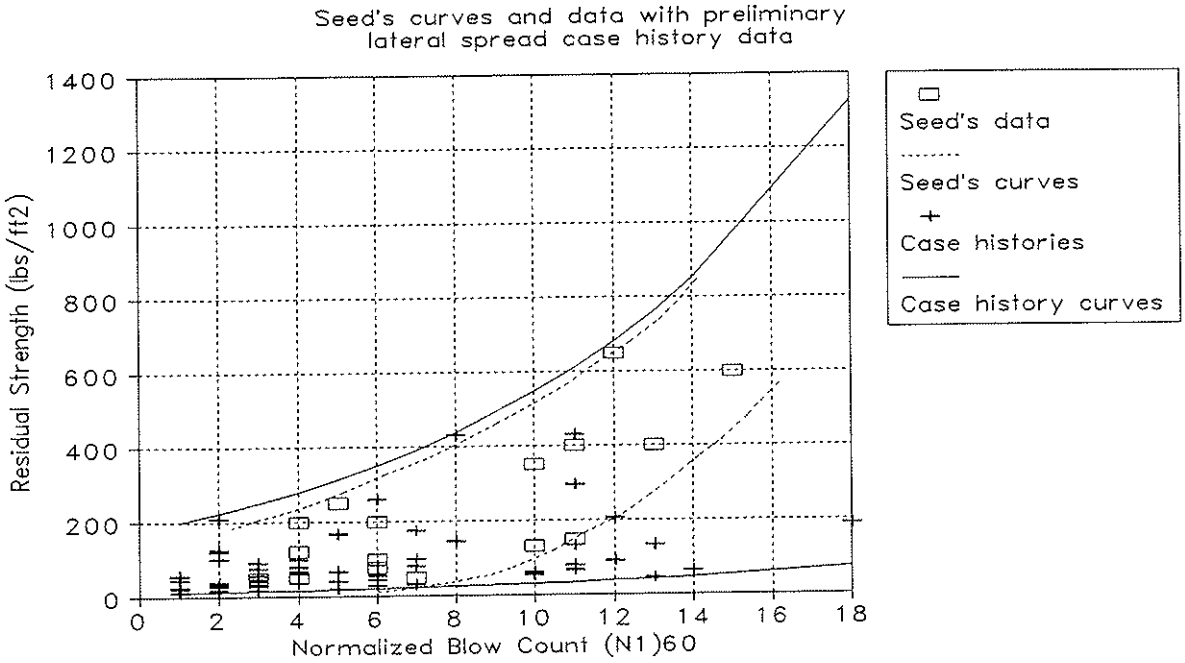

Figure 1.

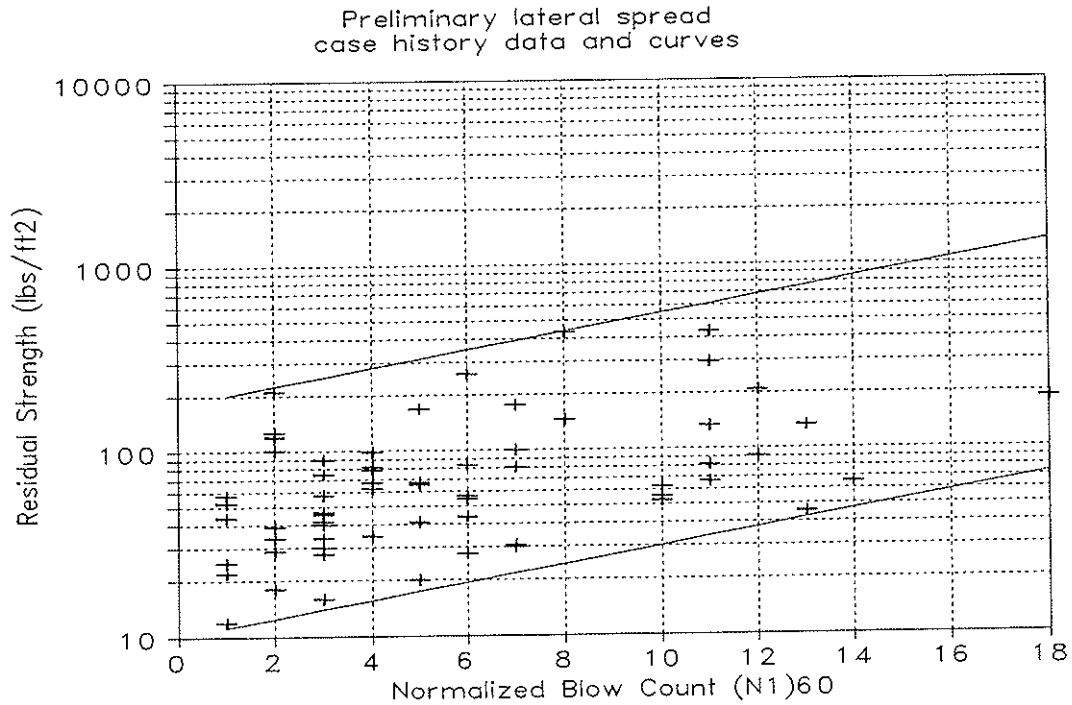

Figure 2.

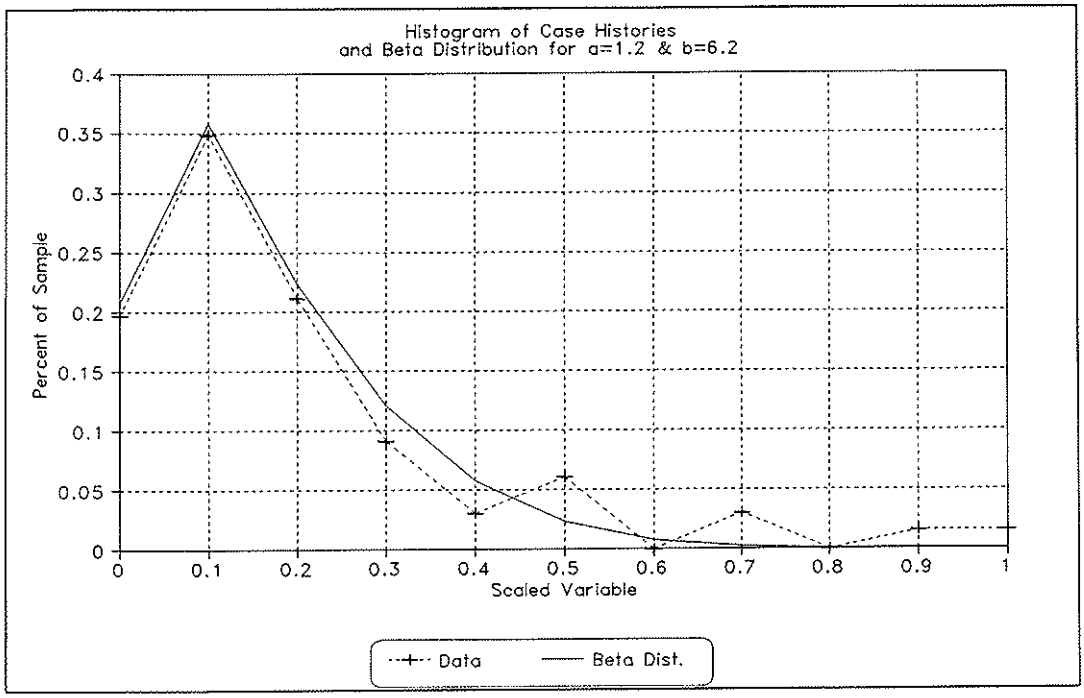

Figure 3.

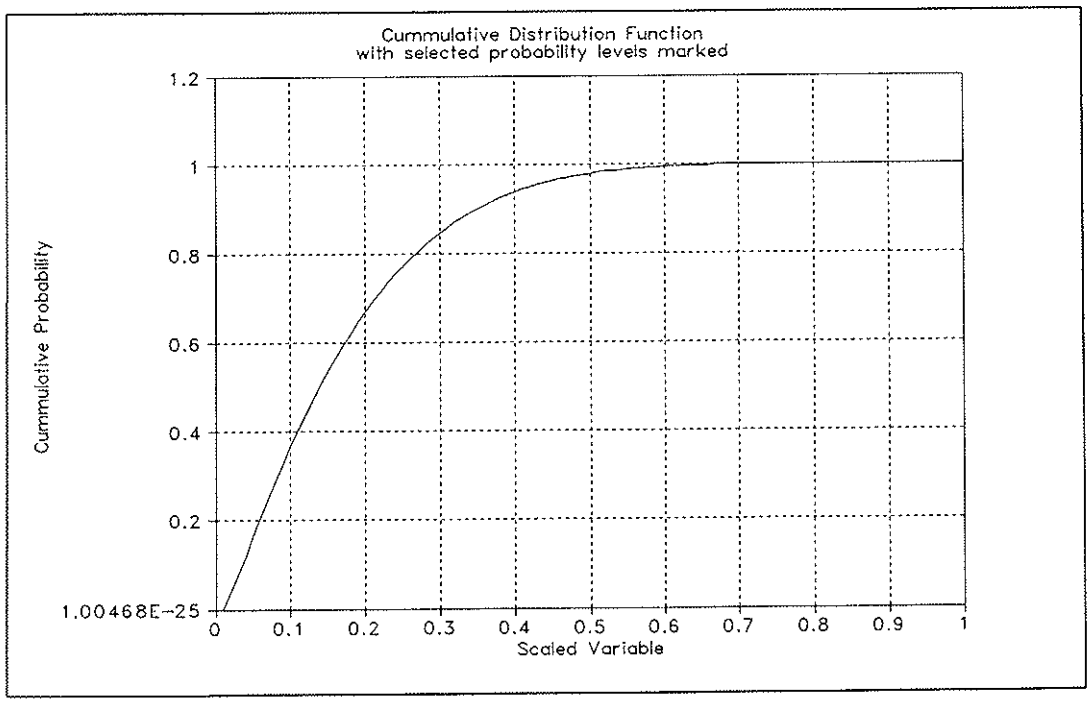

Figure 4.

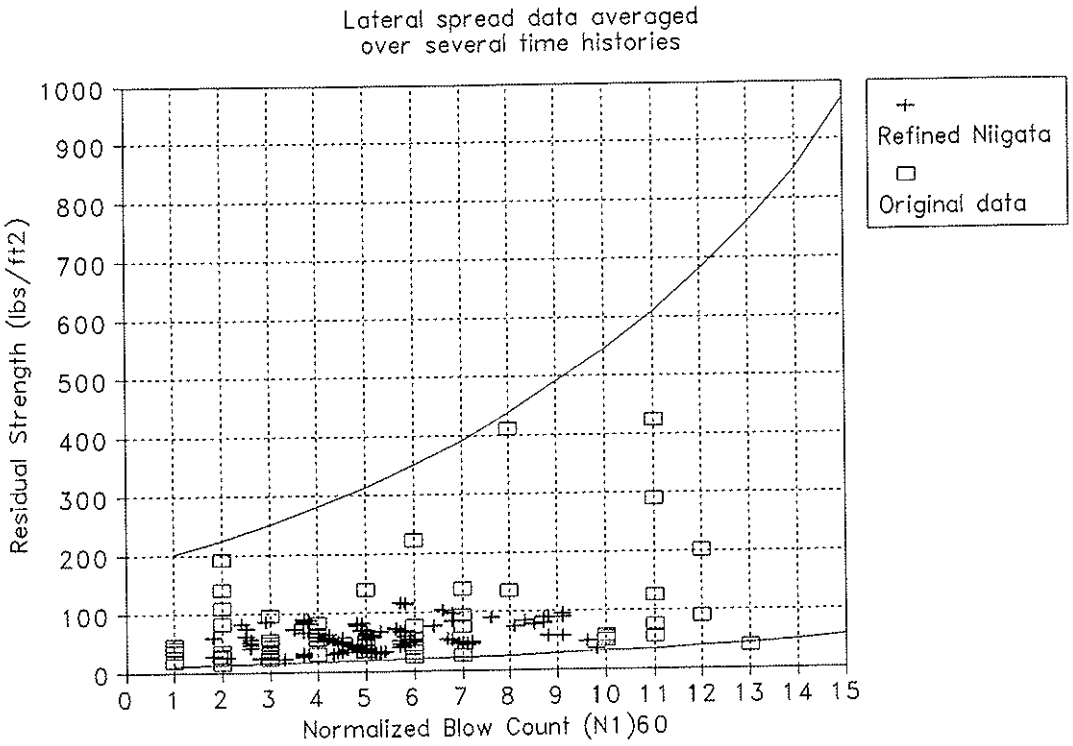
Lateral spread data averaged
over several time histories
Residual Strength (lbs/ft2)
1000
900
800
700
600
500
400
300
200
100
0
0 1 2 3 4 5 6 7 8 9 10 11 12 13 14 15
Normalized Blow Count (N1)60
Refined Niigata
Original data

Figure 5.

APPENDIX D.
Participant Contact Information

PRINCIPAL INVESTIGATOR

Professor Timothy D. Stark
2217 Newmark Civil Engineering Laboratory
University of Illinois at Urbana-Champaign
205 N. Mathews Ave.
Urbana, IL 61801-2352
217-333-7394
217-333-9464 (fax)
e-mail: t-stark1@uiuc.edu

SPONSOR

Dr. Clifford J. Astill
Program Director, Siting and Geotechnical Systems/Earthquake Hazards Mitigation
4201 Wilson Blvd., Room 545
Arlington, VA 22230
703-306-1362
703-306-0291 (fax)
e-mail: castill@nsf.gov

THEORETICAL/CONCEPTUAL ISSUES DISCUSSION GROUP PARTICIPANTS

*Keynote Speaker:

Professor Peter M. Byrne
Department of Civil Engineering
University of British Columbia
Canada V6T 1W5
604-822-2516
604-822-6901 (fax)

Professor J. David Frost
Associate Professor and GT Coordinator
Georgia Institute of Technology
School of Civil and Environmental Engineering
Atlanta, GA 30332-0355
404-894-2280
404-894-2281 (fax)
e-mail: dfrost@ce.gatech.edu

Dr. Marte Gutierrez
Senior Engineer
Norwegian Geotechnical Institute
P.O. Box 3930 Ullevål Hageby
N-0806 Oslo, Norway
9-011-47 22 02 30 00
9-011-47 22 23 04 48 (fax)
e-mail: mg@ngi.no

Dr. Richard M. Iverson
Research Hydrologist
U.S. Geological Survey
David A. Johnston Cascades Volcano Observatory
5400 MacArthur Blvd.
Vancouver, WA 98661
360-696-7772
360-696-7866 (fax)

Mr. Michael G. Jefferies
Golder Associates, Inc.
Landmere Lane, Edwalton
Nottingham, England NG12 4DG
9-011-44-115-9456544
9-011-44-115-9456540 (fax)
e-mail: mjefferies@golder.com

Dr. Joseph P. Koester
U.S. Army Corps of Engineers
Waterways Experiment Station, CEWES-GG-H
3909 Halls Ferry Road
Vicksburg, MS 39180-0631
601-634-2202
601-634-3453 (fax)
e-mail: koestej@ex1.wes.army.mil

****Recording Secretary:**

Professor Steven L. Kramer
Department of Civil Engineering (FX-10)
265 Wilcox Hall
University of Washington
Seattle, WA 98195
206-685-2642
206-685-3836 (fax)
e-mail: kramer@u.washington.edu

Professor Jean H. Prévost
E-306, E-Quad
Department of Civil Engineering
Princeton University
Princeton, NJ 08544
609-258-5424
609-258-1270 (fax)
e-mail: prevost@soil.princeton.edu

Dr. Wen-June Su
Associate Engineering Geologist
Illinois State Geological Survey
615 Peabody Dr.
Champaign, IL 61820
217-333-4747
217-333-2830 (fax)

SHEAR STRENGTH OF LIQUEFIED SOILS FROM LABORATORY AND FIELD TESTS DISCUSSION GROUP PARTICIPANTS

Professor Wayne A. Charlie
Department of Civil Engineering
Colorado State University
211 A Weber Building
Fort Collins, CO 80523
970-491-8584 or 5048
970-491-7727 (fax)
e-mail: wcharlie@vines.colostate.edu

Professor Pedro A. de Alba
University of New Hampshire
College of Engineering & Physical Sciences
Department of Civil Engineering, Kingsbury Hall
Durham, NH 03824-3591
603-862-1417
603-862-2364 (fax)
e-mail: padealba@christa.unh.edu

Mr. Jason E. Hedien
Geotechnical Engineer
Harza Engineering Co.
Sears Tower
233 S. Wacker Dr.
Chicago, IL 60606-6392
312-831-3000
312-831-3999 (fax)

Professor Bruce L. Kutter
University of California at Davis
Department of Civil Engineering
Davis, CA 95616
916-752-8099
916-752-8924 (fax)
e-mail: blkutter@ucdavis.edu

***Keynote Speaker:**

Professor Geoffrey R. Martin
Department of Civil Engineering
University of Southern California
Los Angeles, CA 90089-2531
213-740-9124
213-744-1426 (fax)
e-mail: geomar@mizar.usc.edu

Professor Gholamreza Mesri
University of Illinois at Urbana-Champaign
Department of Civil Engineering
2230 Newmark Civil Engineering Laboratory
205 N. Mathews Ave.
Urbana, IL 61801-2352
217-333-6934
217-333-9464 (fax)

Mr. Scott M. Olson
Graduate Research Assistant
University of Illinois at Urbana-Champaign
Department of Civil Engineering
2214 Newmark Civil Engineering Laboratory
205 N. Mathews Ave.
Urbana, IL 61801-2352
217-333-6941
217-333-9464 (fax)
e-mail: s-olson4@uiuc.edu

Dr. Steven J. Poulos
Principal
GEI Consultants, Inc.
1021 Main Street
Winchester, MA 01890-1970
617-721-4075
617-721-4073 (fax)

Professor Michael F. Riemer
Department of Civil and Environmental Engineering
440 Davis Hall
University of California
Berkeley, CA 94720-1710
510-642-7457
510-642-7476 (fax)
e-mail: riemer@ce.berkeley.edu

****Recording Secretary:**

Professor Peter K. Robertson
Department of Civil Engineering
University of Alberta
Edmonton, Alberta
Canada T6G 2G7
403-492-5106
403-492-8198 (fax)
e-mail: pkrobertson@civil.ualberta.ca

SHEAR STRENGTH OF LIQUEFIED SOILS FROM CASE HISTORIES DISCUSSION GROUP PARTICIPANTS

***Keynote Speaker:**

Dr. Gonzalo Castro
Principal
GEI Consultants, Inc.
1021 Main Street
Winchester, MA 01890-1970
617-721-4036
617-721-4073 (fax)

Professor Ricardo Dobry
Department of Civil Engineering
Rensselaer Polytechnic Institute
Troy, NY 12180-3590
518-276-6934
518-276-4833 (fax)
e-mail: dobryr@rpi.edu

Dr. A. Gus Franklin
U.S. Army Corps of Engineers
Waterways Experiment Station, CEWES-GG-H
3909 Halls Ferry Road
Vicksburg, MS 39180-0631
601-634-2658
601-634-3453 (fax)
e-mail: FRANKLA@ex1.wes.army.mil

Dr. David R. Gillette
Mail Code D-8313
U.S. Bureau of Reclamation
P.O. Box 25007
Denver, CO 80225-0007
303-236-3900 ext. 256
303-236-3900 (fax)
e-mail: DGILLETTE@ibr8gw80.usbr.gov

Dr. Leslie F. Harder, Jr.
Chief, Dam Projects Section
State of California
Department of Water Resources
1416 Ninth Street, P.O. Box 942836
Sacramento, CA 94236-0001
916-653-8055
916-653-0968 (fax)

Professor John C. Horne
Department of Civil Engineering
Clemson University
Clemson, SC 29634-0911
864-656-3322
864-656-2670 (fax)
e-mail: horne@ces.clemson.edu

Professor Izzat M. Idriss
Director, Center for Geotechnical Modeling
2097 Brainer Hall
Department of Civil Engineering
University of California
Davis, CA 95616
916-752-5403
916-758-1104 (fax)
e-mail: imidavis@aol.com

Dr. William F. Marcuson, III
U.S. Army Corps of Engineers
Waterways Experiment Station, CEWES-GG-H
3909 Halls Ferry Road
Vicksburg, MS 39180-0631
601-634-2234
601-634-3453 (fax)
e-mail: marcusw@ex1.wes.army.mil

Professor Timothy D. Stark
2217 Newmark Civil Engineering Laboratory
University of Illinois at Urbana-Champaign
205 N. Mathews Ave.
Urbana, IL 61801-2352
217-333-7394
217-333-9464 (fax)
e-mail: t-stark1@uiuc.edu

Professor Robert V. Whitman
Department of Civil and Environmental Engineering
Massachusetts Institute of Technology
77 Massachusetts Avenue
Cambridge, MA 02139
617-253-7127
617-253-6044 (fax)

****Recording Secretary:**

Professor T. Leslie Youd
Brigham Young University
368 Clyde Building
Provo, UT 84602
801-378-6327
801-378-4449 (fax)
e-mail: tyoud@byu.edu